# Control of Hepatitis C Virus Genome Replication by Viral Factors and Mediators of Host Intrinsic Immunity

**Patricia da Silva Domingues**

A thesis presented for the degree of Doctor of Philosophy

College of Medical, Veterinary and Life Sciences

University of Glasgow

**MRC - University of Glasgow**

**Centre for Virus Research**

**8 Church Street**

**Glasgow**

**G11 5JR**

**February 2013**

# Table of contents

**List of Figures and Tables** ..... **V**

**Acknowledgements** ..... **IX**

**Abbreviations** ..... **X**

**Abstract** ..... **XVI**

**One and Three Letter Amino Acid Abbreviations** ..... **XVIII**

**Author's declaration** ..... **XIX**

**1 Introduction** ..... **1**
1.1 Background ..... 1
1.1.1 Non-A, Non-B Hepatitis ..... 1
1.1.2 Classification of HCV ..... 2
1.1.3 Epidemiology and transmission of HCV ..... 4
1.1.4 Natural history of HCV infection ..... 8
1.1.5 Treatment of HCV infection ..... 10
1.2 HCV virion ..... 13
1.2.1 Genome organisation ..... 14
1.2.2 HCV-encoded proteins ..... 20
1.3 Experimental model systems for studying HCV life cycle ..... 34
1.3.1 *in vitro* models ..... 36
1.3.2 *in vivo* models ..... 40
1.4 HCV life cycle ..... 42
1.4.1 Virus attachment and entry ..... 42
1.4.2 Translation and Replication ..... 49
1.4.3 Assembly and release ..... 52
1.5 Immune responses and HCV infection ..... 57
1.5.1 Innate immune responses ..... 57
1.5.2 Adaptive immune responses ..... 65
1.6 Interferon stimulated gene 15 ..... 68
1.6.1 ISG15, an ubiquitin-like protein ..... 69
1.6.2 ISG15 gene expression ..... 73
1.6.3 Biological function of ISGylation ..... 74
1.7 Aims ..... 78

**2 Material and Methods** ..... **80**
2.1 Materials ..... 80
2.1.1 Bacteria ..... 80
2.1.2 Cells ..... 80
2.1.3 Vectors ..... 81
2.1.4 Clones ..... 81
2.1.5 Cell culture growth media ..... 81

2.1.6 Antisera ..... 82
2.1.7 Synthetic oligonucleotides ..... 83
2.1.8 siRNAs and shRNAs ..... 85
2.1.9 Kits ..... 87
2.1.10 Transfection reagents ..... 87
2.1.11 Interferons and related reagents ..... 88
2.1.12 Commonly used chemical ..... 88
2.1.13 Composition of buffers and solutions ..... 89
2.2 Methods ..... 91
2.2.1 Bacteria cultures ..... 91
2.2.2 Manipulation of DNA ..... 91
2.2.3 Manipulation of RNA ..... 99
2.2.4 Transfection of DNA/RNA into mammalian cells ..... 101
2.2.5 Protein methods ..... 102
2.2.6 Microscopy Methods ..... 103
2.2.7 Cell culture methods ..... 104
2.2.8 Assessment of HCV infection, replication and infectious virus production ..... 106

**3 Expanding HCV *in vitro* model systems ..... 115**
3.1 Introduction ..... 115
3.1.1 Expanding the SGR systems to include other HCV genotypes ..... 115
3.1.2 Hepatocyte-like permissive cell lines for HCV replication ..... 116
3.2 Construction of JFH1 SGRs containing genotype 3 sequences ..... 117
3.2.1 The NS4B C-terminal region is essential for HCV RNA replication 117
3.2.2 Construction of SGRs containing gt3a sequences at the C-terminal region of NS4B (2a3a-NS4B-SGR) ..... 120
3.2.3 Analysis of the replication competence of 2a3a-NS4B-SGRs ..... 127
3.2.4 Construction of 2a3a-NS3-4A-SGR ..... 135
3.2.5 J3a3a replicates efficiently in Huh-7 and Huh-7.5 ..... 135
3.2.6 Construction of JFH1 SGR containing genotype 3a NS3-4A protease variants ..... 137
3.2.7 Analysis of Luc-2a3a-NS3-4A-SGR replication ..... 143
3.3 Characterisation of ability of HepaRG cells to replicate HCV genomes ..... 145
3.3.1 HepaRG cells are not permissive for transient HCV replication .. 145
3.3.2 HepaRG cells can efficiently translate HCV SGR RNAs ..... 147
3.3.3 HCV can replicate in HepaRG cells in stable replication assays .. 148
3.3.4 HepaRG cells are not permissive for HCVcc infection ..... 152
3.3.5 Innate immune responses may dictate the permissiveness of HepaRG cells to viral replication ..... 154
3.4 Discussion ..... 162
3.4.1 Chimeric gt2a/gt3a SGR ..... 162
3.4.2 Permissiveness of HepaRG cells to HCV replication ..... 169

**4 Antiviral activities of ISG15 during HCV infection ..... 173**
4.1 Introduction ..... 173
4.2 Type I IFNs are strong inducers of ISG15 and can efficiently regulate HCV replication ..... 173
4.2.1 Huh-7 and U2OS cells induce ISG15 in response to IFN treatment 173
4.2.2 Type I IFNs efficiently reduce HCV replication in Huh-7 and U2OS cells ..... 177
4.3 siRNA silencing of ISG15 enhances constitutive HCV replication in Huh-7 and U2OS cells ..... 180
4.3.1 ISG15 knockdown partially alleviates IFN-mediated repression of HCV replication ..... 180
4.3.2 ISG15 silencing increases HCV RNA abundance in the absence of exogenous IFN stimulation ..... 180
4.4 shRNA silencing of ISG15 enhances HCV replication during infection . 185
4.4.1 Generation and characterisation of ISG15 shRNA lentiviral cell lines ..... 185
4.4.2 Transient HCV replication in sh6 cells ..... 194
4.4.3 Infection assays in sh6 cells ..... 198
4.5 Discussion ..... 204

**5 Investigation of the ISG15 mechanisms against HCV replication ..... 216**
5.1 Introduction ..... 216
5.2 Effect of ISG15 on viral RNA synthesis ..... 216
5.2.1 Optimisation of 4sU labelling of HCV RNA ..... 218
5.2.2 Labelling of nascent viral RNA during infection assays ..... 227
5.3 Preliminary studies on the conjugation requirements for ISG15 anti-HCV activities ..... 233
5.3.1 Generation of inducible Huh-7 cell lines to express ISG15 WT and mutant protein forms ..... 233
5.3.2 Silencing of ISG15 major E3 ligase, HERC5 ..... 246
5.4 Discussion ..... 250

**6 Final discussion and future perspectives ..... 255**
6.1 Summary ..... 255
6.2 Expanding the range of genotypes for study of HCV infection ..... 256
6.3 The mechanisms of action of ISG15 ..... 257
6.3.1 ISG15, an antiviral or proviral factor in HCV infection? ..... 257
6.3.2 Is conjugation necessary for ISG15 to impair HCV RNA replication? ..... 259

**References ..... 261**

# List of Figures and Tables

### Chapter 1

Figure 1.1 – HCV classification ..... 4
Figure 1.2 – Worldwide distribution of HCV genotypes 1-6 ..... 5
Figure 1.3 – Proposed possible mechanisms of action of ribavirin. ..... 11
Figure 1.4 – The HCV virion. ..... 13
Figure 1.5 – Schematic representation of the HCV genome ..... 14
Figure 1.6 – Model of the secondary and tertiary RNA structures of the 5'UTR of HCV (genotype 1b) ..... 18
Figure 1.7 – Proposed secondary structure of the 3' UTR of HCV (genotype 1b) . 19
Figure 1.8 – HCV *in vitro* model systems ..... 34
Figure 1.9 – Schematic representation of the HCV life cycle. ..... 42
Figure 1.10 - Activation of the interferon response triggered by the detection of viral pathogen-associated molecular patterns (PAMPs) ..... 60
Figure 1.11 - Interferon mediated signalling pathways ..... 63
Figure 1.12 – ISG15 structure. ..... 70
Figure 1.13 – Conjugation of ISG15 to target proteins (ISGylation). ..... 72

### Chapter 3

Figure 3.1- Predicted secondary structure of the NS4B C-terminus and sequence conservation between gt2a and gt3a variants ..... 118
Figure 3.2 – Representation of the gt3 mutants at the C-terminus of NS4B. ... 120
Figure 3.3 - Construction of NS4B C-terminal mutants by site-directed mutagenesis ..... 122
Figure 3.4 – Assessment of replication efficiency of NS4B gt3a mutants ..... 130
Figure 3.5 – Properties of the amino acids at the C-terminus of NS4B. ..... 130
Figure 3.6 – Luc-M1-7 replicates efficiently in Huh-7 cells ..... 133
Figure 3.7 – Replication efficiency of NS4B gt3a mutants ..... 134
Figure 3.8 – Schematic diagram of the JC-1 chimera genome. ..... 136
Figure 3.9 – J3a3a recombinant chimera and its ability to replicate in Huh-7 and Huh-7.5 cells ..... 137
Figure 3.10 – Cloning of the NS3-4A protease region from gt3a into Luc-SGR .. 138

Figure 3.11 – Luc-2a3a-NS3-4A cannot replicate in Huh-7 cells. ..... 143
Figure 3.12 – Transient replication assay of Luc-WT, Luc-GND and Luc-2a3a-NS3-4A electroporated in Huh-7 and Huh-7.5 cells..... 144
Figure 3.13 – HCV SGR replicons cannot replicate in HepaRG cells..... 146
Figure 3.14 - Translation of Luc-SGRs in Huh-7 and HepaRG cells. ..... 148
Figure 3.15 – Colony-forming capacity in Huh-7 and HepaRG cells ..... 149
Figure 3.16 – Stable HCV replication in HepaRG cells ..... 151
Figure 3.17 - Infection of Huh-7 cells with UV-inactivated virus..... 153
Figure 3.18 – HepaRGs are not permissive to HCV infection ..... 154
Figure 3.19 – dsRNA signalling and activation of type I IFN pathways..... 155
Figure 3.20 - Type I IFNs are strong inducers of ISG15 ..... 156
Figure 3.21 – Extracellular responses to poly-I:C in HepaRG cells. ..... 159
Figure 3.22 – Intracellular responses to poly-I:C in HepaRG cells..... 159
Figure 3.23 – ISG15 is upregulated during transient HCV replication in HepaRG cells..... 161
Figure 3.24 – Replication efficiency of genotype 3 NS4B mutants ..... 164
Figure 3.25 – Helical wheel projections of JFH1 (left panel) and Glasgow-3 (right panel) NS4B Helix 2 ..... 165
Figure 3.26 – Schematic representation of the amino acid sequence found at the NS4B/NS5A boundary ..... 167

**Chapter 4**

Figure 4.1 – Stable HCV replication in Huh-7 and U2OS cells ..... 174
Figure 4.2 – Type I IFNs are strong inducers of ISG15 ..... 176
Figure 4.3 – Type I IFNs efficiently reduce HCV replication ..... 177
Figure 4.4 – ISG15 silencing alleviates the IFN-mediated reduction of HCV RNA ..... 181
Figure 4.5 – ISG15 silencing promotes HCV replication ..... 183
Figure 4.6 – NS5A turnover levels in Huh-7/SGR cells ..... 184
Figure 4.7 – ISG15 silencing promotes HCV replication ..... 184
Figure 4.8 – Design and construction of pLKO-ISG15-specific shRNA lentiviral plasmids..... 191
Figure 4.9 – Map showing the features of the lentiviral vectors. [A] pLKO-shRNA vectors ..... 192

Figure 4.10 – Generation of lentiviral cell lines stably expressing ISG15 shRNAs ..... 193
Figure 4.11 – Characterisation of Huh-7 cells expressing ISG15 specific shRNAs ..... 196
Figure 4.12 – Transient HCV replication assay in shISG15 expressing cell lines. 197
Figure 4.13 – JC-1 infection efficiency in Huh-7 and shCtrl cell lines..... 200
Figure 4.14 – ISG15 silencing promotes HCV replication..... 201
Figure 4.15 – IFN antiviral activities during HCV infection in ISG15 depleted cells ..... 203
Figure 4.16 – Protein modification by ubiquitin (Ubiquitination) and ISG15 (ISGylation)..... 205
Figure 4.17 – Expression levels of ISG15 in Huh-7 and Huh-7.5 cells ..... 214
Figure 4.18 – Analysis of HERC5 silencing in U2OS/SGR cells ..... 214

**Chapter 5**

Figure 5.1 – Metabolic tagging of nascent RNA..... 217
Figure 5.2 – Schematic representation method used to determine absolute quantification of total and newly transcribed viral RNA..... 219
Figure 5.3 – Calculation of HCV RNA copy number ..... 220
Figure 5.4 – Amplification plot of IVT SGR standards (A) and the derived standard curve (B) ..... 223
Figure 5.5 – Labelling and quantification of newly transcribed viral RNA during HCV replication ..... 225
Figure 5.6 – Cell viability of Huh-7 exposed to increasing concentrations of 4sU ..... 226
Figure 5.7 – Labelling and quantification of newly transcribed viral RNA during HCV infection ..... 229
Figure 5.8 – Labelling and quantification of newly transcribed viral RNA during HCV infection ..... 230
Figure 5.9 – Labelling and quantification of newly transcribed viral RNA during HCV infection ..... 232
Figure 5.10 – Map of the lentivirus vectors used to express WT (GG) and mutant (AA) ISG15 from a cDNA fragment under the control of a tetracycline inducible promoter (A) and eGFPnls..... 235

Figure 5.11 – Construction of pLKO.dCMV.TetO.FLAG.ISG15-GG/AA lentiviral plasmids ..... 239
Figure 5.12 – Immunofluorescence analysis of FLAG expression ..... 240
Figure 5.13 – Generation of inducible lentiviral cell lines to express FLAG-ISG15-GG and –AA proteins ..... 243
Figure 5.14 – Analysis of the expression of FLAG protein in inducible lentiviral cells ..... 245
Figure 5.15 – Western blot analysis of ISG15 and FLAG protein expression in Huh-7-FLAG-ISG15-GG and –AA cell lines ..... 245
Figure 5.16 – Analysis of HERC5 silencing in Huh-7/SGR cells ..... 249

## Tables

Table 1 – Summary of the findings regarding ISG15 activities on HCV replication. ..... 211
Table 2 – Copy number of HCV IVT standards. ..... 222
Table 3 – Standards vs CT. ..... 222

# Acknowledgements

I would like to thank Prof. Duncan McGeoch and Prof. Massimo Palmarini for the opportunity to undertake my PhD studies at the CVR.

I am greatly indebted to my amazing supervisors, John McLauchlan and Chris Boutell for their enormous patience, guidance and ability to deal with my crazy ideas. But most of all, I thank them for their outstanding supervision of my practical and written work. I would like to express my gratitude to John for his kind and caring nature towards all those depending on him and for always being there for me during the many stressful times of my PhD.

I would like to thank my parents and my sister for their never ending love and support through all these years away from home. Without them I would never have come this far in my scientific career. I also extend my gratitude to my grandparents and loved ones that are no longer with us, who always motivated me to follow my dreams.

Thanks to all the past and present members of John's group for creating a great working atmosphere, especially Graham Hope, Gaie Brown and Paul Targett-Adams for their scientific expertise and friendship. Also, an extended thank you to other members of the CVR (in particular, Michelle Pearson, Charles McGinley, Anne Catchpole, Fiona Graham, Steven McFarlane) for their constant support even with the most unusual demands! I would like to thank Prof. Roger Everett and Dr. Arvind Patel for providing me with crucial reagents.

I am very grateful to Allan, Seamus and Jolanda for making the late working nights so much fun. And also, to the members of the Oh Kami karate Club, especially to Rachael and Andrew for their love and the much need coffee breaks!

Last but not least, I am very grateful to my new supervisor Ben for his patience and support during the final stage of writing my thesis.

# Abbreviations

| | |
|---|---|
| °C | degrees centigrade |
| % | percentage |
| μ | micro ($10^{-6}$) |
| 4sU | 4-thiouridine |
| ADRP | adipocyte differentiation related protein |
| ALT | alanine aminotransferase |
| Amp | ampicillin |
| Apo | apolipoprotein |
| APS | ammonium persulphate |
| ATP | adenosine-5'-triphosphate |
| Blast | blasticidin |
| bp | base pair(s) |
| BPB | bromophenol blue |
| BrUTP | 5-bromouridine 5'-triphosphate |
| BSA | bovine serum albumin |
| BVDV | bovine viral diarrhoea virus |
| C- | carboxy-terminus |
| CCAM | cell culture adaptive mutation |
| cDNA | complementary DNA |
| CHO | Chinese hamster ovary (cells) |
| CLDN | claudin (receptor) |
| cn | copy number |
| CTP | cytidine-5'-triphosphate |
| DAB | diaminobenzidine |
| DAPI | 4',6-diamidino-2-phenylindole |
| $dH_2O$ | deionised molecular biology grade water |
| DMEM | Dulbecco's modified Eagles media |

| | |
|---|---|
| DMSO | dimethyl sulphoxide |
| DNA | deoxyribonucleic acid |
| ds | double-stranded |
| DV | dengue virus |
| EDTA | ethylenediaminetetra acetic acid |
| EGF | epidermal growth factor |
| eIF | eukaryotic translation initiation factor |
| EM | electron microscopy |
| EMCV | encephalomyocarditis virus |
| ER | endoplasmic reticulum |
| FCS | foetal calf serum |
| FFU | focus-forming unit(s) |
| FITC | fluorescein isothiocyanate |
| FRAP | fluorescence recovery after photobleaching |
| g | gram(s) or gravitational force |
| GAG | glycosaminoglycan |
| GFP | green fluorescent protein |
| GTP | guanosine-5'-triphosphate |
| h | hour(s) |
| HAV | hepatitis A virus |
| HBV | hepatitis B virus |
| HCC | hepatocellular carcinoma |
| HCl | hydrochloric acid |
| HCV | hepatitis C virus |
| HCVcc (virus) | HCV cell culture-derived virus |
| HCVpp | HCV pseudoparticles |
| HDL | high-density lipoprotein |
| HIV | human immunodeficiency virus |

| | |
|---|---|
| HL | hydrophobic loop |
| HRP | horseradish peroxidase |
| HVR | hypervariable region |
| IF | indirect immunofluorescence |
| IFN | interferon |
| IFNAR | interferon alpha receptor |
| IFNGR | interferon gamma receptor |
| Ig | immunoglobulin |
| IRES | internal ribosome entry site |
| IRF3 | IFN regulatory factor 3 |
| ISG | IFN-stimulated gene |
| JFH | Japanese fulminant hepatitis |
| Kan | kanamycin |
| kb | kilobase pair(s) |
| KDa | kilodalton(s) |
| l | litre(s) |
| LCS | low-complexity sequence |
| LD | lipid droplet |
| LDL | low-density lipoprotein |
| LEL | large extracellular loop |
| LVP | lipoviroparticle |
| ml | millilitre ($10^{-3}$) |
| M | molar |
| MAF | membrane-associated foci |
| MBN | mung bean nuclease |
| MDA5 | melanoma differentiation-associated gene 5 |
| ME | mercaptoethanol |
| min | minute(s) |

| | |
|---|---|
| miRNA | micro RNA |
| mRNA | messenger RNA |
| MTOC | microtubule organising centre |
| MTP | microsomal triglyceride transfer protein |
| MW | membranous web |
| n | nano ($10^{-9}$) |
| N- | amino terminus |
| NS | non-structural proteins |
| NANBH | non-A, non-B hepatitis |
| NBM | nucleotide-binding motif |
| Neo/G418 | neomycin phosphotransferase |
| NS | non-structural |
| NTP | nucleoside triphosphate |
| OCLN | occludin (receptor) |
| ORF | open reading frame |
| *E.coli* | *Escherichia coli* |
| PAGE | polyacrylamide gel electrophoresis |
| PAMP | pathogen-associated molecular pattern |
| PBS | phosphate-buffered saline |
| PCR | polymerase chain reaction |
| PFA | paraformaldehyde |
| PI | protease inhibitor |
| PKR | protein kinase R |
| PRR | pattern recognition receptor |
| Puro | puromycin |
| RC | replication complex |
| RdRp | RNA-dependent RNA polymerase |
| RGB | running gel buffer |

| | |
|---|---|
| RIG-I | retinoic-acid-inducible gene I |
| RLU | relative light unit(s) |
| RNA | ribonucleic acid |
| RNAi | RNA interference |
| rpm | rotations per minute |
| RSV | respiratory syncytial virus |
| RTP | ribavirin triphosphate |
| RT-PCR | reverse transcription PCR |
| RT-qPCR | reverse transcription quantitative real-time PCR |
| S | Structural proteins |
| sec | second(s) |
| SDS | sodium dodecyl sulphate |
| SEL | small extracellular loop |
| SGB | stacking gel buffer |
| SGR | subgenomic replicon |
| siRNA | small inhibitory RNA |
| shRNA | short hairpin RNA |
| SP | signal peptidase |
| SPP | signal peptide peptidase |
| SR-BI | scavenger receptor class B member I |
| ss | single-stranded |
| SUMO | small ubiquitin modifier |
| STAT | signal transducer and activator of transcription |
| STAT-C | specifically targeted antiviral therapy for hepatitis C |
| $TCID_{50}$ | median tissue culture infective dose |
| TEMED | N'N'N'N'-tetramethylethylene-diamine |
| TMA | transcription-mediated amplification |
| TMD | transmembrane domain |

| | |
|---|---|
| TRBP | TAR RNA-binding protein |
| TRIS | 2-amino-2-(hydroxymethyl)-1,3-propanediol |
| TRITC | tetramethyl rhodamine isothiocyanate |
| TTP | thymidine-5'-triphosphate |
| ub | ubiquitin |
| ubl | ubiquitin-like protein |
| UTP | uridine-5'-triphosphate |
| UTR | untranslated region |
| UV | ultraviolet |
| VLDL | very-low density lipoprotein |
| VLP | virus-like particle |
| v/v | volume/volume ratio |
| WT | wild-type |
| w/v | weight/volume ratio |
| YFV | yellow fever virus |
| YT | yeast tryptose |

# Abstract

Hepatitis C virus (HCV) is a worldwide public health problem affecting an estimated 170 million individuals. Studies on the replication of the HCV genome have been facilitated by the development of selectable subgenomic replicons (SGRs) replicating in the human hepatoma cell line Huh-7. This system represents a powerful tool for studying viral RNA synthesis, but is limited by the HCV strains that can replicate in cell culture as well as the cell lines that can support replication. Improving these models would aid our current understanding of the role of intrinsic host and viral factors required for viral replication as well as providing valuable tools for the screening and identification of new antiviral compounds. Currently, replicon systems are available for genotype (gt) 1a, 1b and 2a isolates, which are able to replicate viral RNA both transiently and continuously in Huh-7 cells. In the UK, infection with gt3 accounts for about 44% of cases and has a similar prevalence to gt1. The lack of cell culture systems for gt3 has hampered studies on its pathogenesis and responsiveness to novel anti-HCV therapeutics.

Given that construction of a SGR entirely from gt3 sequences has previously failed, our approach examined the feasibility of replacing sequences at the C-terminus of NS4B and the NS3/4A protease from the JFH1 SGR with those from the Glasgow-3 gt3a isolate. The approach adopted in these studies identified amino acids that vary between gt2a and gt3a at the C-terminus of NS4B, which can be tolerated without impairing HCV RNA replication. By contrast, cloning of NS3-4A sequences into the JFH1-SGR (Luc-2a3a-NS3-4A) abolished any detectable transient replication in Huh-7 cells. However, delayed replication was evident in Huh-7.5 cells, a clonal derivative of Huh-7 cells.

A further aim was to expand the cell lines permissive for HCV RNA replication. To date, only Huh-7 cells are highly permissive for viral replication and virus production in culture. Huh-7 cells are hepatoma cells, and may not fully recapitulate the features of hepatocytes during normal infection by HCV. Therefore, the permissiveness of HepaRG cells, a cell line which retains many features of fully functional hepatocytes, to HCV replication was examined. Despite the ability to translate viral RNA, HepaRG cells were unable to initiate HCV RNA replication in short-term assays. Nevertheless, assessment of

replication using colony forming assays did reveal that stable replication of SGR RNAs could be achieved in HepaRG cells, under selective pressure with an antibiotic. Thus, adaptation of the JFH1 SGR to the HepaRG cell environment may be required for efficient genome synthesis. Similar to the results with transient replication assays, HepaRG cells were not susceptible to infection by HCV.

HCV typically establishes a chronic infection that can be successfully eradicated by interferon-alpha (IFN$\alpha$) based therapies. However, the underlying mechanisms leading to viral clearance by IFN$\alpha$ are poorly understood. From a siRNA library screen, ISG15 was identified as an interferon-stimulated gene that modulated HCV RNA replication. In this study, the contribution of ISG15 to clearance of HCV infection was examined in greater detail. siRNA-mediated depletion of ISG15 from both Huh-7 and U2OS cells, which harboured the subgenomic replicon, repressed ISG15 expression, resulting in a suppression of the antiviral activity of IFN$\alpha$. Moreover, lowering the expression of ISG15 increased viral RNA levels in Huh-7 and U2OS cells in the absence of IFN. These data indicate that ISG15 plays an inhibitory role during HCV replication both by augmenting IFN-mediated antiviral activity and in a mechanism independent from IFN-activation. Further experiments using the infectious HCV system confirmed these results and demonstrated that infection of Huh-7 cells stably expressing short hairpin RNA (shRNA) directed against ISG15 resulted in higher levels of HCV RNA, when compared with shRNA-Ctrl cells. Together, these findings imply a role for ISG15 in limiting HCV replication. The mechanism used by ISG15 to modulate HCV infection is not known. Following the above findings, studies were conducted to determine whether ISG15 can affect the rates of synthesis or degradation of viral RNA. By metabolically labelling newly synthesised transcripts, it was shown that cells stably expressing ISG15 shRNAs generated higher levels of viral RNA compared with control cells. This increase in the levels of newly synthesised viral RNA mirrored the differences in total steady-state levels of viral RNA in both cell lines, indicating that ISG15 can negatively regulate the rate of viral RNA synthesis. Since ISG15 is an ubiquitin-like protein and can form conjugates with an array of other proteins, the requirements of ISG15 conjugation for its anti-HCV activities were also explored.

# One and Three Letter Amino Acid Abbreviations

| Amino acid | Three letter code | One letter code |
|---|---|---|
| Alanine | Ala | A |
| Arginine | Arg | R |
| Asparagine | Asn | N |
| Aspartic acid | Asp | D |
| Cysteine | Cys | C |
| Glutamine | Gln | Q |
| Glutamic acid | Glu | E |
| Glycine | Gly | G |
| Histidine | His | H |
| Isoleucine | Ile | I |
| Leucine | Leu | L |
| Lysine | Lys | K |
| Methionine | Met | M |
| Phenylalanine | Phe | F |
| Proline | Pro | P |
| Serine | Ser | S |
| Threonine | Thr | T |
| Tryptophan | Trp | W |
| Tyrosine | Tyr | Y |
| Valine | Val | V |

# Author’s declaration

All work presented in this thesis was obtained by the author’s own efforts, unless otherwise stated.

# 1 Introduction

## 1.1 Background

### 1.1.1 Non-A, Non-B Hepatitis

Viral hepatitis is a clinical condition which describes inflammation of the liver caused by viral infection. Originally, two types of viral hepatitis were recognized to describe infections caused by hepatitis A virus (named “infectious hepatitis”) or by hepatitis B virus (termed “serum hepatitis”) (Bayer *et al.*, 1968; Feinstone *et al.*, 1973). With the advent of serological tests for HAV and HBV, it became clear that some patients with transfusion-associated hepatitis suffered from a different form of hepatitis. These patients did not have serological markers for either HAV or HBV, hence this transfusion-associated hepatitis was called non-A, non-B hepatitis (NANBH) (Feinstone *et al.*, 1975).

Studies in chimpanzees, showed that NANBH was caused by a transmissible agent, as inoculation of these animals with serum from patients diagnosed with NANBH resulted in enhancement of ALT levels similar to that seen in patients (Alter *et al.*, 1978). Moreover, serum from infected chimpanzees was able to infect a second line of animals. The agent responsible for NANBH was sensitive to organic solvents and lost its infectivity after treatment with chloroform, indicative of a virus containing a lipid envelope (Feinstone *et al.*, 1983). Further analysis from transmission studies in chimpanzees revealed that the NANBH agent caused distinctive membranous tubules in hepatocytes from infected animals (Shimizu *et al.*, 1979). Simultaneously, other studies demonstrated that the infectivity of NANBH was not reduced on passage of the inoculum through an 80nm filter (Bradley *et al.*, 1985). Collectively, these observations indicated that the causative agent for NANBH was probably a small enveloped virus, which was capable of inducing the formation of membranous tubules in infected cells.

Despite this progress, conventional immunological methods failed to identify viral antigens and antibodies associated with NANBH. It was not until 1989 when Choo and co-workers, using recombinant DNA cloning technologies, identified the causative agent of NANBH (Choo *et al.*, 1989). In their approach, small cDNA fragments were amplified from infectious material derived from

chronically infected chimpanzees and cloned into bacteriophage λgt11 to create an expression library that was screened with sera from chronic NANBH patients. From this screen, one positive clone (5-1-1) proved to be derived from the NANB genome. Using Southern blot analysis, the 5-1-1 cDNA clone was shown not to hybridise to either control human DNA or to DNA derived from NANBH-infected chimpanzees, thereby demonstrating that this cDNA clone was not derived from the host genome. Total RNA extracted from the liver of infected chimpanzees specifically hybridised to both cDNA clone 5-1-1 and 81 (a larger overlapping clone isolated from the same library), but not with total RNA extracted from control, uninfected chimpanzees (Choo *et al.*, 1989). Furthermore, extracted nucleic acids from ultracentrifuged pellets of NANBH chimpanzee plasma lost the hybridization signal after treatment with ribonuclease but not with deoxyribonuclease, indicating that the infectious agent contained an RNA genome. Moreover, NANBH virus carried a single-stranded RNA molecule, since only one of the strands in clone 81 hybridized to the viral genome. Using Northern blot analysis the length of the viral genome was estimated to be about 10,000 nucleotides. Sequencing of clone 5-1-1 revealed that it contained one continuous long open reading frame (ORF) of positive-sense. The infectious agent of NANBH was then designated hepatitis C virus (HCV) (Choo *et al.*, 1989).

### 1.1.2 Classification of HCV

HCV was described as an enveloped positive-sense, single-stranded RNA virus and, due to its ability to induce membrane tubule formation, it was originally suggested to be related to the *Togaviridae* or *Flaviviridae*. From analysis of HCV amino acid sequences, greater similarity was found with members of the two genera of the *Flaviviridae* family (*Pestivirus* and *Flavivirus*). This led to the classification of HCV as a member of the *Flaviviridae* family (Miller & Purcell, 1990). Later, gene organisation and hydrophobicity profiles indicated that HCV was closer to the *Pestivirus* genus than the Flaviviruses (Choo *et al.*, 1991). Subsequently, HCV was classified as a separate genus (*Hepacivirus*) within the *Flaviviridae* (Robertson *et al.*, 1998) (Figure 1.1).

HCV has been divided into six closely related major genetic groups or genotypes (numbered 1 to 6) (Simmonds, 2004). Each of these genotypes is equally divergent, differing by about 30-35% at the nucleotide level, leading to approximately 30% amino acid sequence differences between the encoded polyproteins (Simmonds, 2004). Numerous subtypes (designated by a, b, c,..), corresponding to the more closely related sequences within some of genotypes (differing from each other by >15%) have also been described for HCV. The different HCV genotypes are also associated with distinct geographical distributions and with various groups at risk of infection (Simmonds, 2004).

The HCV-encoded RNA polymerase (section 1.2.2.2-V) possesses no proofreading or 5'-3' exonuclease activity, and therefore introduces mutations into the viral genome during replication. Consequently, neutral and adaptive evolution occurs during the course of chronic infection within an individual. These genetic variants within an infected individual have been referred to as quasispecies (Martell *et al.*, 1992). Accordingly, quasispecies are closely related viral genomes that differ from each other by up to 5% at the nucleotide level.

In addition to HCV, the genus *Hepacivirus* comprises also GB virus-B (GBV-B) and possibly canine hepacivirus (CHV) (Figure 1.1). GBV-B was isolated from plasma of an individual GB with unexplained hepatitis. However, this virus apparently did not originate from GB and doesn't seem to infect humans or chimpanzees, although it can cause acute hepatitis in infected tamarins and other New World monkey species (Bukh *et al.*, 2001; Stapleton *et al.*, 2011). More recently, CHV was identified in respiratory samples of domestic dogs (Kapoor *et al.*, 2011). CHV is the first non-primate hepacivirus discovered. Comparative phylogenetic analysis has confirmed that this virus is the closest genetic relative of HCV, however there is still some debate as to whether it should be classified as its own *Hepacivirus* species (Bukh, 2011).

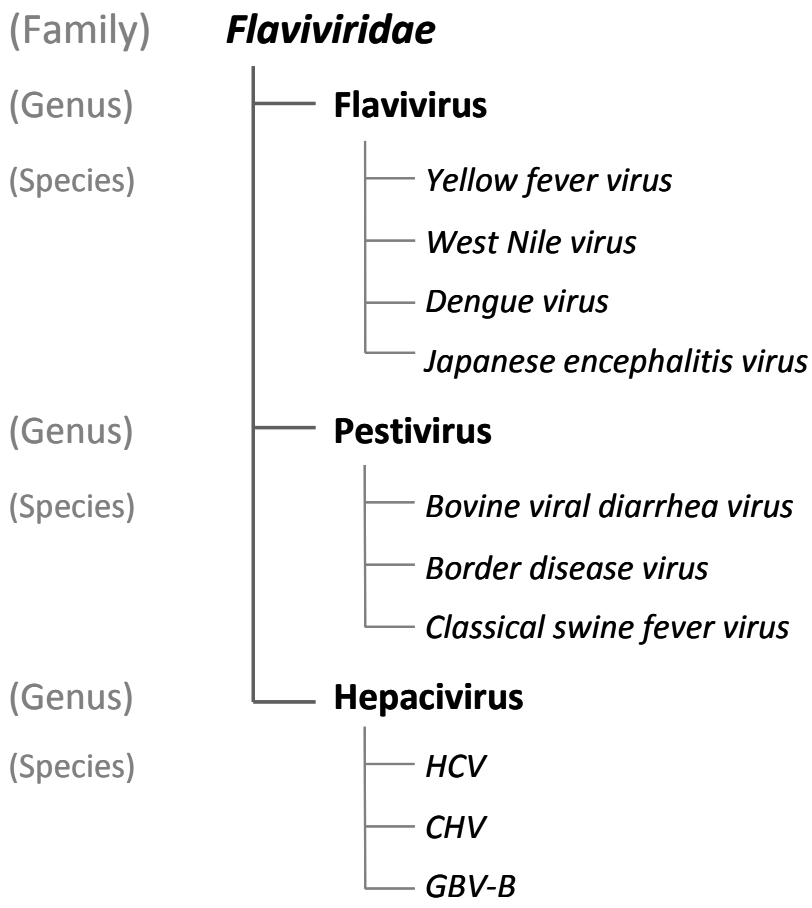


**Figure 1.1 – HCV classification. Three genera have been identified within the Flaviviridae family: *Flavivirus*, *Pestivirus* and *Hepacivirus*. HCV belongs to the *Hepacivirus* genus together with GBV-B. Recently CHV has been proposed to belong to the genus *Hepacivirus*.**

### 1.1.3 Epidemiology and transmission of HCV

Since its discovery, HCV has been recognised as a global health problem. It is estimated to affect 2-4% of the world's population (Alter, 2007). HCV is estimated to infect 0.6-1% of the population in UK, but almost 2% of the population in USA (Thomson, 2009). In Europe, prevalence ranges from 1.5% to 5%. Countries with the highest prevalence are found in Africa (>10%) and Asia (3-4%). Studies have shown that HCV positivity is particularly high in Egypt, with viral antibodies detected in 15-20% of the general population.

Prevalence of each genotype varies widely and can also be mapped geographically (Figure 1.2). For example, the dominant genotype found in Europe, USA and China is genotype 1. Genotype 4 is the most common genotype in Africa and the Middle East. Genotypes 5 and 6 are rare and found in isolated geographic areas; genotype 5 in South Africa and genotype 6 in Hong Kong and Southeast Asia. Recent data from the Health Protection Agency (HPA) indicates that the prevalence of genotype 3a is roughly similar to that for genotype 1 in the UK (HPA, 2011).

.

**Figure 1.2 – Worldwide distribution of HCV genotypes 1-6. The distribution of the six HCV genotypes is highlighted across the globe. Pie charts generated for each genotype (based on the sequences available at http:hcv.lanl.gov) are shown.**

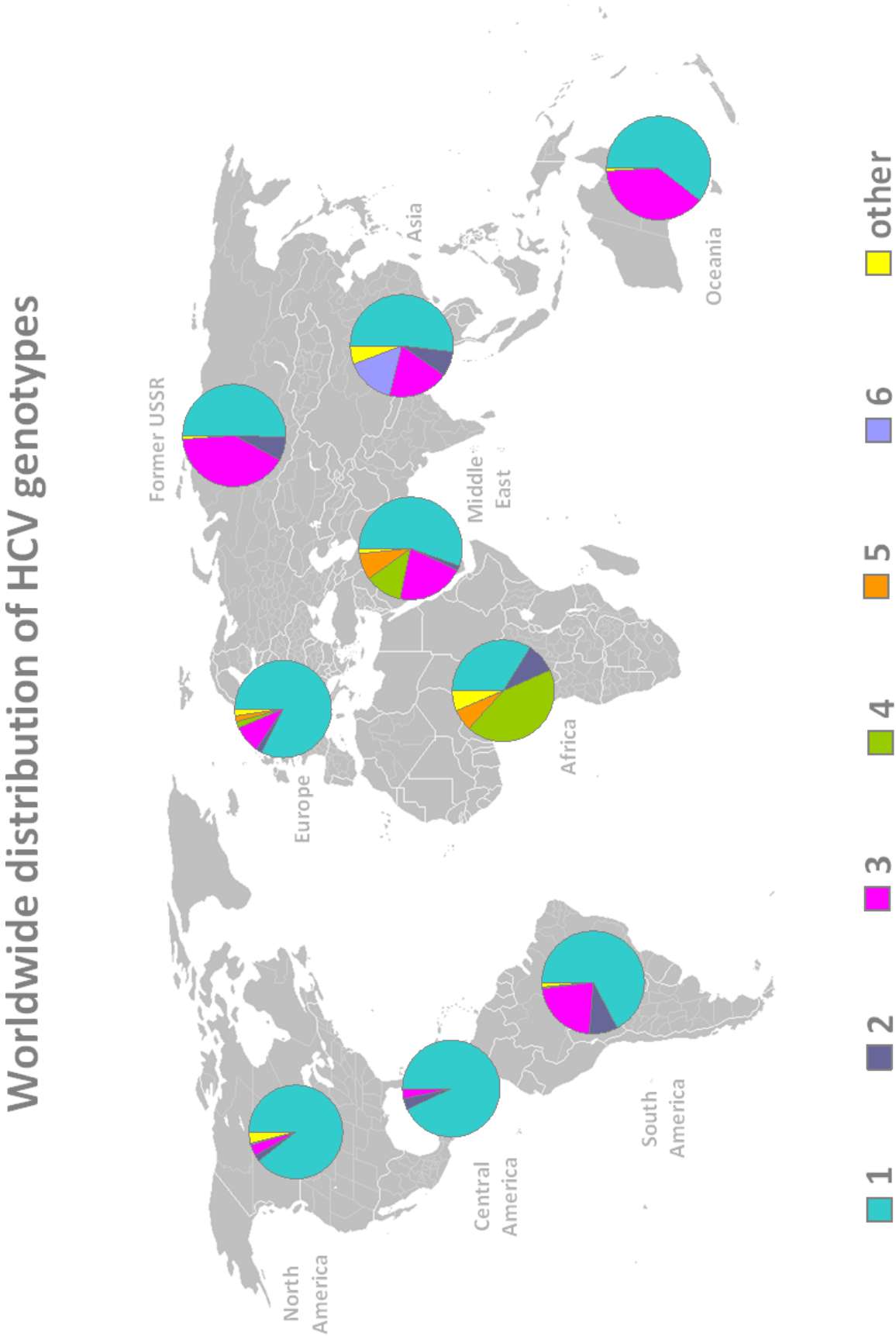
Worldwide distribution of HCV genotypes
Former USSR
Asia
Oceania
Middle East
Europe
Africa
North America
Central America
South America
1
2
3
4
5
6
other

HCV is transmitted predominantly by direct percutaneous exposure to infected blood, mainly through blood transfusions, intravenous drug use (IDU) or unsafe medical and surgical procedures (Shepard *et al.*, 2005). Transfusion-associated cases occurred prior to routine donor screening in blood banks, but this route of infection has been effectively eliminated in Western countries. However, in developing countries there is an ongoing risk of HCV transmission through transfused blood due to the lack of resources to implement adequate donor screening. The number of cases of acute HCV among injecting drug users has recently declined in the US and Europe because of implementation of harm reduction policies, syringe exchange programs, counseling of injecting drug users regarding protection from infection and changes in injecting behavior.

Transmission can also occur through alternative percutaneous modes like tattooing and body piercing as a consequence of using inadequately sterilized equipment. Some cases of acute HCV have been related to sexual transmission; however the degree to which the virus is transmitted through this route is debatable. An epidemic of acute hepatitis C has been reported among HIV-infected men who have sex with men (MSM) (Danta *et al.*, 2007). This route of transmission is higher than in heterosexual couples and, HIV and HCV co-infection is currently estimated to affect 4-5 millions of people worldwide (Alter, 2006). Given that transmission of HIV shares the same route, an increasing incidence of HCV infection in HIV-infected MSM can lead to serious health problems in the coming years and has serious implications on rapid transmission of drug-resistant variants as well as efficacy of future therapies (Thomson *et al.*, 2011a; Thomson *et al.*, 2011b).

IDU and to a lesser extent sexual transmission represents the main risks for acute HCV in western countries. The picture is however different in developing countries, in which social and cultural differences result in a very different set of risk factors for HCV. Nosocomial and iatrogenic transmission, occupational exposure, sexual and intrafamilial transmission in addition to IDU contribute to acute HCV cases in developing countries.

## 1.1.4 Natural history of HCV infection

HCV infection is a leading cause of chronic hepatitis, compensated and decompensated cirrhosis, and hepatocellular carcinoma. As a result, it is the most common indication for liver transplantation (Seeff, 2002). Initial infection leads to the establishment of an acute phase which, in the majority of cases, progresses to a chronic infection.

### 1.1.4.1 Acute Hepatitis C

Acute HCV infection is rarely identified, as the majority of infected individuals have mild or no symptoms. However, in 20 to 30% of infected individuals, acute infection can be accompanied by clinical symptoms, most of which are similar to other forms of hepatitis (flu-like symptoms, fever, jaundice, dark urine, fatigue, nausea, vomiting, loss of appetite and abdominal pain) (Lemon *et al.*, 2007). Acute infection can lead to fulminant hepatitis but this condition is rare.

HCV infection can be self-limiting and may spontaneously resolve. It is estimated that spontaneous clearance of acute HCV infection occurs in 15 to 20% of cases. However, in a single source outbreak of HCV infection of a group of healthy women, up to 50% of the cases resolved infection spontaneously (Pestka *et al.*, 2007). Although it is difficult to determine these acutely infected patients who will spontaneously resolve infection, several clinical features have been associated with spontaneous clearance: 1) age - patients less than 40 years of age including children are more likely to undergo spontaneous resolution; 2) gender - women are more likely to resolve infection than men; 3) clinical symptoms - jaundice is a good predictor of spontaneous viral clearance, presumably because it reflects an effective host immune response, capable of eradicating the virus; 4) co-infections - individuals with co-infections, for example HIV, are less likely to spontaneously clear HCV.

Most studies have suggested that cellular immune responses play a crucial role in spontaneous resolution of acute HCV. Clearance of HCV is associated with the development of robust and multispecific CD4+ and CD8+ T-cell responses (Thimme *et al.*, 2002). Persistence of HCV infection presumably occurs when the innate responses are weak or antagonised, thus diminishing their direct antiviral effects (Seeff, 2009).

#### 1.1.4.2 Chronic Hepatitis C

It is thought that up to 80% of acute infections become persistent, culminating in a chronic state. Most patients with chronic hepatitis C are asymptomatic, however more severe symptoms can develop over a 5–35 year period in as many as 20% of infected patients. The most common symptom is intermittent fatigue, with others reporting right upper quadrant abdominal pain, nausea and poor appetite. These patients can eventually develop serious liver diseases such as hepatic fibrosis, cirrhosis and steatohepatitis. Among those with cirrhotic livers, 1- 4% develop hepatocellular carcinoma (HCC) (Heller & Rehermann, 2005).

Progression to liver fibrosis is affected by many factors such as alcohol consumption, obesity, diabetes mellitus, gender and age of acquiring infection. Additionally, the degree of inflammation and fibrosis on liver biopsy, immunosuppression and genetic profile, HIV or HBV coinfection and comordid conditions are important factors influencing the course of chronic HCV infection. Chronic HCV is also associated with extrahepatic manifestations. Among them, the most common is mixed cryoglobulinemia (Charles & Dustin, 2009).

The various HCV genotypes also exhibit differences in HCV pathology and influence progression to liver complications. For example, higher rates of progression to chronicity have been associated with people infected with genotype 1 (Amoroso *et al.*, 1998). Moreover, a relationship between genotype 3 infections and hepatic steatosis has also been identified (Mihm *et al.*, 1997; Rubbia-Brandt *et al.*, 2001; Rubbia-Brandt *et al.*, 2000). Although additional factors may be involved, this hepatic manifestation was suggested to be associated with genotype 3 infections, as improvement of steatosis was observed after elimination of the virus with interferon (IFN) (Castera *et al.*, 2004; Kumar *et al.*, 2002).

### 1.1.5 Treatment of HCV infection

A protective vaccine against HCV does not exist and the current standard of care consists of a combination of Pegylated interferon-$\alpha$ (Peg-IFN$\alpha$) and ribavirin (RBV). This therapy is administered for 24-48 weeks, depending on the HCV genotype and baseline viraemia (NICE, 2004). Cure of infection is characterised by a sustained virologic response (SVR), which is defined as absence of HCV in the peripheral blood 24 weeks after cessation of treatment. With these regimens, approximately 70-80% of patients infected with genotypes 2 or 3 achieve SVR, whereas only 40-50% of patients infected with genotypes 1 or 4 successfully respond to therapy (Soriano *et al.*, 2009). Moreover, Peg-IFN$\alpha$/RBV therapy is frequently associated with side effects, including myalgia, fever, headaches, depression and anaemia (Fried *et al.*, 2002). For those patients who develop cirrhosis and HCC, liver transplantation is the only available option. However, infection of the grafted organ occurs in all cases due to circulating virus and progression to serious liver disease is more rapid. Moreover, these patients respond less efficiently to therapy.

The exact mode by which this combination therapy eradicates HCV infection is still not clear. IFN$\alpha$ belongs to the family of type I IFNs, host-cell synthesised cytokines, which play a central role in the innate immune response. In addition to their antiviral properties, type I IFNs have antiproliferative and immunomodulatory properties. The antiviral properties of these cytokines are described in more detail in section 1.5.1.1. Briefly, IFN$\alpha$ creates an antiviral state in the cells through inducing expression of IFN-stimulated genes (ISGs). It is

thought that the proteins encoded by these ISGs will mediate the antiviral activities of IFNα and play an essential role in clearance of infection. The mechanism of viral clearance by these ISG proteins is not yet understood.

RBV is a broad-spectrum antiviral nucleoside analogue, capable of being incorporated into viral RNA during replication and can therefore prematurely terminate synthesis of viral RNA. The exact mode of action of ribavirin is not known. However, a combination of different mechanisms have been proposed (Paeshuyse *et al.*, 2011): 1) immunomodulatory activities; 2) modulation of the ISG expression; 3) inhibition of inosine 5'-monophosphate dehydrogenase (IMPDH) by ribavirin 5'-monophosphate (RMP); 4) inhibition of eIF4E; 5) inhibition of the RNA-dependent RNA polymerase by ribavirin 5'-triphosphate (RTP) and 6) induction of viral mutagenesis (Figure 1.3).

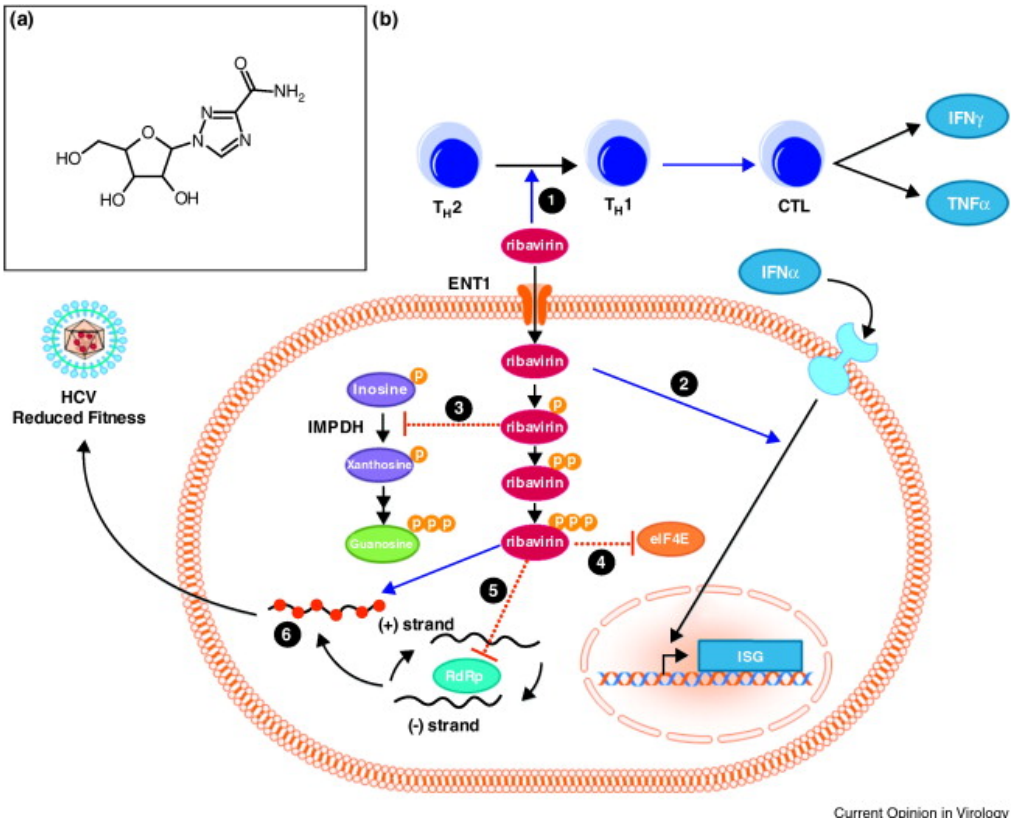


**Figure 1.3 – Proposed possible mechanisms of action of ribavirin. [A] Structural formula of ribavirin. [B] Schematic diagram indicating the proposed mechanisms of action of ribavirin: (1) modulation of the TH1 and TH2 responses, (2) stimulation of ISG expression, (3) inhibition of IMPDH, (4) inhibition of the eukaryotic translation initiation factor eIF4E, (5) direct inhibition of the viral RdRP, (6) viral mutagenesis. The red dotted lines indicate an inhibitory or negative effect; blue arrows indicate a stimulatory or positive effect. ISG: interferon stimulated gene, CTL: cytotoxic T lymphocyte, IMPDH: inosine 5'-monophosphate dehydrogenase, HCV: hepatitis C virus, RdRp: RNA-dependent RNA polymerase, INFα: interferon-alpha, INFγ: interferon-gamma, TNFα: tumour necrosis factor alpha, ENT1: equilibrative nucleoside transporter 1. Extracted from Paeshuyse *et al.*, 2011.**

Over the past decade, the focus has been to refine the use of current therapies through an increased understanding of how viral kinetics predicts the success or failure of treatment. A major contribution was the discovery of a group of single nucleotide polymorphisms (SNPs) in the region of the interleukin-28B gene (IL-28B, type III IFN) (Mangia *et al.*, 2010; Ridruejo *et al.*, 2011; Thompson *et al.*, 2010). These studies have shown that patients with a CC genotype of the IL-28B polymorphism achieve higher SVR (more than 2-fold) after treatment with Peg-IFN$\alpha$/RBV, compared to patients with the CT or TT genotype.

Through developments with *in vitro* systems that have given a greater understanding of the HCV lifecycle, it has been possible to identify a number of potential new targets for direct acting antivirals (DAAs; antiviral agents targeting viral functions) and host-targeted agents (HTA; which inhibit host cell activities known to be required for viral replication). Among the DAAs, the NS3/4A protease inhibitors (PI), telaprevir and boceprevir, have recently been approved for treatment of patients infected with HCV genotype 1 (Jacobson *et al.*, 2011; Poordad *et al.*, 2011; Ramachandran *et al.*, 2012). PI monotherapy is associated with a rapid emergence of drug-resistance viral variants, therefore current treatment strategies require co-administration with Peg-IFN$\alpha$/RBV. These regimens have shown improved efficacy (60–75% SVR) compared with current standard of care in genotype 1-infected individuals. Interestingly, triple therapy also shows good efficacy in patients who previously failed to respond to therapy (Bacon *et al.*, 2011). A number of other DAAs and HTAs are at the preclinical or early to late clinical development stage. These include other NS3/4A protease inhibitors, nucleoside/nucleotide analogues and non-nucleoside inhibitors of the HCV RNA-dependent RNA polymerase (RdRp), inhibitors of the HCV NS5A protein, and cyclophilin inhibitors.

Drug resistance remains a potential problem for any new DAA against HCV. Because of the error-prone nature of the HCV RNA-dependent RNA polymerase and the generation of a vast number of quasispecies, drug resistance inevitably occurs in patients treated with antiviral drugs targeting distinct HCV specific enzymes and may limit their efficacy. Indeed, some studies have shown that amino acid changes within NS3-4A protease, such as R155, A156 and D168,

confer resistance to all protease inhibitors currently in clinical development (Romano *et al.*, 2012). Thus, further work is required to understand the molecular basis of drug resistance, in order to develop drugs that can act in a broader spectrum of resistant viral variants.

## 1.2 HCV virion

HCV particles isolated from the sera of infected patients and from HCVcc particle preparations generated in cell culture demonstrated heterogeneity in their density. HCV particles have a spherical morphology and initial filtration studies with patient-derived material, indicated that they were 50 to 80nm in diameter (Bradley *et al.*, 1985; He *et al.*, 1987). Although advances with the production of infectious virions in tissue culture systems have been made, the biochemical and morphological features of HCV particles remain elusive. The density of HCV serum particles (HCVsp) depends on the method of analysis and on the patient sample. Electron microscopic analyses performed on cell-culture derived HCV indicates that mature, enveloped virions are 55-60nm in diameter (Gastaminza *et al.*, 2010; Wakita *et al.*, 2005).

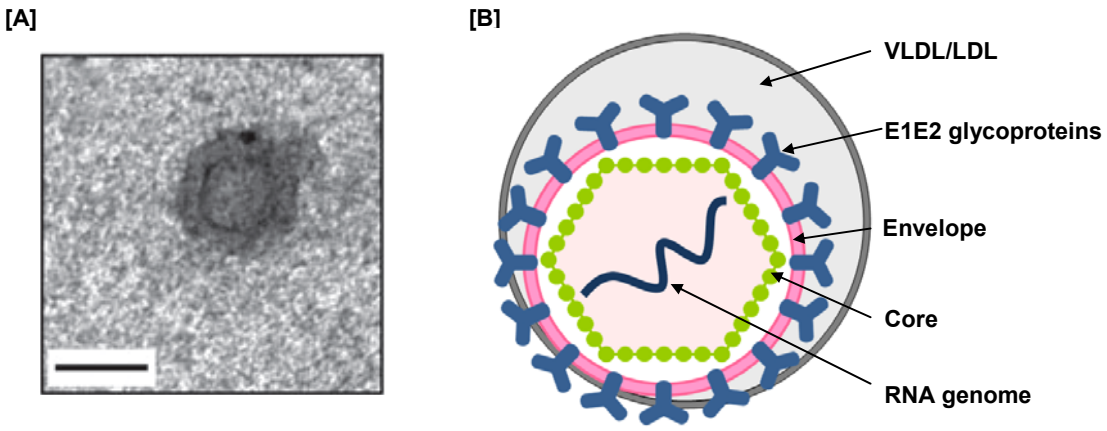


**Figure 1.4 – The HCV virion. [A] Electron micrograph of HCV virion shown by immunogold labelling; scale bar 50nm (Wakita *et al.*, 2005). [B] Schematic representation of the HCV particle and its components: the single-stranded RNA genome enclosed within the capsid composed of core protein. An envelope layer derived from host cell membranes surrounds the viral capsid and the HCV glycoprotein E1/E2 heterodimers are embedded within it. The virion is proposed to be associated with VLDL/LDL, generating lipoviroparticles (LVP).**

Density gradient analyses have shown that viral RNA exists within low- and high-density fractions (Andre *et al.*, 2005). This is probably due to the tight association of virions with host cell components, most notably lipoproteins (Andre *et al.*, 2002; Gastaminza *et al.*, 2008; Gastaminza *et al.*, 2006).

Association appears to occur during assembly, since HCV formation and secretion depend on components of very low density lipoprotein (VLDL) assembly and secretion pathways, including apolipoprotein B and E (apoB and apoE) and microsomal triglyceride transfer protein (Chang *et al.*, 2007; Gastaminza *et al.*, 2008; Huang *et al.*, 2007). Most particles containing viral RNA that are secreted from HCV-infected cells are poorly infectious and fractionate at high densities such as ~1.14g/ml. By contrast, highly infectious HCVcc are found within low density fractions of 1.09-1.1g/ml (Lindenbach *et al.*, 2005). Moreover, only the low-density fractions derived from HCV-positive human serum exhibits high infectivity in chimpanzees (Bradley *et al.*, 1991). The mature virion is thought to consist of a genome-containing nucleocapsid that is surrounded by an outer envelope (Figure 1.4). The envelope consists of a lipid membrane in which the viral glycoproteins E1 and E2 are embedded.

### 1.2.1 Genome organisation

The HCV genome is ~9600 nucleotides long and encodes a single open reading frame (ORF) flanked by two untranslated regions (UTRs) at the 5' and 3' termini (Figure 1.5). The ORF encodes a large polyprotein (~3000 amino acids) that is proteolytically cleaved by viral and cellular proteases to produce 10 viral proteins. The amino-terminal (N-terminal) one-third of the polyprotein encodes the virion structural (S) proteins, core (C) and the glycoproteins E1 and E2, followed by the non-structural (NS) proteins (NS2, NS3, NS4A, NS4B, NS5A, NS5B). Separating the S and NS proteins is p7, a short hydrophobic polypeptide.

**Figure 1.5 – Schematic representation of the HCV genome containing two untranslated regions (UTR) at the 5' and 3' ends flanking a single open reading frame (upper panel). Translation of the viral RNA generates a single polyprotein (central panel) that is processed by host and viral proteases to generate the individual mature proteins (lower panel). The host proteases SPP (blue arrowhead) and SP (red arrowhead) generate the structural proteins and the NS2/NS3 autoprotease (orange arrowhead) and NS3/4A protease (green arrowhead) cleave the polyprotein at the indicated boundaries. The topology of HCV proteins relative to the ER membrane is represented in the lower panel.**

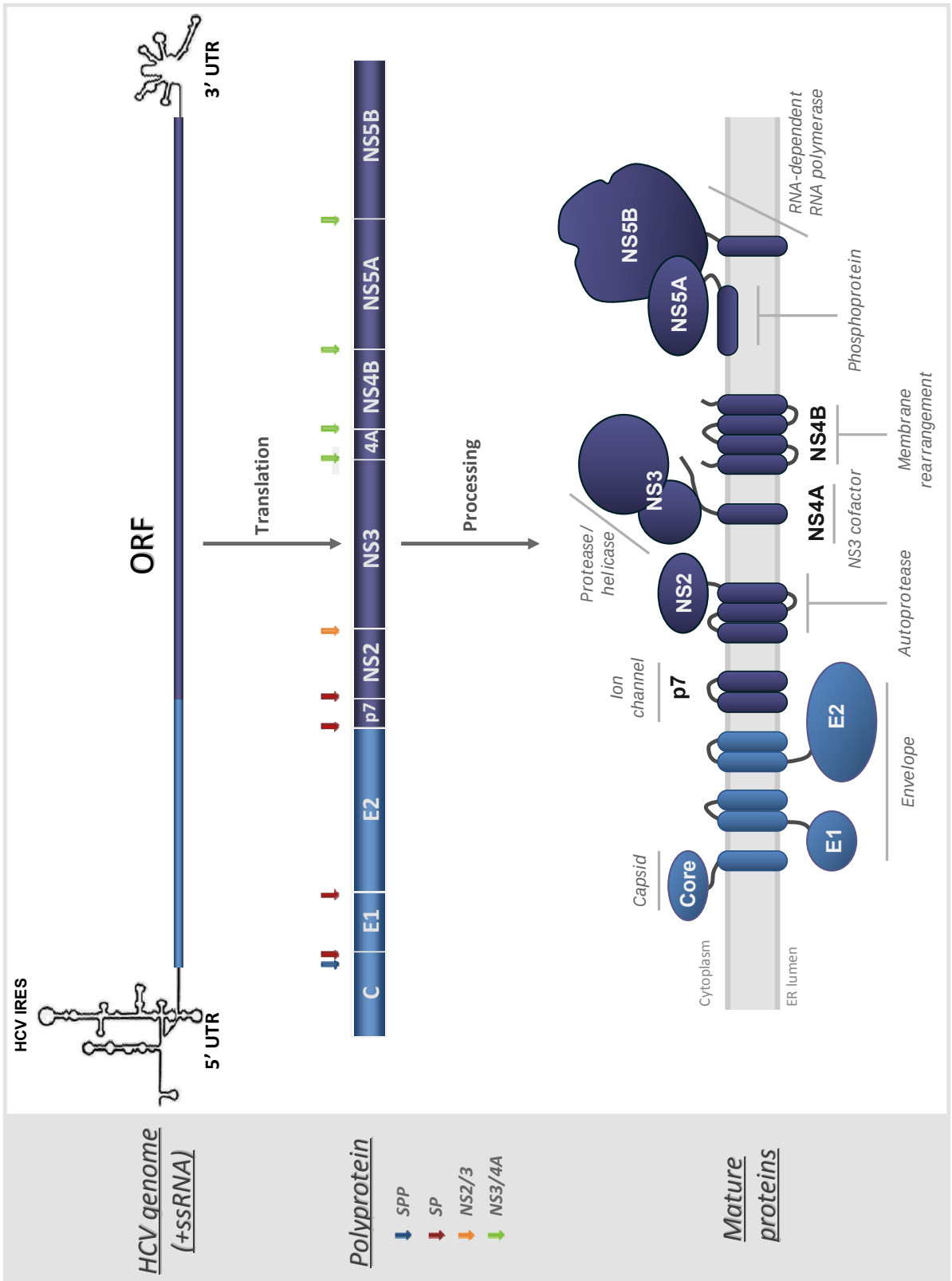
HCV genome (+ssRNA)
HCV IRES
5' UTR
ORF
3' UTR
Translation
Polyprotein
C
E1
E2
p7
NS2
NS3
4A
NS4B
NS5A
NS5B
SPP
SP
NS2/3
NS3/4A
Processing
Mature proteins
Capsid
Core
Cytoplasm
ER lumen
Ion channel
p7
Protease / helicase
NS3
NS2
Autoprotease
NS4A
NS3 cofactor
NS4B
Membrane rearrangement
Envelope
E1
E2
Phosphoprotein
NS5A
RNA-dependent RNA polymerase
NS5B

#### 1.2.1.1 5' and 3' UTR regions

##### I. 5' UTR and HCV IRES

The 5′ UTR is highly conserved among various isolates (Bukh *et al.*, 1992). The 5′ UTR is ~341 nucleotides in length and contains an internal ribosomal entry site (IRES) (Bukh *et al.*, 1992; Honda *et al.*, 1999). Based on NMR and X-ray crystallography analysis, the 5' UTR is predicted to contain four highly structured domains (domains I-IV) and a pseudoknot (Berry *et al.*, 2011; Honda *et al.*, 1996a; Honda *et al.*, 1996b; Lukavsky *et al.*, 2003; Lukavsky *et al.*, 2000). The HCV IRES spans domains II, III and IV of the 5' UTR, and together with the first 24-40 nucleotides of the core-coding sequence specifically interacts with the 40S ribosomal subunit and eIF3 to initiate cap-independent translation of viral RNA (He *et al.*, 2003; Honda *et al.*, 1996b; Kieft *et al.*, 2001; Pestova *et al.*, 1998). The pseudoknot domain is located at the centre of the HCV IRES, connecting domains II and III with the AUG-containing domain IV (Boehringer *et al.*, 2005; Spahn *et al.*, 2001) (Figure 1.6). This domain is the most highly structured region of the IRES and is therefore required for efficient translation (Berry *et al.*, 2010; Kieft *et al.*, 2001). Additionally, core is predicted to contain four highly conserved RNA secondary structures within the region encoding the first 62 amino acids of the protein. Within these structures two stem-loops (SL47 and SL87) are important for efficient translation and replication of the viral RNA both *in vitro* and *in vivo* (McMullan *et al.*, 2007).

In addition to its involvement in translation, the 5' UTR is essential for genome replication. Several reports indicated that domains I and II are sufficient for viral RNA replication, although the efficiency of this process is enhanced by the presence of the complete 5' UTR (Friebe *et al.*, 2001; Kim *et al.*, 2002). Several host factors can associate with the HCV 5' UTR and these interactions regulate translation and replication of the viral genome. The polypyrimidine tract binding protein (PTB), La autoantigen and poly (rC)-binding protein are some of the factors known to bind to the 5' UTR that also influence viral RNA replication (Ali & Siddiqui, 1995; 1997; Fukushi *et al.*, 2001). Moreover, PTB and La autoantigen are required for translation (Domitrovich *et al.*, 2005; Fukushi *et al.*, 2001). More recently, interactions between the liver-specific microRNA, miR-122, which binds at two sites in the HCV 5′ UTR, were identified as essential for maintaining HCV RNA abundance during infection in cultured cells and in infected chimpanzees (Jopling *et al.*, 2008; Jopling *et al.*, 2005; Lanford *et al.*, 2010; Machlin *et al.*, 2011). miR-122 is thought to protect HCV RNA from nucleolytic degradation or inhibit the activation of enzymes that induce innate immune responses, thereby enhancing viral replication (Machlin *et al.*, 2011).

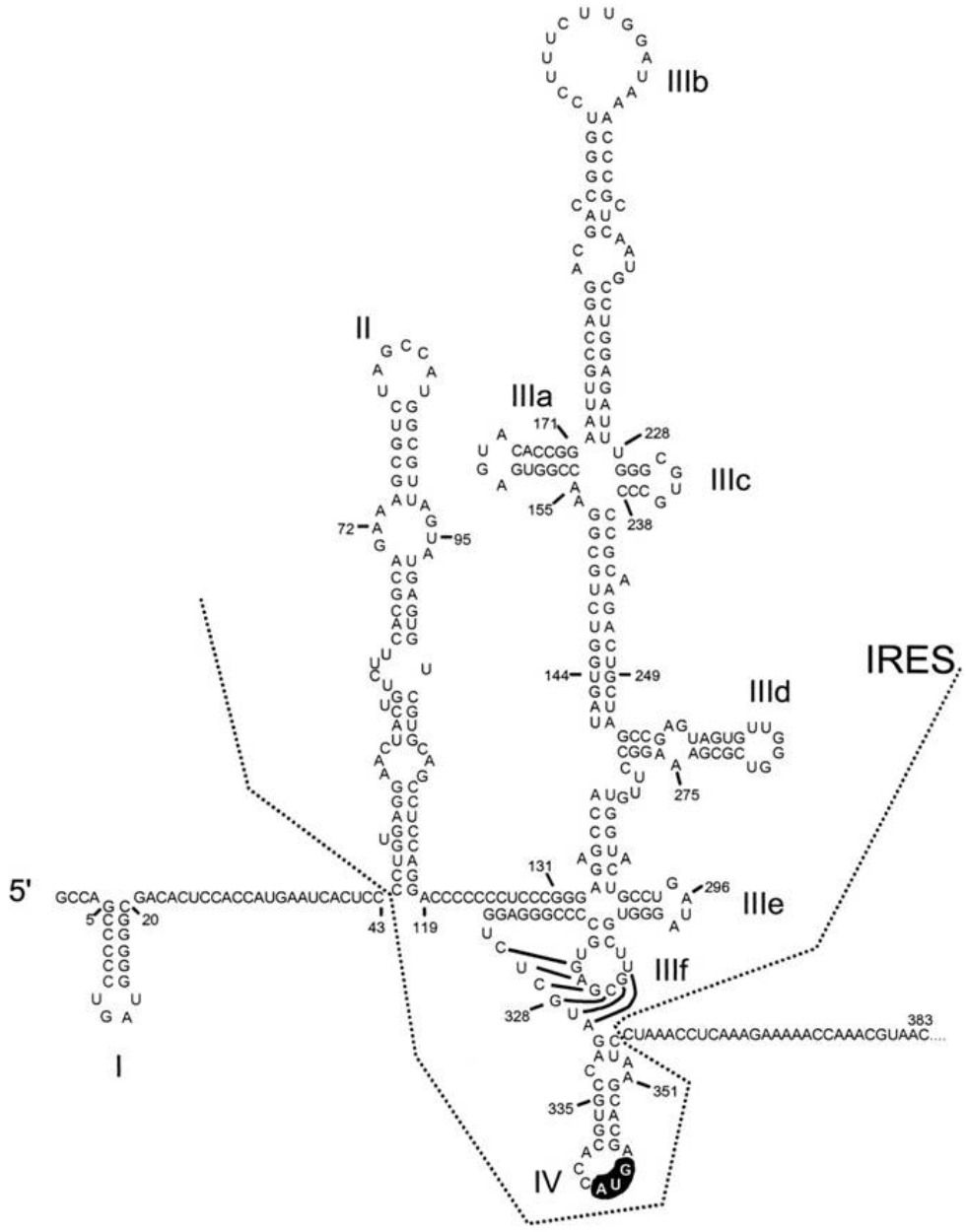


**Figure 1.6 – Model of the secondary and tertiary RNA structures of the 5'UTR of HCV (genotype 1b). The major structural domains (I to IV) and subdomains (IIIa to IIIf) together with a small region corresponding to the core-coding sequence, are represented. The initiation AUG codon within stem-loop IV is highlighted. The HCV IRES extends from domains II to IV and is also represented. Extracted from Honda *et al.*, 1999.**

## II. 3' UTR

The 3' UTR varies between 200 and 235 nt in length, and forms a tripartite structure which includes a short variable region, a poly(U/UC) tract (approximately 80 nt in length), and a highly conserved X-tail region (98 nt in length) (Ito & Lai, 1997; Kolykhalov *et al.*, 1996; Tanaka *et al.*, 1996) (Figure 1.7). The X-tail region comprises three stable stem–loop structures (designated SL1-SL3) that are almost invariant among HCV genotypes. The variable region is composed of two stem loops (VSL1 and VSL2) and, contrary to the X-tail region, is dispensable for viral RNA replication (Friebe & Bartenschlager, 2002). The poly (U/UC) tract is variable in length and composition, consisting of uridine residues that are interdispersed with occasional cytidine residues. The minimum length of this segment is 26 nt in order to direct viral RNA replication (Friebe & Bartenschlager, 2002). Deletion studies have shown that the 3'X-tail region, as well as the 52 nt upstream of the poly(U/C) tract, are crucial for RNA replication both *in vitro* and *in vivo* (Friebe & Bartenschlager, 2002; Yanagi *et al.*, 1999; Yi & Lemon, 2003). Additionally, the variable region within the poly (U) tract and a part of the X-tail region stimulate IRES-mediated translation of viral RNA (Song *et al.*, 2006).

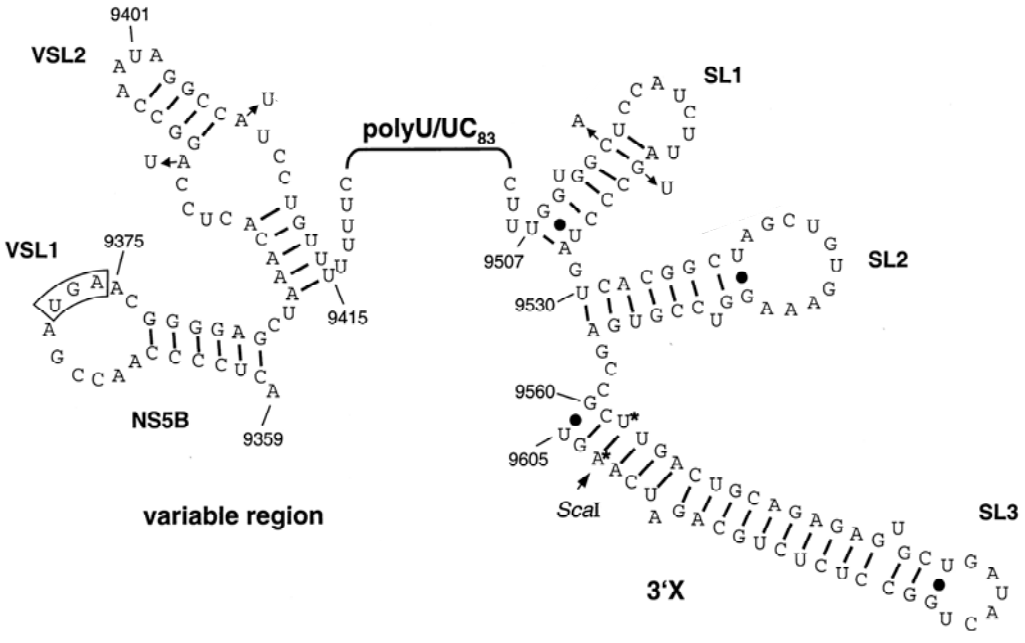


**Figure 1.7 – Proposed secondary structure of the 3' UTR of HCV (genotype 1b). Represented are the two stem-loops within the variable region (VSL1 and VSL2) the 83 nucleotide poly(U/UC) tract and the three stem-loops in the 3'X (SL1, SL2 and SL3). The stop codon of the polyprotein ORF is boxed. Extracted from Friebe & Bartenschlager, 2002.**

## 1.2.2 HCV-encoded proteins

### 1.2.2.1 Structural proteins

#### I. Core

Core protein is located at the N-terminus of the polyprotein and is released as a 191 residue precursor (23 KDa) by host signal peptidase (SP). SP cleaves at the N-terminal end of E1, leaving core anchored in the ER membrane (Hussy *et al.*, 1996; Moradpour *et al.*, 1996; Santolini *et al.*, 1994). Complete maturation of core requires further processing at the C-terminus by a cellular signal peptide peptidase (SPP), which releases the protein (21KDa) from the ER membrane allowing its attachment to lipid droplets (LDs) (McLauchlan *et al.*, 2002).

The amino acid sequence of core is highly conserved among HCV genotypes. The mature form of the protein is estimated to be between 177 and 179 aa (Ogino *et al.*, 2004), and consists of two domains distinguished by markedly different amino acid compositions and hydrophobicity profiles (Hope & McLauchlan, 2000; McLauchlan, 2000): a N-terminal domain D1 (~120 aa) and a C-terminal domain D2 (~60 aa). Domain D1 is characterized by a high proportion of positively-charged amino acids. This domain is thought to interact with viral RNA, but has also been shown to interact with a variety of cellular components (McLauchlan, 2000). One of the best characterized of these is the interaction with the DEAD-box RNA helicase DDX3, which occurs via residues 24-35 of core. Disrupting interaction with DDX3 via mutating key residues within the core binding region has no effect on HCV propagation *in vitro*, indicating that this virus-host interaction may be pathogenesis-related (Angus *et al.*, 2010). Domain D2 has membrane-binding characteristics and is responsible for targeting core to the surface of LDs (Boulant *et al.*, 2005). It has been proposed that the folding of domain D2 occurs in a membrane environment and is critical for folding of domain D1 (Boulant *et al.*, 2005). Structural analysis of D2 revealed two amphipathic $\alpha$-helices (helix-1 and helix-2), separated by a non-structured hydrophobic segment (hydrophobic loop, HL). Mutagenesis studies have demonstrated that both helices are required for the attachment of core to LDs (Boulant *et al.*, 2006).

## II. E1 and E2

HCV encodes two glycoproteins, E1 and E2 (30KDa and ~68KDa, respectively), present as a heterodimer at the virion surface, which are essential for viral binding and entry into host cells. Both proteins are type I transmembrane glycoproteins, composed of a large N-terminal ectodomain, responsible for virus attachment to cell receptors, and a short C-terminal transmembrane domain, involved in anchoring the glycoproteins in a lipid bilayer (Cocquerel *et al.*, 1999; Op De Beeck & Dubuisson, 2003). E1 and E2 are released from the polyprotein precursor through SP-mediated cleavage at the C/E1, E1/E2 and E2/p7 boundaries (Dubuisson *et al.*, 2002). During their synthesis, E1 and E2 ectodomains are translocated into the ER lumen (Deleersnyder *et al.*, 1997).

The ectodomains of HCV envelope glycoproteins E1 and E2 are highly modified by N-linked glycans. E1 and E2 contain up to 6 and 11 glycosylation sites, respectively (Lavie *et al.*, 2007). These modifications are believed to be involved in protein folding, receptor interactions to facilitate entry and shield the virion glycoproteins from neutralising antibodies during infection (Goffard *et al.*, 2005; Helle *et al.*, 2007; Lavie *et al.*, 2007). Studies using both the HCVpp and HCVcc systems (section 1.3.1-I and -III) have demonstrated that the intracellular forms of E1 and E2 assemble as stable noncovalent heterodimers (Deleersnyder *et al.*, 1997; Krey *et al.*, 2010; Op De Beeck *et al.*, 2004). In contrast, it was recently shown that E1 and E2 proteins change their oligomeric state after incorporation into the virus particle and form large covalent complexes stabilised by disulphide bridges (Vieyres *et al.*, 2010).

The structural organization of E2 has been obtained, based on disulphide mapping studies and modelling on the known *Flavivirus* glycoprotein E structure (Krey *et al.*, 2010). According to this model, E2 is predicted to contain three separate domains (I, II and III). Domain I structural analysis revealed a bipartite composition, consisting of eight β-strands followed by hypervariable region 1 (HVR1), which is the most genetically variable segment of the E2 protein, as well as highly conserved residues involved in CD81 binding (Krey *et al.*, 2010; Weiner *et al.*, 1991). HVR1 is implicated in facilitating E2/SR-BI mediated viral entry and escape from anti-HCV neutralising antibodies (Bartosch *et al.*, 2003b;

Weiner *et al.*, 1991). HVR1 is suggested to exist as a polypeptide loop exposed on the surface of the virion where it functions as an immunological decoy to shield the more conserved regions of the glycoproteins, such as the CD81 binding pocket (Weiner *et al.*, 1991). HCV lacking the HRV1 region was found to retain infectivity, however this was shown to be strongly attenuated both *in vivo* and *in vitro*, supporting a functional role of this region in viral entry (Bartosch *et al.*, 2003b; Callens *et al.*, 2005). Despite the sequence variability of HVR1, the physico-chemical properties of the residues at each position and the conformation of HVR1 are highly conserved among genotypes. Due to the basic nature of HVR1, this region has been shown to play a role in modulating virus entry (Callens *et al.*, 2005). Domain II is proposed to be relatively unstructured, containing another hypervariable region (HVR2). The most conserved region in domain II (aa 502 to 520) is suggested to act as a fusion loop and thereby involved in receptor binding (Roccasecca *et al.*, 2003). DI is connected to DIII by a linker region called the intergenotypic variable region (IgVR) and DIII is connected to the TM domain by the flexible stem region.

While E2 has been shown to mediate direct binding of HCV to cell surface receptors and entry, little is known about the contribution of E1 to HCV infection, mostly due to difficulties in purifying this protein. The association between E1 and E2 is essential for HCVpp entry (Bartosch *et al.*, 2003a; Drummer *et al.*, 2003; Hsu *et al.*, 2003). Several studies have identified conserved regions within E1 and E2 which may be involved in mediating membrane fusion (Flint *et al.*, 1999; Lavillette *et al.*, 2007; Perez-Berna *et al.*, 2006). Mutagenesis analysis of putative fusion peptides within the E1 coding region revealed that interaction between E1 and E2 is presumably required for proper E2 glycosylation and consequently, HCVcc and HCVpp entry (Russell *et al.*, 2009). However, the mechanism by which E1 mediates this post-translational event in E2 remains unknown.

**III. P7**

The HCV p7 protein is a small, integral membrane protein of 63 amino acids that resides at the junction between the S and NS regions of the HCV polyprotein. Although most cleavage events in the HCV polyprotein precursor proceed to completion during or immediately after translation, proteolysis at

the E2-p7 and p7-NS2 junctions are delayed, leading to the production of an E2-p7-NS2 precursor (Dubuisson *et al.*, 1994). The E2-p7-NS2 precursor is liberated by SP-mediated cleavage at the E1/E2 boundary and the autoproteolytic cleavage mediated by NS2-3 protease at the NS2/NS3 boundary (Lin *et al.*, 1994a; Santolini *et al.*, 1995). Processing between E2 and p7 is also incomplete resulting in the production of fully processed E2 and uncleaved E2-p7 (Lin et al., 1994). p7 monomers comprise two transmembrane domains organized as $\alpha$-helices that are connected by a short basic loop (Montserret *et al.*, 2010). Both the N- and C-termini are exposed to the ER lumen, with the hydrophilic loop facing the cytosol (Carrere-Kremer *et al.*, 2002; Patargias *et al.*, 2006).

p7 is believed to self-organize in lipid membranes to form ion-conducting channels or pores that modify the permeability of the cell membrane to ions and other molecules (Griffin *et al.*, 2003). Due to its ability to sustain ion fluxes, p7 has been included into the family of viral proteins known as viroporins. Viroporins are small, virus-encoded polypeptides that interact with membranes and comprise at least one transmembrane segment. Moreover, oligomerization is an essential prerequisite for their ability to modify the membrane's permeability (Gonzalez & Carrasco, 2003). Electron microscopy studies suggest that p7 monomers assemble into both hexameric and heptameric structures in lipid bilayers (Clarke *et al.*, 2006; Griffin *et al.*, 2003; Luik *et al.*, 2009).

p7 is not required for RNA replication (Lohmann *et al.*, 1999). However it is critical for release of infectious virions both *in vitro* and *in vivo* (Jones *et al.*, 2007; Sakai *et al.*, 2003). It is likely to play an important role in later stages of viral assembly and potentially for cell entry. Recent studies showed that the ion channel activity of the protein is enhanced at low pH, suggesting that p7 channels may be gated by acidic pH and facilitate the transport of protons (StGelais *et al.*, 2007). Furthermore, substitution of M2 with p7 facilitated the transport of the influenza HA protein to the cell surface in a cell-based assay (Griffin *et al.*, 2004). Thus, p7 may operate in an M2-like fashion to facilitate HCV particle production. Based on these observations it suggests that p7 plays a role in protecting the glycoproteins from low pH during assembly, however it has also been hypothesised that p7 is required for proper folding of the glycoproteins. Furthermore, recent evidence suggests that the proton-selective

ion-channel activity of p7 prevents the acidification of intracellular virions during their transit through otherwise acidic intracellular compartments (Wozniak *et al.*, 2010). Several inhibitor compounds inhibit p7 ion channel activity *in vitro*, thereby resulting in a reduction of infectious virus particles (Griffin *et al.*, 2008; Steinmann *et al.*, 2007). The essential role of p7 in the virus life cycle has rendered it an attractive target for antiviral development.

#### 1.2.2.2 Non-structural proteins

##### I. NS2

NS2 is a 24kDa dimeric integral membrane protein, composed of two functionally and topologically distinct domains: a N-terminal membrane-binding domain (MBD) and a C-terminal cytosolic globular protease domain (Lorenz *et al.*, 2006). Moreover, the X-ray crystal structure of the protease domain revealed a dimer with 2 composite active sites (Lorenz *et al.*, 2006). Recently, using NMR analysis, the secondary structure of the N-terminal MBD has been solved and is proposed to contain three transmembrane $\alpha$-helices (TM1-3), connected by flexible loop regions (Jirasko *et al.*, 2008; Jirasko *et al.*, 2010).

Before cleavage from the polyprotein, NS2 participates in the protease activity responsible for cleavage at the NS2/NS3 junction (Lorenz *et al.*, 2006; Santolini *et al.*, 1995; Yamaga & Ou, 2002). As mentioned earlier, the N-terminus of NS2 is released from the E2-p7-NS2 precursor by SP-mediated cleavage at the C-terminus of p7 (Lin et al., 1994). The catalytic activity of NS2-3 autoprotease requires the N-terminal one-third of NS3 (Grakoui *et al.*, 1993). Mutation of the amino acid residues at the NS3-4A catalytic triad does not affect NS2-3-mediated cleavage of NS2/NS3, indicating that this event does not require NS3-4A protease activity (Grakoui *et al.*, 1993; Hijikata *et al.*, 1993). Co-immunoprecipitation studies revealed stable interaction of NS2 with NS3, p7 and E2, whereas with NS5A this interaction was shown to be weaker (Jirasko *et al.*, 2010). Apart from its protease activity, NS2 appears to play a crucial role for production of infectious virus particles. Mutagenesis studies have demonstrated that deletion or substitution mutations within NS2 significantly affect the production of infectious virus (Jones *et al.*, 2007; Phan *et al.*, 2009). Studies using intergenotypic chimeras also showed that the production of infectious virus

is highly dependent upon the specific position of the chimeric junction site within NS2 (Pietschmann *et al.*, 2006; Yi *et al.*, 2007). Moreover, the S168 residue of NS2 has been shown to be involved in regulating a post-particle assembly step in infectious virus production (Yi *et al.*, 2009). The defects in virus production caused by mutation of this residue could however be rescued by trans-complementation of ectopically expressed NS2 (Yi *et al.*, 2009). Collectively, these observations suggest a role for NS2 in a later step of virion formation.

### II. NS3 and NS4A

NS3 a is 70KDa multifunctional protein composed of two domains, an N-terminal chymotrypsin-like serine protease domain (aa 1-180) and a C-terminal RNA helicase/NTPase domain (aa 181-631). The NS3 protease domain adopts a chymotrypsin-like fold, composed of two $\beta$-barrel domains. The small NS4A peptide (6KDa) forms a very stable heterodimer with NS3 and functions as a cofactor for NS3 serine protease activity (Bartenschlager *et al.*, 1995; Lin *et al.*, 1995). The interaction of NS3 with the central region of NS4A (aa 21-32) is required for proper folding of NS3 (Kim *et al.*, 1996). NS3 by itself has no transmembrane domain, but the N-terminal hydrophobic region of NS4A forms a transmembrane $\alpha$-helix which is required for integral membrane association of the NS3-4A complex to the ER (Wolk *et al.*, 2000). Mutagenic analysis of the C-terminal acid region of NS4A (aa 40-54) demonstrated genetic interactions between NS4A, NS3 and NS4B protein and that are essential for RNA replication (Phan *et al.*, 2011). Moreover, amino acid changes at the C-terminus of NS4A which did not affect RNA replication, were shown to block assembly of infectious particles, indicating that NS4A plays important roles not only in RNA replication but also virus assembly (Phan *et al.*, 2011). In addition to its role in NS3 cofactor activity, NS4A has also been demonstrated to regulate the phosphorylation status of NS5A (Lindenbach *et al.*, 2007). The NS3-4A protease is responsible for polyprotein cleavage at four sites: NS3-4A, NS4A-4B, NS4B-5A and NS5A-5B (Failla *et al.*, 1994; Gallinari *et al.*, 1998; Lin *et al.*, 1994b). Cleavage mediated by NS3-4A follows a preferential order: first cleavage in *cis* at the NS3/4A site, followed by subsequent proteolysis in *trans*. Rapid processing is achieved at the NS5A/NS5B junction, producing the NS4A-NS4B-NS5A intermediate. Cleavage

then takes place between NS4A and NS4B, to generate a NS4B-NS5A precursor. The final cleavage event mediated by NS3-4A occurs between NS4B and NS5A.

In addition to its role in the processing of the polyprotein and viral replication, the NS3-4A protease is also a key player in disrupting innate defence mechanisms. NS3-4A cleaves and thereby inactivates a mitochondrial protein, the caspase recruitment domain containing crucial adaptor molecule Cardif (also known as MAVS, IPS-1 or VISA), in the RIG-I viral RNA sensing pathway (Li *et al.*, 2005b; Loo *et al.*, 2006; Meylan *et al.*, 2005). NS3-4A also targets TRIF (toll/IL-1 receptor homology (TIR) domain-containing adaptor inducing IFNβ), a key adaptor molecule in the TLR3 dsRNA sensing pathway (Ferreon *et al.*, 2005; Li *et al.*, 2005a). More recently, another cellular protein has been identified as a target for NS3-4A protease activity, the T-cell protein tyrosine phosphatase (TC-PTP) (Brenndorfer *et al.*, 2009). Epithelial growth factor (EGF) stimulation causes TC-PTP to exit from the nucleus and to dephosphorylate the EGF receptor, leading to decreased downstream activation of the phosphatidylinositol 3-kinase (PI3K)-Akt pathway (Tiganis *et al.*, 1999). Thus, cleavage of TC-PTP by NS3-4A resulted in enhancement of EGF-induced signalling and increased basal Akt activity, which is critical for efficient replication of HCV (Brenndorfer *et al.*, 2009). This has been suggested to impact on development of hepatocellular carcinoma.

The NS3 helicase/NTPase domain is a member of the DEXH/D-box subgroup of helicase superfamily 2 (Gorbalenya *et al.*, 1989; Tai *et al.*, 1996). The crystal structure of the HCV helicase reveals a Y-shaped molecule composed of 3 subdomains (Kim *et al.*, 1998; Yao *et al.*, 1997). The NS3 helicase/NTPase has been implicated in several functions, including RNA binding, ATP hydrolysis, and unwinding of RNA. Kinetic analyses indicate that the NS3 helicase unwinds double-stranded RNA in highly coordinated cycles, triggered by ATP binding, of discrete steps of 11 base pairs. During replication, the NS3 helicase has been suggested to translocate along the RNA substrate by changing protein conformation. Gu and Rice (2010), obtained the crystal structures for a series of NS3 helicase structural transition states, including ground-state and transition-state ternary complexes (Gu & Rice, 2010). These structures recapitulated the helicase activity along the reaction pathways of ATP binding and hydrolysis,

revealing the molecular basis of action of the NS3 helicase (Gu & Rice, 2010). The NS3 helicase activity can be modulated by interactions between the serine protease and helicase domains (Beran *et al.*, 2009; Frick *et al.*, 2004; Pang *et al.*, 2002). Indeed the kinetics of duplex RNA unwinding is slower for the isolated helicase domain as compared with the full-length NS3 protein. The presence of NS4A enhances productive RNA binding of a full-length NS3-4A complex (Frick *et al.*, 2004). Additionally, NS3 helicase interaction with other NS proteins, NS5A and NS5B, appears to also modulate its activity.

### III. NS4B

NS4B is a 27KDa integral membrane protein. The precise membrane topology is still unknown, however it is predicted to contain a N-terminal region (aa 1–69), four transmembrane domains (aa 70–190) in the central region of the protein and a C-terminal region (aa 191–261) (Hugle *et al.*, 2001; Lundin *et al.*, 2003). Both the N- and C-terminal regions of the protein are thought to reside on the cytosolic side of the ER. The N-terminal region is predicted to contain two two amphipathic $\alpha$-helices, designated AH1 and AH2 (Elazar *et al.*, 2004; Gouttenoire *et al.*, 2009a). AH1 is believed to mediate targeting of NS4B to the ER by a co-translational mechanism (Elazar *et al.*, 2004). AH2 on the other hand, has been proposed to translocate across the membrane into the ER lumen by a post-translational mechanism, leading to the formation of a fifth transmembrane domain (TMX) (Lundin *et al.*, 2006). AH2 has also been proposed to oligomerise with itself and to mediate lipid vesicle aggregation (Cho *et al.*, 2010). The central region of NS4B is predicted to harbour four transmembrane domains (TM1-4), which are connected via three transmembrane loops. The loop connecting TM2 and TM3 is predicted to be oriented towards the cytosolic side of ER (Lundin *et al.*, 2003). This loop contains a nucleotide-binding motif (aa 129-135), which has been implicated in GTPase and ATPase activities (Einav *et al.*, 2004; Thompson *et al.*, 2009). Mutation at this motif which would disrupt the NS4B GTPase and ATPase activities resulted in a decrease in viral replication, indicating that these activities are important for RNA synthesis (Einav *et al.*, 2004; Thompson *et al.*, 2009). Han *et al* (2011) recently identified two conserved dimerization motifs (GXXXG and S/T cluster) within the NS4B transmembrane domains TM2,3 and TM1 (Han *et al.*, 2011). These motifs were

essential for NS4B function and regulate its ability to interact with membranes. Mutagenesis analysis within these motifs demonstrated that both regions were critical for virus replication (Han *et al.*, 2011). The C-terminal region of NS4B is thought to reside in the cytoplasm (Hugle *et al.*, 2001; Lundin *et al.*, 2003). This region is well conserved and is predicted to contain two $\alpha$-helices, H1 (aa201 to 213) and H2 (aa228 to 253). H1 has not been shown to mediate interaction of the C-terminus of NS4B with membranes. However, mutagenesis analysis within this helix, demonstrated that it is important for virus replication (Jones *et al.*, 2009; Paredes & Blight, 2008; Paul *et al.*, 2011). By contrast, H2 associates with membranes (Aligo *et al.*, 2009; Gouttenoire *et al.*, 2009b; Liefhebber *et al.*, 2009). This helix is less well-conserved than H1, however mutation of some residues in H2 result in impairment of replication, indicating that H2 is also essential for virus replication (Aligo *et al.*, 2009; Jones *et al.*, 2009). The C-terminus of NS4B also contains an arginine-rich motif (192RR193), which may mediate binding of NS4B to viral RNA (Einav *et al.*, 2008). At the end of the C-terminus, two cysteine residues (C257 and C261) have been suggested to undergo palmitoylation (Yu *et al.*, 2006). Although the precise role of this modification is not clear, it has been suggested to be involved in NS4B oligomerization.

Ectopic expression of NS4B typically induces rearrangement of the ER membrane, producing vesicular or pocket-like structures referred to as the "membranous web" or "membrane-associated foci" (MAF) (Egger *et al.*, 2002; Gosert *et al.*, 2003; Gretton *et al.*, 2005). These structures can be visualised by electron microscopy and are thought to be the sites where replication complex assembly takes place (Gao *et al.*, 2004). Initial observations using immunofluorescence analysis demonstrated that viral proteins involved in viral replication localize to these punctate structures (Elazar *et al.*, 2004; Hugle *et al.*, 2001). Moreover, these punctate sites on the ER were also shown to co-localise with viral RNA (El-Hage & Luo, 2003; Gosert *et al.*, 2003; Moradpour *et al.*, 2004; Targett-Adams *et al.*, 2008). Thus, the membrane rearrangements induced by NS4B are likely to play a central role in viral RNA replication.

Aside from its role in creating the environment suitable for HCV RNA synthesis, NS4B has also been suggested to play a direct role in viral replication. Site-directed mutagenesis studies within NS4B revealed that specific amino acid changes lead to enhanced as well as abolished phenotype on viral RNA replication (Blight, 2011; Jones *et al.*, 2009; Lindstrom *et al.*, 2006; Paredes & Blight, 2008; Paul *et al.*, 2011). Moreover, studies on cell culture adaptive mutations have highlighted that adaptive mutations were found within NS4B and greatly enhanced RNA replication efficiency in cell culture (Lohmann *et al.*, 2003; Lohmann *et al.*, 2001).

The interactions of HCV proteins with cellular membranes is thought to result in the activation of ER stress pathways (Tardif *et al.*, 2002). NS4B may play an important role in this process due to its multispanning membrane topology and its capacity to alter cellular membranes. Several studies suggested that NS4B expression may cause ER stress and induce the unfolded protein response (UPR). The induction of UPR by NS4B, and presumably other NS proteins, is thought to contribute positively to HCV infection by facilitating replication of viral RNA (Li *et al.*, 2009; Zheng *et al.*, 2005).

**IV. NS5A**

NS5A is a hydrophilic phosphoprotein that exists in two isoforms, basally phosphorylated (56KDa) and hyperphosphorylated (58KDa) forms. NS5A is predicted to comprise three distinct domains (I-III), separated by low complexity sequences (LCS I and LCS II) (Moradpour *et al.*, 2005; Tellinghuisen *et al.*, 2004). Domain I (aa 1-213), is the most conserved region between the NS5A sequences from all HCV genotypes. It comprises an amphipathic $\alpha$-helix (AH; aa 5-25) and a zinc binding motif (ZBM), that is required for the RNA binding activities of NS5A (Brass *et al.*, 2002; Huang *et al.*, 2005; Liu *et al.*, 2006; Tellinghuisen *et al.*, 2004). NS5A localizes to the site where RNA synthesis takes place via the amphipathic $\alpha$-helix membrane anchor subdomain (Brass *et al.*, 2002; Penin *et al.*, 2004; Sapay *et al.*, 2006). Analysis of the crystal structure of domain I revealed that it forms a dimer with a claw-like shape that can accommodate a single-stranded RNA molecule (Tellinghuisen *et al.*, 2005). More recently, an alternative dimer structure has been reported. According to this structure, although the domain I of NS5A still forms a dimer, the claw-like shape is absent

and the residues involved in RNA binding are exposed between the flat surfaces (Love *et al.*, 2009). The differences observed between the two structures are thought to result from two functional states of membrane-tethered NS5A. However, further characterisation is required for the support of this hypothesis. Interestingly, Foster *et al* (2010) have shown that not only domain I, but also domains II and III can bind to viral RNA, although domain I and II retain higher binding affinity than domain III. Moreover, they demonstrated that domain I can specifically bind to the polypyrimidine tract of the viral 3' UTR suggesting a role of NS5A, presumably with other cellular and viral factors, in viral genome replication (Foster *et al.*, 2010; Foster *et al.*, 2011). The role of LCS I and II of NS5A in the HCV replication cycle is unknown. LCS II contains two closely-spaced polyproline motifs that have been shown to bind to SH3-domain containing proteins (e.g., Grb2, amphiphysin II/Bin1 and the Src-family of tyrosine kinases) (Macdonald *et al.*, 2004; Nanda *et al.*, 2006; Zech *et al.*, 2003). Mutagenesis analysis of these proline motifs (PM1 and PM2) revealed that PM2 was dispensable for HCV RNA replication or other stages of the virus life cycle, whereas mutation of the P342 in PM1 led to a decrease in virus replication, suggesting a role of this motif in replication and virus production (Hughes *et al.*, 2009a). Thus, the two proline motifs within LSCII are likely to play distinct roles in the HCV life cycle. LSCI in the other hand, has been proposed to be essential for efficient RNA replication. Appearance of replicon enhancing mutations were found in the C-terminal part of domain I and LCS I supporting a role for these regions in RNA replication (Blight *et al.*, 2000; Lohmann *et al.*, 2003).

Domain II (aa 250-342), is less well conserved than domain I and was shown to be flexible and disordered (Liang *et al.*, 2006; Liang *et al.*, 2007). Domain II contains a region referred to as the interferon-sensitivity-determining-region (ISDR), which has been suggested to interact with and antagonize the activity of the interferon-induced, double-stranded RNA-dependent protein kinase (PKR) (Gale *et al.*, 1998; Gale *et al.*, 1997). Domain III (aa 355-447) is mostly unstructured and is the most variable region in NS5A among HCV genotypes. Domain III is dispensable for RNA replication, as this region can tolerate insertions of large sequences, such as those encoding for the green fluorescent protein (GFP), without dramatic effects on RNA replication (Moradpour *et al.*, 2004). By contrast, large deletions in this domain were shown to significantly

impair virus infectivity, indicating that domain III of NS5A plays a role in virion assembly (Appel *et al.*, 2008; Hughes *et al.*, 2009b; Masaki *et al.*, 2008; Tellinghuisen *et al.*, 2008b).

NS5A has been shown to interact with core protein and to associate with LDs. The functional importance of the core-NS5A interaction on the same organelles is not fully understood. However, mutagenesis analysis have shown that domain I of NS5A is required for its association with LDs, and this interaction was shown to be crucial for infectious virus production (Miyanari *et al.*, 2007). Moreover, deletions in domain III impaired virus production, however these did not prevent attachment of NS5A to LDs. Instead, deletions in domain III abolished the association of NS5A with core protein on LDs (Appel *et al.*, 2008).

Several studies have focused on determining the NS5A phosphorylation sites and their functional role in the virus life cycle. The basal phopho-isoform of NS5A has been mapped at the centre of the molecule (aa 2200-2250) and near its C-terminus (aa 2351-2419) (Huang *et al.*, 2007b). Hyperphosphorylation of NS5A (p58 isoform) is suggested to occur on serine residues found within LCSI, as well as domains II and III. Cell culture adaptive mutations that increase RNA replication resulted in a decrease in hyperphosphorylation, suggesting that NS5A phosphorylation may regulate viral replication (Blight *et al.*, 2000). Moreover, deletion of serine residues in LCSI led to reduced NS5A hyperphosphorylation, which enhanced viral replication (Appel *et al.*, 2005; Evans *et al.*, 2004). Phosphorylation of domain III is thought to be required for the NS5A-core interaction and thus is essential for virion formation (Masaki *et al.*, 2008; Tellinghuisen *et al.*, 2008a). Indeed, mutagenesis analysis on a phosphoacceptor residue (S457) within this domain did not alter RNA replication efficiency, but blocked the production of infectious virus (Tellinghuisen *et al.*, 2008a). Hyperphosphorylation of NS5A is dependent on the presence of other NS proteins within the same polyprotein, such as NS3, NS4A and NS4B (Kaneko *et al.*, 1994). This suggests that these proteins are likely to interact with the cellular machinery to promote NS5A phosphorylation (Koch & Bartenschlager, 1999; Neddermann *et al.*, 1999). Collectively, these observations indicate that the phosphorylation status of NS5A may act as a regulatory switch between viral replication and presumably virion assembly.

NS5A interacts with the human vesicle-associated membrane protein-associated protein A (hVAP-A), a SNARE-like membrane protein, via the region of NS5A involved in hyperphosphorylation (Evans *et al.*, 2004; Gao *et al.*, 2004). hVAP-A, an ER/Golgi-localized protein involved in intracellular vesicle trafficking, has been shown to be essential for viral RNA synthesis (Evans *et al.*, 2004). Several reports suggest that disruption of NS5A hyperphosphorylation disrupts its interaction with VAP-A and consequently results in downregulation of HCV RNA replication (Evans *et al.*, 2004; Gao *et al.*, 2004). In addition, studies utilizing chemical inhibitors of protein kinases have demonstrated that inhibition of casein kinase 1$\alpha$ (CKI$\alpha$) led to reduction of NS5A hyperphosphorylation, resulting in increased viral RNA replication levels (Neddermann *et al.*, 2004). CKI$\alpha$ requires pre-phosphorylation of residues near sites of phosphorylation in NS5A for productive modification, suggesting that other kinases also play a role in NS5A phosphorylation (Quintavalle *et al.*, 2007).

NS5A can interact with numerous host-signalling pathways (Macdonald & Harris, 2004). As stated earlier, NS5A can interact and interfere with the activity of the interferon-induced double-strand RNA-dependent protein kinase (PKR) (Gale *et al.*, 1998; Gale *et al.*, 1997). PKR is involved in phosphorylation of the translation initiation factor eIF2$\alpha$, which in turn results in blockage of protein translation (Williams, 2001). Binding of NS5A to PKR prevents PKR-dependent shutdown of protein synthesis, thereby allowing HCV translation to continue. In addition, NS5A has been shown to interact and regulate other signalling cascades involved in regulation of cell growth, such as the Ras-Erk and PI3K-AKT pathways (Macdonald *et al.*, 2003; Macdonald *et al.*, 2005; Mankouri *et al.*, 2008; Street *et al.*, 2004).

**V. NS5B**

NS5B is the RNA-dependent RNA polymerase (RdRP) and therefore the catalytic centre of the HCV RC. This protein uses the viral genomic RNA as a template for generation of a complementary negative-stranded RNA intermediate. The negative-stranded RNA is then used as the template for the synthesis of molar excess of positive-stranded progeny RNA molecules. NS5B is composed of an N-terminal catalytic domain and a C-terminal TM segment

responsible for membrane association (Lee *et al.*, 2004; Schmidt-Mende *et al.*, 2001). Similar to other RdRp polymerases, NS5B possesses palm, fingers and thumb domains. The palm domain contains the active site of the enzyme, whereas the fingers and the thumb modulate the interaction with the RNA molecule. Interactions between the fingers and thumb domains result in a fully encircled catalytic site, creating a tunnel in which a single-stranded RNA molecule is directly guided to the active site (Ago *et al.*, 1999; Bressanelli *et al.*, 1999; Lesburg *et al.*, 1999).

As stated earlier, the genotype 2 isolate JFH1 replicates with higher efficiency in cell culture than any isolate from other genotypes. In a study by Simister *et al* ( 2009), it was demonstrated that the higher replication efficiency of JFH1 to replicate is linked with greater capacity for the NS5B RdRP to initiate *de novo* RNA synthesis (Simister *et al.*, 2009). Comparison analysis with other genotype 2 RdRp demonstrated that the improved activity of JFH1 RdRp results from a more closed structural conformation which promotes greater interaction affinity with the single-stranded RNA viral genome and consequently improves initiation of *de novo* synthesis of RNA replication (Simister *et al.*, 2009). Further analysis, identified a key residue (I405), residing at the thumb domain, which is responsible for the enhanced efficiency of JFH1 RdRp (Schmitt *et al.*, 2011). Mutation of this residue in the genotype 1b RdRp sequence, improved significantly replication efficiency of this isolate in cell culture (Schmitt *et al.*, 2011; Scrima *et al.*, 2012).

The RNA-dependent RNA polymerase activity appears to be modulated by interaction with other proteins. NS5A has been demonstrated to interact with NS5B and this interaction is critical for viral RNA replication (Shimakami *et al.*, 2004). Cyclophilin B, a peptidyl-prolyl cis-trans-isomerase, can also interact with the C-terminal region of NS5B and appears to stimulate its RNA binding activity (Watashi *et al.*, 2005). However, more recently Kaul *et al* (2009) have demonstrated that in fact cyclophilin A, and not cyclophilin B, is essential for replication and production of infectious particles (Kaul *et al.*, 2009). In addition, other cellular proteins have been demonstrated to interact with NS5B and to influence HCV RNA replication activity. For example, NS5B is phosphorylated by a protein kinase C-related kinase, PRK2, and this phosphorylation event is involved in regulating HCV RNA replication (Kim *et al.*, 2004). More recently, it

was found that high RdRp activity is enhanced by a "kissing-loop" interaction between an RNA element present in NS5B (5BSL3.2) and the SL2 in the 3' UTR region (Friebe *et al.*, 2005; Murayama *et al.*, 2010).

## 1.3 Experimental model systems for studying HCV life cycle

Since its discovery in 1989, research into the HCV life cycle and host-virus interactions that influence viral pathogenicity and outcome have been hampered by the lack of experimental HCV cell culture infection systems and suitable small animal models. However, from the late 1990s onwards, considerable progress has been made in developing models systems to study different aspects of the virus life cycle. Three laboratory-based models in particular have improved our understanding of HCV biology. These include HCV subgenomic replicons (SGR), pseudotyped particles (HCVpp) and the HCV cell culture system (HCVcc). More recently, small animal models have been developed which permit *in vivo* studies on HCV infection and assessment of the activity of new antiviral compounds. These include the uPA/SCID and $Fah^{-/-}/Rag2^{-/-}/IL2rg^{-/-}$ mouse models.

**Figure 1.8 – HCV *in vitro* model systems. [I.] HCVpp allows for the study of HCV entry. Recombinant retrovirus particles that contain HCV envelope glycoproteins on their surface are produced in HEK-293T cells by cotransfecting plasmids encoding the HCV glycoproteins, retroviral or lentiviral core and polymerase proteins and a proviral genome harbouring a reporter gene. Following infection of permissive cell lines, the retrovirus genomes express a reporter gene, such as luciferase, allowing for a quantitative measure of cell entry. [II.] HCV SGRs, allow for the study of viral RNA replication in cell culture. Bicistronic replicon RNAs, encoding a selectable marker, under control of the HCV IRES in the first cistron and the HCV non-structural NS3-NS5B proteins under the control of the encephalomyocarditis virus (EMCV) IRES in the second cistron, are electroporated into Huh-7 cells and derived sub-lines. RNA replication results in the expression of the selectable marker and allows for selection of cell colonies that support viral RNA replication. [III.] HCVcc allows for the study of the entire HCV lifecycle. This system uses either JFH1 HCV genomic RNA or chimeric versions of this genome. Electroporation of these RNAs into permissive cell lines allows for viral RNA replication and the production of infectious particles that can infect naïve cells. Productive infection can be monitored by several methods allowing the detection of intracellular viral RNA or protein levels. Reproduced from Tellinghuisen *et al.* (2007).**

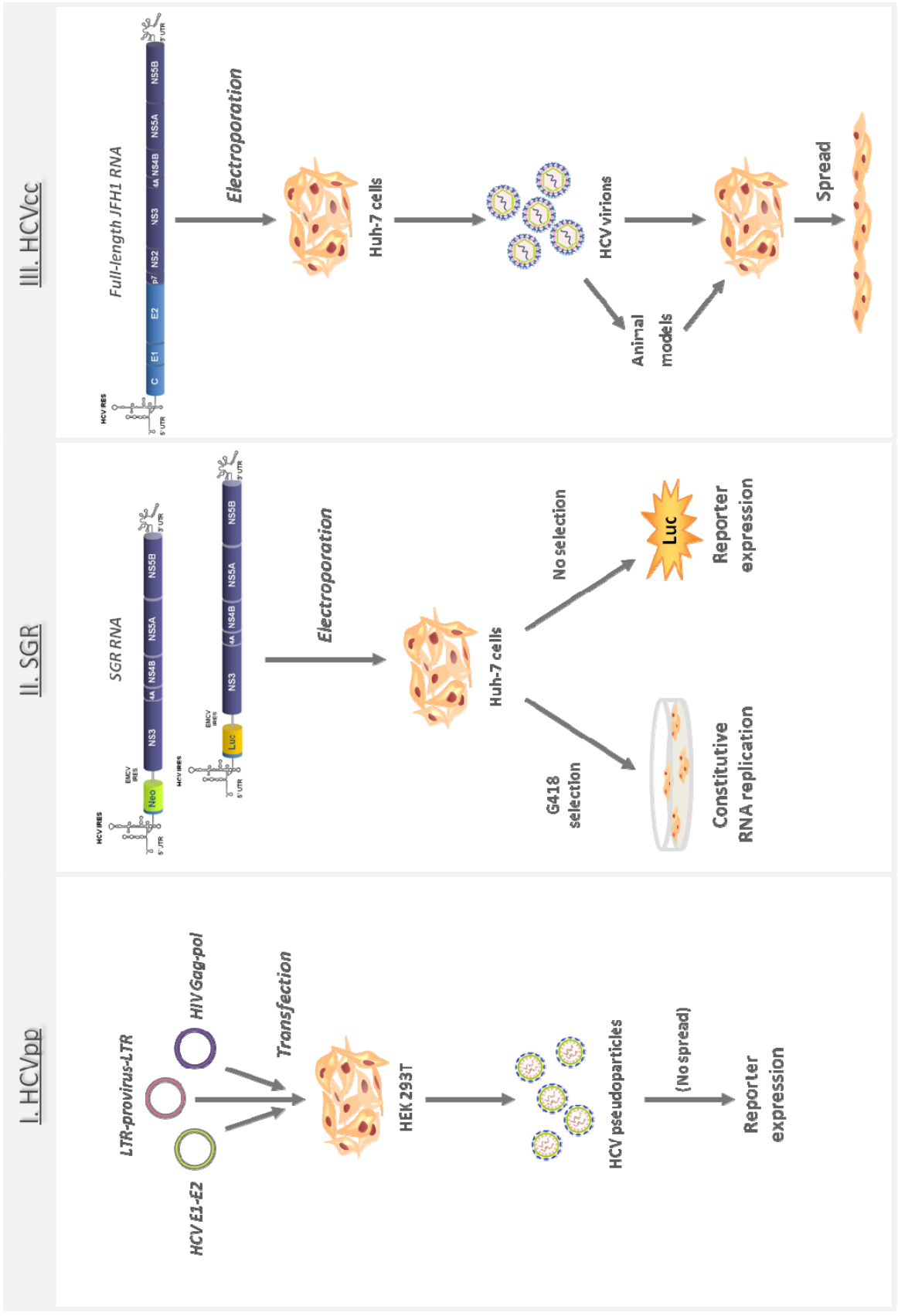
I. HCVpp
LTR-provirus-LTR
HIV Gag-pol
HCV E1-E2
Transfection
HEK 293T
HCV pseudoparticles
(No spread)
Reporter expression
II. SGR
SGR RNA
Neo
Luc
Electroporation
Huh-7 cells
No selection
G418 selection
Luc
Reporter expression
Constitutive RNA replication
III. HCVcc
Full-length JFH1 RNA
Electroporation
Huh-7 cells
HCV virions
Animal models
Spread

### 1.3.1 *in vitro* models

#### I. HCV pseudoparticles (HCVpp)

To study the process of HCV entry, the HCV pseudoparticle (HCVpp) system was generated using HCV glycoproteins which are exposed at the surface of retroviral particles (Bartosch *et al.*, 2003a; Drummer *et al.*, 2003; Hsu *et al.*, 2003). HCVpp are produced by cotransfection of 293T cells with three expression vectors encoding the HCV E1E2 proteins, the Gag-Pol proteins from either human immunodeficiency virus or murine leukemia virus, and a retroviral genome carrying a reporter marker gene (e.g luciferase or GFP). The marker gene packaged into HCVpp enables easy evaluation of infectivity mediated by HCV glycoproteins. This system has been developed using HCV glycoproteins from genotypes 1a, 1b, 2a, 3a, 4a, 5a and 6a, allowing the analysis of cross- and genotype-specific neutralization (Lavillette *et al.*, 2005; Owsianka *et al.*, 2005). Several reports have demonstrated that HCVpp has tropism for liver cells and the ability of anti-E2 antibodies in neutralising HCVpp has allowed studies on virus binding, attachment and internalization as well as the identification of the HCV receptors required for entry in the cells (Bartosch *et al.*, 2003b; Evans *et al.*, 2007; Ploss *et al.*, 2009).

#### II. Sub-genomic replicons (SGR)

Shortly after the cloning of the HCV genome in 1989 (Choo *et al.*, 1989), the first apparent full-length HCV RNA generated was not successful in replicating viral sequences *in vitro*. These clones lacked the 3' UTR region of the genome which was essential for efficient replication. In 1997, Kolykhalov *et al* (1997) generated the first full-length functional HCV cDNA clone, which included the 3' UTR region. This full-length HCV RNA (H77 strain) was infectious in chimpanzees, however it was unable to replicate *in vitro* (Kolykhalov *et al.*, 1997). In 1999, Lohmann *et al*, overcame the *in vitro* replication barrier with the development of the first HCV replicon system based on sequences from Con-1, a genotype 1b strain of the virus (Lohmann *et al.*, 1999). These HCV SGR RNAs were engineered as bicistronic constructs, in which the region encoding core to NS2 was replaced by a coding sequence for a selectable antibiotic resistant marker (neomycin phosphotransferase, *neo*). This gene was under the control of

the HCV IRES, and was followed downstream by an heterologous IRES from encephalomyocarditis virus (EMCV), to drive translation of the downstream HCV NS3 to NS5B coding region derived from the Con-1 consensus genome. The first 48 nucleotides of the core coding sequence located at the 3'end of the HCV IRES were linked in-frame with the *neo* gene to ensure complete IRES activity. Upon transfection of human hepatoma Huh-7 cells with *in vitro* transcribed HCV SGRs, followed by selection with G418, a small number of resistant colonies of cells supporting autonomous HCV replication were obtained (Lohmann *et al.*, 1999). Although this SGR system was a major breakthrough in propagating HCV in cell culture, replication of these RNAs was relatively inefficient.

Sequence analysis of Con-1-derived HCV RNAs replicating in cell clones after G418 selection identified the presence of cell culture adaptive mutations. These mutations were located across all NS coding regions (NS3, NS4B, NS5A and NS5B). Introduction of selected subsets of these mutations into the original consensus Con-1 sequence resulted in enhancement of RNA replication by several orders of magnitude (Blight *et al.*, 2000; Krieger *et al.*, 2001). Full-length HCV replicons have also been generated using Con-1 cell culture adapted sequences, which are able to replicate in Huh-7 cells. However, replication efficiency was lower than that observed in SGRs and no virus production was observed in these cells (Pietschmann *et al.*, 2002). In these full-length replicons, the presence of adaptive mutations was detrimental to viral particle assembly. In addition, inoculation of chimpanzees with a full-length Con1 replicon containing adaptive mutations failed to establish a productive infection (Bukh *et al.*, 2002). Some of these mutations are not found in natural isolates in HCV-infected patients, suggesting that they represent a specific adaptation to the Huh-7 cell environment.

In addition to cell culture adaptive mutations, cell permissiveness also influenced the ability of HCV SGR RNA to replicate *in vitro*. Several cell lines have been reported to support HCV replication, however Huh-7 cells still remained the most permissive line. Later, highly permissive clones of Huh-7 cells were generated that supported higher viral replication levels. To that end, a subpopulation of Huh-7 cells harbouring higher levels of HCV SGRs were cured of the replicon by co-culturing the cells with IFN. From this approach, two cell lines were generated, Huh-7-Lunet and Huh-7.5 (Blight *et al.*, 2002; Friebe *et al.*,

2005). Similarly, an additional subclone (Huh-7.5.1) was generated by curing Huh-7.5 cells of replicating HCV. Reintroduction of replicon RNAs into these "cured" cell lines resulted in much higher RNA replication levels when compared with the parental Huh-7 cell line (Blight et al., 2002). The reasons for higher replication in these cells is not fully understood, but was thought to result from a partial impairment of their antiviral immune responses (Lanford *et al.*, 2003). Indeed, Huh-7 cells were shown to be defective dsRNA signaling through TLR3 pathway (Li *et al.*, 2005). In addition to the defect in TLR3 signalling, Huh-7.5 cells were also found to contain a mutation in the RIG-I CARD domain, which blocked down-stream signalling and activation of IRF-3 (Sumpter *et al.*, 2005).

With the developments obtained from generating highly permissive cell lines as well as cell culture adapted HCV RNAs, further improvements to the SGR model have been achieved. For example, the *neo* resistance marker could be replaced by other antibiotic markers as well as reporter genes (Bartenschlager *et al.*, 2003). The latter was a major improvement to this system, since measurement of replication activity in transient assays and high throughput screening of antiviral compounds was made possible. Moreover, other SGRs containing NS3-NS5B consensus sequences derived from other HCV strains (such as H77 strain, genotype 1a) were also developed (Blight *et al.*, 2003). Similar to Con-1 SGR, H77 SGRs also required adaptive mutations for efficient replication in Huh-7 cells (Blight *et al.*, 2003; Yi & Lemon, 2004).

Using a similar approach to that used for Con-1, an HCV genotype 2a replicon was generated using strain JFH-1, isolated from the serum of a Japanese patient with fulminant HCV (Kato *et al.*, 2003). JFH-1 subgenomes replicated with higher efficiency in Huh-7 cells, producing 60 times more drug-resistance colonies than the original Con-1-derived replicons harbouring highly adaptive mutations (Kato *et al.*, 2003). Unlike Con-1 replicons, JFH1 replicons did not require adaptive mutations to achieve high levels of replication. In addition, JFH1 replicons containing the luciferase reporter gene gave much improved levels of replication in transient assays compared to equivalent Con-1 replicons (Targett-Adams & McLauchlan, 2005). Given the higher replication efficiency of strain JFH1, the JFH1 SGR also replicated in cell lines other than Huh-7 cells, such as human cell lines of hepatic or nonhepatic origin (HepG2, IMY-N9, HeLa, HEK 293) and mouse embryonic fibroblasts (Chang *et al.*, 2006; Date *et al.*, 2004; Kato *et al.*, 2005).

**III. HCV cell culture-derived virions (HCVcc)**

The successful development of the SGR system was followed a major breakthrough in the propagation of HCV *in vitro* using HCV strain JFH1. Prior to availability of this system, the sole source of HCV infectious particles was either the sera from infected patients or chimpanzees. Following the efficiency in replication achieved by the JFH1 SGRs, RNA derived from the full-length JFH1 cDNA resulted in production of infectious virus, termed HCVcc, following transfection into Huh-7 cells (Lindenbach *et al.*, 2005; Wakita *et al.*, 2005; Zhong *et al.*, 2005). This HCVcc-derived virus was infectious in both naive Huh-7 cells and in chimpanzees. The success with isolation of JFH1 has allowed the development of chimeric viruses, in which the structural genes of JFH1 are replaced with those of Con1, H77 and J6 sequences of genotypes 1b, 1a and 2a, respectively (Pietschmann *et al.*, 2006; Yi *et al.*, 2007). The most efficient of these chimeras is JC-1 and consists of genotype 2 strain J6- and JFH1-derived sequences. This chimera is capable of yielding infectious titres up to 1000-fold higher than JFH1 (Pietschmann *et al.*, 2006). This *in vitro* model, reproducing the entire life cycle of HCV in Huh-7 cells, has enabled extensive research into various areas of HCV biology.

### 1.3.2 *in vivo* models

Although the development of *in vitro* model systems has represented a substantial advance in the understanding of HCV biology, the range of cells and viral strains that can be utilised is very limited. In addition, studies on adaptive immune responses, which determine the outcome of HCV infection, cannot be addressed with such models. To date, the chimpanzee is the only immunocompetent animal model available to study HCV. Chimpanzees support HCV infection and replication, and allow the recapitulation of the complete viral life cycle for all six HCV genotypes (Bukh *et al.*, 2010). Chimpanzees have innate and adaptive immune responses similar to those observed in humans and therefore, are highly relevant to study the natural course of HCV infection. However, experiments in chimpanzees are no longer permitted due to ethical concerns in most countries. Although HCV is unable to infect mice, advances have been made in developing susceptible humanized mouse models. The most successful small animal model currently available for HCV infection is the human liver uPA/SCID mouse. These mice are immunodeficient (SCID – severe combined immunodeficient) and have liver-specific expression of the urokinase plasminogen activator (Alb-uPA), which allows repopulation of the liver with transplanted human hepatocytes. Human liver uPA/SCID mice are susceptible to HCV infection and they produce infectious virions to levels similar to those found in humans and chimpanzees (Lindenbach *et al.*, 2006; Mercer *et al.*, 2001; Meuleman & Leroux-Roels, 2008). The major drawbacks with this system are that the mice are immunodeficient, thus precluding studies on most aspects of immunity and pathogenesis, and the low success rate with xenotransplantation of human liver. Since the development of the uPA-SCID mouse system, there have been further improvements to the model. For example, $Fah^{-/-}/Rag2^{-/-}/IL2rg^{-/-}$ mice which contain a partially reconstituted human immune system, has resolved some of the limitations observed with the uPA/SCID mouse (Bissig *et al.*, 2010). This model has other limitations, such as absence of antibody responses due to the lack of reconstitution of fully functional B cells (Bissig *et al.*, 2007). Thus, studies on mechanisms of immune escape from neutralizing antibodies or the evaluation of B cell vaccines are not possible with $Fah^{-/-}/Rag2^{-/-}/IL2rg^{-/-}$ mice.

More recently, further developments were made to create fully immunocompetent humanised mouse models. In a study by Dorner *et al* (2011), it was demonstrated that expression of the two human genes, CD81 and occludin, in fully immunocompetent mice, was sufficient to render these mice susceptible to HCV infection (Dorner *et al.*, 2011). Although, this model is limited to HCV entry it presents a useful alternative to the chimpanzee model for studies on virus neutralization, virus-receptor interaction and the development of novel therapeutics for blocking virus entry. More recently, Washburn *et al* (2011), developed the AFC8-hu HSC/Hep mice which represent the first mouse model with both human immune and liver cells. Infection of these mice with HCV appears to induce human immune responses (Washburn *et al.*, 2011). Thus, major advances made with AFC8-hu HSC/Hep mice will allow further studies on HCV pathogenesis and in the development of improved therapeutics for HCV infection.

## 1.4 HCV life cycle

HCV is a hepatotropic pathogen that reaches the liver through sinusoidal blood vessels to infect its primary target cells, which are hepatocytes. Infection occurs through a series of sequential stages: I) attachment to the cells; II) entry by receptor-mediated endocytosis; III) translation of incoming viral genome(s); IV) polyprotein processing and replication complex formation; V) RNA replication; VI) assembly of new virions and VII) release of virions from the cells. After binding and entry, the remainder of the HCV life cycle takes place in the cytoplasm of hepatocytes. Each of these steps is represented in (Figure 1.9) and described in the following paragraphs.

### 1.4.1 Virus attachment and entry

#### I. HCV liver uptake and attachment to hepatocytes

HCV is transmitted predominantly through direct exposure to blood or blood products. Following exposure, HCV establishes a productive infection in hepatocytes. Hepatocytes are shielded from the bloodstream by Kupffer cells, liver sinusoidal endothelial cells (LSECs) and hepatic stellate cells. HCV is thought to enter the liver through the sinusoidal blood and is captured by the LSECs to facilitate infection of hepatocytes. However, little is understood about these early events in infection.

**Figure 1.9 – Schematic representation of the HCV life cycle. Attachment of HCV to cell-surface receptors leads to receptor-mediated endocytosis into a low-pH vesicles. Following membrane fusion, the viral genome is released into the cytoplasm. The incoming viral genome is a positive single-stranded RNA molecule and functions as a template for translation of the HCV-sense polyprotein, which is further processed to produce the mature viral proteins. Viral RNA replication occurs within membrane-associated replication complexes. Replicated RNA is used for further production of viral proteins or is encapsidated. The viral particles are thought to use the cellular secretory pathway for maturation and release of HCV virions.**

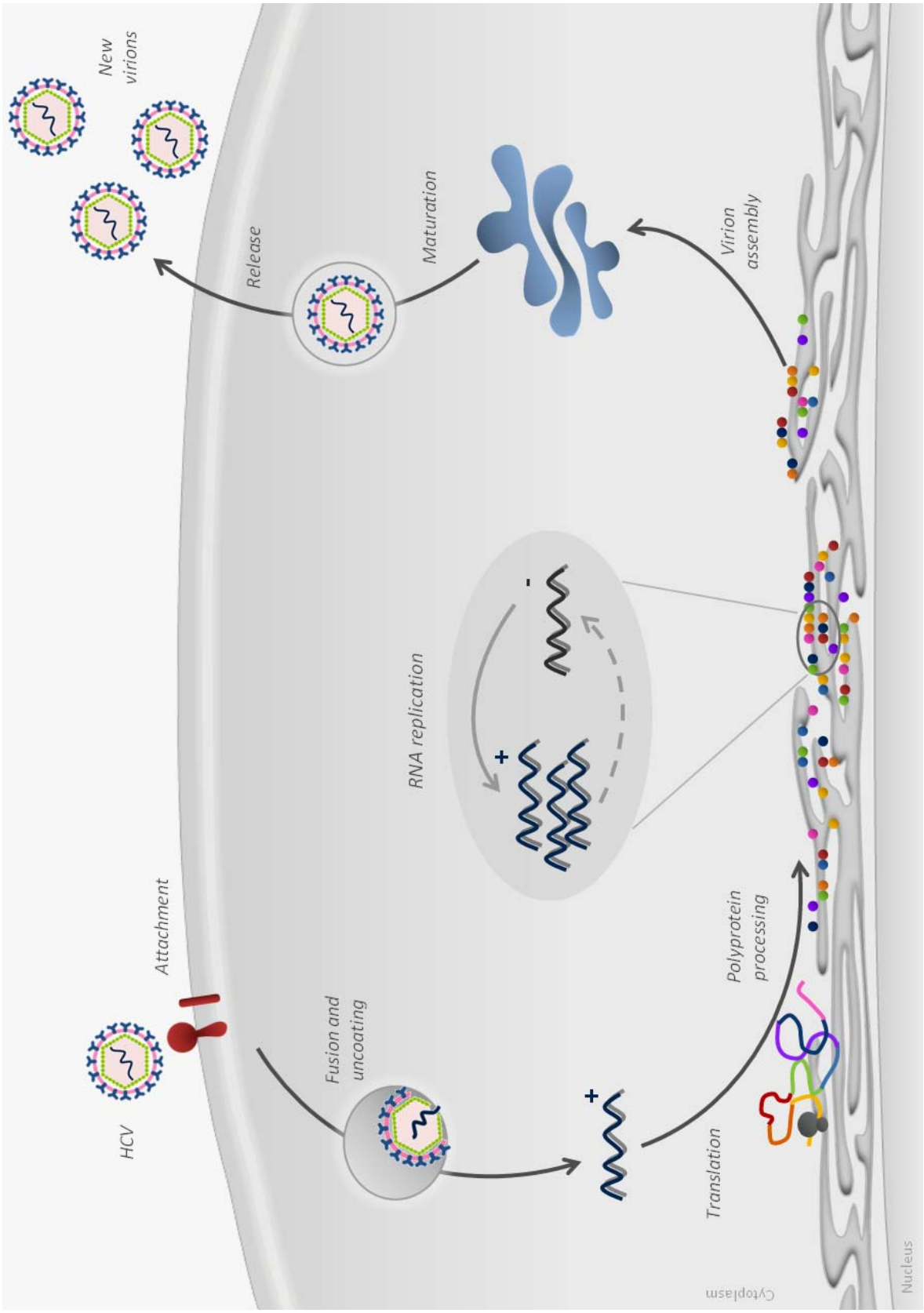
New virions
Release
Maturation
Virion assembly
Attachment
RNA replication
Fusion and uncoating
Polyprotein processing
HCV
Translation
Cytoplasm
Nucleus

As mentioned earlier, HCV particles exist in association with lipoproteins and thus circulate as lipoviroparticles (LVPs; section 1.2). HCV LVPs may cross from the liver endothelium through interaction with a set of capturing receptors called C-lectins (DC-SIGN and L-SIGN). DC-SIGN (dendritic-cell-specific ICAM-3 grabbing non-integrin) and L-SIGN (liver/lymph node-specific ICAM-3 grabbing non-integrin) are highly expressed in Kupffer cells and LSECs, respectively, and have been suggested to mediate transcytosis of HCV particles from the blood to the underlying hepatocytes. Several reports support this hypothesis and revealed that HCV E2 protein can bind with high affinity to both DC-SIGN and L-SIGN (Gardner *et al.*, 2003; Lai *et al.*, 2006; Pohlmann *et al.*, 2003). Loss of this interaction greatly inhibits virus uptake, suggesting that these lectins may be used for capturing HCV to the hepatocytes.

Once HCV has transversed the endothelium, two receptors [glycosaminoglycans (GAGs) and low density lipoprotein receptor (LDL-R)] have been implicated in capturing and concentrating the virus at the basal surface of hepatocytes. GAGs are thought to represent, an initial, low affinity interaction between HCV particles and the cell surface (Barth *et al.*, 2003; Koutsoudakis *et al.*, 2006). GAGs such as heparin sulphate proteoglycan (HSPG) do bind recombinant E2 glycoprotein (Barth *et al.*, 2003). Cells treated with heparinase, an enzyme responsible for cleaving heparin sulphate molecules, resulted in reduced binding of recombinant E2 and HCVcc entry into the cells (Barth *et al.*, 2003; Koutsoudakis *et al.*, 2006). In addition to GAGs, many groups have suggested that the LDL-R is involved in HCV entry (Agnello *et al.*, 1999; Germi *et al.*, 2002; Molina *et al.*, 2007). It has been shown that endocytosis of HCV correlates with the presence of LDL-R and this process is inhibited using anti-LDL-R antibodies. Additional evidence for the role of LDL-R in HCV entry has also emerged from experiments in which knockdown of LDL-R in primary hepatocytes resulted in loss of HCV infectivity (Molina *et al.*, 2007; Owen *et al.*, 2009).

## II. Entry

Following attachment, internalisation of virus particles requires a series of interactions with at least four cell receptors. These include the scavenger receptor class B type I (SR-BI) (Scarselli *et al.*, 2002), the tetraspanin CD81 (Pileri *et al.*, 1998) and two tight junction proteins, claudin-1 (CLDN1) (Evans *et al.*, 2007) and occludin (OCLN) (Benedicto *et al.*, 2009; Liu *et al.*, 2009; Ploss *et al.*, 2009).

SR-BI is highly expressed in hepatic cells, where it functions as a lipoprotein receptor that mediates selective cholesterol ester uptake from high-density lipoprotein (HDL) (Krieger, 2001; Reynolds *et al.*, 2008). SR-BI is a 82KDa glycoprotein, consisting of a highly glycosylated large extracellular loop anchored to the plasma membrane at both the N- and C-termini by transmembrane domains with short extensions into the cell cytoplasm. SR-BI was initially identified as a receptor for HCV entry through its ability to bind to a soluble recombinant form of E2 glycoprotein (Scarselli *et al.*, 2002). Receptor competition assays further demonstrated that anti-SR-BI antibodies that inhibited soluble recombinant E2, could prevent HCVpp infectivity (Bartosch *et al.*, 2003b). Additionally, siRNA-mediated silencing of SR-BI in Huh-7 cells resulted in a reduction of HCVpp infectivity (Lavillette *et al.*, 2005). Binding of E2 to SR-BI requires the HVR1 domain of E2 and deletion of this region results in loss of binding to the receptor (Scarselli *et al.*, 2002). Consistently, HCV virions incubated with anti-HVR1 antibodies inhibited E2 binding to SR-BI, thereby reducing infectivity in cell culture. These studies demonstrate an important role for SR-BI in HCV entry (Bartosch *et al.*, 2003b).

CD81 was the first receptor, which was identified as mediating HCV entry (Pileri *et al.*, 1998). It is a member of the tetraspanin family of transmembrane proteins. The protein has an apparent molecular weight of 26KDa and consists of four transmembrane domains, separated by two extracellular loops [small (SEL) and large (LEL)] and short cytoplasmic N- and C-terminal regions. Initial evidence that CD81 was a binding receptor for HCV come from studies demonstrating that solubilised forms of E2 protein could bind to CD81 (Pileri *et al.*, 1998). In addition, the same group showed that this interaction was mediated through the LEL of CD81, as expression of the recombinant form of the

LEL bound to HCV (Pileri *et al.*, 1998). Anti-CD81 antibodies or silencing of CD81 using siRNAs inhibited HCVcc and HCVpp infection of primary human hepatocytes and hepatoma cell lines (Bartosch *et al.*, 2003b; Molina *et al.*, 2008; Wakita *et al.*, 2005; Zhang *et al.*, 2004). Further evidence supporting the role of CD81 in HCV entry was obtained from studies where human hepatoma cell lines (HepG2 and HH29 cells), which were previously resistant to infection, became permissive to HCVpp upon ectopic expression of CD81 (Bartosch *et al.*, 2003b; Lavillette *et al.*, 2005; Zhang *et al.*, 2004).

Inhibition studies using anti-SR-BI and anti-CD81 antibodies have suggested that SR-BI may act concomitantly with CD81 (Zeisel *et al.*, 2007). Since HCVcc could bind CHO cells expressing SR-BI but not CD81, it is suggested that HCVcc may attach to SR-BI before CD81 (Evans *et al.*, 2007). Although CD81 can interact with a soluble form of E2, it does not appear to be able to interact directly with mature HCV virions, indicating that binding to other receptors may alter the virion conformation to reveal CD81 binding sites. Sharma *et al* (2011) reported that CD81 LEL induced changes in glycoprotein E1E2 conformation, as evidenced by an altered reactivity of the proteins with conformation-specific antibodies (Sharma *et al.*, 2011). In support of this hypothesis, interaction of SR-BI with E2 has been suggested to induce a conformational change in the HCV glycoproteins, which is essential for binding to the subsequent cell receptors. Indeed, deletion of HVR1 in E2 resulted in loss of SR-BI dependency and led to an increase in HCVcc binding to CD81 (Bankwitz *et al.*, 2010). The authors hypothesised that HVR1 may mask conserved CD81 binding epitopes and shield them from neutralising antibodies. In addition, mutagenesis studies on E2-specific N-linked glycan residues showed increased E2-CD81 association, suggesting that a conformational change in E2 may be required to promote high-affinity association with CD81.

After attachment to CD81, virions are directed to tight junctions, where interaction with CLDN1 and OCLN occurs, to facilitate cellular uptake. CLDN1 and OCLN are expressed at the interface between basolateral and apical membranes, and are involved in regulating paracellular transport of solutes and generate apical-basal cell polarity (Shin *et al.*, 2006). CLDN1 consists of four transmembrane domains and two extracellular loops. The first extracellular loop is required for HCVpp entry (Evans *et al.*, 2007). Although no direct interaction

has been observed between HCV glycoproteins and CLDN1, several studies have revealed that CD81 interacts with CLDN1, suggesting that these factors can act in a cooperative manner during entry (Evans *et al.*, 2007; Harris *et al.*, 2008; Krieger *et al.*, 2010). Furthermore, in nonpolarised or partially polarised cells this CD81-CLDN1 interaction occurs outside of cell junctions before infection and appears to influence the entry process (Harris *et al.*, 2010; Harris *et al.*, 2008). Disruption of CD81-CLDN1 association with anti-CLDN1 antibodies reduced E2 association with the cell surface and resulted in loss of HCV infectivity (Krieger *et al.*, 2010). Recently, two receptor tyrosine kinases, epidermal growth factor receptor (EGFR) and ephrin receptor A2, have been reported as cofactors for HCV cell entry (Lupberger *et al.*, 2011). These receptors were suggested to mediate HCV entry by regulating CD81-CLDN1 association and viral glycoprotein-dependent membrane fusion. Blocking the receptor kinase activity greatly reduced HCV infection both *in vitro* and *in vivo* (Lupberger *et al.*, 2011).

Another tight junction protein, OCLN, has been implicated in HCV entry (Benedicto *et al.*, 2009; Liu *et al.*, 2009; Ploss *et al.*, 2009). Similar to CLDN1, OCLN has four transmembrane domains and two extracellular loops. Contrary to CLDN1, a direct interaction between OCLN and the E2 from HCVcc particles has been demonstrated (Liu *et al.*, 2009b). This interaction is apparently essential for HCV entry since silencing of OCLN in cells permissive for HCV entry, resulted in a reduction of both HCVcc and HCVpp infectivity (Ploss *et al.*, 2009). Furthermore, knockdown of OCLN in a cell-cell fusion assay, where fusion activity depended on cell surface expression of the E1E2 glycoprotein complex, diminished fusion activity, suggesting that OCLN may participate in the HCV fusion process (Benedicto *et al.*, 2009).

More recently, the Niemann-Pick C1-like 1 cholesterol absorption receptor (NPC1L1) has been suggested as an entry factor for HCV (Sainz *et al.*, 2012). NPC1L1 is a cell surface cholesterol sensing receptor expressed on the apical surface of intestinal enterocytes and human hepatotyces, including Huh-7 cells. NPC1L1 is an entry factor used by HCV, that functions after binding, but at or before fusion (Sainz *et al.*, 2012). However, the requirement of this receptor for HCV entry requires further confirmation, as expression of SR-BI, CD81, CLDN1 and OCLN in murine and hamster cells rendered these cells permissive for HCV infection (Ploss *et al.*, 2009).

Similar to other flaviviruses, HCV entry is thought to be mediated by clathrin-mediated endocytosis, with delivery of the viral nucleocapsid into the cytoplasm via early endosomes (Blanchard *et al.*, 2006). Treatment of cells with agents that disrupt clathrin-coated pit formation or siRNA-mediated silencing of clathrin, reduced both HCVpp and HCVcc entry (Blanchard *et al.*, 2006; Meertens *et al.*, 2006). Once internalized, the virus glycoproteins are proposed to fuse with the membrane of early endosomes (Meertens *et al.*, 2006). This mechanism is dependent on low pH, with an optimum at about 5.5 (Lavillette *et al.*, 2006). Furthermore, experiments using drugs that inhibited acidification of endosomes have shown that low pH in endosomes is required for both HCVpp and HCVcc cell entry (Blanchard *et al.*, 2006; Hsu *et al.*, 2003; Koutsoudakis *et al.*, 2006; Meertens *et al.*, 2006).

Investigation of fusion determinants indicated that three discrete regions of both E1 and E2 proteins participate in the intracellular membrane fusion process (Lavillette *et al.*, 2007). The process of entry may also be dependent on an intact and dynamic microtubule network and for early post-fusion steps of infection (Roohvand *et al.*, 2009). It is suggested that core protein may play a role in this process through its interaction with tubulin, which resulted in enhanced microtubule polymerization (Roohvand *et al.*, 2009). This interaction could mediate the transport of the HCV nucleocapsid to sites where genome translation takes place and subsequently where the viral RNA would be released into the cytoplasm.

## 1.4.2 Translation and Replication

### III. Translation of incoming genomes

Uncoating of viral nucleocapsids results in release of the viral genome into the cell cytoplasm. The viral genome serves as a template for synthesis of the HCV precursor polyprotein. In contrast to cellular mRNAs, which require a 5'-cap structure for recruitment of both eIF4F (eukaryotic initiation factor 4F) complex and the small (40S) subunit of the ribosome to initiate translation, HCV RNA lacks a 5'-cap and uses an IRES to mediate cap-independent translational initiation (Wang *et al.*, 1993). IRES-mediated translation is initiated by direct binding of a vacant 40S ribosomal subunit to the IRES and positioning of the polyprotein start codon into the 40S P site (Kieft *et al.*, 2001; Otto & Puglisi, 2004). Compared to capped cellular mRNAs, the HCV IRES can capture the 40S ribosomal subunit in the absence of any known initiation factors previously identified as required for ribosome binding to an mRNA. However, integration of two eukaryotic initiation factors (eIF2 and eIF3) into the IRES-40S complex, is necessary for efficient protein synthesis of the viral RNA (Pestova *et al.*, 1998). After interaction of the HCV IRES with the 40S ribosomal subunit, this complex binds to eIF3, followed by recruitment of the eIF-2:Met-tRNAi:GTP complex to generate a 48S-like complex (Ji *et al.*, 2004). Upon hydrolysis of GTP, the initiation factors are released allowing attachment of the 60S ribosomal subunit to the 48S complex. This generates a functional IRES-80S complex, which can initiate viral protein synthesis.

### IV. Polyprotein processing and RC formation

Translation of the HCV genome generates a large precursor polyprotein, which is targeted to the ER membrane and thereafter processed by cellular and viral proteases to generate the mature forms of structural and non-structural viral proteins (section 1.2.2). Host signal peptidase cleaves at the C-terminal end of the signal peptide between core and E1, releasing an immature form of core and creating the N-terminus for E1 (Hussy *et al.*, 1996; Moradpour *et al.*, 1996; Santolini *et al.*, 1994). Core is further processed within the signal sequence at its C-terminus by host signal peptide peptidase to yield the mature form of the protein (McLauchlan *et al.*, 2002). Additional signal peptidase

cleavages occur at the boundaries between E1-E2, E2-p7, p7-NS2, yielding E1, E2, p7 and the N-terminus of NS2 (Dubuisson *et al.*, 2002). E1 and E2 undergo further maturation through N-glycosylation and conformation of the glycoproteins. HCV NS proteins are processed by two viral proteases: the zinc-dependent NS2/3 auto-protease that cleaves NS3 from NS2, and the NS3/4A protease which processes the polyprotein at the NS3-NS4A junction and subsequent downstream junctions, NS4A-NS4B, NS4B-NS5A, and NS5A-NS5B (section 1.2.2.2).

Similar to many positive-sense RNA viruses, HCV induces dramatic remodelling of intracellular membranes to generate specialised compartments in which RNA replication takes place. For replication to occur, the viral genome, together with viral and host proteins is recruited to these specialised compartments in order to create the viral replication complex (RC). The HCV RC is thought to assemble on intracellular ER membranes through dynamic deformation of those membranes, which generate vesicles-like structures, known as the membranous web [MW; (Egger *et al.*, 2002; Gosert *et al.*, 2003)]. Membrane alterations induced by the expression of HCV proteins were systematically studied by inducibly expressing the entire HCV polyprotein and individual viral components (Egger *et al.*, 2002). In this study, it was found that expression of the HCV polyprotein induces distinct membrane alterations. Formation of the MW was induced by NS4B alone and very similar in morphology to the “sponge-like inclusions” previously observed using electron microscopy in the liver of HCV-infected chimpamzees (Pfeifer *et al.*, 1980). It is believed that membrane alterations provide 1) physical support and organisation of the RC, 2) compartmentalization and concentration of viral products essential for replication and 3) protection of the viral RNA from host defences.

As mentioned above, NS4B is sufficient to induce rearrangement of the ER membrane, by an as yet unknown mechanism (Egger *et al.*, 2002; Gosert *et al.*, 2003). The precise composition of the HCV RC is not known, but it includes NS proteins (NS3-4A, NS4B, NS5A, and NS5B), cellular components and newly synthesized RNA molecules. Metabolic labelling of the nascent viral RNA with BrUTP in the presence of actinomycin D confirmed that the RC at the MW is the site of viral RNA synthesis (Gosert et al., 2003). By immunofluorescence microscopy, MWs appear as dot-like structures with diameters of up to several microns (Gosert *et al.*, 2003).

### V. Mechanism of RNA replication

The synthesis of new viral genomes is thought to occur in the MW and is catalysed by NS5B, the viral RdRp. Replication proceeds through the synthesis of a complementary negative-strand RNA by NS5B, using the positive-strand genome RNA as a template. Then, negative-strand RNA serves as a template to produce numerous strands of positive-sense RNA (Lohmann *et al.*, 1999; Takehara *et al.*, 1992). During this process, dsRNA intermediates are formed, which can be visualised at RC sites in actively replicating cells (Targett-Adams *et al.*, 2008). The positive-strand RNA is produced in a 5-10 fold excess compared with negative-strand RNA, and is used as the template for further polyprotein translation, synthesis of new intermediates of replication and packaging into new virus particles (Quinkert *et al.*, 2005). Several host and viral factors have been shown to modulate viral RNA synthesis. Some of these factors have been described previously in sections 1.2.1.1-I&II and 1.2.2.2-II to -V and are involved in regulating a range of cellular processes. These factors can directly influence the activity of RdRp [e.g., cyclophilin A (Kaul *et al.*, 2009), and the protein kinase PRK2 (Kim *et al.*, 2004)] or interfere with the activity of different components of the replication complex to modulate viral RNA replication.

### 1.4.3 Assembly and release

The final stages of the HCV life cycle include the assembly of virions and their release from cells. As mentioned earlier, the HCV virion is thought to consist of a nucleocapsid, in which core encapsidates and protects the viral genome, and an outer envelope composed of a lipid membrane containing the E1E2 glycoproteins. In addition, the mature virion is thought to associate with VLDL/LDL, generating lipoviroparticles (LVP). Although little is known about the molecular mechanisms governing nucleocapsid formation and release of virions, much of what is known about these later steps of the HCV life cycle has been established through the development of the HCVcc model.

#### VI. Nucleocapsid assembly

Nucleocapsid assembly involves the formation of the capsid by oligomerization of the core protein and encapsidation of genomic RNA. Core protein has a central role in assembly as it is the constitutive unit of the nucleocapsid. After full maturation of core by SPP, the protein is targeted to lipid droplets (LDs; McLauchlan *et al.*, 2002). This association is mediated by the D2 domain of core and is required for virus production (Boulant *et al.*, 2007; Miyanari *et al.*, 2007). Confocal microscopy analyses with fluorescent reporters identified crucial residues for core-LD association within D2 (Boulant *et al.*, 2006). Live cell imaging of virus-producing cells has been used to visualize core during the HCV assembly process (Counihan *et al.*, 2011). Using this method, fluorescently labelled core was found to move to the surface of large, immotile LDs soon after translation. During the peak of virus assembly core formed polarized caps on these LDs that were frequently in close apposition to ER-localized core, indicating that core may transfer between the ER and LDs at these sites (Counihan *et al.*, 2011). Similarly, 3D reconstruction of confocal images during infection demonstrated that core gradually decorates the surface of LDs and the extent of LD coverage by core correlated with the production of infectious particles (Boulant *et al.*, 2007).

In addition to being located around LDs, core protein also induces their redistribution from a dispersed distribution within the cytoplasm to the perinuclear region (Boulant *et al.*, 2008). The loading of core onto LDs has been shown to displace adipocyte differentiation related protein (ADRP), an abundant protein on the LD surface. ADRP maintains the normal dispersed cytoplasmic distribution of LDs and its displacement by core protein during infection causes LDs to re-localise in aggregates at close to the microtubule organising centre (Boulant *et al.*, 2008). Viral RNA is replicated at the ER, and the LD redistribution is believed to create the microenvironment that coordinates interaction between core and RCs during assembly (Boulant *et al.*, 2008; Miyanari *et al.*, 2007). Several studies have shown that core is also involved in the recruitment of NS proteins and RNA replication complexes to sites adjacent to LDs; for example, NS2, NS3, NS4AB, NS5A, NS5B localize around LDs in infected cells (Boulant *et al.*, 2008; Jirasko *et al.*, 2010; Ma *et al.*, 2011; Miyanari *et al.*, 2007; Popescu *et al.*, 2011). Electron microscopy images showed that, although core is tightly associated with LDs, NS2, NS5A, E2 and E1 also colocalize in close proximity to LDs (Miyanari *et al.*, 2007; Popescu *et al.*, 2011). Furthermore, *in situ* hybridization analyses indicate that positive- and negative-strand viral RNAs are found at the proximity of LDs (Miyanari *et al.*, 2007). In contrast, viruses containing defective mutations in core-LD association do not show accumulation of the other viral elements around LDs (Miyanari *et al.*, 2007; Popescu *et al.*, 2011). The trafficking of core between LD and ER membranes and the consequent presence of other viral proteins around the LDs is essential to the assembly process.

Mutational analyses have demonstrated important roles for p7 and the non-structural proteins in assembly and release of infectious HCV. In addition to core protein, NS5A has been reported to associate with LDs and to co-localise with core on these organelles (Miyanari *et al.*, 2007). Mutations within domain I of NS5A have established that this domain is required for its association with LDs, and this interaction is crucial for infectious virus production (Miyanari *et al.*, 2007). Also, deletions in domain III impaired virus production by disrupting the NS5A-core protein association on LDs but did not affect attachment of NS5A to LDs (Appel *et al.*, 2008). Moreover, another study found that mutagenesis of a cluster of serine residues within domain III impaired NS5A basal phosphorylation,

resulting in a decrease in NS5A-core interactions, which disrupted virus production (Masaki *et al.*, 2008).

Several studies have identified regions or residues within the NS2 protein essential for infectious virus production (Jirasko *et al.*, 2010; Jones *et al.*, 2007; Ma *et al.*, 2011; Popescu *et al.*, 2011; Yi *et al.*, 2009). NS2 directly interacts with multiple viral proteins including E1E2, p7, NS3 and NS5A, and immunofluorescence analysis have shown that NS2 co-localises with these proteins at the LD-ER interface, suggesting that it may provide an important link between replication complexes and the structural proteins during the assembly process (Jirasko *et al.*, 2010; Popescu *et al.*, 2011). Since no direct interaction has been identified between NS2 and core, it has been hypothesised that an interplay might exist between the core-NS5A and NS2-NS5A interactions during assembly (Jirasko *et al.*, 2010; Ma *et al.*, 2011; Stapleford & Lindenbach, 2011). In addition, p7 recruits both core and NS2 to sites adjacent to replication complexes (Boson *et al.*, 2011; Tedbury *et al.*, 2011). Mutagenesis studies on conserved residues of p7, which are important for ion channel activity, have shown that p7 is required for production of infectious virus (Jones *et al.*, 2007; Steinmann *et al.*, 2007). However, the exact function of p7 during virion assembly remains to be elucidated. In a recent study, p7 inhibited the acidification of intracellular compartments, presumably to protect intracellular virions during their maturation or secretion (Wozniak *et al.*, 2010). Thus, HCV assembly is a complex process that requires multiple interactions between the structural and non-structural proteins, which are apparently orchestrated at LD-associated ER-membrane structures.

In addition to viral factors, a number of host proteins have been implicated in HCV morphogenesis, for example the heat shock cognate protein 70 (HSC70), annexin A2 (ANXA2) and the diacylglycerol acyl transferase 1 (DGAT1) enzyme (Backes *et al.*, 2010; Herker *et al.*, 2010; Parent *et al.*, 2009). HSC70 was initially identified by mass spectrometric analysis as a host factor associated with HCVcc virions. HSC70 is thought to be required for an early step in infection given that HCVcc infection could be inhibited by anti-HSC70 antibodies (Parent *et al.*, 2009). Furthermore, silencing of HSC70 using siRNAs revealed that HSC70 is not required for viral RNA replication, but is important for production of infectious particles (Parent *et al.*, 2009). Proteome analysis of HCV replication

complexes identified ANXA2 as an associated host factor presumably involved in viral replication (Backes *et al.*, 2010). Although ANXA2 colocalized with viral non-structural proteins, silencing of the gene did not affect RNA replication. Instead, reduction of ANXA2 expression significantly impaired assembly of infectious virus (Backes *et al.*, 2010). Moreover, although no interaction between NS5A and ANXA2 was observed, these two proteins did colocalize, suggesting that NS5A was responsible for the recruitment of ANXA2 to HCV replication sites and together contribute to virion morphogenesis, by an unknown mechanism. DGAT1, which catalyzes the final step of triglyceride synthesis and is crucial for LD biogenesis, has been shown to interact with core protein (Herker *et al.*, 2010). This interaction appears to be essential for trafficking of core to LDs and disrupting this process by depletion of the DGAT1 gene inhibits virion assembly (Herker *et al.*, 2010).

Although core is essential for formation of HCV virions, the mechanism of how virus particles are assembled is still not fully understood. An important step in this process is the multimerization of core, presumably followed by capsid construction and packaging of the RNA genome into viral particles. Recently Kushima *et al* (2010) suggested that the nucleocapsid-like particle of HCV is composed of a disulfide-bonded core protein complex (Kushima *et al.*, 2010). Moreover, they identified that residue C128 is responsible for the formation of the disulfide bond between core monomers. Mutation of this residue led to loss of the disulfide-bonded core and consequently resulted in inhibition of HCV virus particle formation, indicating that disulfide-bonded core protein complex is required for the efficient virion assembly (Kushima *et al.*, 2010).

### VII. Virus release

It is suggested that the maturation and secretion of HCV particles is tightly linked to VLDL assembly. Initial observations were obtained from analysis of the composition of membrane vesicles containing HCV replication complexes (Huang *et al.*, 2007a). This study revealed that, in addition to the non-structural proteins involved in virus replication, these membranes were highly enriched in proteins involved in the VLDL secretion pathway (apoB, apoE and microsomal triglyceride transfer protein [MTP]) (Huang *et al.*, 2007a). Inhibition of MTP activity or silencing of apoB indicated that these factors which are involved in

the VLDL secretion pathway, also may facilitate the production of infectious HCV particles (Huang *et al.*, 2007a). Furthermore, drug inhibition studies on the maturation of high-density intracellular HCV particles to secreted particles revealed that blocking transport between ER and Golgi compartments, led to the degradation of intracellular high-density HCV particles in a post-ER compartment and in a non-proteasomal manner (Gastaminza *et al.*, 2008). In addition, these studies also demonstrated that inhibition of MTP activity and silencing of ApoB prevented the assembly of infectious particles at an early stage (Gastaminza *et al.*, 2008). Several reports have demonstrated that apoE also associates with HCVcc particles and down-regulation of apoE using siRNAs suppresses infectious virus production (Benga *et al.*, 2010; Chang *et al.*, 2007; Jiang & Luo, 2009). In addition, HCV infectivity was also impaired by anti-apoE antibodies, suggesting that HCV virions are assembled as apoE-enriched lipoprotein particles (Chang *et al.*, 2007). ApoE was found to interact with NS5A in HCV-infected cells, suggesting that apoE is required for an early step of virion assembly, and its recruitment by NS5A is important for viral assembly and release of infectious viral particles (Benga *et al.*, 2010; Cun *et al.*, 2010; Jiang & Luo, 2009). Compared to apoE, the importance of apoB and MTP activity in the assembly and secretion of infectious HCV is somewhat contradictory. Some studies demonstrated that siRNA-mediated depletion of apoB from infected cells resulted in inhibition of virus production, whereas treatment with MTP inhibitors reduced both HCV assembly and secretion (Gastaminza *et al.*, 2008; Huang *et al.*, 2007a). By contrast, other studies found that the levels of apoB and MTP activity had no influence on the assembly and release of HCVcc (Benga *et al.*, 2010; Chang *et al.*, 2007; Jiang & Luo, 2009). The exact reasons for these differences are still not fully understood. Nonetheless, the VLDL assembly pathway is required for release of HCV infectious virus and apoE is believed to be a critical component of this pathway.

## 1.5 Immune responses and HCV infection

The immune defences against invading pathogens are divided into two major arms: innate or non-specific immune responses and adaptive or specific immune responses. The innate immune system is the first line of defence and is composed of proteins (e.g. interferons) and cells (e.g. dendritic cells and natural killer cells). Although non-specific, innate immune responses have the advantage of being constitutively present and therefore, ready to mobilize following infection. The adaptive immune system acts as a secondary line of defence and is dependent on appropriate innate immune stimuli. This system is normally silent, but when activated is capable of mounting a targeted response to the infecting pathogens. The adaptive immune system is further divided into two types: humoral immunity, mediated by antibodies produced by B-cells and, cellular immunity, mediated by T-cells. The following sections present a brief overview of the immune responses during the course of HCV infection and describe some of the mechanisms used by the virus to evade such defences, which determine the outcome of infection.

### 1.5.1 Innate immune responses

#### 1.5.1.1 Interferons and HCV infection

More than 50 years ago, Lindenmann (1957) reported a phenomenon of viral interference to describe conditions which disrupted virus infectivity (Lindenmann *et al.*, 1957). In their work, they found that infection of chicken embryo cells with influenza virus, whether active or inactive, produced and released a new factor into the surrounding fluid. This new factor, termed interferon (IFN), interfered with virus growth and conferred resistance to infection in non-infected cells.

Since their discovery IFNs have been intensively studied, and now represent a large family of secreted proteins that exhibit strong antiviral activities and immunomodulatory properties. IFNs are classified, according to their cellular origin and to the types of receptors they bind, into three groups designated type I, II and III IFNs (Pestka *et al.*, 2004; Stark *et al.*, 1998). Type I IFNs in humans comprise 13 IFN$\alpha$ species and single species of IFN$\beta$, IFN$\kappa$, IFN$\varepsilon$ and IFN$\omega$ (Pestka *et al.*, 2004). All type I IFNs bind to the same IFN$\alpha/\beta$ receptor (IFNAR) which

consists of two subunits, IFNAR1 and IFNAR2 (Figure 1.11). The function of type I IFNs, in particular IFNα and β is well characterized and they are essential for mounting a robust host response against viral infection. Indeed, mice deficient in IFNAR demonstrate increased susceptibility to infection with several viruses when compared with wild-type mice (Muller *et al.*, 1994). In addition to their ability to inhibit viral infection, type I IFNs are also known to exert multiple immunoregulatory effects on NK and T cells (Gonzalez-Navajas *et al.*, 2012). Type II IFNs comprise a single member, IFNγ, which also exhibits antiviral activities. Contrary to type I IFNs, IFNγ is not produced by virus-infected cells, but is expressed at high levels by activated T cells and NK cells. IFNγ binds to its own receptor (IFNGR), which is composed of two subunits (IFNGR1/2) (Figure 1.11). The more recently described IFNs are type III IFNs and include three gene products IFNλ1, IFNλ2 and IFNλ3, also known as IL29, IL28A and IL28B, respectively (Kotenko *et al.*, 2003; Sheppard *et al.*, 2003). Similar to type I IFNs, these IFNs are induced upon viral infection and possess antiviral activities. Type III IFNs signal through the IFNλ receptor which is composed of IL-10R2 and IFNλR1 (Figure 1.11). Analysis of the crystal structure of type III IFNs, revealed that these IFNs are markedly different from type I or II IFNs and structurally related to members of the IL-10 family (Gad *et al.*, 2009).

### I. Induction of type I IFNs during viral infection

IFNα/β are produced by almost all cell types and are highly upregulated in response to viral infection. The signaling pathways that lead to the induction of these IFNs are dependent on the detection of viral signatures generated during infection [pathogen-associated molecular patterns (PAMPs)] by host-specialised receptors [pattern-recognition receptors (PRRs)]. In hepatocytes, three major classes of PRRs are recognised: 1) the Toll-like receptors (TLRs), that are mainly located in endosomes and the cell surface, and include TLR3, TLR7, TLR8 and TLR9; 2) the retinoic-acid-inducible gene I-like receptors (RLRs), that are located in the cytoplasm and include retinoic acid-inducible gene I (RIG-I), melanoma differentiation-associated gene 5 (MDA5) and laboratory of genetics and physiology 2 (LGP2), and 3) the nucleotide oligomerization domain [NOD]-like receptors (NLRs), that are also present in the cytoplasm (Thompson *et al.*, 2011). Among these PRRs, TLR3 and RIG-I can recognise HCV genome signatures

and mediate downstream signalling which results in IFNα/β production (Saito *et al.*, 2008b; Sumpter *et al.*, 2005; Wang *et al.*, 2009). TLR3 can recognise dsRNA and induce type I IFN expression in a manner that is dependent on "TIR-domain-containing adaptor protein inducing IFNβ" (TRIF). Although TLR3 has been suggested to sense HCV infection, the role of this PRR is less well characterised than RIG-I, since *in vitro* studies on HCV infection are dependent on Huh-7 cells that are deficient in TLR3 signalling (Li *et al.*, 2005a). However, activation of TLR3 signalling by HCV RNA has been demonstrated by ectopically expressed TLR3 (Wang *et al.*, 2009). Induction of type I IFNs through RIG-I signalling is initiated by recognition of viral 5'triphosphate RNA as well as the poly-uridine motif at the viral 3' UTR (Saito *et al.*, 2007; Saito *et al.*, 2008b). This binding leads to a conformational change of the sensor and results in interaction with IFNβ-promoter stimulator 1, IPS-1 (also called MAVS, Cardif or VISA), which mediates downstream signalling through recruitment of TBK1 and IKK1 kinases. Both TLR3 and RIG-I signalling pathways can then activate the transcription factors IRF-3/IRF-7 and NF-κB. After dimerization of IRF-3/IRF-7, these factors translocate into the nucleus, bind to the IFNα/β promoters and initiate transcription of the IFNα/β genes. Although viral infection is sensed in hepatocytes, HCV antagonises IFN production at multiple levels (Lau *et al.*, 2008; Loo *et al.*, 2006). The viral protease NS3/4A has been reported to target and cleave IPS-1, blocking downstream signalling of IFNβ (Bellecave *et al.*, 2010; Li *et al.*, 2005c; Meylan *et al.*, 2005). In addition, NS3/4A cleaves TRIF, which is essential for TLR3-dependent signalling (Li *et al.*, 2005b).

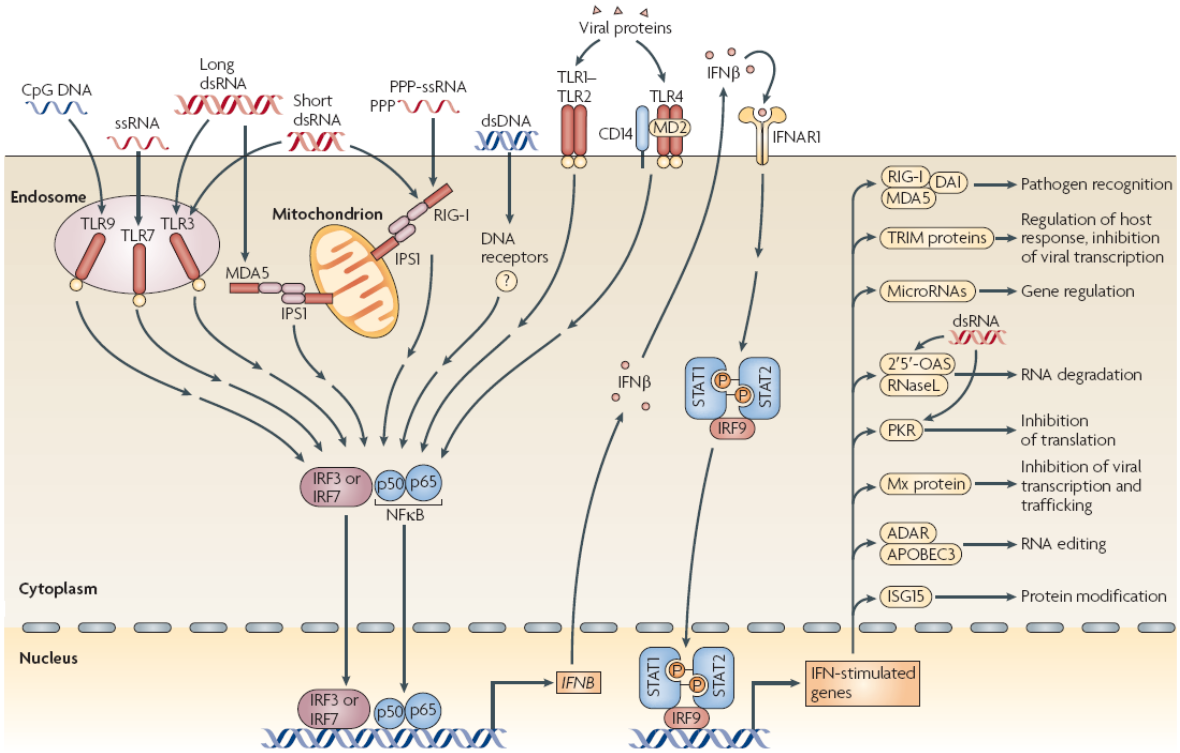


**Figure 1.10 - Activation of the interferon response triggered by the detection of viral pathogen-associated molecular patterns (PAMPs). All of the pattern-recognition receptors (PRRs) initiate signalling pathways that converge at the activation of the transcription factors interferon (IFN)-regulatory factor 3 (IRF3), IRF7 and/or nuclear factor-κB (NFκB); this leads to the expression of IFNβ. IFNβ then initiates an antiviral effector programme in the infected cell and neighbouring cells, which involves the expression of numerous IFN-stimulated genes (ISGs). Some of the ISGs, such as RIG-I (retinoic-acid-inducible gene I), MDA5 (melanoma differentiation-associated gene 5), DAI (DNA-dependent activator of IRFs), some microRNAs and the TRIM (tripartite motif-containing) family of proteins, are involved in the amplification and regulation of the IFN response. Other ISGs, such as 2′5′-oligoadenylate synthetase (OAS) and ribonuclease L (RNaseL), IFN-inducible dsRNA-dependent protein kinase (PKR), myxovirus resistance (Mx) protein, adenosine deaminase RNA-specific (ADAR) and apolipoprotein B mRNA-editing enzyme, catalytic polypeptide 3 (APOBEC3), are involved in antiviral mechanisms that interfere with the life cycle of individual viruses. IFNAR1, interferon-α receptor; IPS1, *IFNB*-promoter stimulator 1; ISG15, IFN-stimulated protein of 15 kDa; MD2, myeloid differentiation protein 2; PPP, 5′ triphosphate; ssRNA, single-stranded RNA; STAT, signal transducer and activator of transcription; TLR, Toll-like receptor. Extracted from Bowie & Unterholzner, 2008.**

## II. IFN signalling pathways and their targeting by HCV infection

IFN$\alpha/\beta$ signal through a common heterodimer receptor (IFNAR1 and IFNAR2) which is expressed in most tissues. The intracellular domains of these two receptors are associated with the Janus protein tyrosine kinases (Jak PTKs), Tyk2 and Jak1, respectively (Figure 1.11). Activation of Jak1 and Tyk2 kinases phosphorylates IFNARs and leads to the recruitment and phosphorylation of "signal transducers and activators of transcription" (STATs) family members. Activation of STAT heterodimers (STAT1 and STAT2) by IFN$\alpha/\beta$ mediates recruitment of the IFN-regulatory factor 9 (IRF9) to form the IFN-stimulated gene factor 3 (ISGF3) complex (STAT1-STAT2-IRF9). This complex translocates into the nucleus and binds to IFN-stimulated response elements (ISREs) located in gene promoters to activate the transcription of hundreds of ISGs (IFN-stimulated genes). Most of the type I ISGs encode proteins with antiviral activities, such as MxA guanosine triphosphatase, double-stranded RNA-activated protein kinase (PKR), 2'-5' oligoadenylate synthetase (2'-5'OAS), RNase L, inducible nitric oxide synthase (iNOS/NOS-2), indoleamine 2,3-dioxygenase (IDO), IFN-stimulated gene 15 (ISG15), GTPase Mx1 (myxovirus resistance 1), and others. Additionally, ISG products can mediate immunomodulatory, metabolic and proapoptotic actions that suppress virus infection and stimulate the adaptive immune response (Pasare & Medzhitov, 2004; Stetson & Medzhitov, 2006). During acute HCV infection, IFN$\beta$ is secreted by infected cells and leads to a strong induction of ISGs. Some of these gene products have been suggested to have direct anti-HCV activities, such as PKR, ISG56, ISG20, ADAR1 and viperin (Horner & Gale, 2009).

While NS3/4A is involved in blocking IFN induction by cleaving signalling molecules, other viral proteins have been reported to antagonize IFN signalling by targeting the Jak/STAT pathway and blocking the expression of ISGs (Bode *et al.*, 2007). In general, expression of HCV proteins seems to be associated with inhibition of STAT1 activities or degradation of STAT1 and disruption of ISG transcription (Blindenbacher *et al.*, 2003; Heim *et al.*, 1999; Lin *et al.*, 2005). Other studies have demonstrated that core protein in particular is capable of interferering with STAT1 activation or with its ability to interact with the ISGF3 complex (de Lucas *et al.*, 2005). However, the exact mechanism by which core

interferes with STAT1 activities is still not understood. Expression of core has also been associated with increased expression of "suppressor of cytokine signalling-3" (SOCS3) (Bode *et al.*, 2003). SOCS3 belongs to a family of proteins involved in negative regulation of Jak/STAT signalling. Induction of SOCS3 by core is thought to impair Jak-dependent activation of STATs and consequently antagonise IFN actions. HCV proteins have also been shown to directly antagonise expression or function of ISGs. Activation of the antiviral protein kinase PKR by dsRNA leads to the phosphorylation of the eukaryotic initiation factor 2$\alpha$ (eIF2$\alpha$). This PKR-mediated phosporylation mediates inhibition of translation, cellular proliferation and induces apoptosis in infected cells (Gil *et al.*, 2006). It has been suggested that HCV E2 and NS5A target activation and the downstream effects of PKR. Unglycosylated forms of E2 protein have been reported to interact with PKR and block PKR-mediated phosphorylation of eIF2$\alpha$, preventing IFN-induced shut-down of translation (Pavio *et al.*, 2002; Taylor *et al.*, 1999). In addition, NS5A also confers suppression of PKR activation. NS5A is thought to directly interact with PKR through the IFN sensitivity-determining region (ISDR) at the C-terminus of the protein (Gale *et al.*, 1997). Blocking PKR activity correlates with the degree of IFN-resistance in infected patients undergoing IFN-based treatment. However, this correlation in patients is apparently inconsistent and requires further *in vivo* validation.

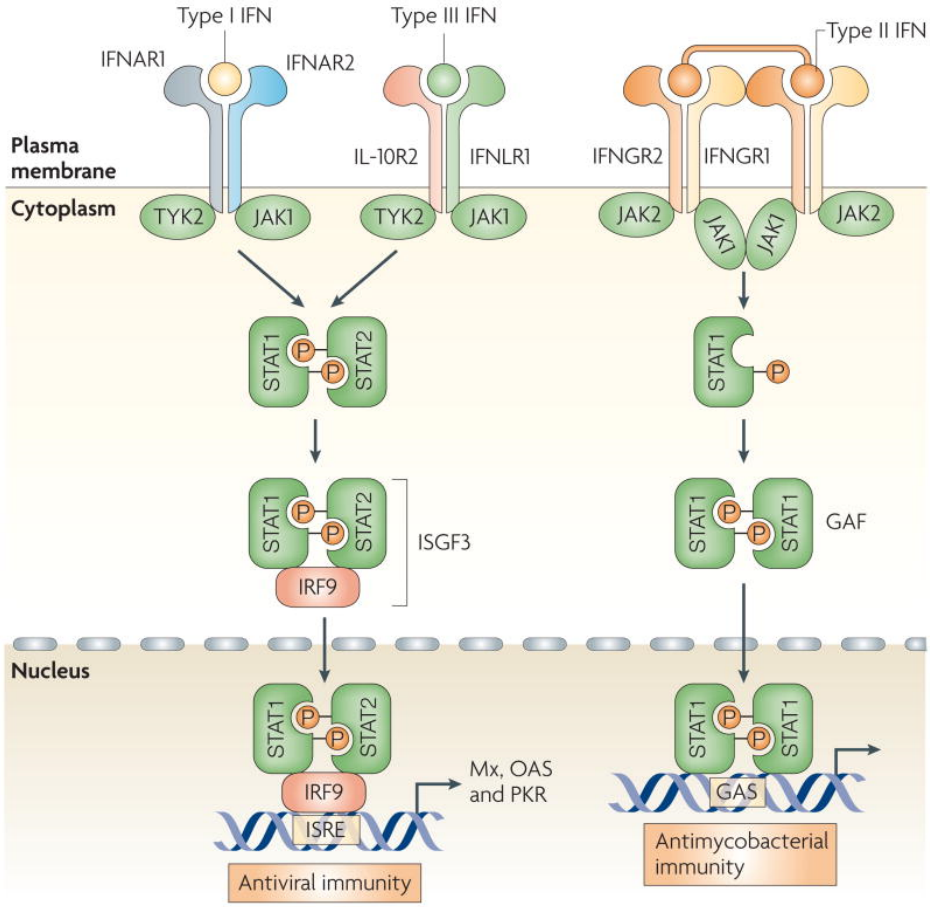


**Figure 1.11 - Interferon mediated signalling pathways. The action of the interferons is mediated through three receptor complexes. Type I IFNs bind to a heterodimer of IFNα receptor 1 (IFNAR1) and IFNAR2; IFNλ subtypes bind to the interleukin-10 receptor 2 (IL-10R2) and IFNLR1 (IFNλ receptor heterodimer 1); and a tetramer consisting of two IFNGR2 (IFNγ receptor 2) chains and two IFNGR1 chains recognises dimers of the type II IFNγ. Extracted from Sadler & Williams, 2008.**

### 1.5.1.2 Natural Killer (NK) cells and HCV infection

NK cells are unique lymphocytes of the innate immune system which are critical for controlling viral infection. They are enriched in human liver, have cytotoxic potential and can secrete several cytokines, such as tumour necrosis factor-α (TNFα) and IFNγ (Doherty *et al.*, 1999; Ferlazzo *et al.*, 2002). Additionally, NK cells can cross-talk with dendritic cells, which is essential for regulation of adaptive responses (Gerosa *et al.*, 2002). NK cells express surface binding proteins (killer cell immunoglobulin-like receptors or KIRs) that can bind to ligands on the surface of most cells. Activation of NK cells and their functions in controlling infection are regulated by both activating and inhibitory KIRs and their corresponding HLA ligands.

NK cells have been reported to play a role in innate immune responses during HCV infection (Cheent & Khakoo, 2011). However, the level of NK cell responsiveness is dependent on genetic factors and correlates with HCV clearance (Khakoo *et al.*, 2004). HCV is able to interfere with NK antiviral functions through E2 interaction with the CD81 receptor on NK cells. This interaction inhibits NK function and results in decreased IFNγ production (Crotta *et al.*, 2002; Tseng & Klimpel, 2002). However, in the context of infectious virions, efficient crosslinking of E2 with CD81 on NK cells has not been observed and *in vitro* exposure of NK cells to high concentrations of HCVcc did not impair their functions (Yoon *et al.*, 2009). More recently, Amadei *et al* (2010), also demonstrated that NK cells are activated during the acute phase of HCV infection and can more strongly produce IFNγ and exert cytotoxicity, than in uninfected controls (Amadei *et al.*, 2010).

### 1.5.1.3 Dendritic cells and HCV infection

Dendritic cells (DCs) are specialised, antigen-presenting cells of the innate immune system, that are able to link and regulate innate and adaptive immune systems. They are often regarded as sentinels that capture antigens on the periphery of different tissues. Processing of these antigens results in their presentation in the context of major histocompatibility complex molecules (MHC) to either T- or B-cells (Steinman, 2001). DCs comprise different forms and subsets, including plasmocytoid-DCs (pDCs) and myeloid-DCs (mDCs). DCs express

a variety of PRRs, such as TLRs, through which they sense and process viral antigens and become active (Creagh & O'Neill, 2006). Activation of mDCs leads to the production of interleukins -12 and -15 (IL-12 and IL-15), which can induce the expression of IFNγ in NK cells and promote CD4+ T-cell differentiation. By contrast, pDCs are important effectors of the innate responses to viral infections, as they are the major source of type I IFNs in the body and can produce large amounts of IFNα (Liu *et al.*, 2009a).

The frequency and number of DC subsets in the blood and their ability to produce IFNα is lower in patients infected with HCV, when compared with uninfected individuals (Longman *et al.*, 2005; Ulsenheimer *et al.*, 2005). By contrast, other studies have shown normal levels of IFNα expression by DCs in chronic HCV-infected patients (Decalf *et al.*, 2007). The reasons for the discrepancy in these correlations are still not clear. IL-12 secretion by mDCs has been shown to be defective in cells obtained from HCV-infected patients (Della Bella *et al.*, 2007; Dolganiuc *et al.*, 2006; Kanto *et al.*, 2004). Instead, these cells secrete enhanced levels of IL-10, which in turn results in suppression of IL-12 and IFNα production in mDCs. Suppression of cytokines results in defective activation and proliferation of T-cells, allowing HCV to persist. Moreover, *in vitro* studies using the HCVcc system demonstrated that increased IL-10 expression in infected DCs also resulted in loss of their ability to stimulate CD4+ or CD8+ T-cell responses (Saito *et al.*, 2008a).

### 1.5.2 Adaptive immune responses

Elimination of viruses requires, in the majority of cases, coordination of multiple immune mechanisms and activation of strong adaptive immunity. Contrary to innate responses, adaptive immune responses take several weeks to develop in infected patients. These responses are divided into two major arms, humoral immunity (mediated by antigen-specific B-cells) and cellular immunity (mediated by T-cells).

### 1.5.2.1 Cellular immunity

Cellular immune responses are mediated by helper or CD4+ T-cells and cytolytic or CD8+ T-cells. CD8+ cells are the main effector cells and eliminate viral infections through cytolytic (secretion of perforin and granzymes) and noncytolytic (secretion of cytokines such as IFN$\gamma$ and TNF$\alpha$) mechanisms. CD4+ or helper cells are so-called because their main function is to ensure optimal responses by other T-cells (such as CD8+ T-cells), B cells and other phagocytes to mount a strong response against infection (Swain *et al.*, 2011). Activation of T-cells is mediated through the recognition of virus-derived peptides, which are displayed by the major histocompatibility complexes I and II (MHC I and II; also known as HLA when referred to humans) on the surface of antigen presenting cells (Neefjes *et al.*, 2011). MHC I molecules are present in most cells and are recognised, along with the antigens they present, by CD8+ T-cells. MHC II molecules are mainly found in specialised cells, such as dendritic cells, macrophages and B cells, and are mainly recognised by CD4+ T-cells.

During acute HCV infection, T-cell-mediated responses are delayed and CD4+ and CD8+ T cells subsets only detected at 8-12 weeks after infection (Thimme *et al.*, 2002; Thimme *et al.*, 2001). However, these responses have been implicated in successful control of infection and clearance of virus. Immunisation of chimpanzees with viral proteins (non-structural proteins which are not normally targeted by neutralising antibodies) resulted in protection against infection (Folgori *et al.*, 2006). Additionally, animal studies showed that depletion of CD4+ or CD8+ T-cells resulted in prolonged or persistent infection upon challenging the animals with HCV (Grakoui *et al.*, 2003; Shoukry *et al.*, 2003).

CD8+ T-cell responses target multiple epitopes in all viral proteins (structural and non-structural) (Cooper *et al.*, 1999). Although the respective role of CD4+ and CD8+ subsets in viral clearance is not fully understood, cooperation between CD4+ and CD8+ T-cells is known to be required for clearance of infection. Several studies have suggested that self-limiting acute HCV infection is associated with strong and multispecific (8-12 epitopes) CD8+ T-cell responses (Gruner *et al.*, 2000; Lechner *et al.*, 2000). Similarly, strong and multispecific CD4+ T-cell responses is a major determinant for resolution of

infection. Moreover, HCV-specific CD4+ T-cells are important for the outcome of infection, as loss of CD4+ helper activity has been associated with poor CD8+ T-cell function (Kaplan *et al.*, 2007; Urbani *et al.*, 2006). Additionally, depletion of CD4+ T-cells from chimpanzees resulted in failure of CD8+ T-cell-mediated control of HCV infection (Grakoui *et al.*, 2003). By contrast, progression of HCV infection into a chronic stage is associated with either weak or mono-specific CD4+ or CD8+ T-cell responses (Missale *et al.*, 1996; Thimme *et al.*, 2001).

Despite the multispecificity of T cell-mediated responses, persistence of HCV infection and progression towards chronicity is common. Emergence of viruses with escape mutations has been proposed to be the main mechanism of evasion of CD4+ and CD8+ mediated responses (Petrovic *et al.*, 2012). For instance, animal studies have demonstrated that amino acid substitutions in HCV epitopes inhibited CD4+ and CD8+ T-cell recognition and escaped T-cell-mediated responses, whereas those with no substitutions, efficiently cleared infection (Erickson *et al.*, 2001; Meyer-Olson *et al.*, 2004).

#### 1.5.2.2 Humoral immunity

Humoral immune responses are activated by the recognition of viral antigens and are mediated by antibodies. Acute HCV infection is accompanied by the production of virus-specific antibodies. Similar to cellular immune responses, appearance of virus-specific antibodies is delayed in acute infection, notably 8 to 20 weeks after initiation of viral replication (Logvinoff *et al.*, 2004). Antibodies generated during infection can target all viral proteins, however the majority of antibodies with virus-neutralising activities are mapped against the viral envelope proteins (E1 and E2) (Choo *et al.*, 1994).

Although initial studies in chimpanzees demonstrated that serum from HCV-infected animals could neutralise virus infectivity *in vitro* and protect animals against challenge with HCV (Farci *et al.*, 1994), direct evidence supporting the involvement of antibody-mediated clearance of infection is sparse. Resolution of HCV infection has been observed in both chimpanzees and humans without seroconversion (Christie *et al.*, 1997; Cooper *et al.*, 1999; Post *et al.*, 2004). By contrast, in a single-source outbreak of HCV comprising young healthy females infected with the same HCV genotype, viral clearance was associated with rapid

induction of neutralizing antibodies in the early phase of infection (Pestka *et al.*, 2007). After resolution of infection, this antibody response was lost. Chronic HCV infection was accompanied by delayed induction of neutralizing antibodies and reduced or lack of capacity to neutralize the virus at early stages of infection (Pestka *et al.*, 2007). However, from this study there were no data on cellular responses and it was not clear whether the neutralizing antibodies had a central role in resolving infection or it was associated with strong cellular immune responses.

Despite the presence of neutralizing antibodies, persistent infection can be explained by several mechanisms, including the circulation of highly variable viral genomes (quasispecies) and continuous selection of escape variants, association of HCV glycoproteins with HDL proteins, direct cell-to-cell transfer of virus and glycosylation of E1/E2 proteins to shield neutralizing antibodies (Edwards *et al.*, 2012).

## 1.6 Interferon stimulated gene 15

The biological response of IFNs against viral infections involves the upregulation of hundreds of interferon-stimulated genes (ISGs). One of the most strongly induced genes upon type I IFN stimulation is ISG15. ISG15 was identified more than 30 years ago by Farrell et al, (1979) as a 15KDa protein induced following IFN stimulation of Ehrlich ascites tumour cells (Farrell *et al.*, 1979). In 1986, the first human sequence of ISG15 was cloned from IFN-treated Daudi cells (Blomstrom *et al.*, 1986). Further studies indicated that the full-length mRNA sequence encoded a polypeptide of 165 amino acids, generating a protein of about 18KDa (Reich *et al.*, 1987). In the same year, Haas et al reported the induction of a low molecular weight protein following IFN treatment of A549 and murine L929 cells (Haas *et al.*, 1987). They demonstrated that this protein reacted with antibodies against ubiquitin and named it ubiquitin cross-reactive protein (UCRP). Further analysis revealed, that the UCRP and ISG15 sequences were identical, thus identifying ISG15 as the first member of new family of ubiquitin-like proteins (Loeb & Haas, 1992).

### 1.6.1 ISG15, an ubiquitin-like protein

ISG15 is expressed as an inactive precursor protein of 165 aa in length. The maturation process of ISG15 is mediated by proteolytic cleavage of the 8 C-terminal amino acids (Potter *et al.*, 1999). This cleavage exposes a C-terminal LRLRGG motif which is conserved in the mature form of ubiquitin (ub) protein and other ubiquitin-like proteins (ubls), such as SUMO and NEDD8 (Haas *et al.*, 1987). As with other members of this family of proteins, ISG15 is capable of conjugating to other proteins through the C-terminal LRLRGG motif (Loeb & Haas, 1992). The structure of ISG15 consists of two ubiquitin-like domains, each of which exhibit approximately 30% homology with ub (Loeb & Haas, 1992) (Figure 1.12). The crystal structure of ISG15 was solved by Narasimhan *et al* (2005), and demonstrated that each domain folds into a β-grasp structure, with 5 β-sheets and 1 α-helix, connected by a 6 residue extended linker (hinge region) (Narasimhan *et al.*, 2005). Each ISG15 domain also shares a similar 3-dimensional structure with ub and two other ub-like modifiers, NEDD8 and SUMO (Narasimhan *et al.*, 2005). The two ISG15 domains, although essential for ISG15 conjugation, have different roles in this process. The N-terminal domain of ISG15 is required for the efficient E3 ligase-mediated transfer of ISG15 from the E2 enzyme UbCH8 to its substrates, but is dispensable for the activation and trans-thiolation steps (Chang *et al.*, 2008). On the other hand, the C-terminal domain of ISG15 is sufficient to link ISG15 to the E1 enzyme UbE1L and the E2 enzyme UbCH8 (Chang *et al.*, 2008).

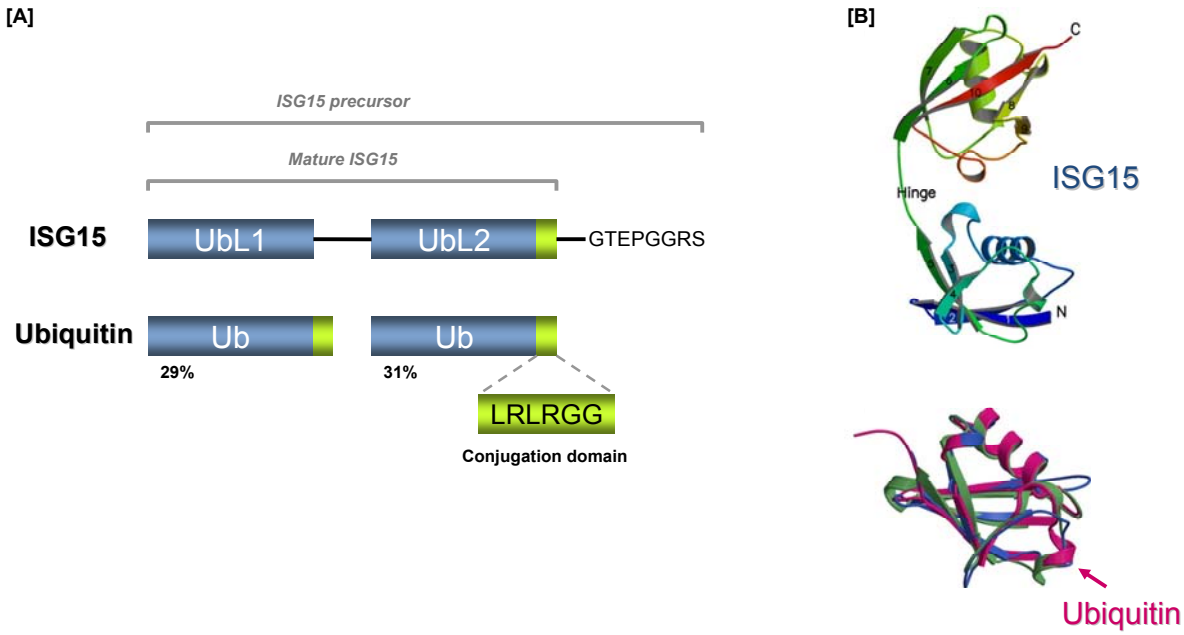


**Figure 1.12 – ISG15 structure. [A] ISG15 is expressed as a precursor protein (17KDa) which is further processed by specific proteases to yield the mature, 15KDa protein. ISG15 contains two ubiquitin-like (UBL) domains, each of which sharing 29% and 31% sequence homology with ubiquitin, respectively. The C-terminal UBL encodes the conserved di-Gly residues similar to ubiquitin and other ubiquitin-like proteins. [B] ISG15 secondary structure. Upper panel is represented a ribbon diagram of ISG15 showing two separate domains, with colour ramped from blue (N-terminus, N) to red (C-terminus, C) through green (Hinge). The two ubiquitin-like domains (each in β-grasp fold) are oriented differently and connected by a hinge. Lower panel shows an overlay of ribbon diagrams for ubiquitin (pink) with the N- (blue) and C-terminal (green) domains of ISG15 to emphasize the marked similarities in their respective β-grasp folds. Adapted from Narasimhan *et al* (2005).**

Similar to ubiquitination, ISG15 conjugation (ISGylation) is a 3-step process that requires a sequential action of multiple enzymes, involving activation, conjugation and ligation that are performed by E1, E2 and E3 enzymes respectively (Figure 1.13). The ISG15 activating enzyme is the Ub-activating E1-like protein UbE1L (also known as UbA7) (Yuan & Krug, 2001). Cells or mice lacking UbE1L fail to form ISG15 conjugates upon stimulation, indicating that UbE1L is required for ISGylation (Kim *et al.*, 2006; Malakhov *et al.*, 2003; Yuan & Krug, 2001). UbE1L charges ISG15 by forming a high-energy thiolester intermediate and then transfers ISG15 and the thiolester linkage to the subsequent E2 enzymes. The E2 conjugating enzymes involved in ISGylation are UbcH8 and UbcH6 (Kim *et al.*, 2004a; Takeuchi *et al.*, 2005; Zhao *et al.*, 2004). These enzymes also participate in Ub conjugation, indicating possible cross-talk between ISGylation and ubiquitination. E2 enzymes subsequently transfer ISG15

to specific E3 ligases, which in turn mediate the formation of an isopeptide bond between ISG15 and the ε-amino group of lysine residues of the target proteins. To date, three E3 ligases have been identified for ISG15: the HECT domain and RCC1-like domain containing protein 5 (HERC5) (Dastur *et al.*, 2006), the estrogen-responsive finger protein EFP (also known as TRIM25) (Zou & Zhang, 2006) and the human homolog of *Drosophila ariadne* (HHARI) (Okumura *et al.*, 2007). In contrast to EFP and HHARI, which target ISG15 to specific proteins (14-3-3σ and 4EHP proteins, respectively), HERC5 does not have strong substrate specificity and mediates conjugation of ISG15 to the majority of substrates. siRNA-mediated knockdown of HERC5 abrogated the majority of ISG15 conjugates, confirming its role as a major E3 ligase for ISG15 (Dastur *et al.*, 2006).

As with ub, ISG15 can be removed from conjugated proteins through the action of deconjugating or deubiquitination enzymes (DUBs). In the case of ub, multiple proteins have deconjugation activity, but with ISG15 only one protein, UBP43 (or USP18), possesses deconjugation activity *in vitro* (Malakhov et al., 2002). Other ubiquitin-specific DUBs have been suggested to possess de-ISGylation activities (e.g. USP2, USP5, USP13, and USP14), although with lower affinity than UBP43 (Catic *et al.*, 2007). The components of the ISGylation system identified so far, including UbE1L, UbcH6/8, HERC5, EFP and UBP43, are all inducible by IFN.

Given the role of ub in protein degradation, it was initially thought that ISG15 could influence protein turnover. In a study reported by Liu et al, (2003), treatment with proteasome inhibitors (MG132 or lactacystin) resulted in increased levels of ISG15 conjugates (Liu *et al.*, 2003). Using ATP-depleting agents in cells treated with proteasome inhibitors, they were able to show that the increase in ISG15 conjugates, but not ubiquitin conjugates, was dependent on the presence of ATP. Thus, the formation of ISG15 conjugates in the presence of proteasome inhibitors required *de novo* ISGylation, indicating that ISG15 does not mark proteins for degradation through the proteasome pathway (Liu *et al.*, 2003). Instead it is thought that ISG15 conjugation may alter subcellular localization, structure, stability or activity of target proteins (Yeh *et al.*, 2000).

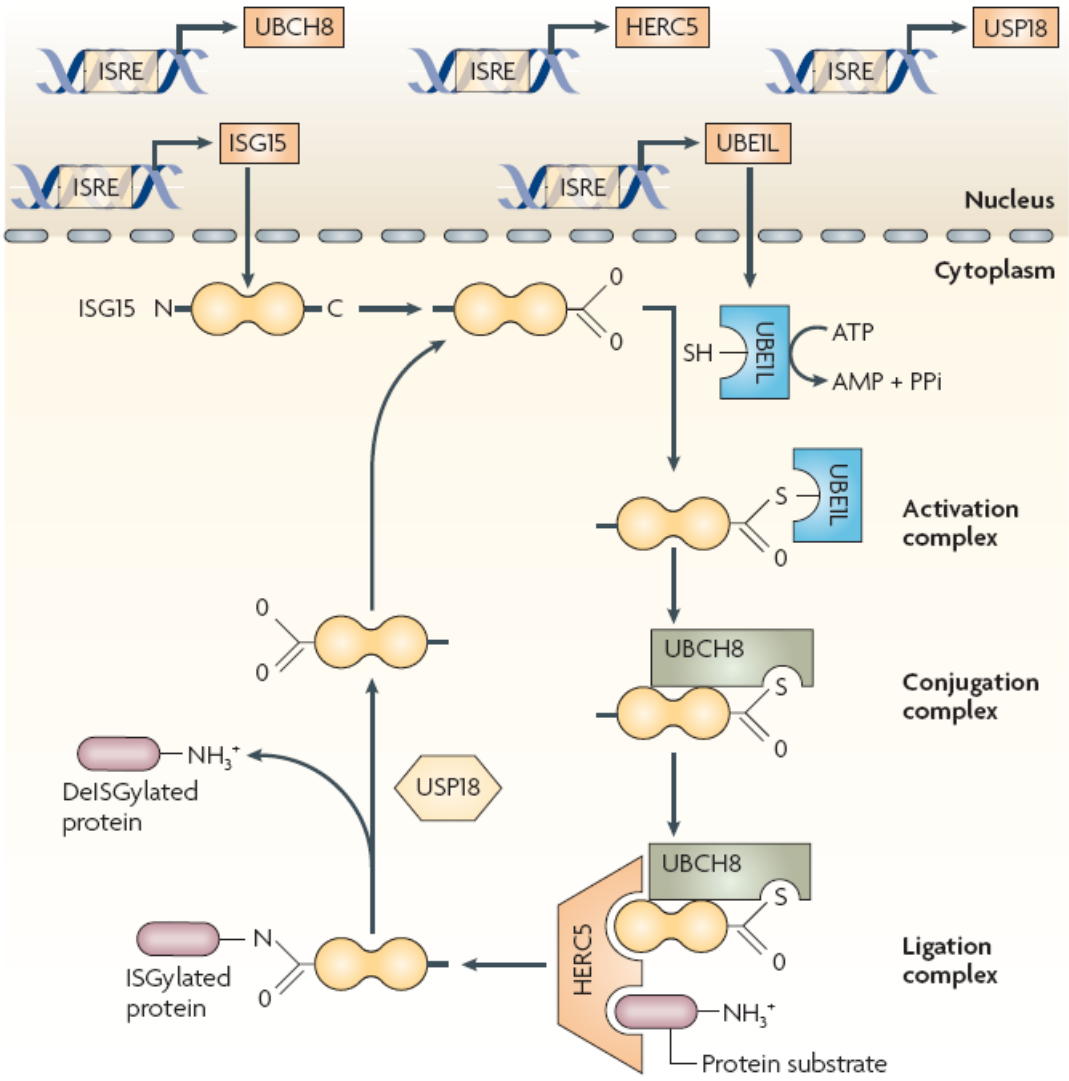


**Figure 1.13 – Conjugation of ISG15 to target proteins (ISGylation). The expression of ISG15, the E1-activating enzyme UBE1L, multiple E2-conjugating enzymes (e.g. UBCH8) and E3-ligase enzymes (e.g. HERC5) is coordinately induced by type I IFNs through IFN-stimulated response elements (ISREs). E1, E2 and E3 proteins sequentially catalyse the conjugation of ISG15 to numerous protein substrates to modulate pleiotropic cellular responses to inhibit virus production. ISGylation is reversibly regulated by ISG15 specific-proteases (USP18), which are also induced by IFNs. Extracted from Sadler & Williams, 2008.**

### 1.6.2 ISG15 gene expression

Induction of ISG15 expression is primarily triggered by type I IFNs. The ISG15 promoter region contains two IFN-stimulated response elements (ISREs), similar to all genes induced by type I interferons (Reich *et al.*, 1987). ISG15 expression is also triggered by different cell stress or stimuli, in particular those induced by viral or bacterial infections but also treatment with retinoic acid, campothecin and following irradiation. Some of these stresses activate transcription factors, such as IRF-3 and ISGF3, which can directly bind and activate the ISG15 promoter and upregulate expression of ISG15 (Mossman *et al.*, 2001; Nicholl *et al.*, 2000). Given that IRF-3 can activate ISG15 transcription, ISG15 can also be produced in an IFN-independent manner following activation of cytoplasmic sensors with dsRNA (Memet *et al.*, 1991). In addition, lipopolysccharide (LPS) has been demonstrated to strongly stimulate ISG15, via the IRF-3 or p38 MAP kinase and NF-kB activation pathways (Li *et al.*, 2001; Malakhova *et al.*, 2002; Manthey *et al.*, 1998).

The ISG15 promoter region contains also a PU.1 binding site. Therefore, ISG15 expression can also be induced by PU.1, a B- and myeloid-cell specific transcriptor factor, which overlaps with the ISG15 ISRE sequence (Meraro *et al.*, 2002). Shortening of telomere length also regulates ISG15 expression. Lou *et al* (2009) demonstrated that ISG15 expression, both mRNA and protein, is linked with telomere length and that expression increases with short telomeres (Lou *et al.*, 2009). However, the mechanisms by which this activation is regulated and its functional consequences are not well understood.

ISG15 and its conjugates are highly expressed in several tumor tissues and cell lines (Andersen *et al.*, 2006; Desai *et al.*, 2006). For example, ISG15 expression is increased in bladder cancers compared with normal bladder tissue, and this expression positively correlates with the degree of tumor progression (Andersen *et al.*, 2006). Interestingly, in breast cancer cell lines, the increased levels of ISG15 were found to be associated with decreased levels of polyubiquitinated proteins/degradation (Desai *et al.*, 2006). Silencing of ISG15 in these cells increased the levels of polyubiquitinated proteins, suggesting an antagonistic role of ISG15 in regulating ubiquitin-mediated protein degradation (Desai *et al.*, 2006).

## 1.6.3 Biological function of ISGylation

The identification of the protein targets for ISGylation is fundamental to elucidate the biological role of ISG15 protein modification. Using a combination of affinity purification and mass spectrometry, several groups have identified some of the target proteins for ISGylation (Giannakopoulos *et al.*, 2005; Malakhov *et al.*, 2003; Zhao *et al.*, 2005). A large number of those proteins function in diverse cellular pathways, including translation, glycolysis, cell motility, protein modification, intracellular protein trafficking, RNA splicing, chromatin remodelling, cytoskeletal organization, and stress responses (Giannakopoulos *et al.*, 2005; Malakhov *et al.*, 2003; Zhao *et al.*, 2005). Other ISG15-modified proteins are involved in type I IFN signalling pathways, such PKR, MxA, RIG-I, PLCγ1, JAK1, ERK1 and STAT1 (Malakhov *et al.*, 2003; Zhao *et al.*, 2005), suggesting a role of protein ISGylation in type I IFN-induced immune responses.

### 1.6.3.1 Regulation of immune responses by ISG15

Upon interferon treatment, ISG15 can be detected both in the free and conjugated forms. Several observations have indicated a role of ISG15 and ISGylation in regulating immune responses. For example, RIG-I was identified as a target protein for ISGylation (Kim *et al.*, 2008; Zhao *et al.*, 2005). ISGylation of RIG-I results in reduced levels of basal and virus-induced IFN production. In addition, cells lacking the ISG15 UbE1L enzyme showed higher levels of RIG-I protein than normal cells. Based on these observations, ISG15 conjugation of RIG-I is suggested to function as negative feedback loop which regulates RIG-I mediated signalling to maintain a balance between innate immune response and hypersensitivity during antiviral response. On the other hand, ISG15 can also positively regulate IFN signalling pathways through the ISGylation of IRF-3. ISGylation of this factor was shown to prevent its ubiquitination and degradation, indicating a positive feedback mechanism for the induction of the host antiviral response by ISGylation-dependent stabilization of IRF-3 (Lu *et al.*, 2006).

Additionally, free ISG15 is secreted from cells possibly to act as a cytokine or chemokine. This secreted form of ISG15 stimulates IFNγ production in cells expressing T-cell surface receptor-associated molecules, such as CD3, CD4, and CD8 (Recht *et al.*, 1991). Moreover, secreted ISG15 stimulates neutrophil recruitment, maturation of dendritic cells and differentiation and proliferation of NK cells (D'Cunha *et al.*, 1996a; Owhashi *et al.*, 2003).

#### 1.6.3.2 Antiviral activities of ISG15

The strong induction of ISG15 in response to IFN treatment or viral infection suggests a role for ISG15 in antiviral defence. Although initial studies in mice lacking ISG15 or UBE1L revealed no apparent defect in defence against vesicular stomatitis virus (VSV) and lymphocytic choriomeningitis virus (LCMV) (Kim *et al.*, 2006; Osiak *et al.*, 2005), a growing body of work strongly suggests a role for ISG15 in defence against other viral pathogens.

**I. Sindbis virus**

Evidence for the involvement of protein ISGylation in antiviral response came from studies using recombinant chimeric Sindbis virus systems. Mice lacking the IFNα/β receptor (IFNα/β $R^{-/-}$) abrogated the expression of ISG15 and ISG15 conjugates and were more susceptible to Sindbis virus infection, when compared to normal mice (Lenschow *et al.*, 2005). Moreover, this antiviral effect of ISG15 on virus infection was shown to be dependent on its ability to conjugate to target proteins. Overexpression of the ISG15-LRLRGG protein (i.e. the mature form of ISG15) attenuated viral infection in IFNα/β $R^{-/-}$ mice, whereas expression of a mutant (LRLRAA) ISG15 form abrogated the antiviral effect of the protein (Lenschow *et al.*, 2005). Later, the same group using ISG15 knockout mice, showed that the gene is important for resistance to not only Sindbis virus infection, but also to infections with influenza A and B viruses, herpes simplex virus 1 and murine gamma herpesvirus 68 (Lenschow *et al.*, 2007). Consistent with these observations, another group showed that mice lacking UbE1L are more susceptible to infection with Sindbis virus (Giannakopoulos *et al.*, 2009). In addition, mutation of a critical residue (Arg 151) for the interaction of ISG15 with UbE1L, abrogated the antiviral effect of ISG15 (Giannakopoulos *et al.*, 2009). Together, these studies suggest an

important role for protein ISGylation in antiviral defence against Sindbis virus infection and other viruses.

## II. Ebola virus and HIV-1

As with many viruses, type I IFNs can inhibit viral replication. Overexpression of ISG15 and the activating enzyme UbE1L, can mimic the IFN-mediated inhibition of human immunodeficiency virus 1 (HIV-1) assembly and release (Okumura *et al.*, 2006). Overexpression of ISG15 alone without UbEL1 was not inhibitory, indicating that ISG15 conjugation is required for its effects on HIV-1 release. Moreover, HIV-1 released from ISG15-expressing cells was rescued by expression of the ISG15 deconjugating enzyme, UBP43 (USP18) (Okumura *et al.*, 2006). In addition, expression of UbEL1 or UbEL1 and ISG15 inhibits the ubiquitination of HIV-1-encoded Gag polypeptide and the cellular factor Tsg101, which results in disruption of the Gag-Tsg101 interaction and consequently prevention of assembly and release of HIV-1 virions from infected cells (Okumura *et al.*, 2006). Furthermore, siRNA-mediated silencing of ISG15 during IFN treatment enabled HIV-1 release (Okumura *et al.*, 2006).

Similar to HIV-1, overexpression of ISG15 or UbE1L and UbcH8, also resulted in inhibition of budding of the Ebola virus VP40 virus-like particles (VLPs) (Okumura *et al.*, 2008). Efficient release of VP40 VLPs requires interactions with host proteins such as Tsg101 and Nedd4, an E3 ubiquitin ligase. IFN treatment or expression of ISG15 were shown to significantly inhibit the release of virus particles via the VP40 pathway (Malakhova & Zhang, 2008; Okumura *et al.*, 2008). ISG15 covalently bound to and negatively regulated Nedd4 Ub-E3 ligase activity (Malakhova & Zhang, 2008; Okumura *et al.*, 2008). This interaction between ISG15 and Nedd4 was shown to prevent ubiquitination of Ebola VP40 protein and subsequent VP40-mediated virus production from the cells (Malakhova & Zhang, 2008; Okumura *et al.*, 2008). Transfection of ISG15-specific siRNAs rescued budding of VP40 VLPs (Okumura *et al.*, 2008). Together, these observations confirmed a direct inhibitory role of ISG15 on Ebola VP40 VLP budding.

### III. Influenza viruses

As mentioned above ISG15 knock-out mice are more susceptible to infection by several viruses, including influenza A and B viruses (Lenschow *et al.*, 2007). Inhibition of UbE1L and UbcH8, the ISG15 E1 and E2 enzymes, in A549 cells resulted in inhibition of ISG15 conjugates, which significantly alleviated the IFN-induced antiviral activity against influenza A virus (Hsiang *et al.*, 2009). Distinct from its effects on late stages of HIV-1 and Ebola virus replication, the antiviral effect of ISG15 on influenza A was evident predominantly at early times of infection (Hsiang *et al.*, 2009). The antiviral mechanism of ISG15 against influenza A virus was suggested to result from its interaction and inhibition of one of the viral proteins, NS1 (Tang *et al.*, 2010; Zhao *et al.*, 2010).

Similar to these observations on influenza A virus, mice lacking the ISG15 UbE1L enzyme were more susceptible to influenza B virus infection, indicating that ISG15 antiviral activity to both influenza A and B viruses is mediated through its ability to form conjugates (Lai *et al.*, 2009). The NS1 protein from influenza B virus (NS1B) was shown to bind ISG15, and NS1B-ISG15 interaction resulted in inhibition of ISG15 conjugation activities and alleviation of viral replication (Yuan & Krug, 2001).

### IV. HCV

ISG15 has been proposed to have dual activities during HCV infection. Initial studies aimed at identifying predictors of host response to therapy revealed that expression of a subset of ISGs, including MxA, PKR, 2'5'-OAS, ISG15, and interleukin 8, were significantly upregulated in chronically infected HCV patients prior to starting therapy (MacQuillan *et al.*, 2003). In addition, patients who fail to respond to therapy have higher levels of ISG15 gene expression as well as other genes involved in the ISGylation system, such as UPB43 (USP18), when compared with liver tissue from patients who do respond (Randall *et al.*, 2006). *In vitro* studies demonstrated that siRNA-mediated silencing of USP18, which results in an increase in ISG15 conjugates, potentiated the ability of IFN to inhibit HCV RNA replication and virus production (Randall *et al.*, 2006). Consistent with this idea, Kim & Yoo (2010), demonstrated that expression of ISG15 and the ISG15 conjugation machinery resulted in inhibition

of HCV replication in cells harbouring a genotype 1b replicon (Kim & Yoo, 2010). In addition, they showed that ISG15 was able to conjugate to the wild-type, but not a mutant form of NS5A protein. These data suggested that the antiviral activity of ISG15 during HCV replication was mediated by ISGylation of the NS5A protein. Furthermore, cotransfection of ISG15 and ISG15 conjugation enzymes enhanced the IFN-mediated decrease of HCV replication (Kim & Yoo, 2010).

By contrast, other studies suggested a proviral activity of ISG15 during HCV replication (Chen *et al.*, 2010; Chua *et al.*, 2009). In these studies, depletion of ISG15 or UbE1L expression by siRNAs, followed by IFN$\alpha$ treatment resulted in a reduction in HCV RNA levels and virus production (Chen *et al.*, 2010; Chua *et al.*, 2009). Broering et al, (2010) also showed that siRNA silencing of ISG15 suppressed HCV replication in both murine and human cells harbouring a genotype 1b replicon (Broering *et al.*, 2010). Moreover, both silencing and over-expression of ISG15 significantly decreased and increased, respectively, HCV replication in infected Huh-7.5 cells. Silencing of ISG15 during IFN, Ribavirin or IFN/Ribavirin treatment enhanced their antiviral effects on HCV replication (Broering *et al.*, 2010). Together, these observations suggest that ISG15 is required for HCV replication and suppression of ISG15 expression results in decreased viral replication.

## 1.7 Aims

The aims of the project were divided into two lines of investigation. The first aim was to expand the existing *in vitro* model systems for studying HCV replication and infection. To that end, studies were initiated to explore the feasibility of developing a subgenomic replicon that included sequences from a HCV genotype 3a isolate (Glasgow-3 strain) and to expand analysis of viral RNA synthesis in an alternative permissive cell line. For the first approach, sequences in the highly efficient genotype 2a JFH1 subgenomic replicon were replaced with those from the Glasgow-3 strain. In the second approach, HepaRG cells, which are liver-derived cells that retain features of mature hepatocytes, were used to examine their ability to support viral RNA synthesis.

From a previous siRNA library screen, the interferon-stimulated gene ISG15 was identified as a modulator of HCV RNA replication. Hence, the second part of the project was to focus on determining the contribution of ISG15 to clearance of HCV. Two cells lines that support HCV replication, Huh-7 and U2OS cells, were employed to examine the role of ISG15 using both siRNA- and shRNA-mediated gene knockdown in SGR and HCVcc-infected cells. Finally, the mechanism through which ISG15 modulates HCV infection was analysed. In these studies, the importance of ISG15 conjugation to its antiviral activity was examined along with whether ISG15 affected the rates of synthesis or degradation of viral RNA during replication.

# 2 Material and Methods

## 2.1 Materials

### 2.1.1 Bacteria

| Cells | Source |
|---|---|
| XL10-Gold Ultracompetent | QuickChange Lightning Site-directed mutagenesis (Stratagene) |
| DH5$\alpha$ Chemical competent | NEB |

### 2.1.2 Cells

| Cells | Description | Source |
|---|---|---|
| Huh-7 | Human hepatoma cell line | Nakabayashi *et al*, 1982 |
| Huh-7.5 | Human hepatoma cell line | Blight *et al*, 2002 |
| HepaRG | Human hepatocyte cell line | Gripon *et al*, 2002 |
| U2OS | Human osteosarcoma cell line | American Type Culture Collection |
| Huh-7 (5-15) | Human hepatoma genotype 1b replicon cell line | Lohmann *et al*, 2003 |
| HEK-293T | Human Embryonic Kidney cell line | American Type Culture Collection |

### 2.1.3 Vectors

| Plasmid | Source |
|---|---|
| pGEM-T Easy | Promega |
| pCMV-FLAG-UbcH7 | Dr. Emilia Vanni (CVR) |
| pOTB7-ISG15 | Gene services |
| pLKO.dCMV.TetO.mcs | Prof. Roger Everett (CVR) |
| pLKOneo.CMV.EGFPnls.TetR | Prof. Roger Everett (CVR) |
| pLKO-shPML1 | Prof. Roger Everett (CVR) |

### 2.1.4 Clones

| Plasmid | Source |
|---|---|
| pSGR-JFH1 | Prof. Takaji Wakita (National Institute of Infectious Diseases, Japan) |
| pSGR-Blast-JFH1 | Dr. Arvind Patel (CVR) |
| pSGR-luc-JFH1 | Dr. John McLauchlan (CVR) |
| pSGR-neo-luc-JFH1 | Dr. John McLauchlan (CVR) |
| pJFH1 | Prof. Takaji Wakita (National Institute of Infectious Diseases, Japan) |
| pJ6-JFH1 (JC-1) | Dr. Arvind Patel (CVR) |

### 2.1.5 Cell culture growth media

Huh-7, Huh-7.5, U2OS and HEK-293T cell lines were cultured in Dulbecco's Modified Eagle Medium (DMEM, Invitrogen Life Technologies), supplemented with 10% foetal bovine serum (FBS), 100U/ml of penicillin and 100µg/ml of streptomycin.

HepaRG cells were cultured in William's E medium (WEM, Invitrogen Life Technologies), supplemented with 10% foetal bovine serum gold (PAA), 2mM L-glutamine, 100U/ml of penicillin, 100µg/ml of streptomycin, 5µg/ml of insulin and 0.5µM hydrocortisone.

### 2.1.6 Antisera

#### I. Primary Antibodies

| Antibody | Type | Dilution | | Source |
|---|---|---|---|---|
| | | IF | WB | |
| Anti-NS5A | Sheep polyclonal | 1:5000 | 1:1000 | Prof. Mark Harris (University of Leeds) |
| Anti-dsRNA | Mouse monoclonal | N/A | 1:200 | Scicons (Hungary) |
| Anti-ISG15 | Mouse monoclonal | N/A | 1:100 | Dr. Ernest Borden (Cleveland Clinic Foundation, Ohio) |
| Anti-ISG15 | Rabbit polyclonal | 1:50 | 1:50 | Santa Cruz |
| Anti-Phospho-Stat1 (Tyr701) | Rabbit monoclonal | N/A | 1:1000 | Cell Signalling |
| Anti-HERC5 | Rabbit polyclonal | N/A | 1:1000 | Enzo Life sciences |
| Anti-Actin | Mouse monoclonal | N/A | 1:1000 | Sigma |

#### II. Secondary Antibodies

| Antibody | Type | Dilution | | Source |
|---|---|---|---|---|
| | | IF | WB | |
| Anti-mouse IgG-HRP | Goat polyclonal | N/A | 1:2000 | Sigma |
| Anti-sheep IgG-HRP | Goat polyclonal | N/A | 1:2000 | Sigma |
| Anti-rabbit IgG-HRP | Goat polyclonal | N/A | 1:2000 | Sigma |
| Anti-rabbit-Alexa 488 | Donkey polyclonal | 1:2000 | N/A | Invitrogen Life Technologies |
| Anti-rabbit-Alexa- | Donkey | 1:2000 | N/A | Invitrogen Life |

| | | | | |
|---|---|---|---|---|
| 594 | polyclonal | | | Technologies |
| Anti-sheep-Alexa-488 | Donkey polyclonal | 1:2000 | N/A | Invitrogen Life Technologies |
| Anti-sheep-Alexa-594 | Donkey polyclonal | 1:2000 | N/A | Invitrogen Life Technologies |

### 2.1.7 Synthetic oligonucleotides

The oligonucleotides represented in the following table, used for PCR amplification, SDM (site-directed mutagenesis) or Seqn (sequencing) analysis, were ordered from Sigma.

| Oligo name | Use | Forward/ Reverse | Sequence (5'→3') |
|---|---|---|---|
| EcoRI-4B | PCR | Fwd | ACCGAATTCGCCTCTAGGGCGGC TCTCATC |
| 4B/5A-SacI | PCR | Rev | GGTGAGCTCCTGTCAAGATGGTG CAAACCC |
| 4B-M1 (SDM1) | SDM | Fwd | CCAGAGGAAACCACGTCTCCCCTA CTCACTACG |
| 4B-M1 (SDM1) | SDM | Rev | CGTAGTGAGTAGGGGAGACGTGG TTTCCTCTGG |
| 4B-M2 (SDM2) | SDM | Fwd | CCTACTCACTACGTGCCGGAGTC GGATGCG |
| 4B-M2 (SDM2) | SDM | Rev | CGCATCCGACTCCGGCACGTAGT GAGTAGG |
| 4B-M3 (SDM3) | SDM | Fwd | CGGAGTCGGATGCGGCGGCGCG TGTGACC |
| 4B-M3 (SDM3) | SDM | Rev | GGTCACACGCGCCGCCGCATCCG ACTCCG |
| 4B-M5 (SDM5) | SDM | Fwd | CGTGTGACCCAACTACTTAGCTCT CTTACTATAACC |
| 4B-M5 (SDM5) | SDM | Rev | GGTTATAGTAAGAGAGCTAAGTA GTTGGGTCACACG |
| 4B-M6 (SDM6) | SDM | Fwd | GCCTACTCAGAAGACTCCACCAAT GGATAACTGAGGACTGCCC |

| | | | |
|---|---|---|---|
| 4B-M6 (SDM6) | SDM | Rev | GGGCAGTCCTCAGTTATCCATTG GTGGAGTCTTCTGAGTAGGC |
| 4B-M7 (SDM7) | SDM | Fwd | CTCCACCAATGGATAAATGAGGA CTGCCCCATC |
| 4B-M7 (SDM7) | SDM | Rev | GATGGGGCAGTCCTCATTTATCC ATTGGTGGAG |
| 4B-M8 (SDM8) | SDM | Fwd | GGATAAATGAGGACTGCCCCTCC CCATGCTCCGGATCCTGGC |
| 4B-M8 (SDM8) | SDM | Rev | GCCAGGATCCGGAGCATGGGGAG GGGCAGTCCTCATTTATCC |
| 4B-M9 (SDM9) | SDM | Fwd | GCGGCGGCGCGTGTGACCGCACT ACTTAGCTCTCTTAC |
| 4B-M9 (SDM9) | SDM | Rev | GTAAGAGAGCTAAGTAGTGCGGT CACACGCGCCGCCGC |
| 4B-M10 (SDM10) | SDM | Fwd | CTACTTAGCTCTCTTACTGTAACC AGCCTACTCAGAAGAC |
| 4B-M10 (SDM10) | SDM | Rev | GTCTTCTGAGTAGGCTGGTTACA GTAAGAGAGCTAAGTAG |
| 4B-M11 (SDM11) | SDM | Fwd | CAATGGATAAATGAGGACTACCC CTCCCCATGCTCCGG |
| 4B-M11 (SDM11) | SDM | Rev | CCGGAGCATGGGGAGGGGTAGT CCTCATTTATCCATTG |
| 4B-M8 (SDM8) | SDM | Fwd | GGATAACTGAGGACTGCCCCTCC CCATGCTCCGGATCCTGGC |
| 4B-M8 (SDM8) | SDM | Rev | GCCAGGATCCGGAGCATGGGGAG GGGCAGTCCTCAGTTATCC |
| 4B-M8 & M11 (only) | SDM | Fwd | AATTGGATAACTGAGGACTACCC CTCCCCATGCTCCGG |
| 4B-M8 & M11 (only) | SMD | Rev | CCGGAGCATGGGGAGGGGTAGT CCTCAGTTATCCAATT |
| 4B-M11/∆8 | SDM | Fwd | CAATGGATAAATGAGGACTACCC CATCCCATGCTCCGG |
| 4B-M11/∆8 | SDM | Rev | CCGGAGCATGGGATGGGGTAGTC CTCATTTATCCATTG |
| PmeI/NcoI-NS3 | PCR | Fwd | GTTTAAACCATGGCTCCGATCACA GCATAC |

| | | | |
|---|---|---|---|
| NS3-SanDI | PCR | Rev | GGGACCCAGTTGGAGCATGCAAG TAC |
| NS3_Mut/NcoI | SDM | Fwd | GTTATGTGGACTGTCTATCATGG TGCAGGCTCAAG |
| NS3_Mut/NcoI | SDM | Rev | CTTGAGCCTGCACCATGATAGAC AGTCCACATAAC |
| ISG15_HindIII | PCR | Fwd | ACCAAGCTTATGGGCTGGGACCT GAC |
| ISG15/WT_XbaI/BamHI | PCR | Rev | GGTGGATCCTCTAGATTAGCCTC CCCGCAGGCGCAG |
| ISG15/dN_XbaI/BamHI | PCR | Rev | GGTGGATCCTCTAGATTAGGCTG CCCGCAGGCGCAG |
| Kozak-Flag | PCR | Fwd | AAAAAGCTAGCTCTACCATGGACT ACAAAGACG |
| ISG15-seqn | Seqn | Fwd | TGAAGCAGCAAGTGAGCGGG |
| ISG15_His-HindIII1 | PCR | Fwd | CACCATCACCACAAGCTTATGGGC TGGGACCTGACG |
| ISG15_NheI-Kozak-His2 | PCR | Fwd | ACCGCTAGCTCTACCATGCATCAT CACCATCACCAC |
| HCV JFH1 probe | qPCR | probe | AAAGGCCTTGTGGTACTG |
| JFH1 qPCR Fwd | qPCR | Fwd | TCTGCGGAACCGGTGAGTAC |
| JFH1 qPCR Rev | qPCR | Rev | GCACTCGCAAGCGCCCTATC |

### 2.1.8 siRNAs and shRNAs

Scrambled negative control (siCtrl), human ISG15 (siISG15) and human HERC5 (siHERC5) siRNAs were supplied by Ambion (Applied Biosystems). 1nM of each siRNA was supplied by the manufacturer and resuspended in $dH_2O$ to yield a stock concentration of 100µM (siCtrl) or 50µM (ISG15 and HERC5 siRNAs). Each cellular gene was targeted by 3 siRNAs directed against different regions of the mRNA sequence.

The designed shRNAs targeting different regions of the ISG15 mRNA were ordered from Sigma. The respective shRNA control was provided by Prof. Roger Everett.

| Name | Sequence |
|---|---|
| siRNA Negative Control (siCtrl) | Supplied by Applied Biosystems |
| ISG15 siRNA 1 | Supplied by Applied Biosystems |
| ISG15 siRNA 2 | Supplied by Applied Biosystems |
| ISG15 siRNA 3 | Supplied by Applied Biosystems |
| HERC5 siRNA 1 | Supplied by Applied Biosystems |
| HERC5 siRNA 2 | Supplied by Applied Biosystems |
| HERC5 siRNA 3 | Supplied by Applied Biosystems |
| ISG15 shRNA 1 (sh1) | gatccGCGCAGATCACCCAGAAGATTCAAGAGATCTTCTGGGTGATCTGCGCTTTTTTACGCGTg (5'→3')<br>gCGCGTCTAGTGGGTCTTCTAAGTTCTCTAGAAGACCCACTAGACGCGAAAAAATGCGCActtaa (3'→5') |
| ISG15 shRNA 2 (sh2) | gatccGGCGCAGATCACCCAGAAGTTCAAGAGACTTCTGGGTGATCTGCGCCTTTTTTACGCGTg (5'→3')<br>gCCGCGTCTAGTGGGTCTTCAAGTTCTCTGAAGACCCACTAGACGCGGAAAAAATGCGCActtaa (3'→5') |
| ISG15 shRNA 3 (sh3) | gatccGCGACGAACCTCTGAACATTTCAAGAGAATGTTCAGAGGTTCGTCGCTTTTTTACGCGTg (5'→3')<br>gCGCTGCTTGGAGACTTGTAAAGTTCTCTTACAAGTCTCCAAGCAGCGAAAAAATGCGCActtaa (3'→5') |
| ISG15 shRNA 4 (sh4) | gatccGAACATCCTGGTGAGGAATTTCAAGAGAATTCCTCACCAGGATGTTCTTTTTTACGCGTg (5'→3')<br>gCTTGTAGGACCACTCCTTAAAGTTCTCTTAAGGAGTGGTCCTACAAGAAAAAATGCGCActtaa (3'→5') |
| ISG15 shRNA 5 (sh5) | gatccGCGGGCTGGAGGGTGTGCATTCAAGAGATGCACACCCTCCAGCCCGCTTTTTTACGCGTg (5'→3')<br>gCGCCCGACCTCCCACACGTAAGTTCTCTACGTGTGGGAGGTCGGGCGAAAAAATGCGCActtaa (3'→5') |
| ISG15 shRNA 6 (sh6) | gatccGCACCGTGTTCATGAATCTTTCAAGAGAAGATTCATGAACACGGTGCTTTTTTACGCGTg (5'→3')<br>gCGTGGCACAAGTACTTAGAAAGTTCTCTTCTAAGTACTTGTGCCACGAAAAAATGCGCActtaa (3'→5') |
| Ctrl shRNA (shCtrl) | accgTTATCGCGCATATCACGCGTTCAAGAGACGCGTGATATGCGCGATAACTTTTTc (5'→3') |

### 2.1.9 Kits

| Kit | Source |
|---|---|
| KOD Hot Start DNA Polymerase kit | Novagen |
| TaqMan Reverse Transcription reagents | Applied Biosystems |
| QuickChange Lightning Site-directed mutagenesis kit | Stratagene |
| T7 RiboMax Express Large Scale RNA production system | Promega |
| PureLink HiPure plasmid Midi prep kit | Invitrogen Life Technologies |
| QIAquick gel extraction kit | Qiagen |
| RNeasy Mini Kit | Qiagen |
| RNeasy Midi Kit | Qiagen |
| RNeasy MinElute Cleanup Kit | Qiagen |
| uMACS Streptavidin Kit | Miltenyi Biotech |
| MaXtract 2ml Phase Lock High-density tubes | Qiagen |
| Luciferase assay system | Promega |
| Enhanced Chemiluminescence Plus Western Blotting Detection system | Amersham Biosciences |

### 2.1.10 Transfection reagents

| Reagent | Source |
|---|---|
| Opti-MEM I | Gibco |
| Lipofectamine RNAiMAX | Invitrogen Life Technologies |
| Lipofectamine 2000 | Invitrogen Life Technologies |
| PLUS reagent | Invitrogen Life Technologies |
| Polybrene | Sigma |

### 2.1.11 Interferons and related reagents

| Reagent | Description | Source |
|---|---|---|
| hIFNα | α-Interferon, Human, recombinant, *E.coli* | Merck |
| hIFNβ | β-Interferon, Human, recombinant, CHO cells | Calbiochem |
| hIFNγ | Interferon-γ, Human, recombinant, *E.coli* | Roche |
| Poly-I:C | - | Invivogen |

### 2.1.12 Commonly used chemical

| Chemical | Abbreviation | Source |
|---|---|---|
| 2-Mercaptoethanol | β-ME | Sigma |
| 37.5:1 acrylamide/bis solution | - | Bio-RAD |
| 4',6-diamidino-2-phenylindole | DAPI | Promega |
| Agarose | - | Melford |
| Ammonium persulphate | APS | Bio-RAD |
| Ampicillin | Amp | Melford |
| Bromophenol blue | BPB | BDH |
| Chloroform | - | Sigma |
| Ethanol | EtOH | Fisher Scientific |
| Ethidium Bromide | EtBr | Sigma |
| Glucose | - | BDH |
| Glycine | - | BDH |
| Methanol | MeOH | BDH |
| N,N,N',N'-Tetramethylethylene-diamine | TEMED | Sigma |
| Neomycin phosphotransferase | G418 | Melford |
| Phenol | - | Sigma |
| Propan-2-ol | - | BDH |
| Sodium chloride | NaCl | BDH/ ABI |

| | | |
|---|---|---|
| Sodium dodecyl sulphate | SDS | BDH |
| Sodium hydroxide | NaOH | BDH |
| Sucrose | - | BDH |
| Tween 20 | - | Sigma |
| N,N-Dimethylformamide | DMF | Sigma |
| EZ-link Biotin-HPDP | - | Pierce |
| Chloroform/Isoamylalcohol(24:1) | - | Fluka |
| Tris-EDTA | TE | Sigma |
| Tris NaCl EDTA buffer solution | STE | Fluka |
| Dithiothreitol | DTT | BioUltra |

## 2.1.13 Composition of buffers and solutions

### 2.1.13.1 Bacteria growth media

| Solution | Composition |
|---|---|
| Luria-Bertani (LB) - broth | 170mM NaCl, 10g/l Bactopeptone, 5g/l yeast extract |
| 2YT-Broth (Yeast tryptose Broth) | 85mM NaCl, 16g/l Bactopeptone, 10g/l yeast extract |
| LB-agar | LB-broth plus 1.5% (w/v) agar |

### 2.1.13.2 Tissue culture

| Solution | Composition |
|---|---|
| Trypsin | 0.25% (w/v) Difco trypsin dissolved in PBS(A), 0.0005% (w/v) phenol red |
| Versene | 0.6mM EDTA in PBS(A), 0.002% (w/v) phenol red |
| PBS(A) | 170mM NaCl, 3.4mM KCl, 10mM $Na_2HPO_4$, 1.8mM $KH_2PO_4$, Tris-HCl (pH 7.2) |

### 2.1.13.3 DNA manipulation and luciferase assay buffers

| Solution | Composition |
|---|---|
| Gel loading buffer | 5x TBE, 50% sucrose, 1 µg/ml BPB |
| TBE (10x) | 0.9M Tris-HCl, 0.9M boric acid, 0.02M EDTA |
| Equilibration buffer (EQ1) | 0.1M sodium acetate (pH 5.0), 0.6M NaCl, 0.15% (v/v) Triton X-100 |
| Resuspension buffer (R3) | 50mM Tris-HCl (pH 8.0), 10mM EDTA, 100µg/ml RNase A |
| Lysis buffer (L7) | 0.2M NaOH, 1% (w/v) SDS |
| Precipitation buffer (N3) | 3.1M potassium acetate (pH 5.5) |
| Wash buffer (W8) | 0.1M sodium acetate (pH 5.0), 825mM NaCl |
| Elution buffer (E4) | 100mM Tris-HCl (pH 8.5), 1.25M NaCl |
| Luciferase lysis buffer | 25mM Tris-phosphate (pH 7.8), 2mM DTT, 2mM 1,2-diaminocyclohexane-N,N,N',N'-tetraacetic acid, 10% glycerol, 1% Triton X-100 |

### 2.1.13.4 SDS-PAGE and Western Blot analysis

| Solution | Composition |
|---|---|
| Sample loading buffer | 31% stacking gel buffer, 31% glycerol, 21% SDS (25%), 9% 2-mercaptoethanol, 1µg/ml BPB, 8% $H_2O$ |
| Gel running buffer | 25mM Tris-HCl, 200mM glycine, 0.1% (w/v) SDS |
| Resolving buffer | 1.5M Tris-HCl (pH 8.9), 0.4% SDS |
| Stacking buffer | 0.5M Tris-HCl (pH 6.8), 0.4% SDS |
| Towbin buffer | 25mM Tris-HCl (pH 8.0), 200mM glycine, 20% (v/v) methanol |
| PBS(A) | 170mM NaCl, 3.4mM KCl, 10mM $Na_2HPO_4$, 1.8mM $KH_2PO_4$, Tris-HCl (pH 7.2) |
| PBS-T | PBS(A) plus 0,05% (v/v) Tween 20 |
| Blocking buffer | 5% (w/v) Marvel milk in PBS-T |

# 2.2 Methods

## 2.2.1 Bacteria cultures

Depending on the application, different strains of *E. coli* were used. Once transformed, the bacteria were recovered in 2YT-broth media and then grown in LB agar plates or in LB-broth medium, supplemented with appropriate antibiotics (100µg/ml Amp or 25µg/ml Chloramphenicol). The LB-agar was poured into 90mm dishes and allowed to set at room temperature. The bacterial cultures were plated onto the LB-agar plates using a glass spreader, inverted and incubated at 30°C or 37°C for approximately 20 or 16h, respectively.

For growing bacteria cultures from LB-agar plates to minipreps (Section 2.2.2.9) or midipreps (Section 2.2.2.10), single colonies were picked using a pipette tip and used to inoculate 2ml (minipreps) or 150-500ml LB-broth medium (midipreps), supplemented with appropriate antibiotics. The cultures were incubated with rotation (180rpm) at 30°C or 37°C.

To ensure that a single bacterial colony was expanded from miniprep to midiprep culture, the streak plate procedure was used. Briefly, bacteria were picked from the miniprep culture using a sterile wire loop and spread over the surface of a fresh LB-agar plate (supplemented with appropriate antibiotic). The agar plates were incubated as before and single colonies grown into midiprep cultures.

## 2.2.2 Manipulation of DNA

### 2.2.2.1 Polymerase Chain Reaction (PCR)

For amplification of viral or human gene (ISG15) cDNAs, the KOD Hot Start DNA Polymerase PCR kit (Novagen) was used. The product of these reactions was utilised for cloning into appropriate vectors and site-directed mutagenesis (Section 2.2.2.2). The reactions were performed in a ThermoHybaid PX2 Thermal Cycler as follows:

**Reaction components**

| Components | Volume (µl) |
|---|---|
| 10x KOD buffer | 5 |
| Template DNA | 1 |
| Fwd primer (10uM) | 1 |
| Rev primer (10uM) | 1 |
| dNTPs (2mM) | 5 |
| $MgSO_4$ | 2 |
| KOD polymerase | 1 |
| $dH_2O$ | 34 |

**Cycling conditions (viral cDNAs)**

| Stage | Temperature | Time | Number of cycles |
|---|---|---|---|
| Initial denaturation | 94˚C | 2min | 1 |
| Denaturation | 94˚C | 15sec | 30 |
| Primer annealing | 63˚C | 30seconds | |
| Extension* | 72˚C | 20sec | |
| Hold | 4˚C | ∞ | 1 |

**typically, 1minute/Kbp*

**Cycling conditions (ISG15 cDNA)**

| Stage | Temperature | Time | Number of cycles |
|---|---|---|---|
| Initial denaturation | 94˚C | 2min | 1 |
| Denaturation | 94˚C | 20sec | 30 |
| Primer annealing | 63˚C | 30sec | |
| Extension* | 72˚C | 1 or 2min | |
| Hold | 4˚C | ∞ | 1 |

**typically, 1minute/Kbp*

Products of the entire PCR reaction were separated by agarose gel electrophoresis (Section 2.2.2.11-I) and the band of interest was purified by QIAquick spin column methodology (Section 2.2.2.11-II).

### 2.2.2.2 Site-directed mutagenesis

Mutagenesis reactions were performed using the QuikChange® Lightning Site-Directed Mutagenesis kit (Stratagene). Forward and reverse primers for mutagenesis (Section 2.1.7) were designed to incorporate the desired mutation(s) in the middle of the primer sequence and were between 25 and 45 bases in length. PCR reactions were performed in a ThermoHybaid PX2 Thermal Cycler as follows:

**Reaction components**

| Components | Volume (µl) |
|---|---|
| 10x reaction buffer | 5 |
| dsDNA template | 1 |
| Fwd primer (125ng) | 1 |
| Rev primer (125ng) | 1 |
| dNTP mix | 1 |
| QuickSolution reagent | 1.5 |
| QuickChange Lightning Enzyme | 1 |
| $dH_2O$ | 38.5 |

**Cycling conditions**

| Stage | Temperature | Time | Number of cycles |
|---|---|---|---|
| Initial denaturation | 95°C | 2min | 1 |
| Denaturation | 95°C | 1min | 18 |
| Primer annealing | 60°C | 30sec | |
| Extension | 68°C | 5min | |

| | | | |
|---|---|---|---|
| Final extension | 68°C | 5min | 1 |
| Hold | 4°C | ∞ | 1 |

Following PCR, 10U of *Dpn*I was added to digest the non-mutated dam-methylated parental DNA. The reactions were mixed by pipetting, centrifuged at 8000g for 15sec, followed by incubation at 37ºC for 1h. *Dpn*I-treated DNA was then transformed into 50µl XL10-Gold Ultracompetent cells (Section 2.2.2.8).

#### 2.2.2.3 Cloning of PCR products

**I. pGEM-T Easy cloning system (Promega)**

Amplification of DNA using a non-proofreading polymerase such as *Taq* DNA polymerase (which lacks 3'→5' exonuclease activity) yields products that contain a single 3' terminal nucleotide overhang (commonly an A residue). The T-vectors, such as pGEM-T Easy vector, contain a complementary 3' single T overhang and are used for cloning of products with A-residue overhangs.

**II. dA tailling**

PCR products generated from proofreading DNA polymerases such as KOD polymerase have blunt ends and usually have to be introduced into blunt-ended vectors. For cloning of such blunt-ended PCR fragments into T-vectors it is necessary to introduce A overhangs at the 3' end termini. To that end, 2µl of 10x Taq buffer, 2µl of 2mM dATP and 1µl of Taq polymerase were added to the PCR product (15µl final volume). The reaction was incubated at 70°C for 20min, followed by purification of the PCR product by QIAquick spin column methodology (Section 2.2.2.11-II).

**III. Ligation reactions**

In a standard ligation reaction, DNA vectors (usually pGEM-T Easy vector) and purified PCR product were combined at 1:3 molar ratio. Typically, 1µl of pGEM-T Easy vector, 3µl of DNA fragment, 5µl of 2x ligase buffer were mixed with 1U T4 DNA ligase and water added to a final volume of 10µl. The ligation

mix was mixed briefly and incubated overnight at 4ºC. The ligated DNA was then used for transforming bacteria (Section 2.2.2.7).

#### 2.2.2.4 Restriction enzyme digestion

Restriction digestions were prepared by adding 10U enzyme per 0.5-1µg of DNA and using the appropriate buffer (according to the supplier specifications, NEB or Roche). All the reactions were performed at 37ºC (unless otherwise specified) for 2h. Following the restriction reaction, DNA was purified by QIAquick spin column methodology (Section 2.2.2.11-II).

#### 2.2.2.5 Dephosphorylation of linearised plasmid DNA

In a ligation reaction, the DNA ligase catalysis the formation of phosphodiester bonds between the 5' phosphate and the 3'- hydroxyl groups. To prevent recirculation of digested DNA vector, the 5' phosphate is usually removed from the vector using calf intestinal phosphatase (CIP). Following restriction digestion of DNA vectors, 4U of CIP was added and the mixture was incubated for 30min at 37ºC. The digested DNA was then purified using QIAquick spin column methodology (Section 2.2.2.11-II).

#### 2.2.2.6 Mung Bean nuclease treatment

Prior to *in vitro* transcription (Section 2.2.3.1) of viral RNAs, the SGR or full-length HCV cDNA plasmids were linearised using *Xba*I endonuclease. Restriction enzymes like *Xba*I produce 3' end overhangs, which have been reported to interfere with the T7 and SP6 mediated transcription (Schenborn & Mierendorf, 1985). DNA templates containing 3' end overhangs were shown to synthesised extraneous RNA transcripts, which were complementary to the expected RNA transcripts. This is thought to be caused by self-annealing of the 3' overhang end of the DNA template and consequently lead the initiation of transcription by T7 or SP6 polymerases at additional sites other than the promoter region. Thus to avoid this synthesis of extraneous RNA transcripts, the ends of the linearised plasmid were removed prior to transcription. Therefore, after phenol/chloroform purification and ethanol precipitation of linearised DNA (Section 2.2.2.11-III & IV), the DNA was treated with 2U of Mung Bean Nuclease (Promega) in 1x reaction buffer for 30min at 30ºC.

#### 2.2.2.7 Transformation of competent DH5α cells

Competent *E. coli* DH5α cells were used for cloning plasmid DNA or ligation reactions. Typically, 1µg of plasmid DNA, or 7-15µl of ligation reaction were used per transformation reaction (50µl of bacteria). The DNA was added to pre-chilled bacteria (30min on ice) and then heat-pulsed at 42°C for 2min. Subsequently, the transformation mix was immediately placed on ice for 1min and then transferred into 300µl 2YT-broth media (pre-heated at 37°C). The cells were incubated at 37°C with rotation (180rpm) for 45min and then plated on LB-agar plates, supplemented with appropriate antibiotic. The plates were inverted and incubated at 30°C or 37°C for approximately 20 or 16h, respectively.

#### 2.2.2.8 Transformation of XL10-Gold Ultracompetent Cells

For transformation of *Dpn*I-treated DNA (Section 2.2.2.2), XL10-Gold Ultracompetent cells were used. 45µl of cells (gently thawed on ice) were utilised for each transformation, to which 2µl β-ME was added. After 2min incubation on ice, 4µl of *Dpn*I-treated DNA was added to the competent bacteria and incubated on ice for further 30min. The transformation mix was then heat-pulsed at 42°C for 50sec, followed by 2min incubation on ice. Pre-heated 2YT-Broth (42°C, 500µl) was added to the mix, followed by incubation at 37°C for 1h with rotation (180rpm). 250µl of the transformation mix was plated on LB-agar plates, supplemented with appropriate antibiotic, and then incubated at 37°C for approximately 16h.

#### 2.2.2.9 Small-scale preparation of DNA (Minipreps)

Single colonies of transformed bacteria were grown in 2ml of LB-broth media. To prepare DNA, 200µl of each bacterial culture was transferred to a centrifuge tube, 200µl of lysis buffer was added and the mixture vortexed briefly. 200µl of precipitation buffer (section 2.1.13.3) was added to the mixture, mixed by vortexing and the cellular debris pelleted by centrifugation at 10000g for 2min. The supernatant was transferred to a new centrifuge tube containing 600µl of 100% isopropanol to precipitate the DNA. The samples were centrifuged at 10000g for 5min. The DNA pellet was washed once with 500µl of 70% ethanol, allowed to dry at room temperature, and resuspended in 20µl of water. The purified DNA was then analysed by restriction enzyme digestion.

#### 2.2.2.10 Large-scale preparation of DNA (Midipreps)

Large scale preparation of plasmid DNA was performed by using a PureLink™ HiPure Plasmid DNA Purification Kit (Invitrogen) according to the manufacturer's protocol.

Bacteria (typically in 150-500ml cultures) were pelleted by centrifugation at 4000g for 10min and resuspended in 4ml of R3 buffer (resuspension buffer). Cells were lysed by addition of 4ml of L7 buffer (lysis buffer), mixed immediately by inversion and incubated for 5min at room temperature. 4ml of N3 buffer (precipitation buffer) was added, mixed by inversion and the solution incubated for 10min at room temperature. The solution was then filtered, and the filtrate transferred to HiPure Midi columns (previously equilibrated with 10ml of EQ1 – equilibration buffer). The solution passed through the column by gravity flow and the DNA was retained on the filtration cartridge inserted into the column. The columns were washed 2x with 10ml of W8 buffer (wash buffer) and then transferred to polypropylene tubes to elute the DNA by adding 5ml of E4 buffer (elution buffer). The DNA was precipitated by adding 3.5mL of 100% isopropanol, mixed by vortexing and incubated for 10min at room temperature. The DNA was pelleted by centrifugation at 6500g for 30min. The pellet was washed with 3ml of 70% ethanol followed by centrifugation at 6500g for 5min. The pellet was resuspended in 50-200µl of water and stored at -20ºC.

#### 2.2.2.11 Separation and purification of DNA fragments

##### I. Agarose gel electrophoresis

The DNA fragments yielded by PCR or from restriction enzyme digestions were separated according to their molecular length by agarose gel electrophoresis. Agarose gels were prepared containing 1-2% agarose melted in 0.5% TBE buffer. Ethidium bromide was added to the gel mix at a final concentration of 0.05µg/ml. The DNA samples were mixed with loading buffer and then loaded onto the gel. Molecular weight markers (100bp or 1Kbp, NEB) were used for identification of the sizes of DNA fragments. For visualization of the DNA, the gels were exposed to UV-light (long or short-wave depending on the application) and photographed using a BioRad gel documentation system.

### II. Purification of DNA fragments from agarose gels

Purification of DNA fragments from agarose gels was performed using a QIAquick Spin Kit (Qiagen). The appropriate DNA fragments were excised from the gel using a scalpel blade and then transferred into a 1.5ml centrifuge tube. 3 volumes of QG buffer were added per 1 volume of gel and the tubes were placed at 60°C to dissolve the gel. The sample was added to a QIAquick Spin Column and centrifuged at 10000g for 1min. The DNA that bound to the column was washed with 700µl PE buffer and centrifuged at 10000g for 1min. The PE buffer was discarded, the columns placed in a fresh tube and centrifuged as before to completely remove any residual PE buffer. The columns were transferred into a clean centrifuge tube and, to elute the DNA, 30µl of elution buffer was added to each column. After 1min incubation at room temperature columns were centrifuged at 10000g for 1min. The recovered DNA was immediately used for further cloning steps or stored at -20°C.

### III. Phenol-chloroform purification

Digested DNA was purified by adding an equal volume of 1:1 phenol/chloroform solution to the sample. After vigorous mixing by vortexing, the solution was centrifuged at 10000g for 1min to separate the organic (containing proteins) and aqueous layers (containing nucleic acids). The aqueous layer (upper part) was transferred to a fresh centrifuge tube and an equal amount of 100% chloroform was added. The solution was vortexed as before and centrifuged at 10000g for 1min to separate organic and aqueous layers. The aqueous layer was transferred into a fresh tube and DNA was precipitated by ethanol precipitation (Section 2.2.2.11-IV).

### IV. Ethanol precipitation

DNA was precipitated by adding 2.5 volumes of 100% ethanol and 1/20 volume of NaCl (5M). The solution was mixed by vortexing and incubated at 4ºC for 5-10min. DNA was pelleted by centrifugation at 10000g for 5min. The pellet was washed once with 75% ethanol and centrifuged at 10000g for 2min. The supernatant was removed and the pellet resuspended in an appropriate volume of water after drying.

#### 2.2.2.12 Sequencing analysis of DNA

Nucleotide sequences were determined by automated nucleotide sequencing performed by The Sequencing Service (School of Life Sciences, University of Dundee, Scotland). Analysis of the resulting sequences was performed using Vector NTI (Invitrogen) or CLC Genomics Workbench 4.

### 2.2.3 Manipulation of RNA

#### 2.2.3.1 *In vitro* transcription of linearised DNA

*In vitro* transcripts were generated from previously linearised HCV SGR or full-length cDNA (section 2.2.2.6) using the T7 RiboMAX™ Express Large Scale RNA Production System (Promega). Each reaction mixture typically contained 2x T7 RiboMax buffer, 1µg of linearised/MB-treated DNA, 2µl of T7 RNA polymerase and RNase-free water made up to a 20ul total reaction volume. The reactions were incubated at 37°C for 1-2h. To remove the DNA template from the transcription reactions, 1U of RNase-free DNase was added per µg of DNA and incubated at 37°C for 15min. For purification and precipitation of the transcribed RNA, the RNeasy Mini Kit (Qiagen) was used.

#### 2.2.3.2 RNA cleanup (RNeasy Mini Kit, Qiagen)

Firstly, RNase-free water was added to the *in vitro* transcribed reaction to adjust the volume to 100µl. 350µl of RLT buffer was then added and the solution was mixed by pipetting. Subsequently, 250µl of 100% ethanol was added, the solution mixed again before transfer to a RNeasy mini spin column. After centrifugation at 10000g for 15sec, the flow-through was discarded. 500µl of RPE was added to the column and then centrifuged as before. A second wash with 500µl of RPE was performed by centrifuging the columns at 10000g for 2min. The flow-through was discarded and the columns were centrifuged again at 10000g for 1min to remove any residual flow-through or RPE buffer. The collection tube and the flow-through were discarded and the column transferred to a new tube. To elute the RNA, 25-50µl of RNase-free water was added to the column and incubated for 1min at room temperature. Then, the columns were centrifuged for 1min at 10000g and the eluted RNA collected and stored at -70°C.

### 2.2.3.3 Extraction of RNA from mammalian cells (small-scale)

Extraction of RNA from up to $10^7$ cells was performed using the RNeasy Mini Kit (Qiagen); such extractions produced up to 100µg of RNA. Before lysis, the culture media was removed and cells were washed once with PBS(A). The cells were lysed by adding 300-600µl RLT buffer directly to the wells and incubated for 2min at room temperature. The lysate was homogenized by pipetting and then transferred into a fresh tube. 1 volume of 70% ethanol (typically 300-600µl) was added to each homogenised sample and mixed well by pipetting. The samples were transferred into a RNeasy spin column and centrifuged at 10000g for 15sec. The flow-through was discarded and 700µl of RW1 buffer (wash buffer) was added to the column. After centrifugation at 10000g for 15sec, the flow-through was discarded and the columns transferred into new tubes. 500µl of RPE buffer was added to the column and centrifuged at 10000g for 15sec. A second wash with 500µl of RPE buffer was performed followed by centrifugation for a longer time, 2min at 10000g. The flow-through was discarded and the columns were centrifuged again at 10000g for 1min to remove any residual flow-through or RPE buffer. The collection tube and the flow-through were discarded and the column transferred to a new tube. To elute the RNA, 50µl of RNase-free water was added to the column and incubated for 1min at room temperature. Then, the columns were centrifuged for 1min at 10000g and the eluted RNA collected and stored at -70°C.

### 2.2.3.4 Extraction of RNA from mammalian cells (large scale)

Extraction of up to 1mg of RNA from up to $10^8$ cells was performed using the RNeasy Midi Kit (Qiagen). Before lysis, the culture media was removed and cells were washed once with PBS(A). The cells were lysed by adding 3ml RLT buffer directly to the dishes and incubated for 2min at room temperature. The lysate was homogenized by pipetting and the samples then transferred into a fresh 15ml tube. 1 volume of 70% ethanol (typically 3ml) was added to each homogenised sample and mixed thoroughly by shaking vigorously. The samples were transferred into an RNeasy Midi column and centrifuged at 4500g for 5min. The flow-through was discarded and 4ml of RW1 buffer (wash buffer) was added to the column. After centrifugation at 4500g for 5min, the flow-through was discarded and 2.5ml of RPE buffer (wash buffer containing ethanol) was added to

the column and centrifuged at 4500g for 2min. A second wash with 2.5ml of RPE buffer was performed at 4500g for 5min. The flow-through and the tubes were discarded and the columns transferred into new 15ml RNase-free tubes. To elute the RNA, 150µl of RNase-free water was added to the column and incubated for 5min at room temperature. The columns were centrifuged for 3min at 4500g. A second elution step was performed by adding 200µl of RNase-free water to the columns. The columns were centrifuged as before and the eluted RNA transferred into new RNase-free centrifuge tubes and stored at -70°C.

## 2.2.4 Transfection of DNA/RNA into mammalian cells

### 2.2.4.1 Transfection of DNA/RNA into mammalian cells using lipofectamine

Prior to DNA/RNA transfection (e.g. expression plasmids or poly-I:C), cells were seeded on the appropriate culture plates and allowed to settle for 24h at 37ºC. Depending on the culture plates used, 0.5-1µg DNA/RNA and 2-10µl of Lipofectamine 2000 (Invitrogen) were diluted separately in 250µl of Opti-MEM I (Gibco) and incubated at room temperature for 5min. The diluted DNA and Lipofectamine 2000 were combined and incubated at room temperature for further 20min. The DNA-Lipofectamine 2000 mixture was added to the plated cells and incubated at 37ºC for the appropriate length of time.

### 2.2.4.2 Electroporation of viral RNA into mammalian cells

Trypsinized cells, typically grown in 175cm$^2$ culture flasks, were counted using a haemocytometer. The appropriate volume of cells (containing 3.5x10$^6$ cells) was transferred into 15ml centrifuge tubes and centrifuged at 200g for 5min at room temperature. The media was decanted and the cells washed by resuspension in 10ml of PBS(A). The cells were centrifuged as before and the PBS(A) decanted. The pelleted cells were resuspended in 400ul PBS(A) and transferred into 4mm electroporation cuvettes along with 5-10µg of *in vitro* transcribed viral RNA. Cells were electroporated (250V and 950uF) using a BioRad GenePulser Xcell. The contents of each cuvette were resuspended in appropriate media (complete DMEM or WEM media) and seeded onto culture flasks or plates.

## 2.2.5 Protein methods

### 2.2.5.1 Sodium dodecyl sulfate - polyacrylamide gel electrophoresis (SDS-PAGE)

Proteins were resolved by SDS-PAGE electrophoresis, based on the method described by Laemmli (1970). Resolving gels were prepared using acrylamide solution at a final concentration of 8-12.5% in 1x resolving gel buffer. Addition of APS (0.1%) and TEMED (0.08%) initiated polymerisation and the solution was immediately poured into the gel assembly apparatus (using Bio-Rad Miniprotein II Apparatus), leaving a gap of ~2 cm from the top. The solution was then overlaid with $H_2O$. When polymerisation was complete, the water was discarded and excess water at the gel surface was absorbed carefully with filter paper. Stacking gel was prepared using acrylamide at a final concentration of 5% in 1x stacking gel buffer. Polymerisation was initiated upon the addition of APS (0.1%) and TEMED (0.08%), and the solution immediately overlaid onto the resolving gel. A 10-15 tooth Teflon comb was used to form wells in the stacking gel. The gel was allowed to polymerise before removal of the comb. The gels were placed in holders, transferred to an electrophoresis tank and submerged in 1x gel running buffer.

Before loading the protein samples on the gel, they were boiled for 10min at 100ºC. The wells in the gels were washed 2x with a syringe and 10-20µl (depending on the combs used) of each sample was loaded. High range protein markers (Amersham) were also included for protein size determination and empty wells were filled with an equal volume of boiling mix. Electrophoresis was performed at 120V until the required separation of protein markers and samples was achieved. Gels were then removed from the apparatus for Western blot analysis.

### 2.2.5.2 Western blot analysis

After SDS-PAGE electrophoresis, the resolved proteins were transferred to HybondTM-ECL™ nitrocellulose membranes using a Bio-Rad mini-transblot apparatus. The gel containing cassette, together with an ice container, were placed in the transblot apparatus and filled with Towbin buffer. Transfer was performed at 60V for approximately 2h.

#### 2.2.5.3 Immunodetection

Following transfer, the nitrocellulose membrane was incubated with blocking buffer for 1h at room temperature. After three washes with PBS-T the membranes were probed with appropriate antibody (diluted in 5% milk/PBS-T), by overnight incubation at 4ºC. The membranes were washed again six times with PBS-T (20min per wash) and then probed with appropriate secondary antibody (diluted in 2% milk/PBS-T) for 1h at room temperature. Finally the membrane was washed again six times with PBS-T (20min per wash; the last two washes with only PBS(A)).

Proteins were detected using Enhanced Chemiluminescence Plus Western Blotting Detection System (Amersham Biosciences). Following 2-5min incubation with ECL Plus reagent solution, the membranes were placed between mellanine sheets and the proteins visualised by exposure to Kodak X-OMAT S films which were developed using a Konica film-processing unit SRX-101a.

#### 2.2.5.4 Stripping of antibodies from nitrocellulose membranes

In order to re-probe nitrocellulose membranes, they were incubated in stripping buffer (1% SDS, 0.2M glycine, pH 2.5) for 30min at room temperature with agitation. Membranes were then washed three time with PBS-T (10min per wash) and blocked with 5% milk/PBS-T. Membranes were re-probed as described above. Only one stripping step was performed per membrane.

### 2.2.6 Microscopy Methods

#### 2.2.6.1 Indirect Immunofluorescence

Naive, replicon or infected cells seeded on 13mm glass coverslips were fixed for 10min with 100% methanol at -20ºC. The methanol was removed and the cells washed three times with PBS(A). The cells were incubated with primary antibody, at an appropriate dilution in PBS(A), for 2h at room temperature. The cells were washed with PBS(A), and stained with secondary antibody (diluted at 1:1000) conjugated with either FITC, TRITC or Cy5 for 1h at room temperature. The nuclei were stained by the addition of DAPI (diluted 1:2000 in PBS(A)). Finally, the cells were washed with PBS(A) three times, followed by two washes

with water. The coverslips were mounted on a glass slide (in Citifluor glycerol/PBS) and sealed with nail varnish prior to examination with a Zeiss Laser Scanning LSM510 META inverted confocal microscope (Carl Zeiss Ltd., UK). The images were analyzed using LSM510 software.

## 2.2.7 Cell culture methods

### 2.2.7.1 Propagation of cell lines

Huh-7, Huh-7.5, U2OS and HEK-293T cells were cultured in complete DMEM media and incubated at 37ºC with 5% $CO_2$. HepaRG cells were cultured in complete WEM media under the same temperature and $CO_2$ conditions. Cells harbouring SGR containing the neomycin/blasticidin resistance genes were cultured in the presence of 0.5mg/ml to 1mg/ml of G418 or 0.5µg/ml of Blasticidin. Cells were grown in tissue culture flasks (80cm$^2$ and 175cm$^2$), and the media was changed every 3-4 days. When the cells reached confluence, they were trypsinised for detachment, resuspended in 10ml media and a proportion (1:5 to 1:10) was used to seed a new flask or used for experiments.

### 2.2.7.2 Freezing cells

Cryogenic preservation of cell cultures was used to preserve stocks of cell lines. A culture flask of confluent cells was trypsinised and resuspended in the appropriate medium (DMEM or WEM depending on the cell line). Cryoprotection of cells was achieved by adding DMSO (to a final concentration of 10% (v/v)) and foetal calf serum (to 50% (v/v)). The cell suspension was then aliquoted in cryogenic vials (1ml/each), and kept at -70ºC overnight. The following day, cell aliquots were transferred to liquid nitrogen (-180ºC) for long term storage.

### 2.2.7.3 Lentivirus transduction of cell lines

Generation of lentiviruses and transduction of Huh-7 cells was used for either the production of cell lines with stable knockdown of protein expression or for expression of tagged proteins. Depletion of endogenous protein expression was based on RNAi-mediated gene silencing, which used lentiviral plasmids to express short hairpin RNA (shRNA) molecules.

On the day preceding transfection, HEK-293T cells were seeded in 60mm tissue culture dishes, in growth media containing 10% heat-inactivated serum (30min at 56°C) and 0.1% penicillin/streptomycin (P/S), at a density of approximately $1.5\times10^6$ cells per dish. For each transfection, 4.5µg of each plasmid DNA (the plasmid DNA of interest and two helper plasmids for production of lentiviral particles, pCMV.DR8.91 and pVSV-G) were mixed with 300µl of serum-free DMEM and 10µl of PLUS reagent. The DNA-PLUS mixtures were incubated for 15min at room temperature. 300µl of serum-free DMEM and 14µl of Lipofectamine2000 reagent were then added to the DNA-PLUS mixture and the whole mixture was incubated at room temperature for a further 15min. The media from HEK-293T cells was removed and kept at 37°C (conditioned media) and the cells washed once with serum-free DMEM. 1ml of serum-free media was added to the transfection mixture, before transferring to the cells, which were then incubated for 3h at 37°C. Following the incubation period, the cells were overlaid with 3ml of conditioned media. The cells were allowed to recover for 4-6h and media was changed to fresh DMEM (containing 30% FBS and 1% P/S). The lentiviral particles were produced from the cells over a period of 40 to 60h, before supernatants were harvested.

#### 2.2.7.4 Transduction of cell lines with lentivirus

On the day before transduction with lentivirus stocks, $6\times10^5$ Huh-7 cells were seeded onto 60mm dishes. At 60h post-transfection, the supernatants from HEK-293T cells containing lentiviral particles were harvested and centrifuged at 200g for 5min to remove cell debris. The supernatants were then filtered using a 0.45µm filter. 1ml of the supernatant, together with 5µg of polybrene, was added to Huh-7 cells, which were then incubated for 1h at 37°C, with gentle agitation every 10-15min. This procedure was repeated by adding a further 3ml of lentivirus supernatant containing polybrene to Huh-7 cells and incubated overnight. Finally, Huh-7 cells were overlaid with fresh media supplemented with 5µg/ml polybrene. Transduced cells were selected using the appropriate antibiotics (initially 1µg/ml puromycin, and subsequently increased to 10ug/ml, or 1mg/ml G418, depending on the plasmid). The resulting cell lines produced are detailed in the following table:

| Name | Description | Selection |
|---|---|---|
| shCtrl | Huh-7+pLKO.dCMV.Control-shRNA | Puromycin |
| sh1 | Huh-7+pLKO.dCMV.ISG15-shRNA1 | Puromycin |
| sh2 | Huh-7+pLKO.dCMV.ISG15-shRNA2 | Puromycin |
| sh3 | Huh-7+pLKO.dCMV.ISG15-shRNA3 | Puromycin |
| sh4 | Huh-7+pLKO.dCMV.ISG15-shRNA4 | Puromycin |
| sh5 | Huh-7+pLKO.dCMV.ISG15-shRNA5 | Puromycin |
| sh6 | Huh-7+pLKO.dCMV.ISG15-shRNA6 | Puromycin |
| ISG15-FLAG-GG | Huh-7+pLKO.dCMV.TetR.eGFP+ pLKO.dCMV.TetO.FLAG-ISG15-GG | Neomycin/ puromycin |
| ISG15-Flag-AA | Huh-7+pLKO.dCMV.TetR.eGFP+ pLKO.dCMV.TetO.FLAG-ISG15-AA | Neomycin/ puromycin |

## 2.2.8 Assessment of HCV infection, replication and infectious virus production

### 2.2.8.1 Analysis of HCV RNA replication (SGR)

#### I. Luciferase assays

Transient replication assays were performed by electroporation of *in vitro* transcribed replicon RNA expressing the luciferase reporter into mammalian cells (Section 2.2.4.2). Linearized DNA was used to direct *in vitro* transcription of replicon RNA, and 5-10µg of the transcription reaction was electroporated into cells. Typically, $8x10^4$ or $1x10^5$ cells were seeded into each well after electroporation (depending on the cell line), in a 24-well plate format. Luciferase assays were performed at 4, 24, 48 and 72h post-electroporation.

For determination of luciferase activity, cells were washed once with PBS(A) and lysed with 100µl cold 1x cell lysis buffer (Promega). After 2min incubation, 50µl of lysate was mixed with 100µl of luciferase assay reagent in a 1.5ml microcentrifuge tube. The solutions were mixed briefly and the luciferase activity measured using a Glomax™ 20/20 Luminometer.

**II. Colony forming assays**

Colony forming assays were performed by electroporation of neomycin- or blasticidin-selective replicon RNA into mammalian cells. *In vitro* transcribed *Neo* or *Blast* replicon RNAs were used to electroporated $3.5x10^6$ cells (Section 2.2.4.2). 24-48h after electroporation, media was replaced with fresh media supplemented with 0.5 to 1mg/ml of G418 or 0.5µg/ml of Blasticidin (depending on the HCV replicon used). 3 to 4 weeks after electroporation, drug-resistant colonies were stained with Coomassie Brillant blue (CBB). The medium was removed from the culture dish and the cells washed once with PBS(A). Colonies were stained with 10ml of CBB for 20min. The CBB was removed and the colonies washed well with water and allowed to dry.

### 2.2.8.2 Analysis of HCV Infectivity (HCVcc)

**I. Preparation of virus**

*In vitro* transcribed full-length genomic viral RNA (10µg) was used to electroporate Huh-7 cells (Section 2.2.4.2). The transfected cells were seeded on 90mm tissue culture dishes and incubated at 37°C for the required time period (72h for JFH1 or 48h for JC-1 virus). The medium containing infectious virions was harvested and centrifuged at 200g for 5min to sediment any residual cell debris, before infectivity was determined (Section 2.2.8.2-II).

**II. 50% tissue culture infectivity dose ($TCID_{50}$)**

For quantification of virus infectivity, limiting dilution assays using the $TCID_{50}$ assay as described by Lindenbach (2005) were employed. The $TCID_{50}$ assay measures the dilution of virus that will infect 50% of replicate cell cultures. To determine the virus titre by $TCID_{50}$ assay, Huh-7 cells were seeded at a density of $3x10^3$ (in 100µl complete DMEM) per well in flat-bottomed 96-well plates (Nunc). 48 or 72h later, serial 3-fold dilutions of cell medium were added, with 8 wells per dilution. Up to 72h later, the medium was removed, the cells were fixed with ice-cold methanol and incubated at -20°C for 20min. The cells were then washed 3x with PBS(A) and probed with anti-NS5A antibody (1:5000 dilution) in PBS(A) for 1h at room temperature. The cells were washed again 3x

with PBS(A) and incubated with the appropriate FITC-conjugated secondary antibody (1:2000 dilution) in PBS(A) for 1h at room temperature. After three washes in PBS(A) and two washes with water, the cells were overlaid with 100µl of $dH_2O$ before visualization under a fluorescent microscope to determine the number of positive wells at each dilution. The wells containing at least one NS5A-expressing cell were counted as positive, and the $TCID_{50}$ was calculated according to the Reed & Muench formula (Lindenbach, 2005).

#### 2.2.8.3 RNA interference

**I. Reverse transfection of mammalian cells with siRNA**

To verify the effect of cellular genes (e.g. ISG15, HERC5) on virus replication, target siRNAs were transfected into Huh-7/SGR and U2OS/SGR cells using lipofectamine RNAiMAX reagent. Transfections were performed in 24- or 12-well plates (depending on the experiment). For each well (e.g. 24-well plate), 100µl Opti-MEM I was mixed with 1µl lipofectamine RNAiMAX and the siRNAs were added to the transfection mixture. For transfection of negative control (scrambled) siRNA, 1µl of siCtrl mix (final concentration 50 nM) was added to the wells. For the target siRNAs, 0.5µl of a mixture of 3 siRNAs, targeting the same gene (final concentration 75nM), was used. The transfection mixture was gently mixed by pipetting, added to the wells and incubated for 20min at room temperature. Wells were then seeded with $8x10^4$ cells in 900µl of DMEM, giving a total volume of 1ml in each well. At appropriate times after transfection (24 or 48h, depending on the experiment), the supernatant was removed and the cells washed once with PBS(A) before: i) lysis in RLT buffer (Section 2.2.3.3) for RT-qPCR assays (Section 2.2.8.5); ii) lysis with BM for Western blotting analysis (Section 2.2.5) or iii) fixed with methanol for indirect immunofluorescence analysis (Section 2.2.6.1).

**II. Mammalian cell lines constitutively expressing shRNAs**

The lentiviral cell lines developed in sections 2.2.7.3 & 2.2.7.4 were used to assess the effect of ISG15 depletion, using short hairpin RNAs. These cells were used for electroporation with viral subgenomic RNA or infection with virus. Depending on the experiment (specified where appropriate in Chapter 5), these

cells were used for: i) transient HCV replication assays (Section 2.2.8.1-I); ii) measuring HCV and ISG15 expression levels in the presence or absence of exogenous IFN treatment by RT-qPCR assay (Section 2.2.8.5) and Western blotting analysis (Section 2.2.5) or iii) assessing the rates of viral RNA synthesis and degradation (Section 2.2.8.4).

### 2.2.8.4 4sU labelling and purification of nascent viral RNA

Metabolic labelling of newly transcribed viral RNA was performed using the method previously described by (Dolken *et al.*, 2008). The protocols for labelling and purification are described below in 3 stages.

#### I. 4sU labelling of nascent viral RNA

Cells were cultured in 90mm tissue culture dishes (2 plates per sample) in order to guarantee sufficient material for subsequent pull-down of labelled RNA (ideally 50 to 150µg of total RNA). Cells were seeded at a density of $5.5x10^5$ or $8x10^5$ per 90mm culture dish (depending on whether the cells were cultured for 72 or 48h, respectively) 24h prior to infection with JC-1 (moi=0.8). After plating, the cells were either: i) infected and labelled with 100µM 4sU for 24h; ii) infected for 24h and labelled with 100µM 4sU for a further 24h; or iii) infected for 24h, then pulse-labelled with 200µM 4sU for 6h followed by monitoring for loss of labelled RNA for 48h. To start labelling, 4sU was prepared in cell culture medium at the required concentration (100µM for up to 24h labelling; 200µM for up to 12h labelling) and the mixture added immediately to the cells, following by incubation at 37°C for the appropriate time. The medium was then removed from the cells, washed once with PBS(A) and the cells were immediately lysed by adding 3ml of RLT buffer. Total RNA was isolated and purified following the method described in Section 2.2.3.4.

#### II. Biotinylation of newly transcribed RNA

For isolation of labelled transcripts, the total RNA extracted from the cells was biotinylated, using a modified form of biotin (EZ-link Biotin-HPDP, Pierce) which has affinity for thiol groups (4sU). To biotinylate labelled transcripts, the following components were added per µg of RNA, 2µl of Biotin-HPDP (1mg/ml

dissolved in DMF), 1µl of 10x Biotinylation Buffer (100mM Tris pH 7.4, 10mM EDTA) and up to 6µl of RNase-free water; typically, 60µg of total RNA was used for biotinylation reactions. Reactions were incubated for 1.5h at room temperature with rotation. To remove unincorporated biotin-HPDP, two rounds of chloroform extraction were performed, using Qiagen MaXtract 2ml Phase Lock gel kit, according to manufacturer's instructions. Prior to use, the Qiagen MaXtract 2ml Phase Lock tubes (hereafter referred to as Phase lock tubes) were centrifuged at 10000g for 1min to pellet the gel matrix. The biotinylation reaction was added to the Phase lock tubes (600µl total volume for 60µg RNA reaction), then an equal volume of chloroform/isoamyl acohol (24:1) was added to each tube and shaken vigorously. After incubation for 2-3min, the Phase lock tubes were centrifuged at 10000g for 5min. The upper phase was transferred into a new Phase lock tube and a second round of chloroform extraction was performed as before. The upper phase from the second chloroform extraction was transferred into a new tube and the RNA precipitated by adding 1/10 volume of NaCl (5M) and an equal volume of 100% isopropanol (due to some loss during the extraction procedure, the sample volume was approximately 500µl). After centrifugation at 20000g for 30min at 4°C, the supernatant was removed, the pellet washed with an equal volume of 75% ethanol and centrifuged at 20000g for 10min. Finally, the supernatant was carefully removed and the RNA resuspended in 100µl of 1x TE.

**III. Streptavidin isolation of biotinylated RNA**

Following biotinylation, the RNA samples (in a volume of 100µl) were denatured at 65°C for 10min and immediately placed on ice for a further 5min. 100µl of streptavidin beads were then added to the RNA samples and incubated with rotation for 15min at room temperature. For separation of RNA/streptavidin complexes, the samples were applied to the µMacs columns and placed into a magnetic stand. The columns were then washed 3x with 0.9ml of washing buffer (100mM Tris-HCl, pH7.5, 10mM EDTA, 1M NaCl, 0.1% Tween20) at 65°C and the flow-through (which contained >90% unbound RNA) was retained on ice. The columns were washed again 3x with 0.9ml washing buffer at room temperature and the eluates discarded. To elute the RNA which was bound to the columns, two separate quantities of 100µl Elution Buffer (100mM DTT) were added to the columns. To purify the bound and eluted RNA as well as RNA in the

flow-through, the RNeasy MiniElute Kit (Qiagen) was used. 700µl of RLT buffer was added to each sample and mixed by pipetting. 500µl of 100% ethanol was added to the diluted RNA, mixed thoroughly by pipetting and the mixture transferred to a RNeasy MiniElute spin column. After centrifugation for 15sec at 8000g, the flow-through, together with the collection tube, was discarded. The spin columns were transferred to new tubes and 500µl of RPE buffer (wash buffer containing ethanol) was added to each column. The columns were centrifuged at 8000g for 15sec and flow-through discarded. Another wash was performed by adding 80% ethanol to the columns followed by centrifugation at 8000g for 2min. The flow-through and the collection tubes were discarded, the columns were transferred to a new collection tube and centrifuged again at 10000g for 1min to remove any residual flow-through or ethanol. The collection tube and the flow-through were discarded and the column transferred to a new tube. To elute the RNA, 30ul (bound and eluted RNA samples) or 18ul (flow-through RNA samples) of RNase-free water was added to the column and incubated for 1min at room temperature. The columns were centrifuged for 1min at 10000g and the eluted RNA collected and stored at -70°C. All the RNA fractions (total, newly transcribed and pre-existing/flow-through) were then analysed by RT-qPCR (Section 2.2.8.5).

#### 2.2.8.5 Reverse Transcription-Quantitative PCR (RT-qPCR)

RT-qPCR was a two-step process involving the reverse transcription of RNA followed by a real-time PCR amplification using either relative or absolute quantification procedures.

##### I. cDNA synthesis

Reverse transcription of viral and cellular RNAs was performed using the TaqMan Reverse Transcription Reagents Kit (Applied Biosystems). For each reaction 1µl of RNA was reverse transcribed in a ThermoHybaid PX2 Thermal Cycler as follows:

**Reaction components (final volume of 20µl)**

| Components | Volume (µl) |
|---|---|
| 10x RT buffer | 2 |
| $MgCl_2$ (25mM) | 4.4 |
| dNTPs (10mM) | 4 |
| Random Hexamers (50µM) | 1 |
| RNase inhibitor (20U/µl) | 0.4 |
| Multiscribe Reverse Transcriptase (50U/µl) | 0.5 |
| $dH_2O$ | 6.7 |
| RNA | 1 |

**Cycling conditions**

| Stage | Temperature | Time | Number of cycles |
|---|---|---|---|
| Primer annealing | 25°C | 10min | 1 |
| Extension | 37°C | 60min | 1 |
| RT inactivation | 95°C | 5min | 1 |
| Hold | 4°C | ∞ | 1 |

## II. Real-Time PCR

### Relative Quantification (RQ)

The relative quantity of viral or cellular RNA from electroporated or infected cells was determined by a RQ reaction. The cDNA obtained from the reverse transcription of total intracellular RNA (Section 2.2.3.3 and 2.2.3.4) was amplified using target HCV-, ISG15-, USP18-, HERC5-specific and control GAPDH-specific primers (Applied Biosystems) in the presence of FAM™ (target-specific) and VIC® (control-specific) labelled MGB probes. The JFH1 probe and primer sequences were located in the 5' UTR of the viral genome. Each sample was run in triplicate as a singleplex reaction. The reaction mixes are described below

along with the reaction cycle conditions performed on an Applied Biosystems 7500 Fast Real-Time PCR System using Fast Universal PCR conditions:

**Real-Time PCR Reaction Mix for JFH1 RNA**

| Components | Volume (µl) |
|---|---|
| 18µm Forward Primer (Final 900nm) | 1 |
| 18µm Reverse Primer (Final 900nm) | 1 |
| 5µm FAM JFH1 Probe (250nm) | 1 |
| TaqMan Fast Universal Mix (2x) | 10 |
| $dH_2O$ | 5 |
| cDNA | 2 |

**Real-Time PCR Reaction Mix for ISG15, USP18, HERC5 and GAPDH RNA:**

| Components | Volume (µl) |
|---|---|
| Probe | 1 |
| TaqMan Fast Universal Mix (2x) | 10 |
| $dH_2O$ | 7 |
| cDNA | 2 |

**Cycling conditions**

| Stage | Temperature | Time | Number of cycles |
|---|---|---|---|
| Denaturation | 95°C | 20sec | 1 |
| Primer annealing | 95°C | 3sec | 40 |
| Extension | 60°C | 30sec | |

The HCV or cellular target signals were normalised to the endogenous GAPDH control and the data was analysed using Applied Biosystems software (SDS version 1.3.1), according to the manufacturer's instructions.

**Absolute Quantification (AQ)**

The absolute quantity of viral transcripts from the RNA fractions obtained from the 4sU experiments was determined by an AQ reaction. The cDNA obtained from the reverse transcription (Section 2.2.8.5-I) of viral RNA was amplified using the HCV-specific primer/FAM probe combination described for RQ (Section 2.2.8.5-II). *In vitro* transcribed JFH1 genomic RNA of known concentration was used as a standard. Serially-diluted standard cDNAs and undiluted sample cDNAs were analysed in triplicate and real-time reactions were amplified and analysed using the same Fast Universal PCR conditions as for RQ reactions (Section 2.2.8.5.II).

### 2.2.8.6 Resazurin assay

For measuring the impact of labelling Huh-7 cells with 4sU nucleoside on cell viability, the resazurin assay was used. Resazurin is a redox dye with both colorimetric and fluorimetric properties, which changes relative to cellular metabolic activity. This assay is based on the ability of viable or metabolically active cells to convert the non-fluorescent redox dye (resazurin, blue) into a fluorescent reduced product (resorufin, red). This conversion occurs intracellularly and is undertaken by the activity of mitochondrial enzymes.

The resazurin assay was performed at 2, 16, 24, 48h after 4sU labelling. At each time-point, the media was replaced with 500ul of fresh media containing resazurin (1:50 from a 1mg/ml stock) and the cells incubated at 37°C for 6h. After the incubation period, 100ul of resazurin-containing media was transferred into a black 96 well plate. The fluorescence was measured in a Varioskan Flash (Thermo Scientific) using the following settings: 544nm excitation wavelength (typically between 530 and 560nm) and 590nm absorbance wavelength.

# 3 Expanding HCV *in vitro* model systems

## 3.1 Introduction

With the advent of subgenomic replicons (SGRs), it became possible to study HCV RNA synthesis in cell culture (Lohmann *et al.*, 1999). The first generation of functional HCV replicons was derived from a consensus Con1 cDNA clone which was able to replicate under selective pressure in Huh-7 human hepatoma cells (Lohmann *et al.*, 1999). Subsequently, other viable replicons were constructed from both genotype 1a (Blight *et al.*, 2000) and 2a strains of the virus (Kato *et al.*, 2003). The genotype 2a replicons were established from a consensus sequence of strain JFH1, which was isolated from a 32-year-old Japanese patient with fulminant hepatitis (Kato *et al.*, 2003). These JFH1 replicons could replicate more efficiently in Huh-7 cells than the Con1 replicons and did not require cell culture adaptive mutations to achieve high replication levels.

The SGR system represents a powerful tool to study RNA replication in cell culture, although there is a remaining need to develop systems that include other HCV genotypes and to expand viral RNA synthesis in alternative permissive cell lines with natural host-like environments. These systems would provide improved models to 1) understand the underlying mechanisms and the role of host and viral factors required for viral replication of different HCV genotypes and 2) screen for novel anti-viral drugs and provide a platform for testing of resistance variants from patients.

### 3.1.1 Expanding the SGR systems to include other HCV genotypes

Although the development of the SGR system was a major breakthrough to study HCV RNA replication, it is limited by the availability of HCV isolates that can replicate viral RNA in tissue culture cells (namely genotypes 1a, 1b and 2a). In an attempt to expand the repertoire of HCV SGR systems, we aimed to construct a SGR with sequences from genotype 3 (gt3).

Currently, gt3 strains account for 44% of HCV infections in the UK (Brant *et al.*, 2010) and thus have a similar prevalence to gt1 strains (45%). Chronic HCV infection has been associated with liver steatosis (virally- or metabolically-induced) and this has been suggested to be an important risk factor for progression to other liver diseases. Virus-induced steatosis is more frequent and more severe in patients infected with HCV gt3 (Adinolfi *et al.*, 2001) and reduces the response to antiviral therapies (Shah *et al.*, 2011). In addition, gt3 infection also carries a greater chance of developing accelerated liver fibrosis (Bochud *et al.*, 2009). The correlations and consequences of HCV-induced steatosis in patients infected with gt3 on viral replication, disease progression and lower response to antiviral therapies have not been fully addressed. An *in vitro* system that enabled replication of gt3 strains would aid development of an understanding of the characteristics of gt3 infections. However, previous attempts to construct subgenomic replicons entirely from gt3 sequences have failed (Hubb, 2008). Therefore, we sought to explore the feasibility of replacing sequences in the highly efficient JFH1 SGRs, with those from an isolate from Glasgow, as a first step in strategically designing a gt3 replicon.

### 3.1.2 Hepatocyte-like permissive cell lines for HCV replication

For many years, researchers have sought to improve HCV cell culture models to try to recapitulate the events which occur during natural HCV infection *in vivo*. Primary human hepatocytes potentially represent the best model for studying HCV in culture. However, primary cell lines are limited by their availability, growth potential and survival time. Moreover, they require elaborate isolation procedures and can exhibit considerable donor variability.

Thus, the focus of the second part of the studies presented in this chapter was to test the ability of HCV JFH1-SGRs to replicate in HepaRG, a human hepatocyte cell line. This cell line was originally isolated from a female HCV-infected patient with hepatocellular carcinoma (Gripon *et al.*, 2002). The cells exhibit hepatocyte-like morphology and support HBV infection in a similar fashion to primary human hepatocytes. In addition, HepaRG cells have the ability to differentiate into both hepatocyte-like and billiary-like epithelial cells when cultured under appropriate conditions (Parent *et al.*, 2004). HepaRG cells also express several liver-specific factors and have a similar gene expression

pattern to primary human hepatocytes (Hart *et al.*, 2010). In this context, HepaRG cells could provide a useful alternative to primary cells for studying HCV due to better availability and unlimited proliferation.

## 3.2 Construction of JFH1 SGRs containing genotype 3 sequences

As mentioned above, the use of SGR systems is limited by the availability of HCV isolates that replicate viral RNA in tissue culture cells. Previous attempts to construct replicons entirely from gt3 sequences have failed (Hubb, 2008). Hence, we aimed to examine the feasibility of replacing sequences in the highly efficient JFH1 SGR (gt2a), with those from a gt3 isolate from Glasgow (Shaw *et al.*, 2003). Attention was focused on the C-terminal end of NS4B and the NS3/4A protease complex. The NS4B C-terminus was selected as a recent study had been published from our group (Jones *et al.*, 2009) that had identified mutations in this region with varying effects on HCV RNA replication. In the case of NS3/4A, Imhof and Simmonds (2010) had shown that virus production was not blocked by introducing gt3 sequences into the full-length infectious JFH1 chimeric clone (JC-1). To examine whether gt3 sequences were functional in replication, a SGR expressing luciferase as a reporter (Luc-JFH1, hereafter referred as Luc-WT), was used since it allows rapid and transient assessment of viral RNA synthesis. The Luc-WT SGR is a bicistronic construct which contains a firefly luciferase reporter gene in the first cistron under the control of the HCV IRES and the JFH1 NS3 to NS5B region in the second cistron under the control of a heterologous IRES from EMCV (Targett-Adams & McLauchlan, 2005). Assaying for luciferase activity is based on the assumption that enzyme levels directly correlate with the replication levels of replicon RNAs (Targett-Adams & McLauchlan, 2005).

### 3.2.1 The NS4B C-terminal region is essential for HCV RNA replication

Previous work from our group (Jones *et al.*, 2009) demonstrated that the C-terminal region of NS4B can tolerate several mutations without affecting replication. Hence, the capacity to replace residues in the C-terminal region of JFH1 NS4B with corresponding gt3 amino acids without abrogating replication was assessed.

NS4B is a hydrophobic protein which is able to interact with and rearrange the ER membrane to form sites where replication complex (RC) assembly takes place (called the membranous web, MW) (Egger *et al.*, 2002; Gosert *et al.*, 2003; Hugle *et al.*, 2001). NS4B is predicted to comprise four transmembrane domains (TMDs) in the central region of the protein (aa ~70 to 190), flanked by N- and C-terminal regions located at the cytosolic side of the ER membrane (Figure 3.1-A) (Elazar *et al.*, 2004; Lundin *et al.*, 2003). The N-terminal region (aa 1 to ~69) of NS4B is less conserved among HCV genotypes than the rest of the protein. This region is predicted to contain an amphipathic $\alpha$-helix (aa 6 to 29), and a fifth TMD (termed TMX) which has been suggested to translocate into the ER membrane by a post-translational mechanism (Gouttenoire *et al.*, 2009a; Lundin *et al.*, 2003).

The C-terminal region of NS4B (aa 191 to 261) is relatively well conserved between HCV genotypes and is predicted to possess two $\alpha$-helical segments, H1 (aa192 to 227) and H2 (aa228 to 253) (Figure 3.1). Recent studies on this region have suggested that H2 has an amphipathic $\alpha$-helix which can mediate membrane association, suggesting that NS4B membrane association is mediated not only by the TMD but also by the amphipathic $\alpha$-helices at the N- and C-terminal domains (Elazar *et al.*, 2004; Gouttenoire *et al.*, 2009b; Liefhebber *et al.*, 2009; Lindstrom *et al.*, 2006).

**Figure 3.1- Predicted secondary structure of the NS4B C-terminus and sequence conservation between gt2a and gt3a variants. [A] A schematic representation of the predicted secondary structure of NS4B at the ER membrane. NS4B is predicted to contain four transmembrane domains (1-4), flanked by N- (aa 1 to ~69) and C- terminal (aa 191 to 261) regions oriented to the cytosolic side of the ER. Represented are the amphipathic $\alpha$-helix (aa 6 to 29), a fifth TMX at the N-terminal region, as well as the NBM (nucleotide binding motif) (aa 129 to 135). The two predicted helices H1 (aa 201 to 213) and H2 (aa 228 to 253) at the C-terminal region are also shown. [B] Sequences from the C-terminal region of NS4B, derived from strain JFH1 (GeneBank AB047639) and from Glasgow-3 strain (Shaw *et al.*, 2003) were aligned using CLC workbench 4. Regions 1 and 2 represent conserved and less well conserved sequences between the two genotypes, respectively. Grey boxes within Regions 1 and 2 indicate helices H1 and H2, respectively.**

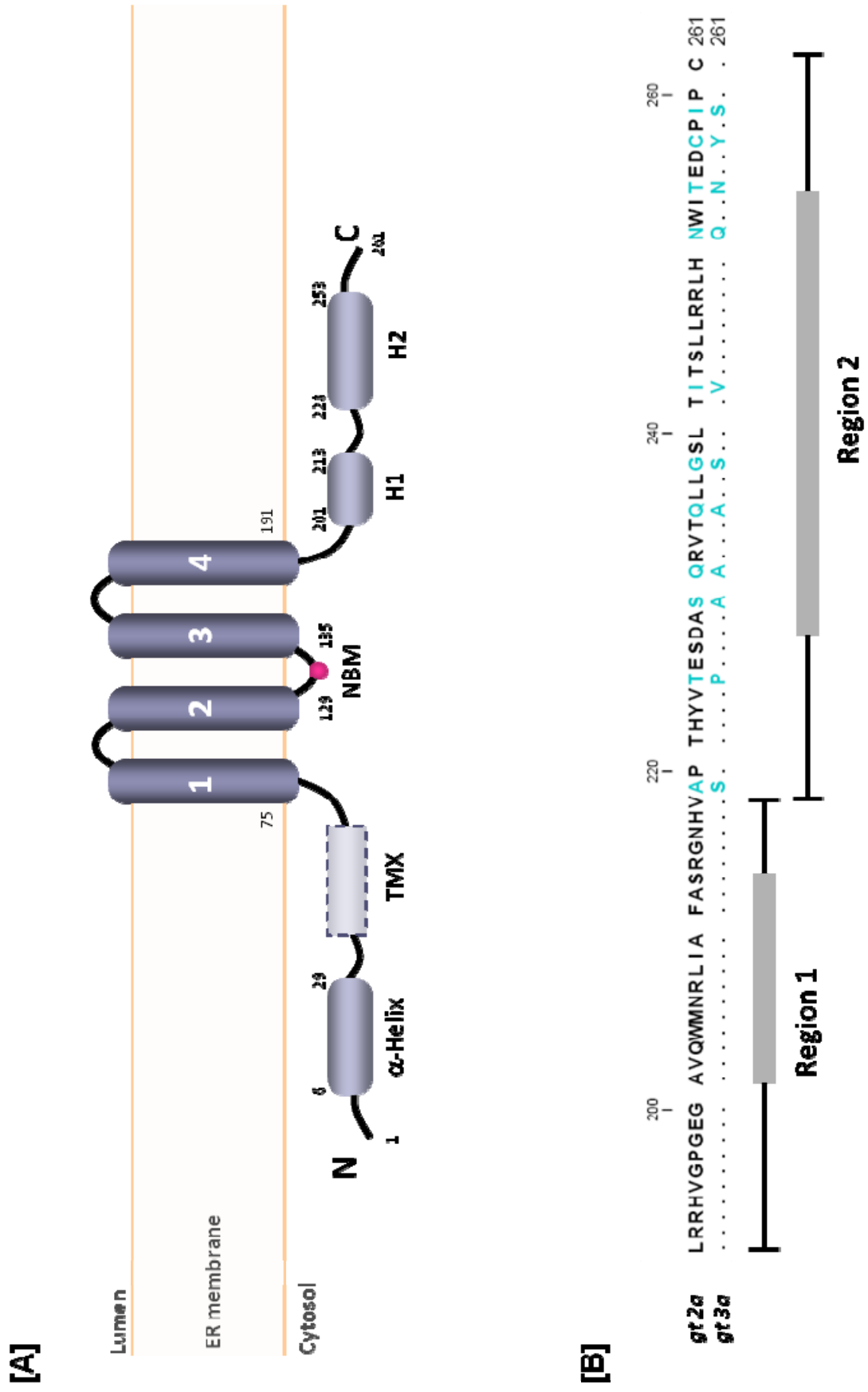
[A]
Lumen
ER membrane
Cytosol
N
C
α-Helix
TMX
NBM
H1
H2
1
6
29
75
123
135
191
201
213
223
253
261
1
2
3
4
[B]
gt2a
gt3a
200
220
240
260
LRRHVGPGEG AVQWMNRLIA FASRGNHVAP THYVTESDAS QRVTQLLGSL TITSLLRRLH NWITEDCPIP C 261
. . . . . S. . . . . P. . . . . A A. . . A. . S. . . V. . . . . Q. . N. . Y. S. . 261
Region 1
Region 2

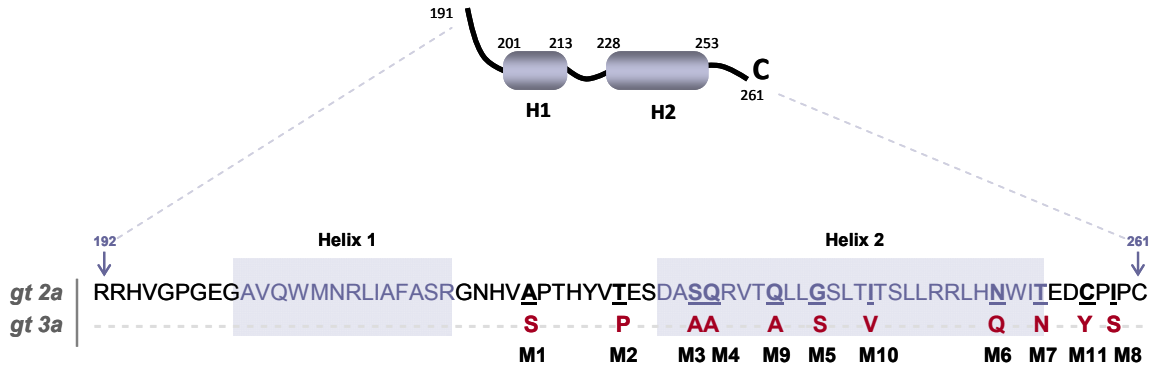


**Figure 3.2 – Representation of the gt3 mutants at the C-terminus of NS4B. Schematic representation of the amino acid sequence of the NS4B C-terminal region of gt2a and gt3a (Glasgow-3 strain). Amino acids substituted with gt3a variants are underlined and numbered M1-M11.**

### 3.2.2 Construction of SGRs containing gt3a sequences at the C-terminal region of NS4B (2a3a-NS4B-SGR)

Alignment of the C-terminal region of NS4B from strain JFH1 (gt2a, GenBank AB047639) and HCV-strain Glasgow-3 (gt3a, (Shaw *et al.*, 2003)) revealed that it can be separated into two segments Region 1 and Region 2, which contain $\alpha$-helices H1 and H2 respectively. Region 1 was completely conserved (comprising aa 191 to 218) whereas region 2 (comprising aa 219 to 261) differed at 11 amino acid positions (Figure 3.1-B). Using this information, the variable amino acids in Region 2 in strain JFH1 NS4B were converted to encode the corresponding Glasgow-3 residues (Figure 3.2). These mutations were introduced into a 266bp *Bam*HI-*Bam*HI DNA fragment spanning NS4B and NS5A sequences by site-directed mutagenesis (SDM), before introduction into a replicon called Luc-SGR-JFH1/M4. Luc-SGR-JFH1/M4 was generated in a previous study from our group (referred to as M9 in Jones *et al.*, 2009). This construct contained a Gln to Ala mutation at position 231, which corresponds to the Glasgow-3 sequence at this position (Figure 3.1-B and Figure 3.2). Substitution from Gln to Ala had no impact on viral replication and thus Luc-SGR-JFH1/M4 was used as the parent plasmid into which the remaining gt3a mutations were introduced.

The overall strategy used to construct the Luc-2a3a-NS4B replicons from Luc-SGR-JFH1/M4 is represented in Figure 3.3 and is described as follows:

- PCR amplification of the complete NS4B (783bp) and the first 31bp of NS5A coding regions from Luc-SGR-JFH1/M4, using the EcoRI-4B_Fwd and 4B/5A-SacI_Rev primers, which inserted *Eco*RI and *Sac*I restriction sites at the 5' and 3' ends respectively of the amplified fragment (*Eco*RI-NS4B-*Sac*I; Figure 3.3-A).

- Insertion of *Eco*RI-NS4B-*Sac*I into the pGEM-T Easy vector using *Eco*RI and *Sac*I restriction sites to generate pGEM-NS4B/M4 (Figure 3.3-B).

- The NS4B gt3a mutants were inserted into pGEM-NS4B/M4 by SDM using the primers shown in Figure 3.3-D and the strategy is described as follows (the numbers below correspond to the circled numbers in Figure 3.3-C):

  1. Insertion of M1, M2 and M3 into pGEM-NS4B/M4 within the *Bam*HI-*Bst*XI region to yield pGEM-NS4B-M1-4.

  2. Insertion of M6, M7 and M8 into pGEM-NS4B/M4 within the *Bst*XI-*Bam*HI region to yield pGEM-NS4B-M4/6-8.

  3,4,5. Using *Bst*XI and *Sac*I restriction sites (Figure 3.3-C, upper panel), *Bst*XI-M6-8-*Sac*I was excised from pGEM-NS4B-M4/6-8 and inserted into the pGEM-NS4B-M1-4 backbone, generating pGEM-NS4B-M1-8/$\Delta$5.

  6. Insertion of M5 into the pGEM-NS4B-M1-8/$\Delta$5 construct. This insertion resulted also in loss of the *Bst*XI restriction site.

  7,8,9. Sequential insertion of M9, M10 and M11 into pGEM-NS4B-M1-8, resulting in the final pGEM-NS4B-M1-11 construct.

- Finally, using the *Bam*HI restriction sites, the NS4B mutants were excised from pGEM-NS4B-M1-11 and inserted into Luc-JFH1 to yield Luc-M1-11 (Figure 3.3-E).

- In addition to the final Luc-M1-11 construct, mutants generated at intermediate SDM stages were also inserted into the Luc-SGR replicon (Figure 3.3-F) following the same cloning strategy (Figure 3.3-E).

**Figure 3.3- Construction of NS4B C-terminal mutants by site-directed mutagenesis. [A] PCR amplification of NS4B and the first 31bp of the NS5A coding region from Luc-SGR-JFH1/M4 using the forward "EcoRI-4B_Fwd" and reverse "4B/5A-SacI_Rev" oligonucleotide primers. [B] Insertion of the amplified fragment, EcoRI-NS4B-SacI, into the pGEM-T Easy vector. [C] Representation of the restriction sites and locations of mutations at the 266bp BamHI-BamHI fragment within the EcoRI-NS4B-SacI region (upper panel). NS4B nt sequence numbered 1 to 783: *Bam*HI (position 521), *Bst*XI (position 709) and *Bam*HI (position 4, within the NS5A coding region). Insertion of M1 to 11 by SDM into pGEM-NS4B vector (lower panel): 1) Insertion of M1-3; 2) Insertion of M6-8; 3,4,5) Cloning of M6-8 into pGEM-M1-4 vector using the *Bst*XI and *Sac*I restriction sites; 6) Insertion of M5 into pGEM-M1-8/Δ5; 7,8,9) Insertion of M9, 10 and 11 into pGEM-M1-8 construct. [D]) Sequence and position of the SDM oligos used to generate M1 to M11 in the NS4B coding region. [E] Cloning of the 3' terminal region of NS4B containing the gt3a mutants into Luc-SGR using BamHI-BamHI restriction sites. [F] Table representing all final Luc-SGRs generated at final or intermediate SDM stages. SDM, site-directed mutagenesis; nt, nucleotides; aa, amino acids.**

**[A]**

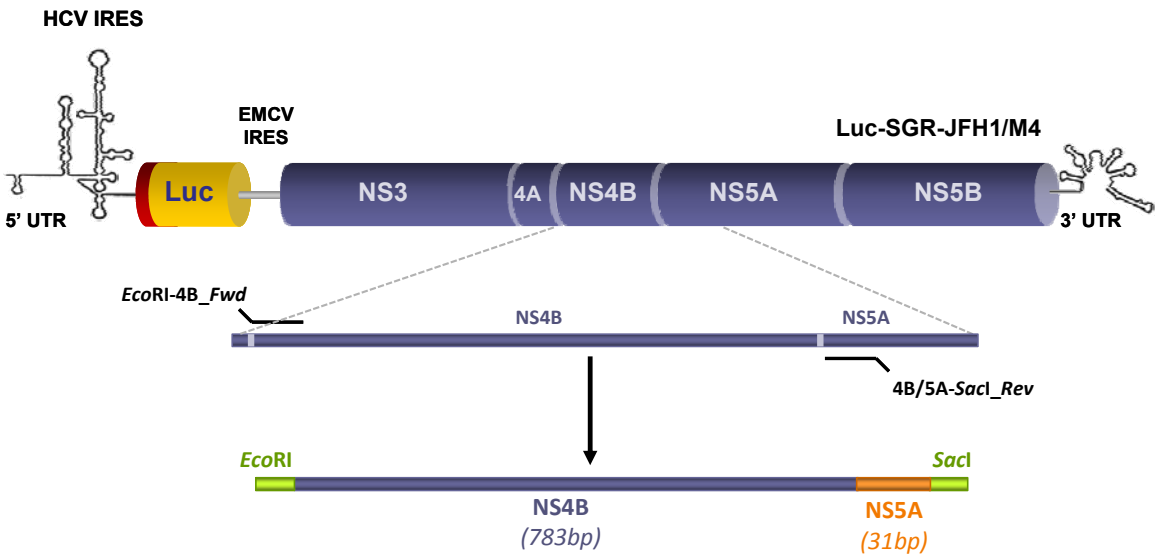


| | |
|---|---|
| *Eco*RI-4B_*Fwd*: | **5'- ACC GAA TTC GCC TCT AGG GCG GCT CTC ATC -3'** (*Eco*RI) |
| 4B/5A-*Sac*I_*Rev*: | **5'- GGT GAG CTC CTG TCA AGA TGG TGC AAA CCC -3'** (*Sac*I) |

**[B]**

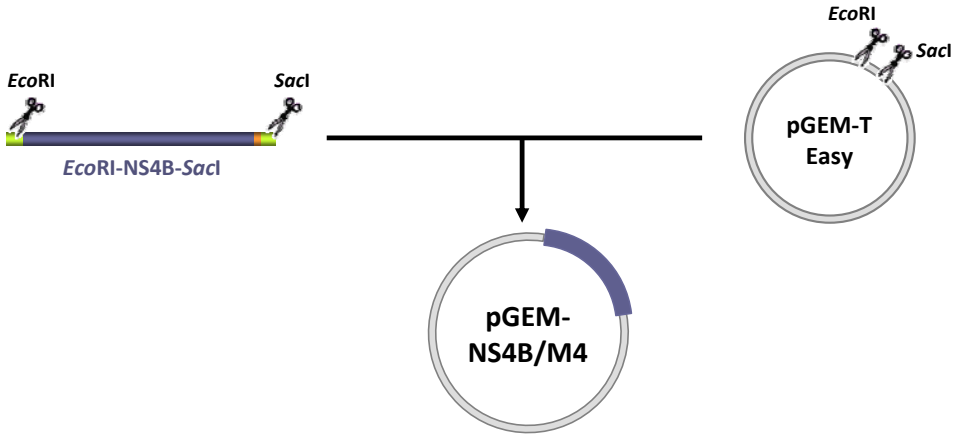

[C]

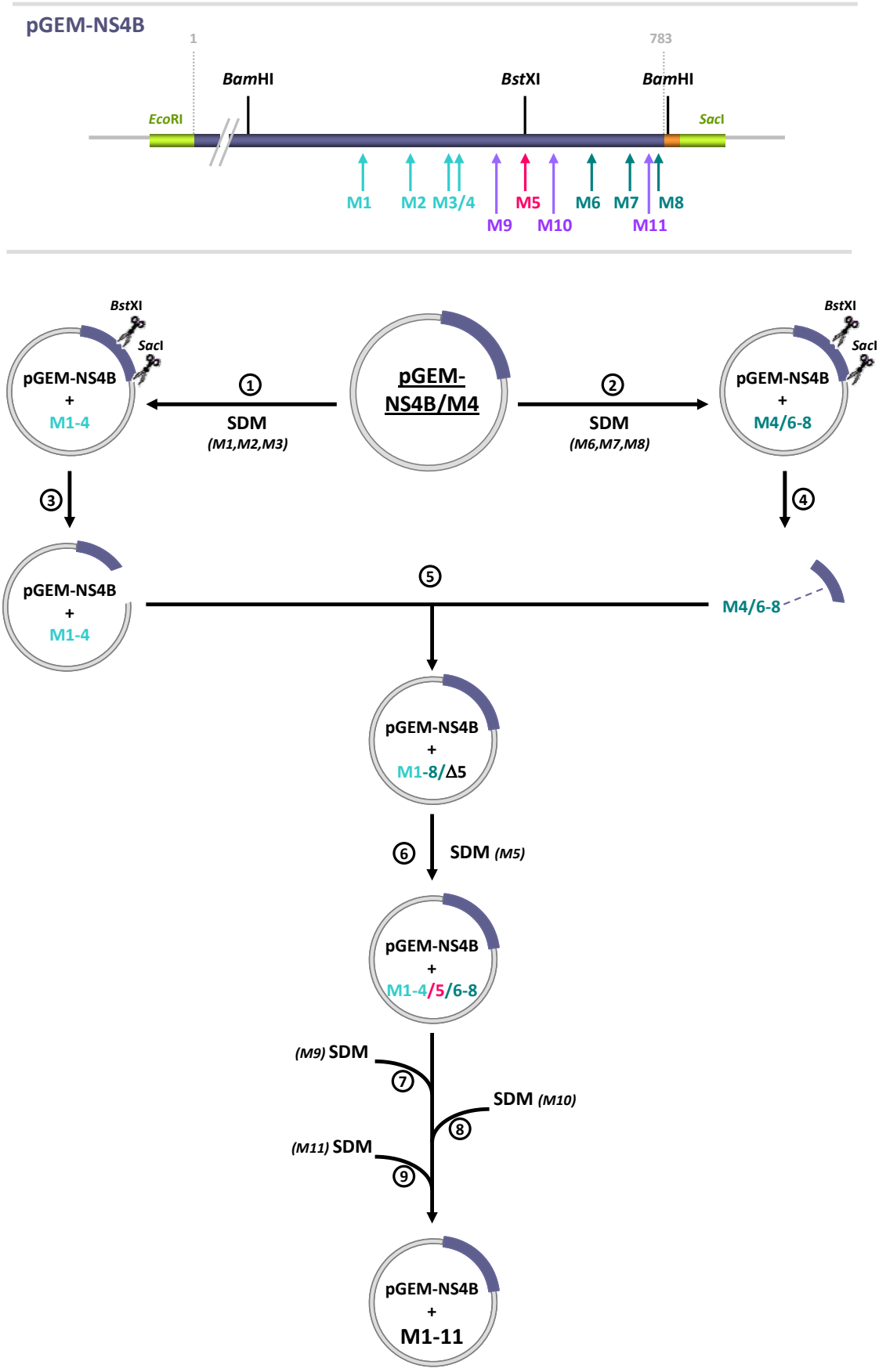
pGEM-NS4B
1
783
BamHI
BstXI
BamHI
EcoRI
SacI
M1
M2
M3/4
M5
M6
M7
M8
M9
M10
M11
BstXI
SacI
pGEM-NS4B + M1-4
1
SDM (M1,M2,M3)
pGEM-NS4B/M4
2
SDM (M6,M7,M8)
BstXI
SacI
pGEM-NS4B + M4/6-8
3
4
pGEM-NS4B + M1-4
5
M4/6-8
pGEM-NS4B + M1-8/Δ5
6
SDM (M5)
pGEM-NS4B + M1-4/5/6-8
(M9) SDM
7
SDM (M10)
8
(M11) SDM
9
pGEM-NS4B + M1-11

**[D]**

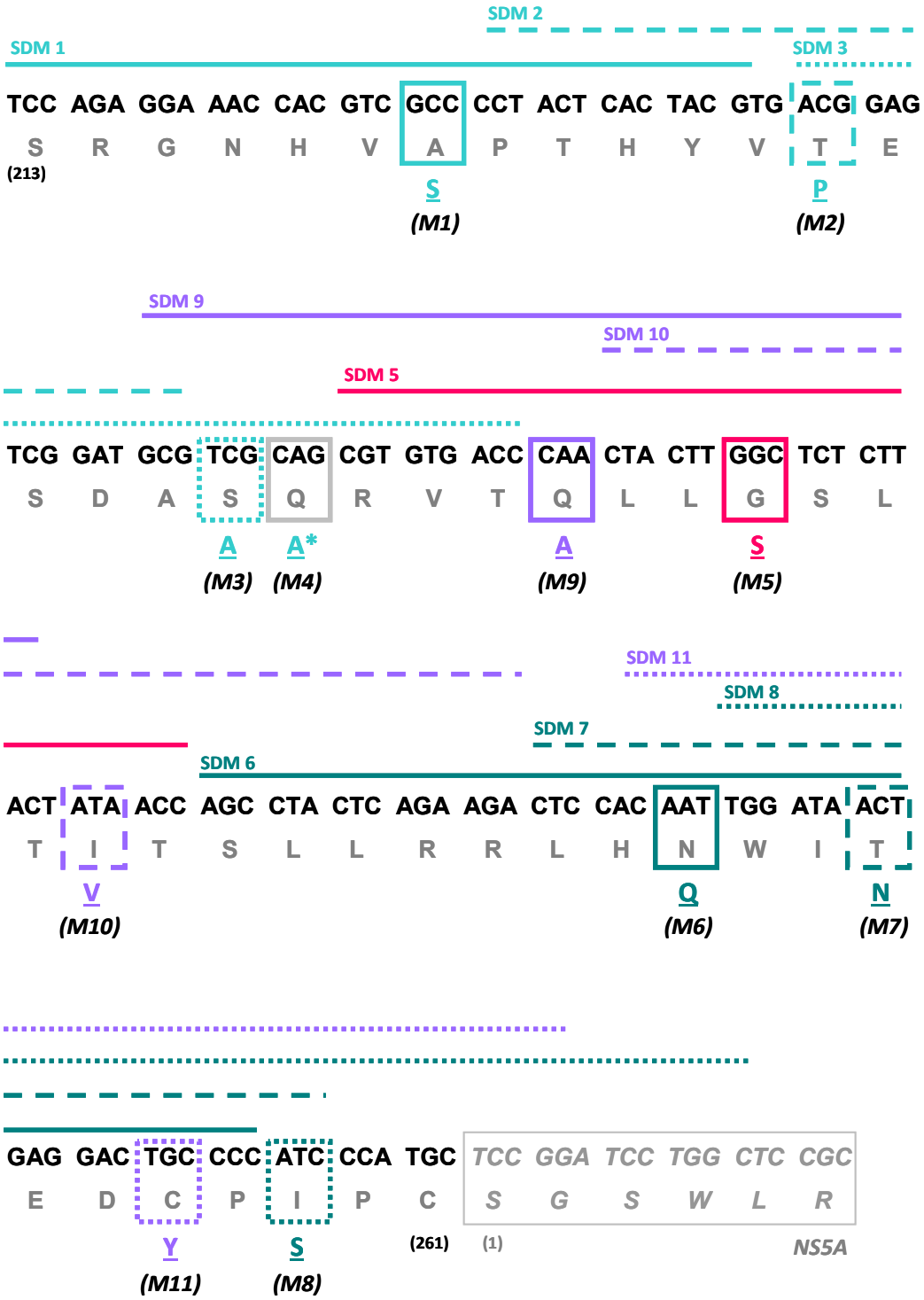
SDM 2
SDM 1
SDM 3
TCC AGA GGA AAC CAC GTC GCC CCT ACT CAC TAC GTG ACG GAG
S R G N H V A P T H Y V T E
(213)
S
(M1)
P
(M2)
SDM 9
SDM 10
SDM 5
TCG GAT GCG TCG CAG CGT GTG ACC CAA CTA CTT GGC TCT CTT
S D A S Q R V T Q L L G S L
A
(M3)
A*
(M4)
A
(M9)
S
(M5)
SDM 11
SDM 8
SDM 7
SDM 6
ACT ATA ACC AGC CTA CTC AGA AGA CTC CAC AAT TGG ATA ACT
T I T S L L R R L H N W I T
V
(M10)
Q
(M6)
N
(M7)
GAG GAC TGC CCC ATC CCA TGC TCC GGA TCC TGG CTC CGC
E D C P I P C S G S W L R
Y
(M11)
S
(M8)
(261)
(1)
NS5A

**[E]**

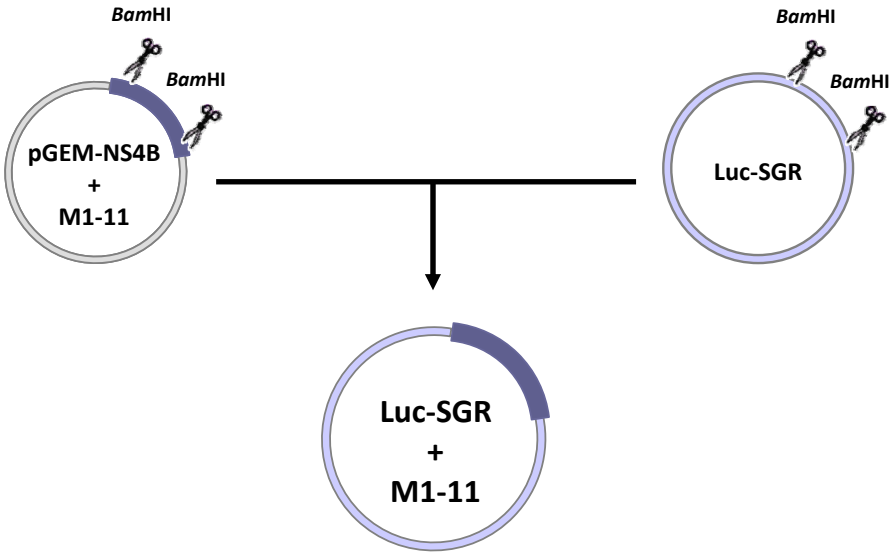


**[F]**

| NS4B mutants | pGEM-T constructs | Luc-SGR constructs |
|---|---|---|
| M1, M2, M3, M4 | pGEM-NS4B+M1-4 | Luc-M1-4 |
| M6, M7, M8 | pGEM-NS4B+M4/6-8 | Luc-M4/6-8 |
| M1, M2, M3, M4, M6, M7, M8 | pGEM-NS4B+M1-8/Δ5 | Luc-M1-8 /Δ5 |
| M1, M2, M3, M4, M5, M6, M7, M8 | pGEM-NS4B+M1-8 | Luc-M1-8 |
| M1, M2, M3, M4, M5, M6, M7, M8, M9 | pGEM-NS4B+M1-9 | Luc-M1-9 |
| M1, M2, M3, M4, M5, M6, M7, M8, M9, M10 | pGEM-NS4B+M1-10 | Luc-M1-10 |
| M1, M2, M3, M4, M5, M6, M7, M8, M9, M10, M11 | pGEM-NS4B+M1-11 | Luc-M1-11 |

### 3.2.3 Analysis of the replication competence of 2a3a-NS4B-SGRs

#### I. Luc-SGR containing all NS4B gt3a mutants does not replicate efficiently

To determine whether introduction of gt3a sequences into the C-terminus of NS4B was tolerated in the context of the JFH1 replicon, transcribed RNA from Luc-M1-11 was electroporated into Huh-7 cells and the luciferase activity was measured for up to 72h (Figure 3.4), as an indirect assessment of replication efficiency. RNAs encoding Luc-WT and Luc-GND (a replication defective replicon encoding a GDD to GND mutation in the NS5B sequence (Kato *et al.*, 2003) were also electroporated into cells and used as positive and negative controls respectively. The luciferase values indicated that replication of Luc-WT increased at all time points after electroporation (Figure 3.4-A). By contrast, the luciferase values decreased for Luc-GND, indicating the inability of this construct to replicate. For Luc-M1-11 the luciferase values declined between 4 to 48h, similar to the pattern for Luc-GND (Figure 3.4-A). Between 48 and 72h there was a small recovery in luciferase activity (~2 fold), suggesting perhaps some ability of this construct to replicate, although enzyme levels were very low.

Since M1-11 gave such low levels of replication, intermediate Luc-SGRs constructed during SDM (Figure 3.3-C & F) were examined to determine whether single mutations or a combination of mutations could account for the lack of replication. Starting from the constructs with a higher to lower number of gt3 changes, Luc-M1-10, Luc-M1-9 and Luc-M1-8 constructs (which excluded M11, M10-11 and M9-11, respectively) were tested. As shown in Figure 3.4-A, removal of M11, M10 or M9 from Luc-M1-11 still gave decreased luciferase activity over 72h similar to Luc-GND. In addition, the small recovery detected previously with the Luc-M1-11 replicon between 48 and 72h was now lost with all of the constructs (Luc-M1-10, Luc-M1-9 and Luc-M1-8) (Figure 3.4-A). Therefore, removal of M11, M10 or M9 from Luc-M1-11 did not restore replication.

## II. M8 negatively affects replication in the context of the remaining gt3 mutations

To examine the other mutations that may impair replication, constructs containing mutants M1-4 and M4/6-8 (located at the N- and C-terminus of region 2 of NS4B, respectively (Figure 3.3-C)) were tested. M5 was not present in these constructs as it was only introduced after combining M1-4 and M6-8 in the same vector (see SDM strategy Figure 3.3-C). RNA transcripts from Luc-M1-4 and Luc-M4/6-8 were electroporated into Huh-7 cells and the activity of luciferase was measured as described before. The luciferase values indicated that M1-4 could replicate efficiently over 72h, in a similar manner to the WT replicon (Figure 3.4-B). On the other hand, luciferase activity declined in the first 24h after electroporation for Luc-M4/6-8 and between 24 and 72h a small recovery in activity (~2 fold) was detected. Thus, separating the mutations in Luc-M1-8 roughly in half was able to at least partially overcome the negative impact on replication. In addition, these results suggested that the mutation(s) responsible for the reduced replication competence of Luc-M1-11 were located most probably between M5-8 (i.e., M5, M6, M7 or M8, or a combination of these mutations). From among these mutants, attention was focused on M8 as it is located in close proximity to the NS4B/NS5A cleavage site and thus could affect proteolysis at this site by NS3/4A (Figure 3.3-C & D). Substitution of Ile with Ser is also a significant change in the physicochemical characteristics at position 259 (hydrophibic to polar residue) (Figure 3.5-A) and this could have a detrimental effect on NS4B function.

Similarly, M5 was another candidate because absence of this mutation in Luc-M1-4 and Luc-M4/6-8 constructs either completely or partially restored replication to WT-like levels (Figure 3.4-B). Moreover, substitution of Gly to Ser added another hydrophilic amino acid (aa) in the central region of H2 (Figure 3.5-A). Although this change did not result in a change to the hydropathy pattern within the H2 (Figure 3.5-B), it could possibly negatively impact on H2 interactions with other aa within NS4B or other viral proteins.

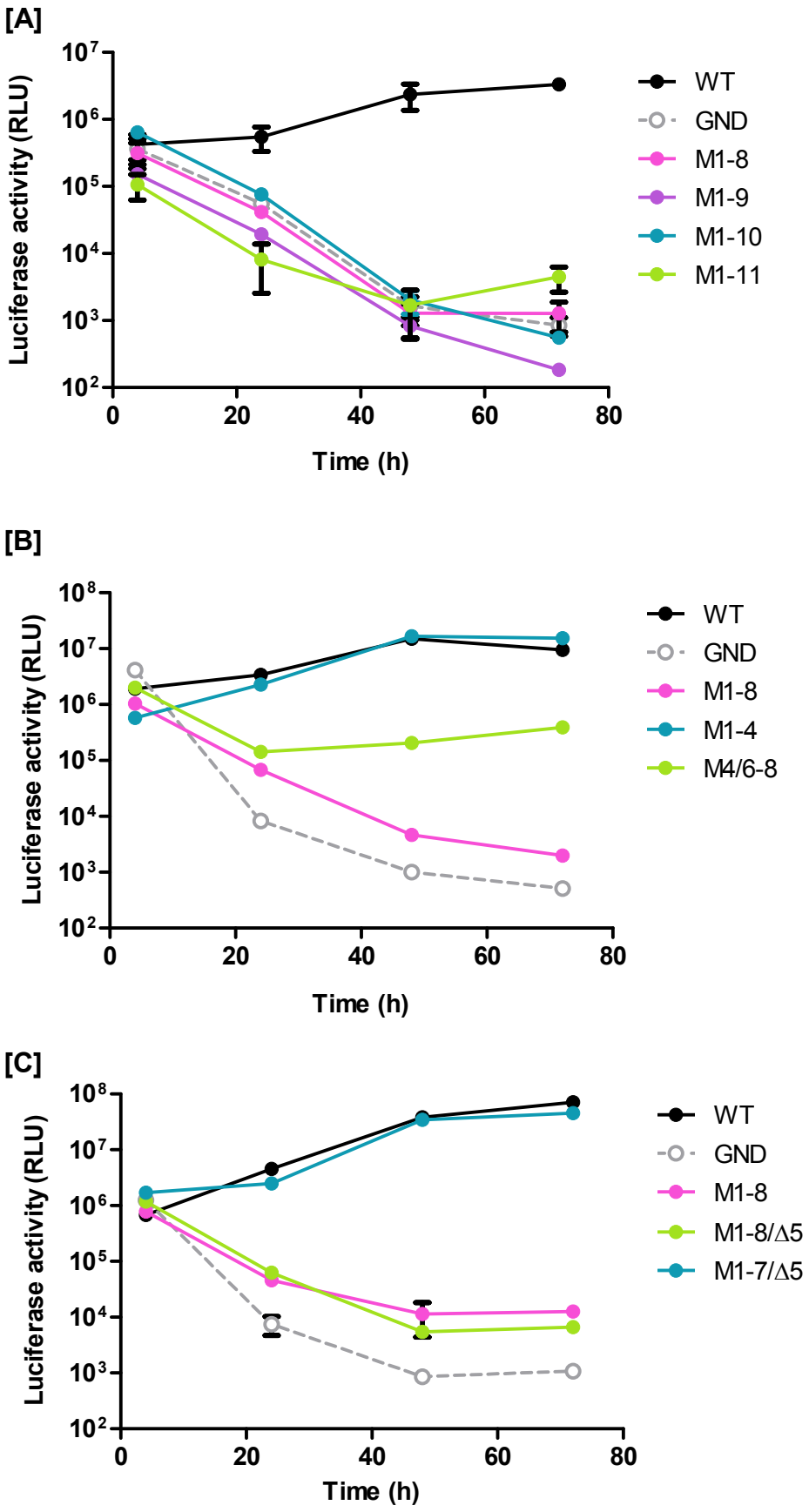
[A]
Luciferase activity (RLU)
$10^7$
$10^6$
$10^5$
$10^4$
$10^3$
$10^2$
0
20
40
60
80
Time (h)
WT
GND
M1-8
M1-9
M1-10
M1-11
[B]
Luciferase activity (RLU)
$10^8$
$10^7$
$10^6$
$10^5$
$10^4$
$10^3$
$10^2$
0
20
40
60
80
Time (h)
WT
GND
M1-8
M1-4
M4/6-8
[C]
Luciferase activity (RLU)
$10^8$
$10^7$
$10^6$
$10^5$
$10^4$
$10^3$
$10^2$
0
20
40
60
80
Time (h)
WT
GND
M1-8
M1-8/Δ5
M1-7/Δ5

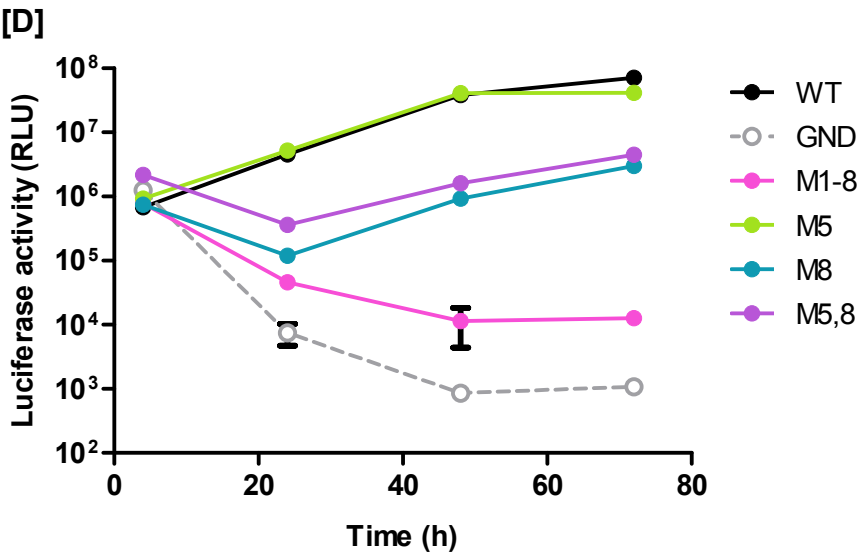


**Figure 3.4 – Assessment of replication efficiency of NS4B gt3a mutants. Huh-7 cells were electroporated with Luc-SGR RNAs containing all or different combinations of gt3 mutants. The cells were lysed at 4, 24, 48 and 72h after electroporation and the extracts used for measuring luciferase activity. [A] M1-8, M1-9, M1-10 and M1-11; [B] M1-8, M1-4 and M6-8; [C] M1-8, M6-8, M1-8/Δ5 and M1-7/Δ5; [D] M1-8, M5, M8 and M5,8; [E] M1-8, M1-9/Δ8, M1-10/Δ8 and M1-11/Δ8. RLU, relative light units.**

**Figure 3.5 – Properties of the amino acids at the C-terminus of NS4B. [A] Analysis of aa residues within gt2 and gt3 sequences. Represented are aa 228 to 261 spanning M3 to M11. [B] Hydrophobicity plot of gt2a (upper panel) and gt3a M1-8 (lower panel) at the C-terminus of NS4B, using CLC Genomics Workbench 4 (based on Kyle-Doolittle algorithm). Positive values represent hydrophobic regions.**

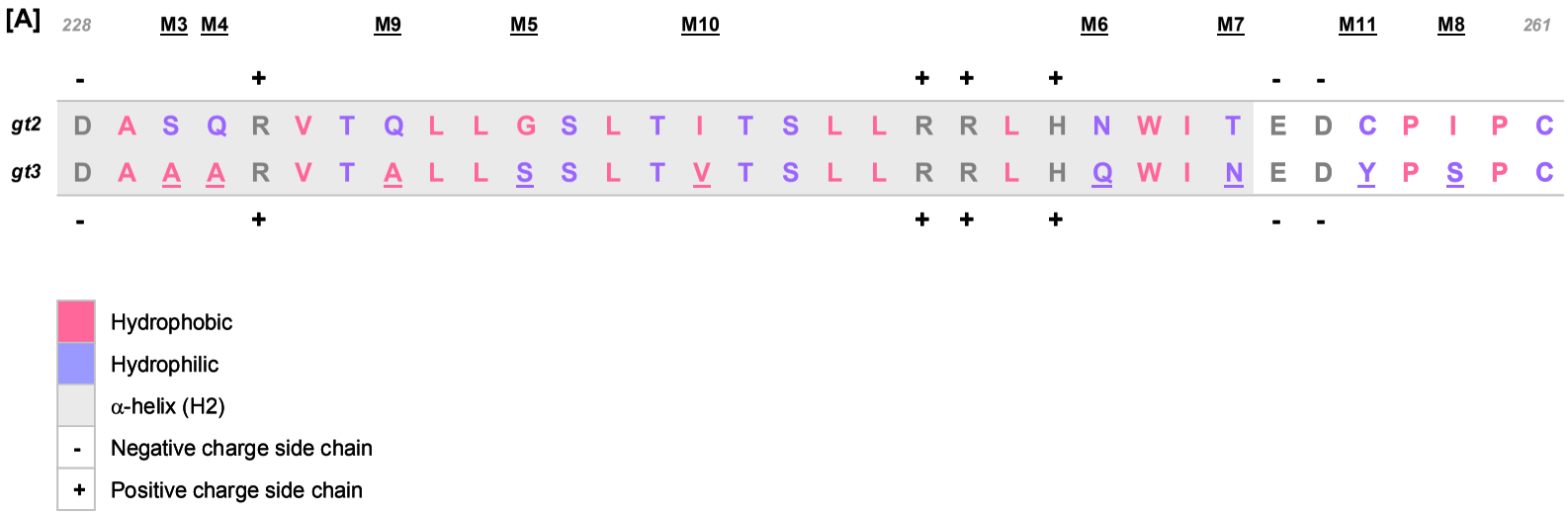
[A]
228
M3 M4
M9
M5
M10
M6
M7
M11
M8
261
gt2 D A S Q R V T Q L L G S L T I T S L L R R L H N W I T E D C P I P C
gt3 D A A A R V T A L L S S L T V T S L L R R L H Q W I N E D Y P S P C
Hydrophobic
Hydrophilic
α-helix (H2)
Negative charge side chain
Positive charge side chain

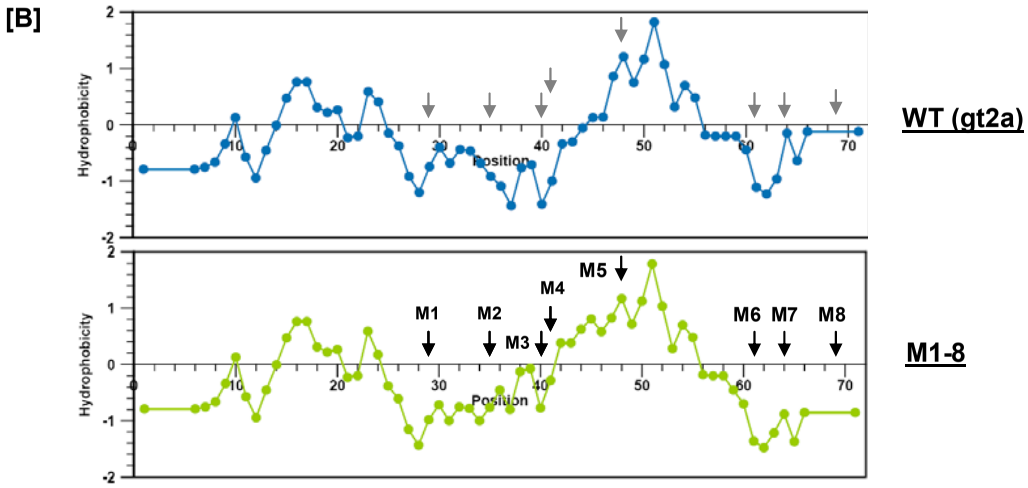
[B]
Hydrophobicity
Position
M1
M2
M3
M4
M5
M6
M7
M8
WT (gt2a)
M1-8

To examine both possibilities, Luc replicons containing M1-8 including or excluding M5 (Luc-M1-8 and Luc-M1-8/Δ5 respectively) and M1-7, excluding M5 and M8 (Luc-M1-7/Δ5), were constructed (following the same strategy described in Figure 3.3-C). RNA transcripts from Luc-M1-8/Δ5 and Luc-M1-7/Δ5 were electroporated into Huh-7 cells and the activity of luciferase was measured for up to 72h as before. For comparative purposes Luc-M1-8 was tested in addition to the Luc-WT and –GND controls. As shown in Figure 3.4-C, luciferase values declined over the 72h period for Luc-M1-8/Δ5, following the same pattern as Luc-GND and Luc-M1-8, suggesting that M5 did not impair replication. However removal of M5 and M8 (Luc-M1-7/Δ5) restored luciferase activity to levels similar to Luc-WT over the 72h period (Figure 3.4-C). Furthermore, the effect of M5 and M8 individually (Luc-M5 and Luc-M8 respectively) or a combination of both mutants (Luc-M5,8) on replication was assessed. As shown in Figure 3.4-D, luciferase values for Luc-M5 increased over 72h similar to the levels for Luc-WT. By contrast, luciferase activity declined in the first 24h after electroporation for Luc-M8 and Luc-M5,8, and then recovered between 24 and 72h, although activity did not reach the same levels as for Luc-WT (~15 to 23 fold lower). Thus, M5 alone did not apparently account for the lack of replication by M1-8. However, deletion of M5 and M8 in the context of the remaining NS4B mutations (Luc-M1-7/Δ5) restored WT-like replication, suggesting that M8 was the mutation responsible for reduced replication competence of Luc-M1-8.

To further confirm these results, a Luc replicon Luc-M1-7, containing M5 and excluding M8 was constructed and its ability to replicate assessed as before. As shown in Figure 3.6-A, the luciferase levels increased throughout the 72h period for Luc-M1-7 in a similar fashion as observed for Luc-WT. In addition, examination of viral protein synthesis at 72h after electroporation by Western blot analysis, revealed high levels of NS5A protein in M1-7 (Figure 3.6-B), close to levels produced by Luc-WT. Thus, the C-terminal region of NS4B could tolerate mutations M1 to M7 without significantly affecting HCV RNA replication but inclusion of M8 into the NS4B sequences led to either no or very little RNA synthesis (Figure 3.6).

Since removal of M8 (Luc-M1-7) restored replication, the remaining mutations M9, M10 and M11 were added back to this construct (Luc-M1-9/Δ8, Luc-M1-10/Δ8 and Luc-M1-11/Δ8) and their ability to replicate was assessed. As shown in Figure 3.4-E, luciferase activity still decreased in the first 24h for Luc-M1-9/Δ8 or in the first 48h for Luc-M1-10/Δ8 and Luc-M1-11/Δ8. Following those times, luciferase activity increased up to 72h for all of the constructs (Figure 3.7), although did not achieve similar luciferase activity as for Luc-WT (~670, ~300 and ~17 fold lower than WT in Luc-M1-11, Luc-M1-10 and Luc-M1-9, respectively). Nonetheless, the data indicate that as many as 10 gt3a-specific mutations could be introduced into the C-terminal region of NS4B and some HCV RNA replication could be retained.

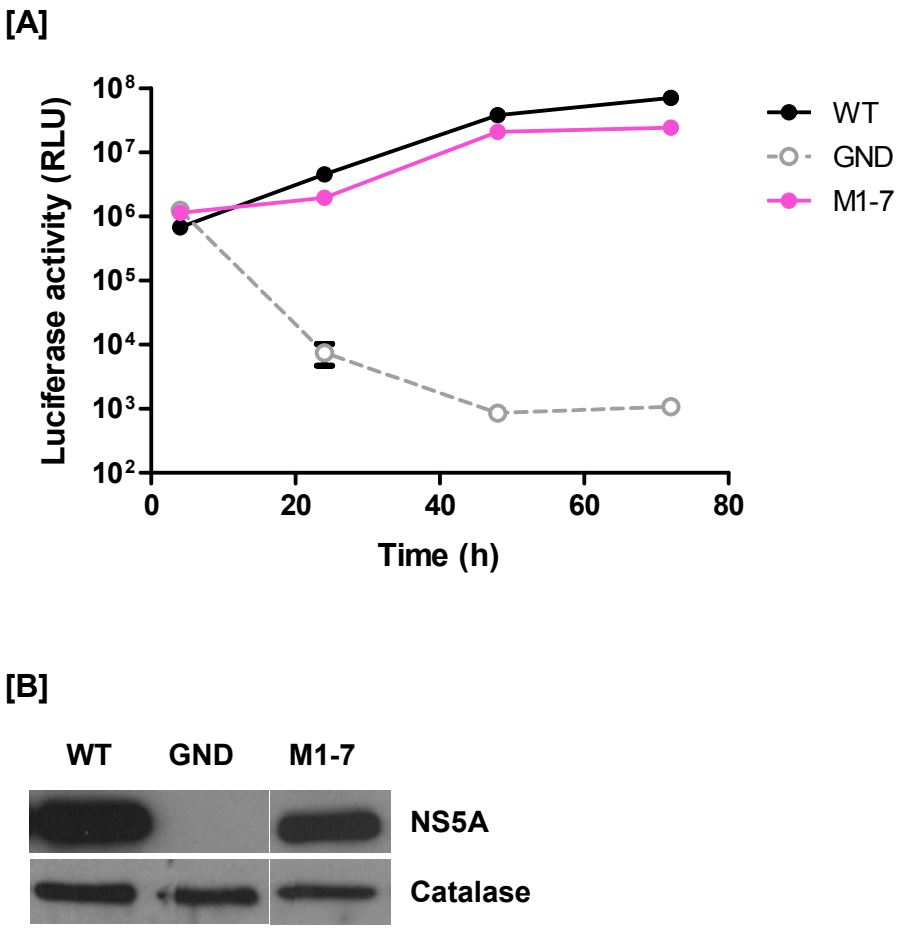


**Figure 3.6 – Luc-M1-7 replicates efficiently in Huh-7 cells. Huh-7 cells were electroporated with Luc-SGR RNAs containing Luc-WT, Luc-GND or M1-7. The cells were lysed at 4, 24, 48 and 72h after electroporation and the extracts used for measuring the luciferase activity [A]; [B] Extracts from cells electroporated with Luc-WT, GND or M1-7 were prepared at 72 h post-electroporation and examined for NS5A expression using anti-NS5A and anti-catalase antisera RLU, relative light units.**

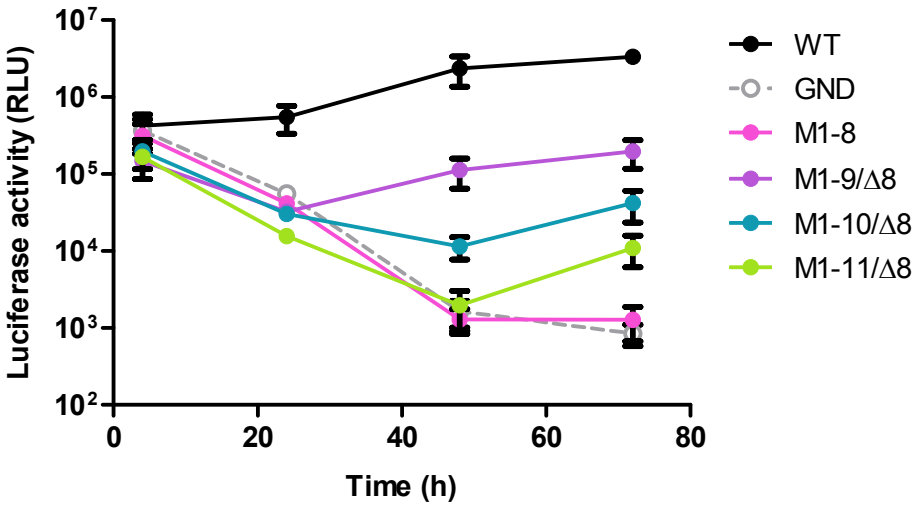


**Figure 3.7 – Replication efficiency of NS4B gt3a mutants. Huh-7 cells were electroporated with Luc-SGR RNAs containing M1-8, M1-9/Δ8, M1-10/Δ8 and M1-11/Δ8. The cells were lysed at 4, 24, 48 and 72h after electroporation and the extracts used for measuring luciferase activity. RLU, relative light units**

### 3.2.4 Construction of 2a3a-NS3-4A-SGR

As mentioned at the beginning of this section, in parallel with the gt3 substitutions at the C-terminus of NS4B, the study also examined the impact of inserting gt3 sequences for the NS3/4A protease complex into the sub-genomic replicon. In a recent study, it was shown that virion production could be achieved by inserting the NS3 protease and the NS4A cofactor from the six major genotypes into the JC-1 chimeric version of JFH1, which produces high levels of infectious virus in Huh-7.5 cells (Imhof & Simmonds, 2010). Thus, in the second part of this study, we aimed to clone the NS3 protease and NS4A cofactor regions from J3a3a [JC-1 chimera containing NS3/4A sequences from HCV-strain Glasgow-3 (Imhof & Simmonds, 2010), Figure 3.9] into the Luc-JFH1 replicon and assess its ability to replicate.

NS3 is composed of two functional and discrete units, an N-terminal chymotrypsin-like serine protease domain and a C-terminal RNA helicase/NTPase domain (Bartenschlager *et al.*, 1993; Kim *et al.*, 1997). NS4A is a small hydrophobic protein (6KDa) that forms a stable complex with the NS3 protease domain to promote anchoring to cellular membranes through an N-terminal hydrophobic peptide, thereby facilitating cleavage of the HCV polyprotein at the NS3/NS4A, NS4A/NS4B, NS4B/NS5A and NS5A/NS5B junctions (Bartenschlager *et al.*, 1993; Grakoui *et al.*, 1993). In addition, the NS3/4A protease can antagonise antiviral mechanisms during HCV infection. NS3/4A cleaves IPS-1, the interferon $\beta$ (IFN$\beta$) promoter stimulator-1, and TRIF, a TLR3 adaptor protein (Li *et al.*, 2005b; Li *et al.*, 2005c; Loo *et al.*, 2006). Cleavage of these molecules prevents IPS-1- and TRIF-dependent signal transduction which is essential to stimulate IFN$\alpha$ and $\beta$ expression.

### 3.2.5 J3a3a replicates efficiently in Huh-7 and Huh-7.5

The NS3-4A intergenotypic chimeric constructs developed by Imhof and Simmonds (2010) were characterised in Huh7.5 cells. These cells have been previously reported to give higher levels of replication as well as generate a higher titre of infectious virus when compared with parental Huh-7 cells (Pietschmann *et al.*, 2006), which were the cells used in the current study.

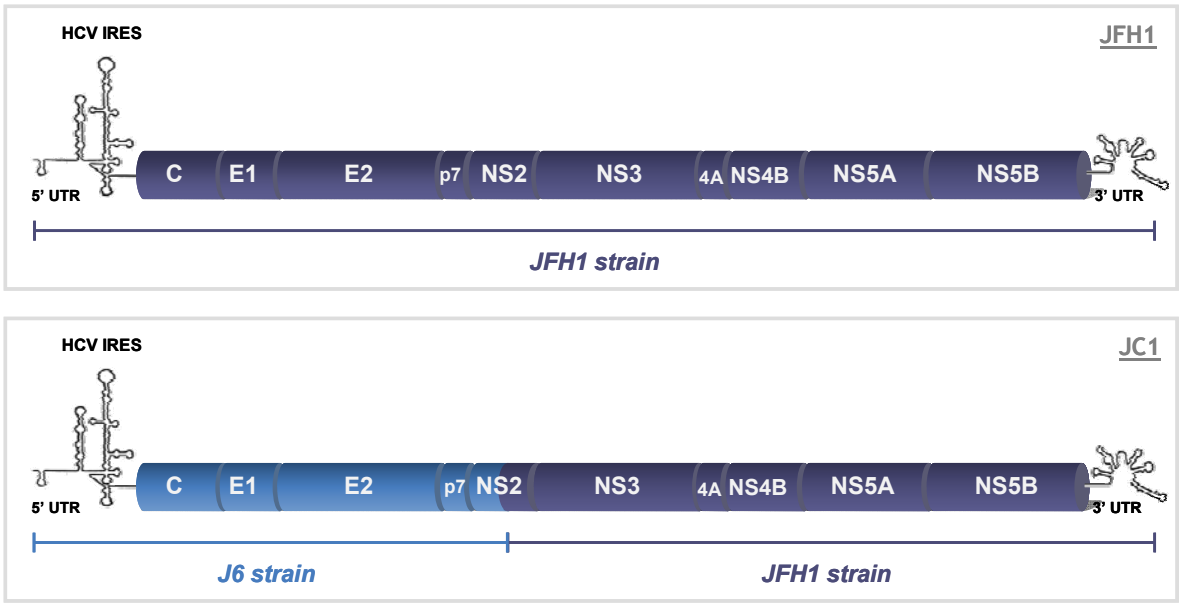


**Figure 3.8 – Schematic diagram of the JC-1 chimera genome. In the upper and lower panels are represented the JFH1 and JC-1 genome respectively. JC-1 chimera contains sequences from strain J6, spanning core to part of the NS2 coding regions, and from JFH1 strain for the remaining coding regions.**

To rule out the possibility that Huh-7 and Huh-7.5 cells give different replication efficiencies for J3a3a and any Luc-SGR derived constructs, RNA transcripts from J3a3a and JC-1 (used as control, Figure 3.8) were electroporated into the two cell lines. At 48h post-electroporation, levels of viral RNA were examined by RT-qPCR analysis. As shown in Figure 3.9-B, the levels of JC-1 RNA were about 6-fold higher in Huh-7.5 cells, when compared with the parental Huh-7 cells, as previously reported (Pietschmann *et al.*, 2006). This suggested that J3a3a could replicate in Huh-7 cells, although less efficiently than in Huh-7.5 cells. Nonetheless, these data indicate that J3a3a can synthesise viral RNA in Huh-7 cells.

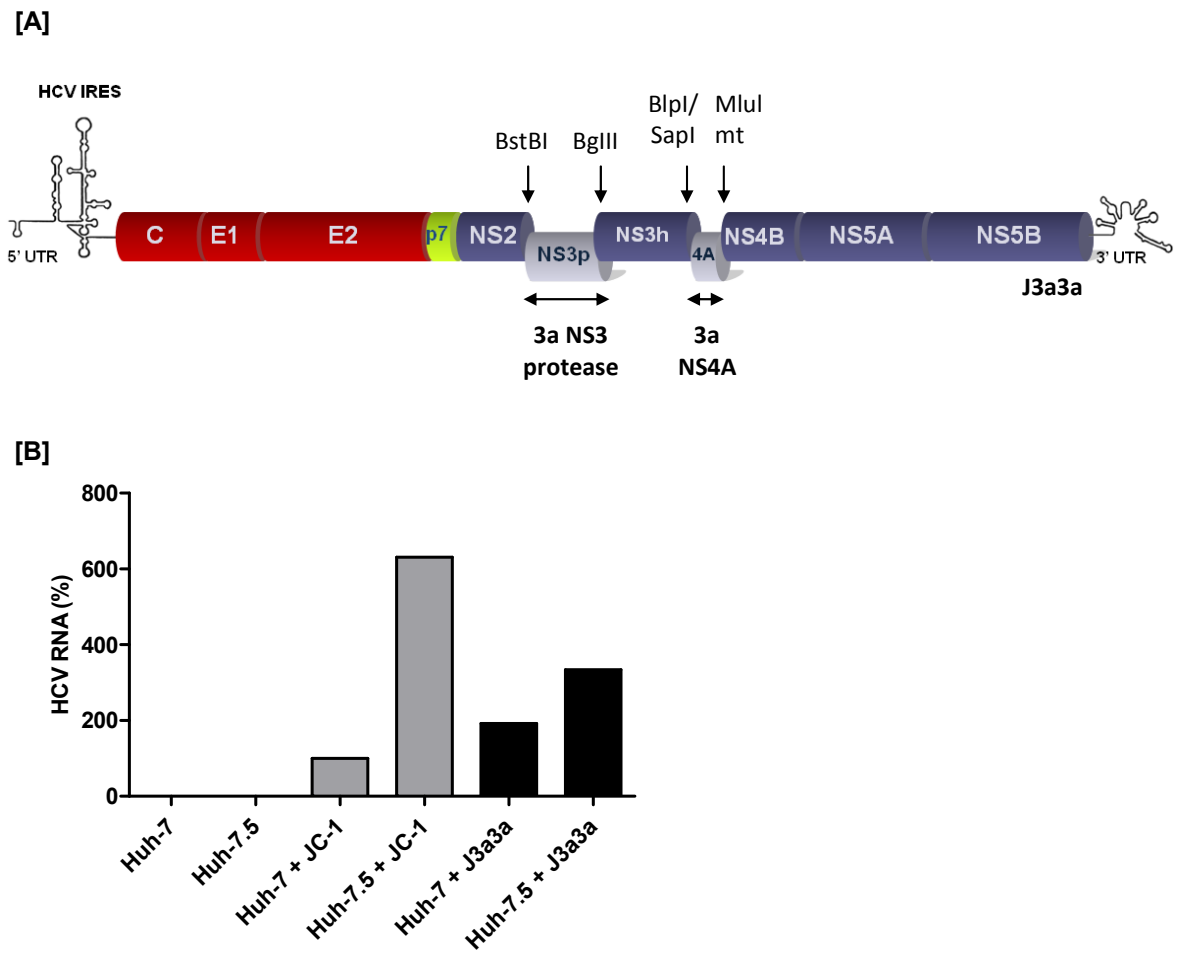


**Figure 3.9 – J3a3a recombinant chimera and its ability to replicate in Huh-7 and Huh-7.5 cells. [A] Schematic representation of the genomic map of the J3a3a chimera. Represented are the naturally occurring (*Bst*BI, *Bgl*II, *Blp*I and *Sap*I) or mutated (*Mlu*I) restriction sites used to clone the gt3a NS3 protease and NS4A cofactor coding regions in the JC-1 backbone construct (adapted from (Imhof & Simmonds, 2010)). [B] RT-qPCR analysis of J3a3a and JC-1 RNA levels in Huh-7 and Huh-7.5 cells. HCV RNA levels were normalised against endogenous levels of GAPDH mRNA expression.**

### 3.2.6 Construction of JFH1 SGR containing genotype 3a NS3-4A protease variants

To construct a SGR containing the gt3a NS3 protease and NS4A coding sequences (Figure 3.10, A-D), the NS3 protease region was amplified from the J3a3a chimera, using the oligonucleotide primers "PmeI/NcoI-NS3_Fwd" (which inserted two new restriction sites, *Pme*I and *Nco*I, at the 5' end of the fragment) and "NS3-SanDI_Rev" (which inserted a *San*DI restriction site at the 3' end of the fragment) (Figure 3.10-A). This fragment, PmeI/NcoI-NS3-SanDI, was then inserted into pGEM-T Easy to yield pGEM-PmeI/NcoI-NS3-SanDI. Subsequently, a second *Nco*I restriction site in the NS3 coding region was mutated in pGEM-PmeI/NcoI-NS3-SanDI by SDM (Figure 3.10-B), to allow the use of the newly

inserted *Nco*I site in later cloning steps. Using *Bgl*II and *San*DI restriction sites, the region encoding the NS4A cofactor was excised from the J3a3a chimera (BglII-NS3-NS5A-SanDI) and inserted into pGEM-PmeI/NcoI-NS3-SanDI vector to yield pGEM-PmeI/NcoI-NS3-NS5A-SanDI (Figure 3.10-C).

Having generated a plasmid containing the relevant NS3 protease and NS4A coding sequences from gt3a, the strategy for constructing a SGR encoding these sequences is outlined in Figure 3.10-D. The process was as follows:

1) pGEM-PmeI_EMCV-NS3-NS5A_SanDI was produced by combining 3 DNA fragments: PmeI-NcoI fragment containing the EMCV IRES generated from pLuc-SGR (numbered ① in Figure 3.10-D); XmnI-PmeI and XmnI-NcoI fragments from pGEM-PmeI/NcoI-NS3-NS5A-SanDI (numbered ② and ③ in Figure 3.10-D). Ligation of these 3 DNA fragments produced plasmid pGEM-PmeI-EMCV-NS3-NS5A-SanDI (Figure 3.10-D).

2) Using the *Pme*I and *San*DI restriction sites, a DNA fragment containing the EMCV-NS3-NS5A segment was excised from pGEM-PmeI-EMCV-NS3-NS5A-SanDI and inserted into the Luc-SGR, to generate Luc-SGR-2a3a-NS3/4A (Figure 3.10-D).

**Figure 3.10 – Cloning of the NS3-4A protease region from gt3a into Luc-SGR. [A] PCR amplification of NS3 protease coding region from J3a3a and insertion of *Pme*I/*Nco*I (3' end) and *San*DI (5' end) restriction sites using the forward "PmeI/NcoI-NS3_Fwd" and reverse "NS3-SanDI_Rev" oligos. [B] 1) Insertion of PmeI/NcoI-NS3-SanDI into the pGEM-T Easy vector; 2) deletion of a second *Nco*I restriction site by SDM. [C] Cloning of NS4A region: 1) digestion of J3a3a vector with *Bgl*II and *San*DI and 2) insertion of *Bgl*II-NS3-NS5A-*San*DI fragment into pGEM-PmeI/NcoI-NS3-SanDI. [D] Cloning of NS3-4A region from pGEM-T Easy vector into Luc-SGR: 1) Excision of EMCV IRES from Luc-SGR using PmeI and NcoI restriction sites; 2) Digestion of pGEM-PmeI/NcoI-NS3-NS5A-SanDI vector with XmnI, PmeI and NcoI; 3) Ligation of PmeI-EMCV IRES-NcoI, *Xmn*I-*Pme*I and *Nco*I-*Xmn*I fragments; 4) Using PmeI and SanDI, gt3a NS3-4A region was excised from pGEM-PmeI-EMCV-NS3-NS5A-SanDI and inserted into Luc-SGR. SDM, site-directed mutagenesis.**

**[A]**

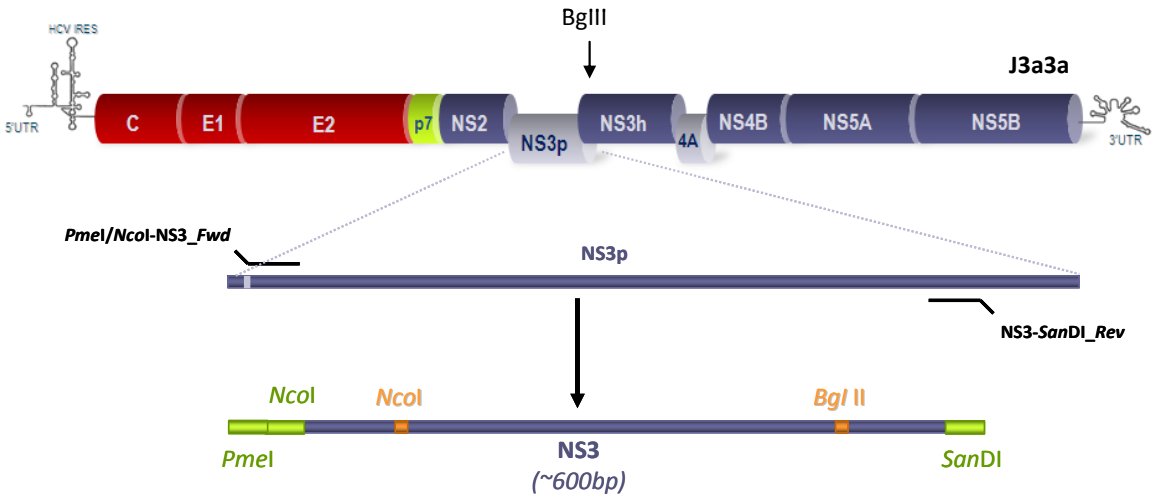


| | |
|---|---|
| *Pme*I/NcoI-NS3_*Fwd*: | **5'- GTT TAA ACC ATG GCT CCG ATC ACA GCA TAC -3'** (***Pme*I** ***Nco*I**) |
| NS3-*San*DI_*Rev*: | **5'- GGG ACC CAG TTG GAG CAT GCA AGT AC -3'** (***San*DI**) |

[B]

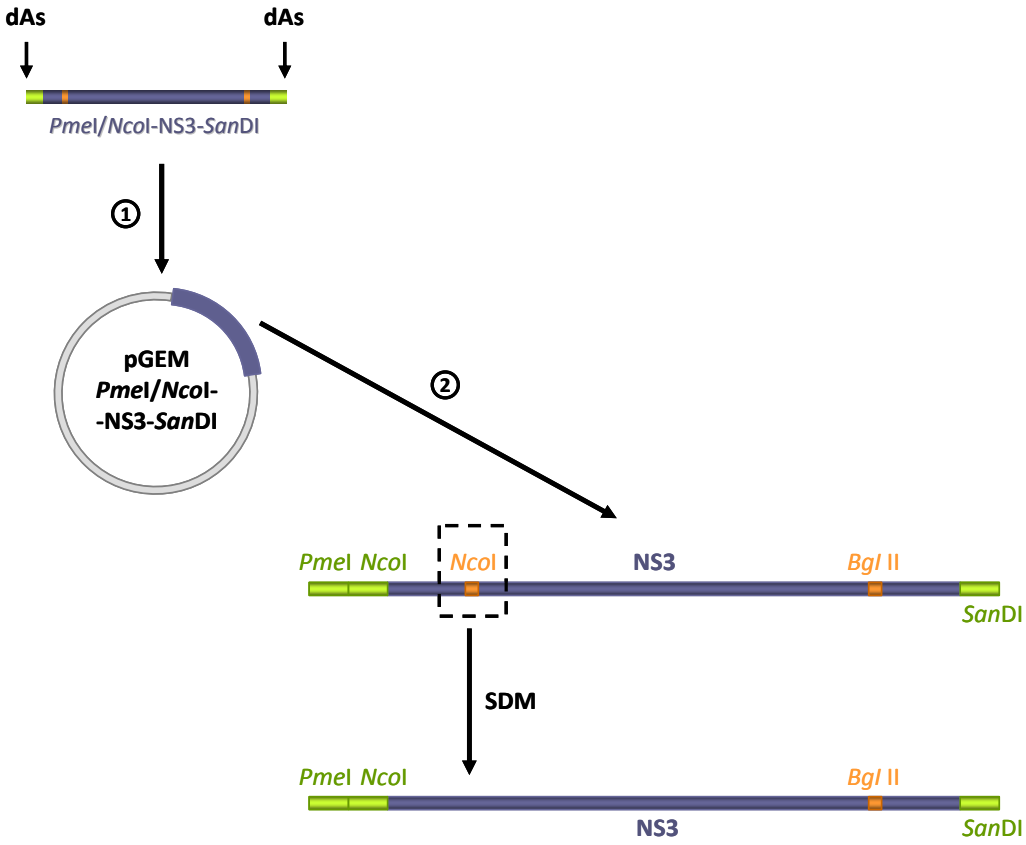


NS3_Mut/*NcoI_Fwd*: **5'- GTT ATG TGG ACT GTC TAT CAT GGT GCA GGC TCA AG-3'**

NS3-Mut/*NcoI_Rev*: **5'- CT TGA GCC TGC ACC ATG ATA GAC AGT CCA CAT AAC-3'**

**[C]**

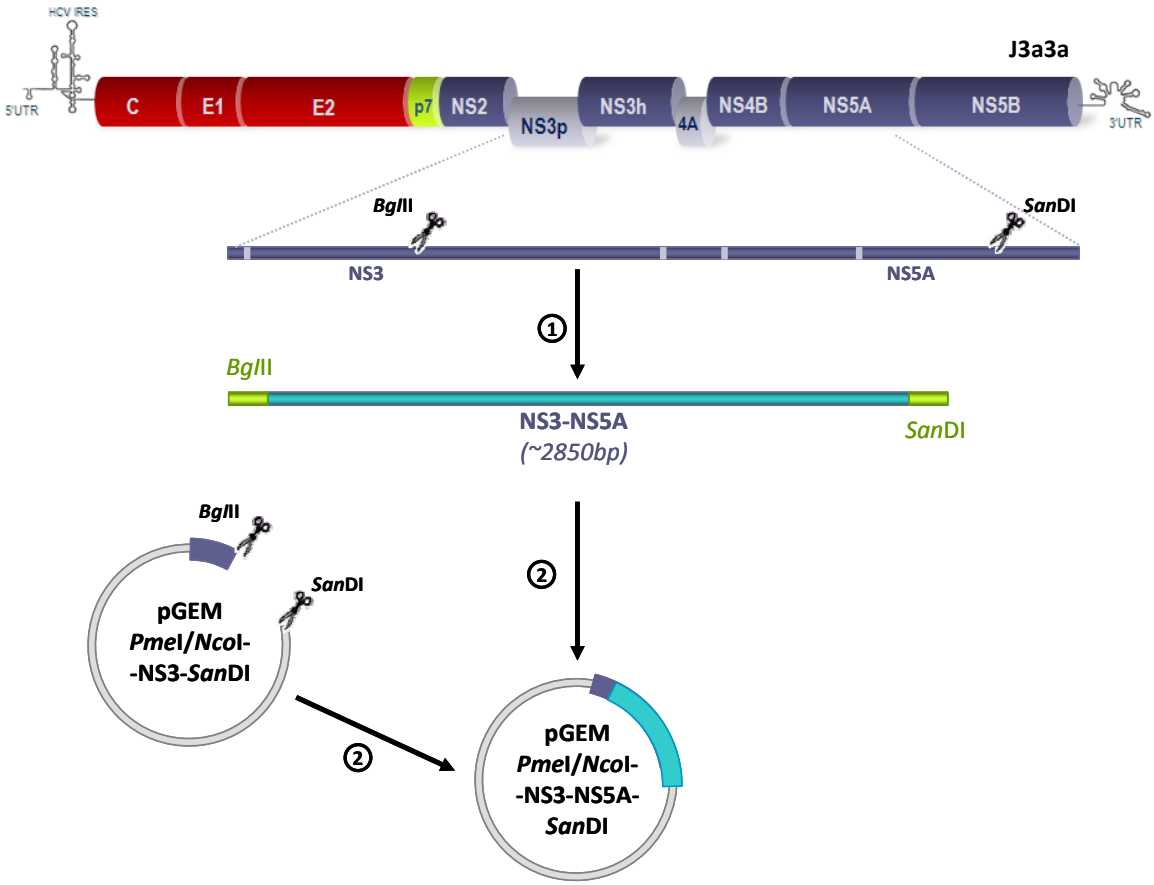
HCV IRES
5'UTR
C
E1
E2
p7
NS2
NS3p
NS3h
4A
NS4B
NS5A
NS5B
3'UTR
J3a3a
BglII
SanDI
NS3
NS5A
1
BglII
NS3-NS5A
(~2850bp)
SanDI
BglII
SanDI
pGEM
PmeI/NcoI-
-NS3-SanDI
2
2
pGEM
PmeI/NcoI-
-NS3-NS5A-
SanDI

**[D]**

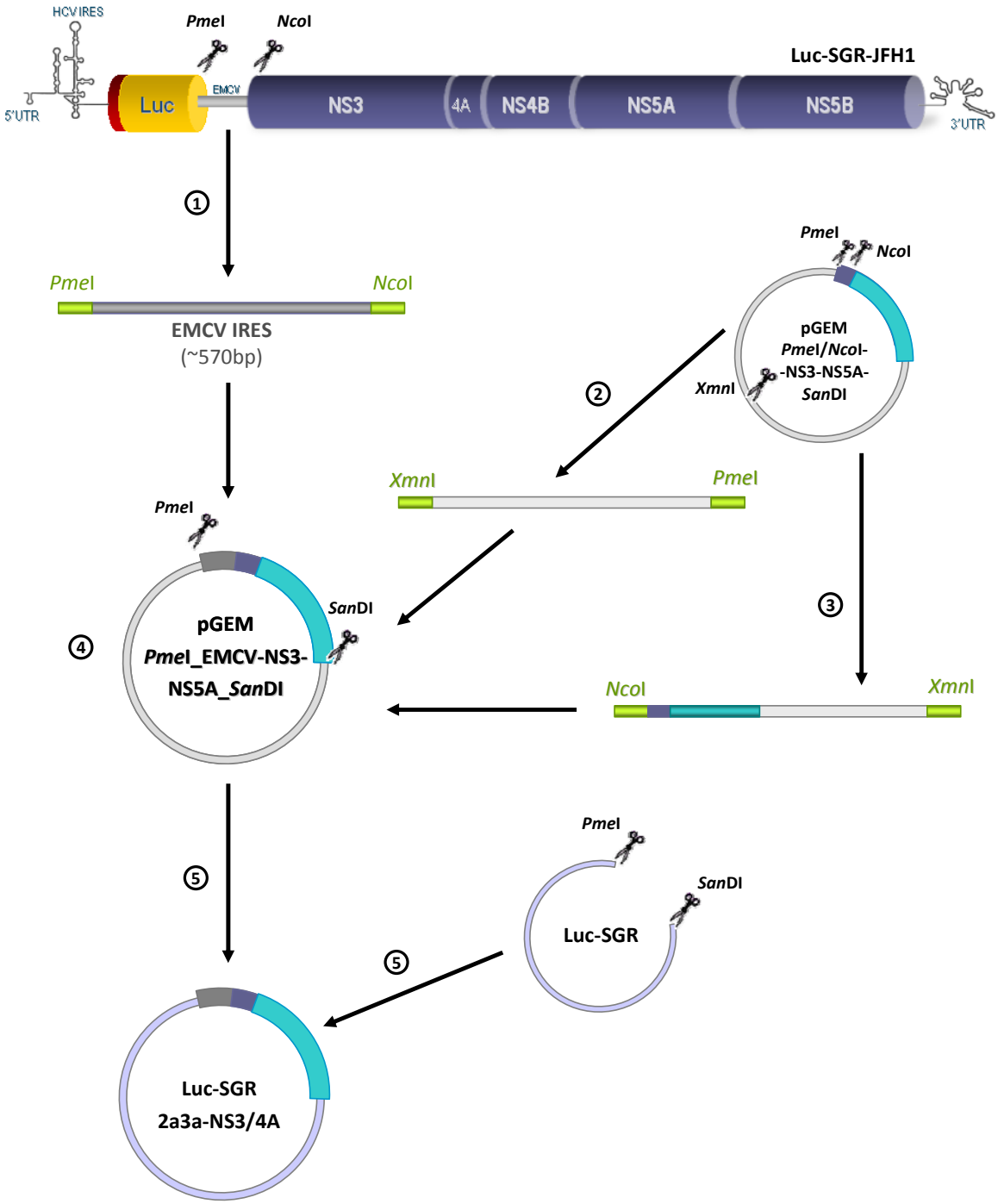
HCV IRES
PmeI
NcoI
Luc-SGR-JFH1
5'UTR
Luc
EMCV
NS3
4A
NS4B
NS5A
NS5B
3'UTR
1
PmeI
NcoI
EMCV IRES
(~570bp)
PmeI
NcoI
pGEM
PmeI/NcoI-
-NS3-NS5A-
SanDI
XmnI
2
XmnI
PmeI
PmeI
SanDI
pGEM
PmeI_EMCV-NS3-
NS5A_SanDI
4
3
NcoI
XmnI
5
PmeI
SanDI
Luc-SGR
5
Luc-SGR
2a3a-NS3/4A

### 3.2.7 Analysis of Luc-2a3a-NS3-4A-SGR replication

To determine whether the introduction of NS3 and NS4A gt3a sequences affected transient replication of the JFH1 SGR, RNA from Luc-2a3a-NS3-4A was electroporated into Huh-7 cells and the activity of luciferase was measured for up to 72h (Figure 3.11). RNAs from Luc-WT and Luc-GND were also electroporated into cells and used as positive and negative controls respectively.

Luciferase activity from Luc-WT and Luc-GND followed the same pattern as seen previously. Thus, enzyme activity increased between 4 and 72h for Luc-WT whereas luciferase values from Luc-GND decreased over the corresponding period. Luc-2a3a-NS3-4A gave the same pattern of luciferase activity as Luc-GND, indicating that replacement of the JFH1 NS3 protease and NS4A cofactor with gt3a sequences in Luc-WT was not tolerated in short-term transient assays in Huh-7 cells.

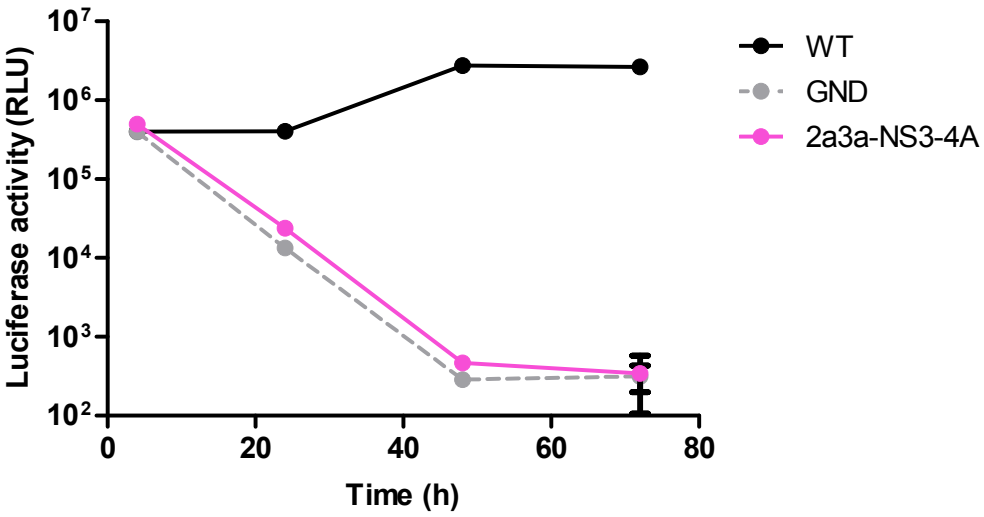


**Figure 3.11 – Luc-2a3a-NS3-4A cannot replicate in Huh-7 cells. Huh-7 cells were electroporated with WT, GND and 2a3a-NS3-4A Luc-SGRs. The cells were lysed at 4, 24, 48 and 72h after electroporation and the extracts used for measuring the luciferase activity. RLU, relative light units.**

Given that Huh-7.5 cells generally support higher levels of HCV replication than Huh-7 cells, it was thought that Luc-2a3a-NS3-4A might also replicate better in Huh-7.5 cells. To that end, RNA transcripts from Luc-WT, Luc-GND and Luc-2a3a-NS3-4A were electroporated into both cell lines and luciferase activity assessed at 4, 24, 48 and 72h after electroporation. As shown in Figure 3.12, the luciferase activity in both Huh-7/WT and Huh-7.5/WT cells increased from 4 to 72h after electroporation. By contrast for Luc-GND, the luciferase values decreased throughout all time points in both cells lines. As before, luciferase activity from Luc-2a3a-NS3-4A gave similar levels to Luc-GND in Huh-7 cells, indicating its inability to replicate. When electroporated into Huh-7.5 cells, Luc-2a3a-NS3-4A activity decreased between 4 and 48h. However, a 5- to 6-fold increase in luciferase activity was detected between 48 and 72h, suggesting that Luc-2a3a-NS3-4A could replicate in Huh-7.5, although with much lower efficiency than the WT replicon. These data were reproducible in further experiments (J. Liefhebber, *pers. comm.*).

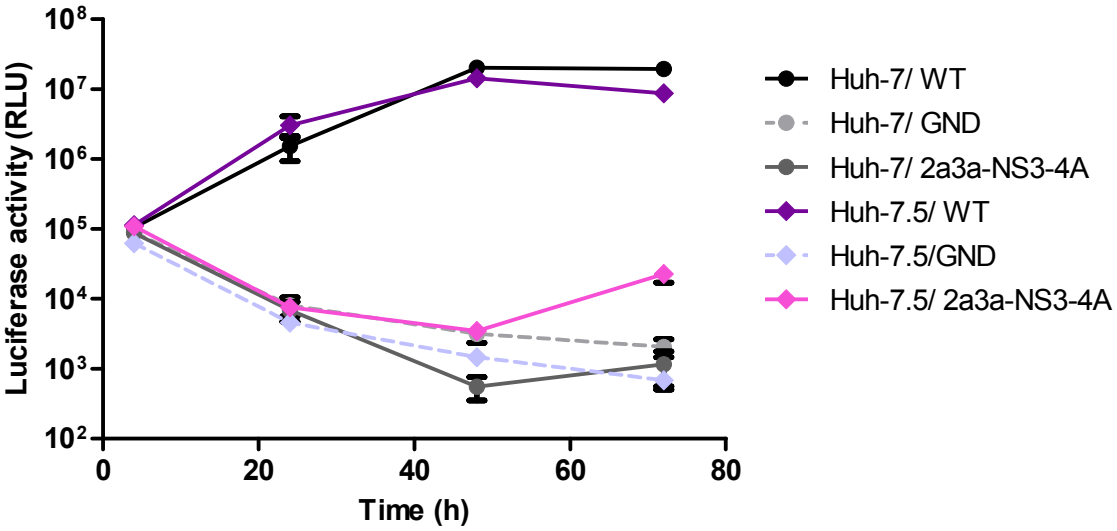


**Figure 3.12 – Transient replication assay of Luc-WT, Luc-GND and Luc-2a3a-NS3-4A electroporated in Huh-7 and Huh-7.5 cells; the cells were lysed at 4, 24, 48 and 72h after electroporation and the extracts used for measuring the luciferase activity. RLU, relative light units.**

## 3.3 Characterisation of ability of HepaRG cells to replicate HCV genomes

As mentioned previously, *in vitro* studies on HCV infection and replication have been possible due to the use of permissive Huh-7 and Huh-7-derived cell lines that support the virus life cycle. Despite the advantages of these cells, they do not fully recapitulate all aspects of HCV replication in naturally infected hepatocytes. To gain a better understanding of HCV-host interactions, alternative cellular models which exhibit more hepatocyte-like characteristics than Huh-7 cells are needed. In this context, we sought to investigate the feasibility of replicating HCV RNAs in HepaRG cells, which have a similar gene expression pattern to primary human hepatocytes and human liver tissue (Hart *et al.*, 2010).

### 3.3.1 HepaRG cells are not permissive for transient HCV replication

To investigate whether HepaRG cells could support HCV replication, Luc-WT was used since it allows rapid and transient assessment of viral RNA synthesis. RNA transcripts from Luc-WT and Luc-GND were introduced into Huh-7 and HepaRG cells and luciferase activity in cell extracts was assayed at time intervals up to 72h after electroporation (Figure 3.13-A). Luciferase values generated by Luc-WT in Huh-7 cells (Huh-7-WT) decreased slightly between 4 and 24 h and then increased (about 6 fold) until 72h after electroporation. By contrast, luciferase values decreased throughout all the time points for Luc-GND (Huh-7-GND), as shown in previous experimental data. In HepaRG cells, the luciferase values produced by both the Luc-WT and Luc-GND replicons (HepaRG-WT and -GND, respectively) followed a similar pattern to Huh-7-GND between 4 and 72h (Figure 3.13-A).

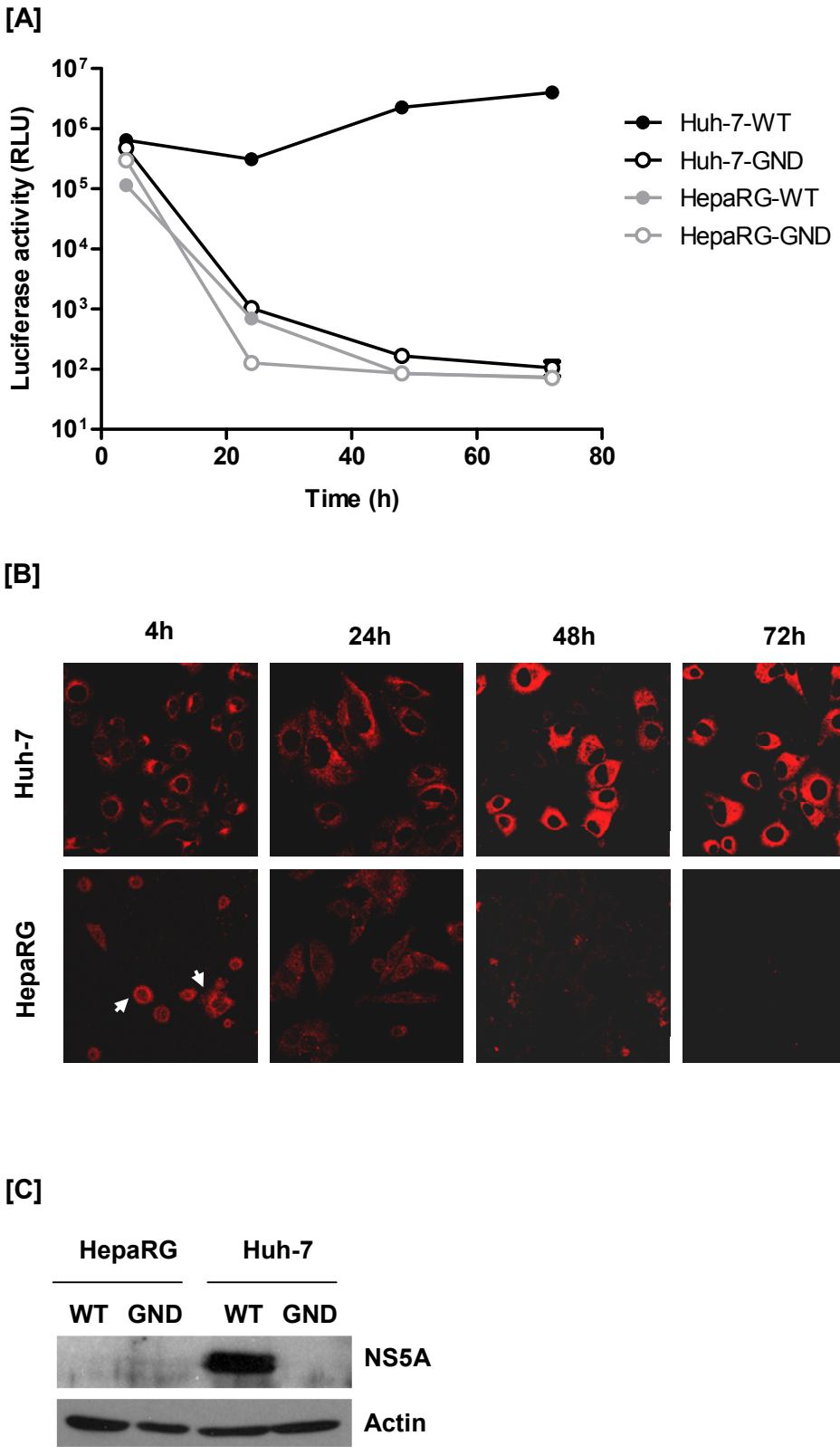


**Figure 3.13 – HCV SGR replicons cannot replicate in HepaRG cells. [A] Huh-7 and HepaRG cells were electroporated with *in vitro* transcribed Luc-WT and Luc-GND RNAs. Cell extracts were assayed for luciferase activity at 4, 24, 48 and 72h after electroporation. RLU, relative light units. [B] Intracellular localization of NS5A protein: Huh-7 and HepaRG cells containing Luc-WT replicons were fixed at 4, 24, 48 and 72h after electroporation and the cells stained for NS5A protein using anti-NS5A antisera. White arrows indicate NS5A expressing cells. [C] Extracts from Huh-7 and HepaRG cells electroporated with Luc-WT and Luc-GND were prepared at 72h post-electroporation and examined by Western blot analysis with anti-NS5A and anti-actin antisera.**

The correlation between luciferase activity and viral protein synthesis in both Huh-7 and HepaRG cells with Luc-WT was examined by indirect immunofluorescence and Western blot analysis. Immunofluorescence analysis revealed that NS5A expression could be detected in Huh-7 cells electroporated with Luc-WT RNA as early as 4h and 24h, and the abundance of intracellular protein increased by 48h and 72h (Figure 3.13-B). By contrast, NS5A expression was barely detectable at early time-points (Figure 3.13-B, white arrows indicate NS5A expressing cells) in HepaRG cells and by 48h and 72h expression of the protein was not observed.

Detection of NS5A protein by Western blot analysis was only examined at 72h post-electroporation (Figure 3.13-C). Analysis of cell extracts revealed that expression of NS5A was readily observed in Huh-7-WT, however in Huh-7-GND, NS5A was not detected. NS5A expression from either the Luc-WT or -GND replicons was not found in HepaRG cells. Analysis of the abundance of actin in each sample revealed that approximately equivalent amounts of cell protein were present in the extracts. These results are in agreement with the data from the luciferase assays and together indicate that HepaRG cells cannot support HCV RNA synthesis during transient assays.

### 3.3.2 HepaRG cells can efficiently translate HCV SGR RNAs

To determine whether the lack of HCV replication in HepaRG cells could be linked to low efficiency in the translation of input replicon RNAs, Luc-WT RNA was electroporated into Huh-7 and HepaRG cells and the extent of translation was determined between 1 and 8h, which is prior to the onset of detectable replication (typically 12-14h in Huh-7 cells (Jones *et al.*, 2007)). As shown in Figure 3.14, luciferase values in Huh-7 cells increased about 25-fold between 1 and 4h after electroporation. After 4h, luciferase activity decreased slightly and reached a plateau by 8h. In HepaRG cells, the luciferase values closely followed the same pattern as in Huh-7 cells during the first 4h after electroporation, but the enzyme levels were about 5-fold lower. In the following 4h (between 4 and 8h after electroporation) luciferase activity continued to rise, reaching levels at 8h which were almost identical to those in Huh-7 cells. These results suggest that the inability of HepaRG cells to support transient HCV replication is not linked to an inability to translate input viral RNA.

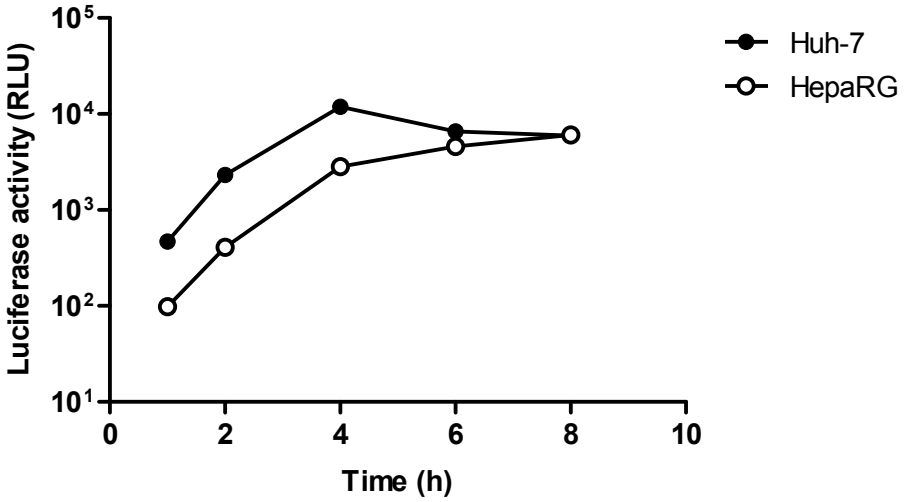


**Figure 3.14 - Translation of Luc-SGRs in Huh-7 and HepaRG cells. Huh-7 and HepaRG cells were electroporated with *in vitro* transcribed Luc-WT RNA and assayed for luciferase activity at 1, 2, 4, 6 and 8h after electroporation. RLU, relative light units.**

### 3.3.3 HCV can replicate in HepaRG cells in stable replication assays

To further investigate whether HepaRG cells could support HCV replication, RNA transcripts from subgenomic replicons carrying the neomycin resistance gene were electroporated into cells and their ability to form drug-resistant colonies was assessed by 3–4 weeks after electroporation. In these experiments, RNA was made from SGR constructs in which the neomycin selectable marker gene (*neo*) replaced the Luc reporter gene (Neo-SGR-WT and –GND), thereby permitting selection of drug-resistant colonies in the presence of G418.

To determine whether HepaRG cells could form drug-resistant colonies, Neo-SGR-WT and -GND RNA transcripts (hereafter referred as Neo-WT and Neo-GND respectively) were electroporated into Huh-7 and HepaRG cells and incubated for 3-4 weeks in the continuous presence of G418 to select for cells that were neomycin resistant. After 3-4 weeks, the drug-resistant colonies were stained with Coomassie Brilliant blue. From the results shown in Figure 3.15, the colony-forming capacity in both cell lines was visibly different and by comparison with Huh-7 cells, HepaRG cells had a lower capacity to form neomycin resistant colonies. Nevertheless, the ability to recover drug-resistant colonies with HepaRG cells suggested that the Neo-WT replicon could constitutively replicate, albeit at a much lower efficiency compared to Huh-7 cells. Thus, contrary to the data from the experiments with transient assays,

HepaRG cells could support HCV replication in an assay that relied on constitutive replication.

Following the above results, it was possible to select a population of drug-resistant HepaRG cells containing HCV replicons. To expand the range of antibiotics that could be used for selection, another replicon was used that replaced the *neo* gene with the blasticidin resistance gene (*blast*). In parallel experiments, growth of HepaRG cells in the presence of blasticidin gave more rapid cell killing as compared to G418 (data not shown). Preliminary data with populations of cells harbouring the blasticidin-resistant replicon (Blast-SGR-WT) also revealed detection of NS5A while the protein was rarely found in cells with the neo replicon (data not shown). As a consequence, further experiments were performed on blasticidin-resistant HepaRG replicon cells.

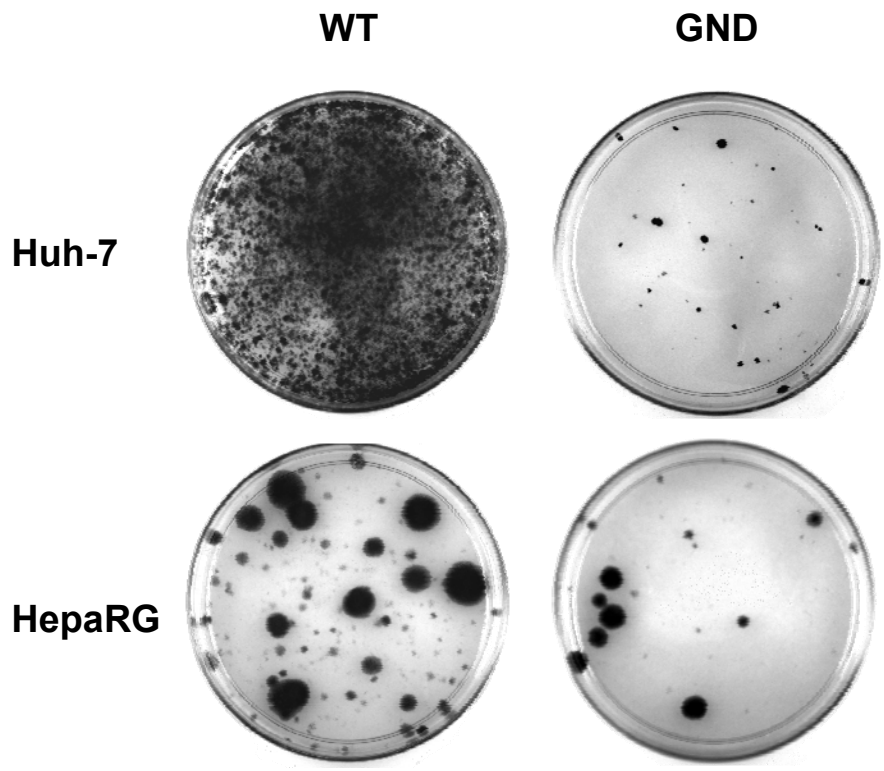


**Figure 3.15 – Colony-forming capacity in Huh-7 and HepaRG cells. Huh-7 and HepaRG cells were electroporated with G418-selectable replicons (Neo-WT and Neo-GND). After 3-4 weeks of incubation with the antibiotic, drug-resistant colonies were stained with Coomassie Brilliant blue.**

To characterize the HCV subgenomic replicon in HepaRG cells, a population of blasticidin-resistant cells (hereafter referred to as HepaRG-SGR) was examined for the presence of NS5A protein and dsRNA by indirect immunofluorescence (Figure 3.16-A). The presence of viral dsRNA was analysed using the J2 antibody, previously described as an indicator of putative sites of RNA replication (Targett-Adams *et al.*, 2008). For comparative purposes, Huh-7 replicon cells (Huh-7-SGR) were used as control. Huh-7-SGR and HepaRG-SGR cells were fixed and probed with anti-NS5A antisera and monoclonal J2 antibody. In Huh-7-SGR cells, immunofluorescence analysis revealed that most of the cells were positive for NS5A expression (~99% of the cells) and the viral protein was widely distributed throughout the cell cytoplasm. The distribution of dsRNA in these cells was punctate and in some areas colocalization of J2 and NS5A was evident (Figure 3.16-A-i). By contrast, in HepaRG-SGR cells, only 5 to 10% of the cell population expressed NS5A protein. In these cells, NS5A was also distributed throughout the cell cytoplasm, but exhibited a more punctuate localization than in Huh-7 cells. The distribution of dsRNA in most of the HepaRG-SGR cells followed the distribution of NS5A, and contrary to Huh-7-SGR cells, J2 and NS5A colocalized to a greater extent in these cells (Figure 3.16-A-ii).

Expression of NS5A protein was also examined by Western blot analysis. Extracts from Huh-7-SGR cells revealed the presence of high levels of NS5A protein. By contrast, much lower, but detectable amounts of NS5A were observed in HepaRG-SGR cells (Figure 3.16-B). In addition, NS5A in the HepaRG-SGR cells was present as two species, representing the hypo- (56 kDa) and hyperphosphorylated (58 kDa) forms of the protein, which are typically found in cells containing the replicon. In Huh-7-SGR cells, it was not possible to identify two species due to the excessive amount of protein detected.

In addition to these results, steady-state levels of replicon RNA were monitored for up to 14 passages during establishment of the respective Huh-7-SGR and HepaRG-SGR cell lines by RT-qPCR analysis. As shown in Figure 3.16-C, the range in viral RNA levels in Huh-7 cells were 7- to 33-fold greater than those in HepaRG cells. Nonetheless, replicon RNA could be detected in HepaRG-SGR cells during the establishment of the replicon cell line and together with the results from the colony-forming experiments, suggest that HepaRG cells can support HCV replication in long-term replication assays.

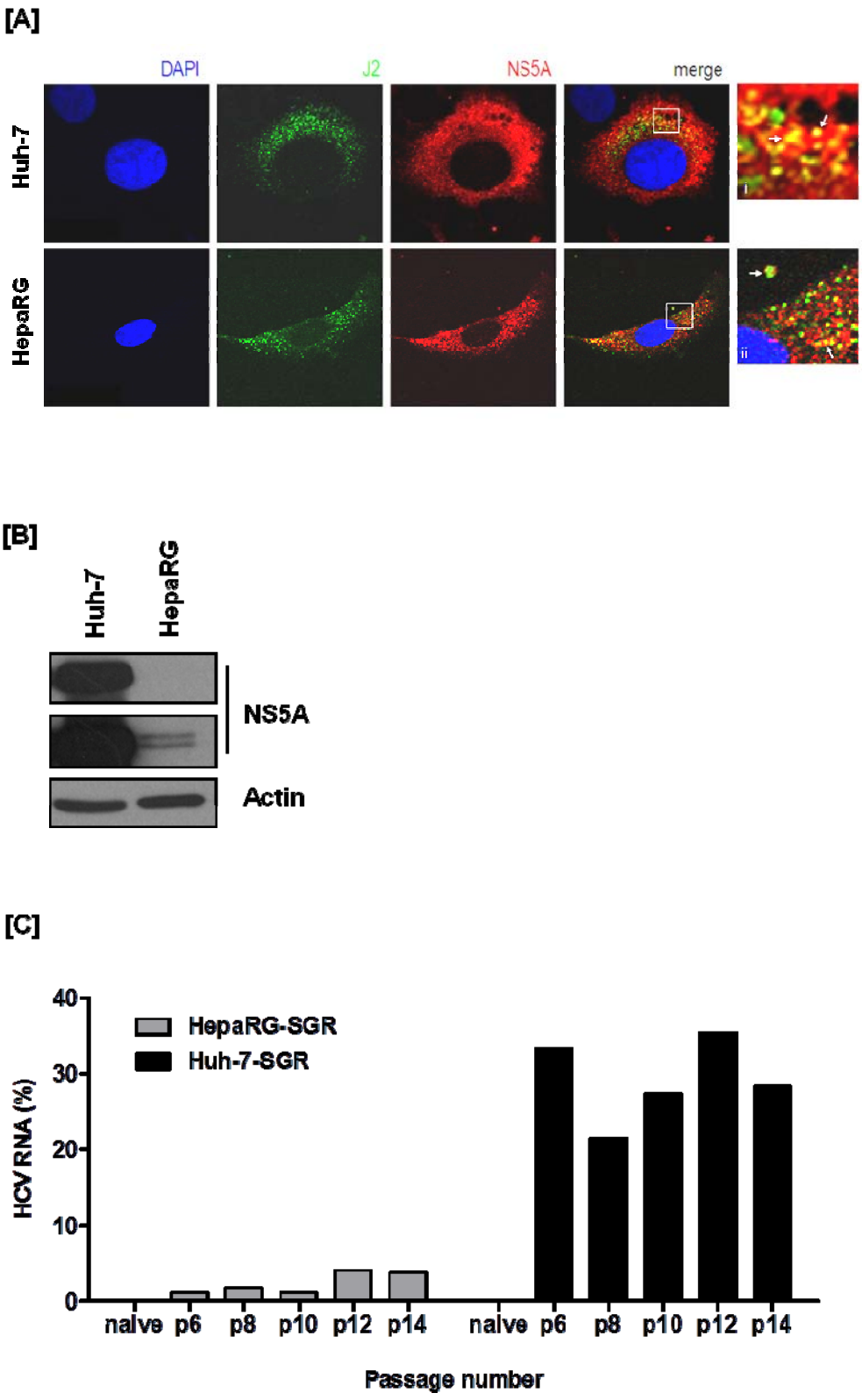


**Figure 3.16 – Stable HCV replication in HepaRG cells. [A] Immunofluorescence analysis of NS5A and dsRNA localisation in Huh-7 and HepaRG replicon cells. For visualization of nuclei, the cells were stained with DAPI. Boxed regions are shown enlarged in panels i and ii (right side of respective cells). Arrows indicate colocalization of dsRNA and NS5A in replicon-containing cells. [B] Cell extracts from Huh-7 and HepaRG replicon cells were probed with NS5A and actin antisera. Upper NS5A blot represents a lower exposure time, and the lower NS5A blot represents a higher exposure time. [C] RT-qPCR analysis of steady-state levels of replicon RNA in Huh-7 and HepaRG replicon-containing cells during early passages. HCV RNA levels were normalised against endogenous levels of GAPDH mRNA.**

### 3.3.4 HepaRG cells are not permissive for HCVcc infection

To determine the permissiveness of HepaRG cells to HCV infection, JC-1 virus was used (Figure 3.8). To generate a stock of infectious virus, Huh-7 cells were electroporated with JC-1 RNA and the supernatant was removed at 48h. The virus titre was estimated as $6.5x10^4$virus/ml by $TCID_{50}$ analysis and then used as the inoculum to infect Huh-7 and HepaRG cells. In order to include a negative control for virus production, the inoculum was exposed to UV light to inactivate the virus. As shown in Figure 3.17-A, the UV-inactivated inocula lost the ability to establish infection in Huh-7 cells, when compared with non-inactivated stock. Quantitative analysis of intracellular viral RNA further confirmed that only the non-inactivated inoculum retained the ability to replicate in Huh-7 cells (Figure 3.17-B).

Using this information, JC-1 and JC-1/UV (virus exposed to UV light for 2 minutes) were used to infect Huh-7 and HepaRG cells at a moi of 0.4. At 6, 24 and 48h after infection, RNA was extracted from cells and viral RNA levels were assessed by RT-qPCR. As shown in Figure 3.18, JC-1 replicated efficiently in Huh-7 cells, as the RNA levels increased throughout the infection period. By contrast, the UV-inactivated virus did not produce detectable levels of viral RNA over the same time period. In HepaRG cells, viral RNA was only detected at 6h after infection and in the following 24 and 48h these levels decreased, similar to the JC-1/UV virus, indicating that HepaRG cells could not support infection and replication of JC-1.

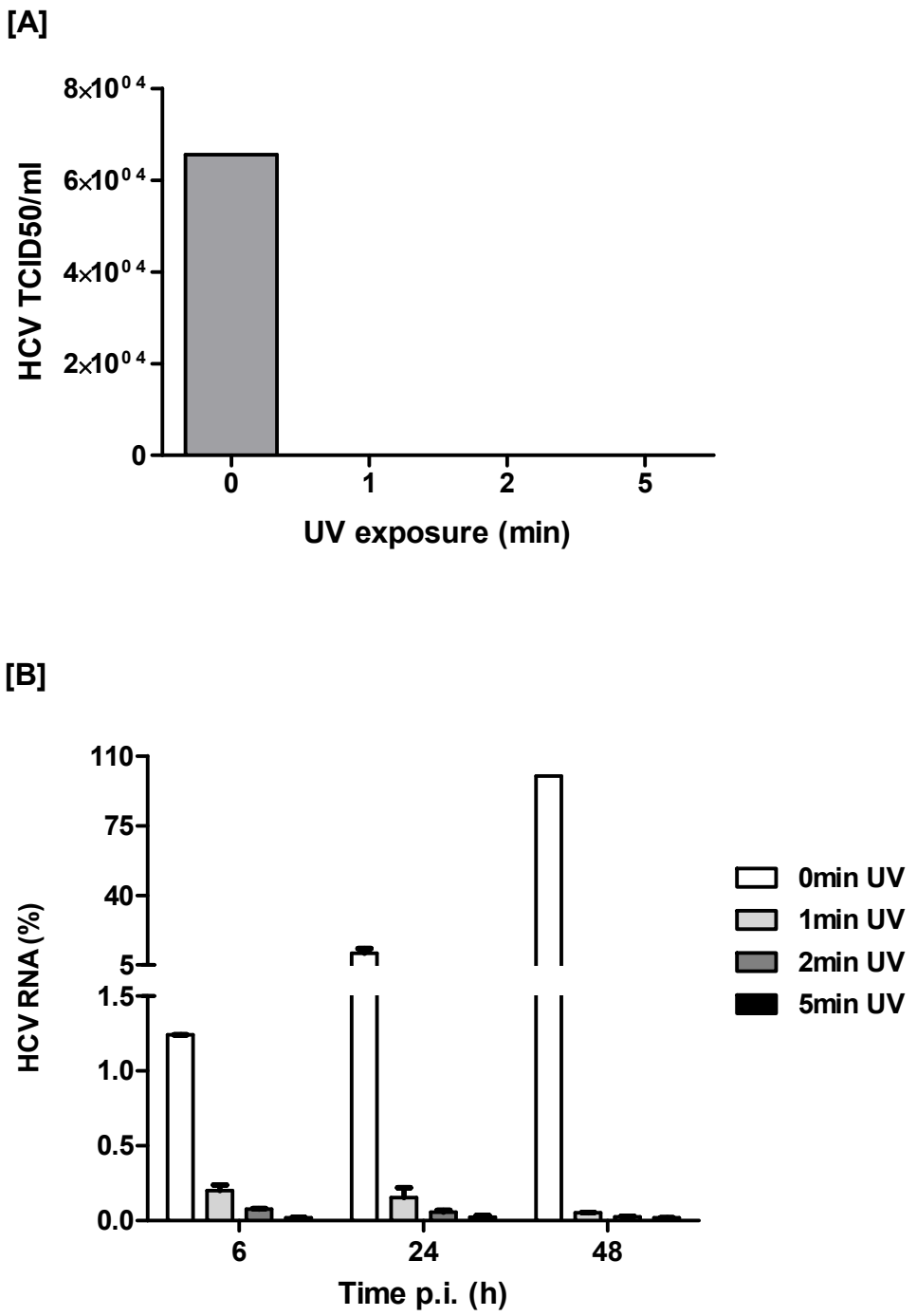


**Figure 3.17 - Infection of Huh-7 cells with UV-inactivated virus. Huh-7 cells were infected with JC-1 or JC-1/UV for up to 48h. [A] TCID50/ml of JC-1 inocula exposed to 0, 1, 2 and 5min of UV light. [B] Levels of HCV RNA were determined by RT-qPCR analysis normalised against abundance of GAPDH mRNA.**

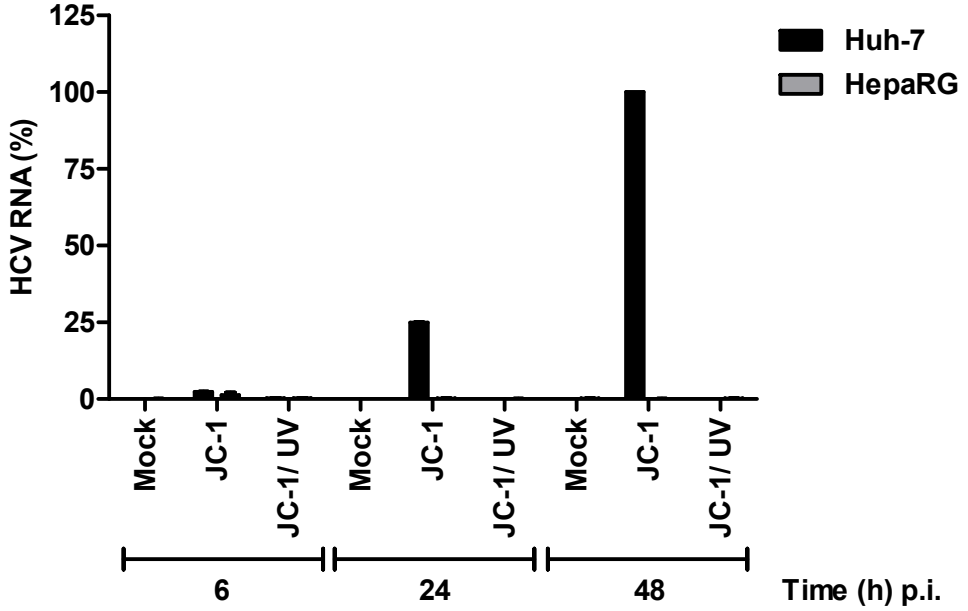


**Figure 3.18 – HepaRGs are not permissive to HCV infection. Huh-7 and HepaRG cells were infected with JC-1 or JC-1/UV for up to 48h. Levels of HCV RNA were determined by RT-qPCR analysis and normalised against abundance of GAPDH mRNA.**

### 3.3.5 Innate immune responses may dictate the permissiveness of HepaRG cells to viral replication

The permissiveness of Huh-7 cells to HCV infection and replication *in vitro* is thought to be linked with an impaired antiviral response (Keskinen *et al.*, 1999; Li *et al.*, 2005a). By contrast, HepaRG cells may retain the ability to mount a robust antiviral response upon HCV replication. To investigate whether the reduced permissiveness of HepaRG cells to HCV infection and replication could be linked with an intact innate response, IFN-regulated pathways were examined in these cells.

The innate immune system represents the first line of defence against invading viral pathogens. Following infection, recognition of conserved molecular signatures expressed by the virus (pathogen associated molecular patterns, PAMPs) are recognised by specialised pattern recognition receptor molecules (PRR), such has TLR3 and RIG-I. This interaction initiates TLR3- and RIG-I-dependent signalling pathways leading to induction and release of type I IFNs (Figure 3.19). Binding of type I IFNs to IFNα/β receptors (IFNR1/2) on the cell surface activates Jak/STAT signalling pathways and stimulation of a wide array of IFN-stimulated genes (ISGs) (Figure 3.19). Most of these genes encode antiviral proteins which can mediate antiviral activities and are likely to influence the outcome of infection.

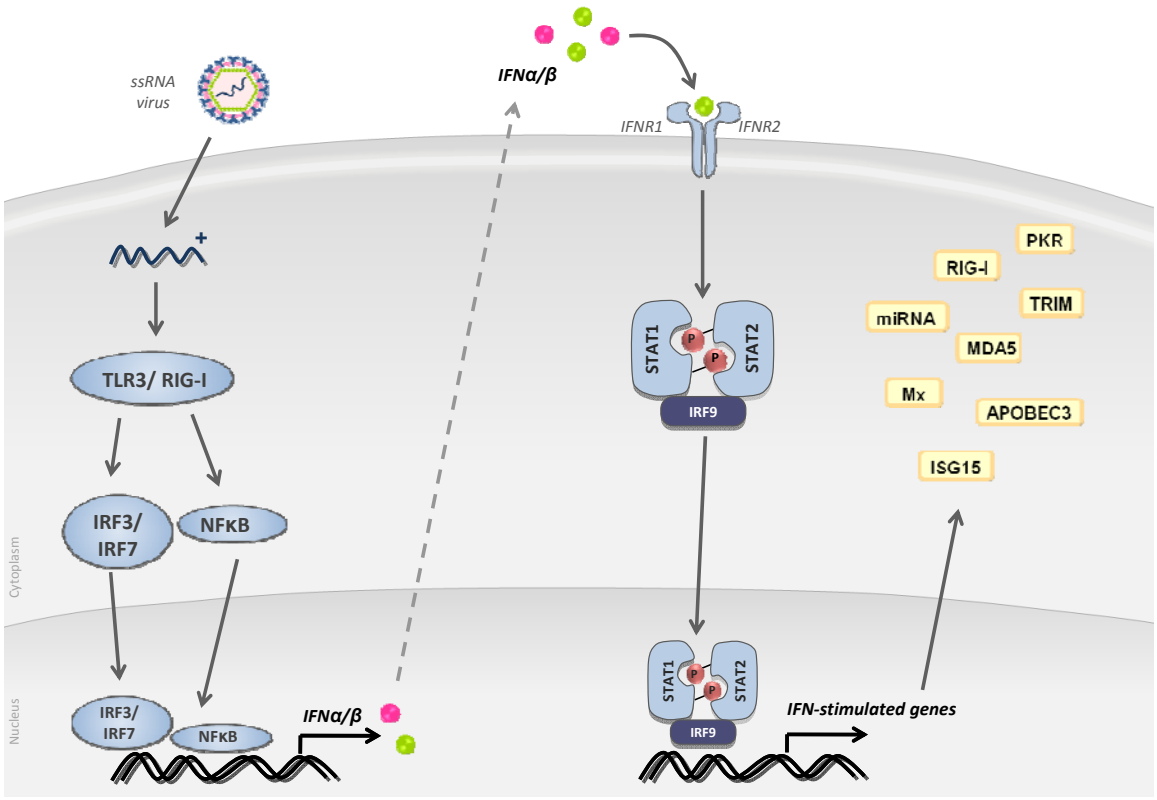


**Figure 3.19– dsRNA signalling and activation of type I IFN pathways. Upon infection, viral RNA can signal through RIG-I/TLR3-dependent pathways and induce the production of IFNα/β. IFNα/β bind to type I IFN receptors at the cell surface and activate Jak/STAT signalling cascade, which induces the synthesis of hundreds of IFN-stimulated genes (ISGs).**

#### 3.3.5.1 IFN signalling through the JAK/STAT pathway is functional in HepaRG cells

To analyse the kinetics of type I and type II IFN-inducible gene expression, HepaRG and Huh-7 cells were treated with increasing doses of IFNα, β and γ. At 48h after treatment, ISG induction was assessed my measuring ISG15 RNA and protein expression levels. As shown in Figure 3.20-A, ISG15 mRNA increased in a dose-dependent manner in response to IFNα and β in Huh-7 cells, but was less efficiently induced by IFNγ. Similarly ISG15 mRNA expression increased in HepaRG cells following treatment with IFNα and β, but to a lesser extent with IFNγ. However, the ISG15 levels detected in HepaRG cells were ~4-fold (IFNα treated) and ~2-fold lower (IFNβ treated) than in Huh-7 cells (Figure 3.20-C). Analysis of protein synthesis revealed that following IFNα and β treatment, high levels of both conjugated and free ISG15 protein were detected in both Huh-7 and HepaRG cells (Figure 3.20-B & D). Similar to the RNA data, IFNγ proved to be a poor inducer of ISG15 protein. Thus, these data indicate that IFN signalling through Jak/STAT pathway is intact in both Huh-7 and HepaRG cells.

**Figure 3.20- Type I IFNs are strong inducers of ISG15. HepaRG and Huh-7 cells were treated with increased doses (0, 50, 100 and 200U/ml) of IFNα, β and γ. At 48h after treatment cells extracts were used for RT-qPCR analysis of ISG15 mRNA expression (A – Huh-7 and C – HepaRG cells) and Western blot analysis (B – Huh-7 and D – HepaRG cells) of ISG15 free and conjugated forms using anti-ISG15 antisera.**

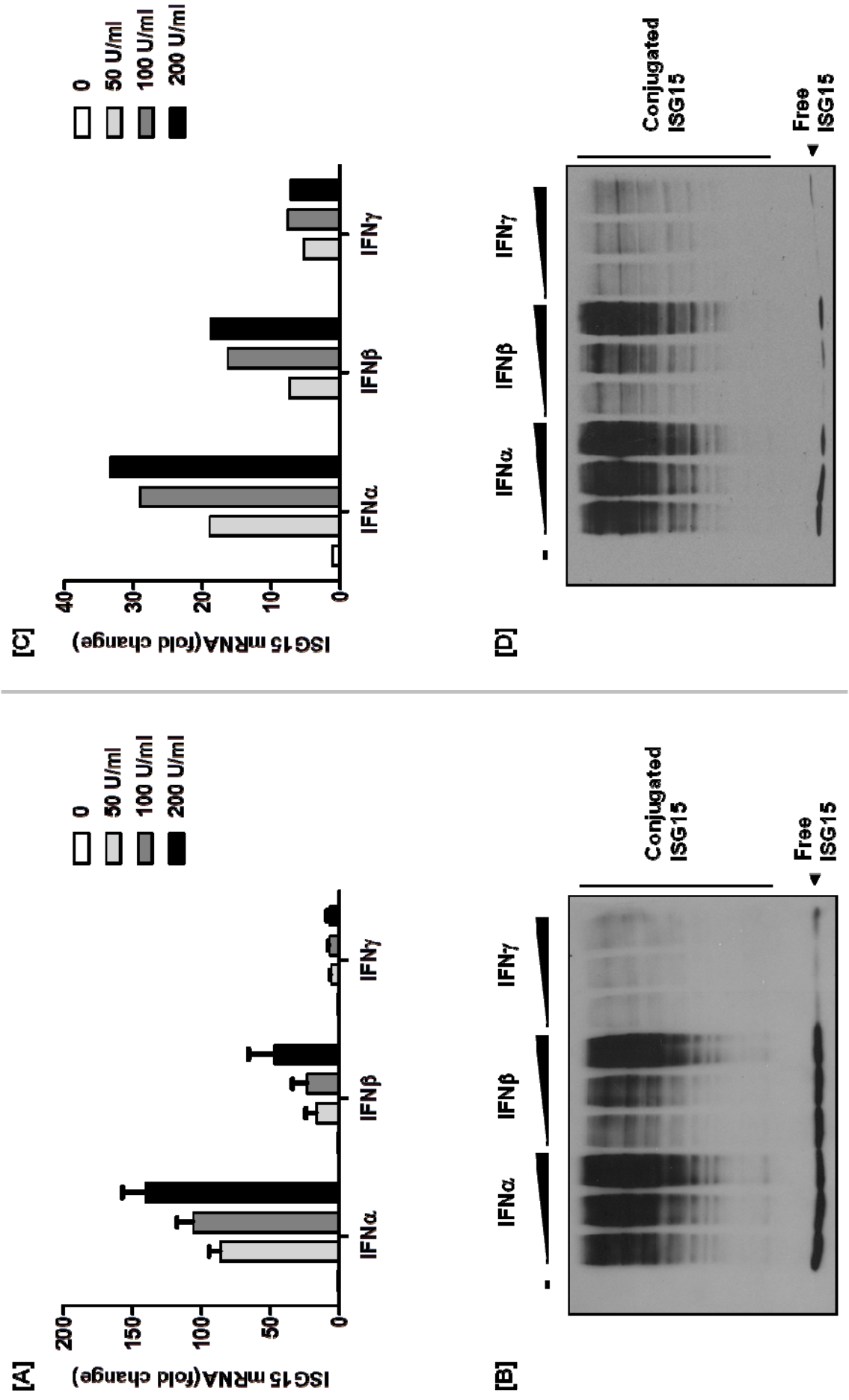
[A]
ISG15 mRNA(fold change)
0
50
100
150
200
0
50 U/ml
100 U/ml
200 U/ml
IFNα
IFNβ
IFNγ
[B]
IFNα
IFNβ
IFNγ
-
Conjugated ISG15
Free ISG15
[C]
ISG15 mRNA(fold change)
0
10
20
30
40
0
50 U/ml
100 U/ml
200 U/ml
IFNα
IFNβ
IFNγ
[D]
IFNα
IFNβ
IFNγ
-
Conjugated ISG15
Free ISG15

### 3.3.5.2 HepaRG cells sense extracellular and intracellular poly-I:C and induce the expression of ISG15

To further characterise the responsiveness of HepaRGs cells, they were treated with poly-I:C. Poly-I:C is a synthetic analogue of dsRNA which is recognised by TLR3 (extracellular) or RIG-I/MDA5 (intracellular) receptors. Activation of these receptors promotes the induction of type I IFNs and consequently the expression of ISGs. For comparative purposes, Huh-7 cells were used in these experiments, as they have been previously shown to be defective for poly-I:C signalling through TLR3 (Li *et al.*, 2005a).

Poly-I:C was added to monolayers of HepaRG and Huh-7 cells and at 6, 24 and 48h, ISG15 expression was analysed by RT-qPCR. As shown in Figure 3.21, poly-I:C failed to induce ISG15 at any time-point in Huh-7 cells. By contrast, ISG15 expression increased about 20-fold by 6h after poly-I:C treatment in HepaRG cells, when compared with mock-treated cells (Figure 3.21); by 24 and 48h ISG15 expression decreased. Thus, contrary to Huh-7 cells in which TLR3 is defective, HepaRG cells retained the ability to sense extracellular poly-I:C, suggesting that TLR3 signalling is intact in these cells.

To examine whether cytoplasmic signalling responses were intact in HepaRG cells, poly-I:C was transfected into the cells, to mimic intracellular dsRNA generated during viral replication. For comparative purposes, in addition to HepaRG and Huh-7 cells, Huh-7.5 cells were also used in these experiments. Huh-7 cells contain a functionally intact RIG-I signalling pathways whereas Huh-7.5 cells are defective in this pathway as a result of a point mutation within RIG-I CARD-like homology domain (Sumpter *et al.*, 2005). HepaRG, Huh-7 and Huh-7.5 cells were transfected with 5ug/ml of poly-I:C and the ability to induce ISG15 expression was analysed at 24h by RT-qPCR. As shown in Figure 3.22, ISG15 levels increased ~160 fold in response to poly-I:C in HepaRG cells, when compared to the levels in mock-treated cells. Interestingly, high levels of ISG15 were induced in response to poly-I:C transfection in Huh-7 cells, indicating that TLR3-independent signalling was used for sensing dsRNA in these cells, such as the RIG-I pathway. As expected, Huh-7.5 cells which are defective in both TLR3 and RIG-I signalling, did not respond to intracellular poly-I:C (Figure 3.21). Thus, in contrast to Huh-7 cells, HepaRG cells can sense and respond to both

extracellular and intracellular poly-I:C, indicating that innate signalling pathways are intact in these cells.

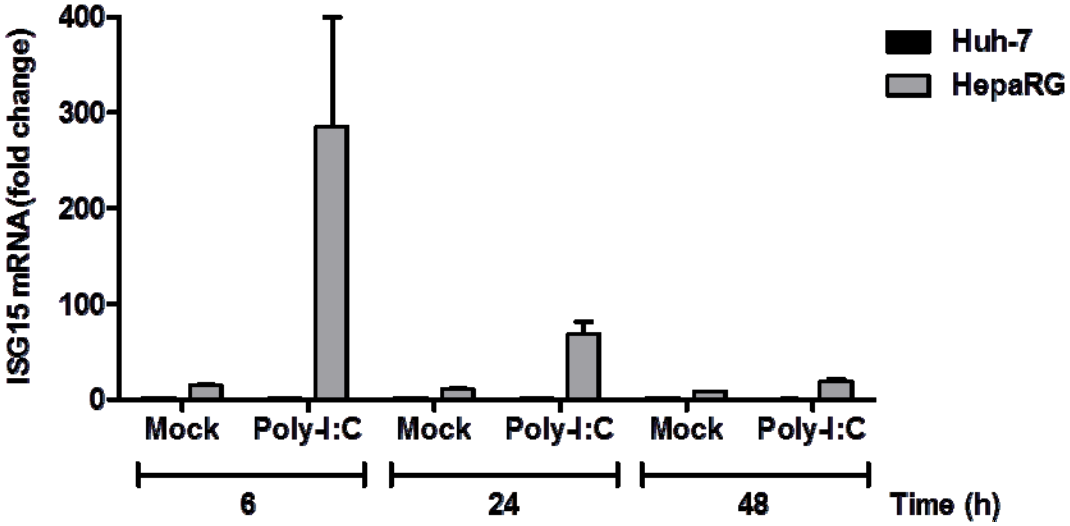


**Figure 3.21– Extracellular responses to poly-I:C in HepaRG cells. Huh-7 and HepaRG cells were treated with poly-I:C (100ug/ml) and IFNα (10U/ml) and at 6, 24 and 48h after treatment cells extracts were used for RT-qPCR analysis of ISG15 mRNA expression.**

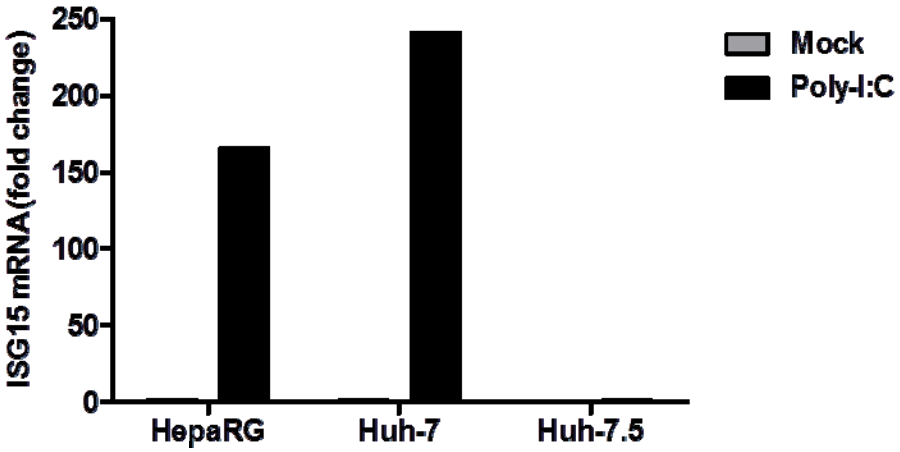


**Figure 3.22 – Intracellular responses to poly-I:C in HepaRG cells. HepaRG, Huh-7 and Huh-7.5 were electroporated with 5ug/ml poly-I:C and 24h after, ISG15 expression was analysed by RT-qPCR.**

### 3.3.5.3 HepaRG cells induce ISG15 expression in response to viral RNA

To examine whether HCV RNA could elicit an induction in the IFN signalling cascade, Luc-WT and –GND RNAs were electroporated into Huh-7 and HepaRG cells and ISG15 RNA levels were monitored by RT-qPCR. To assess HCV RNA replication, luciferase activity was measured between 4 and 48h. As shown in Figure 3.23, luciferase activity decreased slightly between 4 and 12h in Huh-7 for Luc-WT (Huh-7 WT) and between 12h and 48h increased about 6-fold. By contrast, luciferase values decreased throughout all the time points for Luc-GND (Huh-7 GND). In HepaRG cells, luciferase activity for both the Luc-WT and Luc-GND replicons (HepaRG WT or GND, respectively) was lower than in Huh-7 cells and followed a similar pattern to Huh-7 GND between 4 and 48h, consistent with previous results (Figure 3.13-A). Analysis of ISG15 RNA by RT-qPCR, revealed that basal levels did not change throughout the 48h period in Huh-7-WT or Huh-7-GND, when compared with mock-electroporated cells (Figure 3.23). By contrast, in HepaRG cells the basal levels of ISG15 in mock-electroporated cells were 6- to 10-fold higher than the respective Huh-7 cells. Moreover, ISG15 RNA increased between 2- to 3-fold between 4 and 12h in HepaRG cells; by 24 and 48h those levels had decreased to levels similar to mock-electroporated cells. Taken together, in contrast to Huh-7 cells, HepaRGs had the ability to sense and respond to HCV RNA. Hence, the low permissiveness to replicate HCV RNAs in HepaRG cells may be partially explained by innate immune responses in these cells.

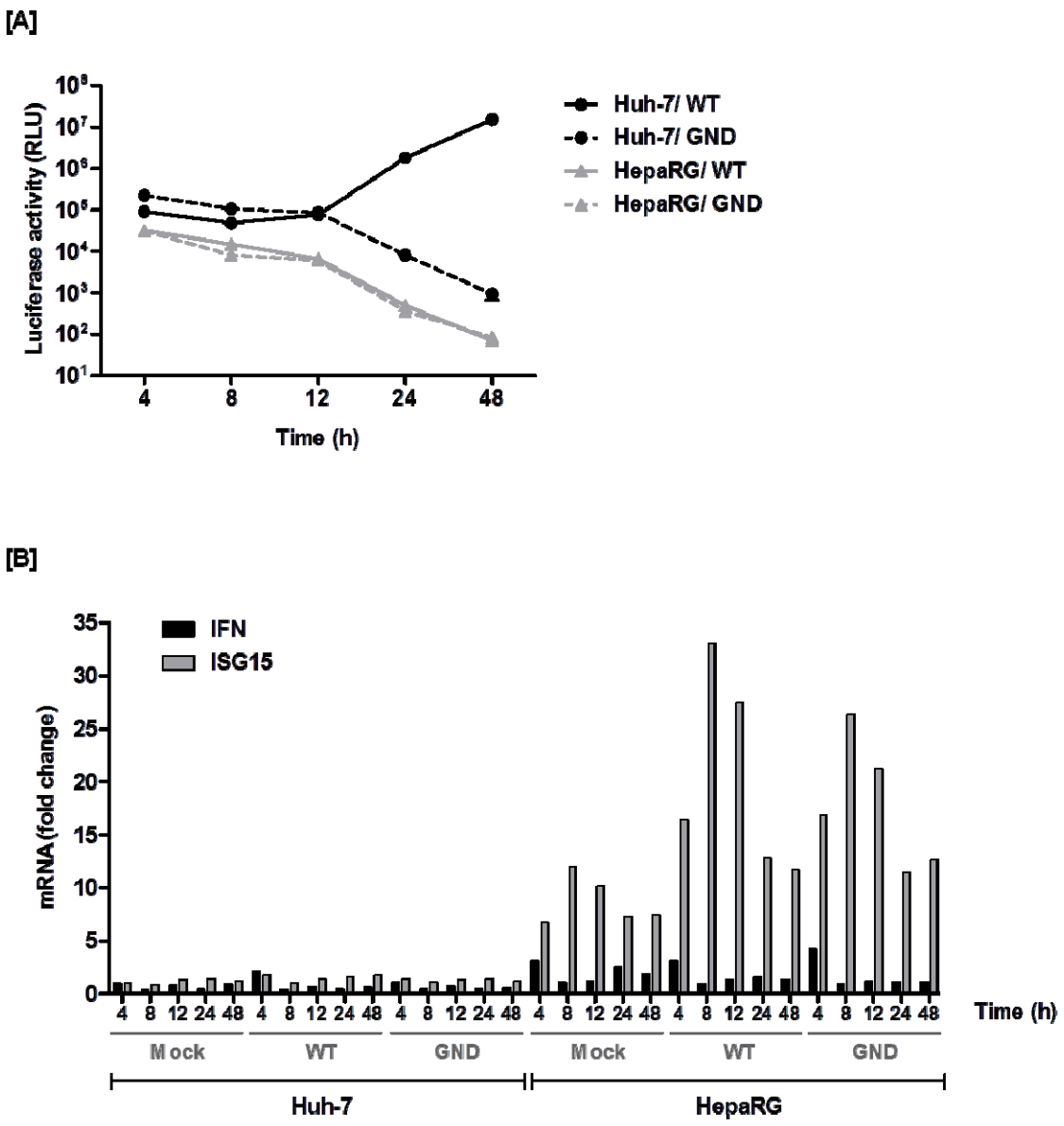


**Figure 3.23– ISG15 is upregulated during transient HCV replication in HepaRG cells. [A] Huh-7 and HepaRG cells were electroporated with in vitro transcribed Luc-WT and Luc-GND RNA; Cell extracts were assayed for luciferase activity at 4, 8, 12, 24 and 48h after electroporation. RLU, relative light units. [B] Levels of ISG15 and IFNβ mRNA were determined by RT-qPCR analysis normalised against abundance of GAPDH mRNA.**

## 3.4 Discussion

The advent of replicons based on natural HCV isolates and cell lines that could support viral RNA replication has made it possible to study the factors governing the mechanisms required for synthesis of the HCV genome as well as providing a tool for screening and identification of lead compounds for antiviral therapeutics. Currently, replicon systems are available for gt 1a, 1b and 2a isolates, which are able to replicate viral RNA both transiently and continuously in Huh-7 cells. Out of the predicted 170 million individuals infected with HCV, estimates for those carrying gt3 strains are uncertain although it is the second most predominant genotype after gt1. Moreover, it is widely distributed across the globe. In the UK, infection with gt3 accounts for about 44% of cases and has a similar prevalence to gt1. The lack of cell culture systems for gt3 has hampered studies on its pathogenesis and responsiveness to novel anti-HCV therapeutics. Previous attempts to construct a gt3 replicon using sequences from a Glasgow gt3a isolate failed to replicate in cells *in vitro* (Hubb, 2008). Our approach focused on replacing amino acid sequences from the C-terminus of NS4B and NS3/4A protease from the JFH1 SGR with those from the Glasgow-3 gt3a isolate. In addition, we also sought to expand the cell lines permissive for HCV RNA replication. Thus far, only Huh-7 cells are highly permissive for viral replication and virus production in culture. As stated earlier, although these cells are derived from the liver, they are also hepatoma cells and thus may not fully recapitulate the features of hepatocytes during normal infection by HCV. In the second part of the studies presented in this chapter, the key objective was to determine the permissiveness of HepaRG cells, a cell line which retains many features of fully functional hepatocytes, to HCV replication.

### 3.4.1 Chimeric gt2a/gt3a SGR

Eleven amino acid changes were required to convert the C-terminus of NS4B from a JFH1 sequence into gt3. Introduction of these changes into the JFH1 luciferase replicon (Luc-M1-11) effectively abolished replication, with only a slight rise in luciferase activity by 72h after electroporation (Figure 3.4-A). All of these changes lay in Region 2 at the C-terminus of NS4B; by contrast, the sequences in Region 1 were fully conserved (Figure 3.24-A). This suggests two functionally distinct regions at the C-terminus of NS4B. Interestingly, 7 out of

the 11 amino acid differences reside in predicted Helix 2 (Figure 3.24-A). Analysis of helical wheel projections of Helix 2 containing the gt3a substitutions (Figure 3.25) indicated that the variable sequences are not strictly located to a particular face of the helix. Perhaps the most interesting feature in this analysis is the positions of M9 and M10, which do slightly impair replication. The amino acids at these positions are located about 2 helical turns from each other. Therefore, substitution at these sites may impede genotype-specific interactions of H2 with either viral or host factors. There is evidence that palmitoylation occurs at cysteine residues at positions 257 and 261 (Yu *et al.*, 2006). M11 is located at position 257 and is a Tyr residue in the gt3a sequence, which would block palmitoylation at this site. Yu et al demonstrated that palmitoylation at residue Cys 261 affects oligomerisation of NS4B, which might be linked to membranous web formation. It is possible that, in our study, substitution at position 257 impairs replication also through affecting oligomerisation of the protein.

The most deleterious variant amino acid was found at position 259 (M8; Ile to Ser). This substitution is located at the P3 position at the boundary sequence for cleavage of NS4B/NS5A (Figure 3.26). NS3-dependent cleavage sites consist of an acidic amino acid at P6 position, a Cys or Thr at the P1 position and a Ser or Ala at the P1' position (Bartenschlager *et al.*, 1995). However, changes in amino acid residues located at the P3 and P4 positions within the NS4B/NS5A boundary sequence also affect efficient proteolysis at this site (Kim *et al.*, 2000). Moreover, Herod et al, (2012) demonstrated that increased rate of cleavage at the NS4B/NS5A boundary can be achieved by mutations at the P3 and P4 sites (Herod *et al.*, 2012). This increase in cleavage efficiency at the NS4B/NS5A boundary also resulted in a lethal effect on viral replication. Thus, it is possible that the negative impact of mutation I259S at P3 is a result of changes in the rate of cleavage between NS4B and NS5A segments in the viral polyprotein. Interestingly, introduction of compensatory mutations at P1'-P3' slowed the rate of cleavage at this boundary and also restored replication (Herod *et al.*, 2012). Analysis of the gt3a sequence at the N-terminus of NS5A, revealed that a change at the P3' position is required to convert gt2a to a gt3a sequence (Figure 3.26, Ser to Asp). Future studies that substituted Asp for Ser at position P3' would help to address this question.

[A]

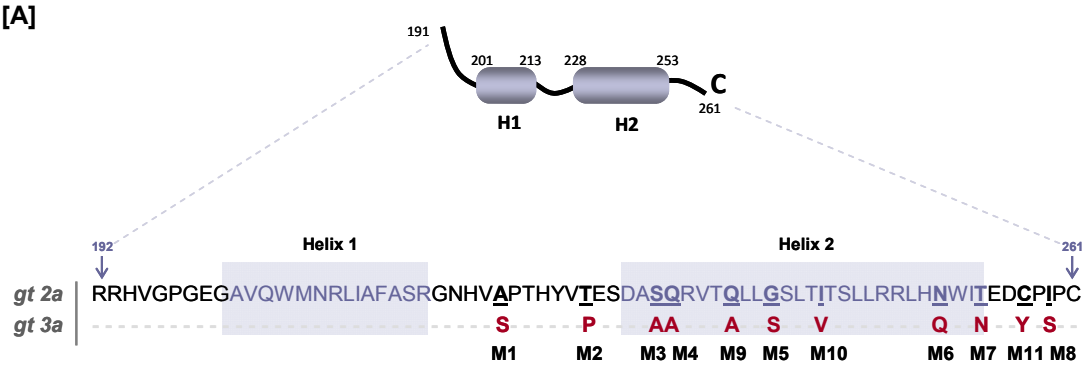


[B]

| Luc-SGR constructs | NS4B mutants | Replication |
|---|---|---|
| Luc-M1-11 | M1, M2, M3, M4, M5, M6, M7, M8, M9, M10, M11 | +/- |
| Luc-M1-10 | M1, M2, M3, M4, M5, M6, M7, M8, M9, M10 | - |
| Luc-M1-9 | M1, M2, M3, M4, M5, M6, M7, M8, M9 | - |
| Luc-M1-8 | M1, M2, M3, M4, M5, M6, M7, M8 | - |
| Luc-M1-7 | M1, M2, M3, M4, M5, M6, M7 | +++ |
| Luc-M8 | M8 | ++ |
| Luc-M1-11/Δ8 | M1, M2, M3, M4, M5, M6, M7, M9, M10, M11 | + |
| Luc-M1-10 /Δ8 | M1, M2, M3, M4, M5, M6, M7, M9, M10 | ++ |
| Luc-M1-9 /Δ8 | M1, M2, M3, M4, M5, M6, M7, M9 | ++ |


**Figure 3.24 – Replication efficiency of genotype 3 NS4B mutants. [A] Schematic representation of the amino acid sequence of the NS4B C-terminal region of gt2a and gt3a. Amino acids substituted with gt3a variants are underlined and numbered M1-M11. [B] Summary of effect of mutations on viral replication using green or "++++" as WT-like replication and red or "-" as GND replication deficient. Intermediate colours represent different degrees of replication in relation to both WT and GND.**

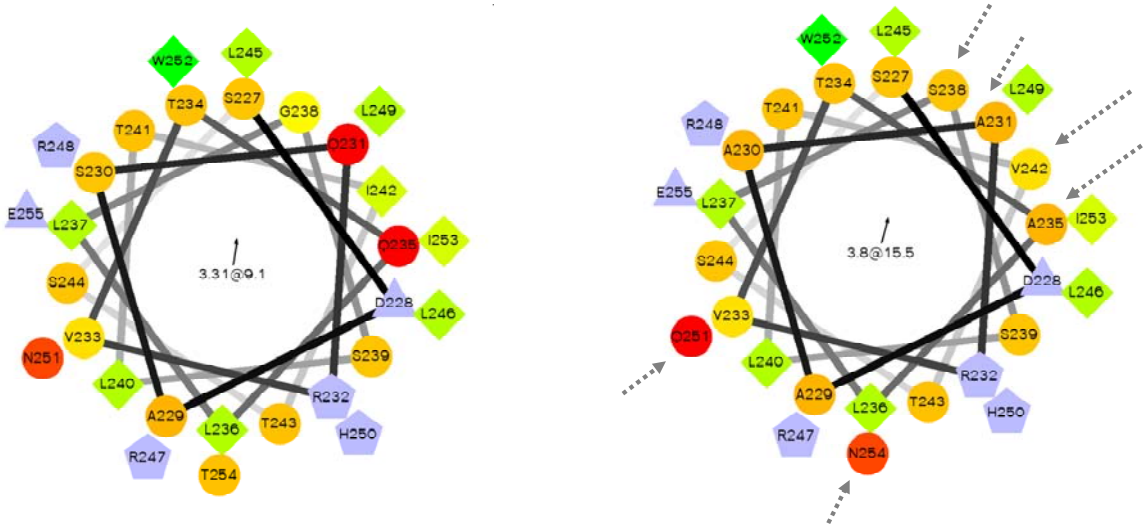


**Helix 2 - JFH1 sequence** **Helix 2 – gt3 sequence**

**Figure 3.25 – Helical wheel projections of JFH1 (left panel) and Glasgow-3 (right panel) NS4B Helix 2. Grey dashed arrows represent the positions on the helix of the gt3a changes. Physicochemical properties of amino acids are represented: circles - hydrophilic residues; diamonds - hydrophobic residues; triangles - potentially negatively charged; pentagons - potentially positively charged. The most hydrophobic residues are shown in green. The amount of green decreases proportionally to the hydrophobicity, with zero hydrophobicity coded as yellow. Hydrophilic residues are represented in red and the amount of red decreases proportionally to the hydrophilicity. The helical wheel projections of Helix 2 of NS4B were generated using a program available online http://rzlab.ucr.edu/scripts/wheel/wheel.cgi.**

Although expression of NS4B alone is able to modify membranes, it also engages in protein-protein interactions with other HCV proteins and host factors as well as protein-RNA interactions. While it is not yet known whether these or additional interactions with the C-terminus are important for efficient RNA replication, it is possible that the lack of RNA replication by Luc-M1-11 is the result of suboptimal protein-protein interactions mediated by the C-terminus of NS4B. The mechanisms involved in membrane changing by NS4B to create sites for RC assembly are not understood, but are likely to be dependent on multimerization and complex interactions between viral and host proteins. For example, interactions between NS5A and NS4B have been demonstrated to be essential to maintain the membranous web and the efficiency of replication (Paul *et al.*, 2011). Recent studies demonstrated that membranous web integrity was maintained by the activity of an ER-localised lipid kinase, PI4KIII$\alpha$ (Berger *et al.*, 2009; Reiss *et al.*, 2011). Moreover, NS5A was shown to recruit and activate PI4KIII$\alpha$, which leads to an accumulation of PI4P at sites of HCV replication

(Reiss *et al.*, 2011). Silencing of PI4KIIIα significantly reduced HCV replication in both replicon-bearing cells and in cells infected with HCVcc, confirming that PI4KIIIα is essential for HCV replication (Lim & Hwang, 2011). The region encoding the last 67 amino acids of NS4B and first 91 amino acids of NS5A was shown to be the minimal functional segment able to restore a low level of replication in cells depleted for PI4KIIIα (Vaillancourt *et al.*, 2012). Moreover, NS4B S258P and NS5A R70S substitutions were required to rescue a low level of replication in PI4KIIIα-deficient cells (Vaillancourt *et al.*, 2012). It is interesting to speculate that changes which may modulate NS4B-NS5A interactions may also affect the ability of NS5A to recruit and activate PI4KIIIα, thereby resulting in a lethal defect on replication. Thus, it would be interesting to investigate whether the deleterious changes at the C-terminus of NS4B in this study could result from such a mechanism.

Changes at the C-terminus of NS4B have also been demonstrated to influence mobility and post-translational modification of NS5A (Jones *et al.*, 2009). As stated earlier, NS5A exists as hypo- and hyperphosphorylated forms, and hyperphosphorylation has been suggested to act as a modulating switch between RNA synthesis and assembly of virus particles. NS4B may play a critical role in this process and its ability to generate membrane rearrangements is linked with hyperphosphorylation status of NS5A. Amino acid changes at the C-terminus of NS4B that disrupted foci formation, also increased mobility of NS5A (Jones *et al.*, 2009). The Jones *et al.* (2009) study emphasises the importance of the integrity of NS4B-NS5A interactions for virus replication and presumably for optimal interactions between NS5A and other viral/host proteins. Although mutation of Cys257 to Ala (referred to as M15 in Jones *et al.*, 2009) did not affect viral replication, it is possible that in our study this change, together with the remaining substitutions, affected the optimal interaction of NS4B with NS5A, and consequently protein-protein interactions of NS4B with other viral or host proteins.

In conclusion, the approach adopted in these studies identified amino acids that vary between gt2a and gt3a at the C-terminus of NS4B that can be tolerated without impairing HCV RNA replication. Deleterious amino acid changes were also found, which would form the basis for further analysis to determine whether compensatory mutations outside of this region could restore replication. This approach has been successful in other mutagenesis studies (Paul *et al.*, 2011) and is therefore feasible. Given the data reported by Paul et al, it would seem appropriate to perhaps examine firstly the gt3a sequences in NS5A that differ from gt2a. This could help build a map of genetic interactions for specific genotypes and thus aid our understanding of the spectrum of interactions that occur in the replication complex.

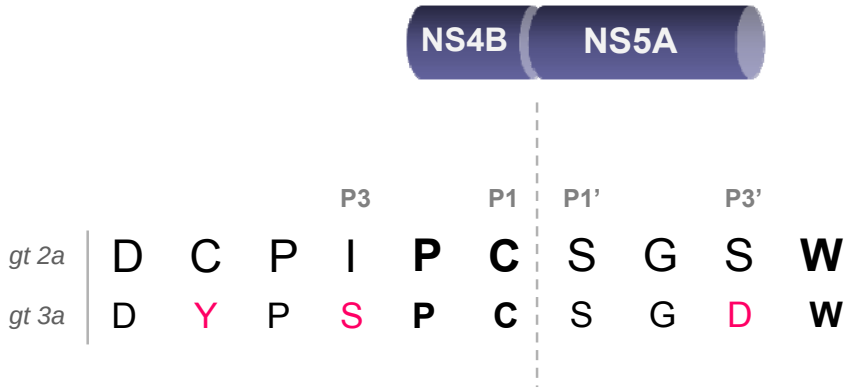


**Figure 3.26 – Schematic representation of the amino acid sequence found at the NS4B/NS5A boundary. The upper and lower sequences are those found in gt2a (JFH1 strain) and gt3a (Glasgow-3 strain). The amino acid variations between the two genotypes are shown in red and in bold are represented conserved amino acids between all HCV genotypes.**

The approach used in the current study to construct a gt3 SGR was extended to include the gt3 sequences encoding the NS3/4A viral protease. Our results with the Luc-2a3a-NS3-4A-SGR provided further valuable information on the effect of gt3a sequences in the non-structural region on genome synthesis. We found that, cloning of these sequences into the JFH1-SGR (Luc-2a3a-NS3-4A) abolished any detectable transient replication by 72h in Huh-7 cells. However, delayed replication was evident between 48 and 72h in Huh-7.5 cells. These findings are similar to those reported by (Imhof & Simmonds, 2010). They found that the J3a3a chimera (construct JC-1 containing NS3-4A sequences from gt3a) yielded very low levels of replication in Huh-7 cells as detected by cells positive for NS5A expression. Indeed, NS5A-positive cells were not found prior to day 5 after electroporation of RNA. In Huh-7.5 cells, there was an eclipse phase of 6 days before NS5A was detected in 80% of the cells. Hence, in both Huh-7 and Huh-7.5 cells, any replication is apparently delayed but eventually more robust in Huh-7.5. In the case of Huh-7.5 cells, J3a3a required an adaptive mutation (L1663A) in the NS4A membrane segment to permit continuous spread in culture. Time constraints did not allow introduction of this mutation into Luc-2a3a-NS3-4A to determine whether it would direct higher or earlier RNA replication in Huh-7.5 cells or indeed enable detection of replication in Huh-7 cells. Clearly, such an approach would address whether the mutation is able to influence either replication (as detected in the SGR system) or virus assembly (as detected with J3a3a in the infectious virus system).

A separate topic is the question as to why Huh-7 cells show either no or very low replication of Luc-2a3a-NS3-4A whereas Huh-7.5 cells do apparently support some replication. Huh-7 cells and their derivatives are the most permissive cells for HCV replication and some studies have linked such an ability to the lack of dsRNA sensing through TLR3 (Li *et al.*, 2005a). In the case of Huh-7.5 cells, which are derived from Huh-7 cells, they lack not only TLR3 but also activation of IRF-3 through RIG-I signalling. A point mutation within RIG-I CARD-like homology domain was found in Huh-7.5 cells, resulting in defective RIG-I-mediated activation of IRF-3 (Sumpter *et al.*, 2005). As stated previously (section 3.2.4), the HCV NS3/4A protease can antagonise antiviral mechanisms during HCV infection by cleavage of the adaptor molecules MAVS (RIG-I signalling) and TRIF (TLR3 signalling). Cleavage of these molecules prevents

stimulation of type I IFNs and therefore prevents IFN-mediated control of HCV replication. It is possible that in the context of a gt2a backbone, gt3a NS3-4A kinetics of cleavage of MAVS is reduced, which renders this antiviral pathway sufficiently active to inhibit RNA replication. If that would be the case, it is interesting to hypothesize that blocking IFN activation, by means of lack of signalling through both RIG-I and TLR3 (as in the case in Huh-7.5 cells), may allow Luc-2a3a-NS3-4A-SGR to replicate. Further studies that are directed at determining whether replication of Luc-2a3a-NS3-4A in Huh-7.5 cells is ablated under conditions where the RIG-I and TLR3 pathways are restored would help to address this question.

Having demonstrated that converting separately the C-terminus of NS4B and the NS3/4A complex to gt3a in the JFH1 SGR could enable replication, it would have been interesting to combine the chimeras and examine whether replication was either increased or decreased. The possible interactions between NS4B and NS5A are described above. It is also known that functional NS3/4A interacts with other viral proteins. For example, Paredes & Blight (2008) have previously demonstrated a genetic interaction between the NS3 protease and the C-terminal region of NS4B, and that this interaction is important for viral replication. Moreover, this interaction was abolished with amino acid changes residing between aa 254 and 258, which abolished replication. It is possible that other amino acids outside of this small segment but within the C-terminal domain of NS4B also are involved in interactions with the NS3 protease. The constructs and data from the studies presented here would provide a platform for such analysis.

### 3.4.2 Permissiveness of HepaRG cells to HCV replication

Several cell lines, including primary and human hepatoma cells, have been evaluated for their ability to support HCV replication in cell culture (Lindenbach *et al.*, 2005; Wakita *et al.*, 2005). Despite such efforts, thus far only Huh-7 cells have proven to be optimal for both replication and virion production. Other hepatoma cell lines, such as Huh-6 and HepG2 cells, are also permissive for HCV replication, however the efficiency in replicating viral RNA and production of infectious virus is lower than in Huh-7 cells (Date *et al.*, 2004). Huh-7 cells are liver-derived and, at least, appear capable of mimicking the environment in

hepatocytes that permits productive infection. However, they are also derived from tumour cells and therefore their differentiation status is likely to differ substantially from human hepatocytes. For example, some studies have demonstrated that Huh-7 cells and derived cells differ substantially, at the level of cellular miRNA expression profiles and allelic variations within the IL28B gene (Bensadoun *et al.*, 2011; Ehrhardt *et al.*, 2011). The IL28B polymorphism is a predictive marker for outcome of HCV infection. Therefore, variations within this genotype between hepatoma cell lines used for *in vitro* studies and human hepatocytes may lead to different observations regarding the biology of HCV infection and antiviral compound efficiencies. In an attempt to examine HCV replication in cells that more closely reflect events in mature hepatocytes, we investigated HepaRG cells since they are derived from hepatic progenitor cells and exhibit features of fully functional mature hepatocytes (Cerec *et al.*, 2007). Gene expression profiles revealed that the mRNA content in HepaRG cells more closely reflects primary hepatocytes and human liver tissues than HepG2 cells, the most frequently used liver cell line (Hart *et al.*, 2010). Given that HepaRG cells are derived from hepatocellularcarcinoma liver tissue, their karyotype presents a few abnormalities, more specifically in chromosome 7 and a translocation from chromosome 22 to 12 (Gripon *et al.*, 2002). However, the remainder of the chromosomes do not shown significant differences with primary hepatocytes (Hart *et al.*, 2010).

Despite being able to translate viral RNA, HepaRG cells were unable to initiate HCV RNA replication following transfection of SGR RNA. Nevertheless, assessment of replication using colony forming assays did reveal some stable replication of SGR RNAs in HepaRG cells, under selective pressure with an antibiotic. Such results suggest adaptation of JFH1 SGR to the HepaRG cell environment may be required for efficient genome synthesis. However, replication was at least 10-fold less than in Huh-7 cells and eventually the HepaRG-SGR cells did not prove capable of long-term maintenance beyond a few weeks. Therefore, it did not prove possible to determine any adaptive changes in the JFH1-SGR that permitted continuous replication in HepaRG cells.

Similar to the results from transient replication assays, HepaRG cells were not susceptible to infection with JC-1 virus, since no replication was detected up to 48h after infection, when compared with Huh-7 cells. HepaRG cells have been reported to be permissive for infection with HCV particles derived from serum (HCVsp) of infected patients (Ndongo-Thiam *et al.*, 2011). However, the authors observed that HepaRG cells were susceptible to HCVsp infection only when they exhibit a differentiated and depolarized epithelial phenotype. Consistent with our observations, infection with JFH1 virus apparently yielded only weak transient replication (Ndongo-Thiam *et al.*, 2011). HepaRG cells do possess some unique features such that they can differentiate into hepatocyte-like or biliary-like cells under appropriate culture conditions. It would be interesting to determine whether the permissiveness of HepaRG cells to either SGR replication or infection with HCVcc would improve by growing them under conditions where they would adopt a more biliary- or hepatocyte-like phenotype.

There are other reasons that may dictate the permissiveness of a cell line to viral replication and extensive attention has been directed to the identification of cellular factors required for efficient HCV replication. The human microRNA 122 (mir122), a liver-specific factor involved in lipid metabolism, was previously identified as a required factor for robust HCV replication in Huh-7 cells (Jopling *et al.*, 2005). Recent findings have shown that cell lines which exhibited low permissiveness for HCV replication, such as Hep3B and HEK 293T cells, would support HCV replication and secretion of infectious particles upon exogenous expression of mir122 (Da Costa *et al.*, 2012; Kambara *et al.*, 2012). Thus, it is possible that insufficient levels of mir122 are present in HepaRG cells and this contributes to their lower competence for replicating HCV RNAs.

Alternatively, low permissiveness could result from the presence of cellular inhibitory factors, such as those involved in mounting a robust innate or intrinsic response to infection. In the case of Huh-7 cells, transcription of type I IFNs through the TLR3 signalling cascade is defective and this has been suggested to be linked with their higher permissiveness to HCV replication (Li *et al.*, 2005a). Similarly, Huh7.5 cells, have a further defect in RIG-I signalling, which apparently renders this cell line more permissive for viral replication than the parental Huh-7 cells. Based on these observations, it is possible that lower

permissiveness of HepaRG cells for HCV replication could result from a robust innate response.

Our data demonstrated that HepaRG cells possess fully functional TLR3 and RIG-I signalling pathways, as ISG15 mRNA expression was induced upon stimulation with extracellular or intracellular poly-I:C, a dsRNA analogue. Huh-7 cells only responded to intracellular poly-I:C, whereas Huh-7.5 cells did not respond to either extracellular or intracellular poly-I:C, consistent with previously reports (Li *et al.*, 2005a). Surprisingly, transfection of viral RNA into Huh-7 and HepaRG cells did not mediate observable changes in the expression levels of IFNβ mRNA in either cell line. Although no changes in IFN induction were observed, ISG15 was induced in response to viral RNA in HepaRG cells. This could suggest that ISG15, possibly along with other interferon-stimulated factors, could play a role in regulating initiation of virus replication. Further studies that would block the interferon-stimulating pathways would help to address this question. Paramyxovirus V proteins have been previously described to counter the IFN signalling pathways (Goodbourn & Randall, 2009). This control was shown to be mediated by targeting STAT1 for proteasome degradation and disruption of induction of ISGs (Parisien *et al.*, 2002). Recently, Andrus *et al.* (2011) demonstrated that expression of the parainfluenza virus V protein in human foetal liver cells significantly enhanced productive HCVcc infection (Andrus *et al.*, 2011). In addition, regulation of IFN induction was demonstrated to be disabled by the BVDV N-terminal protease fragment (Npro) (Hilton *et al.*, 2006). Npro specifically blocks the activity of IRF-3, which is essential for IFN promoter activation. Thus, a feasible approach for addressing the impact of IFN signalling pathways in HepaRG cells permissiveness could be tested through expression of either V or Npro viral proteins.

# 4 Antiviral activities of ISG15 during HCV infection

## 4.1 Introduction

As shown in the previous chapter, cell line permissiveness to HCV replication is not only regulated by viral factors, but may also be controlled by the activities of host factors. In particular, ISG15 was shown to possibly play a role in determining permissiveness of HepaRG cells to HCV replication. From a siRNA library screen developed in our group to identify novel host proteins involved in HCV replication (Jones *et al.*, 2010), ISG15 had been identified as a modulator of HCV RNA synthesis. Since ISG15 has antiviral activities in other virus systems (see Chapter 1, section 1.6), we sought to investigate and characterise its role during clearance of HCV infection, and determine its mechanism of action.

## 4.2 Type I IFNs are strong inducers of ISG15 and can efficiently regulate HCV replication

To investigate the role of ISG15 in controlling HCV replication, Huh-7 and U2OS cells (human osteosarcoma) were used. U2OS cells have previously been shown to support HCV replication, albeit at lower efficiency than Huh-7 cells (Targett-Adams & McLauchlan, 2005). U2OS SGR cells yield ~10-fold less viral RNA and lower expression of the viral protein NS5A than Huh-7 cells (Figure 4.1).

### 4.2.1 Huh-7 and U2OS cells induce ISG15 in response to IFN treatment

To examine whether the ISG15 gene in Huh-7 and U2OS cells responded to IFN stimulation, naïve cells were treated with increasing amounts of IFN$\alpha$, $\beta$ and $\gamma$ (0, 50, 100 and 200U/ml). At 48h after treatment, ISG15 induction was assessed at both RNA and protein levels by RT-qPCR and Western blot analysis, respectively. As shown in Figure 4.2, the basal levels of ISG15 in both cell types were very low. Exposure of Huh-7 cells to IFN increased ISG15 RNA by up to 140- and 50-fold in response to IFN$\alpha$ and $\beta$, respectively (Figure 4.2-A). In U2OS cells, treatment with IFN$\alpha$ and $\beta$ resulted in 40- and 20-fold increases in ISG15 mRNA levels (Figure 4.2-C). As expected (see Chapter 3, section 3.3.5.1), IFN$\gamma$ failed to induce high levels of ISG15 in either cell line. The rise in ISG15 RNA levels was

mirrored at the protein level in Huh-7 cells, where both conjugated and unconjugated forms of ISG15 protein were readily detected following IFN$\alpha/\beta$ treatment (Figure 4.2-B). In U2OS cells, lower levels of unconjugated ISG15 were detected following type I IFN treatment compared to Huh-7 cells (Figure 4.2-D). Interestingly, considerably few ISG15 protein conjugates were produced in U2OS cells. Nonetheless, these data do indicate that IFN signalling through the Jak/STAT pathway is intact in Huh-7 and U2OS cells and ISG15 could be strongly induced in response to type I IFNs.

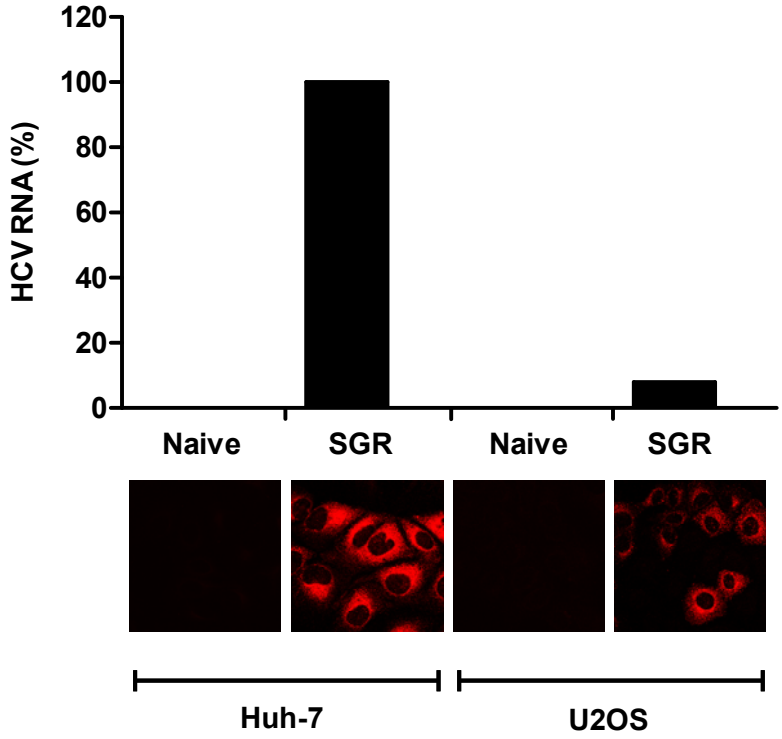


**Figure 4.1– Stable HCV replication in Huh-7 and U2OS cells. RT-qPCR analysis of steady-state levels of replicon RNA in Huh-7 and U2OS replicon-containing cells. HCV RNA levels were normalised against endogenous levels of GAPDH mRNA (upper graph). Immunofluorescence analysis of NS5A expression in Huh-7 and U2OS replicon cells (lower panels).**

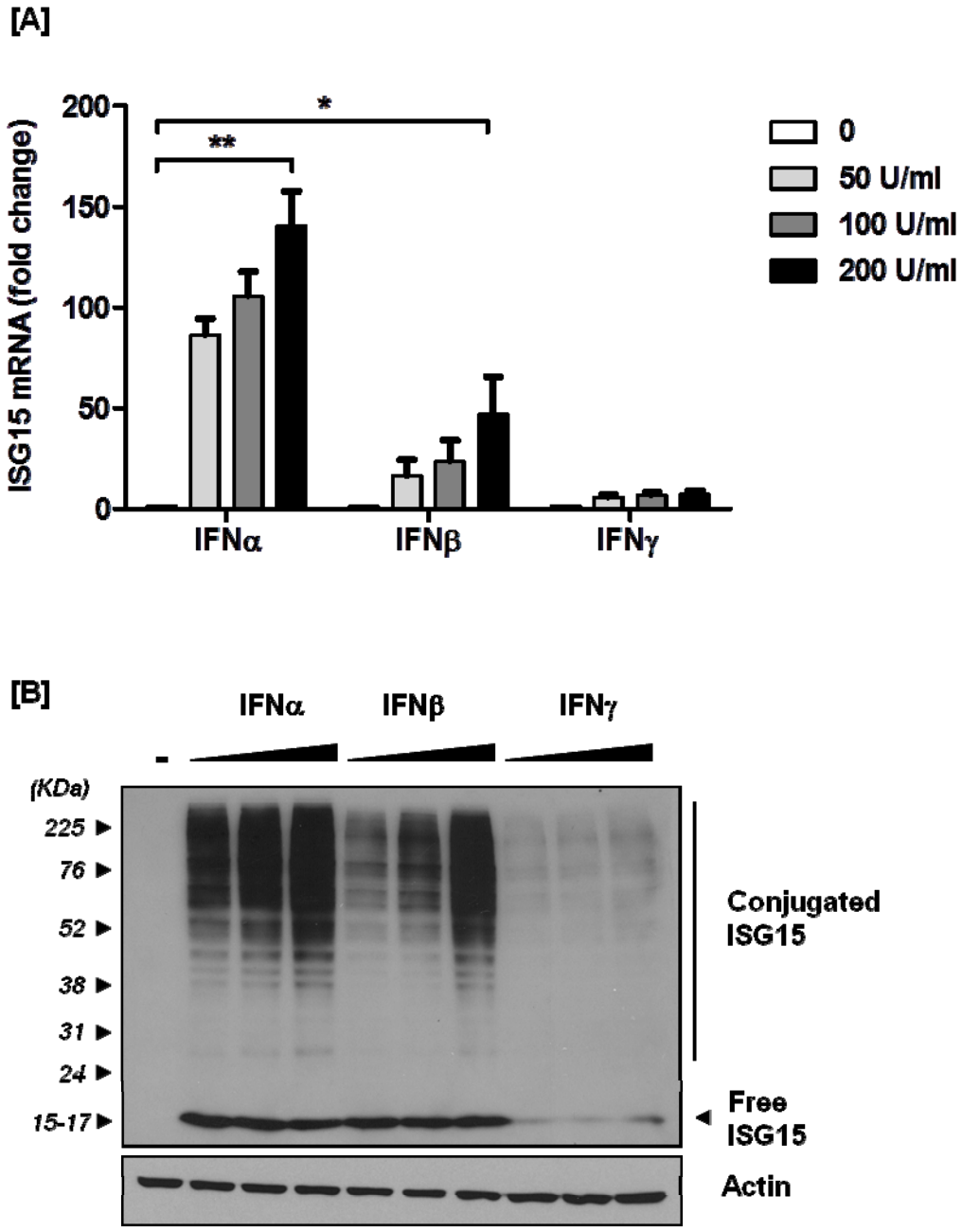
[A]
ISG15 mRNA (fold change)
200
150
100
50
0
*
**
0
50 U/ml
100 U/ml
200 U/ml
IFNα
IFNβ
IFNγ
[B]
IFNα
IFNβ
IFNγ
-
(KDa)
225
76
52
38
31
24
15-17
Conjugated ISG15
Free ISG15
Actin

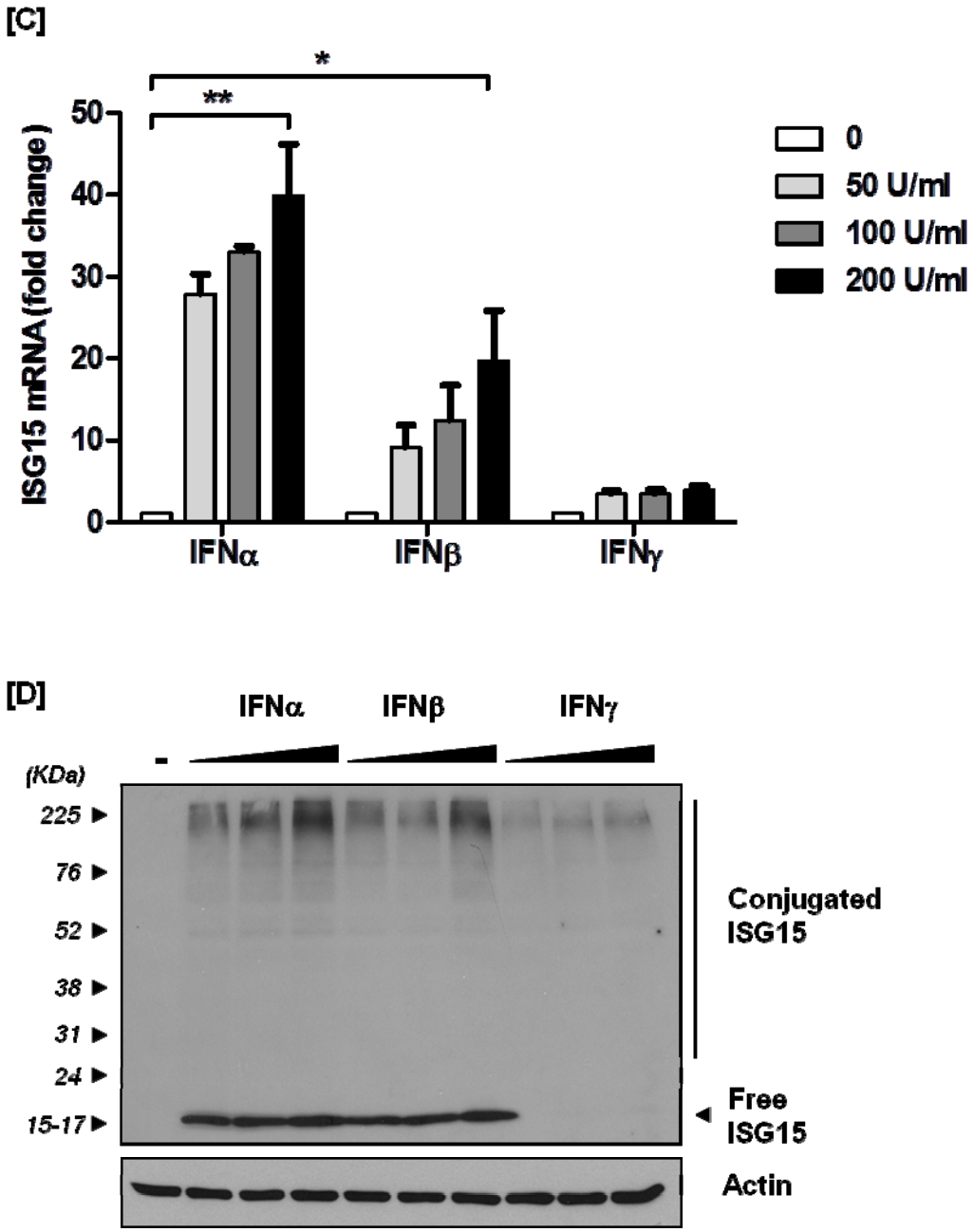


**Figure 4.2 – Type I IFNs are strong inducers of ISG15. Huh-7 and U2OS cells were treated with increasing doses (0, 50, 100 and 200U/ml) of IFNα, β and γ. At 48h after treatment cells extracts were used for RT-qPCR analysis of ISG15 mRNA expression in Huh-7 (A*) and U2OS (C) cells and Western blot analysis of ISG15 free and conjugated forms using anti-ISG15 antisera in Huh-7 (B*) and U2OS (D) cells. Actin expression was examined using anti-actin antisera. *The data used in panels A) and B) are duplicated from Figure 3.20-A&B. Unpaired t test statistical comparison of IFNα, β and γ efficacy in inducing ISG15 mRNA expression are shown: * $p<0.05$ and ** $p<0.005$.**

### 4.2.2 Type I IFNs efficiently reduce HCV replication in Huh-7 and U2OS cells

To examine the effects of type I and II IFNs on HCV replication *in vitro*, naïve- and replicon-bearing Huh-7 and U2OS cells were treated with 200U/ml IFNα, β and γ. 48h after treatment, viral replication was assessed by measuring HCV RNA and protein expression. As observed in Figure 4.3 (A and D), all IFNs decreased viral RNA levels in both Huh-7 and U2OS replicon cells, although in Huh-7 SGR cells differing efficiencies were observed. In Huh-7 cells, IFNα and β had the greatest impact on replication, reducing HCV RNA levels by 85-90% respectively. NS5A expression was also reduced to a greater extent by type I IFNs in Huh-7/SGR cells, when compared with the effects of IFNγ (Figure 4.3-C). By contrast in U2OS SGR cells, all IFNs reduced viral RNA levels and NS5A expression to a similar extent (Figure 4.3-D&F). The higher efficiency of IFNγ in reducing viral RNA in U2OS SGR cells, could be explained by the fact that these cells support lower replication than Huh-7 cells (Figure 4.1). Hence, the differential effect of the three IFNs on replication was not observed in U2OS SGR cells. Since IFNα and β induced higher expression of ISG15 and reduced HCV replication more efficiently in Huh-7 cells, there was a possible correlation between ISG15 and IFN antiviral efficacy. Interestingly, upregulation of ISG15 RNA following IFNα and β treatment in naïve Huh-7 and U2OS cells was ~5.5 to 7.5 and ~1.5 to 2 fold lower than in the respective replicon cells (Figure 4.3-B and E). This enhanced rise in ISG15 RNA in replicon cells was not accompanied by a corresponding increase in either free or conjugated forms of ISG15 protein following IFNα/β treatment. Instead protein levels were similar to those found in naïve Huh-7 and U2OS cells respectively (Figure 4.3-C and F).

Thus, from these observations it suggests that 1) type I IFNs, can more efficiently reduce HCV replication than IFNγ in Huh-7 cells, 2) ISG15 may contribute to the IFNα/β-mediated repression of HCV replication.

**Figure 4.3 – Type I IFNs efficiently reduce HCV replication. The effects of different IFNs on ISG15 expression and HCV RNA replication were examined by treating naïve or SGR cells with 200U/ml of each IFN for 48h. RT-qPCR analysis of HCV replicon RNA in Huh-7 and Huh-7/SGR (A) or U2OS and U2OS/SGR (D) and ISG15 mRNA levels in Huh-7 and Huh-7/SGR (B) or U2OS and U2OS/SGR [E] are shown. [C] and [F] indicate Western blot analysis of ISG15, NS5A and actin proteins in Huh-7 and Huh-7/SGR or U2OS and U2OS/SGR, respectively. Unpaired t test statistical comparison of IFNα, β and γ efficacy in reducing HCV RNA levels are shown: * p<0.05, ** p<0.005 and *** p<0.0005.**

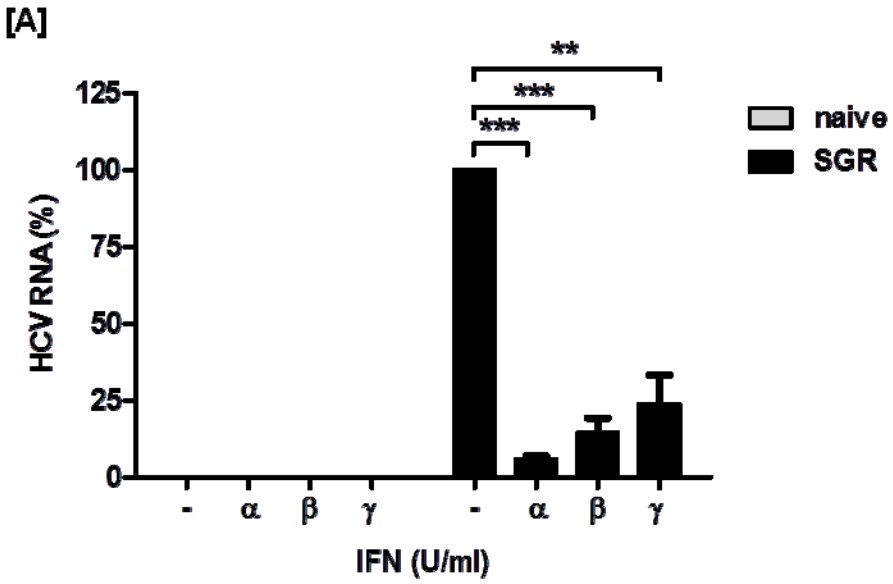
[A]
**
***
***
125
100
75
50
25
0
HCV RNA (%)
naive
SGR
- α β γ - α β γ
IFN (U/ml)

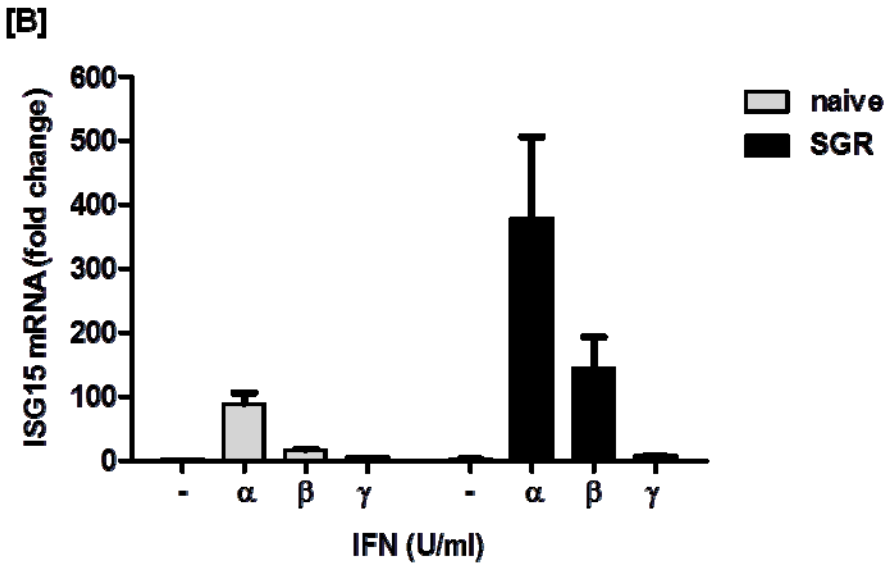
[B]
600
500
400
300
200
100
0
ISG15 mRNA (fold change)
naive
SGR
- α β γ - α β γ
IFN (U/ml)

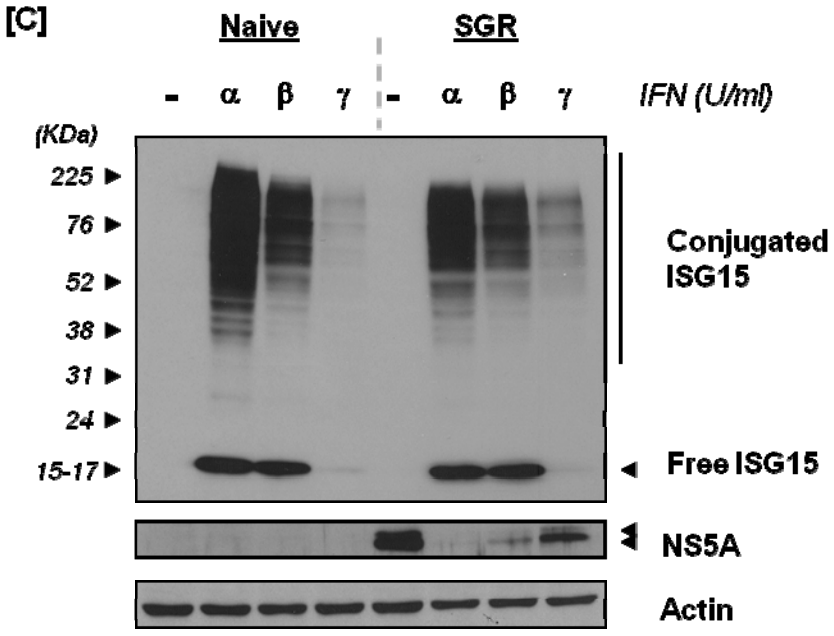
[C]
Naive
SGR
- α β γ - α β γ IFN (U/ml)
(KDa)
225
76
52
38
31
24
15-17
Conjugated ISG15
Free ISG15
NS5A
Actin

[D]

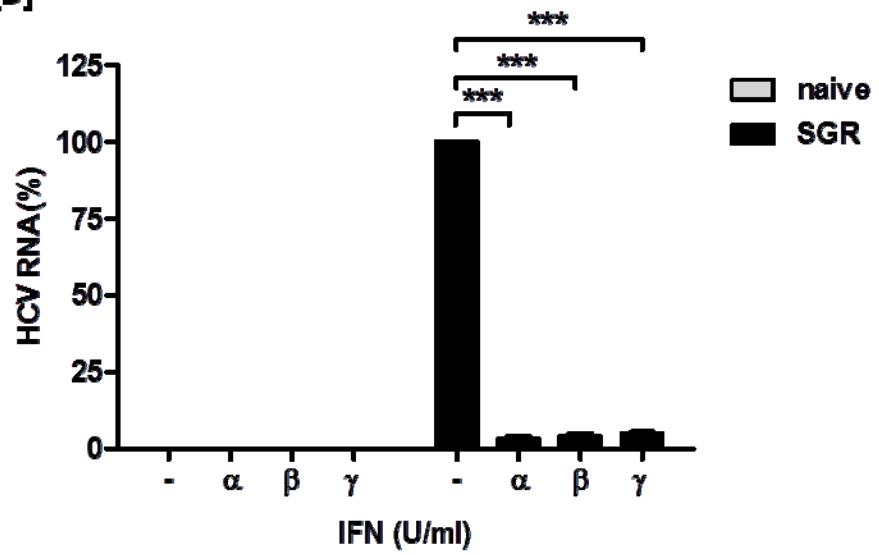
***
***
***
125
100
75
50
25
0
HCV RNA(%)
naive
SGR
- α β γ - α β γ
IFN (U/ml)

[E]

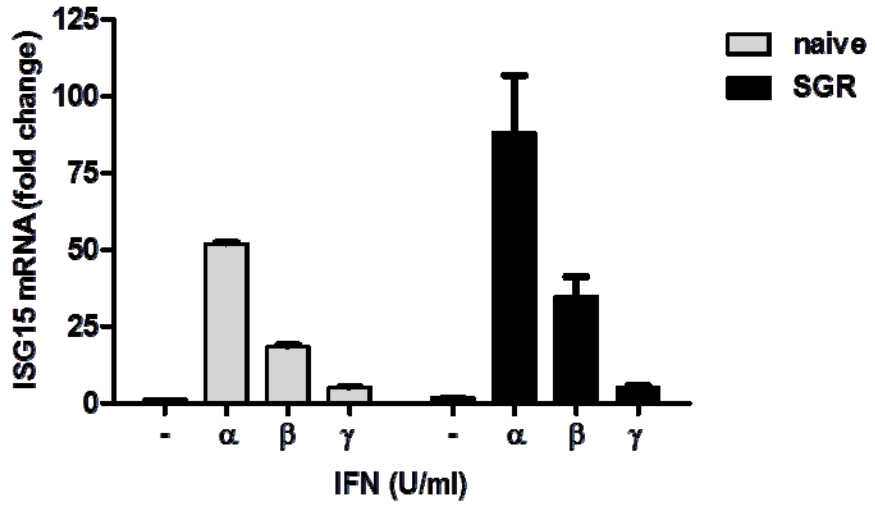
125
100
75
50
25
0
ISG15 mRNA(fold change)
naive
SGR
- α β γ - α β γ
IFN (U/ml)

[F]

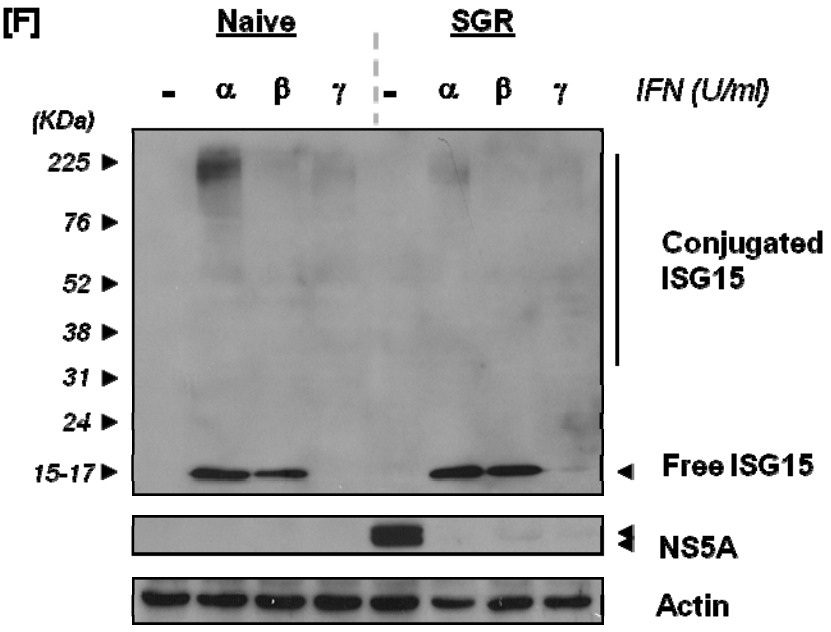
Naive
SGR
- α β γ - α β γ IFN (U/ml)
(KDa)
225
76
52
38
31
24
15-17
Conjugated ISG15
Free ISG15
NS5A
Actin

## 4.3 siRNA silencing of ISG15 enhances constitutive HCV replication in Huh-7 and U2OS cells

### 4.3.1 ISG15 knockdown partially alleviates IFN-mediated repression of HCV replication

To examine whether ISG15 could contribute to repression of HCV replication mediated by IFNα, its expression was abrogated during IFN stimulation. To that end, Huh-7 and U2OS SGR cells were transfected with a pool of ISG15 (siISG15) or scrambled (siCtrl) siRNAs for 24h, followed by treatment with IFNα (200U/ml) for a further 48h. Transfection of siRNAs against ISG15 resulted in a reduction of ISG15 mRNA stimulation upon IFNα treatment by 3-5 fold in both Huh-7/SGR and U2OS/SGR cells, when compared with the siCtrl-transfected cells (Figure 4.4-A). This effect was specific for ISG15 mRNA, as the levels of USP18 stimulation following IFNα treatment did not decrease upon transfection of siISG15 in either Huh-7 or U2OS/SGR cells (Figure 4.4-B). Instead, ISG15 knock-down enhanced USP18 levels in both cell lines. Quantification of HCV RNA levels in siCtrl-transfected cells demonstrated a reduction of ~90 to 95% in viral RNA following IFNα treatment when compared with untreated Huh-7/SGR and U2OS/SGR cells (Figure 4.4-C). However, the decrease in ISG15 stimulation observed in IFNα-treated Huh-7/SGR and U2OS/SGR cells transfected with siISG15, gave a lower decrease in HCV RNA levels. These data suggested that ISG15 may contribute to IFN-mediated repression of HCV replication.

### 4.3.2 ISG15 silencing increases HCV RNA abundance in the absence of exogenous IFN stimulation

In addition to IFN-dependent antiviral activities, many ISGs are expressed at low basal levels and have a role in facilitating surveillance and response to virus infection before IFN is induced.

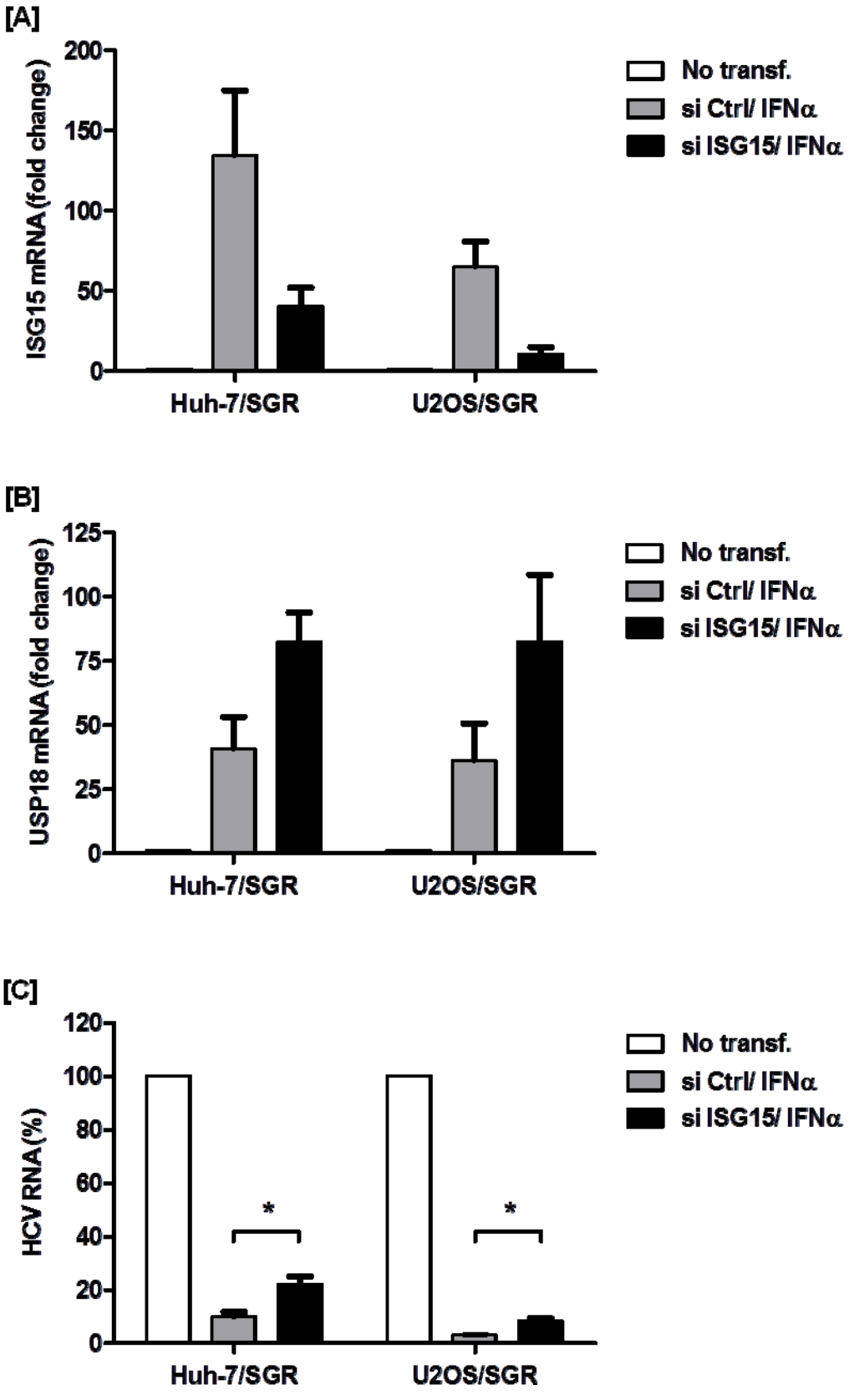


**Figure 4.4 – ISG15 silencing alleviates the IFN-mediated reduction of HCV RNA. Huh-7 and U2OS replicon cell lines were transfected with ISG15-specific and scrambled siRNAs (siCtrl) for 24h, followed by treatment with IFNα for 48h. RT-qPCR analysis in Huh-7/SGR (left panel) and U2OS/SGR (right panel), is shown for ISG15 (A), USP18 (B) and HCV RNA (C) levels respectively. Unpaired t test statistical comparison of IFNα efficacy in reducing HCV RNA levels in siCtrl and siISG15 transfected cells are shown, where * indicates $p<0.05$.**

To investigate whether basal levels of ISG15 play a role in lowering viral RNA levels, ISG15 expression was reduced in Huh-7/SGR and U2OS/SGR cells using ISG15 (siISG15) and scrambled siRNAs (siCtrl), in the absence of exogenous IFN$\alpha$ stimulation. 48h after siRNA transfection, the effect on HCV replication was assessed by examining viral RNA and protein synthesis. As shown in Figure 4.5 (A and C), transfection of ISG15 siRNAs resulted in a 1.8- to 2-fold reduction in the basal levels of ISG15 transcripts in Huh-7/SGR and U2OS/SGR cells respectively, when compared with the siCtrl-transfected cells. This decrease in ISG15 mRNA resulted in a 30 to 150% increase in viral RNA levels in Huh-7 and U2OS cells respectively, when compared with siCtrl-transfected cells (Figure 4.5-B&D). This effect was also found in viral protein levels in U2OS/SGR cells as silencing of ISG15 resulted in a small but observable increase in NS5A expression (Figure 4.5-E). By contrast, there was no visible rise in NS5A expression in Huh-7/SGR cells. It was possible that a 30% rise in RNA would impact on increased levels of NS5A expression, however these changes may be too small to be detected by Western blot analysis. Alternatively, if NS5A were produced at its maximum in Huh-7/SGR cells, then small changes in viral RNA may not be seen at the protein level. To investigate whether the latter possibility was the case, Huh-7/SGR cells were treated with MG132 (proteasome inhibitor) and NS5A expression analyzed for up to 8 or 20h after treatment. As shown in Figure 4.6, blocking protein degradation did not result in an increase of NS5A levels, even at longer MG132 incubation times. However, actin protein levels did decrease during MG132 treatment at later times, indicating that NS5A could have increased when protein degradation was blocked. Alternatively, inhibition of proteasome activity may have caused cell toxicity, without having a direct impact on NS5A levels. Overall, these data indicate that NS5A expression may not normally rise in siISG15-transfected cells to levels higher than those observed in untreated Huh-7/SGR cells.

In similar experiments using a genotype 1b replicon, Huh-7/5-15 (gt1b SGR) cells were transfected with siRNAs against ISG15 and the effect on viral replication assessed by RT-qPCR analysis. Transfection of siISG15 into Huh-7/5-15 cells resulted in a modest reduction of ISG15 expression by 1.5-fold, when compared with the levels in siCtrl-transfected cells (Figure 4.7-A). Consequently, only a 20% rise in viral RNA was detected in the siISG15-transfected cells (Figure

4.7-B). Nevertheless, the data indicated that ISG15 exerted an inhibitory effect on HCV RNA for both gt1b and -2a replicons.

Overall, the data from these and the previous experiments demonstrated that silencing ISG15 increased HCV RNA levels in both Huh-7/SGR and U2OS/SGR cells, suggesting an inhibitory role for ISG15 on HCV replication both in an IFN-dependent and -independent manner.

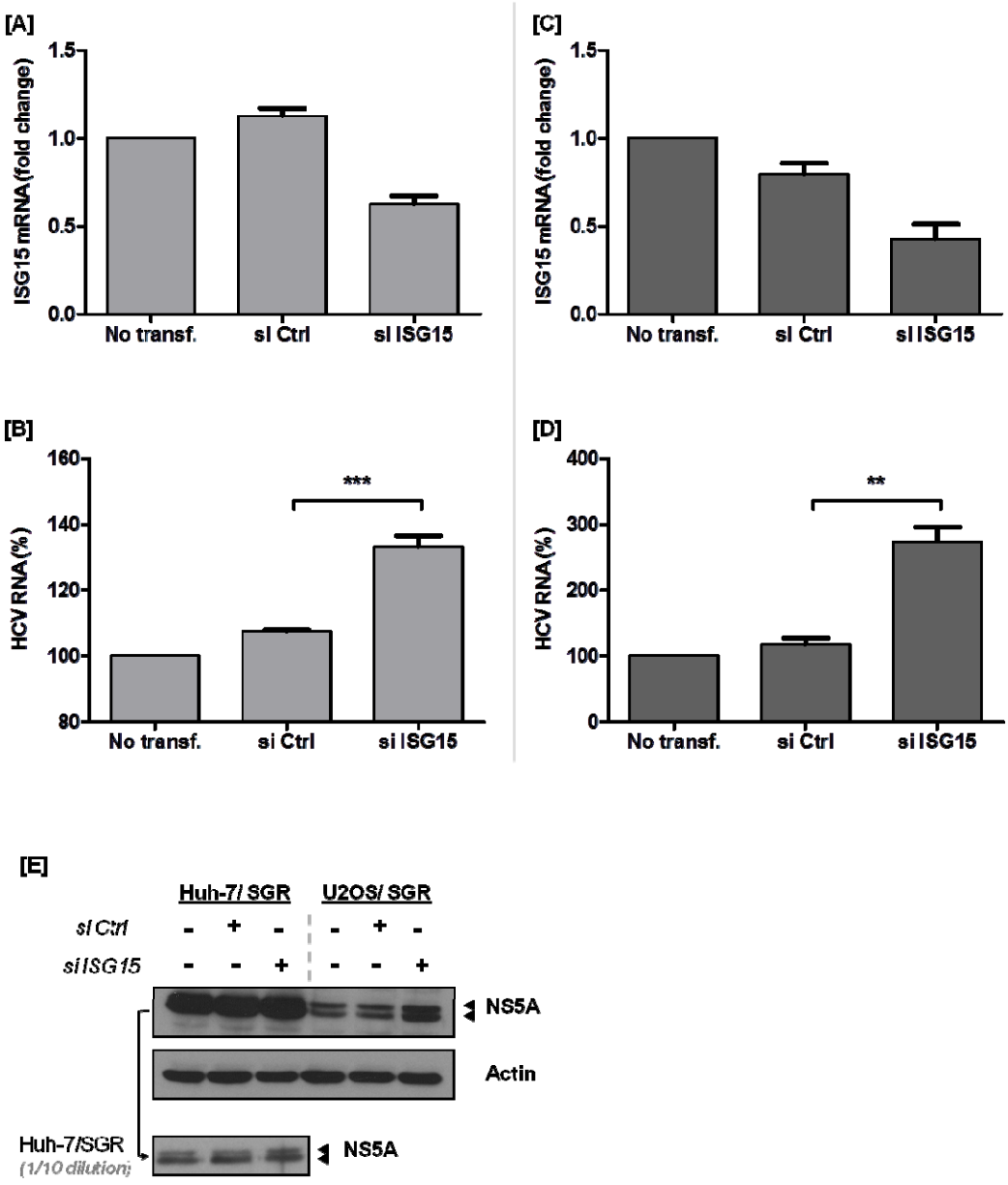


**Figure 4.5 – ISG15 silencing promotes HCV replication. Huh-7/SGR and U2OS/SGR cells were transfected with ISG15-specific and scrambled siRNAs for 48h. The abundance of ISG15 mRNA (A and C) and HCV RNA (B and D) were determined at 48h post-transfection by RT-qPCR in Huh-7/SGR (A and B) and U2OS/SGR (C and D) cells. (ISG15 and HCV RNA levels normalised against GAPDH). [E] Western blot analysis of NS5A and actin proteins in Huh-7/SGR (left panel) and U2OS/SGR (right panel). Lower panel represents 1:10 dilution of NS5A expression levels in Huh-7/SGR cells. Unpaired t test statistical comparison of siCtrl and siISG15 impact on HCV RNA levels are shown: ** p<0.005 and *** p<0.0005.**

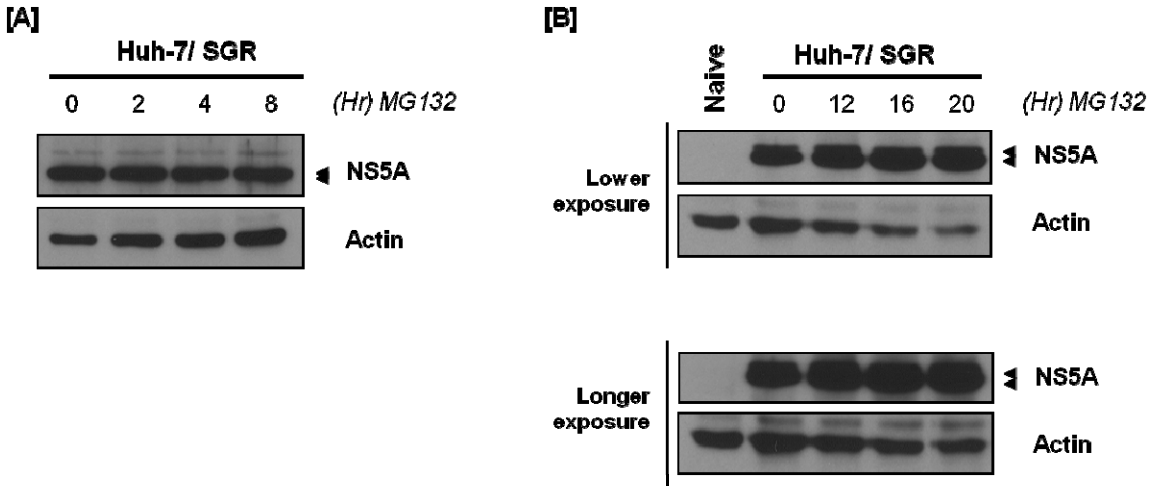


**Figure 4.6 – NS5A turnover levels in Huh-7/SGR cells. Huh-7 SGR cells were treated with proteasome inhibitor MG132 at 10uM for up to 8h (A) or 20h (B). Western blot analysis of NS5A and actin expression during MG132 treatment; lower panels show longer exposure of NS5A and actin.**

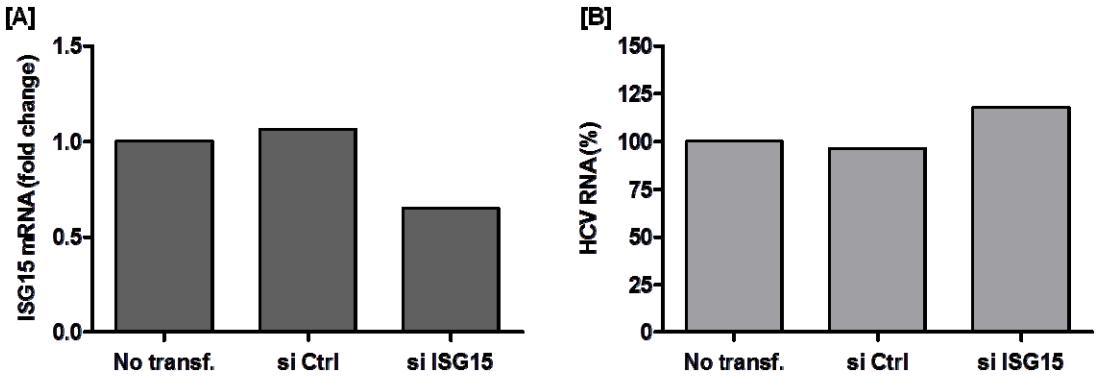


**Figure 4.7 – ISG15 silencing promotes HCV replication. Huh-7/5-15 cells (gt1b SGR) were transfected with ISG15-specific and scrambled siRNAs at a final concentration of 10nM, for 48h. The abundance of ISG15 mRNA (A) and HCV RNA (B) were determined at 48h post-transfection by RT-qPCR in the absence of exogenous IFN stimulation. ISG15 and HCV RNA levels normalised against abundance of GAPDH mRNA.**

## 4.4 shRNA silencing of ISG15 enhances HCV replication during infection

To further examine the processes by which ISG15 may impair not only viral replication but also infection, the study was extended to include use of infectious HCVcc. For this analysis, U2OS cells were not used since they are refractory to HCV infection and virion production.

To avoid any off-target effects resulting from siRNA transfection and the inherent toxicity that can accompany transfection, an alternative approach was used to silence ISG15. This method utilized a lentivirus system to create cell lines that constitutively expressed short-hairpin RNAs (shRNAs) that would inhibit endogenous ISG15 expression. The following section describes the strategy used to design ISG15 shRNAs as well as construction and validation of the resulting shRNA lentiviral cell lines.

### 4.4.1 Generation and characterisation of ISG15 shRNA lentiviral cell lines

To identify appropriate shRNA sequences that would target ISG15, siRNA sequences supplied by different manufacturers (and including the ISG15 siRNAs used in section 4.3 [Ambion siRNA#1 to #3]), were aligned with the ISG15 coding region (Figure 4.8-A). From this alignment, it was possible to identify 4 distinct siRNA clusters across the gene (numbered I to IV in Figure 4.8-A). To maximise the likelihood of selecting a shRNA with efficient targeting, 6 consensus sequences were designed (Figure 4.8-B) according to the following criteria:

1) The shRNA targeting region was based on siRNA sequences with a length of 19bp.
2) Each sequence contained between 40 and 70% GC content and started with G or A, as RNA polymerase III prefers to initiate transcription with a puridine.
3) Sequences with 4 consecutive bases or 7 consecutive GC doublets were avoided, as their presence may create intra-molecular secondary structure or reduce specificity of the target sequence.

4) No shRNA sequences with internal loops and palindromic sequences were selected.

5) GC content was higher at the 5' end than at the 3' end.

6) Each shRNA sequence ended with 6Ts (polymerase III termination signal).

shRNA sequences were further modified to contain 5' and 3' terminal sequences compatible with insertion into *Bam*HI and *Eco*RI sites (Figure 4.8-C). These sequences were introduced to allow their insertion into the pLKO plasmid (Figure 4.8-C and D). The central region of the shRNAs contained the sense and antisense siRNA sequences (#1 to #6) connected by a loop region (TTCAAGAGA). The antisense siRNA region was followed by a poly-T motif and an additional restriction site (*Mlu*I), which was used for diagnostic restriction analysis. In parallel for comparative purposes, a shRNA composed of a scrambled sequence was also created (Figure 4.8-C). Sense and antisense oligonucleotides for each shRNA were synthesised and subsequently annealed (Figure 4.8-D). The pLKO acceptor vector (pLKO-shPML) was digested with *Bam*HI and *Eco*RI, thereby allowing insertion of duplexes encoding each ISG15 shRNA (#1 to #6) as well as shCtrl (Figure 4.8-D). The generated constructs were designated pLKO-shISG15#1 to #6 and pLKO-shCtrl.

In order to produce lentiviral stocks to transduce cells (Figure 4.10), HEK-293T cells were transfected with each of the pLKO-shISG15 plasmids together with plasmids that would generate lentivirus components (pCMV-DR8.91 and pVSV-G, Figure 4.9), according to the method described in Chapter 2 (sections 2.2.7.3 and 2.2.7.4). At 60h after transfection, the supernatants were harvested and used to transduce monolayers of Huh-7 cells (Figure 4.10). Cell lines that incorporated the shRNA sequences were selected by culturing cells in the presence of puromycin. The generated cell lines were named Huh-7-shISG15-1 to -6 (hereafter referred as to sh1, sh2, sh3, sh4, sh5 and sh6) and Huh-7-shCtrl (hereafter referred as to shCtrl). Following continuous growth, only four cell lines survived (sh1, sh5, sh6 and shCtrl), which were used to further validate any knock-down in ISG15 expression. Given the low basal levels of ISG15 RNA and protein in Huh-7 cells, validation of knock-down efficiency by the shRNAs was examined by treating the cells with IFN$\alpha$. Thus, the inhibitory effect of each shRNA on ISG15 could be tested under conditions that normally stimulate

expression of the gene. Moreover, the effect of the shRNAs in each of the 3 cell lines was compared with knockdown by the siRNA against ISG15. In these experiments, levels of both ISG15 RNA (by RT-qPCR) and protein (by Western blot and indirect immunofluorescence analysis) were examined (Figure 4.11). The results revealed that ISG15 induction by IFN$\alpha$ was not considerably affected in siCtrl and shCtrl Huh-7 cells (Figure 4.11). Compared with cells transfected with siCtrl, siISG15 lowered RNA expression by 4-fold (Figure 4.11-A). The cell line expressing the ISG15 shRNA 1 (sh1) did not repress induction of ISG15, as compared to the shCtrl cells (Figure 4.11-A). sh5 and sh6 cell lines on the other hand inhibited ISG15 expression by 2- and 4-fold, respectively. The sh6 cell line gave comparable levels of ISG15 inhibition to siISG15 following IFN$\alpha$ stimulation. This knockdown was specific for ISG15 as levels of USP18 (also called UBP43), the ISG15 IFN-inducible deconjugating enzyme for ISG15, were not reduced in cells either transfected with ISG15 siRNA or in sh1, sh5 and sh6 cells (Figure 4.11-B). Indeed, inhibition of ISG15 during IFN stimulation appeared to enhance USP18 levels, in agreement with the data presented in Figure 4.4.

Western blot analysis of cell extracts revealed stimulation of both conjugated and free ISG15 protein in Huh-7, siCtrl, shCtrl and sh1 cell lines in response to IFN$\alpha$ treatment (Figure 4.11-C). By contrast, cells either transfected with siISG15 or sh6 cells gave barely detectable expression of both single and conjugated ISG15 protein, consistent with the RNA data; sh5 cells did produce ISG15 protein but at slightly lower levels than shCtrl cells. Similarly, immunofluorescence analysis revealed that ISG15 was widely distributed throughout the cell cytoplasm and nucleus in Huh-7, siCtrl, shCtrl, sh1 and sh5 cells following IFN stimulation (Figure 4.11-D). However, in siISG15-transfected cells and sh6 cells, expression was greatly abrogated and ISG15 protein was barely detected. Thus, ISG15 expression could be efficiently inhibited following IFN stimulation using shRNA methodology, with no visible effects on cell viability and growth. The cell line which gave efficient knockdown of ISG15 to similar or greater levels compared to siRNAs was sh6. This cell line, together with the shCtrl cells, were selected for use in subsequent experiments.

[A]

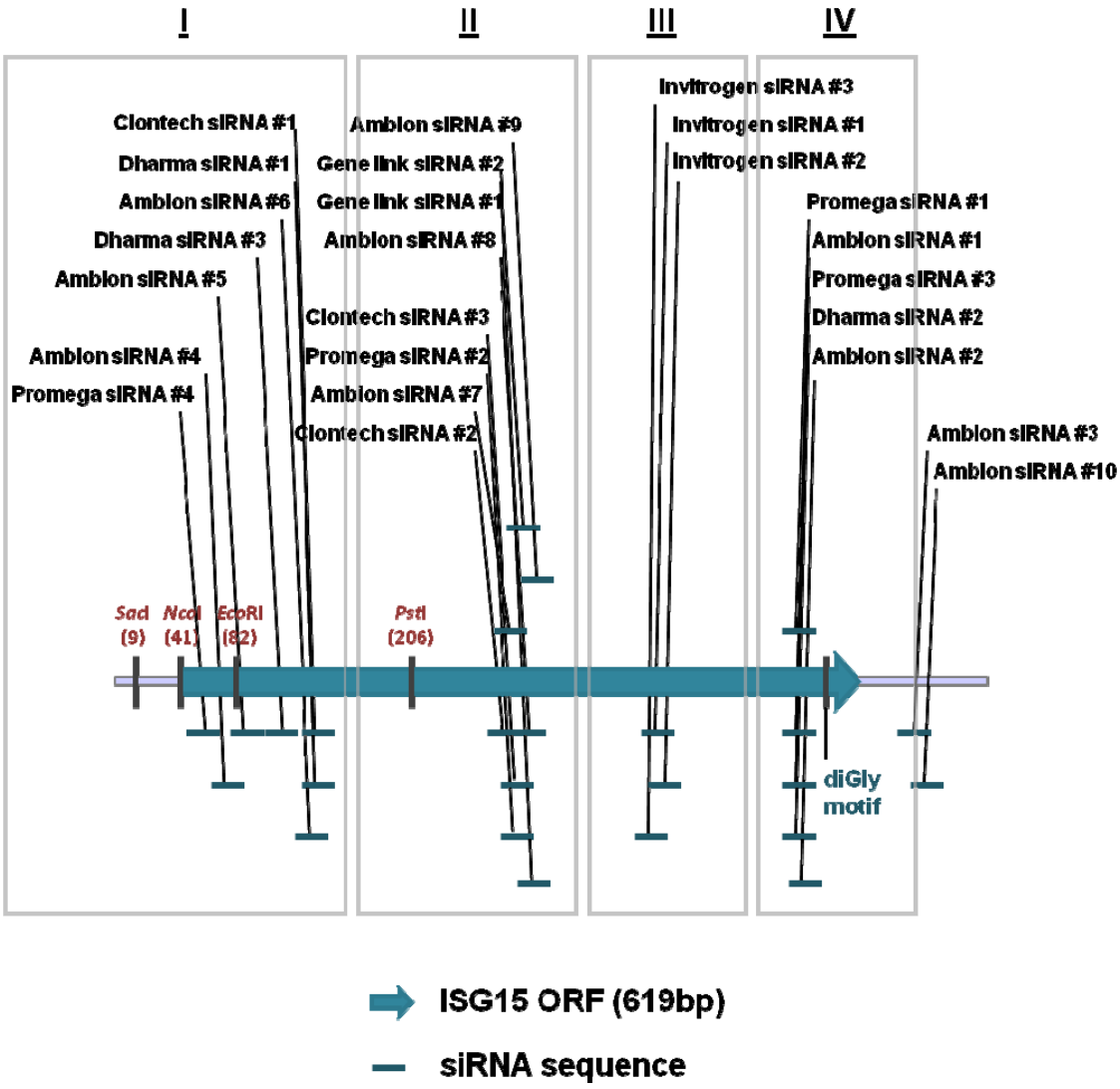
I
II
III
IV
Clontech siRNA #1
Dharma siRNA #1
Ambion siRNA #6
Dharma siRNA #3
Ambion siRNA #5
Ambion siRNA #4
Promega siRNA #4
Ambion siRNA #9
Gene link siRNA #2
Gene link siRNA #1
Ambion siRNA #8
Clontech siRNA #3
Promega siRNA #2
Ambion siRNA #7
Clontech siRNA #2
Invitrogen siRNA #3
Invitrogen siRNA #1
Invitrogen siRNA #2
Promega siRNA #1
Ambion siRNA #1
Promega siRNA #3
Dharma siRNA #2
Ambion siRNA #2
Ambion siRNA #3
Ambion siRNA #10
SacI (9)
NcoI (41)
EcoRI (82)
PstI (206)
diGly motif
ISG15 ORF (619bp)
siRNA sequence

**[B]**


I
CGCAGATCACCCAGAAGAT -Clontech siRNA #1
GCGCAGATCACCCAGAAGA -Dharma siRNA #1
AAGGCGCAGATCACCCAGAAG -Ambion siRNA #6
(#1) GCGCAGATCACCCAGAAGA
(#2) GGCGCAGATCACCCAGAAG
II
GGTGGACAAATGCGACGAA -Clontech siRNA#2
CGACGAACCTCTGAACATC -Clontech siRNA#3
GCGACGAACCTCTGAACAT -Promega siRNA#2
AAATGCGACGAACCTCTGAAC -Ambion siRNA#7
AACCTCTGAACATCCTGGTGA -Ambion siRNA#8
CTCTGAACATCCTGGTGAGGAAT -Gene link siRNA#1
TCTGAACATCCTGGTGAGGAATA -Gene link siRNA#2
AACATCCTGGTGAGGAATAAC -Ambion siRNA#9
(#3) GCGACGAACCTCTGAACAT
(#4) GAACATCCTGGTGAGGAAT
III
GCAAGTGAGCGGGCTGGAGGGTGTG -Invitrogen siRNA #3
GCGGGCTGGAGGGTGTGCAGGACGA -Invitrogen siRNA #1
GGCTGGAGGGTGTGCAGGACGACCT -Invitrogen siRNA #2
(#5) GCGGGCTGGAGGGTGTGCA
IV
GAGCACCGTGTTCATGAAT -Promega siRNA#1
GCACCGTGTTCATGAATCT -Ambion siRNA#1
GCACCGTGTTCATGAATCT -Promega siRNA#3
GCACCGTGTTCATGAATCT -Dharma siRNA#2
CCGTGTTCATGAATCTGCG -Ambion siRNA#2
(#6) GCACCGTGTTCATGAATCT

**[C]**

| shRNA | *Bam*HI siRNA sense sequence | Loop | siRNA antisense seqn | Poly-T | *Mlu*I | *Eco*RI |
|---|---|---|---|---|---|---|
| **#1** | 5‘ –gatccGCGCAGATCACCCAGAAGATTCAAGAGATCTTCTGGGTGATCTGCGCTTTTTTACGCGTg------3'<br>3’ ------gCGCGTCTAGTGGGTCTTCTAAGTTCTCTAGAAGACCCACTAGACGCGAAAAAAATGCGCActtaa- 5’ | | | | | |
| **#2** | 5'-gatccGGCGCAGATCACCCAGAAGTTCAAGAGACTTCTGGGTGATCTGCGCCTTTTTTACGCGTg-------3‘<br>3‘------gCCGCGTCTAGTGGGTCTTCAAGTTCTCTGAAGACCCACTAGACGCGGAAAAAAATGCGCActtaa-5' | | | | | |
| **#3** | 5'-gatccGCGACGAACCTCTGAACATTTCAAGAGAATGTTCAGAGGTTCGTCGCTTTTTTACGCGTg------3'<br>3'------gCGCTGCTTGGAGACTTGTAAAGTTCTCTTACAAGTCTCCAAGCAGCGAAAAAATGCGCActtaa-5' | | | | | |
| **#4** | 5'-gatccGAACATCCTGGTGAGGAATTTCAAGAGAATTCCTCACCAGGATGTTCTTTTTTACGCGTg-------3'<br>3'------gCTTGTAGGACCACTCCTTAAAGTTCTCTTAAGGAGTGGTCCTACAAGAAAAAATGCGCActtaa-5' | | | | | |
| **#5** | 5'-gatccGCGGGCTGGAGGGTGTGCATTCAAGAGATGCACACCCTCCAGCCCGCTTTTTTACGCGTg------3'<br>3'------gCGCCCGACCTCCCACACGTAAGTTCTCTACGTGTGGGAGGTCGGGCGAAAAAAATGCGCActtaa-5' | | | | | |
| **#6** | 5'-gatccGCACCGTGTTCATGAATCTTTCAAGAGAAGATTCATGAACACGGTGCTTTTTTACGCGTg------3'<br>3'------gCGTGGCACAAGTACTTAGAAAGTTCTCTTCTAAGTACTTGTGCCACGAAAAAATGCGCActtaa-5' | | | | | |
| **Ctrl** | 5'-gatccTTATCGCGCATATCACGCGTTCAAGAGACGCGTGATATGCGCGATAATTTTTTACGCGTg------3'<br>3'------gAATAGCGCGTATAGTGCGCAAGTTCTCTGCGCACTATACGCGCTATTAAAAAATGCGCActtaa-5' | | | | | |

**[D]**

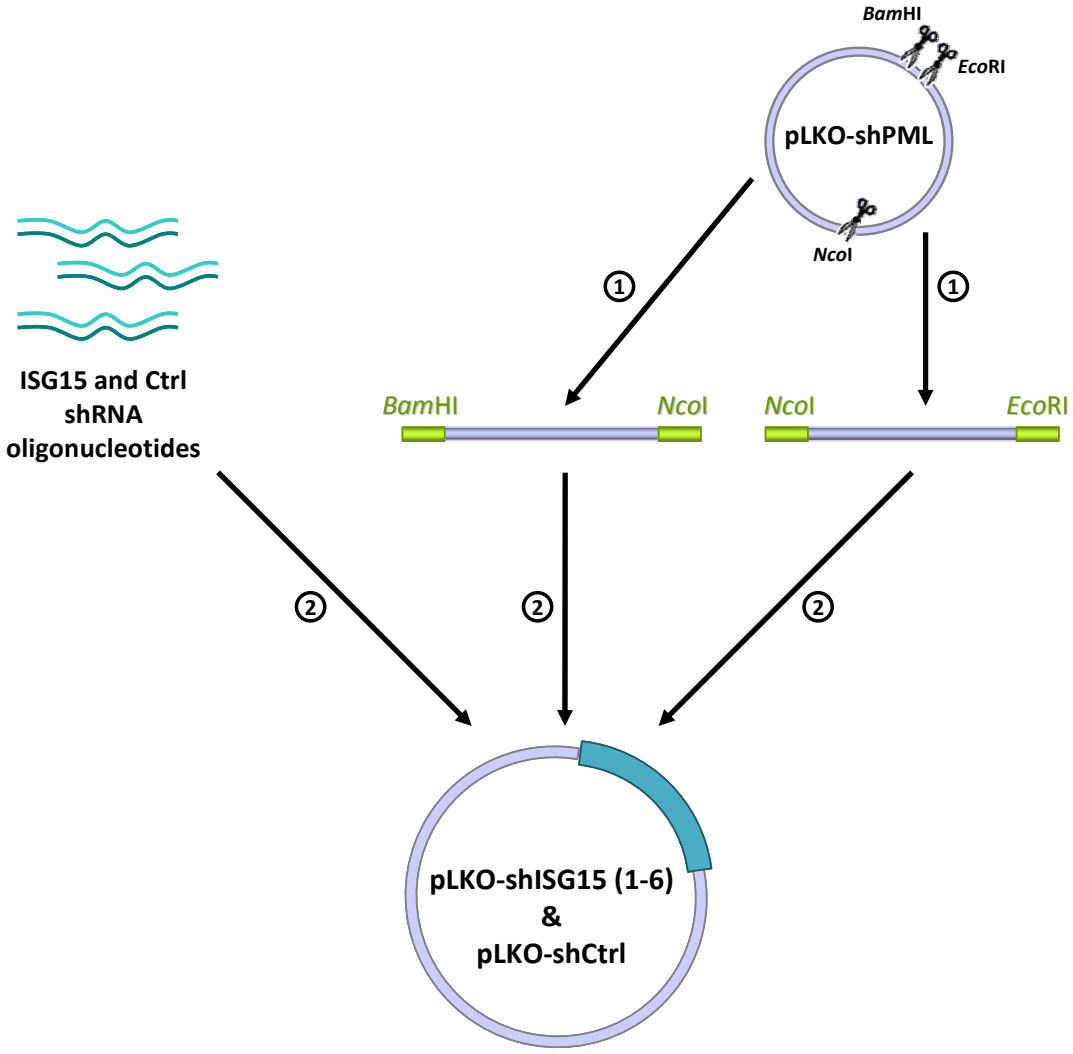


**Figure 4.8 – Design and construction of pLKO-ISG15-specific shRNA lentiviral plasmids. [A] Alignment of siRNA sequences to the ISG15 gene. I to IV represent the 4 clusters resulting from the siRNA alignments. [B] Consensus siRNA sequences used to generate 6 ISG15 shRNAs. [C] shRNAs generated for targetting ISG15. [D] Construction of pLKO-shISG15 vectors: 1) Digestion of pLKO-shPML with *Bam*HI, *Nco*I and *Eco*RI enzymes, generating *Bam*HI-*Nco*I and *Nco*I-*Eco*RI DNA fragments; 2) Ligation of *Bam*HI-*Nco*I, *Nco*I-*Eco*RI and each ISG15 shRNA or Ctrl shRNA, to generate pLKO-shISG15 (1 to 6) and –shCtrl vectors.**

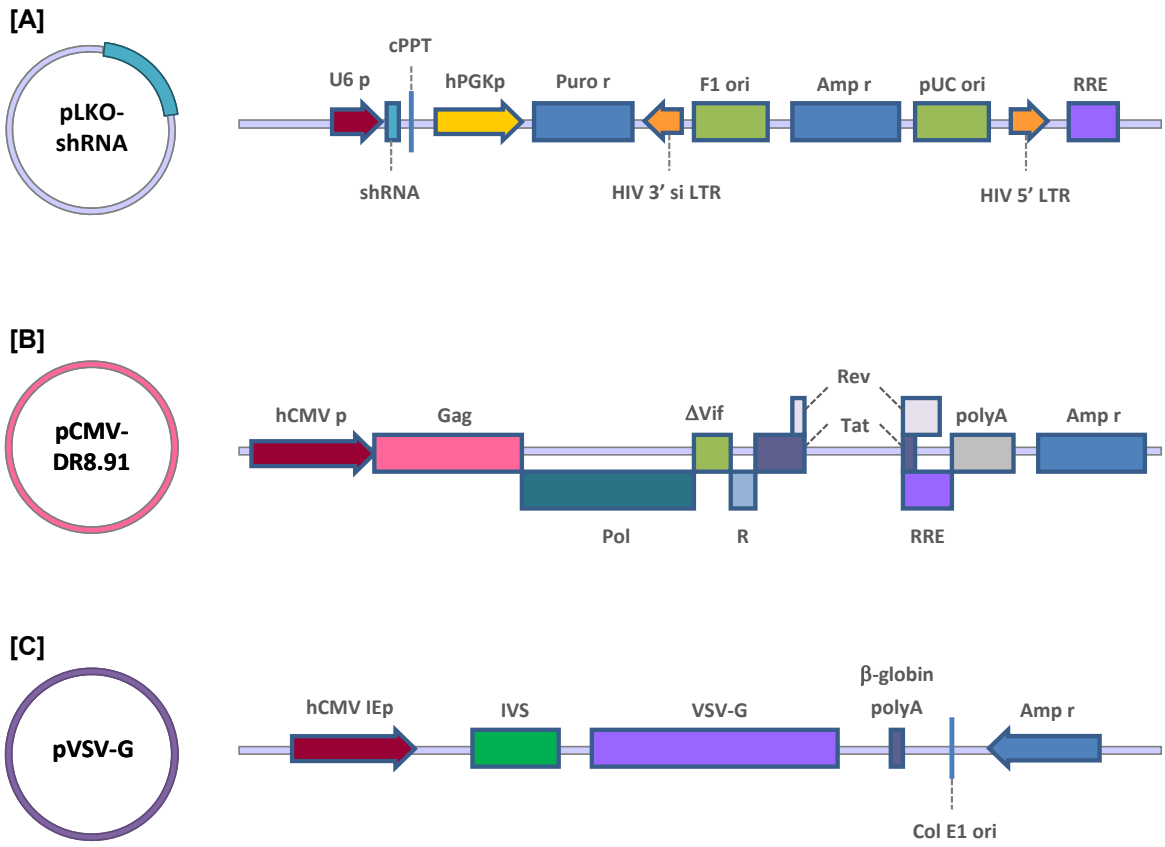


**Figure 4.9 – Map showing the features of the lentiviral vectors. [A] pLKO-shRNA vectors. Lentiviral packaging vectors pCMV-Dr8.91 [B] and pVSV-G [C]. The lentivirus features are represented and include RRE – rev response element, cPPT – polypurine tract, LTR - long terminal repeats, si – self-inactivating, hCMV IEp – human cytomegalovirus immediate early promoter, hPGKp – human phosphoglycerate kinase promoter, IVS – intervening sequence, VSV-G – vesicular stomatitis virus glycoprotein. The vector also contains a gene for puromycin (Puro r) and ampicillin resistance (Amp r). The site of shRNA sequence insertion is indicated as shRNA.**

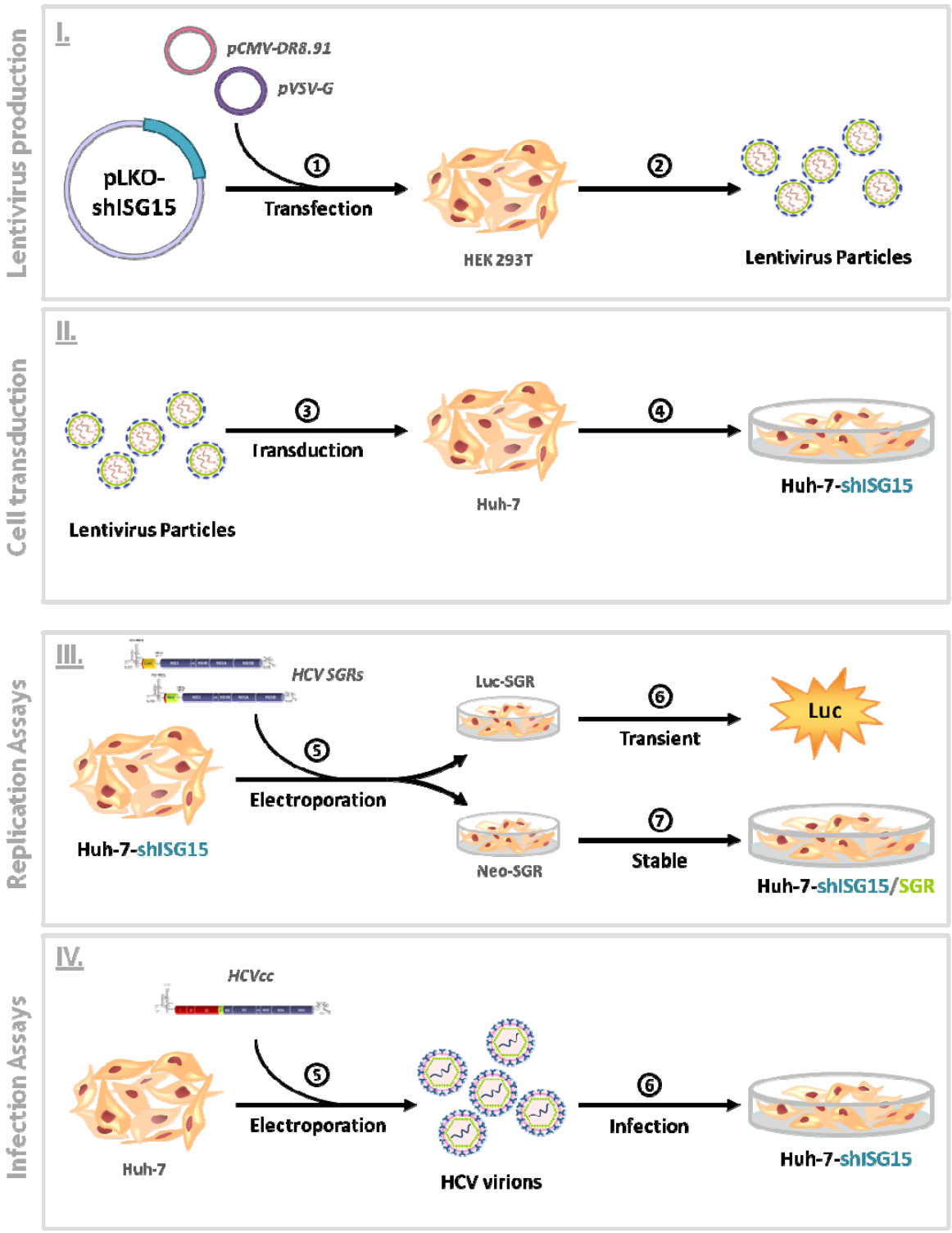


**Figure 4.10 – Generation of lentiviral cell lines stably expressing ISG15 shRNAs. Lentiviruses were produced by transfection of pLKO-shRNA vectors together with pCMV-DR8.91 and pVSV-G packaging vectors into 293T cells (I). At 60h post-transfection, the supernatant containing lentivirus particles was used to transduce Huh-7 cells (II). The stable cell lines were generated by puromycin selection of shRNA expressing cells and used for HCV replication (III; luciferase assays and stable replication assays) and infection assays (IV). Detailed protocol descriptions in Chapter 2, sections 2.2.7.3 and 2.2.7.4.**

### 4.4.2 Transient HCV replication in sh6 cells

To examine whether the effect of reducing ISG15 levels could be assessed in transient replication assays, Luc-WT and –GND transcripts were electroporated into Huh-7, shCtrl and sh6 cell lines and replication was assessed for up to 72h, by measuring luciferase activity (Figure 4.12-A). In addition, to verify the effect of IFN during transient replication in these cell lines, 100U/ml of IFNα was added at 24h after electroporation. Luciferase activity for Luc-WT in Huh-7 cells (Huh-7/WT) increased at all time points after electroporation (Figure 4.12-B). By contrast, luciferase values decreased throughout all the time points for Luc-GND (Huh-7/GND). In shCtrl and sh6 cells, the luciferase values produced by the Luc-WT (shCtrl/WT and sh6/WT) followed a similar pattern to Huh-7/WT between 4 and 72h. The correlation between luciferase activity and viral protein synthesis was examined at 72h post-electroporation by Western blot analysis (Figure 4.12-C). Examination of cell extracts revealed that NS5A protein was detected in Huh-7/WT, whereas in Huh-7/GND cells, NS5A expression was not observed. NS5A was found at similar levels in shCtrl/WT and sh6/WT cells, although its abundance was slightly lower than in Huh-7/WT cells.

As shown in Figure 4.12-B, addition of IFNα at 24h after electroporation resulted in a 34-fold reduction of luciferase activity at 72h in Huh-7/WT. Luciferase activity in Huh-7/GND cells treated with IFNα followed similar levels as untreated Huh-7/GND. Treatment with IFNα resulted in a 20- and 14-fold reduction in viral replication in shCtrl/WT and sh6/WT respectively between 24 and 72h under the same treatment conditions as in Huh-7 cells (Figure 4.12-B). These data suggested that silencing of ISG15 possibly alleviated some of the IFNα-mediated reduction in viral replication. Western blot analysis of cell extracts at 72h after electroporation revealed that, in response to IFNα treatment, high levels of both conjugated and free ISG15 protein were induced in Huh-7/WT, Huh-7/GND and shCtrl cells (Figure 4.12-C). As expected, induction of ISG15 in sh6 cells was abrogated. Although luciferase activity was detected at 48h after IFN treatment (72h after electroporation), NS5A expression was not detected in any of the cell lines by Western blot analysis (Figure 4.12-C).

Taken together, the small differences observed in luciferase activity as a result of the repression of ISG15 expression following IFN treatment in sh6 cells suggested that ISG15 silencing may partially alleviate IFNα repression of viral replication in transient assays. However, it was concluded that this assay may not be sensitive enough to study the effects of ISG15 on HCV replication. Hence, the significance of the results was inconclusive.

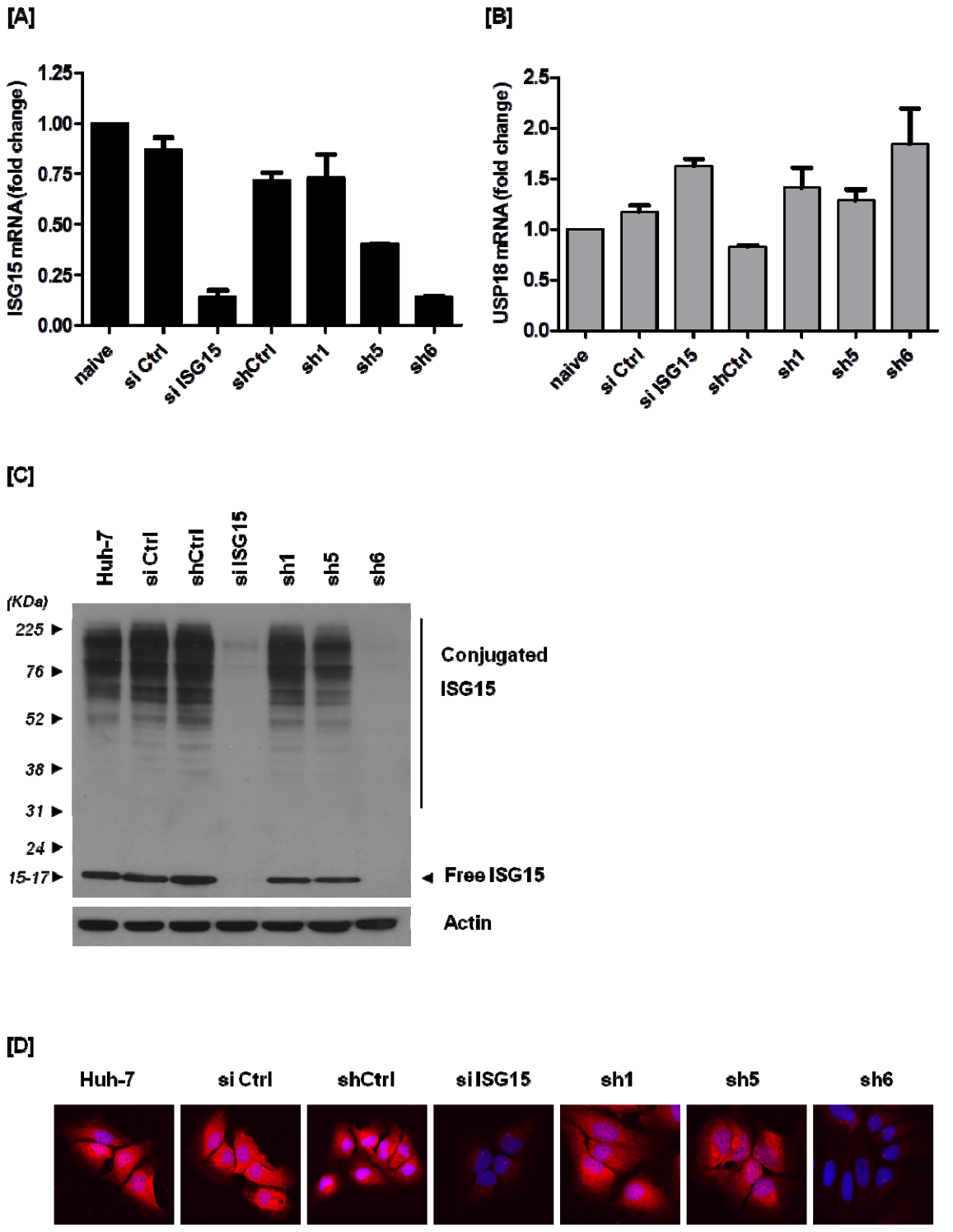


**Figure 4.11 – Characterisation of Huh-7 cells expressing ISG15 specific shRNAs. Three Huh-7 lentiviral cell lines that express ISG15-specific shRNAs were generated and validated for their ability to deplete ISG15 expression, following exposure to 200U/ml of IFNα for 24h. RT-qPCR analysis of ISG15 (A) and USP18 (B) mRNA levels normalised against GAPDH abundance. C) Western blot analysis of cell extracts using monoclonal antibodies against ISG15 and actin. D) Indirect immunofluorescence analysis using ISG15 antibody and DAPI for nuclear staining.**

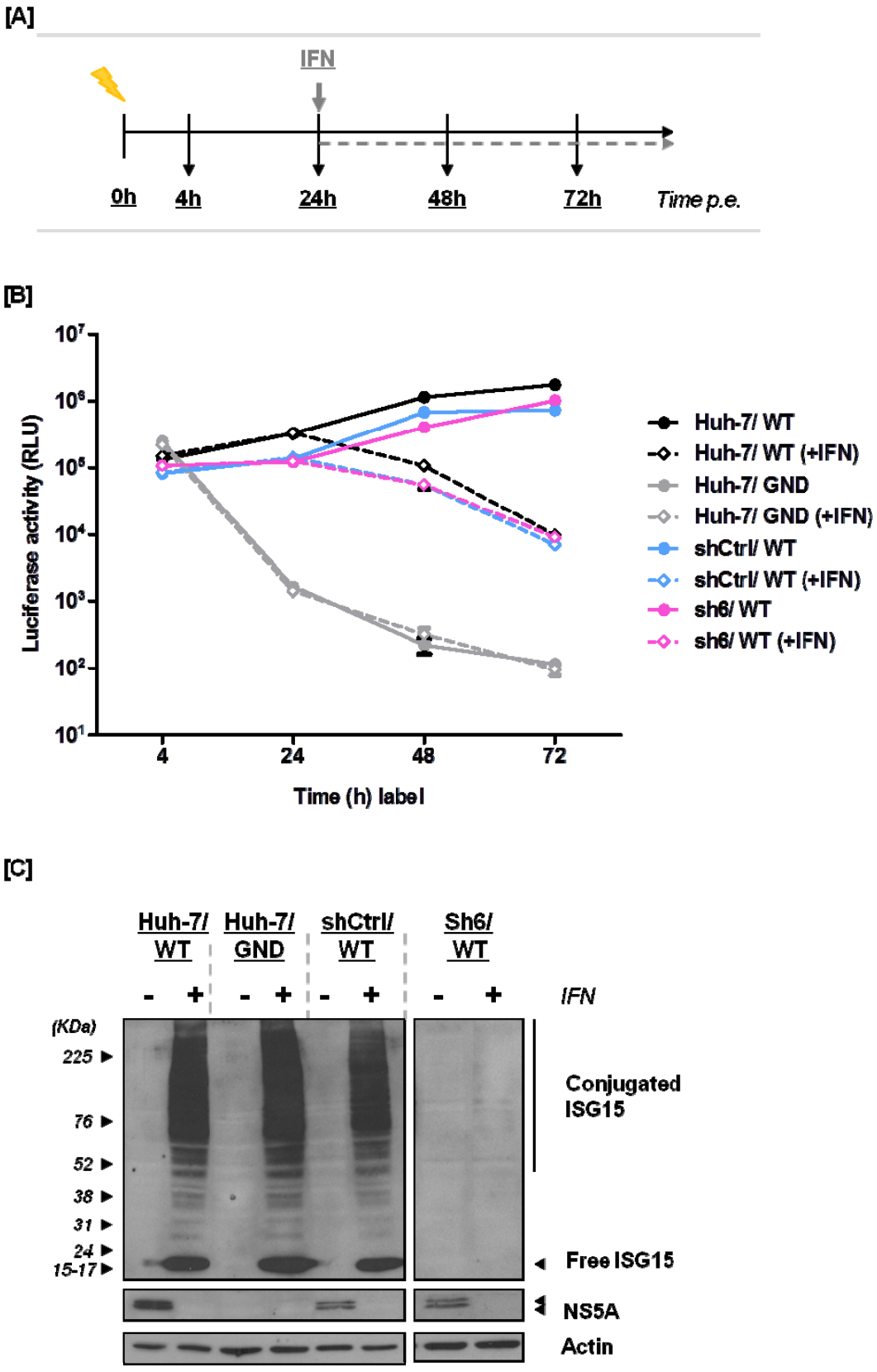


**Figure 4.12 – Transient HCV replication assay in shISG15 expressing cell lines. [A] Outline of the experiment. [B] Huh-7, shCtrl and sh6 cells were electroporated with Luc-WT and Luc-GND RNAs. At 24h after electroporation cells were treated with 100U/ml of IFNα or left untreated. Cell extracts were assayed for luciferase activity at 4, 24, 48 and 72h after electroporation. RLU, relative light units. [C] Cell extracts were prepared at 72h post-electroporation and examined by Western blot analysis with anti-ISG15, anti-NS5A and anti-actin antisera.**

### 4.4.3 Infection assays in sh6 cells

With the assay used in the previous section, translation and replication efficiencies of viral RNA could be monitored in a transient manner by electroporation of *in vitro* synthesised HCV RNA into cells. Given the somewhat low sensitivity of this system for examining differences exerted by ISG15 silencing on viral replication, a different approach using infectious virus was employed to address this question. This system is biologically more relevant than transient replication assays, as it allows the study of not only replication but the complete cycle of viral infection. Moreover, it avoids any problems associated with electroporation of cells with large amounts of RNA.

To examine whether expression of shCtrl could affect the infectious process, Huh-7 and shCtrl cell lines were compared initially for their ability to support infection and replication of JC-1 virus. To that end, viral stocks were generated by electroporating JC-1 RNA into Huh-7 cells, as described before (Chapter 2, section 2.2.8.2). The supernatant from the JC-1 RNA-electroporated cells was titrated ($5x10^5$ $TCID_{50}$/ml) and then used as the inoculum to infect Huh-7 and shCtrl cells at a MOI of 1. At 4, 24 and 48h after infection, replication was assessed by measuring viral RNA and protein levels. As shown in Figure 4.13-A, JC-1 RNA levels in shCtrl cells were similar to those in Huh-7 cells between 4h and 48h post-infection. Immunofluorescence analysis revealed that expression of NS5A protein was similar in both cell lines at 48h post-infection (Figure 4.13-B). Together, these data suggest that shCtrl cells were able to support viral replication at a similar efficiency to parental Huh-7 cells.

Following the above experiment, shCtrl and sh6 cells were infected with JC-1 virus at a range of MOIs (0.2, 0.4 and 0.8), to investigate the role of ISG15 on HCV replication during productive infection. HCV RNA levels and ISG15 expression was assessed at 24h and 48h after infection by RT-qPCR analysis. As shown in Figure 4.14-A, uninfected sh6 cells had lower ISG15 basal mRNA levels, when compared with the levels in shCtrl cells. Moreover, ISG15 mRNA levels remained consistently low in sh6 cells throughout infection. Interestingly, between 24 and 48h after infection, a reduction in ISG15 transcript levels was observed in shCtrl cells, when compared with the levels in uninfected cells. At the later time point, ISG15 levels in shCtrl cells approached those in sh6 cells (Figure 4.14-A). In the case of viral RNA, higher levels were found in sh6 as compared to shCtrl cells, particularly at 48h (Figure 4.14-B). The increase in viral RNA in sh6 cells was not dependent on MOI (Figure 4.14-B). These results indicated that lowering the abundance of ISG15 leads to a rise in HCV RNA levels, suggesting that ISG15 partially regulates viral replication during infection.

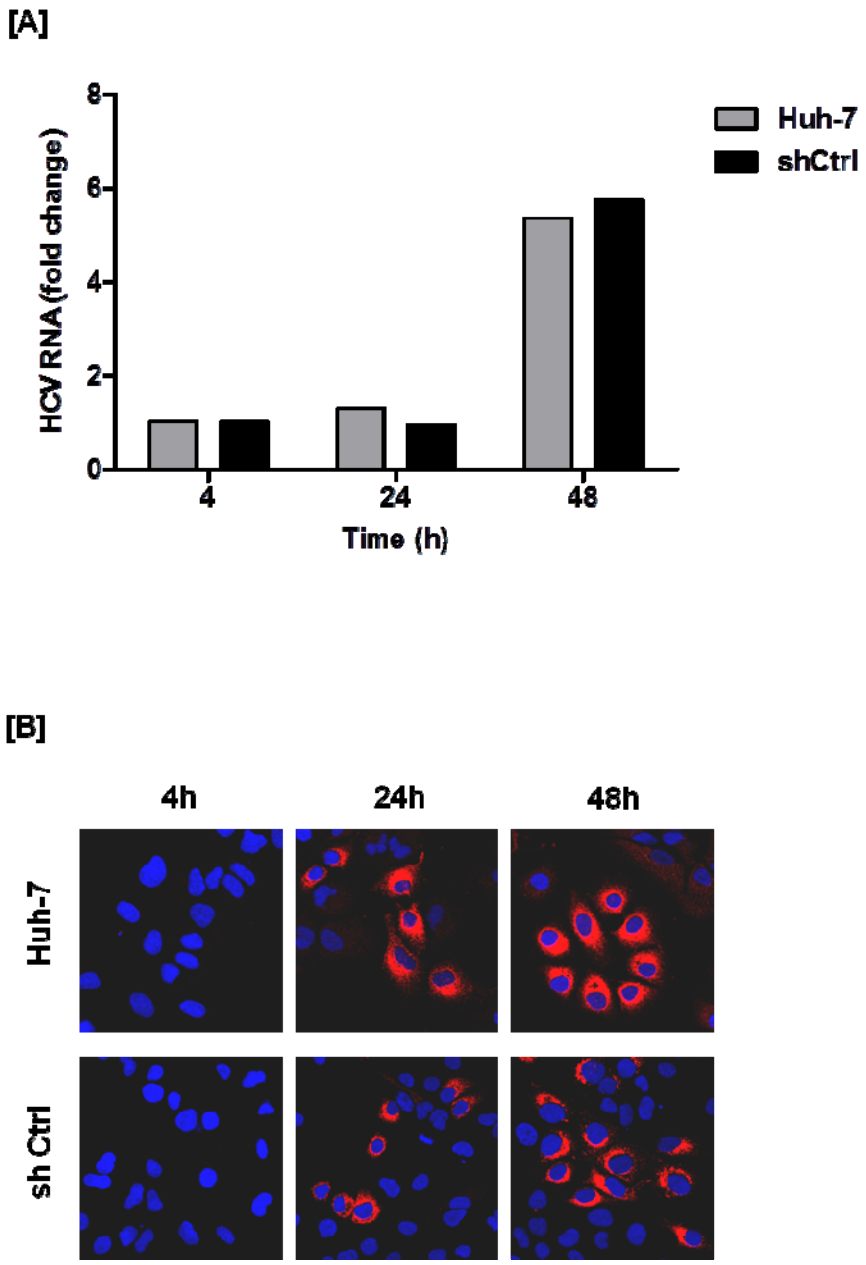


**Figure 4.13 – JC-1 infection efficiency in Huh-7 and shCtrl cell lines. Huh-7 and shCtrl cells were infected with JC-1 virus at a MOI of 1 for 4, 24 and 48h. [A] Levels of HCV RNA were determined by RT-qPCR analysis normalised against abundance of GAPDH mRNA. [B] Immunofluorescence analysis of NS5A expression (Red). For visualization of nuclei, the cells were stained with DAPI.**

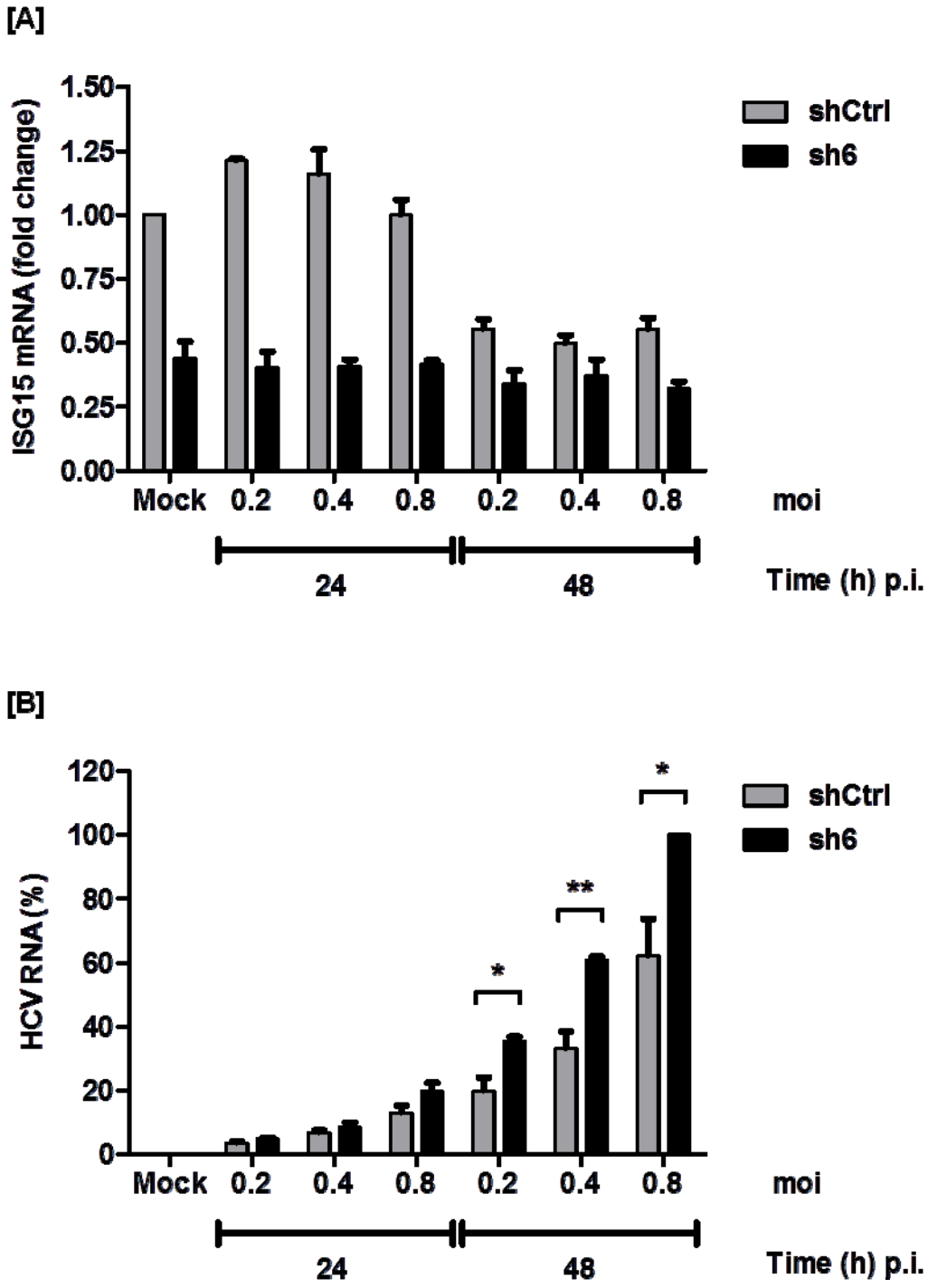


**Figure 4.14 – ISG15 silencing promotes HCV replication. Huh-7 shCtrl and sh6 cells were infected at MOIs of 0.2, 0.4 and 0.8 for up to 48h. Levels of ISG15 [A] and HCV RNA [B] were determined by RT-qPCR analysis and normalised against abundance of GAPDH mRNA. Unpaired t test statistical comparison of HCV RNA levels in shCtrl and sh6 cells are shown: * $p<0.05$ and ** $p<0.005$.**

To examine whether the impact of ISG15 on HCV replication could be detected in the presence of IFN, shCtrl and sh6 cell lines were infected with JC-1 virus at a MOI of 0.8 in the presence or absence of 10U/ml of IFNα. At 6, 24 and 48h, replication was assessed by measuring viral RNA and protein expression levels. As shown in Figure 4.15-A, ISG15 basal levels in untreated shCtrl and sh6 cells were low, and in sh6 cells these levels were further reduced compared with shCtrl cells. Consistent with the data from the previous experiments, abundance of JC-1 RNA was higher in sh6 cells throughout infection, when compared with shCtrl cells (Figure 4.15-B). Western blot analysis of cell extracts at 48h p.i. revealed that sh6 cells expressed slightly higher levels of NS5A protein, when compared with shCtrl cells (Figure 4.15-C), in agreement with the RNA data.

After IFNα treatment, ISG15 expression increased by 66- and 21-fold in shCtrl and sh6 cells, respectively at 6h. By 24 and 48h, ISG15 levels remained higher than in untreated cells, but were reduced when compared with the levels at 6h. At 6h and, to a less extent at 24h after IFNα treatment (6 and 24h p.i), viral RNA levels were lower in the shCtrl cells when compared with the levels in sh6 cells. Following those times, RNA levels decreased further and, by 48h, JC-1 RNA was slightly lower in sh6 cells than in the respective control cells (Figure 4.15-B). From analysis of cell extracts at the latest time point after IFNα treatment, NS5A expression was not detected in the cell extracts. Thus, ISG15 depletion may partially alleviate the anti-viral activities of IFNα during HCV infection, however those effects were only observed at early time-points following virus inoculation.

Taken together, the data from this and the previous experiments suggest that ISG15 plays an anti-HCV role both in an IFN-dependent (only at early time-points after infection, in the case of HCVcc studies) and -independent manner.

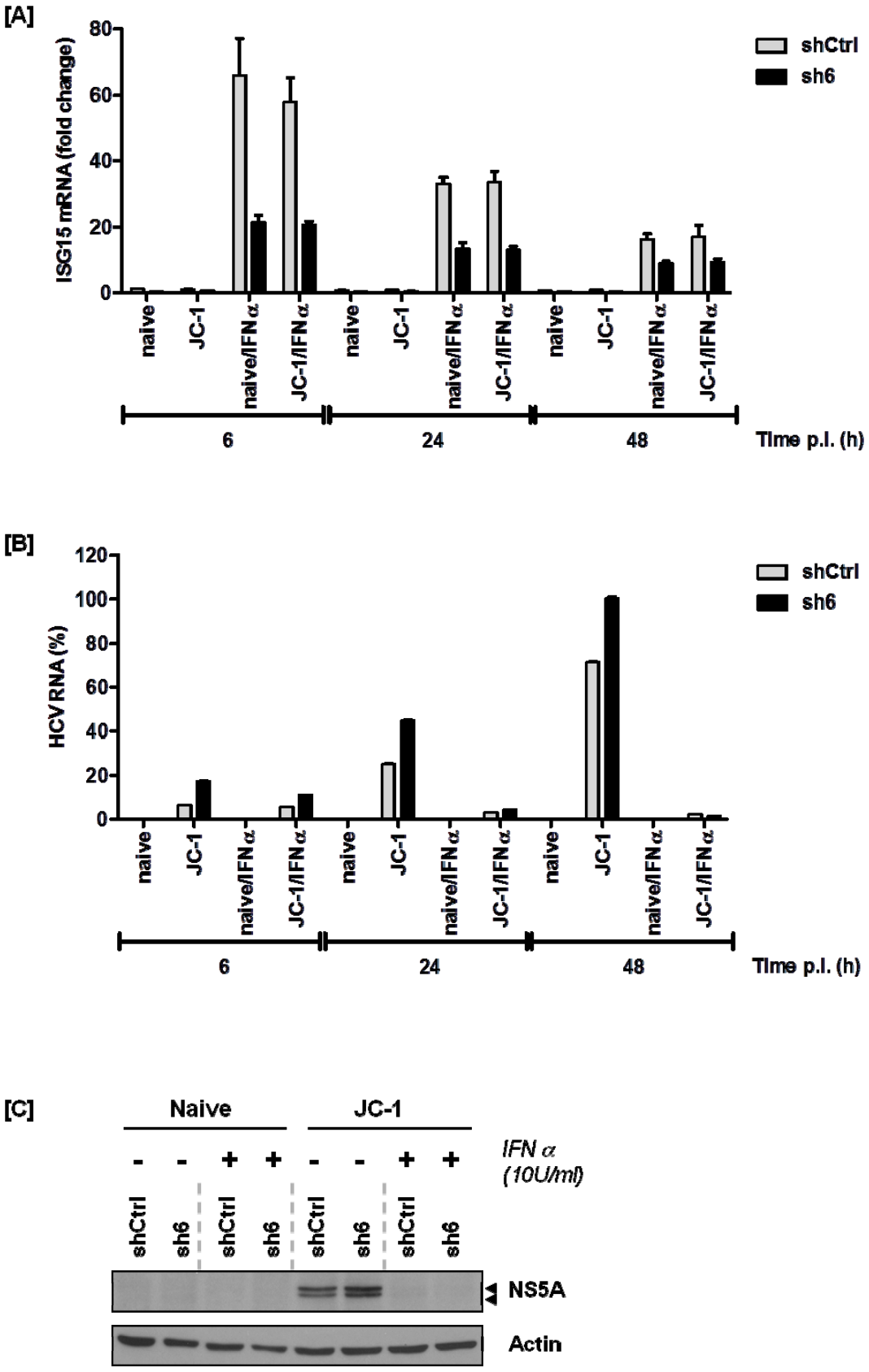


**Figure 4.15 – IFN antiviral activities during HCV infection in ISG15 depleted cells. shCtrl and sh6 cells were infected with JC-1 virus at MOIs of 0.2, 0.4 and 0.8 for up to 48h in the presence or absence of 10U/ml of IFNa. Levels of ISG15 (A) and HCV (B) RNA were determined by RT-qPCR analysis and normalised against abundance of GAPDH mRNA. [C] cell extracts were prepared at 48h after infection and examined by Western blot analysis with anti-NS5A and anti-actin antisera.**

## 4.5 Discussion

In this study, it was found that ISG15 has an inhibitory role during HCV replication. siRNA-mediated depletion of ISG15 from both Huh-7/SGR and U2OS/SGR cells repressed ISG15 expression, which resulted in a suppression of the antiviral activity of IFNα. Moreover, lowering the expression of ISG15 by transfection of siRNAs into SGR cells increased viral RNA levels in Huh-7 and U2OS cells (Figure 4.5) in the absence of IFN. These data indicate that ISG15 plays an inhibitory role during HCV replication both by augmenting IFN-mediated antiviral activity and in a mechanism independent from IFN-activation. Further experiments using the HCVcc system confirmed these results. Infection of Huh-7 cells stably expressing shRNA directed against ISG15 (referred to as sh6 cells), resulted in higher levels of HCV RNA accumulation, when compared with shRNA-Ctrl cells. Together, these findings imply a role of ISG15 in limiting HCV replication.

Type I IFNs play a central role in the innate immune responses to control virus infection. Such responses are in part mediated by a plethora of host genes stimulated by IFN. One of these genes is ISG15 (Farrell *et al.*, 1979). ISG15 encodes a 17-kDa protein which belongs to the family of ub–like proteins and, like other members of this family is capable of forming conjugates to cellular proteins, through a conserved C-terminal di-Glycine motif (Hochstrasser, 2000). Attachment of Ub to proteins (ubiquitination) employs a sequential enzymatic cascade, involving multiple enzymes (Figure 4.16). ISG15 conjugation (ISGylation) is attained through a similar set of reactions, which uses enzymes that are unique to ISG15 conjugation as well as enzymes involved in Ub protein modification [Figure 4.16; (Staub, 2004)].

ISG15 conjugation targets a large number of cellular factors involved in diverse cellular pathways (Loeb & Haas, 1992; Zhao *et al.*, 2005). Many of these substrates are IFNα/β-inducible proteins, including STAT1, Jak1, PKR, MxA and RIG-I, suggesting that ISG15 conjugation might play a role in the innate immune response to both DNA and RNA viruses. Studies using ISG15-deficient mice showed increased susceptibility to infection with several viruses, such as Sindbis virus, herpes simplex virus 1 and murine γ-herpesvirus (Lenschow *et al.*, 2005; Lenschow *et al.*, 2007). In addition, ISG15 has been reported to possess antiviral

activities against Ebola, HIV-1 and Influenza A and B viruses. ISG15 mediates resistance to Ebola virus through ISGylation of the E3 ubiquitin ligase Nedd4, thereby blocking Nedd4 activity and Nedd4-dependent release of virions from cells (Malakhova & Zhang, 2008). Similarly, ISG15 blocks ubiquitination of Gag and Tsg101 proteins (Okumura *et al.*, 2006), thus inhibiting Gag or Tsg101 ubiquitination-dependent release of HIV virions from cells. Moreover, IFN-mediated ISG15 conjugation has been suggested to negatively regulate influenza A virus replication (Hsiang *et al.*, 2009). On the other hand, the influenza B NS1 protein has been reported to bind to ISG15 and block ISGylation of cellular proteins after virus infection (Yuan & Krug, 2001). Thus, there is a growing body of work supporting an important role of ISG15 and ISGylation in the IFN-mediated antiviral response both through the modification of the components of the host immune response and modification of viral proteins.

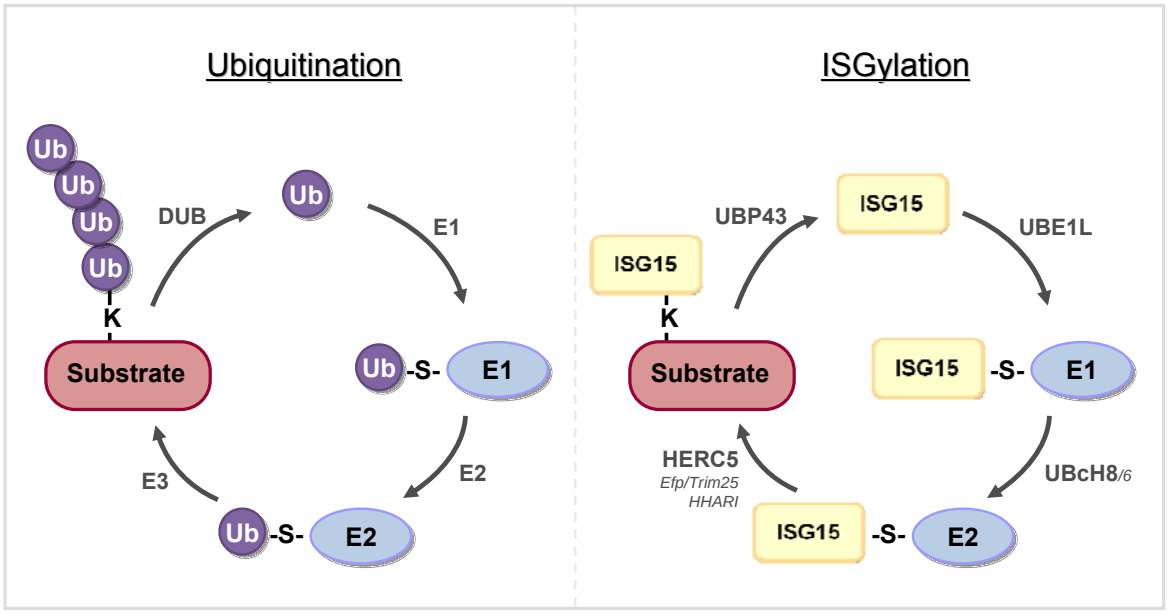


**Figure 4.16 – Protein modification by ubiquitin (Ubiquitination) and ISG15 (ISGylation). Both processes employ similar enzymatic cascades involving E1 activating enzyme (UBE1L), E2 conjugating enzyme (UBcH8/ UBcH6) and an E3 ubiquitin ligase [HERC5, Efp (Trim25) and HHARI]. Ubiquitination and ISGylation are both reversible by the action of deconjugating enzymes, only one of each has been identified in the case of ISG15 (UBP43/USP18). Similarly to ISG15, the proteins involved in ISGylation process is also induced by type I IFNs.**

## I. Lack of ISG15 conjugation in U2OS cells; possible role of HERC5

Exogenous treatment of the two cell lines used in this study, Huh-7 and U2OS cells, with IFN$\alpha$ and $\beta$ induced high expression of both ISG15 mRNA and unconjugated protein. However, U2OS cells produced low amounts of ISG15 conjugates in response to type I IFNs, in contrast to the levels detected in Huh-7 cells. From further analysis, it was found that U2OS cells lack HERC5, the major E3 ligase involved in ISG15 conjugation (Figure 4.18). Thus, the reduced levels of ISG15 conjugates in U2OS cells are likely to result from absence of HERC5. It is presumed that ectopic expression of HERC5 in U2OS cells could restore their ability to produce higher amounts of conjugated ISG15 in response to IFN. Alternatively, other enzyme factors involved in ISGylation in addition to HERC5 may be downregulated or absent in U2OS cells; addressing these two possible explanations for the decreased amounts of conjugated ISG15 in U2OS cells would require further experiments.

Given that silencing of ISG15 in U2OS cells resulted in an increase in HCV RNA levels, it implies that ISG15 plays an inhibitory role against HCV replication in these cells as well as in Huh-7 cells. Since U2OS cells do not produce conjugated ISG15 to the same extent as in Huh-7 cells, it is feasible that different mechanisms may be employed by ISG15 for countering viral replication in the two cells lines. In the case of U2OS cells, free ISG15 may be sufficient for anti-HCV activities, possibly by acting primarily as a transcription factor or cytokine (Recht *et al.*, 1991). By contrast, in Huh-7 cells ISG15 may require conjugation to limit viral replication, either by conjugating to a viral or host protein required for optimal viral replication. Kim & Yoo (2010) have previously demonstrated that the viral protein NS5A is indeed a target for ISGylation. Alternatively, it is possible that ISG15 may act primarily in both cell lines as an unconjugated protein to regulate viral replication. To investigate the conjugation requirements of ISG15 for its anti-HCV activities, preliminary experiments were undertaken and are presented in Chapter 5.

## II. Interplay between ISG15 and USP18

As well as the lack of HERC5 in U2OS cells, it was observed that lowering the expression of ISG15 mRNA levels in both Huh-7 and U2OS cells treated with IFNα resulted in a relative rise in USP18 mRNA levels. Such observations have been reported by others (Chua *et al.*, 2009; Randall *et al.*, 2006). This differential response could imply a feedback mechanism between ISG15 and USP18, the enzyme involved in removal of ISG15 from conjugated forms, and indeed, that transcriptional control of the genes involved in ISGylation are intimately interconnected. ISG15 both positively and negatively regulates activation of type I IFNs, by preventing degradation of IRF-3 or activation of RIG-I, respectively (Kim *et al.*, 2008; Lu *et al.*, 2006). Thus, it is possible that ISG15 and/or ISGylation may also be involved in further regulatory mechanisms to guarantee the optimal response of IFN to invading pathogens.

The activities of IFNs must be tightly regulated to function optimally and provide an adequate response to a stimulus. For example, several mechanisms have been described to coordinate IFN-mediated JAK/STAT signalling. In a study by Sarasin-Filipowicz *et al* (2009) repeated treatment of mice with IFNα led to a refractory activity to further IFNα stimulation (Sarasin-Filipowicz *et al.*, 2009). Previous studies have shown that USP18 plays a role in modulating the antiviral activities of type I IFNs and in IFN-induced desensitization (Murray *et al.*, 2011; Randall *et al.*, 2006). Silencing of USP18 results in prolonged phosphorylation of STAT1, and consequently in an increase in the IFNα-mediated induction of ISG15 and other ISGs (Randall *et al.*, 2006). USP18 has been shown to negatively regulate IFN signalling by binding to IFNR2 and blocking downstream signalling through the JAK/STAT pathway (Malakhova *et al.*, 2006). Further studies that identify the mechanism underlying stimulation of USP18 transcription through impairing ISG15 expression may shed light on the interplay between the genes involved in ISGylation.

### III. The impact of ISG15 on HCV replication

To date, there have been four other studies that have specifically examined the effect of ISG15 on HCV replication and, in some cases, virion production (Broering *et al.*, 2010; Chen *et al.*, 2010; Chua *et al.*, 2009; Kim & Yoo, 2010). Combined with the results presented here, the findings do not provide a consensus on whether ISG15 promotes or disrupts replication; a summary of the findings from each study is presented in Table 1. As well as the summarised information in the table, which illustrates the range of model systems used, there are some points worth noting in terms of differences observed with the data presented in this study. For example, Chen *et al* (2010) found that transfection of a construct expressing ISG15 yielded higher levels of HCV RNA and infectious virus even in the presence of low amounts (up to 1U/ml) of IFN$\alpha$. In their data to support evidence for over-expression of ISG15, they were apparently able to detect conjugated ISG15 without the need to stimulate the levels of the enzymes required for ISGylation and also could detect unconjugated ISG15 in untransfected cells in the absence of IFN$\alpha$. From the data presented here, conjugated forms of ISG15 could not be detected following over-expression of ISG15 alone (Chapter 5). Moreover, unconjugated ISG15 cannot be detected without the addition of IFN. Hence, there are fundamental differences in the characteristics of ISG15 between Chen *et al* (2010) and the results in this study. One striking example of the conflicting data observed was made by Kim & Yoo (2010) who reported decreased levels of replication with the Con-1 replicon in Huh-7 cells, which had been transfected with plasmids expressing ISG15, UbE1L (an E1 activating enzyme for ISG15 conjugation) and UbcH8 (an E2 enzyme for ISG15 conjugation); by contrast in Huh-7.5 cells infected with JFH-1, this combination of vectors enhanced HCV replication (Kim & Yoo, 2010). Thus, it is very likely that the contradictory findings in the data presented in Table 1 are a combination of differences in the replication system used (gts1a, 1b and 2a), the cell lines (Huh-7 from different sources including use of cell lines cured by IFN and a polymerase inhibitor) as well as alternative experimental strategies (e.g. the ranges of IFN employed in the various studies).

Based on the pooled data in Table 1 and the study by Kim & Yoo (2010), analysis of the effects of ISG15 in Huh-7.5 cells harbouring the JFH1 SGR would

have been valuable to determine whether inhibiting ISG15 in these cells had the same effect as in Huh-7 and U2OS cells. However, time constraints did not permit such studies to be performed. Nonetheless, comparative proteome analysis of Huh-7 and Huh-7.5 cells has shown that there are differences between the two cell lines (C. Hinds, *pers. comm.*) and it is known that Huh-7.5 cells express an inactivated, mutated form of RIG-I (Sumpter *et al.*, 2005). In addition, inherent variability between Huh-7 cells from different sources, at the level of permissiveness to HCV replication as well as to response to dsRNA stimuli, has been reported previously (Binder *et al.*, 2007; Sainz *et al.*, 2009a). Indeed, Huh-7 cells from different sources have yielded different host genotypes at the IL28B locus (Bensadoun *et al.*, 2011). In an attempt to partially address variation between cell lines as a possible explanation for the discordant results, the ISG15 expression levels induced by IFN$\alpha$ were examined in three different batches of Huh-7 cells that were available (referred to as Huh-7 A, Huh-7 B and Huh-7 C) and Huh-7.5 cells (Figure 4.17). ISG15 expression levels were very similar in all untreated Huh-7 cells but there were approximately 2-fold higher levels in Huh-7.5 cells (Figure 4.17-B). Treatment with increasing doses of IFN$\alpha$ induced comparable levels of ISG15 mRNA in all cell lines including Huh-7.5 cells (Figure 4.17-A). At the protein level, it was noted that unconjugated ISG15 could be induced to similar levels in all cell lines but the abundance of conjugated protein was considerably less in Huh-7.5 cells (Figure 4.17-C). Moreover, the abundance of phosphorylated STAT1 protein (P-STAT1) was somewhat less in Huh-7.5 cells (Figure 4.17-C). More detailed analysis on the characteristics of the cell lines is needed to provide a possible explanation for the differences in the reported literature and the findings in this study on the impact of ISG15 on HCV replication.

### IV. Approaches for inhibiting ISG15 expression

Given that all of the previous studies had utilised short-term inhibition (by siRNA transfection) or over-expression (by transfection of plasmids expressing ISG15), an alternative approach using shRNAs was adopted to try to overcome possible undesired effects in transient assays. For example, siRNA-mediated silencing can cause effects other than the intended mRNA suppression (commonly regarded as off-target effects). Rao *et al* (2009) has reviewed the

major problems associated with off-target effects for siRNA-mediated gene knockdown (Rao *et al.*, 2009). Briefly, specific off-target effects are observed through partial sequence complementarities of the siRNA construct to mRNA, other than the intended target. These off-target effects are often unrelated to the ability of the siRNA to silence the gene of interest. Improvements have been made in recent years to address these problems, by designing siRNAs with reduced off-target effects. However, in some cases such modifications are sometimes accompanied with a decrease in overall potency of suppression of the siRNA (Snove & Rossi, 2006; Watts *et al.*, 2008). In addition, non-specific off-target effects associated with siRNA silencing can result from immune-mediated responses to exogenous RNAi and cellular toxicity. Some studies have demonstrated that a partial interferon response is induced through activation of TLR3 dsRNA sensors and are often dependent on the siRNA sequence (GU-dependent, 5'-UGUGU-3' and GU-independent, 5'-GUCCUUCAA-3') (Kariko *et al.*, 2004; Sledz *et al.*, 2003). Moreover, siRNAs are delivered into the cells typically via the action of cationic preparations. These facilitate the binding of siRNAs to the cell membrane and promote endocytosis and escape from endosomes. This method improves significantly the transfection efficiency of siRNAs, although it is often associated with increased toxicity.

In the case of shRNAs, sequence-dependent induction of immune responses could also promote non-specific off-target effects. However, shRNAs use the endogenous processing machinery, an advantage over siRNAs in terms of a lower propensity for induction of IFN. In addition, delivery of shRNAs into cells using viral vectors provides higher efficiency in transfection and integration into chromosomal DNA allows selection of stable cell lines that express the inhibitory shRNA. Since transcription of any insert occurs in the nucleus with further processing through endogenous machinery, shRNAs are less susceptible to degradation in the cytoplasm. Thus, higher efficiency in gene silencing by shRNAs can be achieved using low copy numbers and thus fewer off-target effects.

**Table 1 – Summary of the findings regarding ISG15 activities on HCV replication.**

| Study | Effect of ISG15 (-IFN) | Effect of ISG15 (+IFN) | Replication system | Cell lines |
|---|---|---|---|---|
| (Chua *et al.*, 2009) | No effect | Stimulates (increased sensitivity to IFNα at low values of IFN [<10 U/ml]) | • SGR: Con-1 [gt1b];<br>• HCVcc studies: H77-S [gt1a] | • Huh-7 [for Con-1];<br>• Rof-0c [for H77-S; cured replicon cells using polymerase inhibitor] |
| (Broering *et al.*, 2010) | Stimulates | Stimulates | • SGR: Con-1 [gt1b];<br>• HCVcc studies: JC-1 [gt2a chimera] | • MH1 [for Con-1; mouse hepatoma cells];<br>• 'con1' [presumed to be Huh-7 for Con-1];<br>• Huh-7.5 [HCVcc studies] |
| (Chen *et al.*, 2010) | Stimulates | Stimulates | • HCVcc studies: JC-1 [gt2a chimera] | Huh-7.5 |
| (Kim & Yoo, 2010) | Inhibits | Inhibits | • SGR: Con-1 [gt1b] | Huh-7 |
| (Kim & Yoo, 2010) *(Supplementary data)* | Stimulates | Not tested | • HCVcc studies: JFH-1 [gt2a] | Huh-7.5 |
| This study | Inhibits | Inhibits | • SGR: JFH-1 [gt2a] & Con-1 [gt1b];<br>• HCVcc studies: JC-1 [gt2a chimera] | • Huh-7 [for Con-1, JFH-1 SGR/HCVcc];<br>• U2OS [for JFH-1 SGR] |

Using shRNAs, one cell line, sh6, was selected that constitutively expressed lower levels of ISG15 both in the presence and absence of IFNα. Studies with this cell line indicated that electroporation of viral SGR RNA did not result in any increase in HCV replication compared to cells expressing a control shRNA. By contrast, it was possible to reproducibly detect higher viral RNA levels across a

range of multiplicities of infection with infectious JC-1. It is possible that the amount of RNA introduced into cells for transient assays (of the order of as many as $10^6$ copies of *in vitro* transcribed RNA per cell) masked any possible effect of the lower ISG15 levels in sh6 cells. Indeed, ISG15 protein, either in the unconjugated or conjugated form, could not be detected in shCtrl or cells not transduced with lentivirus. With the HCVcc system, the number of infectious genomes entering the cell will be at most 1-2 copies per cell, which is more representative of the infectious process *in vivo*. The fact that infectious assays in sh6 cell did reproduce the data using transiently transfected siRNAs adds weight to the overall conclusion that ISG15 impairs HCV RNA replication in cells that are not stimulated by IFN.

Given that there are caveats even with the shRNA system used, another alternative method for future studies on ISG15 function during HCV infection would be to generate cell lines with a deletion of the gene. Recently, a new technology based on employing gene-targeted zinc-finger nucleases (ZFNs) has been used to produce cell lines with gene-targeted deletions. ZFNs are synthetic fusion proteins consisting of two main functional domains; an engineered zinc finger, which mediates recognition of nucleotide sequences (DNA-binding domain) that is fused to the cleavage domain of the *Fok*I restriction endonuclease (cleavage domain). The *Fok*I restriction endonuclease cleaves the phosphodiester bond in the DNA backbone. ZFNs can be designed to recognise and cleave specific nucleotide sequences in the genome to create double strand DNA breaks (DSB). This event consequently activates the cellular mechanisms of DSB repair, either by error-prone non-homologous end joining (NHEJ) or by stimulation of homologous recombination with a donor DNA template (HDR). Among other applications, this approach using ZFNs exploits NHEJ-derived modifications, which lead to a mutated gene with a knock-out phenotype. The technology has been reported to successfully mediate gene knockout in cultured cells (Santiago *et al.*, 2008). Applying this approach to studies on ISG15 function would be highly beneficial to overcome the limitations on siRNA- and shRNA-meditated targeting.

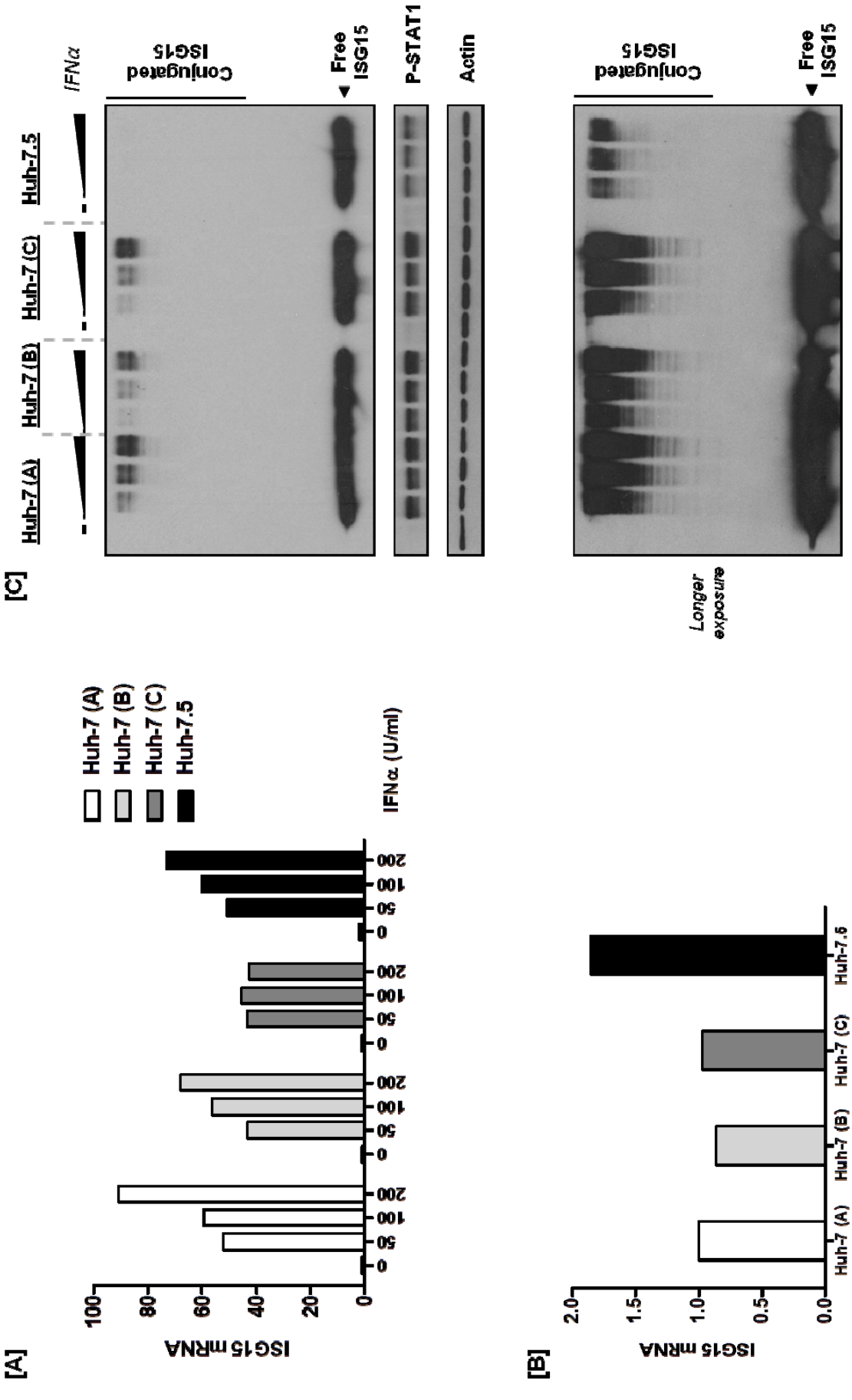
[A]
Huh-7 (A)
Huh-7 (B)
Huh-7 (C)
Huh-7.5
IFNα (U/ml)
ISG15 mRNA
0
20
40
60
80
100
0
50
100
200
[B]
ISG15 mRNA
0.0
0.5
1.0
1.5
2.0
Huh-7 (A)
Huh-7 (B)
Huh-7 (C)
Huh-7.5
[C]
IFNα
Huh-7 (A)
Huh-7 (B)
Huh-7 (C)
Huh-7.5
Conjugated ISG15
Free ISG15
P-STAT1
Actin
Longer exposure

**Figure 4.17 – Expression levels of ISG15 in Huh-7 and Huh-7.5 cells. Three batches of Huh-7 cells (A, B and C) and Huh-7.5 cells were treated with increasing doses (0, 50, 100 and 200U/ml) of IFNα, β and γ. At 48h after treatment cells extracts were used for RT-qPCR analysis of ISG15 mRNA expression [A] and [B] and Western blot analysis of ISG15 free and conjugated forms using anti-ISG15 antisera [C]. Expression of phosphorylated form of STAT1 protein and actin were examined using anti-P-STAT1 and anti-actin antisera.**

**Figure 4.18 – Analysis of HERC5 silencing in U2OS/SGR cells. U2OS/SGR cells were transfected with control, ISG15 and HERC5 siRNAs (siCtrl, siISG15 and siHERC5, respectively) for 24h, followed by treatment with increasing doses (0, 1, 10 and 100 U/ml) of IFNα for 48h. U2OS cells were treated with 0 and 100U/ml IFNα for 48h. RT-qPCR analysis of ISG15 [A] and HERC5 [B] mRNA expression levels. [C] Western blot analysis of ISG15 conjugated and unconjugated forms, HERC5 and actin protein expression levels, using anti-ISG15, anti-HERC5 and anti-actin antisera.**

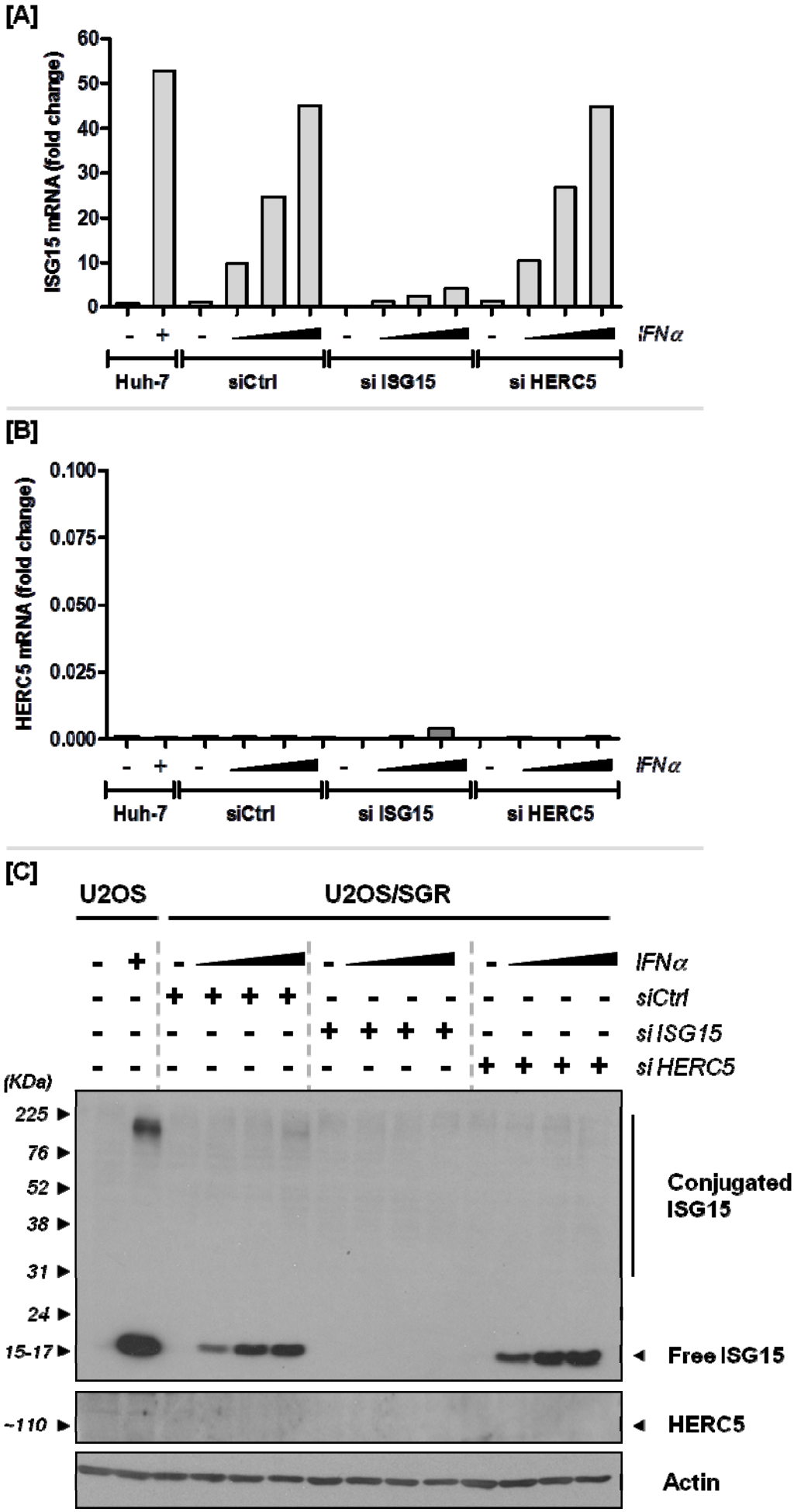
[A]
ISG15 mRNA (fold change)
60
50
40
30
20
10
0
- + - - -
IFNα
Huh-7
siCtrl
si ISG15
si HERC5
[B]
HERC5 mRNA (fold change)
0.100
0.075
0.050
0.025
0.000
- + - - -
IFNα
Huh-7
siCtrl
si ISG15
si HERC5
[C]
U2OS
U2OS/SGR
IFNα
siCtrl
si ISG15
si HERC5
(KDa)
225
76
52
38
31
24
15-17
~110
Conjugated ISG15
Free ISG15
HERC5
Actin

# 5 Investigation of the ISG15 mechanisms against HCV replication

## 5.1 Introduction

Following the observations from the previous sections, we sought to further investigate the antiviral mechanism of ISG15 in HCV replication. To that end two approaches were used to understand the pathways through which ISG15 delivers its activities to control replication, i.e. whether free ISG15 or conjugated ISG15 are required for such functions, and the stage of the viral life cycle that is targeted. To answer the latter question, we sought to investigate whether ISG15 affects the rates synthesis or degradation of viral RNA during HCV replication.

## 5.2 Effect of ISG15 on viral RNA synthesis

To determine the mechanism through which ISG15 modulates HCV replication, the reasons for the differences observed in the steady-state levels of viral RNA between shCtrl- and sh6-infected cells were investigated. For every transcript, steady-state RNA levels result from a balance between RNA synthesis and decay. To examine whether the differences observed in steady-state viral RNA levels could reflect changes in either the relative rates of RNA stability or synthesis, a recently described method for metabolic tagging of *de novo* synthesized transcripts was adopted [(Dolken *et al.*, 2008); Figure 5.1].

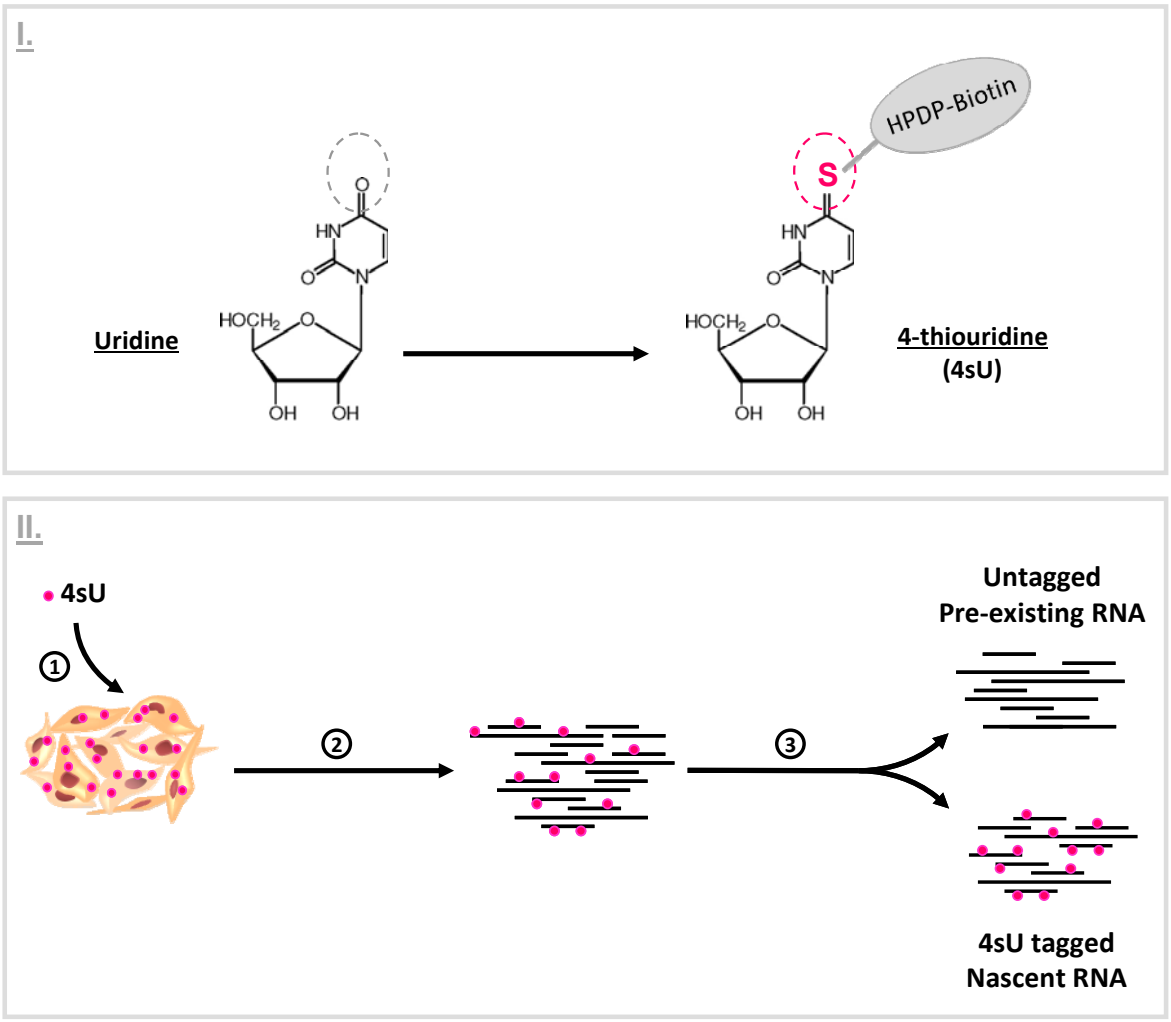


**Figure 5.1– Metabolic tagging of nascent RNA. 4-thiouridine (4sU), a thiol-group containing nucleoside (I.), was used to metabolically label newly transcribed RNA. Following labelling (II.), newly transcribed RNA can be isolated from untagged pre-existing transcripts molecules using thiol-specific biotinylation and purified on streptavidin-coated magnetic beads. The different fractions of RNA can then be quantified using RT-qPCR (absolute quantification). Modified from Friedel & Dolken, 2009.**

In this method, labelling of newly synthesised RNA is achieved by incubating cells in the presence of 4sU (4-thiouridine), a thiol-containing uridine analogue (Figure 5.1-I). The modified nucleoside is readily incorporated into nascent RNA in the place of uridine, with minimal effects on normal cellular gene transcription (Melvin *et al.*, 1978). Newly synthesized transcripts can then be separated from unlabelled RNA using the thiol groups in 4sU-labelled RNAs, which serve as an attachment point for a biotin tag. This interaction allows the subsequent separation of *de novo* synthesised transcripts from the total RNA population using streptavidin-coated magnetic beads.

Under steady-state conditions, RNA synthesis and decay are in equilibrium in order to maintain a pool of stable transcripts. Using the newly transcribed labelled RNA data, together with total RNA ratios and the duration of labelling, RNA half-life can be calculated. Thus, changes in RNA decay and synthesis as well as their impact on total RNA levels can be analysed. In this series of experiments, 4sU-labelling of RNA was applied to determine the abundance of newly synthesised viral transcripts during HCV infection to evaluate the effects of ISG15 silencing on rates of viral RNA synthesis and/or degradation.

### 5.2.1 Optimisation of 4sU labelling of HCV RNA

As reported previously (Rabani *et al.*, 2011), short-term labelling periods can be sufficient for efficient incorporation of 4sU into newly transcribed RNA. To examine the feasibility of labelling nascent viral RNA, cells that constitutively replicated HCV SGR RNAs were used. 4sU was added to the culture medium at a final concentration of 100uM, which has proven to be non-toxic to cells (Friedel & Dolken, 2009). Huh-7/SGR cells were labelled with 4sU for 0, 30, 60 and 120 min, followed by immediate RNA extraction. After isolation of total RNA and thiol-specific biotinylation, total and 4sU-labeled viral RNA was detected and quantified by absolute quantitative PCR of reversed transcribed RNA pools (as described in Chapter 2, section 2.2.8.5). The following sections describe the method used to determine absolute quantification of total and newly transcribed viral RNA and their relative ratios (Figure 5.2).

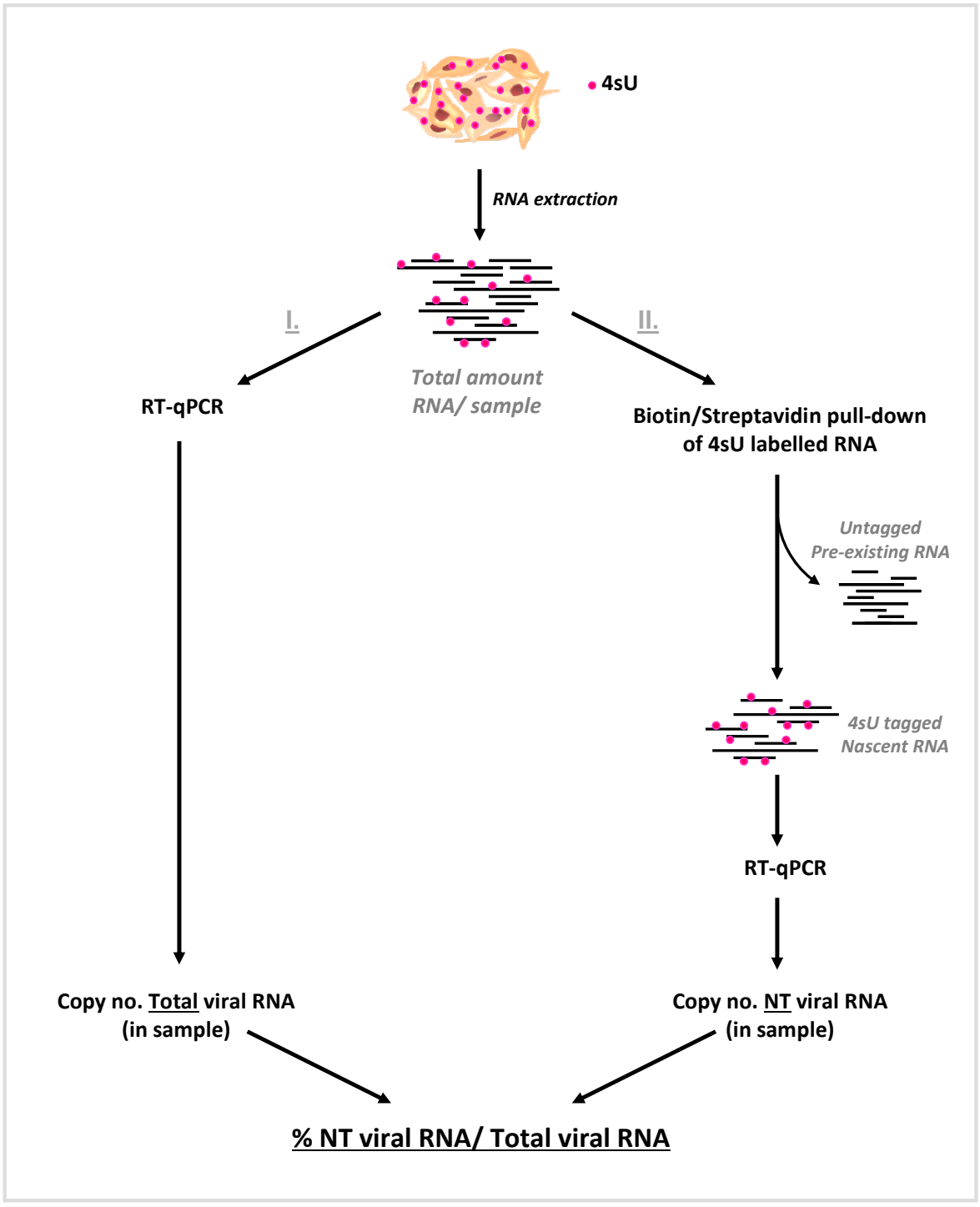


**Figure 5.2 – Schematic representation method used to determine absolute quantification of total and newly transcribed viral RNA. RNA was extracted from 4sU-labelled cells, quantified and used for I) calculation of copy number of total viral RNA (SGR or full-length) in the sample by RT-qPCR; and II) biotinylation of labelled RNA and purified on streptavidin-coated magnetic beads, followed by calculation of copy number of labelled/newly transcribed viral RNA (SGR or full-length) in the sample by RT-qPCR. To determine the relative proportion of newly transcribed viral RNA in each sample, the calculated copy numbers for each RNA fraction (I and II) were combined and expressed as percentage (%) of NT viral RNA per total viral RNA in the sample.**

### 5.2.1.1 Absolute quantification of viral RNA copy number

For calculating the copy number of viral RNA isolated from cells, a standard curve containing a range of known quantities of HCV transcripts was constructed. In these experiments, a standard dilution series was prepared by serial 10-fold dilutions of *in vitro* transcribed (IVT) viral RNA (SGR RNA or in later experiments, full-length RNA). The standard curve, generated by this approach, is represented in Figure 5.4-B. Based on the length of IVT RNA (SGR = 8032bp and JC-1 = 9605bp), the copy number was calculated as shown in Figure 5.3.

$$\text{Molecular Weight } (g/mol) = [(\text{length of RNA [nt]}) \times (320.5\ [\text{Da}])] + 159^{*} \quad [1]$$

$$\text{g/molecule} = \frac{\text{Molecular Weight}}{\text{Mole}} \quad [2]$$

$$\text{Copies of transcript/ ul} = \frac{\text{RNA concentration } (g/ul) \times 10^{-12}}{\text{g/molecule}} \quad [3]$$

**Figure 5.3 – Calculation of HCV RNA copy number. [1] Molecular weight, MW, of viral ssRNA is calculated using the number of nucleotides in one RNA molecule multiplied by the average MW per ribonucleotide (320.5 Da or g/mol). Addition of 159 to the MW takes into account the MW of a 5' triphosphate. [2] The number of molecules in 1 mole is calculated by dividing the MW of viral transcripts by Avogadro's number ($6.02214199 \times 10^{23}$). [3] Using the concentration of viral RNA per sample, and dividing by the number of molecules per mole calculated in [2], the copy of viral RNA transcripts per µl can be calculated.**

The copy number per pg of IVT RNA (e.g SGR RNA) was calculated using the equations represented in Figure 5.3:

$$\text{Molecular Weight} = [(\text{length of RNA [nt]}) \times (320.5\ [\text{Da}])] + 159 \quad [1]$$

$$= [8032 \times 320.5] + 159$$

$$= 2574415\ \text{g/mol}$$

$$\text{g/molecule} = \frac{2574415}{6.02214199 \times 10^{23}} \quad [2]$$

$$= 4.2749 \times 10^{-18}\ \text{g/molecule}$$

$$\text{Copies of transcript/ µl} = \frac{1 \times 10^{-12}}{4.2749 \times 10^{-18}} \quad [3]$$

$$= 233923.6005\ \text{transcripts/µl}$$

From the formulae used in Figure 5.3, the copy number in the serial dilutions of IVT HCV RNA was calculated (Table 2). These values were plotted against the CT values obtained by RT-qPCR (Table 3), giving the standard curve shown in Figure 5.4. From the standard curve, the copy number of viral RNA in unknown samples was derived (either total amount of viral RNA or newly transcribed viral RNA in each sample).

**Table 2 – Copy number of HCV IVT standards.**

| Standard sample | Concentration (pg/µl) | Copies of transcript/µl (SGR RNA) | Copies of transcript/µl (JC-1 RNA) |
|---|---|---|---|
| S1 | 1000 | 233923600.5 | 195615451.9 |
| S2 | 100 | 23392360.05 | 19561545.19 |
| S3 | 10 | 2339236.005 | 1956154.519 |
| S4 | 1 | 233923.6005 | 195615.4519 |
| S5 | 0.1 | 23392.36005 | 19561.54519 |
| S6 | 0.01 | 2339.236005 | 1956.154519 |
| S7 | 0.001 | 233.9236005 | 195.6154519 |
| S8 | 0.0001 | 23.39236005 | 19.56154519 |

**Table 3 – Standards *vs* CT.**

| Standard sample | AVR CT (SGR RNA) | AVR CT (JC-1 RNA) |
|---|---|---|
| S1 | 8.6 | 8.6 |
| S2 | 11.1 | 10.6 |
| S3 | 14.1 | 13.8 |
| S4 | 17.9 | 17.4 |
| S5 | 21.6 | 20.8 |
| S6 | 25.4 | 24.2 |
| S7 | 29.1 | 28.0 |
| S8 | 32.3 | 31.6 |

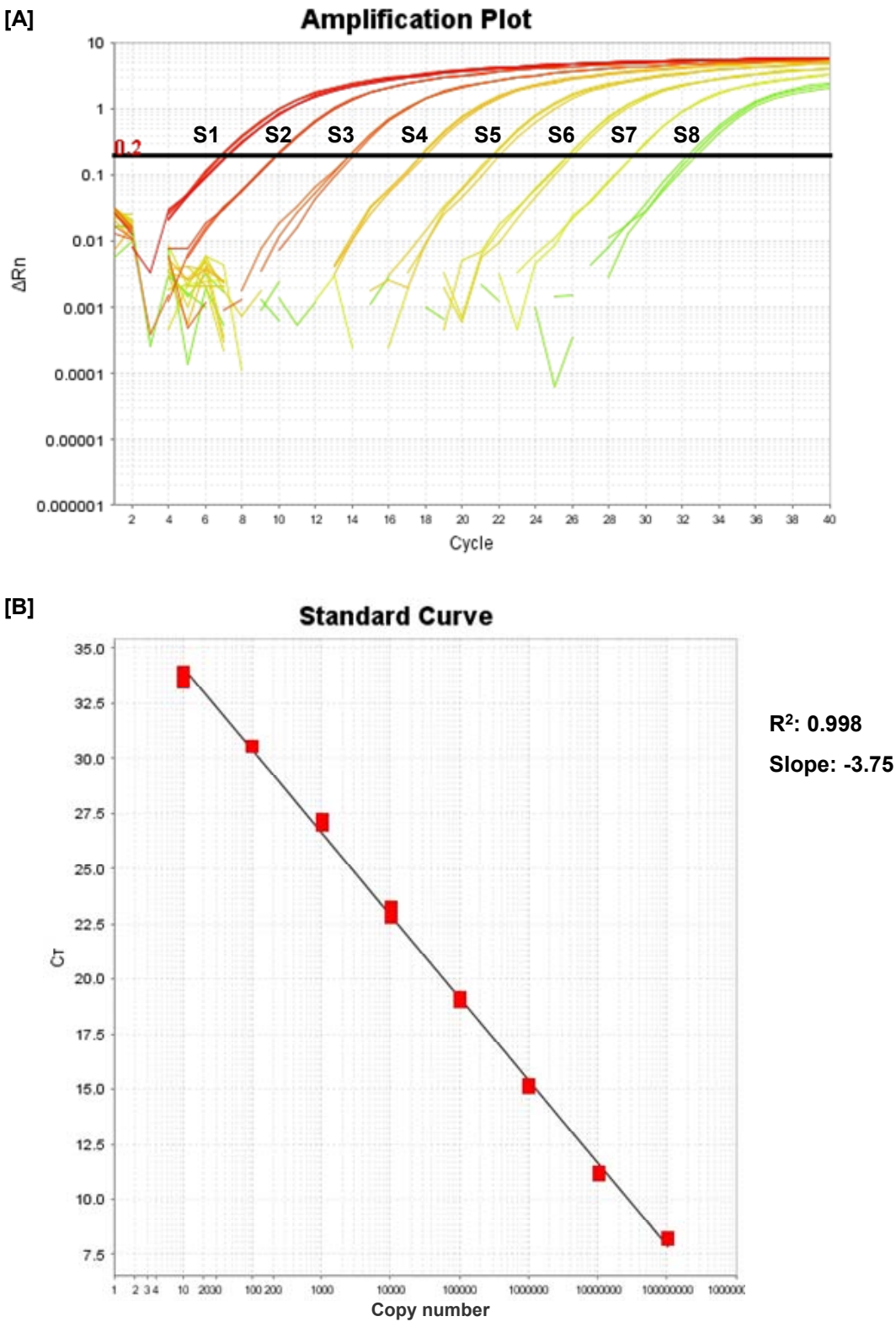


**Figure 5.4 – Amplification plot of IVT SGR standards (A) and the derived standard curve (B). The standard curve is calculated by applying linear regression (best-fit line) in a plot of the Ct values from the standard reactions plotted against standard quantities The regression line formula is Ct=m[log(Qty)]+b, where m is the slope, b is the y-intercept and Qty is the standard quantity. The $R^2$ values indicate the closeness of fit between the standard curve and the individual Ct data points from the standard reaction. A value of 1.00 indicates a perfect fit between the regression line and the data points. The slope indicates the PCR amplification efficiency for the assay. A slope of -3.32 indicates 100% amplification efficiency.**

#### 5.2.1.2 Labelling of newly transcribed viral RNA in Huh-7/SGR cells

To determine whether addition of 4sU affected viral RNA replication, Huh-7/SGR cells were labelled with the nucleoside for up to 2h and RNA was isolated at the times indicated in Figure 5.5-A. Following RT-qPCR analysis, the copy number of total viral transcripts was determined. The data indicated that the number of copies of viral RNA did not change during the labelling period and therefore, it was concluded that addition of 4sU to cells had no dramatic effect on replication (Figure 5.5-B). Labelled RNA also was purified from the total RNA to examine whether there was any evidence of incorporation of the modified nucleoside into replicated HCV RNA (Figure 5.5-C). By 30min, no labelled viral RNA was found, however, it was possible to detect approximately $2x10^7$ HCV transcripts at 1h (equivalent to less than 1% of labelled viral RNA in the overall amount of viral RNA, Figure 5.5-D). This figure rose to $2x10^8$ molecules by 2h after addition of 4sU (equivalent to ~5% viral RNA) (Figure 5.5-C&D). This preliminary experiment revealed that it was possible to label, isolate and quantify viral RNA with 4sU. However, it was concluded that longer labelling times might be necessary for accurate quantification of newly synthesised viral RNA.

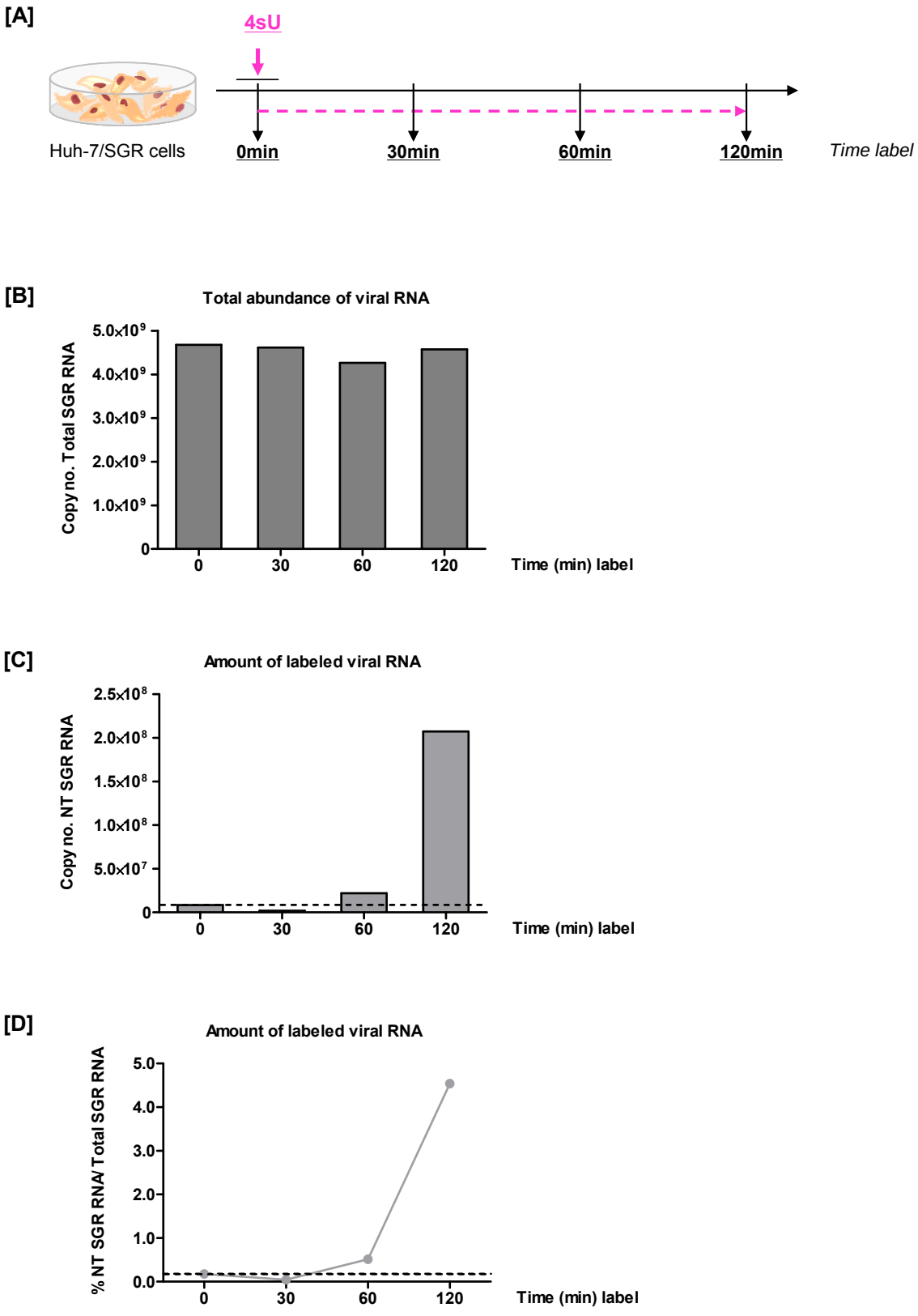


**Figure 5.5 – Labelling and quantification of newly transcribed viral RNA during HCV replication. Huh-7/SGR cells were labelled (100uM 4sU) for 0, 30, 60 and 120min. A) Experimental outline. B) Total abundance of viral RNA. C) Amount of labelled viral RNA. D) Percentage of labelled SGR RNA relative to total viral RNA in the sample. Dashed lines represent cut-off of labelling nascent RNA.**

### 5.2.1.3 Optimization of labelling duration suitable for infection assays

Given that in cells stably expressing the HCV SGR, only ~5% of newly transcribed viral RNA could be labelled in 2h, this number would be expected to be even lower in infected cells, as the levels of viral RNA are less than in stably expressing SGR cells. Thus, in order to guarantee labelling of RNA during viral infection, longer 4sU labelling times and/or higher concentrations were required. To that end, the effect of longer times (2, 16, 24 and 48h) and increased concentrations (0, 50, 100, 200 and 400uM) of 4sU labelling on cell viability were examined in Huh-7 cells using the resazurin reduction assay (as described in Chapter 2, section 2.2.8.6). As shown in Figure 5.6, labelling Huh-7 cells for up to 16h did not affect substantially cell viability at most 4sU concentrations, although at 400uM some negative effects started to appear, as cell viability decreased by about 20% when compared with untreated cells. At 24h, cell viability was partly affected with 50, 100 or 200uM of 4sU, as the values were at or higher than 80% viability. Exposing the cells to 400uM of 4sU on the other hand had a greater effect, reducing viability to 65%. By 48h, all 4sU concentrations were shown to impact on cell viability, as the levels were lower than 80%, and at 400uM cell viability reduced further to about 40%. These results, indicated that was possible to label Huh-7 cells using either 50 or 100uM of 4sU for up to 24h, without substantial effects on cell viability. Thus, for the following infection assays, 100uM 4sU was selected for labelling viral RNA for up to 24h.

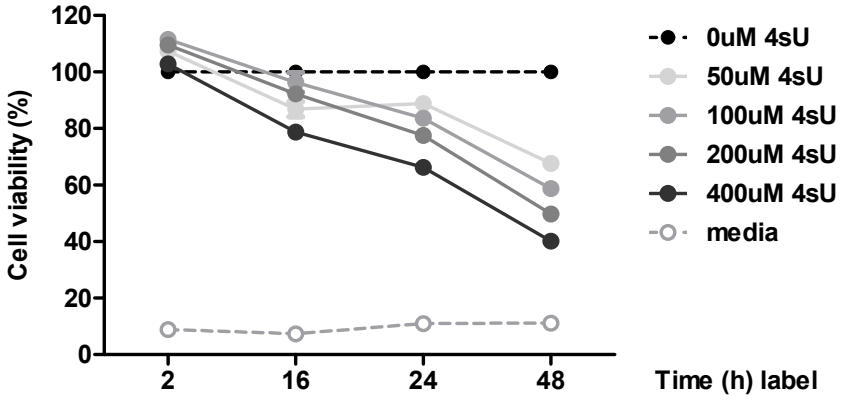


**Figure 5.6 – Cell viability of Huh-7 exposed to increasing concentrations of 4sU. Huh-7 cells were labelled with 0, 50, 100, 200 and 400uM of 4sU for up to 48h. The toxicity associated with 4sU exposure was assessed using the resazurin reduction test. The viable cells retain the ability to reduce resazurin and generate a fluorescent signal. This signal was normalised to the untreated cells and expressed as percentage of viable cells.**

### 5.2.2 Labelling of nascent viral RNA during infection assays

Using the information from the previous section, we sought to examine whether ISG15 affected viral RNA synthesis during HCV infection. As shown before, up to 24h of labelling could be used without reducing cell viability. Therefore, to cover a 48h period, the experimental strategy encompassed two approaches in which cells were labelled with 4sU during either the 24h period immediately following infection or for 24-48h after infection. To that end, shCtrl and sh6 cells were infected with JC-1 virus at a MOI of 0.8 in the presence of 100uM 4sU (Figure 5.7-A). Transcript levels were monitored for up to 24h p.i. and the RNA populations (total and NT viral RNA) quantified as described earlier. Given the variability in the number of viral RNA copies detected between independent experiments, the copy number for viral transcripts in sh6-infected cells at the last time point (in this case 24h) was expressed as 100% and the copy numbers at earlier times in sh6 and shCtrl cells expressed relative to this value. As shown in Figure 5.7-B, the amount of total viral RNA was slightly higher between 6 and 24h p.i in JC-1-infected sh6 cells when compared with the respective shCtrl cells. Analysis of labelled viral RNA indicated that similar levels of viral RNA were generated between 6 and 12h p.i in both shCtrl and sh6 cells (Figure 5.7-C). By 24h p.i., 22% of newly synthesized JC-1 RNA could be detected in shCtrl cells, indicating the higher efficiency in labelling viral RNA during longer 4sU exposure times. In addition, a further 6% increase in the relative amount of NT JC-1 RNA was detected in sh6 cells (28%) when compared to shCtrl cells. Thus, although small differences were observed in total steady-state levels of JC-1 RNA in shCtrl and sh6 cells throughout the first 24h of infection, only at the latest time point were those differences reflected in higher levels of viral RNA synthesis in the sh6 cells. These results indicate that any negative influence of ISG15 on viral RNA synthesis could be detected as early as 24h after infection.

To examine whether ISG15 affects viral RNA synthesis in the second 24h period after infection, shCtrl and sh6 cells were infected with JC-1 virus at a MOI of 0.8 for 24h, followed by labelling with 100uM 4sU for the following 24h (i.e. from 24 to 48h p.i.). Transcript levels were monitored between 24 and 48h p.i. and the RNA populations quantified as described before. In agreement with the data presented earlier (Figure 4.15-A), total levels of viral RNA were consistently higher in sh6 cells when compared with the shCtrl up to 48h p.i (Figure 5.8-B). Similarly, newly transcribed JC-1 RNA levels were also higher in sh6 cells in comparison to shCtrl cells up to 48h p.i, mirroring the differences observed in the total HCV RNA levels (Figure 5.8-C).

To determine whether the higher levels of synthesized viral RNA observed in the sh6 cells were due to increased RNA stability, JC-1 infected shCtrl and sh6 cells were pulse-labelled for 6h with 200uM 4sU at 24h p.i. and the loss of labelled RNA monitored for a further 48h. As before, total levels of JC-1 RNA were consistently higher in sh6 cells when compared with the shCtrl during the period of infection (up to 78h, Figure 5.9-B). The amount of labelled JC-1 RNA present at the end of the labelling period is represented in Figure 5.9-C. In order to better evaluate the differences in the rate of decay of viral RNA (i.e. loss of labelled viral RNA) in infected cells, the data generated in Figure 5.9-C was normalized to the samples corresponding to the time point at which labelling was stopped (i.e. 30h p.i.), in each cell line (Figure 5.9-D). Following this normalization, nonlinear regression (curve) fit analysis was applied (using GraphPad Prism 5 software) in order to verify whether the constant rate (K) of decay of labelled RNA were significantly different in the two cell lines. As shown in Figure 5.9-D, the curves generated from the nonlinear regression were similar and not statistically different in shCtrl and sh6 cells. Since the curves were not significantly different, the data gathered from the pulse-chase experiments suggest that ISG15 does not affect the rate of decay of viral RNA, favouring the conclusion that ISG15 interferes with the synthesis of viral RNA.

[A]

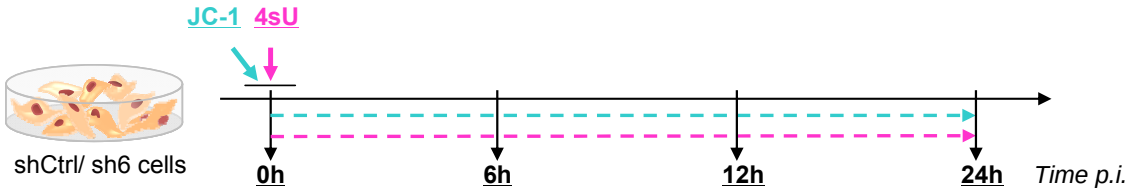


[B]

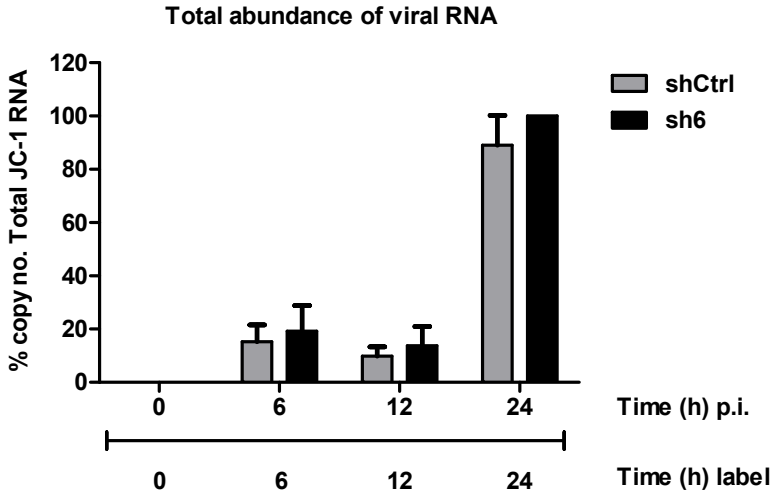


[C]

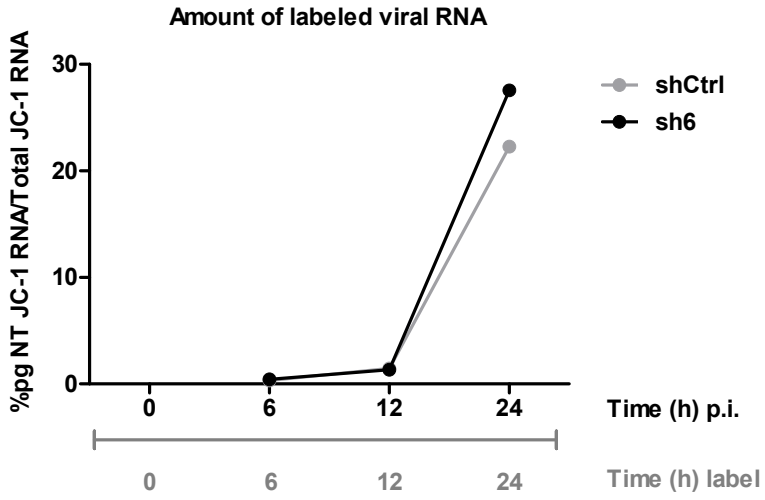


**Figure 5.7 – Labelling and quantification of newly transcribed viral RNA during HCV infection. shCtrl and sh6 cells infected with JC-1 at a MOI of 0.8 in the presence of label (100uM 4sU) for up to 24h. A) Experimental outline. B) Total abundance of viral RNA. C) Rate of synthesis of viral RNA.**

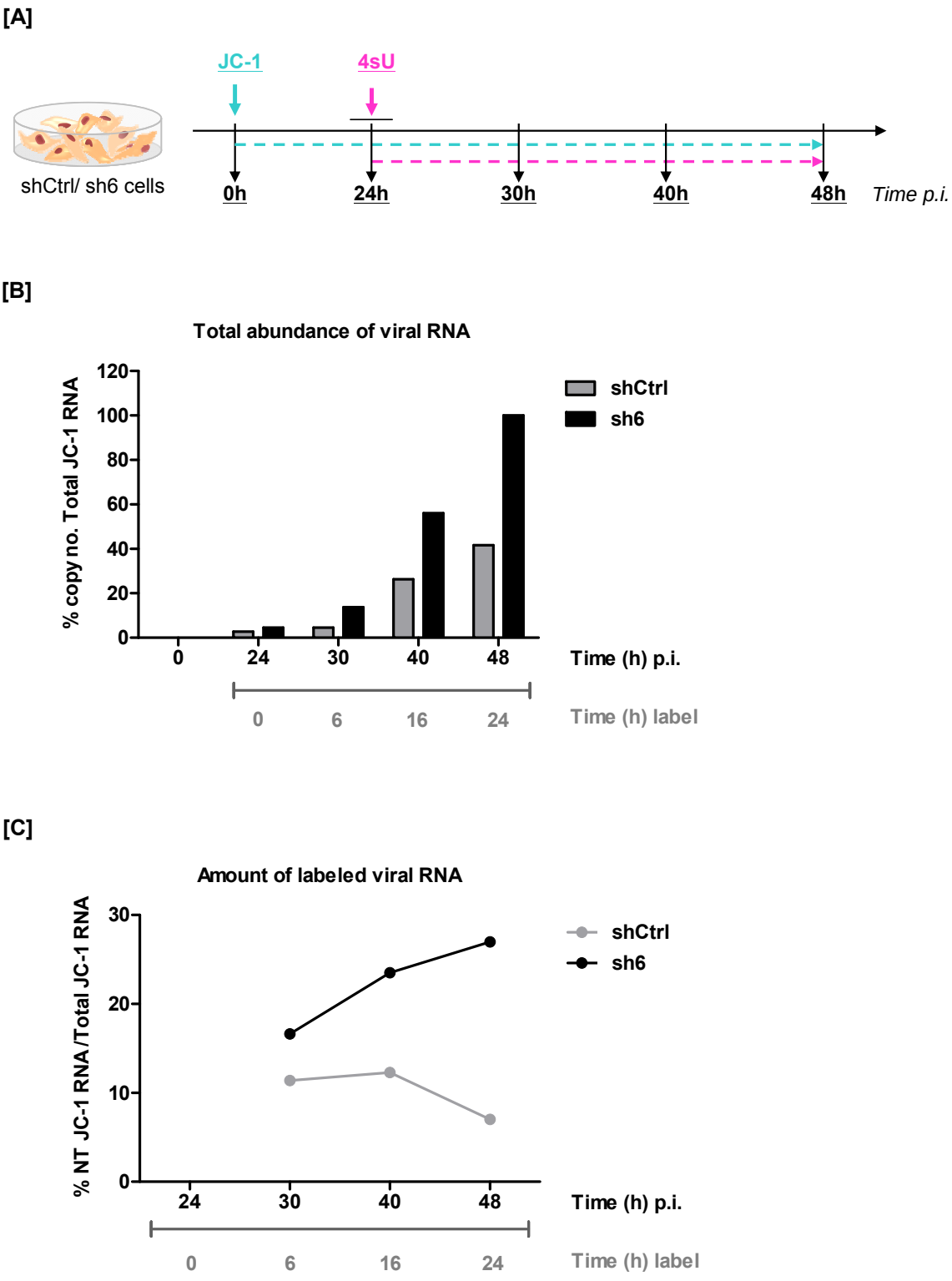


**Figure 5.8 – Labelling and quantification of newly transcribed viral RNA during HCV infection. shCtrl and sh6 cells infected with JC-1 at a MOI of 0.8 and then labeled (100uM 4sU) for up to 24h (48h p.i.). A) Experimental outline. B) Total abundance of viral RNA. C) Rate of synthesis of viral RNA.**

[A]

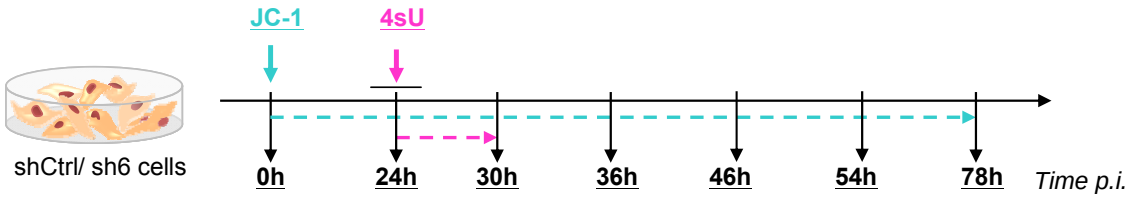
JC-1
4sU
shCtrl/ sh6 cells
0h
24h
30h
36h
46h
54h
78h
Time p.i.

[B]

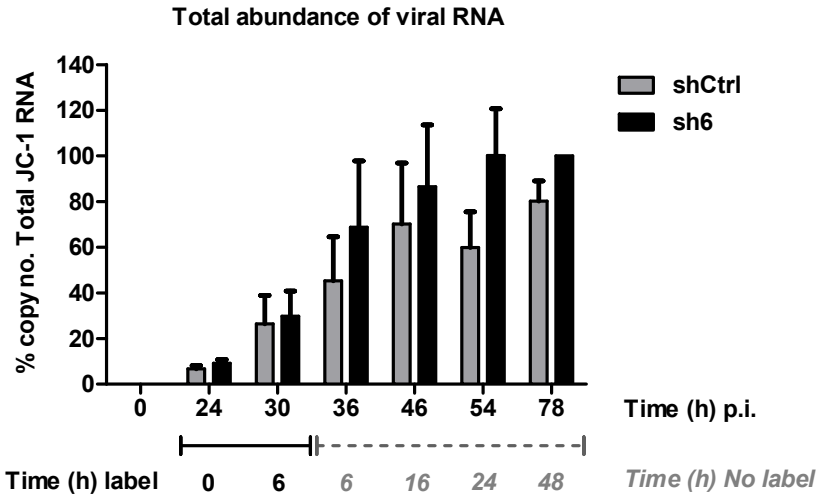
Total abundance of viral RNA
% copy no. Total JC-1 RNA
140
120
100
80
60
40
20
0
shCtrl
sh6
0
24
30
36
46
54
78
Time (h) p.i.
Time (h) label
0
6
6
16
24
48
Time (h) No label

[C]

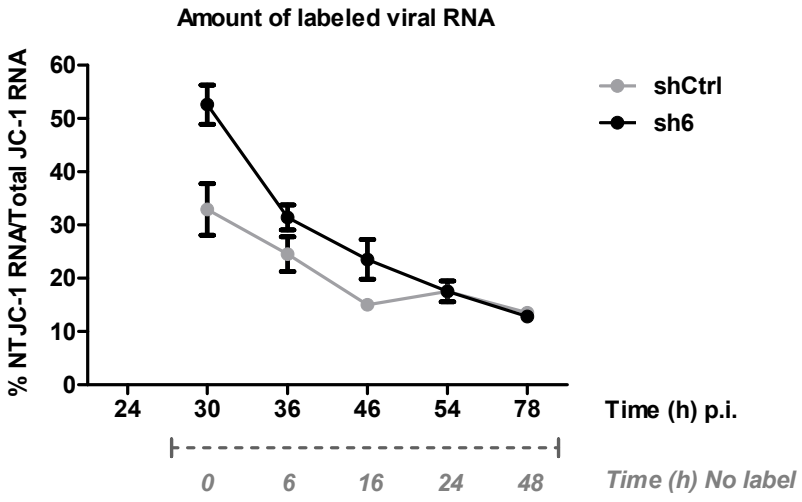
Amount of labeled viral RNA
% NT JC-1 RNA/Total JC-1 RNA
60
50
40
30
20
10
0
shCtrl
sh6
24
30
36
46
54
78
Time (h) p.i.
0
6
16
24
48
Time (h) No label

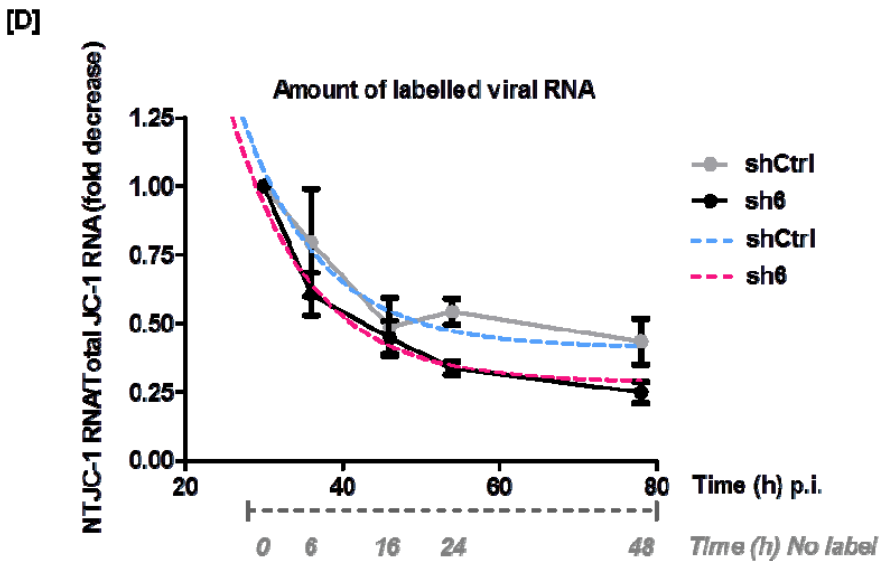


**Figure 5.9 – Labelling and quantification of newly transcribed viral RNA during HCV infection. shCtrl and sh6 cells infected with JC-1 at a MOI of 0.8 for 24h, followed by 6h pulse-label (4sU 200uM). After 6h, the label was removed and the loss of labelling was monitored for up to 48h. A) Experimental outline. B) Total abundance of viral RNA. C) Decay of labelled viral RNA. D) Decay of labelled viral RNA, expressed relative to values at 30h p.i., when labelling was terminated. Dashed lines represent slopes generated from nonlinear regression (curve) fit analysis (using GraphPad Prism 5 software) of the values from shCtrl (blue) and sh6 cells (red).**

## 5.3 Preliminary studies on the conjugation requirements for ISG15 anti-HCV activities

The conjugation status of ISG15 has been linked with its antiviral activities, since it has been shown that it can covalently attach to a variety of cellular proteins, some of which function in the interferon-response pathway (Loeb & Haas, 1992; Zhao *et al.*, 2005). With other viruses, ISG15 conjugation appears to be required for antiviral activities against Sindbis, as well as influenza A and B viruses (Lenschow *et al.*, 2005; Yuan & Krug, 2001). Alternatively, it has also been demonstrated that unconjugated ISG15 mediates resistance to Ebola and HIV-1, by inhibiting ubiquitination of viral proteins involved in egress (Malakhova & Zhang, 2008; Okumura *et al.*, 2006).

### 5.3.1 Generation of inducible Huh-7 cell lines to express ISG15 WT and mutant protein forms

#### 5.3.1.1 Construction of ISG15 expression vectors

To investigate whether conjugated or unconjugated forms of ISG15 are required for reducing HCV RNA replication, cell lines were generated that express wt (GG) and mutant (AA) forms of ISG15. The mutated form has alanine substitutions at the di-GG residues, which are essential for ISG15 conjugation (Figure 5.11-B). Recently, Everett *et al* (2009) developed a tetracycline-inducible system (Tet-On) built into lentivirus vectors, which allowed controlled expression of the protein of interest close to its physiological levels (Everett *et al.*, 2009). This system was used to generate ISG15-inducible cell lines. The strategy employed to construct the tetracycline-inducible ISG15 lentiviral plasmids is detailed in Figure 5.11 and described below.

The expression vector used for cloning the ISG15 cDNA sequence was pLKO.dCMV.TetO.mcs. This plasmid contained, in addition to the elements required for lentivirus production, a tandem TetO operator sequence and dCMV promoter (Figure 5.10). The plasmid pOTB7-ISG15, expressing native ISG15 (GeneBank accession number BC009507) was used as a template for amplification of a DNA fragment encoding ISG15, using the primers listed in Figure 5.11-C. These primers were designed such that the amplified region corresponded to the coding sequence for the mature form of ISG15 protein. To generate the WT form of ISG15 protein (C-terminus ending as LRLRGG) or a mutant version of the protein (LRLRAA), the C-terminal region of ISG15 was amplified using Rev primers which contained either the WT sequence or the respective changes to create the mutant AA sequence (Figure 5.11-A & C). In addition, Fwd and Rev primers introduced *Hind*III and *Xba*I/*Bam*HI restriction sites at the 5' and 3' ends respectively. Each amplified DNA fragment, *Hind*III-ISG15-GG-*Xba*I/*Bam*HI or *Hind*III-ISG15-AA-*Xba*I/*Bam*HI, was then digested with *Hind*III and *Bam*HI and ligated into an intermediate cloning vector pCMV-FLAG-Ubch7 (also digested with *Hind*III and *Bam*HI) to generate the pCMV-FLAG-ISG15-GG and –AA constructs (Figure 5.11-B).

Flag-ISG15-GG and –AA DNA fragments were amplified from the previous constructs using the primers listed in Figure 5.11-D, which inserted an additional *Nhe*I restriction site followed by a Kozak sequence at the 5' end of the FLAG sequence to enhance protein translation. The resultant PCR fragments were digested with *Nhe*I and *Xba*I and ligated into the pLKO.dCMV.TetO.mcs (also digested with *Nhe*I and *Xba*I), to yield the pLKO.dCMV.TetO.FLAG.ISG15-GG and –AA constructs (Figure 5.11-A).

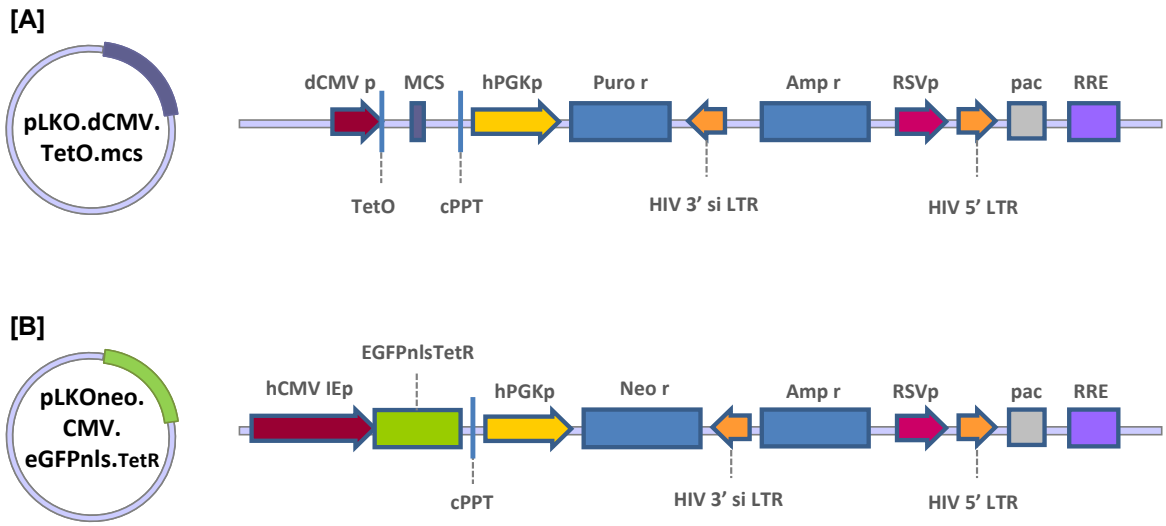


**Figure 5.10 – Map of the lentivirus vectors used to express WT (GG) and mutant (AA) ISG15 from a cDNA fragment under the control of a tetracycline inducible promoter (A) and eGFPnls.TetR fusion protein (B). Additional to some of the features listed in Figure 4.10, these expression vectors also contained: complete (hCMV IEp) or truncated (dCMVp) human cytomegalovirus immediate early promoter; mcs, multiple cloning site, used to insert FLAG-ISG15-GG and –AA cDNA; nls, nuclear localization signal.**

**[A]**

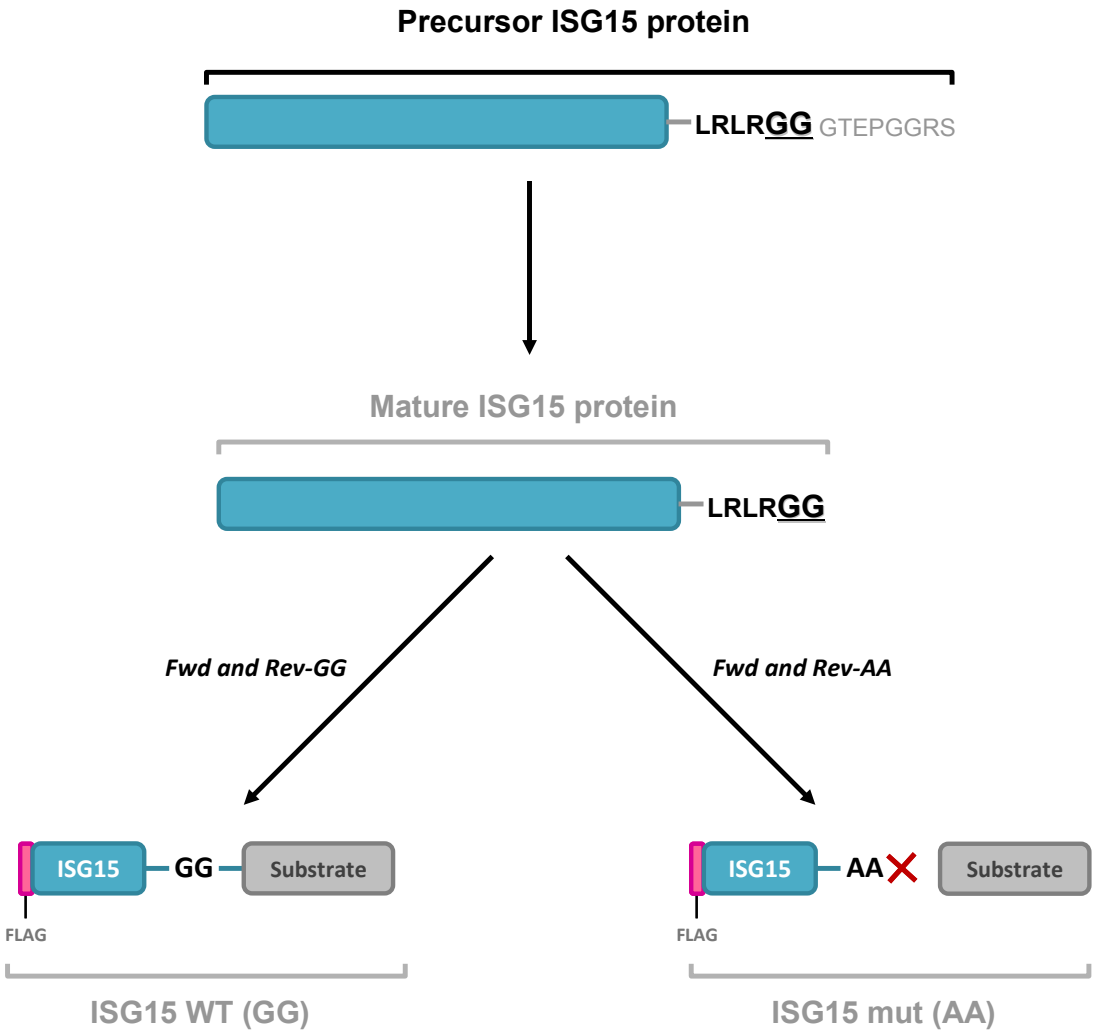
Precursor ISG15 protein
LRLRGG GTEPGGRS
Mature ISG15 protein
LRLRGG
Fwd and Rev-GG
Fwd and Rev-AA
ISG15
GG
Substrate
FLAG
ISG15 WT (GG)
ISG15
AA
Substrate
FLAG
ISG15 mut (AA)

**[B]**

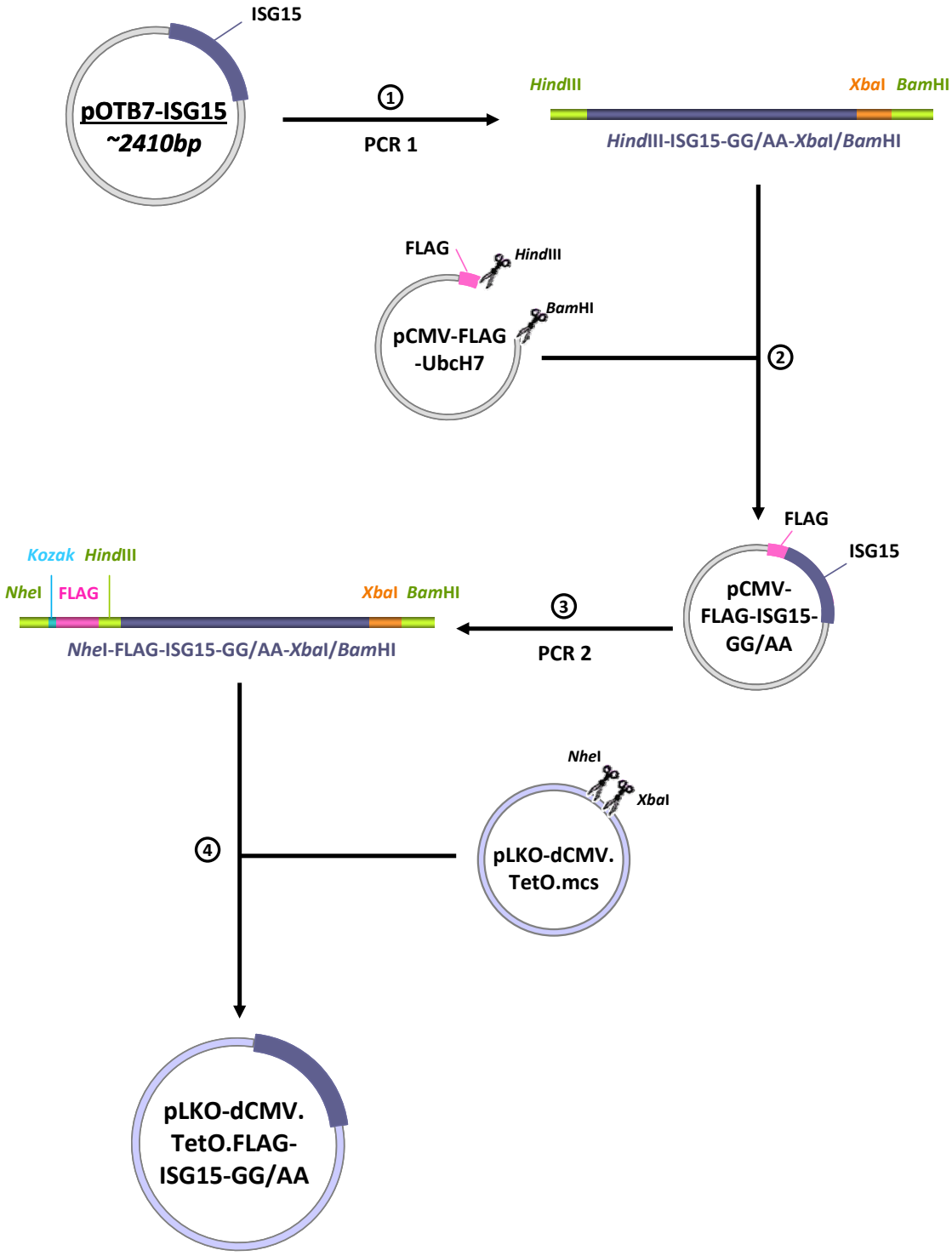
ISG15
pOTB7-ISG15
~2410bp
①
PCR 1
HindIII
XbaI BamHI
HindIII-ISG15-GG/AA-XbaI/BamHI
FLAG
HindIII
BamHI
pCMV-FLAG
-UbcH7
②
FLAG
ISG15
pCMV-
FLAG-ISG15-
GG/AA
③
PCR 2
Kozak HindIII
NheI FLAG
XbaI BamHI
NheI-FLAG-ISG15-GG/AA-XbaI/BamHI
④
NheI
XbaI
pLKO-dCMV.
TetO.mcs
pLKO-dCMV.
TetO.FLAG-
ISG15-GG/AA

**[C]**

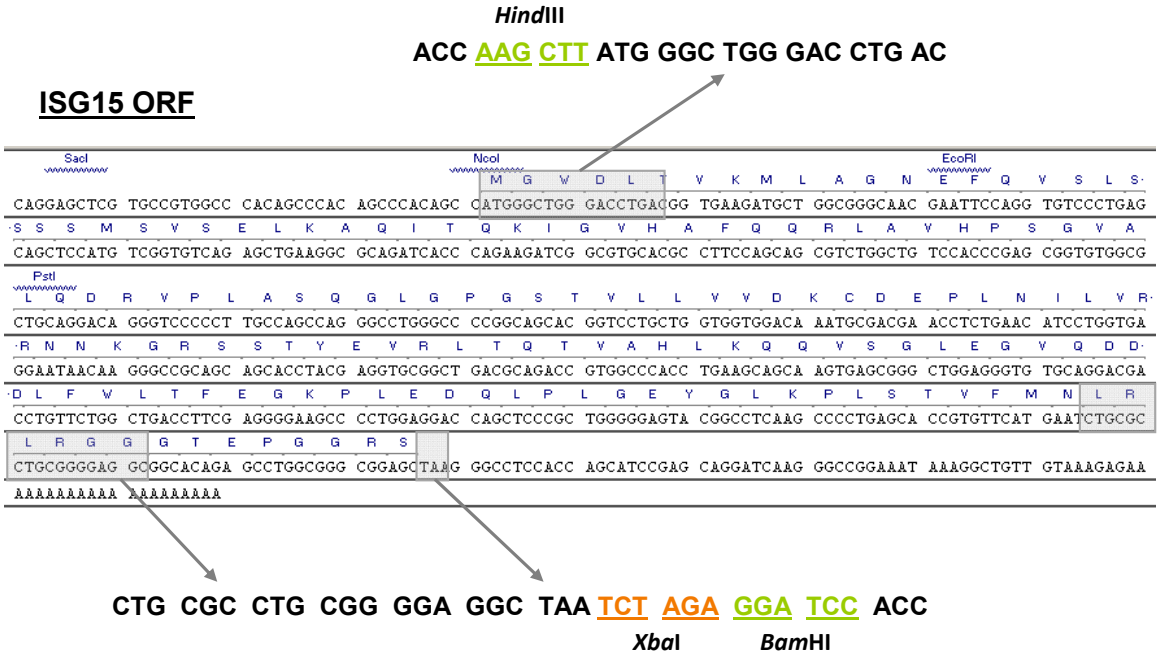


**PCR 1 primers:**

*ISG15_Fwd:* **5'-ACC AAG CTT ATG GGC TGG GAC CTG AC-3'**
***Hind*III**

*ISG15-GG_Rev:* **5'-GGT GGA TCC TCT AGA TTA GCC TCC CCG CAG GCG CAG-3'**
***Bam*HI** ***Xba*I** **Gly Gly**

*ISG15-AA_Rev:* **5'-GGT GGA TCC TCT AGA TTA GGC TGC CCG CAG GCG CAG-3'**
***Bam*HI** ***Xba*I** **Ala Ala**

**[D]**

**PCR 2 primers:**

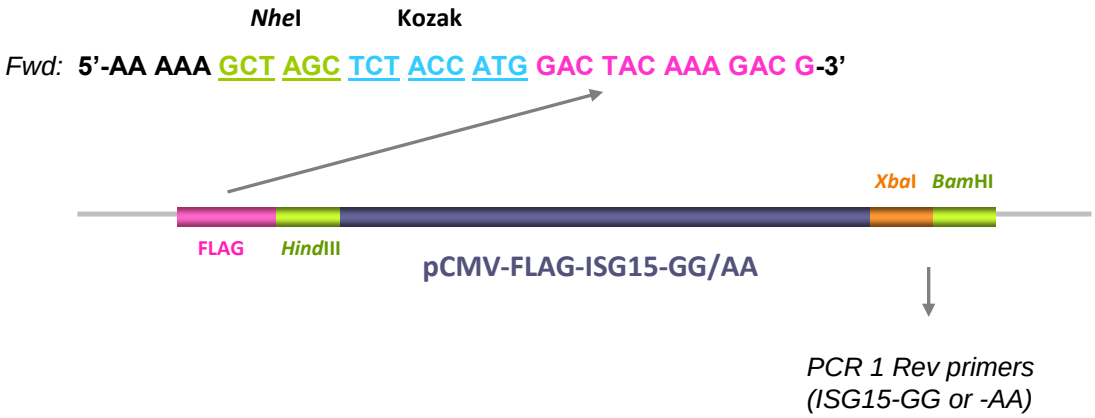


**Figure 5.11 – Construction of pLKO.dCMV.TetO.FLAG.ISG15-GG/AA lentiviral plasmids. [A] Overall strategy to create WT (GG) or mutant (AA) ISG15 protein expression vector. [B] Cloning steps used to insert ISG15 cDNA into pLKO-dCMV.TetO.mcs vectors: 1) PCR amplification of ISG15 cDNA from pOTB7-ISG15 plasmid; 2) digestion of ISG15-GG and -AA cDNA fragment with *Hind*III and *Bam*HI restriction enzymes and insertion into pCMV-FLAG-UbcH7 plasmid; 3) PCR amplification of FLAG-ISG15-GG/AA from pCMV-FLAG-ISG15-GG/AA vector; 4) Digestion of amplified FLAG-ISG15-GG/AA DNA fragment with *Nhe*I and *Xba*I and insertion into pLKO-dCMV.TetO.mcs vector, to generate the final constructs pLKO-dCMV.TetO.FLAG-ISG15-GG and –AA. [C] PCR primers used to amplify ISG15 cDNA from pOTB7-ISG15 vectors (PCR 1) [D] PCR primers used to amplify FLAG-ISG15-GG and –AA DNA fragments from pCMV-FLAG-ISG15-GG/AA vectors (PCR 2).**

To examine whether FLAG-tagged ISG15 protein could be expressed, Huh-7 cells were transfected with pLKO.dCMV.TetO.FLAG.ISG15-GG and -AA plasmids (hereafter referred to as FLAG-ISG15-GG and -AA), alongside pCMV-FLAG-UbcH7 plasmid, as a positive control. After 16h, expression of FLAG protein was assessed by indirect immunofluorescence. As expected, no FLAG was detected in mock-transfected Huh-7 cells (Figure 5.12), whereas in FLAG-UbcH7 transfected cells the tagged protein was expressed and distributed throughout the cell. Similarly, both FLAG-ISG15-GG and -AA transfected cells expressed FLAG-tagged ISG15 to levels close to the FLAG-UbcH7control cells. These data indicated that Flag-ISG15-GG and -AA constructs were capable of expressing the -GG and -AA forms of tagged ISG15.

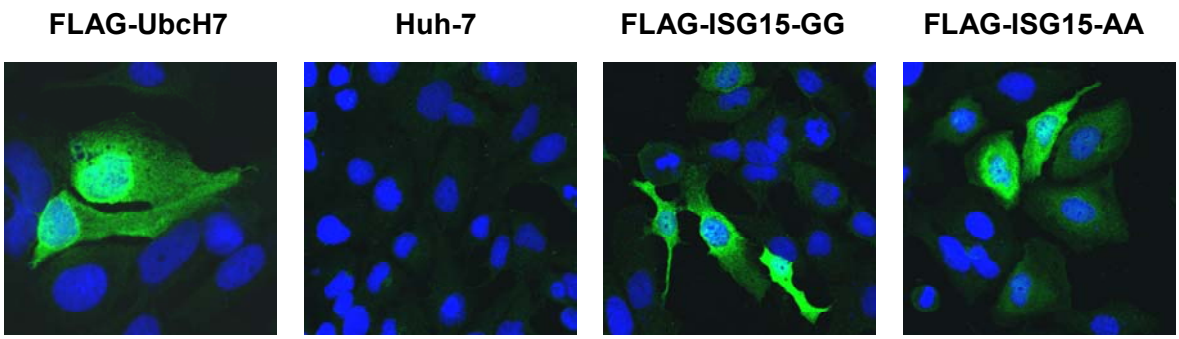


**Figure 5.12 – Immunofluorescence analysis of FLAG expression. Huh-7 cells were transfected with 400ng of pLKO-dCMV.TetO.FLAG-ISG15-GG, pLKO-dCMV.TetO.FLAG-ISG15-AA, plasmids, or pCMV-FLAG-UbcH7, as a positive control. At 16h post-transfection, the cells were fixed and stained for FLAG protein using anti-FLAG antisera.**

#### 5.3.1.2 Generation and characterisation of inducible Huh-7 cell lines expressing WT and mutant ISG15

The purpose of creating the pLKO vectors expressing the WT (GG) or mutant (AA) forms of ISG15 was to create inducible cell lines with the lentivirus system. To create such cell lines, a two step strategy was used. First, a lentiviral cell line expressing the tetracycline repressor was created, and then used as a parental cell line for transfecting the ISG15 lentiviral expressing plasmid, which contains a tetracycline operator sequence. The strategy is described in the following paragraphs and represented in Figure 5.13.

In order to produce lentiviral stocks (Figure 5.13-A), HEK-293T cells were transfected with either pLKO-dCMV-eGFP-TetR or pLKO-dCMV.TetO.FLAG.ISG15-GG and -AA plasmids together with plasmids encoding the lentivirus components (pCMV-DR8.91 and pVSV-G), according to the method described in Chapter 2 (sections 2.2.7.3 and 2.2.7.4). After the first round of transfections, with pLKO-dCMV-eGFP-TetR plasmids, the supernatants were harvested and used to transduce monolayers of Huh-7 cells (Figure 5.13-A-I & II). Cell lines that incorporated the eGFP-TetR sequences were selected by culturing in the presence of neomycin and further sorted according to GFP expression intensity. The generated cell line was named Huh-7-GFP. Subsequently, the supernatants harvested from a second round of transfections, with pLKO-dCMV.TetO.FLAG.ISG15-GG and –AA plasmids, were used to transduce Huh-7-GFP cells (Figure 5.13-III & IV). Cell lines that incorporated the eGFP-TetR as well as

FLAG.ISG15-GG and –AA sequences were selected by culturing in the presence of both puromycin and G418. The generated cell lines were named Huh-7-eGFP-FLAG-ISG15-GG and -AA.

Huh-7-eGFP-FLAG-ISG15-GG and –AA were then treated with tetracycline (1ug/ml) and examined at 24, 48 and 72h for their ability to express FLAG-ISG15 by Western blot analysis (Figure 5.14). Cell extracts from inducible cells expressing FLAG-PIAS protein (Protein Inhibitor of Activated STATs) were used as positive control for FLAG expression. As shown in Figure 5.14, no expression was detected in either FLAG-ISG15-GG or –AA cells, even at longer tetracycline treatment times, when compared with the control. Lower tetracycline concentrations were also tested to rule out the possibility that excess antibiotic could have an inhibitory effect on the inducible system. However, even at lower concentrations (0.1 and 0.5ug/ml) no expression of FLAG protein was observed (data not shown). Thus, the inducible system used to express ISG15 was unsuccessful in Huh-7 cells.

**[A]**

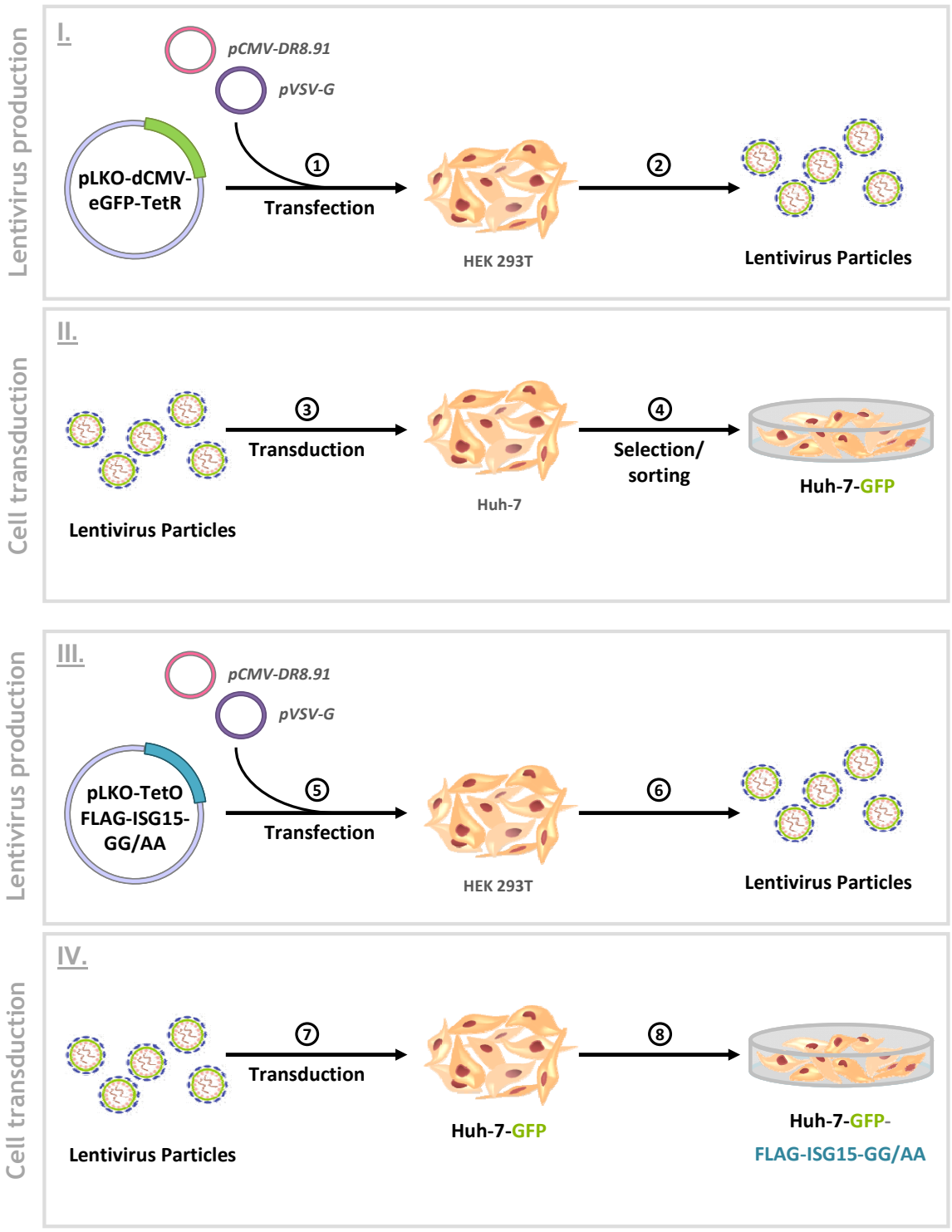
Lentivirus production
I.
pCMV-DR8.91
pVSV-G
pLKO-dCMV-eGFP-TetR
1
Transfection
HEK 293T
2
Lentivirus Particles
Cell transduction
II.
3
Transduction
Lentivirus Particles
Huh-7
4
Selection/ sorting
Huh-7-GFP
Lentivirus production
III.
pCMV-DR8.91
pVSV-G
pLKO-TetO FLAG-ISG15-GG/AA
5
Transfection
HEK 293T
6
Lentivirus Particles
Cell transduction
IV.
7
Transduction
Lentivirus Particles
Huh-7-GFP
8
Huh-7-GFP-FLAG-ISG15-GG/AA

**[B]**

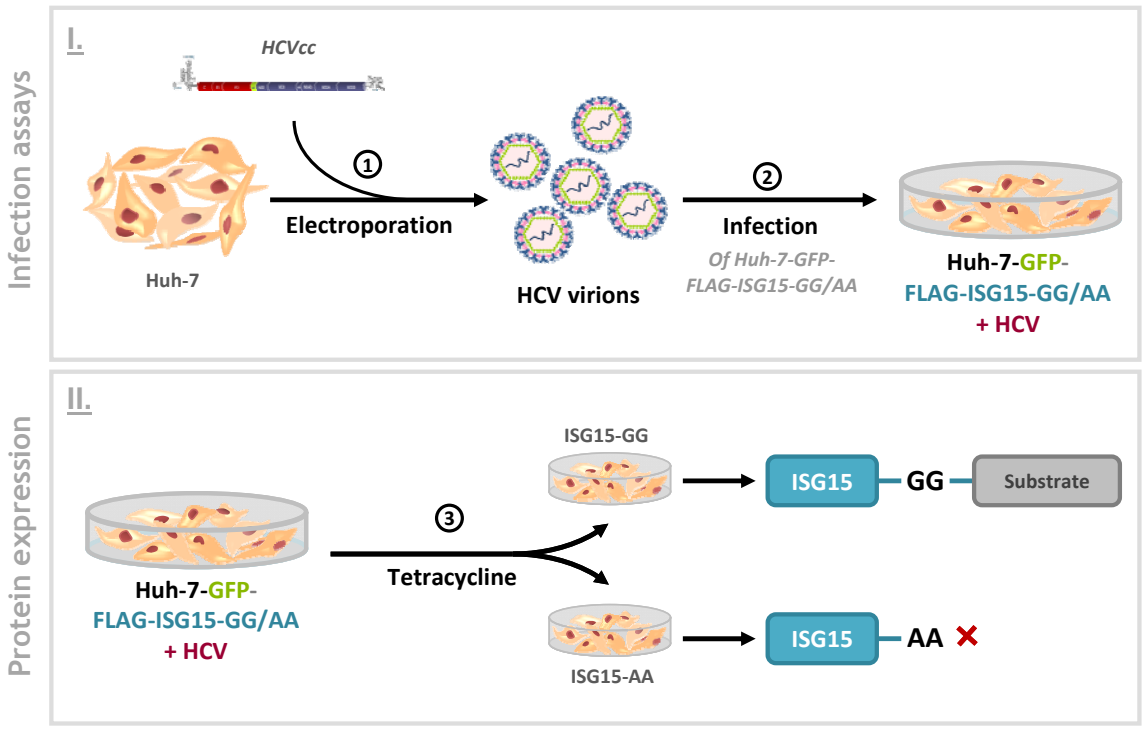


**Figure 5.13 – Generation of inducible lentiviral cell lines to express FLAG-ISG15-GG and –AA proteins. [A] (I) Lentiviruses were produced by transfection of pLKO-dCMV-eGFP-TetR together with pCMV-DR8.91 and pVSV-G packaging vectors into HEK 293T cells. (II) At 60h post-transfection, the supernatant was harvested and used to transducer Huh-7 cells. The cell lines were generated by neomycin selection followed by FACS sorting of eGFP expressing cells (Huh-7-GFP). (III) Lentiviruses were produced by transfection of pLKO-dCMV.TetO.FLAG-ISG15-GG or pLKO-dCMV.TetO.FLAG-ISG15-AA together with the packaging vectors into HEK 293T cells and (IV) the supernatants used to transduce Huh-7-GFP cells as before. Cells potentially expressing the Tet repressor and ISG15 under the control of the Tet operator were selected by puromycin and neomycin resistance. Detailed protocol is described in Chapter 2, sections 2.2.7.3 and 2.2.7.4. [B] The generated cell lines can be used in (I) HCV infection assays and (II) tetracycline induction of FLAG-ISG15-GG and –AA proteins.**

Given the problems encountered in establishing inducible cell lines, an alternative method was use to express ISG15. To that end, the pLKO-TetO-FLAG-ISG15-GG and –AA lentiviral plasmids were utilised, this time without the presence of the TetR plasmid, to transduce naïve Huh-7 cells (as described before). Examination of the derivative cell lines, Huh-7-FLAG-ISG15-GG and –AA, revealed that constitutive expression of ISG15 did not impact on cell viability (data not shown). The ability of Huh-7-FLAG-ISG15-GG and –AA cells to express FLAG-ISG15 was examined by Western blot analysis. As shown in Figure 5.15, two low molecular weight species were detected by the ISG15 antibody, which were presumed to correspond to unconjugated protein. The upper band also was recognised by the FLAG antibody. The appearance of two bands was somewhat unexpected. From the data, it was assumed that the upper species identified by the ISG15 antibody was the FLAG-tagged protein. Since free ISG15 was not detected in naïve cells, it was presumed that the lower species could correspond to FLAG-tagged ISG15, which has been cleaved by a cellular protease, thereby removing the FLAG sequences. Alternatively, its production may result from internal translation initiation at an AUG start codon, downstream from the FLAG sequences. A third, less likely possibility, is that endogenous ISG15 is induced in the ISG15-expressing cell lines. FLAG-ISG15 was more efficiently expressed in the Huh-7-FLAG-ISG15-GG cells, when compared with the levels in the respective –AA cells. As expected, no ISG15 conjugates were observed in the FLAG-ISG15-AA expressing cells, since mutation of the –GG residues would prevent formation of conjugates. In the FLAG-ISG15-GG expressing cells, ISG15 conjugates also were not observed. The reasons for the lack of conjugates in FLAG-ISG15-GG cells is not known, but it could be that, in order to produce ISG15 protein conjugates in these cells in an IFN-independent manner, co-expression of E1, E2 and E3 enzymes might be required.

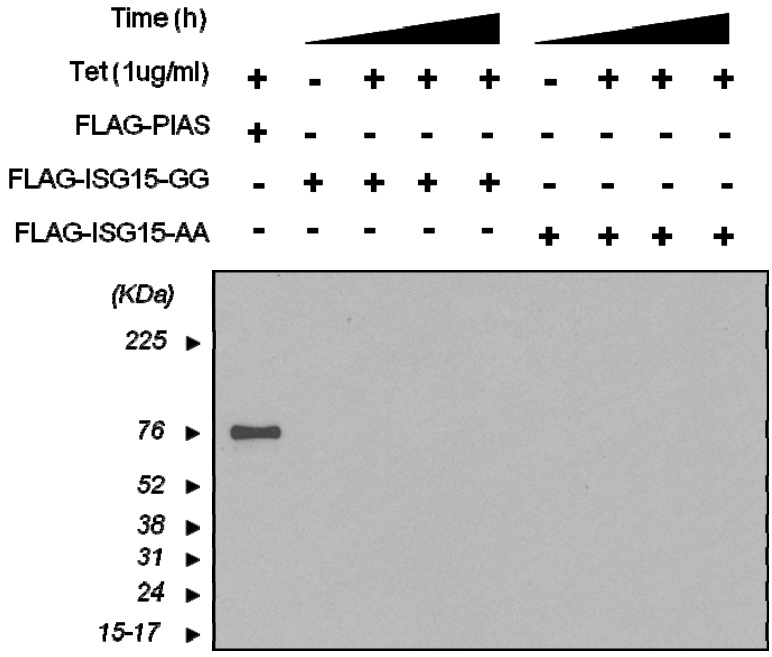


**Figure 5.14 – Analysis of the expression of FLAG protein in inducible lentiviral cells. Huh-7-GFP-FLAG-ISG15-GG and -AA cells were treated with tetracycline (1ug/ml) for 24, 48 and 72h. Expression of FLAG protein was determined by Western blot analysis using anti-FLAG antisera.**

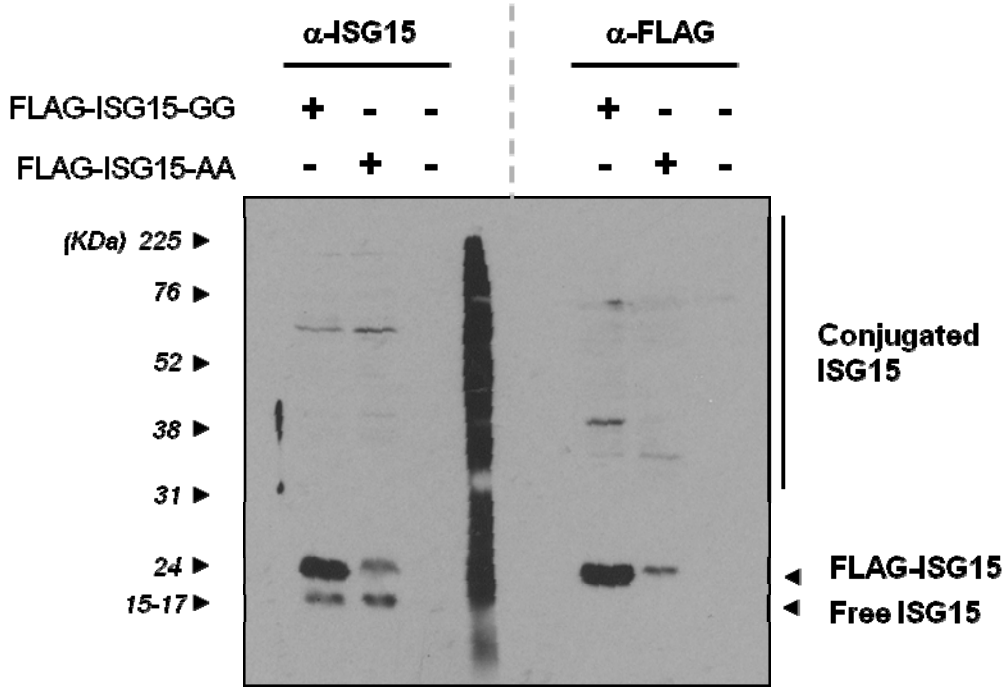


**Figure 5.15 – Western blot analysis of ISG15 and FLAG protein expression in Huh-7-FLAG-ISG15-GG and –AA cell lines, using anti-ISG15 and anti-FLAG antisera. This figure was provided by S. McFarlane.**

### 5.3.2 Silencing of ISG15 major E3 ligase, HERC5

Since it did not prove possible to generate cell lines expressing WT (GG) and mutant (AA) forms of ISG15, an alternative approach was used to investigate the conjugation requirements for ISG15 antiviral activities against HCV. Here, we explored the ability to block ISG15 conjugation both in the presence and absence of IFN induction, by silencing the major ISG15 E3 ligase, HERC5 (Figure 4.16). To that end, Huh-7/SGR cells were transfected with Ctrl, ISG15 and HERC5 siRNAs for 24h, followed by treatment with 0, 1, 10 and 100U/ml IFN$\alpha$. ISG15 and HERC5 expression levels in replicon cells were compared to the levels in the respective naïve cells treated with 0 or 100U/ml IFN$\alpha$ for 48h. The effects on HCV replication were assessed at 48h after IFN$\alpha$ treatment by measuring viral RNA and protein expression levels. As shown in Figure 5.16-A, following IFN$\alpha$ treatment, an 80-fold rise in ISG15 RNA levels was detected in naïve Huh-7 cells. By contrast, about an 8-fold increase was observed in HERC5 RNA levels in Huh-7 cells under the same treatment conditions (Figure 5.16-B). RNA levels of ISG15 and HERC5 in Huh-7/SGR cells transfected with siCtrl yielded the same induction with 100U/ml IFN$\alpha$ as naïve cells (Figure 5.16-A & B). As expected transfection of ISG15 and HERC5 siRNAs in Huh-7/SGR cells specifically attenuated induction of ISG15 and HERC5, respectively, following IFN$\alpha$ stimulation (Figure 5.16-A & B). Interestingly, silencing of HERC5 resulted in an increase in ISG15 transcript levels both in the absence and presence of IFN$\alpha$ (Figure 5.16-A), and the same phenotype was observed on HERC5 levels when ISG15 was repressed (Figure 5.16-B).

Western blot analysis mirrored the ISG15 RNA data such that, following IFN treatment, high levels of conjugated and unconjugated ISG15 protein were found in Huh-7 and in Huh-7/SGR cells transfected with siCtrl (Figure 5.16-D). Silencing of ISG15 in Huh-7/SGR cells blocked expression of any ISG15 protein during IFN$\alpha$ stimulation. Surprisingly, HERC5 silencing did not completely prevent production of ISG15 conjugates in Huh-7/SGR cells. Nonetheless, a small increase in the unconjugated form of ISG15 was observed as a result of HERC5 silencing, suggesting that some conjugation was inhibited in these cells (Figure 5.16-D). The slight reduction in ISG15 conjugation was not due to lack of silencing HERC5, as siHERC5-transfected Huh-7/SGR cells gave apparently complete abrogation of

detectable HERC5 protein (Figure 5.16-D). For HERC5, there was some evidence that increased protein levels were produced with 10U/ml IFNα in cells transfected with siISG15 compared to siCtrl (Figure 5.16-D). However, there was little evidence of enhanced HERC5 protein at the higher doses of cytokine (100U/ml).

Consistent with data shown earlier, silencing of ISG15 in Huh-7/SGR cells resulted in a relative rise in HCV RNA levels in the absence of exogenous IFNα stimulation (Figure 5.16-C). In Huh-7/SGR cells transfected with ISG15, ~2-fold less of a decrease in HCV RNA was observed following 100U/ml of IFNα treatment, but not at lower concentrations, when compared with the levels in the siCtrl cells. HERC5 silencing in Huh-7/SGR cells resulted in a 15% increase in HCV RNA levels, when compared with the control cells (Figure 5.16-C). By contrast, silencing HERC5 followed by IFNα treatment, did not affect the efficiency of IFNα in reducing HCV RNA levels, when compared with siCtrl cells. Western blot analysis revealed that in the absence of exogenous IFNα stimulation no substantial effects were observed in NS5A expression in Huh-7/SGR cells transfected with siCtrl, siISG15 or siHERC5. Following IFNα treatment, a small reduction in NS5A expression was observed with ISG15 siRNA but not HERC5 siRNA transfected cells, when compared with control cells.

These results have shown that 1) silencing of either ISG15 or HERC5 in Huh-7/SGR cells resulted in a corresponding increase in HERC5 or ISG15 RNA levels, respectively; 2) HERC5 silencing reduced, to some extent, production of ISG15 protein conjugates; 3) silencing of HERC5 resulted in a smaller rise in viral RNA levels when compared with the effects of ISG15 silencing in Huh-7/SGR cells in the absence of exogenous IFNα stimulation, and 4) the small reduction on ISG15 conjugate formation did not have an appreciable effect on viral RNA levels following IFNα treatment as observed previously in the cells transfected with ISG15 siRNAs. Together, these data suggest that the IFN-mediated antiviral activities of ISG15 on HCV replication may not be dependent on ISG15 conjugation. However, given that silencing of HERC5, the major E3 ligase for ISGylation, did not completely abrogate the formation of ISG15 conjugates, further experiments are needed to verify whether ISGylation is required for its anti-viral activities against HCV replication.

[A]

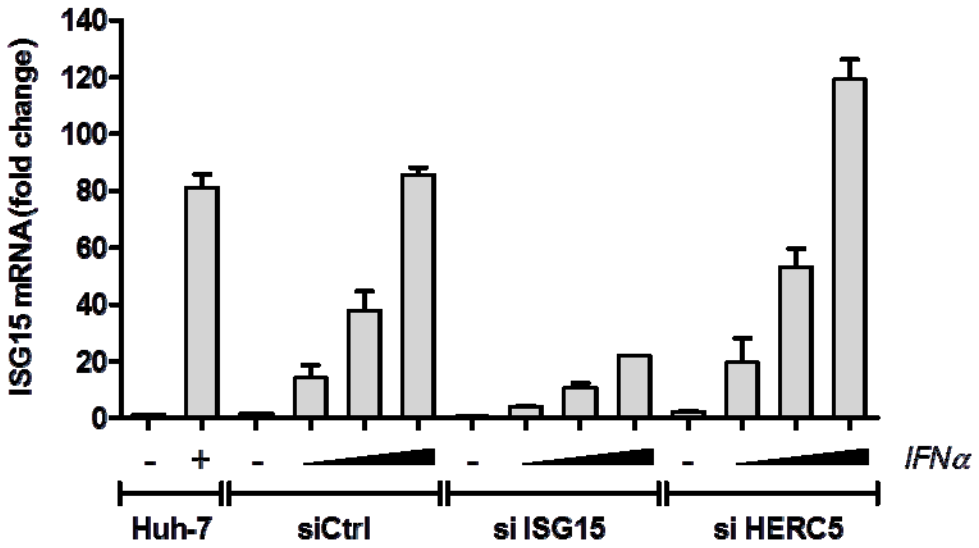
ISG15 mRNA(fold change)
140
120
100
80
60
40
20
0
- + - - -
IFNα
Huh-7
siCtrl
si ISG15
si HERC5

[B]

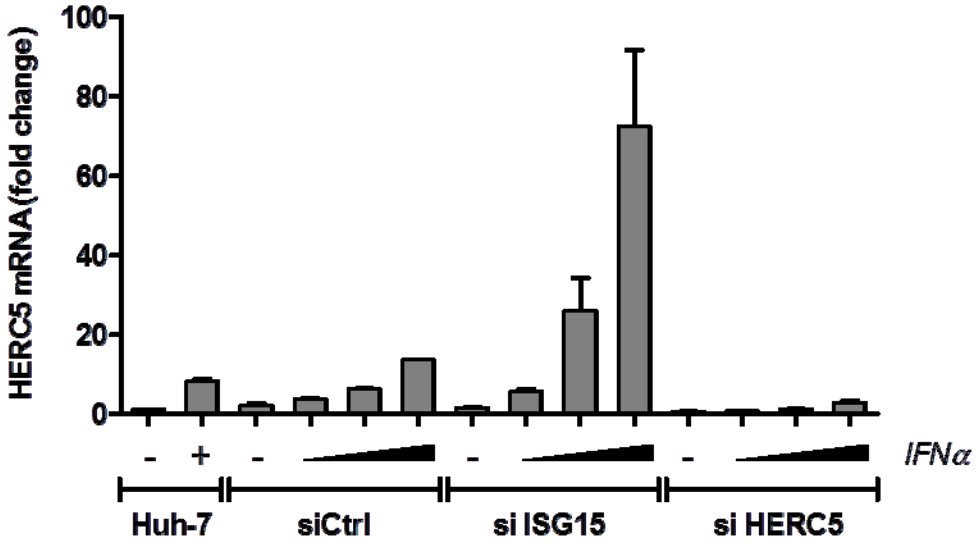
HERC5 mRNA(fold change)
100
80
60
40
20
0
- + - - -
IFNα
Huh-7
siCtrl
si ISG15
si HERC5

[C]

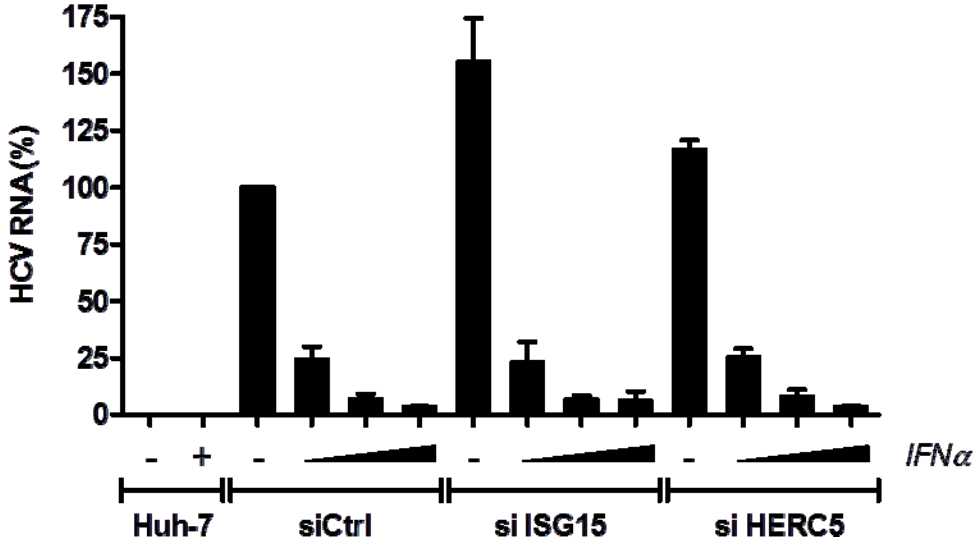
HCV RNA(%)
175
150
125
100
75
50
25
0
- + - - -
IFNα
Huh-7
siCtrl
si ISG15
si HERC5

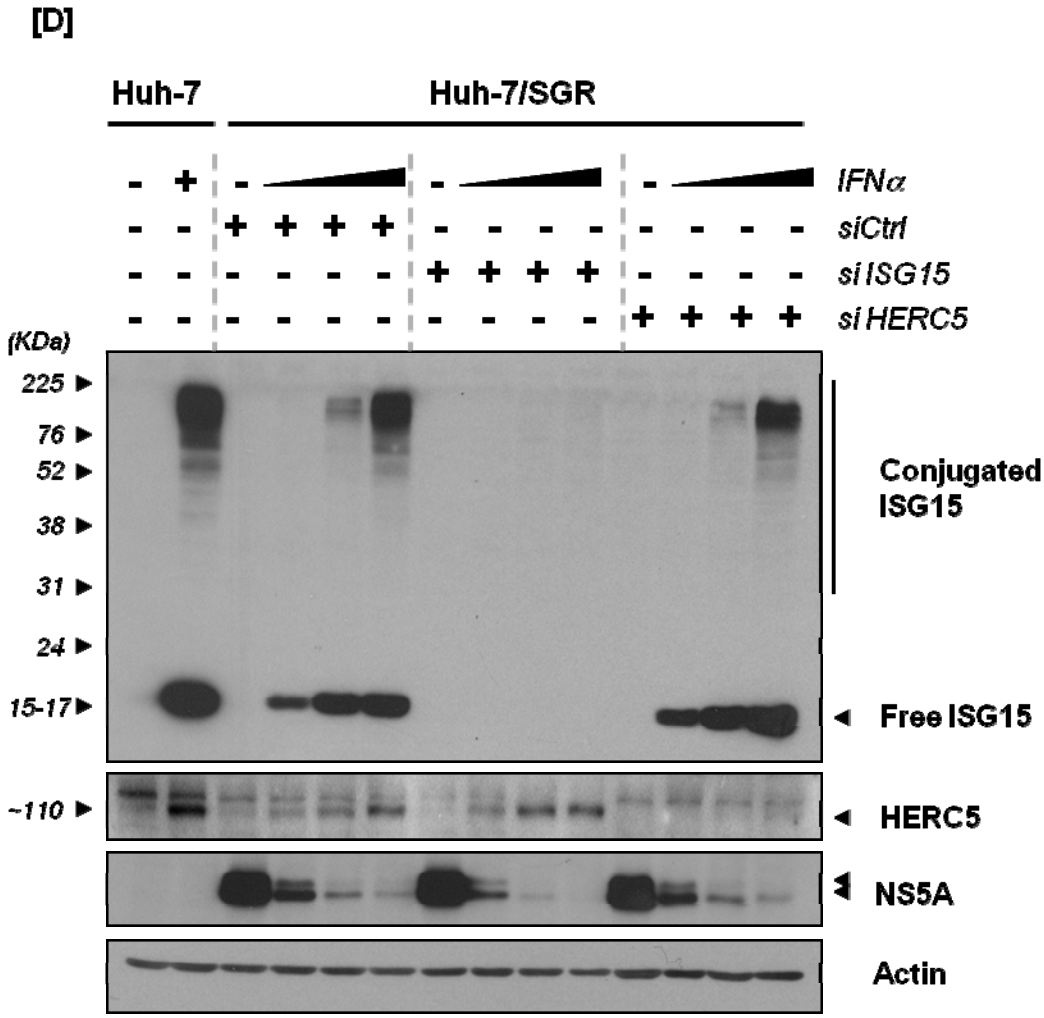


**Figure 5.16 – Analysis of HERC5 silencing in Huh-7/SGR cells. Huh-7/SGR cells were transfected with control, ISG15 and HERC5 siRNAs (siCtrl, siISG15 and siHERC5, respectively) for 24h, followed by treatment with increasing doses (0, 1, 10 and 100 U/ml) of IFNα for 48h. Huh-7 cells were treated with 0 and 100U/ml IFNα for 48h. RT-qPCR analysis of ISG15 [A], HERC5 [B] and HCV [C] RNA expression levels. [D] Western blot analysis of ISG15 conjugated and unconjugated forms, HERC5, NS5A and Actin protein expression levels, using anti-ISG15, anti-HERC5, anti-NS5A and anti-Actin antisera.**

## 5.4 Discussion

Following the findings observed in Chapter 4, the aim of this section was to investigate mechanisms used by ISG15 to limit HCV replication. Two approaches were adopted to determine whether 1) ISG15 affected the rates of synthesis or degradation of viral RNA and 2) ISG15 conjugation was necessary to inhibit HCV RNA replication.

**1) Impact of ISG15 on the rates of viral RNA synthesis or degradation**

Steady-state levels of mRNAs are the result of a tightly regulated balance between *de novo* transcription and mRNA decay. Standard methods such as Northern blot and microarray analysis on total RNA provide a measure of mRNA abundance but do not distinguish between changes in the rates of RNA synthesis or decay. Early studies to investigate rates of transcriptional activity in cells were based on incorporation of radioactive ribonucleosides into RNA. The method relied on analysis of incorporation of $^{3}H$- or $^{14}C$-uridine into mRNA transcripts followed by autoradiography (Forsdyke, 1967; Harwood & Itzhaki, 1973). While this approach was successful, it had the disadvantage of using hazardous radioisotope molecules and required time consuming autoradiography, sometimes taking the order of weeks. An alternative method measured incorporation of bromo-containing nucleosides into nascent mRNA, such as 5-bromouridine (BrU) (Haider *et al.*, 1997; Ohtsu *et al.*, 2008). BrU is taken up by cells and converted to nucleotide phosphates through the ribonucleoside salvage pathway. Quantitation of BrU-tagged RNA can be determined by Northern/Western blot analysis using anti-BrdU monoclonal antibodies (Haider *et al.*, 1997). This approach has also been employed for indirect immunofluorescence studies since BrU-labelled RNA can be detected by staining cells with the same antibodies. Indeed, the method revealed sites of RNA replication in cells harbouring the HCV SGR (Gosert *et al.*, 2003). However, the method does present some limitations, as it is associated with toxicity and the rates of incorporation and isolation of BrU-tagged RNA containing low uridine content are variable.

Improvements to the metabolic tagging of transcribed RNA and downstream purification techniques have been developed in recent years. Thiol-containing nucleosides, such as 4-thiouridine, were described more than 30 years ago, and could readily incorporate into nascent RNA with minimal toxic effects (Melvin *et al.*, 1978). This method can be used for both *in vitro* and *in vivo* studies, since it is well tolerated by mice following injection with 4sU nucleosides (Kenzelmann *et al.*, 2007). Isolation of nascent 4sU-tagged RNA can be achieved using mercury affinity chromatography and further analysed by Affymetrix microarrays (Kenzelmann *et al.*, 2007). More recently, an improved version of the method has been developed in which incorporation of 4sU into nascent RNA was combined with thiol-specific biotinylation and subsequent magnetic separation of total RNA into nascent and pre-existing untagged RNA (Dolken *et al.*, 2008). The three fractions of isolated RNA (labelled, pre-existing and total RNA) are suitable for further analysis using RT-qPCR, microarray and next-generation sequencing (Dolken *et al.*, 2008; Marcinowski *et al.*, 2012; Rabani *et al.*, 2011). Traditionally, assessment of RNA decay could be achieved by blocking global transcription with transcriptional inhibitors, such as actinomycin D (ActD) and monitoring RNA decay over time. These approaches have negative impacts on cellular physiology and may interfere with the determination of the RNA degradation rate. By contrast, 4sU labelling methods allow monitoring of RNA under non-disruptive conditions (Friedel & Dolken, 2009). Thus, use of metabolic labelling of RNA with 4sU nucleosides can enable both the rates of RNA synthesis and decay to be determined.

In the study presented here, the method was applied to labelling newly transcribed HCV RNA and to determine whether ISG15 could affect the rates of synthesis or decay of viral RNA. The results show that it is possible to label newly transcribed viral RNA during infection of Huh-7 cells with infectious virus. While short labelling periods were ideal for detecting changes in cellular mRNA transcripts (Dolken *et al.*, 2008), longer labelling periods were required for accurate detection of HCV labelled RNAs. Huh-7 cells were exposed to 100uM 4sU for up to 24h, which was well tolerated by the cells and there was no apparent significant effect on cell viability. Quantification of the levels of 4sU-labelled viral RNA transcripts demonstrated that in cells stably expressing ISG15 shRNAs (sh6 cells), higher levels of viral RNA were produced (Figure 5.8)

compared with the levels in cells expressing a non-targeting shRNA (shCtrl cells). These changes in the levels of newly synthesised viral RNA mirrored the differences in total steady-state levels of viral RNA in both cells lines, indicating that ISG15 can negatively regulate the amount of viral RNA produced during HCV replication. Furthermore, data from experiments in which infected shCtrl and sh6 cells were pulse-labelled with higher concentrations of 4sU (200uM) for a period of 6h revealed that the rates of loss of labelled viral RNA were similar in both cells. These data suggest that ISG15 does not affect stability of HCV RNA but specifically affects viral RNA synthesis.

In a recent paper by Durfee et al (2010), ISG15 was implicated in broadly targeting newly synthesised proteins. HERC5, the major E3 ligase involved in ISGylation, was shown to localise with ribosomes and thus mediate ISG15 conjugation to newly synthesised proteins (Durfee *et al.*, 2010). It is possible that ISG15 may be able to target some of the viral replicase proteins during translation and prevent their normal function on replication by either disrupting protein–protein interactions between viral and host factors or protein-RNA interactions as part of replication complexes. It may be feasible to isolate HCV replication complexes by immunoprecipitation of 4sU-labelled viral RNAs, which could uncover possible interactions between ISG15 and the viral replicative machinery. Such immunoprecipitates could then be analysed by mass spectrometry or Western blot analysis to identify any factors that are conjugated to ISG15. One previous report has indicated that NS5A is conjugated to ISG15 (Kim & Yoo, 2010) but whether ISGylated NS5A is incorporated into sites of viral RNA replication is not known. Thus, the approach presented here could be developed further to examine the role of ISG15 in regulating HCV replication.

**2) Conjugation requirements for ISG15 anti-HCV activities**

Previous studies have demonstrated that ISG15 plays an antiviral role against Sindbis virus replication, which is dependent on the ability of ISG15 to conjugate to other proteins. By contrast, unconjugated ISG15 has been implicated in controlling replication of other viruses, such as HIV-1 and Ebola virus; these viruses use Gag-mediated and VP40-mediated budding from cells, respectively (Malakhova & Zhang, 2008). ISG15 disrupts ubiquitination of Gag protein, thereby limiting egress of HIV-1 virus (Okumura *et al.*, 2006). In the

case of Ebola, ISG15 binds specifically to Nedd4, an E3 ligase involved in ubiquitination of VP40, to prevent ubiquitination of VP40 and thus blocking egress (Malakhova & Zhang, 2008). In the case of HCV, the precise mode of action of ISG15 is not fully understood. Randall *et al* (2006) demonstrated an increase in ISG15 transcription and protein conjugates by silencing the ISG15 protease USP18. Decreased expression of USP18 resulted in enhancement of the negative effects of IFN against HCV replication (Randall *et al.*, 2006). Consistent with this notion, increased expression of ISG15 and ISG15-conjugation components in HCV replicon cells also resulted in inhibition of HCV replication (Kim & Yoo, 2010). Moreover, ISG15 was shown to directly interact with NS5A protein, suggesting that the anti-HCV activities of ISG15 against HCV were mediated by ISGylation and inhibition of function of NS5A protein (Kim & Yoo, 2010).

Given the data presented in the previous chapter regarding the IFN-dependent and –independent anti-viral role of ISG15 during HCV replication, two approaches were taken to evaluate the conjugation requirements of ISG15 for its anti-HCV activities. As stated earlier, IRF-3 and NF-KB can directly activate transcription of ISG15 following activation of cytoplasmic sensors with dsRNA or LPS (Li *et al.*, 2001; Memet *et al.*, 1991). Therefore, ISG15 can be produced in an IFN-independent manner and may possibly have a role as an early gene in controlling viral infection. To investigate whether these IFN-independent antiviral activities of ISG15 during HCV replication were dependent on its conjugation status, attempts were made to generate tetracycline-inducible cell lines to express a FLAG-tagged WT version of the mature ISG15 protein, which retained the C-terminal di-GG residues involved in conjugation, and a FLAG-tagged mutant version of ISG15 protein, in which these di-GG residues were converted to Ala (FLAG-ISG15-AA); introduction of these two mutations would prevent ISG15 conjugation. Increased protein expression by addition of tetracycline to the cells did not result in induction of ISG15 expression, in either ISG15-GG or ISG15-AA cells. Transient expression of FLAG-ISG15-GG and FLAG-ISG15-AA plasmids confirmed that both constructs were capable of expressing FLAG protein. Further analysis using tetracycline-inducible Huh-7 cells expressing YFP or luciferase revealed that expression of these proteins also failed upon addition of tetracycline (data not shown). Hence, it was concluded

that the tetracycline-inducible system is not well tolerated by Huh-7 cells and the problems encountered with expressing ISG15 are likely to be independent from the nature of the protein. Given those difficulties, Huh-7 cells stably expressing FLAG-ISG15-GG and FLAG-ISG15-AA proteins were generated. These cells apparently tolerated constitutive expression of ISG15 given that no changes in phenotype or cell viability were observed compared to parental Huh-7 cells. Western blot analysis demonstrated that FLAG-tagged unconjugated ISG15 was produced in FLAG-ISG15-GG and FLAG-ISG15-AA Huh-7 cells. However, a lower molecular weight band, presumed to correspond to untagged, free ISG15 protein was also detected. While ISG15 conjugates were not expected in the FLAG-ISG15-AA expressing cells, conjugated forms of ISG15 were also not found in the FLAG-ISG15-GG expressing cells. Thus, expression of ISG15 alone did not lead to production of ISG15 conjugates, indicating that concomitant expression of the E1, E2 and E3 ISG15 enzymes might be required for production of ISG15 conjugates in Huh-7 cells. Moreover, the data suggest that endogenous levels of the ISGylation machinery in the absence of IFN$\alpha$ are insufficient to support ISG15 conjugation.

Parallel to the above approach, the effects of ISG15 conjugation during IFN activation, i.e, when acting as an ISG, were also investigated. To that end, inhibition of ISG15 conjugation during IFN induction, was conducted by silencing HERC5, the major ISG15 E3 ligase. Previous reports have shown that, upon silencing HERC5, the majority of ISG15 conjugates are not produced (Dastur *et al.*, 2006). However, in our experiments silencing of HERC5 did not result in a substantial decrease in the detection of protein conjugates. A small reduction in conjugate formation was detected during IFN treatment but this did not have an appreciable effect on viral replication. By contrast, inhibition of HERC5 expression in the absence of IFN treatment did give a small rise in HCV replication. Thus, any anti-viral activity of ISG15 as a conjugating protein were not conclusively shown from the studies undertaken. Nevertheless, the approaches adopted and results acquired lay the foundation for further work to explore the question of which form of ISG15 regulates HCV replication. Alternative approaches could include silencing of UbE1L, the only E1 enzyme described for ISG15. However, this could also affect other substrates for UbE1L and thus a simple method to study ISG15 conjugation is not immediately obvious.

# 6 Final discussion and future perspectives

## 6.1 Summary

Two main lines of investigation were explored in this thesis that contributed to the understanding of viral and cellular requirements essential for HCV RNA replication in cell culture and the central role of host immune responses in this process. The major findings are summarised below:

I) To expand the range of viral genotypes that can replicate in cell culture, two regions of the JFH1 genome (the C-terminus of NS4B and the NS3P-4A coding segments) were substituted by sequences from a genotype 3a isolate (Glasgow-3 strain). Eleven amino acid changes were required to convert the C-terminus of NS4B from gt2a to gt3a. It was possible to make as many as 10 amino acid changes (Luc-M1-11/ΔM8) while retaining the ability to replicate. Interestingly, insertion of the gt3a NS3P-4A sequences into the JFH-1 SGR produced a replicon that failed to replicate in Huh-7 cells but was capable of some replication in Huh-7.5 cells.

II) The feasibility of using HepaRG cells for studies on replication was explored. No replication could be detected in transient assays but it was possible to generate drug-resistant colonies that harboured the replicon. It was presumed that the low permissiveness of these cells to replication was linked, at least in part, to an intrinsic or innate response. Results showed that ISG15 was upregulated in the cells although there was no evidence for stimulation of IFNβ transcription. Therefore, ISG15 presumably along with other ISGs could perhaps play a role in modulating the permissiveness of HepaRG cells to the initiation of viral replication.

III) ISG15 was identified as an antiviral factor against HCV replication. From experiments using both the SGR and HCVcc systems combined with siRNA and shRNA approaches, knockdown of ISG15 led to an increase in HCV RNA levels. Further studies examining *de novo* labelled viral RNA suggested that ISG15 exerted its anti-viral activity on the rate of viral RNA synthesis and not RNA degradation. In addition to identifying the mechanism of action of ISG15, attempts were made to determine whether conjugation of ISG15 to protein

substrates was needed to reduce viral RNA replication. However, no conclusions could be drawn due to technical problems with the systems used.

## 6.2 Expanding the range of genotypes for study of HCV infection

Since the development of the first sub-genomic replicon for HCV in 1999 by Lohmann *et al* using a Con-1 (gt1b) isolate, a large body of literature has explored various avenues to expand the repertoire of replicon and infectious cDNAs that can be used to examine the viral life cycle. To date, the system that yields the highest levels of replication is based on the JFH-1 (gt2a) strain and chimeric constructs have been generated that incorporate sequences from other genotypes to enable their characteristics to be examined. This approach has yielded valuable insights into the differing properties of the viral proteins from the various genotypes. For example, the NS3 protease from gt3a used in this study has been utilised to demonstrate its lower susceptibility to telaprevir (Imhof & Simmonds, 2011). Such studies are important since telaprevir is not currently prescribed for use in patients infected with HCV gt3 strains. Moreover, incorporation of NS5A sequences from the different HCV genotypes into the JFH-1 backbone has been employed as a strategy to show that gt2a and 3a strains are more resistant to BMS-790052, a drug that is currently undergoing clinical trials (Scheel *et al.*, 2011). The approach adopted in this study was guided largely by previous failed attempts to create a gt3 replicon based on the sequences of the Glasgow-3 isolate. It was possible to modify the C-terminus of NS4B to gt3a sequences with the exception of one substitution, which ablated replication. The constructs generated could provide the platform for further constructs.

Future construction of any chimeras for gt3 replicons should now be considered in light of the recent publication demonstrating replication of SGRs composed entirely of gt3a (strain S52) sequences (Saeed *et al.*, 2012). Replication required introduction of a serine to isoleucine substitution in NS5A (equivalent to S2204I in strain H77), which enabled adaptation of a gt1a replicon (Blight *et al.*, 2003). The strain S52 SGR acquired adaptive mutations in NS3 and NS4B following continuous culture in Huh-7 cells, which improved replicative efficiency. The only sequence difference between S52 and Glasgow-3 at the C-terminus of NS4B is a Lys at position 251 (in S52), which encodes a Gln (in

Glasgow-3). However, substitution at this position (M6) did not affect replication. Further studies could build on the data presented here and that are now available with strain S52 to examine genetic interactions between gt3a sequences. This would help to explore any functional differences between the genotypes. For example, infection with gt3a has been linked with steatosis. In addition, those infected with gt3a strains are more likely to respond to IFN$\alpha$/RBV therapy for reasons that are as yet not understood.

Ultimately, the aim of much HCV research is to be able to examine the infectious process with natural isolates without the need for adaptive mutations. To date, the only strain capable of robust replication and virus production in the absence of any mutations is JFH-1. However, this isolate is somewhat unique since it originated in a patient who developed fulminant hepatitis and thereafter cleared infection. Studies with natural isolates will almost certainly require alternatives to Huh-7 cells. One example of continuous cells capable of infection by HCV is the LH86 line, which was developed from a patient with HCC (Zhu *et al.*, 2007). Creation of 3-D culture systems with Huh-7 cells capable of productive infection by HCVcc has been achieved (Sainz *et al.*, 2009b). There have also been successes with human fetal liver cells (Marukian *et al.*, 2011) and hepatocytes derived from pluripotent stem cells (Roelandt *et al.*, 2012). With the ongoing advances in stem cell technology, it should perhaps be feasible to generate cell lines that can support infection by virus isolated from patient serum.

## 6.3 The mechanisms of action of ISG15

### 6.3.1 ISG15, an antiviral or proviral factor in HCV infection?

During the phase of acute infection, the complex interplay between HCV and the host can lead to two possible outcomes. In one, host immune responses can efficiently inhibit replication and eliminate the virus, resulting in clearance of infection. However, in the majority of the cases, HCV is able to subvert the host immune responses, leading to persistence. HCV has been shown to target host IFN signalling pathways at different levels. In infected cells, NS3/4A-mediated cleavage of signalling factors inhibits IRF-3 activation and NS5A suppresses PKR activity (Gale *et al.*, 1997; Li *et al.*, 2005b; Li *et al.*, 2005c).

Other arms of innate host defence, such as NK cell activation, macrophages and DC function, and consequent activation of adaptive immune responses, can also be controlled by the virus (Edwards *et al.*, 2012; Petrovic *et al.*, 2012; Saito *et al.*, 2008). The efficiency by which HCV controls the different waves of host antiviral response are highly dependent on genetic characteristics of different viral strains and genotypes as well as intrinsic host factors (such as IL28B polymorphisms) (Mangia *et al.*, 2010; Thompson *et al.*, 2010).

The current standard of care for treating chronic HCV infection is based on a combination of Peg-IFN$\alpha$ and ribavirin. This regimen can successfully clear infection in ~50% of the patients. By comparing host genes expressed in liver biopsies from responders and non-responders, it has been possible to identify a subset of four genes that could act as predictors of response to treatment (Dill *et al.*, 2011). All of the genes are IFN-induced and include ISG15. Interestingly, determining the expression of these genes in the liver proved to be a better predictor of response compared to IL28B genotype. Moreover, unpublished studies from our group indicate that IFN-induced genes, including ISG15 and those involved in the ISGylation pathway, are expressed at higher levels in biopsies from infected patients compared to uninfected patients (M. Robinson *et al.*, unpublished). The mechanisms underlying these changes are not known but highlight the importance of studying IFN-regulated genes such as ISG15 with *in vitro* systems.

The data presented in this study and others have reached conflicting conclusions with regard to whether ISG15 acts as a pro- or antiviral factor in HCV infection. Part of the difficulty could result from use of different sources of Huh-7 cells and the use of cells previously carrying but cured of the HCV SGR (e.g. Huh-7.5 cells). Added weight for ISG15 acting as an antiviral factor comes from data obtained with U2OS cells that are also able to support replication. Indeed, knockdown of ISG15 in U2OS cells increased viral RNA cells to a much greater extent compared to Huh-7 cells. It is known that immune cells isolated from cancer patients have defective interferon signalling (Critchley-Thorne *et al.*, 2009) and it is reasonable to assume that tumour-derived cell lines have similar characteristics. Since both U2OS cells and Huh-7 cells are tumour-derived, they would be expected to have impaired interferon signalling pathways and indeed it

is known that Huh-7 cells lack TLR3 and RIG-I is mutated in Huh-7.5 cells. There is not an extensive literature on the use of U2OS cells for interferon signalling studies but the membrane sensor TLR9 is absent from the surface of the cells (Laredj & Beard, 2011). Nevertheless, the fact that the data in the study presented here is reproducible in cells from different tissue lineages gives greater confidence that ISG15 is an antiviral factor. It would be preferable to conduct the studies in other cell lines or indeed primary liver cells. Unfortunately, HepaRG cells were unable to support replication for a sufficiently long period to enable ISG15 knockdown studies. It is known that HCVcc induce ISG expression in human fetal cells and ISG15 is among those that are stimulated upon infection (Marukian *et al.*, 2011). However, replication levels in these cells tend to be low and vary between donors. Manipulation of the cells by expressing the paramyxovirus V proteins to impair STAT signalling does enhance productive infection (Andrus *et al.*, 2011). Therefore, limiting ISG15 expression using the shRNA system could be utilised to conclusively determine its impact in human fetal cells since they have an authentic interferon-response pathway.

### 6.3.2 Is conjugation necessary for ISG15 to impair HCV RNA replication?

One of the important questions not fully addressed in this study was whether conjugated or free ISG15 was responsible for limiting viral RNA replication. The approaches adopted were to generate Huh-7 cells in which HERC5 expression was inhibited using siRNAs and separately, express a mutant form of ISG15 that could not form conjugates; the cells produced using these methods would have allowed analysis not only with the SGR but also the HCVcc system. Although neither approach in Huh-7 cells was successful, HERC5 expression was not detected in U2OS cells and very few conjugated forms of ISG15 were detected in cells stimulated with IFN. Despite the reduced capacity for U2OS cells to produce conjugated ISG15, knockdown of ISG15 had a greater effect on viral RNA levels. This would perhaps suggest that ISGylation is not a prerequisite for ISG15 to exert its antiviral effect and free ISG15 may be sufficient.

The potential role of unconjugated ISG15 has been the subject of considerable debate for more than a fifteen years. Early studies showed that unconjugated ISG15 could be secreted by corneal cells (Taylor *et al.*, 1996) and a range of immune cell types (D'Cunha *et al.*, 1996a; D'Cunha *et al.*, 1996b). Experimental evidence indicated that ISG15 could act as a cytokine, capable of stimulating production of IFNγ from NK and T-cells (D'Cunha *et al.*, 1996a; D'Cunha *et al.*, 1996b). By contrast, data obtained from ISG15$^{-/-}$ mice contradicted these findings and reached the conclusion that ISG15 lacked any cytokine activity (Osiak *et al.*, 2005). However, recent evidence from patients who have mutations in the ISG15 gene and are susceptible to mycobacterial disease apparently confirms the earlier findings that the protein has immunomodulatory properties (Bogunovic *et al.*, 2012). The mutations introduce either a premature stop codon or frameshift into the protein coding region, thereby generating non-functional ISG15. Leukocytes isolated from these patients produced only small amounts of IFNγ after stimulation by mycobacteria. IFNγ stimulation could be restored by addition of human recombinant ISG15. Thus, free ISG15 is a functional factor whose properties have not yet been fully explored. Further experiments that built on the approach to express mutant ISG15 that was incapable of participating in ISGylation would help to address this issue as would attempts to treat infected Huh-7 cells with recombinant ISG15. If the results demonstrated that unconjugated ISG15 could affect HCV replication, this would open entirely new avenues for future research. In addition, ISG15 transcription is elevated in infected liver and also to yet higher levels in those who fail to respond to therapy. If it could be demonstrated that this increased transcription leads to a rise in free ISG15, then further studies would be warranted to determine how it functions in the complex cytokine milieu that resides in the liver.

# References

**Adinolfi, L. E., Gambardella, M., Andreana, A., Tripodi, M. F., Utili, R. & Ruggiero, G. (2001).** Steatosis accelerates the progression of liver damage of chronic hepatitis C patients and correlates with specific HCV genotype and visceral obesity. *Hepatology* **33**, 1358-1364.

**Agnello, V., Abel, G., Elfahal, M., Knight, G. B. & Zhang, Q. X. (1999).** Hepatitis C virus and other flaviviridae viruses enter cells via low density lipoprotein receptor. *Proc Natl Acad Sci U S A* **96**, 12766-12771.

**Ago, H., Adachi, T., Yoshida, A., Yamamoto, M., Habuka, N., Yatsunami, K. & Miyano, M. (1999).** Crystal structure of the RNA-dependent RNA polymerase of hepatitis C virus. *Structure* **7**, 1417-1426.

**Albecka, A., Montserret, R., Krey, T., Tarr, A. W., Diesis, E., Ball, J. K., Descamps, V., Duverlie, G., Rey, F., Penin, F. & Dubuisson, J. (2011).** Identification of new functional regions in hepatitis C virus envelope glycoprotein E2. *J Virol* **85**, 1777-1792.

**Ali, N. & Siddiqui, A. (1995).** Interaction of polypyrimidine tract-binding protein with the 5' noncoding region of the hepatitis C virus RNA genome and its functional requirement in internal initiation of translation. *J Virol* **69**, 6367-6375.

**Ali, N. & Siddiqui, A. (1997).** The La antigen binds 5' noncoding region of the hepatitis C virus RNA in the context of the initiator AUG codon and stimulates internal ribosome entry site-mediated translation. *Proc Natl Acad Sci U S A* **94**, 2249-2254.

**Aligo, J., Jia, S., Manna, D. & Konan, K. V. (2009).** Formation and function of hepatitis C virus replication complexes require residues in the carboxy-terminal domain of NS4B protein. *Virology* **393**, 68-83.

**Alter, H. J., Purcell, R. H., Holland, P. V. & Popper, H. (1978).** Transmissible agent in non-A, non-B hepatitis. *Lancet* **1**, 459-463.

**Alter, M. J. (2006).** Epidemiology of viral hepatitis and HIV co-infection. *J Hepatol* **44**, S6-9.

**Alter, M. J. (2007).** Epidemiology of hepatitis C virus infection. *World J Gastroenterol* **13**, 2436-2441.

**Amadei, B., Urbani, S., Cazaly, A., Fisicaro, P., Zerbini, A., Ahmed, P., Missale, G., Ferrari, C. & Khakoo, S. I. (2010).** Activation of natural killer cells during acute infection with hepatitis C virus. *Gastroenterology* **138**, 1536-1545.

**Amoroso, P., Rapicetta, M., Tosti, M. E., Mele, A., Spada, E., Buonocore, S., Lettieri, G., Pierri, P., Chionne, P., Ciccaglione, A. R. & Sagliocca, L. (1998).** Correlation between virus genotype and chronicity rate in acute hepatitis C. *J Hepatol* **28**, 939-944.

**Andersen, J. B., Aaboe, M., Borden, E. C., Goloubeva, O. G., Hassel, B. A. & Orntoft, T. F. (2006).** Stage-associated overexpression of the ubiquitin-like protein, ISG15, in bladder cancer. *Br J Cancer* **94**, 1465-1471.

**Andre, P., Komurian-Pradel, F., Deforges, S., Perret, M., Berland, J. L., Sodoyer, M., Pol, S., Brechot, C., Paranhos-Baccala, G. & Lotteau, V. (2002).** Characterization of low- and very-low-density hepatitis C virus RNA-containing particles. *J Virol* **76**, 6919-6928.

**Andre, P., Perlemuter, G., Budkowska, A., Brechot, C. & Lotteau, V. (2005).** Hepatitis C virus particles and lipoprotein metabolism. *Semin Liver Dis* **25**, 93-104.

**Andrus, L., Marukian, S., Jones, C. T., Catanese, M. T., Sheahan, T. P., Schoggins, J. W., Barry, W. T., Dustin, L. B., Trehan, K., Ploss, A., Bhatia, S. N. & Rice, C. M. (2011).** Expression of paramyxovirus V proteins promotes replication and spread of hepatitis C virus in cultures of primary human fetal liver cells. *Hepatology* **54**, 1901-1912.

**Angus, A. G., Dalrymple, D., Boulant, S., McGivern, D. R., Clayton, R. F., Scott, M. J., Adair, R., Graham, S., Owsianka, A. M., Targett-Adams, P., Li, K., Wakita, T., McLauchlan, J., Lemon, S. M. & Patel, A. H. (2010).** Requirement of cellular DDX3 for hepatitis C virus replication is unrelated to its interaction with the viral core protein. *J Gen Virol* **91**, 122-132.

**Appel, N., Pietschmann, T. & Bartenschlager, R. (2005).** Mutational analysis of hepatitis C virus nonstructural protein 5A: potential role of differential phosphorylation in RNA replication and identification of a genetically flexible domain. *J Virol* **79**, 3187-3194.

**Appel, N., Zayas, M., Miller, S., Krijnse-Locker, J., Schaller, T., Friebe, P., Kallis, S., Engel, U. & Bartenschlager, R. (2008).** Essential role of domain III of nonstructural protein 5A for hepatitis C virus infectious particle assembly. *PLoS Pathog* **4**, e1000035.

**Backes, P., Quinkert, D., Reiss, S., Binder, M., Zayas, M., Rescher, U., Gerke, V., Bartenschlager, R. & Lohmann, V. (2010).** Role of annexin A2 in the production of infectious hepatitis C virus particles. *J Virol* **84**, 5775-5789.

**Bacon, B. R., Gordon, S. C., Lawitz, E., Marcellin, P., Vierling, J. M., Zeuzem, S., Poordad, F., Goodman, Z. D., Sings, H. L., Boparai, N., Burroughs, M., Brass, C. A., Albrecht, J. K. & Esteban, R. (2011).** Boceprevir for previously treated chronic HCV genotype 1 infection. *N Engl J Med* **364**, 1207-1217.

**Bankwitz, D., Steinmann, E., Bitzegeio, J., Ciesek, S., Friesland, M., Herrmann, E., Zeisel, M. B., Baumert, T. F., Keck, Z. Y., Foung, S. K., Pecheur, E. I. & Pietschmann, T. (2010).** Hepatitis C virus hypervariable region 1 modulates receptor interactions, conceals the CD81 binding site, and protects conserved neutralizing epitopes. *J Virol* **84**, 5751-5763.

**Bartenschlager, R., Ahlborn-Laake, L., Mous, J. & Jacobsen, H. (1993).** Nonstructural protein 3 of the hepatitis C virus encodes a serine-type proteinase required for cleavage at the NS3/4 and NS4/5 junctions. *J Virol* **67**, 3835-3844.

**Bartenschlager, R., Ahlborn-Laake, L., Yasargil, K., Mous, J. & Jacobsen, H. (1995).** Substrate determinants for cleavage in cis and in trans by the hepatitis C virus NS3 proteinase. *J Virol* **69**, 198-205.

**Bartenschlager, R., Kaul, A. & Sparacio, S. (2003).** Replication of the hepatitis C virus in cell culture. *Antiviral Res* **60**, 91-102.

**Barth, H., Schafer, C., Adah, M. I., Zhang, F., Linhardt, R. J., Toyoda, H., Kinoshita-Toyoda, A., Toida, T., Van Kuppevelt, T. H., Depla, E., Von Weizsacker, F., Blum, H. E. & Baumert, T. F. (2003).** Cellular binding of hepatitis C virus envelope glycoprotein E2 requires cell surface heparan sulfate. *J Biol Chem* **278**, 41003-41012.

**Bartosch, B., Bukh, J., Meunier, J. C., Granier, C., Engle, R. E., Blackwelder, W. C., Emerson, S. U., Cosset, F. L. & Purcell, R. H. (2003).** In vitro assay for neutralizing antibody to hepatitis C virus: evidence for broadly conserved neutralization epitopes. *Proc Natl Acad Sci U S A* **100**, 14199-14204.

**Bartosch, B., Dubuisson, J. & Cosset, F. L. (2003).** Infectious hepatitis C virus pseudo-particles containing functional E1-E2 envelope protein complexes. *J Exp Med* **197**, 633-642.

**Bartosch, B., Vitelli, A., Granier, C., Goujon, C., Dubuisson, J., Pascale, S., Scarselli, E., Cortese, R., Nicosia, A. & Cosset, F. L. (2003).** Cell entry of hepatitis C virus requires a set of co-receptors that include the CD81 tetraspanin and the SR-B1 scavenger receptor. *J Biol Chem* **278**, 41624-41630.

**Bayer, M. E., Blumberg, B. S. & Werner, B. (1968).** Particles associated with Australia antigen in the sera of patients with leukaemia, Down's Syndrome and hepatitis. *Nature* **218**, 1057-1059.

**Bellecave, P., Sarasin-Filipowicz, M., Donze, O., Kennel, A., Gouttenoire, J., Meylan, E., Terracciano, L., Tschopp, J., Sarrazin, C., Berg, T., Moradpour, D. & Heim, M. H. (2010).** Cleavage of mitochondrial antiviral signaling protein in the liver of patients with chronic hepatitis C correlates with a reduced activation of the endogenous interferon system. *Hepatology* **51**, 1127-1136.

**Benedicto, I., Molina-Jimenez, F., Bartosch, B., Cosset, F. L., Lavillette, D., Prieto, J., Moreno-Otero, R., Valenzuela-Fernandez, A., Aldabe, R., Lopez-Cabrera, M. & Majano, P. L. (2009).** The tight junction-associated protein occludin is required for a postbinding step in hepatitis C virus entry and infection. *J Virol* **83**, 8012-8020.

**Benga, W. J., Krieger, S. E., Dimitrova, M., Zeisel, M. B., Parnot, M., Lupberger, J., Hildt, E., Luo, G., McLauchlan, J., Baumert, T. F. & Schuster, C. (2010).** Apolipoprotein E interacts with hepatitis C virus nonstructural protein 5A and determines assembly of infectious particles. *Hepatology* **51**, 43-53.

**Bensadoun, P., Rodriguez, C., Soulier, A., Higgs, M., Chevaliez, S. & Pawlotsky, J. M. (2011).** Genetic background of hepatocyte cell lines: are in vitro hepatitis C virus research data reliable? *Hepatology* **54**, 748.

**Beran, R. K., Lindenbach, B. D. & Pyle, A. M. (2009).** The NS4A protein of hepatitis C virus promotes RNA-coupled ATP hydrolysis by the NS3 helicase. *J Virol* **83**, 3268-3275.

**Berger, K. L., Cooper, J. D., Heaton, N. S., Yoon, R., Oakland, T. E., Jordan, T. X., Mateu, G., Grakoui, A. & Randall, G. (2009).** Roles for endocytic trafficking and phosphatidylinositol 4-kinase III alpha in hepatitis C virus replication. *Proc Natl Acad Sci U S A* **106**, 7577-7582.

**Berry, K. E., Waghray, S. & Doudna, J. A. (2010).** The HCV IRES pseudoknot positions the initiation codon on the 40S ribosomal subunit. *Rna* **16**, 1559-1569.

**Berry, K. E., Waghray, S., Mortimer, S. A., Bai, Y. & Doudna, J. A. (2011).** Crystal structure of the HCV IRES central domain reveals strategy for start-codon positioning. *Structure* **19**, 1456-1466.

**Binder, M., Kochs, G., Bartenschlager, R. & Lohmann, V. (2007).** Hepatitis C virus escape from the interferon regulatory factor 3 pathway by a passive and active evasion strategy. *Hepatology* **46**, 1365-1374.

**Bissig, K. D., Le, T. T., Woods, N. B. & Verma, I. M. (2007).** Repopulation of adult and neonatal mice with human hepatocytes: a chimeric animal model. *Proc Natl Acad Sci U S A* **104**, 20507-20511.

**Bissig, K. D., Wieland, S. F., Tran, P., Isogawa, M., Le, T. T., Chisari, F. V. & Verma, I. M. (2010).** Human liver chimeric mice provide a model for hepatitis B and C virus infection and treatment. *J Clin Invest* **120**, 924-930.

**Blanchard, E., Belouzard, S., Goueslain, L., Wakita, T., Dubuisson, J., Wychowski, C. & Rouille, Y. (2006).** Hepatitis C virus entry depends on clathrin-mediated endocytosis. *J Virol* **80**, 6964-6972.

**Blight, K. J. (2011).** Charged residues in hepatitis C virus NS4B are critical for multiple NS4B functions in RNA replication. *J Virol* **85**, 8158-8171.

**Blight, K. J., Kolykhalov, A. A. & Rice, C. M. (2000).** Efficient initiation of HCV RNA replication in cell culture. *Science* **290**, 1972-1974.

**Blight, K. J., McKeating, J. A., Marcotrigiano, J. & Rice, C. M. (2003).** Efficient replication of hepatitis C virus genotype 1a RNAs in cell culture. *J Virol* **77**, 3181-3190.

**Blight, K. J., McKeating, J. A. & Rice, C. M. (2002).** Highly permissive cell lines for subgenomic and genomic hepatitis C virus RNA replication. *J Virol* **76**, 13001-13014.

**Blindenbacher, A., Duong, F. H., Hunziker, L., Stutvoet, S. T., Wang, X., Terracciano, L., Moradpour, D., Blum, H. E., Alonzi, T., Tripodi, M., La Monica, N. & Heim, M. H. (2003).** Expression of hepatitis c virus proteins inhibits interferon alpha signaling in the liver of transgenic mice. *Gastroenterology* **124**, 1465-1475.

**Blomstrom, D. C., Fahey, D., Kutny, R., Korant, B. D. & Knight, E., Jr. (1986).** Molecular characterization of the interferon-induced 15-kDa protein. Molecular cloning and nucleotide and amino acid sequence. *J Biol Chem* **261**, 8811-8816.

**Bochud, P. Y., Cai, T., Overbeck, K., Bochud, M., Dufour, J. F., Mullhaupt, B., Borovicka, J., Heim, M., Moradpour, D., Cerny, A., Malinverni, R., Francioli, P. & Negro, F. (2009).** Genotype 3 is associated with accelerated fibrosis progression in chronic hepatitis C. *J Hepatol* **51**, 655-666.

**Bode, J. G., Brenndorfer, E. D. & Haussinger, D. (2007).** Subversion of innate host antiviral strategies by the hepatitis C virus. *Arch Biochem Biophys* **462**, 254-265.

**Bode, J. G., Ludwig, S., Ehrhardt, C., Albrecht, U., Erhardt, A., Schaper, F., Heinrich, P. C. & Haussinger, D. (2003).** IFN-alpha antagonistic activity of HCV core protein involves induction of suppressor of cytokine signaling-3. *Faseb J* **17**, 488-490.

**Boehringer, D., Thermann, R., Ostareck-Lederer, A., Lewis, J. D. & Stark, H. (2005).** Structure of the hepatitis C virus IRES bound to the human 80S ribosome: remodeling of the HCV IRES. *Structure* **13**, 1695-1706.

**Bogunovic, D., Byun, M., Durfee, L. A., Abhyankar, A., Sanal, O., Mansouri, D., Salem, S., Radovanovic, I., Grant, A. V., Adimi, P., Mansouri, N., Okada, S., Bryant, V. L., Kong, X. F., Kreins, A., Velez, M. M., Boisson, B., Khalilzadeh, S., Ozcelik, U., Darazam, I. A., Schoggins, J. W., Rice, C. M., Al-Muhsen, S., Behr, M., Vogt, G., Puel, A., Bustamante, J., Gros, P., Huibregtse, J. M., Abel, L., Boisson-Dupuis, S. & Casanova, J. L. (2012).** Mycobacterial disease and impaired IFN-gamma immunity in humans with inherited ISG15 deficiency. *Science (New York, NY* **337**, 1684-1688.

**Boson, B., Granio, O., Bartenschlager, R. & Cosset, F. L. (2011).** A concerted action of hepatitis C virus p7 and nonstructural protein 2 regulates core localization at the endoplasmic reticulum and virus assembly. *PLoS Pathog* **7**, e1002144.

**Boulant, S., Douglas, M. W., Moody, L., Budkowska, A., Targett-Adams, P. & McLauchlan, J. (2008).** Hepatitis C virus core protein induces lipid

droplet redistribution in a microtubule- and dynein-dependent manner. *Traffic* **9**, 1268-1282.

**Boulant, S., Montserret, R., Hope, R. G., Ratinier, M., Targett-Adams, P., Lavergne, J. P., Penin, F. & McLauchlan, J. (2006).** Structural determinants that target the hepatitis C virus core protein to lipid droplets. *J Biol Chem* **281**, 22236-22247.

**Boulant, S., Targett-Adams, P. & McLauchlan, J. (2007).** Disrupting the association of hepatitis C virus core protein with lipid droplets correlates with a loss in production of infectious virus. *J Gen Virol* **88**, 2204-2213.

**Boulant, S., Vanbelle, C., Ebel, C., Penin, F. & Lavergne, J. P. (2005).** Hepatitis C virus core protein is a dimeric alpha-helical protein exhibiting membrane protein features. *J Virol* **79**, 11353-11365.

**Bowie, A. G. & Unterholzner, L. (2008).** Viral evasion and subversion of pattern-recognition receptor signalling. *Nat Rev Immunol* **8**, 911-922.

**Bradley, D., McCaustland, K., Krawczynski, K., Spelbring, J., Humphrey, C. & Cook, E. H. (1991).** Hepatitis C virus: buoyant density of the factor VIII-derived isolate in sucrose. *J Med Virol* **34**, 206-208.

**Bradley, D. W., McCaustland, K. A., Cook, E. H., Schable, C. A., Ebert, J. W. & Maynard, J. E. (1985).** Posttransfusion non-A, non-B hepatitis in chimpanzees. Physicochemical evidence that the tubule-forming agent is a small, enveloped virus. *Gastroenterology* **88**, 773-779.

**Brant, L. J., Ramsay, M. E., Tweed, E., Hale, A., Hurrelle, M., Klapper, P. & Ngui, S. L. (2010).** Planning for the healthcare burden of hepatitis C infection: Hepatitis C genotypes identified in England, 2002-2007. *J Clin Virol* **48**, 115-119.

**Brass, V., Bieck, E., Montserret, R., Wolk, B., Hellings, J. A., Blum, H. E., Penin, F. & Moradpour, D. (2002).** An amino-terminal amphipathic alpha-helix mediates membrane association of the hepatitis C virus nonstructural protein 5A. *J Biol Chem* **277**, 8130-8139.

**Brenndorfer, E. D., Karthe, J., Frelin, L., Cebula, P., Erhardt, A., Schulte am Esch, J., Hengel, H., Bartenschlager, R., Sallberg, M., Haussinger, D. & Bode, J. G. (2009).** Nonstructural 3/4A protease of hepatitis C virus activates epithelial growth factor-induced signal transduction by cleavage of the T-cell protein tyrosine phosphatase. *Hepatology* **49**, 1810-1820.

**Bressanelli, S., Tomei, L., Roussel, A., Incitti, I., Vitale, R. L., Mathieu, M., De Francesco, R. & Rey, F. A. (1999).** Crystal structure of the RNA-dependent RNA polymerase of hepatitis C virus. *Proc Natl Acad Sci U S A* **96**, 13034-13039.

**Broering, R., Zhang, X., Kottilil, S., Trippler, M., Jiang, M., Lu, M., Gerken, G. & Schlaak, J. F. (2010).** The interferon stimulated gene 15 functions as a proviral factor for the hepatitis C virus and as a regulator of the IFN response. *Gut* **59**, 1111-1119.

**Bukh, J. (2011).** Hepatitis C homolog in dogs with respiratory illness. *Proc Natl Acad Sci U S A* **108**, 12563-12564.

**Bukh, J., Apgar, C. L., Govindarajan, S. & Purcell, R. H. (2001).** Host range studies of GB virus-B hepatitis agent, the closest relative of hepatitis C virus, in New World monkeys and chimpanzees. *J Med Virol* **65**, 694-697.

**Bukh, J., Meuleman, P., Tellier, R., Engle, R. E., Feinstone, S. M., Eder, G., Satterfield, W. C., Govindarajan, S., Krawczynski, K., Miller, R. H., Leroux-Roels, G. & Purcell, R. H. (2010).** Challenge pools of hepatitis C virus genotypes 1-6 prototype strains: replication fitness and pathogenicity in chimpanzees and human liver-chimeric mouse models. *J Infect Dis* **201**, 1381-1389.

**Bukh, J., Pietschmann, T., Lohmann, V., Krieger, N., Faulk, K., Engle, R. E., Govindarajan, S., Shapiro, M., St Claire, M. & Bartenschlager, R. (2002).** Mutations that permit efficient replication of hepatitis C virus RNA in Huh-7 cells prevent productive replication in chimpanzees. *Proc Natl Acad Sci U S A* **99**, 14416-14421.

**Bukh, J., Purcell, R. H. & Miller, R. H. (1992).** Sequence analysis of the 5' noncoding region of hepatitis C virus. *Proc Natl Acad Sci U S A* **89**, 4942-4946.

**Callens, N., Ciczora, Y., Bartosch, B., Vu-Dac, N., Cosset, F. L., Pawlotsky, J. M., Penin, F. & Dubuisson, J. (2005).** Basic residues in hypervariable region 1 of hepatitis C virus envelope glycoprotein e2 contribute to virus entry. *J Virol* **79**, 15331-15341.

**Carrere-Kremer, S., Montpellier-Pala, C., Cocquerel, L., Wychowski, C., Penin, F. & Dubuisson, J. (2002).** Subcellular localization and topology of the p7 polypeptide of hepatitis C virus. *J Virol* **76**, 3720-3730.

**Castera, L., Hezode, C., Roudot-Thoraval, F., Lonjon, I., Zafrani, E. S., Pawlotsky, J. M. & Dhumeaux, D. (2004).** Effect of antiviral treatment on evolution of liver steatosis in patients with chronic hepatitis C: indirect evidence of a role of hepatitis C virus genotype 3 in steatosis. *Gut* **53**, 420-424.

**Catic, A., Fiebiger, E., Korbel, G. A., Blom, D., Galardy, P. J. & Ploegh, H. L. (2007).** Screen for ISG15-crossreactive deubiquitinases. *PLoS One* **2**, e679.

**Cerec, V., Glaise, D., Garnier, D., Morosan, S., Turlin, B., Drenou, B., Gripon, P., Kremsdorf, D., Guguen-Guillouzo, C. & Corlu, A. (2007).** Transdifferentiation of hepatocyte-like cells from the human hepatoma HepaRG cell line through bipotent progenitor. *Hepatology* **45**, 957-967.

**Chang, K. S., Cai, Z., Zhang, C., Sen, G. C., Williams, B. R. & Luo, G. (2006).** Replication of hepatitis C virus (HCV) RNA in mouse embryonic fibroblasts: protein kinase R (PKR)-dependent and PKR-independent mechanisms for controlling HCV RNA replication and mediating interferon activities. *J Virol* **80**, 7364-7374.

**Chang, K. S., Jiang, J., Cai, Z. & Luo, G. (2007).** Human apolipoprotein e is required for infectivity and production of hepatitis C virus in cell culture. *J Virol* **81**, 13783-13793.

**Chang, Y. G., Yan, X. Z., Xie, Y. Y., Gao, X. C., Song, A. X., Zhang, D. E. & Hu, H. Y. (2008).** Different roles for two ubiquitin-like domains of ISG15 in protein modification. *J Biol Chem* **283**, 13370-13377.

**Charles, E. D. & Dustin, L. B. (2009).** Hepatitis C virus-induced cryoglobulinemia. *Kidney Int* **76**, 818-824.

**Cheent, K. & Khakoo, S. I. (2011).** Natural killer cells and hepatitis C: action and reaction. *Gut* **60**, 268-278.

**Chen, L., Sun, J., Meng, L., Heathcote, J., Edwards, A. & McGilvray, I. (2010).** ISG15, a ubiquitin-like interferon stimulated gene, promotes Hepatitis C Virus production in vitro: Implications for chronic infection and response to treatment. *J Gen Virol*.

**Cho, N. J., Dvory-Sobol, H., Lee, C., Cho, S. J., Bryson, P., Masek, M., Elazar, M., Frank, C. W. & Glenn, J. S. (2010).** Identification of a class of HCV inhibitors directed against the nonstructural protein NS4B. *Sci Transl Med* **2**, 15ra16.

**Choo, Q. L., Kuo, G., Ralston, R., Weiner, A., Chien, D., Van Nest, G., Han, J., Berger, K., Thudium, K., Kuo, C. & et al. (1994).** Vaccination of chimpanzees against infection by the hepatitis C virus. *Proc Natl Acad Sci U S A* **91**, 1294-1298.

**Choo, Q. L., Kuo, G., Weiner, A. J., Overby, L. R., Bradley, D. W. & Houghton, M. (1989).** Isolation of a cDNA clone derived from a blood-borne non-A, non-B viral hepatitis genome. *Science* **244**, 359-362.

**Choo, Q. L., Richman, K. H., Han, J. H., Berger, K., Lee, C., Dong, C., Gallegos, C., Coit, D., Medina-Selby, R., Barr, P. J. & et al. (1991).** Genetic organization and diversity of the hepatitis C virus. *Proc Natl Acad Sci U S A* **88**, 2451-2455.

**Christie, J. M., Healey, C. J., Watson, J., Wong, V. S., Duddridge, M., Snowden, N., Rosenberg, W. M., Fleming, K. A., Chapel, H. & Chapman, R. W. (1997).** Clinical outcome of hypogammaglobulinaemic patients following outbreak of acute hepatitis C: 2 year follow up. *Clin Exp Immunol* **110**, 4-8.

**Chua, P. K., McCown, M. F., Rajyaguru, S., Kular, S., Varma, R., Symons, J., Chiu, S. S., Cammack, N. & Najera, I. (2009).** Modulation of alpha interferon anti-hepatitis C virus activity by ISG15. *J Gen Virol* **90**, 2929-2939.

**Clarke, D., Griffin, S., Beales, L., Gelais, C. S., Burgess, S., Harris, M. & Rowlands, D. (2006).** Evidence for the formation of a heptameric ion channel complex by the hepatitis C virus p7 protein in vitro. *J Biol Chem* **281**, 37057-37068.

**Cocquerel, L., Duvet, S., Meunier, J. C., Pillez, A., Cacan, R., Wychowski, C. & Dubuisson, J. (1999).** The transmembrane domain of hepatitis C virus glycoprotein E1 is a signal for static retention in the endoplasmic reticulum. *J Virol* **73**, 2641-2649.

**Cooper, S., Erickson, A. L., Adams, E. J., Kansopon, J., Weiner, A. J., Chien, D. Y., Houghton, M., Parham, P. & Walker, C. M. (1999).** Analysis of a successful immune response against hepatitis C virus. *Immunity* **10**, 439-449.

**Counihan, N. A., Rawlinson, S. M. & Lindenbach, B. D. (2011).** Trafficking of hepatitis C virus core protein during virus particle assembly. *PLoS Pathog* **7**, e1002302.

**Crotta, S., Stilla, A., Wack, A., D'Andrea, A., Nuti, S., D'Oro, U., Mosca, M., Filliponi, F., Brunetto, R. M., Bonino, F., Abrignani, S. & Valiante, N. M. (2002).** Inhibition of natural killer cells through engagement of CD81 by the major hepatitis C virus envelope protein. *J Exp Med* **195**, 35-41.

**Critchley-Thorne, R. J., Simons, D. L., Yan, N., Miyahira, A. K., Dirbas, F. M., Johnson, D. L., Swetter, S. M., Carlson, R. W., Fisher, G. A., Koong, A., Holmes, S. & Lee, P. P. (2009).** Impaired interferon signaling is a common immune defect in human cancer. *Proc Natl Acad Sci U S A* **106**, 9010-9015.

**Cun, W., Jiang, J. & Luo, G. (2010).** The C-terminal alpha-helix domain of apolipoprotein E is required for interaction with nonstructural protein 5A and assembly of hepatitis C virus. *J Virol* **84**, 11532-11541.

**Da Costa, D., Turek, M., Felmlee, D. J., Girardi, E., Pfeffer, S., Long, G., Bartenschlager, R., Zeisel, M. B. & Baumert, T. F. (2012).** Reconstitution of the entire hepatitis C virus life cycle in non-hepatic cells. *J Virol*.

**Danta, M., Brown, D., Bhagani, S., Pybus, O. G., Sabin, C. A., Nelson, M., Fisher, M., Johnson, A. M. & Dusheiko, G. M. (2007).** Recent epidemic of acute hepatitis C virus in HIV-positive men who have sex with men linked to high-risk sexual behaviours. *Aids* **21**, 983-991.

**Dastur, A., Beaudenon, S., Kelley, M., Krug, R. M. & Huibregtse, J. M. (2006).** Herc5, an interferon-induced HECT E3 enzyme, is required for conjugation of ISG15 in human cells. *J Biol Chem* **281**, 4334-4338.

**Date, T., Kato, T., Miyamoto, M., Zhao, Z., Yasui, K., Mizokami, M. & Wakita, T. (2004).** Genotype 2a hepatitis C virus subgenomic replicon can replicate in HepG2 and IMY-N9 cells. *J Biol Chem* **279**, 22371-22376.

**D'Cunha, J., Knight, E., Jr., Haas, A. L., Truitt, R. L. & Borden, E. C. (1996a).** Immunoregulatory properties of ISG15, an interferon-induced cytokine. *Proc Natl Acad Sci U S A* **93**, 211-215.

**D'Cunha, J., Ramanujam, S., Wagner, R.J., Witt, P.L., Knight, E. Jr., Borden, E.C. (1996b).** In vitro and in vivo secretion of human ISG15, an IFN-induced immunomodulatory cytokine. *J Immunol* **157**,4100-8.

**de Lucas, S., Bartolome, J. & Carreno, V. (2005).** Hepatitis C virus core protein down-regulates transcription of interferon-induced antiviral genes. *J Infect Dis* **191**, 93-99.

**Decalf, J., Fernandes, S., Longman, R., Ahloulay, M., Audat, F., Lefrerre, F., Rice, C. M., Pol, S. & Albert, M. L. (2007).** Plasmacytoid dendritic cells initiate a complex chemokine and cytokine network and are a viable drug target in chronic HCV patients. *J Exp Med* **204**, 2423-2437.

**Deleersnyder, V., Pillez, A., Wychowski, C., Blight, K., Xu, J., Hahn, Y. S., Rice, C. M. & Dubuisson, J. (1997).** Formation of native hepatitis C virus glycoprotein complexes. *J Virol* **71**, 697-704.

**Della Bella, S., Crosignani, A., Riva, A., Presicce, P., Benetti, A., Longhi, R., Podda, M. & Villa, M. L. (2007).** Decrease and dysfunction of dendritic cells correlate with impaired hepatitis C virus-specific CD4+ T-cell proliferation in patients with hepatitis C virus infection. *Immunology* **121**, 283-292.

**Desai, S. D., Haas, A. L., Wood, L. M., Tsai, Y. C., Pestka, S., Rubin, E. H., Saleem, A., Nur, E. K. A. & Liu, L. F. (2006).** Elevated expression of ISG15 in tumor cells interferes with the ubiquitin/26S proteasome pathway. *Cancer Res* **66**, 921-928.

**Diepolder, H. M., Zachoval, R., Hoffmann, R. M., Wierenga, E. A., Santantonio, T., Jung, M. C., Eichenlaub, D. & Pape, G. R. (1995).** Possible mechanism involving T-lymphocyte response to non-structural protein 3 in viral clearance in acute hepatitis C virus infection. *Lancet* **346**, 1006-1007.

**Dill, M. T., Duong, F. H., Vogt, J. E., Bibert, S., Bochud, P. Y., Terracciano, L., Papassotiropoulos, A., Roth, V. & Heim, M. H. (2011).** Interferon-induced gene expression is a stronger predictor of treatment response than IL28B genotype in patients with hepatitis C. *Gastroenterology* **140**, 1021-1031.

**Doherty, D. G., Norris, S., Madrigal-Estebas, L., McEntee, G., Traynor, O., Hegarty, J. E. & O'Farrelly, C. (1999).** The human liver contains multiple populations of NK cells, T cells, and CD3+CD56+ natural T cells with distinct cytotoxic activities and Th1, Th2, and Th0 cytokine secretion patterns. *J Immunol* **163**, 2314-2321.

**Dolganiuc, A., Chang, S., Kodys, K., Mandrekar, P., Bakis, G., Cormier, M. & Szabo, G. (2006).** Hepatitis C virus (HCV) core protein-induced, monocyte-mediated mechanisms of reduced IFN-alpha and plasmacytoid dendritic cell loss in chronic HCV infection. *J Immunol* **177**, 6758-6768.

**Dolken, L., Ruzsics, Z., Radle, B., Friedel, C. C., Zimmer, R., Mages, J., Hoffmann, R., Dickinson, P., Forster, T., Ghazal, P. & Koszinowski, U. H. (2008).** High-resolution gene expression profiling for simultaneous

kinetic parameter analysis of RNA synthesis and decay. *Rna* **14**, 1959-1972.

**Domitrovich, A. M., Diebel, K. W., Ali, N., Sarker, S. & Siddiqui, A. (2005).** Role of La autoantigen and polypyrimidine tract-binding protein in HCV replication. *Virology* **335**, 72-86.

**Dorner, M., Horwitz, J. A., Robbins, J. B., Barry, W. T., Feng, Q., Mu, K., Jones, C. T., Schoggins, J. W., Catanese, M. T., Burton, D. R., Law, M., Rice, C. M. & Ploss, A. (2011).** A genetically humanized mouse model for hepatitis C virus infection. *Nature* **474**, 208-211.

**Drummer, H. E., Maerz, A. & Poumbourios, P. (2003).** Cell surface expression of functional hepatitis C virus E1 and E2 glycoproteins. *FEBS Lett* **546**, 385-390.

**Dubuisson, J., Hsu, H. H., Cheung, R. C., Greenberg, H. B., Russell, D. G. & Rice, C. M. (1994).** Formation and intracellular localization of hepatitis C virus envelope glycoprotein complexes expressed by recombinant vaccinia and Sindbis viruses. *J Virol* **68**, 6147-6160.

**Dubuisson, J., Penin, F. & Moradpour, D. (2002).** Interaction of hepatitis C virus proteins with host cell membranes and lipids. *Trends Cell Biol* **12**, 517-523.

**Durfee, L. A., Lyon, N., Seo, K. & Huibregtse, J. M. (2010).** The ISG15 conjugation system broadly targets newly synthesized proteins: implications for the antiviral function of ISG15. *Mol Cell* **38**, 722-732.

**Edwards, V. C., Tarr, A. W., Urbanowicz, R. A. & Ball, J. K. (2012).** The role of neutralizing antibodies in hepatitis C virus infection. *J Gen Virol* **93**, 1-19.

**Egger, D., Wolk, B., Gosert, R., Bianchi, L., Blum, H. E., Moradpour, D. & Bienz, K. (2002).** Expression of hepatitis C virus proteins induces distinct membrane alterations including a candidate viral replication complex. *J Virol* **76**, 5974-5984.

**Ehrhardt, M., Leidinger, P., Keller, A., Baumert, T., Diez, J., Meese, E. & Meyerhans, A. (2011).** Profound differences of microRNA expression patterns in hepatocytes and hepatoma cell lines commonly used in hepatitis C virus studies. *Hepatology* **54**, 1112-1113.

**Einav, S., Elazar, M., Danieli, T. & Glenn, J. S. (2004).** A nucleotide binding motif in hepatitis C virus (HCV) NS4B mediates HCV RNA replication. *J Virol* **78**, 11288-11295.

**Einav, S., Gerber, D., Bryson, P. D., Sklan, E. H., Elazar, M., Maerkl, S. J., Glenn, J. S. & Quake, S. R. (2008).** Discovery of a hepatitis C target and its pharmacological inhibitors by microfluidic affinity analysis. *Nat Biotechnol* **26**, 1019-1027.

**Elazar, M., Liu, P., Rice, C. M. & Glenn, J. S. (2004).** An N-terminal amphipathic helix in hepatitis C virus (HCV) NS4B mediates membrane association, correct localization of replication complex proteins, and HCV RNA replication. *J Virol* **78**, 11393-11400.

**El-Hage, N. & Luo, G. (2003).** Replication of hepatitis C virus RNA occurs in a membrane-bound replication complex containing nonstructural viral proteins and RNA. *J Gen Virol* **84**, 2761-2769.

**Erickson, A. L., Kimura, Y., Igarashi, S., Eichelberger, J., Houghton, M., Sidney, J., McKinney, D., Sette, A., Hughes, A. L. & Walker, C. M. (2001).** The outcome of hepatitis C virus infection is predicted by escape mutations in epitopes targeted by cytotoxic T lymphocytes. *Immunity* **15**, 883-895.

**Evans, M. J., Rice, C. M. & Goff, S. P. (2004).** Phosphorylation of hepatitis C virus nonstructural protein 5A modulates its protein interactions and viral RNA replication. *Proc Natl Acad Sci U S A* **101**, 13038-13043.

**Evans, M. J., von Hahn, T., Tscherne, D. M., Syder, A. J., Panis, M., Wolk, B., Hatziioannou, T., McKeating, J. A., Bieniasz, P. D. & Rice, C. M. (2007).** Claudin-1 is a hepatitis C virus co-receptor required for a late step in entry. *Nature* **446**, 801-805.

**Everett, R. D., Parsy, M. L. & Orr, A. (2009).** Analysis of the functions of herpes simplex virus type 1 regulatory protein ICP0 that are critical for lytic infection and derepression of quiescent viral genomes. *J Virol* **83**, 4963-4977.

**Failla, C., Tomei, L. & De Francesco, R. (1994).** Both NS3 and NS4A are required for proteolytic processing of hepatitis C virus nonstructural proteins. *J Virol* **68**, 3753-3760.

**Farci, P., Alter, H. J., Wong, D. C., Miller, R. H., Govindarajan, S., Engle, R., Shapiro, M. & Purcell, R. H. (1994).** Prevention of hepatitis C virus infection in chimpanzees after antibody-mediated in vitro neutralization. *Proc Natl Acad Sci U S A* **91**, 7792-7796.

**Farrell, P. J., Broeze, R. J. & Lengyel, P. (1979).** Accumulation of an mRNA and protein in interferon-treated Ehrlich ascites tumour cells. *Nature* **279**, 523-525.

**Feinstone, S. M., Kapikian, A. Z. & Purceli, R. H. (1973).** Hepatitis A: detection by immune electron microscopy of a viruslike antigen associated with acute illness. *Science* **182**, 1026-1028.

**Feinstone, S. M., Kapikian, A. Z., Purcell, R. H., Alter, H. J. & Holland, P. V. (1975).** Transfusion-associated hepatitis not due to viral hepatitis type A or B. *N Engl J Med* **292**, 767-770.

**Feinstone, S. M., Mihalik, K. B., Kamimura, T., Alter, H. J., London, W. T. & Purcell, R. H. (1983).** Inactivation of hepatitis B virus and non-A, non-B hepatitis by chloroform. *Infect Immun* **41**, 816-821.

**Ferlazzo, G., Tsang, M. L., Moretta, L., Melioli, G., Steinman, R. M. & Munz, C. (2002).** Human dendritic cells activate resting natural killer (NK) cells and are recognized via the NKp30 receptor by activated NK cells. *J Exp Med* **195**, 343-351.

**Ferreon, J. C., Ferreon, A. C., Li, K. & Lemon, S. M. (2005).** Molecular determinants of TRIF proteolysis mediated by the hepatitis C virus NS3/4A protease. *J Biol Chem* **280**, 20483-20492.

**Flint, M., Maidens, C., Loomis-Price, L. D., Shotton, C., Dubuisson, J., Monk, P., Higginbottom, A., Levy, S. & McKeating, J. A. (1999).** Characterization of hepatitis C virus E2 glycoprotein interaction with a putative cellular receptor, CD81. *J Virol* **73**, 6235-6244.

**Folgori, A., Capone, S., Ruggeri, L., Meola, A., Sporeno, E., Ercole, B. B., Pezzanera, M., Tafi, R., Arcuri, M., Fattori, E., Lahm, A., Luzzago, A., Vitelli, A., Colloca, S., Cortese, R. & Nicosia, A. (2006).** A T-cell HCV vaccine eliciting effective immunity against heterologous virus challenge in chimpanzees. *Nat Med* **12**, 190-197.

**Forsdyke, D. R. (1967).** Association of attachment to glass with activation of cultured lymphocytes by phytohaemagglutinin. *Biochem J* **104**, 68P.

**Foster, T. L., Belyaeva, T., Stonehouse, N. J., Pearson, A. R. & Harris, M. (2010).** All three domains of the hepatitis C virus nonstructural NS5A protein contribute to RNA binding. *J Virol* **84**, 9267-9277.

**Foster, T. L., Gallay, P., Stonehouse, N. J. & Harris, M. (2011).** Cyclophilin A interacts with domain II of hepatitis C virus NS5A and stimulates RNA binding in an isomerase-dependent manner. *J Virol* **85**, 7460-7464.

**Frick, D. N., Rypma, R. S., Lam, A. M. & Gu, B. (2004).** The nonstructural protein 3 protease/helicase requires an intact protease domain to unwind duplex RNA efficiently. *J Biol Chem* **279**, 1269-1280.

**Friebe, P. & Bartenschlager, R. (2002).** Genetic analysis of sequences in the 3' nontranslated region of hepatitis C virus that are important for RNA replication. *J Virol* **76**, 5326-5338.

**Friebe, P., Boudet, J., Simorre, J. P. & Bartenschlager, R. (2005).** Kissing-loop interaction in the 3' end of the hepatitis C virus genome essential for RNA replication. *J Virol* **79**, 380-392.

**Friebe, P., Lohmann, V., Krieger, N. & Bartenschlager, R. (2001).** Sequences in the 5' nontranslated region of hepatitis C virus required for RNA replication. *J Virol* **75**, 12047-12057.

**Fried, M. W., Shiffman, M. L., Reddy, K. R., Smith, C., Marinos, G., Goncales, F. L., Jr., Haussinger, D., Diago, M., Carosi, G., Dhumeaux, D., Craxi, A., Lin, A., Hoffman, J. & Yu, J. (2002).** Peginterferon alfa-2a plus ribavirin for chronic hepatitis C virus infection. *N Engl J Med* **347**, 975-982.

**Friedel, C. C. & Dolken, L. (2009).** Metabolic tagging and purification of nascent RNA: implications for transcriptomics. *Mol Biosyst* **5**, 1271-1278.

**Fukushi, S., Okada, M., Kageyama, T., Hoshino, F. B., Nagai, K. & Katayama, K. (2001).** Interaction of poly(rC)-binding protein 2 with the 5'-terminal stem loop of the hepatitis C-virus genome. *Virus Res* **73**, 67-79.

**Gad, H. H., Dellgren, C., Hamming, O. J., Vends, S., Paludan, S. R. & Hartmann, R. (2009).** Interferon-lambda is functionally an interferon but structurally related to the interleukin-10 family. *J Biol Chem* **284**, 20869-20875.

**Gale, M., Jr., Blakely, C. M., Kwieciszewski, B., Tan, S. L., Dossett, M., Tang, N. M., Korth, M. J., Polyak, S. J., Gretch, D. R. & Katze, M. G. (1998).** Control of PKR protein kinase by hepatitis C virus nonstructural 5A protein: molecular mechanisms of kinase regulation. *Mol Cell Biol* **18**, 5208-5218.

**Gale, M. J., Jr., Korth, M. J., Tang, N. M., Tan, S. L., Hopkins, D. A., Dever, T. E., Polyak, S. J., Gretch, D. R. & Katze, M. G. (1997).** Evidence that hepatitis C virus resistance to interferon is mediated through repression of the PKR protein kinase by the nonstructural 5A protein. *Virology* **230**, 217-227.

**Gallinari, P., Brennan, D., Nardi, C., Brunetti, M., Tomei, L., Steinkuhler, C. & De Francesco, R. (1998).** Multiple enzymatic activities associated with recombinant NS3 protein of hepatitis C virus. *J Virol* **72**, 6758-6769.

**Gao, L., Aizaki, H., He, J. W. & Lai, M. M. (2004).** Interactions between viral nonstructural proteins and host protein hVAP-33 mediate the formation of hepatitis C virus RNA replication complex on lipid raft. *J Virol* **78**, 3480-3488.

**Gardner, J. P., Durso, R. J., Arrigale, R. R., Donovan, G. P., Maddon, P. J., Dragic, T. & Olson, W. C. (2003).** L-SIGN (CD 209L) is a liver-specific capture receptor for hepatitis C virus. *Proc Natl Acad Sci U S A* **100**, 4498-4503.

**Gastaminza, P., Cheng, G., Wieland, S., Zhong, J., Liao, W. & Chisari, F. V. (2008).** Cellular determinants of hepatitis C virus assembly, maturation, degradation, and secretion. *J Virol* **82**, 2120-2129.

**Gastaminza, P., Dryden, K. A., Boyd, B., Wood, M. R., Law, M., Yeager, M. & Chisari, F. V. (2010).** Ultrastructural and biophysical characterization of hepatitis C virus particles produced in cell culture. *J Virol* **84**, 10999-11009.

**Gastaminza, P., Kapadia, S. B. & Chisari, F. V. (2006).** Differential biophysical properties of infectious intracellular and secreted hepatitis C virus particles. *J Virol* **80**, 11074-11081.

**Germi, R., Crance, J. M., Garin, D., Guimet, J., Lortat-Jacob, H., Ruigrok, R. W., Zarski, J. P. & Drouet, E. (2002).** Cellular glycosaminoglycans and low density lipoprotein receptor are involved in hepatitis C virus adsorption. *J Med Virol* **68**, 206-215.

**Gerosa, F., Baldani-Guerra, B., Nisii, C., Marchesini, V., Carra, G. & Trinchieri, G. (2002).** Reciprocal activating interaction between natural killer cells and dendritic cells. *J Exp Med* **195**, 327-333.

**Giannakopoulos, N. V., Arutyunova, E., Lai, C., Lenschow, D. J., Haas, A. L. & Virgin, H. W. (2009).** ISG15 Arg151 and the ISG15-conjugating enzyme UbE1L are important for innate immune control of Sindbis virus. *J Virol* **83**, 1602-1610.

**Giannakopoulos, N. V., Luo, J. K., Papov, V., Zou, W., Lenschow, D. J., Jacobs, B. S., Borden, E. C., Li, J., Virgin, H. W. & Zhang, D. E. (2005).** Proteomic identification of proteins conjugated to ISG15 in mouse and human cells. *Biochem Biophys Res Commun* **336**, 496-506.

**Gil, L. H., van Olphen, A. L., Mittal, S. K. & Donis, R. O. (2006).** Modulation of PKR activity in cells infected by bovine viral diarrhea virus. *Virus Res* **116**, 69-77.

**Goffard, A., Callens, N., Bartosch, B., Wychowski, C., Cosset, F. L., Montpellier, C. & Dubuisson, J. (2005).** Role of N-linked glycans in the functions of hepatitis C virus envelope glycoproteins. *J Virol* **79**, 8400-8409.

**Gonzalez, M. E. & Carrasco, L. (2003).** Viroporins. *FEBS Lett* **552**, 28-34.

**Gonzalez-Navajas, J. M., Lee, J., David, M. & Raz, E. (2012).** Immunomodulatory functions of type I interferons. *Nat Rev Immunol* **12**, 125-135.

**Goodbourn, S. & Randall, R. E. (2009).** The regulation of type I interferon production by paramyxoviruses. *J Interferon Cytokine Res* **29**, 539-547.

**Gorbalenya, A. E., Donchenko, A. P., Koonin, E. V. & Blinov, V. M. (1989).** N-terminal domains of putative helicases of flavi- and pestiviruses may be serine proteases. *Nucleic Acids Res* **17**, 3889-3897.

**Gosert, R., Egger, D., Lohmann, V., Bartenschlager, R., Blum, H. E., Bienz, K. & Moradpour, D. (2003).** Identification of the hepatitis C virus RNA replication complex in Huh-7 cells harboring subgenomic replicons. *J Virol* **77**, 5487-5492.

**Gouttenoire, J., Castet, V., Montserret, R., Arora, N., Raussens, V., Ruysschaert, J. M., Diesis, E., Blum, H. E., Penin, F. & Moradpour, D. (2009a).** Identification of a novel determinant for membrane association in hepatitis C virus nonstructural protein 4B. *J Virol* **83**, 6257-6268.

**Gouttenoire, J., Montserret, R., Kennel, A., Penin, F. & Moradpour, D. (2009b).** An amphipathic alpha-helix at the C terminus of hepatitis C virus nonstructural protein 4B mediates membrane association. *J Virol* **83**, 11378-11384.

**Grakoui, A., McCourt, D. W., Wychowski, C., Feinstone, S. M. & Rice, C. M. (1993a).** A second hepatitis C virus-encoded proteinase. *Proc Natl Acad Sci USA* **90**, 10583-10587.

**Grakoui, A., McCourt, D. W., Wychowski, C., Feinstone, S. M. & Rice, C. M. (1993b).** Characterization of the hepatitis C virus-encoded serine proteinase: determination of proteinase-dependent polyprotein cleavage sites. *J Virol* **67**, 2832-2843.

**Grakoui, A., Shoukry, N. H., Woollard, D. J., Han, J. H., Hanson, H. L., Ghrayeb, J., Murthy, K. K., Rice, C. M. & Walker, C. M. (2003).** HCV persistence and immune evasion in the absence of memory T cell help. *Science* **302**, 659-662.

**Gretton, S. N., Taylor, A. I. & McLauchlan, J. (2005).** Mobility of the hepatitis C virus NS4B protein on the endoplasmic reticulum membrane and membrane-associated foci. *J Gen Virol* **86**, 1415-1421.

**Griffin, S., Stgelais, C., Owsianka, A. M., Patel, A. H., Rowlands, D. & Harris, M. (2008).** Genotype-dependent sensitivity of hepatitis C virus to inhibitors of the p7 ion channel. *Hepatology* **48**, 1779-1790.

**Griffin, S. D., Beales, L. P., Clarke, D. S., Worsfold, O., Evans, S. D., Jaeger, J., Harris, M. P. & Rowlands, D. J. (2003).** The p7 protein of hepatitis C virus forms an ion channel that is blocked by the antiviral drug, Amantadine. *FEBS Lett* **535**, 34-38.

**Griffin, S. D., Harvey, R., Clarke, D. S., Barclay, W. S., Harris, M. & Rowlands, D. J. (2004).** A conserved basic loop in hepatitis C virus p7 protein is required for amantadine-sensitive ion channel activity in mammalian cells but is dispensable for localization to mitochondria. *J Gen Virol* **85**, 451-461.

**Gripon, P., Rumin, S., Urban, S., Le Seyec, J., Glaise, D., Cannie, I., Guyomard, C., Lucas, J., Trepo, C. & Guguen-Guillouzo, C. (2002).** Infection of a human hepatoma cell line by hepatitis B virus. *Proc Natl Acad Sci U S A* **99**, 15655-15660.

**Gruner, N. H., Gerlach, T. J., Jung, M. C., Diepolder, H. M., Schirren, C. A., Schraut, W. W., Hoffmann, R., Zachoval, R., Santantonio, T., Cucchiarini, M., Cerny, A. & Pape, G. R. (2000).** Association of hepatitis C virus-specific CD8+ T cells with viral clearance in acute hepatitis C. *J Infect Dis* **181**, 1528-1536.

**Gu, M. & Rice, C. M. (2010).** Three conformational snapshots of the hepatitis C virus NS3 helicase reveal a ratchet translocation mechanism. *Proc Natl Acad Sci U S A* **107**, 521-528.

**Haas, A. L., Ahrens, P., Bright, P. M. & Ankel, H. (1987).** Interferon induces a 15-kilodalton protein exhibiting marked homology to ubiquitin. *J Biol Chem* **262**, 11315-11323.

**Haider, S. R., Juan, G., Traganos, F. & Darzynkiewicz, Z. (1997).** Immunoseparation and immunodetection of nucleic acids labeled with halogenated nucleotides. *Exp Cell Res* **234**, 498-506.

**Han, Q., Aligo, J., Manna, D., Belton, K., Chintapalli, S. V., Hong, Y., Patterson, R. L., van Rossum, D. B. & Konan, K. V. (2011).** Conserved GXXXG- and S/T-like motifs in the transmembrane domains of NS4B protein are required for hepatitis C virus replication. *J Virol* **85**, 6464-6479.

**Harris, H. J., Davis, C., Mullins, J. G., Hu, K., Goodall, M., Farquhar, M. J., Mee, C. J., McCaffrey, K., Young, S., Drummer, H., Balfe, P. & McKeating, J. A. (2010).** Claudin association with CD81 defines hepatitis C virus entry. *J Biol Chem* **285**, 21092-21102.

**Harris, H. J., Farquhar, M. J., Mee, C. J., Davis, C., Reynolds, G. M., Jennings, A., Hu, K., Yuan, F., Deng, H., Hubscher, S. G., Han, J. H.,**

**Balfe, P. & McKeating, J. A. (2008).** CD81 and claudin 1 coreceptor association: role in hepatitis C virus entry. *J Virol* **82**, 5007-5020.

**Hart, S. N., Li, Y., Nakamoto, K., Subileau, E. A., Steen, D. & Zhong, X. B. (2010).** A comparison of whole genome gene expression profiles of HepaRG cells and HepG2 cells to primary human hepatocytes and human liver tissues. *Drug Metab Dispos* **38**, 988-994.

**Harwood, R. & Itzhaki, S. (1973).** Utilization of 3 H-5-uridine for RNA synthesis in Ehrlich ascites tumour cells. *Exp Cell Res* **76**, 315-320.

**He, L. F., Alling, D., Popkin, T., Shapiro, M., Alter, H. J. & Purcell, R. H. (1987).** Determining the size of non-A, non-B hepatitis virus by filtration. *J Infect Dis* **156**, 636-640.

**He, Y., Yan, W., Coito, C., Li, Y., Gale, M., Jr. & Katze, M. G. (2003).** The regulation of hepatitis C virus (HCV) internal ribosome-entry site-mediated translation by HCV replicons and nonstructural proteins. *J Gen Virol* **84**, 535-543.

**Heim, M. H., Moradpour, D. & Blum, H. E. (1999).** Expression of hepatitis C virus proteins inhibits signal transduction through the Jak-STAT pathway. *J Virol* **73**, 8469-8475.

**Helle, F., Goffard, A., Morel, V., Duverlie, G., McKeating, J., Keck, Z. Y., Foung, S., Penin, F., Dubuisson, J. & Voisset, C. (2007).** The neutralizing activity of anti-hepatitis C virus antibodies is modulated by specific glycans on the E2 envelope protein. *J Virol* **81**, 8101-8111.

**Heller, T. & Rehermann, B. (2005).** Acute hepatitis C: a multifaceted disease. *Semin Liver Dis* **25**, 7-17.

**Herker, E., Harris, C., Hernandez, C., Carpentier, A., Kaehlcke, K., Rosenberg, A. R., Farese, R. V., Jr. & Ott, M. (2010).** Efficient hepatitis C virus particle formation requires diacylglycerol acyltransferase-1. *Nat Med* **16**, 1295-1298.

**Herod, M. R., Jones, D. M., McLauchlan, J. & McCormick, C. J. (2012).** Increasing rate of cleavage at boundary between non-structural proteins 4B and 5A inhibits replication of hepatitis C virus. *J Biol Chem* **287**, 568-580.

**Hijikata, M., Mizushima, H., Akagi, T., Mori, S., Kakiuchi, N., Kato, N., Tanaka, T., Kimura, K. & Shimotohno, K. (1993).** Two distinct proteinase activities required for the processing of a putative nonstructural precursor protein of hepatitis C virus. *J Virol* **67**, 4665-4675.

**Hilton, L., Moganeradj, K., Zhang, G., Chen, Y. H., Randall, R. E., McCauley, J. W. & Goodbourn, S. (2006).** The NPro product of bovine viral diarrhea virus inhibits DNA binding by interferon regulatory factor 3 and targets it for proteasomal degradation. *J Virol* **80**, 11723-11732.

**Hochstrasser, M. (2000).** Evolution and function of ubiquitin-like protein-conjugation systems. *Nat Cell Biol* **2**, E153-157.

**Hoffmann, R. M., Diepolder, H. M., Zachoval, R., Zwiebel, F. M., Jung, M. C., Scholz, S., Nitschko, H., Riethmuller, G. & Pape, G. R. (1995).** Mapping of immunodominant CD4+ T lymphocyte epitopes of hepatitis C virus antigens and their relevance during the course of chronic infection. *Hepatology* **21**, 632-638.

**Honda, M., Beard, M. R., Ping, L. H. & Lemon, S. M. (1999).** A phylogenetically conserved stem-loop structure at the 5' border of the internal ribosome entry site of hepatitis C virus is required for cap-independent viral translation. *J Virol* **73**, 1165-1174.

**Honda, M., Brown, E. A. & Lemon, S. M. (1996a).** Stability of a stem-loop involving the initiator AUG controls the efficiency of internal initiation of translation on hepatitis C virus RNA. *Rna* **2**, 955-968.

**Honda, M., Ping, L. H., Rijnbrand, R. C., Amphlett, E., Clarke, B., Rowlands, D. & Lemon, S. M. (1996b).** Structural requirements for initiation of translation by internal ribosome entry within genome-length hepatitis C virus RNA. *Virology* **222**, 31-42.

**Hope, R. G. & McLauchlan, J. (2000).** Sequence motifs required for lipid droplet association and protein stability are unique to the hepatitis C virus core protein. *J Gen Virol* **81**, 1913-1925.

**Horner, S. M. & Gale, M., Jr. (2009).** Intracellular innate immune cascades and interferon defenses that control hepatitis C virus. *J Interferon Cytokine Res* **29**, 489-498.

**HPA (2011).** Health protection agency, UK.

**Hsiang, T. Y., Zhao, C. & Krug, R. M. (2009).** Interferon-induced ISG15 conjugation inhibits influenza A virus gene expression and replication in human cells. *J Virol* **83**, 5971-5977.

**Hsu, M., Zhang, J., Flint, M., Logvinoff, C., Cheng-Mayer, C., Rice, C. M. & McKeating, J. A. (2003).** Hepatitis C virus glycoproteins mediate pH-dependent cell entry of pseudotyped retroviral particles. *Proc Natl Acad Sci U S A* **100**, 7271-7276.

**Huang, H., Sun, F., Owen, D. M., Li, W., Chen, Y., Gale, M., Jr. & Ye, J. (2007a).** Hepatitis C virus production by human hepatocytes dependent on assembly and secretion of very low-density lipoproteins. *Proc Natl Acad Sci U S A* **104**, 5848-5853.

**Huang, Y., Staschke, K., De Francesco, R. & Tan, S. L. (2007b).** Phosphorylation of hepatitis C virus NS5A nonstructural protein: a new paradigm for phosphorylation-dependent viral RNA replication? *Virology* **364**, 1-9.

**Huang, L., Hwang, J., Sharma, S. D., Hargittai, M. R., Chen, Y., Arnold, J. J., Raney, K. D. & Cameron, C. E. (2005).** Hepatitis C virus nonstructural protein 5A (NS5A) is an RNA-binding protein. *J Biol Chem* **280**, 36417-36428.

**Hubb, J. R. (2008).** The Interaction of hepatitis C virus and intracellular lipid metabolism. *PhD thesis, University of Glasgow*.

**Hughes, M., Gretton, S., Shelton, H., Brown, D. D., McCormick, C. J., Angus, A. G., Patel, A. H., Griffin, S. & Harris, M. (2009a).** A conserved proline between domains II and III of hepatitis C virus NS5A influences both RNA replication and virus assembly. *J Virol* **83**, 10788-10796.

**Hughes, M., Griffin, S. & Harris, M. (2009b).** Domain III of NS5A contributes to both RNA replication and assembly of hepatitis C virus particles. *J Gen Virol* **90**, 1329-1334.

**Hugle, T., Fehrmann, F., Bieck, E., Kohara, M., Krausslich, H. G., Rice, C. M., Blum, H. E. & Moradpour, D. (2001).** The hepatitis C virus nonstructural protein 4B is an integral endoplasmic reticulum membrane protein. *Virology* **284**, 70-81.

**Hussy, P., Langen, H., Mous, J. & Jacobsen, H. (1996).** Hepatitis C virus core protein: carboxy-terminal boundaries of two processed species suggest cleavage by a signal peptide peptidase. *Virology* **224**, 93-104.

**Imhof, I. & Simmonds, P. (2010).** Development of an intergenotypic hepatitis C virus (HCV) cell culture method to assess antiviral susceptibilities and resistance development of HCV NS3 protease genes from HCV genotypes 1 to 6. *J Virol* **84**, 4597-4610.

**Imhof, I. & Simmonds, P. (2011).** Genotype differences in susceptibility and resistance development of hepatitis C virus to protease inhibitors telaprevir (VX-950) and danoprevir (ITMN-191). *Hepatology* **53**, 1090-1099.

**Ito, T. & Lai, M. M. (1997).** Determination of the secondary structure of and cellular protein binding to the 3'-untranslated region of the hepatitis C virus RNA genome. *J Virol* **71**, 8698-8706.

**Jacobson, I. M., McHutchison, J. G., Dusheiko, G., Di Bisceglie, A. M., Reddy, K. R., Bzowej, N. H., Marcellin, P., Muir, A. J., Ferenci, P., Flisiak, R., George, J., Rizzetto, M., Shouval, D., Sola, R., Terg, R. A., Yoshida, E. M., Adda, N., Bengtsson, L., Sankoh, A. J., Kieffer, T. L., George, S., Kauffman, R. S. & Zeuzem, S. (2011).** Telaprevir for previously untreated chronic hepatitis C virus infection. *N Engl J Med* **364**, 2405-2416.

**Ji, H., Fraser, C. S., Yu, Y., Leary, J. & Doudna, J. A. (2004).** Coordinated assembly of human translation initiation complexes by the hepatitis C virus internal ribosome entry site RNA. *Proc Natl Acad Sci U S A* **101**, 16990-16995.

**Jiang, J. & Luo, G. (2009).** Apolipoprotein E but not B is required for the formation of infectious hepatitis C virus particles. *J Virol* **83**, 12680-12691.

**Jirasko, V., Montserret, R., Appel, N., Janvier, A., Eustachi, L., Brohm, C., Steinmann, E., Pietschmann, T., Penin, F. & Bartenschlager, R. (2008).** Structural and functional characterization of nonstructural protein 2 for its role in hepatitis C virus assembly. *J Biol Chem* **283**, 28546-28562.

**Jirasko, V., Montserret, R., Lee, J. Y., Gouttenoire, J., Moradpour, D., Penin, F. & Bartenschlager, R. (2010).** Structural and functional studies of nonstructural protein 2 of the hepatitis C virus reveal its key role as organizer of virion assembly. *PLoS Pathog* **6**, e1001233.

**Jones, C. T., Murray, C. L., Eastman, D. K., Tassello, J. & Rice, C. M. (2007).** Hepatitis C virus p7 and NS2 proteins are essential for production of infectious virus. *J Virol* **81**, 8374-8383.

**Jones, D. M., Domingues, P., Targett-Adams, P. & McLauchlan, J. (2010).** Comparison of U2OS and Huh-7 cells for identifying host factors that affect hepatitis C virus RNA replication. *J Gen Virol* **91**, 2238-2248.

**Jones, D. M., Gretton, S. N., McLauchlan, J. & Targett-Adams, P. (2007).** Mobility analysis of an NS5A-GFP fusion protein in cells actively replicating hepatitis C virus subgenomic RNA. *J Gen Virol* **88**, 470-475.

**Jones, D. M., Patel, A. H., Targett-Adams, P. & McLauchlan, J. (2009).** The hepatitis C virus NS4B protein can trans-complement viral RNA replication and modulates production of infectious virus. *J Virol* **83**, 2163-2177.

**Jopling, C. L., Yi, M., Lancaster, A. M., Lemon, S. M. & Sarnow, P. (2005).** Modulation of hepatitis C virus RNA abundance by a liver-specific MicroRNA. *Science* **309**, 1577-1581.

**Kambara, H., Fukuhara, T., Shiokawa, M., Ono, C., Ohara, Y., Kamitani, W. & Matsuura, Y. (2012).** Establishment of a novel permissive cell line for the propagation of hepatitis C virus by expression of microRNA miR122. *J Virol* **86**, 1382-1393.

**Kaneko, T., Tanji, Y., Satoh, S., Hijikata, M., Asabe, S., Kimura, K. & Shimotohno, K. (1994).** Production of two phosphoproteins from the NS5A region of the hepatitis C viral genome. *Biochem Biophys Res Commun* **205**, 320-326.

**Kanto, T., Inoue, M., Miyatake, H., Sato, A., Sakakibara, M., Yakushijin, T., Oki, C., Itose, I., Hiramatsu, N., Takehara, T., Kasahara, A. & Hayashi,**

**N. (2004).** Reduced numbers and impaired ability of myeloid and plasmacytoid dendritic cells to polarize T helper cells in chronic hepatitis C virus infection. *J Infect Dis* **190**, 1919-1926.

**Kaplan, D. E., Sugimoto, K., Newton, K., Valiga, M. E., Ikeda, F., Aytaman, A., Nunes, F. A., Lucey, M. R., Vance, B. A., Vonderheide, R. H., Reddy, K. R., McKeating, J. A. & Chang, K. M. (2007).** Discordant role of CD4 T-cell response relative to neutralizing antibody and CD8 T-cell responses in acute hepatitis C. *Gastroenterology* **132**, 654-666.

**Kapoor, A., Simmonds, P., Gerold, G., Qaisar, N., Jain, K., Henriquez, J. A., Firth, C., Hirschberg, D. L., Rice, C. M., Shields, S. & Lipkin, W. I. (2011).** Characterization of a canine homolog of hepatitis C virus. *Proc Natl Acad Sci U S A* **108**, 11608-11613.

**Kariko, K., Bhuyan, P., Capodici, J. & Weissman, D. (2004).** Small interfering RNAs mediate sequence-independent gene suppression and induce immune activation by signaling through toll-like receptor 3. *J Immunol* **172**, 6545-6549.

**Kato, T., Date, T., Miyamoto, M., Furusaka, A., Tokushige, K., Mizokami, M. & Wakita, T. (2003).** Efficient replication of the genotype 2a hepatitis C virus subgenomic replicon. *Gastroenterology* **125**, 1808-1817.

**Kato, T., Date, T., Miyamoto, M., Zhao, Z., Mizokami, M. & Wakita, T. (2005).** Nonhepatic cell lines HeLa and 293 support efficient replication of the hepatitis C virus genotype 2a subgenomic replicon. *J Virol* **79**, 592-596.

**Kaul, A., Stauffer, S., Berger, C., Pertel, T., Schmitt, J., Kallis, S., Zayas, M., Lohmann, V., Luban, J. & Bartenschlager, R. (2009).** Essential role of cyclophilin A for hepatitis C virus replication and virus production and possible link to polyprotein cleavage kinetics. *PLoS Pathog* **5**, e1000546.

**Kenzelmann, M., Maertens, S., Hergenhahn, M., Kueffer, S., Hotz-Wagenblatt, A., Li, L., Wang, S., Ittrich, C., Lemberger, T., Arribas, R., Jonnakuty, S., Hollstein, M. C., Schmid, W., Gretz, N., Grone, H. J. & Schutz, G. (2007).** Microarray analysis of newly synthesized RNA in cells and animals. *Proc Natl Acad Sci U S A* **104**, 6164-6169.

**Keskinen, P., Nyqvist, M., Sareneva, T., Pirhonen, J., Melen, K. & Julkunen, I. (1999).** Impaired antiviral response in human hepatoma cells. *Virology* **263**, 364-375.

**Khakoo, S. I., Thio, C. L., Martin, M. P., Brooks, C. R., Gao, X., Astemborski, J., Cheng, J., Goedert, J. J., Vlahov, D., Hilgartner, M., Cox, S., Little, A. M., Alexander, G. J., Cramp, M. E., O'Brien, S. J., Rosenberg, W. M., Thomas, D. L. & Carrington, M. (2004).** HLA and NK cell inhibitory receptor genes in resolving hepatitis C virus infection. *Science* **305**, 872-874.

**Kieft, J. S., Zhou, K., Jubin, R. & Doudna, J. A. (2001).** Mechanism of ribosome recruitment by hepatitis C IRES RNA. *Rna* **7**, 194-206.

**Kim, D. W., Kim, J., Gwack, Y., Han, J. H. & Choe, J. (1997).** Mutational analysis of the hepatitis C virus RNA helicase. *J Virol* **71**, 9400-9409.

**Kim, J. L., Morgenstern, K. A., Griffith, J. P., Dwyer, M. D., Thomson, J. A., Murcko, M. A., Lin, C. & Caron, P. R. (1998).** Hepatitis C virus NS3 RNA helicase domain with a bound oligonucleotide: the crystal structure provides insights into the mode of unwinding. *Structure* **6**, 89-100.

**Kim, J. L., Morgenstern, K. A., Lin, C., Fox, T., Dwyer, M. D., Landro, J. A., Chambers, S. P., Markland, W., Lepre, C. A., O'Malley, E. T., Harbeson, S. L., Rice, C. M., Murcko, M. A., Caron, P. R. & Thomson, J. A. (1996).** Crystal structure of the hepatitis C virus NS3 protease domain complexed with a synthetic NS4A cofactor peptide. *Cell* **87**, 343-355.

**Kim, K. I., Giannakopoulos, N. V., Virgin, H. W. & Zhang, D. E. (2004a).** Interferon-inducible ubiquitin E2, Ubc8, is a conjugating enzyme for protein ISGylation. *Mol Cell Biol* **24**, 9592-9600.

**Kim, S. J., Kim, J. H., Kim, Y. G., Lim, H. S. & Oh, J. W. (2004b).** Protein kinase C-related kinase 2 regulates hepatitis C virus RNA polymerase function by phosphorylation. *J Biol Chem* **279**, 50031-50041.

**Kim, K. I., Yan, M., Malakhova, O., Luo, J. K., Shen, M. F., Zou, W., de la Torre, J. C. & Zhang, D. E. (2006).** Ube1L and protein ISGylation are not essential for alpha/beta interferon signaling. *Mol Cell Biol* **26**, 472-479.

**Kim, M. J., Hwang, S. Y., Imaizumi, T. & Yoo, J. Y. (2008).** Negative feedback regulation of RIG-I-mediated antiviral signaling by interferon-induced ISG15 conjugation. *J Virol* **82**, 1474-1483.

**Kim, M. J. & Yoo, J. Y. (2010).** Inhibition of hepatitis C virus replication by IFN-mediated ISGylation of HCV-NS5A. *J Immunol* **185**, 4311-4318.

**Kim, S. Y., Park, K. W., Lee, Y. J., Back, S. H., Goo, J. H., Park, O. K., Jang, S. K. & Park, W. J. (2000).** In vivo determination of substrate specificity of hepatitis C virus NS3 protease: genetic assay for site-specific proteolysis. *Anal Biochem* **284**, 42-48.

**Kim, Y. K., Kim, C. S., Lee, S. H. & Jang, S. K. (2002).** Domains I and II in the 5' nontranslated region of the HCV genome are required for RNA replication. *Biochem Biophys Res Commun* **290**, 105-112.

**Knight, E., Jr., Fahey, D., Cordova, B., Hillman, M., Kutny, R., Reich, N. & Blomstrom, D. (1988).** A 15-kDa interferon-induced protein is derived by COOH-terminal processing of a 17-kDa precursor. *J Biol Chem* **263**, 4520-4522.

**Koch, J. O. & Bartenschlager, R. (1999).** Modulation of hepatitis C virus NS5A hyperphosphorylation by nonstructural proteins NS3, NS4A, and NS4B. *J Virol* **73**, 7138-7146.

**Kolykhalov, A. A., Agapov, E. V., Blight, K. J., Mihalik, K., Feinstone, S. M. & Rice, C. M. (1997).** Transmission of hepatitis C by intrahepatic inoculation with transcribed RNA. *Science* **277**, 570-574.

**Kolykhalov, A. A., Feinstone, S. M. & Rice, C. M. (1996).** Identification of a highly conserved sequence element at the 3' terminus of hepatitis C virus genome RNA. *J Virol* **70**, 3363-3371.

**Kotenko, S. V., Gallagher, G., Baurin, V. V., Lewis-Antes, A., Shen, M., Shah, N. K., Langer, J. A., Sheikh, F., Dickensheets, H. & Donnelly, R. P. (2003).** IFN-lambdas mediate antiviral protection through a distinct class II cytokine receptor complex. *Nat Immunol* **4**, 69-77.

**Koutsoudakis, G., Kaul, A., Steinmann, E., Kallis, S., Lohmann, V., Pietschmann, T. & Bartenschlager, R. (2006).** Characterization of the early steps of hepatitis C virus infection by using luciferase reporter viruses. *J Virol* **80**, 5308-5320.

**Krey, T., d'Alayer, J., Kikuti, C. M., Saulnier, A., Damier-Piolle, L., Petitpas, I., Johansson, D. X., Tawar, R. G., Baron, B., Robert, B., England, P., Persson, M. A., Martin, A. & Rey, F. A. (2010).** The disulfide bonds in glycoprotein E2 of hepatitis C virus reveal the tertiary organization of the molecule. *PLoS Pathog* **6**, e1000762.

**Krieger, M. (2001).** Scavenger receptor class B type I is a multiligand HDL receptor that influences diverse physiologic systems. *J Clin Invest* **108**, 793-797.

**Krieger, N., Lohmann, V. & Bartenschlager, R. (2001).** Enhancement of hepatitis C virus RNA replication by cell culture-adaptive mutations. *J Virol* **75**, 4614-4624.

**Krieger, S. E., Zeisel, M. B., Davis, C., Thumann, C., Harris, H. J., Schnober, E. K., Mee, C., Soulier, E., Royer, C., Lambotin, M., Grunert, F., Dao Thi, V. L., Dreux, M., Cosset, F. L., McKeating, J. A., Schuster, C. & Baumert, T. F. (2010).** Inhibition of hepatitis C virus infection by anti-claudin-1 antibodies is mediated by neutralization of E2-CD81-claudin-1 associations. *Hepatology* **51**, 1144-1157.

**Kumar, D., Farrell, G. C., Fung, C. & George, J. (2002).** Hepatitis C virus genotype 3 is cytopathic to hepatocytes: Reversal of hepatic steatosis after sustained therapeutic response. *Hepatology* **36**, 1266-1272.

**Kushima, Y., Wakita, T. & Hijikata, M. (2010).** A disulfide-bonded dimer of the core protein of hepatitis C virus is important for virus-like particle production. *J Virol* **84**, 9118-9127.

**Lai, C., Struckhoff, J. J., Schneider, J., Martinez-Sobrido, L., Wolff, T., Garcia-Sastre, A., Zhang, D. E. & Lenschow, D. J. (2009).** Mice lacking the ISG15 E1 enzyme UbE1L demonstrate increased susceptibility to both mouse-adapted and non-mouse-adapted influenza B virus infection. *J Virol* **83**, 1147-1151.

**Lai, W. K., Sun, P. J., Zhang, J., Jennings, A., Lalor, P. F., Hubscher, S., McKeating, J. A. & Adams, D. H. (2006).** Expression of DC-SIGN and DC-SIGNR on human sinusoidal endothelium: a role for capturing hepatitis C virus particles. *Am J Pathol* **169**, 200-208.

**Lanford, R. E., Guerra, B., Lee, H., Averett, D. R., Pfeiffer, B., Chavez, D., Notvall, L. & Bigger, C. (2003).** Antiviral effect and virus-host interactions in response to alpha interferon, gamma interferon, poly(i)-poly(c), tumor necrosis factor alpha, and ribavirin in hepatitis C virus subgenomic replicons. *J Virol* **77**, 1092-1104.

**Lanford, R. E., Hildebrandt-Eriksen, E. S., Petri, A., Persson, R., Lindow, M., Munk, M. E., Kauppinen, S. & Orum, H. (2010).** Therapeutic silencing of microRNA-122 in primates with chronic hepatitis C virus infection. *Science* **327**, 198-201.

**Laredj, L. N. & Beard, P. (2011).** Adeno-associated virus activates an innate immune response in normal human cells but not in osteosarcoma cells. *J Virol* **85**, 13133-13143.

**Lau, D. T., Fish, P. M., Sinha, M., Owen, D. M., Lemon, S. M. & Gale, M., Jr. (2008).** Interferon regulatory factor-3 activation, hepatic interferon-stimulated gene expression, and immune cell infiltration in hepatitis C virus patients. *Hepatology* **47**, 799-809.

**Lavie, M., Goffard, A. & Dubuisson, J. (2007).** Assembly of a functional HCV glycoprotein heterodimer. *Curr Issues Mol Biol* **9**, 71-86.

**Lavillette, D., Bartosch, B., Nourrisson, D., Verney, G., Cosset, F. L., Penin, F. & Pecheur, E. I. (2006).** Hepatitis C virus glycoproteins mediate low pH-dependent membrane fusion with liposomes. *J Biol Chem* **281**, 3909-3917.

**Lavillette, D., Pecheur, E. I., Donot, P., Fresquet, J., Molle, J., Corbau, R., Dreux, M., Penin, F. & Cosset, F. L. (2007).** Characterization of fusion determinants points to the involvement of three discrete regions of both E1 and E2 glycoproteins in the membrane fusion process of hepatitis C virus. *J Virol* **81**, 8752-8765.

**Lavillette, D., Tarr, A. W., Voisset, C., Donot, P., Bartosch, B., Bain, C., Patel, A. H., Dubuisson, J., Ball, J. K. & Cosset, F. L. (2005).** Characterization of host-range and cell entry properties of the major genotypes and subtypes of hepatitis C virus. *Hepatology* **41**, 265-274.

**Lechner, F., Gruener, N. H., Urbani, S., Uggeri, J., Santantonio, T., Kammer, A. R., Cerny, A., Phillips, R., Ferrari, C., Pape, G. R. & Klenerman, P. (2000).** CD8+ T lymphocyte responses are induced during acute hepatitis C virus infection but are not sustained. *Eur J Immunol* **30**, 2479-2487.

**Lee, K. J., Choi, J., Ou, J. H. & Lai, M. M. (2004).** The C-terminal transmembrane domain of hepatitis C virus (HCV) RNA polymerase is essential for HCV replication in vivo. *J Virol* **78**, 3797-3802.

**Lemon, S., Walker, C. M., Alter, M. J. & Yi, M. (2007).** Hepatitis C. In *Fields Virology*, 5th edn, pp. 1253-1304. Philadelphia: Lipincott Williams & Wilkins.

**Lenschow, D. J., Giannakopoulos, N. V., Gunn, L. J., Johnston, C., O'Guin, A. K., Schmidt, R. E., Levine, B. & Virgin, H. W. t. (2005).** Identification of interferon-stimulated gene 15 as an antiviral molecule during Sindbis virus infection in vivo. *J Virol* **79**, 13974-13983.

**Lenschow, D. J., Lai, C., Frias-Staheli, N., Giannakopoulos, N. V., Lutz, A., Wolff, T., Osiak, A., Levine, B., Schmidt, R. E., Garcia-Sastre, A., Leib, D. A., Pekosz, A., Knobeloch, K. P., Horak, I. & Virgin, H. W. t. (2007).** IFN-stimulated gene 15 functions as a critical antiviral molecule against influenza, herpes, and Sindbis viruses. *Proc Natl Acad Sci U S A* **104**, 1371-1376.

**Lesburg, C. A., Cable, M. B., Ferrari, E., Hong, Z., Mannarino, A. F. & Weber, P. C. (1999).** Crystal structure of the RNA-dependent RNA polymerase from hepatitis C virus reveals a fully encircled active site. *Nat Struct Biol* **6**, 937-943.

**Li, J., Peet, G. W., Balzarano, D., Li, X., Massa, P., Barton, R. W. & Marcu, K. B. (2001).** Novel NEMO/IkappaB kinase and NF-kappa B target genes at the pre-B to immature B cell transition. *J Biol Chem* **276**, 18579-18590.

**Li, K., Foy, E., Ferreon, J. C., Nakamura, M., Ferreon, A. C., Ikeda, M., Ray, S. C., Gale, M., Jr. & Lemon, S. M. (2005a).** Immune evasion by hepatitis C virus NS3/4A protease-mediated cleavage of the Toll-like receptor 3 adaptor protein TRIF. *Proc Natl Acad Sci U S A* **102**, 2992-2997.

**Li, K., Chen, Z., Kato, N., Gale, M., Jr. & Lemon, S. M. (2005b).** Distinct poly(I-C) and virus-activated signaling pathways leading to interferon-beta production in hepatocytes. *J Biol Chem* **280**, 16739-16747.

**Li, X. D., Sun, L., Seth, R. B., Pineda, G. & Chen, Z. J. (2005c).** Hepatitis C virus protease NS3/4A cleaves mitochondrial antiviral signaling protein off the mitochondria to evade innate immunity. *Proc Natl Acad Sci U S A* **102**, 17717-17722.

**Li, S., Ye, L., Yu, X., Xu, B., Li, K., Zhu, X., Liu, H., Wu, X. & Kong, L. (2009).** Hepatitis C virus NS4B induces unfolded protein response and endoplasmic reticulum overload response-dependent NF-kappaB activation. *Virology* **391**, 257-264.

**Liang, Y., Kang, C. B. & Yoon, H. S. (2006).** Molecular and structural characterization of the domain 2 of hepatitis C virus non-structural protein 5A. *Mol Cells* **22**, 13-20.

**Liang, Y., Ye, H., Kang, C. B. & Yoon, H. S. (2007).** Domain 2 of nonstructural protein 5A (NS5A) of hepatitis C virus is natively unfolded. *Biochemistry* **46**, 11550-11558.

**Liefhebber, J. M., Brandt, B. W., Broer, R., Spaan, W. J. & van Leeuwen, H. C. (2009).** Hepatitis C virus NS4B carboxy terminal domain is a membrane binding domain. *Virol J* **6**, 62.

**Lim, Y. S. & Hwang, S. B. (2011).** Hepatitis C virus NS5A protein interacts with phosphatidylinositol 4-kinase type IIIalpha and regulates viral propagation. *J Biol Chem* **286**, 11290-11298.

**Lin, C., Pragai, B. M., Grakoui, A., Xu, J. & Rice, C. M. (1994b).** Hepatitis C virus NS3 serine proteinase: trans-cleavage requirements and processing kinetics. *J Virol* **68**, 8147-8157.

**Lin, C., Lindenbach, B. D., Pragai, B. M., McCourt, D. W. & Rice, C. M. (1994b).** Processing in the hepatitis C virus E2-NS2 region: identification of p7 and two distinct E2-specific products with different C termini. *J Virol* **68**, 5063-5073.

**Lin, C., Thomson, J. A. & Rice, C. M. (1995).** A central region in the hepatitis C virus NS4A protein allows formation of an active NS3-NS4A serine proteinase complex in vivo and in vitro. *J Virol* **69**, 4373-4380.

**Lin, W., Choe, W. H., Hiasa, Y., Kamegaya, Y., Blackard, J. T., Schmidt, E. V. & Chung, R. T. (2005).** Hepatitis C virus expression suppresses interferon signaling by degrading STAT1. *Gastroenterology* **128**, 1034-1041.

**Lindenbach, B. D., Evans, M. J., Syder, A. J., Wolk, B., Tellinghuisen, T. L., Liu, C. C., Maruyama, T., Hynes, R. O., Burton, D. R., McKeating, J. A. & Rice, C. M. (2005).** Complete replication of hepatitis C virus in cell culture. *Science* **309**, 623-626.

**Lindenbach, B. D., Meuleman, P., Ploss, A., Vanwolleghem, T., Syder, A. J., McKeating, J. A., Lanford, R. E., Feinstone, S. M., Major, M. E., Leroux-Roels, G. & Rice, C. M. (2006).** Cell culture-grown hepatitis C virus is infectious in vivo and can be recultured in vitro. *Proc Natl Acad Sci U S A* **103**, 3805-3809.

**Lindenbach, B. D., Pragai, B. M., Montserret, R., Beran, R. K., Pyle, A. M., Penin, F. & Rice, C. M. (2007).** The C Terminus of Hepatitis C Virus NS4A Encodes an Electrostatic Switch That Regulates NS5A Hyperphosphorylation and Viral Replication. *J Virol* **81**, 8905-8918.

**Lindenmann, J., Burke, D. C. & Isaacs, A. (1957).** Studies on the production, mode of action and properties of interferon. *Br J Exp Pathol* **38**, 551-562.

**Lindstrom, H., Lundin, M., Haggstrom, S. & Persson, M. A. (2006).** Mutations of the Hepatitis C virus protein NS4B on either side of the ER membrane affect the efficiency of subgenomic replicons. *Virus Res* **121**, 169-178.

**Liu, B., Woltman, A. M., Janssen, H. L. & Boonstra, A. (2009a).** Modulation of dendritic cell function by persistent viruses. *J Leukoc Biol* **85**, 205-214.

**Liu, S., Yang, W., Shen, L., Turner, J. R., Coyne, C. B. & Wang, T. (2009b).** Tight junction proteins claudin-1 and occludin control hepatitis C virus entry and are downregulated during infection to prevent superinfection. *J Virol* **83**, 2011-2014.

**Liu, M., Li, X. L. & Hassel, B. A. (2003).** Proteasomes modulate conjugation to the ubiquitin-like protein, ISG15. *J Biol Chem* **278**, 1594-1602.

**Liu, S., Ansari, I. H., Das, S. C. & Pattnaik, A. K. (2006).** Insertion and deletion analyses identify regions of non-structural protein 5A of Hepatitis C virus that are dispensable for viral genome replication. *J Gen Virol* **87**, 323-327.

**Loeb, K. R. & Haas, A. L. (1992).** The interferon-inducible 15-kDa ubiquitin homolog conjugates to intracellular proteins. *J Biol Chem* **267**, 7806-7813.

**Logvinoff, C., Major, M. E., Oldach, D., Heyward, S., Talal, A., Balfe, P., Feinstone, S. M., Alter, H., Rice, C. M. & McKeating, J. A. (2004).** Neutralizing antibody response during acute and chronic hepatitis C virus infection. *Proc Natl Acad Sci U S A* **101**, 10149-10154.

**Lohmann, V., Hoffmann, S., Herian, U., Penin, F. & Bartenschlager, R. (2003).** Viral and cellular determinants of hepatitis C virus RNA replication in cell culture. *J Virol* **77**, 3007-3019.

**Lohmann, V., Korner, F., Dobierzewska, A. & Bartenschlager, R. (2001).** Mutations in hepatitis C virus RNAs conferring cell culture adaptation. *J Virol* **75**, 1437-1449.

**Lohmann, V., Korner, F., Koch, J., Herian, U., Theilmann, L. & Bartenschlager, R. (1999).** Replication of subgenomic hepatitis C virus RNAs in a hepatoma cell line. *Science* **285**, 110-113.

**Loo, Y. M., Owen, D. M., Li, K., Erickson, A. K., Johnson, C. L., Fish, P. M., Carney, D. S., Wang, T., Ishida, H., Yoneyama, M., Fujita, T., Saito, T., Lee, W. M., Hagedorn, C. H., Lau, D. T., Weinman, S. A., Lemon, S. M. & Gale, M., Jr. (2006).** Viral and therapeutic control of IFN-beta promoter stimulator 1 during hepatitis C virus infection. *Proc Natl Acad Sci U S A* **103**, 6001-6006.

**Lorenz, I. C., Marcotrigiano, J., Dentzer, T. G. & Rice, C. M. (2006).** Structure of the catalytic domain of the hepatitis C virus NS2-3 protease. *Nature* **442**, 831-835.

**Lou, Z., Wei, J., Riethman, H., Baur, J. A., Voglauer, R., Shay, J. W. & Wright, W. E. (2009).** Telomere length regulates ISG15 expression in human cells. *Aging (Albany NY)* **1**, 608-621.

**Love, R. A., Brodsky, O., Hickey, M. J., Wells, P. A. & Cronin, C. N. (2009).** Crystal structure of a novel dimeric form of NS5A domain I protein from hepatitis C virus. *J Virol* **83**, 4395-4403.

**Lu, G., Reinert, J. T., Pitha-Rowe, I., Okumura, A., Kellum, M., Knobeloch, K. P., Hassel, B. & Pitha, P. M. (2006).** ISG15 enhances the innate antiviral response by inhibition of IRF-3 degradation. *Cell Mol Biol (Noisy-le-grand)* **52**, 29-41.

**Luik, P., Chew, C., Aittoniemi, J., Chang, J., Wentworth, P., Jr., Dwek, R. A., Biggin, P. C., Venien-Bryan, C. & Zitzmann, N. (2009).** The 3-dimensional structure of a hepatitis C virus p7 ion channel by electron microscopy. *Proc Natl Acad Sci U S A* **106**, 12712-12716.

**Lukavsky, P. J., Kim, I., Otto, G. A. & Puglisi, J. D. (2003).** Structure of HCV IRES domain II determined by NMR. *Nat Struct Biol* **10**, 1033-1038.

**Lukavsky, P. J., Otto, G. A., Lancaster, A. M., Sarnow, P. & Puglisi, J. D. (2000).** Structures of two RNA domains essential for hepatitis C virus internal ribosome entry site function. *Nat Struct Biol* **7**, 1105-1110.

**Lundin, M., Lindstrom, H., Gronwall, C. & Persson, M. A. (2006).** Dual topology of the processed hepatitis C virus protein NS4B is influenced by the NS5A protein. *J Gen Virol* **87**, 3263-3272.

**Lundin, M., Monne, M., Widell, A., Von Heijne, G. & Persson, M. A. (2003).** Topology of the membrane-associated hepatitis C virus protein NS4B. *J Virol* **77**, 5428-5438.

**Lupberger, J., Zeisel, M. B., Xiao, F., Thumann, C., Fofana, I., Zona, L., Davis, C., Mee, C. J., Turek, M., Gorke, S., Royer, C., Fischer, B., Zahid, M. N., Lavillette, D., Fresquet, J., Cosset, F. L., Rothenberg, S. M., Pietschmann, T., Patel, A. H., Pessaux, P., Doffoel, M., Raffelsberger, W., Poch, O., McKeating, J. A., Brino, L. & Baumert, T. F. (2011).** EGFR and EphA2 are host factors for hepatitis C virus entry and possible targets for antiviral therapy. *Nat Med* **17**, 589-595.

**Ma, Y., Anantpadma, M., Timpe, J. M., Shanmugam, S., Singh, S. M., Lemon, S. M. & Yi, M. (2011).** Hepatitis C virus NS2 protein serves as a scaffold

for virus assembly by interacting with both structural and nonstructural proteins. *J Virol* **85**, 86-97.

**Macdonald, A., Crowder, K., Street, A., McCormick, C. & Harris, M. (2004).** The hepatitis C virus NS5A protein binds to members of the Src family of tyrosine kinases and regulates kinase activity. *J Gen Virol* **85**, 721-729.

**Macdonald, A., Crowder, K., Street, A., McCormick, C., Saksela, K. & Harris, M. (2003).** The hepatitis C virus non-structural NS5A protein inhibits activating protein-1 function by perturbing ras-ERK pathway signaling. *J Biol Chem* **278**, 17775-17784.

**Macdonald, A. & Harris, M. (2004).** Hepatitis C virus NS5A: tales of a promiscuous protein. *J Gen Virol* **85**, 2485-2502.

**Macdonald, A., Mazaleyrat, S., McCormick, C., Street, A., Burgoyne, N. J., Jackson, R. M., Cazeaux, V., Shelton, H., Saksela, K. & Harris, M. (2005).** Further studies on hepatitis C virus NS5A-SH3 domain interactions: identification of residues critical for binding and implications for viral RNA replication and modulation of cell signalling. *J Gen Virol* **86**, 1035-1044.

**Machlin, E. S., Sarnow, P. & Sagan, S. M. (2011).** Masking the 5' terminal nucleotides of the hepatitis C virus genome by an unconventional microRNA-target RNA complex. *Proc Natl Acad Sci U S A* **108**, 3193-3198.

**MacQuillan, G. C., Mamotte, C., Reed, W. D., Jeffrey, G. P. & Allan, J. E. (2003).** Upregulation of endogenous intrahepatic interferon stimulated genes during chronic hepatitis C virus infection. *J Med Virol* **70**, 219-227.

**Malakhov, M. P., Kim, K. I., Malakhova, O. A., Jacobs, B. S., Borden, E. C. & Zhang, D. E. (2003).** High-throughput immunoblotting. Ubiquitiin-like protein ISG15 modifies key regulators of signal transduction. *J Biol Chem* **278**, 16608-16613.

**Malakhov, M. P., Malakhova, O. A., Kim, K. I., Ritchie, K. J. & Zhang, D. E. (2002).** UBP43 (USP18) specifically removes ISG15 from conjugated proteins. *J Biol Chem* **277**, 9976-9981.

**Malakhova, O., Malakhov, M., Hetherington, C. & Zhang, D. E. (2002).** Lipopolysaccharide activates the expression of ISG15-specific protease UBP43 via interferon regulatory factor 3. *J Biol Chem* **277**, 14703-14711.

**Malakhova, O. A., Kim, K. I., Luo, J. K., Zou, W., Kumar, K. G., Fuchs, S. Y., Shuai, K. & Zhang, D. E. (2006).** UBP43 is a novel regulator of interferon signaling independent of its ISG15 isopeptidase activity. *Embo J* **25**, 2358-2367.

**Malakhova, O. A. & Zhang, D. E. (2008).** ISG15 inhibits Nedd4 ubiquitin E3 activity and enhances the innate antiviral response. *J Biol Chem* **283**, 8783-8787.

**Mangia, A., Thompson, A. J., Santoro, R., Piazzolla, V., Tillmann, H. L., Patel, K., Shianna, K. V., Mottola, L., Petruzzellis, D., Bacca, D., Carretta, V., Minerva, N., Goldstein, D. B. & McHutchison, J. G. (2010).** An IL28B polymorphism determines treatment response of hepatitis C virus genotype 2 or 3 patients who do not achieve a rapid virologic response. *Gastroenterology* **139**, 821-827, 827 e821.

**Mankouri, J., Griffin, S. & Harris, M. (2008).** The hepatitis C virus non-structural protein NS5A alters the trafficking profile of the epidermal growth factor receptor. *Traffic* **9**, 1497-1509.

**Manthey, C. L., Wang, S. W., Kinney, S. D. & Yao, Z. (1998).** SB202190, a selective inhibitor of p38 mitogen-activated protein kinase, is a powerful regulator of LPS-induced mRNAs in monocytes. *J Leukoc Biol* **64**, 409-417.

**Marcinowski, L., Lidschreiber, M., Windhager, L., Rieder, M., Bosse, J. B., Radle, B., Bonfert, T., Gyory, I., de Graaf, M., Prazeres da Costa, O., Rosenstiel, P., Friedel, C. C., Zimmer, R., Ruzsics, Z. & Dolken, L. (2012).** Real-time Transcriptional Profiling of Cellular and Viral Gene Expression during Lytic Cytomegalovirus Infection. *PLoS Pathog* **8**, e1002908.

**Martell, M., Esteban, J. I., Quer, J., Genesca, J., Weiner, A., Esteban, R., Guardia, J. & Gomez, J. (1992).** Hepatitis C virus (HCV) circulates as a population of different but closely related genomes: quasispecies nature of HCV genome distribution. *J Virol* **66**, 3225-3229.

**Marukian, S., Andrus, L., Sheahan, T. P., Jones, C. T., Charles, E. D., Ploss, A., Rice, C. M. & Dustin, L. B. (2011).** Hepatitis C virus induces interferon-lambda and interferon-stimulated genes in primary liver cultures. *Hepatology* **54**, 1913-1923.

**Masaki, T., Suzuki, R., Murakami, K., Aizaki, H., Ishii, K., Murayama, A., Date, T., Matsuura, Y., Miyamura, T., Wakita, T. & Suzuki, T. (2008).** Interaction of hepatitis C virus nonstructural protein 5A with core protein is critical for the production of infectious virus particles. *J Virol* **82**, 7964-7976.

**McLauchlan, J., Lemberg, M. K., Hope, G. & Martoglio, B. (2002).** Intramembrane proteolysis promotes trafficking of hepatitis C virus core protein to lipid droplets. *Embo J* **21**, 3980-3988.

**McMullan, L. K., Grakoui, A., Evans, M. J., Mihalik, K., Puig, M., Branch, A. D., Feinstone, S. M. & Rice, C. M. (2007).** Evidence for a functional RNA element in the hepatitis C virus core gene. *Proc Natl Acad Sci U S A*.

**Meertens, L., Bertaux, C. & Dragic, T. (2006).** Hepatitis C virus entry requires a critical postinternalization step and delivery to early endosomes via clathrin-coated vesicles. *J Virol* **80**, 11571-11578.

**Melvin, W. T., Milne, H. B., Slater, A. A., Allen, H. J. & Keir, H. M. (1978).** Incorporation of 6-thioguanosine and 4-thiouridine into RNA. Application to isolation of newly synthesised RNA by affinity chromatography. *Eur J Biochem* **92**, 373-379.

**Memet, S., Besancon, F., Bourgeade, M. F. & Thang, M. N. (1991).** Direct induction of interferon-gamma- and interferon-alpha/beta-inducible genes by double-stranded RNA. *J Interferon Res* **11**, 131-141.

**Meraro, D., Gleit-Kielmanowicz, M., Hauser, H. & Levi, B. Z. (2002).** IFN-stimulated gene 15 is synergistically activated through interactions between the myelocyte/lymphocyte-specific transcription factors, PU.1, IFN regulatory factor-8/IFN consensus sequence binding protein, and IFN regulatory factor-4: characterization of a new subtype of IFN-stimulated response element. *J Immunol* **168**, 6224-6231.

**Mercer, D. F., Schiller, D. E., Elliott, J. F., Douglas, D. N., Hao, C., Rinfret, A., Addison, W. R., Fischer, K. P., Churchill, T. A., Lakey, J. R., Tyrrell, D. L. & Kneteman, N. M. (2001).** Hepatitis C virus replication in mice with chimeric human livers. *Nat Med* **7**, 927-933.

**Meuleman, P. & Leroux-Roels, G. (2008).** The human liver-uPA-SCID mouse: a model for the evaluation of antiviral compounds against HBV and HCV. *Antiviral Res* **80**, 231-238.

**Meyer-Olson, D., Shoukry, N. H., Brady, K. W., Kim, H., Olson, D. P., Hartman, K., Shintani, A. K., Walker, C. M. & Kalams, S. A. (2004).** Limited T cell receptor diversity of HCV-specific T cell responses is associated with CTL escape. *J Exp Med* **200**, 307-319.

**Meylan, E., Curran, J., Hofmann, K., Moradpour, D., Binder, M., Bartenschlager, R. & Tschopp, J. (2005).** Cardif is an adaptor protein in the RIG-I antiviral pathway and is targeted by hepatitis C virus. *Nature* **437**, 1167-1172.

**Mihm, S., Fayyazi, A., Hartmann, H. & Ramadori, G. (1997).** Analysis of histopathological manifestations of chronic hepatitis C virus infection with respect to virus genotype. *Hepatology* **25**, 735-739.

**Miller, R. H. & Purcell, R. H. (1990).** Hepatitis C virus shares amino acid sequence similarity with pestiviruses and flaviviruses as well as members of two plant virus supergroups. *Proc Natl Acad Sci U S A* **87**, 2057-2061.

**Missale, G., Bertoni, R., Lamonaca, V., Valli, A., Massari, M., Mori, C., Rumi, M. G., Houghton, M., Fiaccadori, F. & Ferrari, C. (1996).** Different clinical behaviors of acute hepatitis C virus infection are associated with different vigor of the anti-viral cell-mediated immune response. *J Clin Invest* **98**, 706-714.

**Miyanari, Y., Atsuzawa, K., Usuda, N., Watashi, K., Hishiki, T., Zayas, M., Bartenschlager, R., Wakita, T., Hijikata, M. & Shimotohno, K. (2007).** The lipid droplet is an important organelle for hepatitis C virus production. *Nat Cell Biol* **9**, 1089-1097.

**Molina, S., Castet, V., Fournier-Wirth, C., Pichard-Garcia, L., Avner, R., Harats, D., Roitelman, J., Barbaras, R., Graber, P., Ghersa, P., Smolarsky, M., Funaro, A., Malavasi, F., Larrey, D., Coste, J., Fabre, J. M., Sa-Cunha, A. & Maurel, P. (2007).** The low-density lipoprotein receptor plays a role in the infection of primary human hepatocytes by hepatitis C virus. *J Hepatol* **46**, 411-419.

**Molina, S., Castet, V., Pichard-Garcia, L., Wychowski, C., Meurs, E., Pascussi, J. M., Sureau, C., Fabre, J. M., Sacunha, A., Larrey, D., Dubuisson, J., Coste, J., McKeating, J., Maurel, P. & Fournier-Wirth, C. (2008).** Serum-derived hepatitis C virus infection of primary human hepatocytes is tetraspanin CD81 dependent. *J Virol* **82**, 569-574.

**Montserret, R., Saint, N., Vanbelle, C., Salvay, A. G., Simorre, J. P., Ebel, C., Sapay, N., Renisio, J. G., Bockmann, A., Steinmann, E., Pietschmann, T., Dubuisson, J., Chipot, C. & Penin, F. (2010).** NMR structure and ion channel activity of the p7 protein from hepatitis C virus. *J Biol Chem* **285**, 31446-31461.

**Moradpour, D., Brass, V. & Penin, F. (2005).** Function follows form: the structure of the N-terminal domain of HCV NS5A. *Hepatology* **42**, 732-735.

**Moradpour, D., Englert, C., Wakita, T. & Wands, J. R. (1996).** Characterization of cell lines allowing tightly regulated expression of hepatitis C virus core protein. *Virology* **222**, 51-63.

**Moradpour, D., Evans, M. J., Gosert, R., Yuan, Z., Blum, H. E., Goff, S. P., Lindenbach, B. D. & Rice, C. M. (2004).** Insertion of green fluorescent protein into nonstructural protein 5A allows direct visualization of functional hepatitis C virus replication complexes. *J Virol* **78**, 7400-7409.

**Mossman, K. L., Macgregor, P. F., Rozmus, J. J., Goryachev, A. B., Edwards, A. M. & Smiley, J. R. (2001).** Herpes simplex virus triggers and then disarms a host antiviral response. *J Virol* **75**, 750-758.

**Muller, U., Steinhoff, U., Reis, L. F., Hemmi, S., Pavlovic, J., Zinkernagel, R. M. & Aguet, M. (1994).** Functional role of type I and type II interferons in antiviral defense. *Science* **264**, 1918-1921.

**Murayama, A., Weng, L., Date, T., Akazawa, D., Tian, X., Suzuki, T., Kato, T., Tanaka, Y., Mizokami, M., Wakita, T. & Toyoda, T. (2010).** RNA

polymerase activity and specific RNA structure are required for efficient HCV replication in cultured cells. *PLoS Pathog* **6**, e1000885.

**Murray, E. J., Burden, F., Horscroft, N., Smith-Burchnell, C. & Westby, M. (2011).** Knockdown of USP18 increases alpha 2a interferon signaling and induction of interferon-stimulating genes but does not increase antiviral activity in Huh7 cells. *Antimicrob Agents Chemother* **55**, 4311-4319.

**Nanda, S. K., Herion, D. & Liang, T. J. (2006).** The SH3 binding motif of HCV [corrected] NS5A protein interacts with Bin1 and is important for apoptosis and infectivity. *Gastroenterology* **130**, 794-809.

**Nakabayashi, H., Taketa, K., Miyano, K., Yamane, T. & Sato, J. (1982).** Growth of human hepatoma cells lines with differentiated functions in chemically defined medium. *Cancer Res* **42**, 3858–3863.

**Narasimhan, J., Wang, M., Fu, Z., Klein, J. M., Haas, A. L. & Kim, J. J. (2005).** Crystal structure of the interferon-induced ubiquitin-like protein ISG15. *J Biol Chem* **280**, 27356-27365.

**Ndongo-Thiam, N., Berthillon, P., Errazuriz, E., Bordes, I., De Sequeira, S., Trepo, C. & Petit, M. A. (2011).** Long-term propagation of serum hepatitis C virus (HCV) with production of enveloped HCV particles in human HepaRG hepatocytes. *Hepatology* **54**, 406-417.

**Neddermann, P., Clementi, A. & De Francesco, R. (1999).** Hyperphosphorylation of the hepatitis C virus NS5A protein requires an active NS3 protease, NS4A, NS4B, and NS5A encoded on the same polyprotein. *J Virol* **73**, 9984-9991.

**Neddermann, P., Quintavalle, M., Di Pietro, C., Clementi, A., Cerretani, M., Altamura, S., Bartholomew, L. & De Francesco, R. (2004).** Reduction of hepatitis C virus NS5A hyperphosphorylation by selective inhibition of cellular kinases activates viral RNA replication in cell culture. *J Virol* **78**, 13306-13314.

**Neefjes, J., Jongsma, M. L., Paul, P. & Bakke, O. (2011).** Towards a systems understanding of MHC class I and MHC class II antigen presentation. *Nat Rev Immunol* **11**, 823-836.

**Nicholl, M. J., Robinson, L. H. & Preston, C. M. (2000).** Activation of cellular interferon-responsive genes after infection of human cells with herpes simplex virus type 1. *J Gen Virol* **81**, 2215-2218.

**Ogino, T., Fukuda, H., Imajoh-Ohmi, S., Kohara, M. & Nomoto, A. (2004).** Membrane binding properties and terminal residues of the mature hepatitis C virus capsid protein in insect cells. *J Virol* **78**, 11766-11777.

**Ohtsu, M., Kawate, M., Fukuoka, M., Gunji, W., Hanaoka, F., Utsugi, T., Onoda, F. & Murakami, Y. (2008).** Novel DNA microarray system for analysis of nascent mRNAs. *DNA Res* **15**, 241-251.

**Okumura, A., Lu, G., Pitha-Rowe, I. & Pitha, P. M. (2006).** Innate antiviral response targets HIV-1 release by the induction of ubiquitin-like protein ISG15. *Proc Natl Acad Sci U S A* **103**, 1440-1445.

**Okumura, A., Pitha, P. M. & Harty, R. N. (2008).** ISG15 inhibits Ebola VP40 VLP budding in an L-domain-dependent manner by blocking Nedd4 ligase activity. *Proc Natl Acad Sci U S A* **105**, 3974-3979.

**Okumura, F., Lenschow, D. J. & Zhang, D. E. (2008).** Nitrosylation of ISG15 prevents the disulfide bond-mediated dimerization of ISG15 and contributes to effective ISGylation. *J Biol Chem* **283**, 24484-24488.

**Okumura, F., Zou, W. & Zhang, D. E. (2007).** ISG15 modification of the eIF4E cognate 4EHP enhances cap structure-binding activity of 4EHP. *Genes Dev* **21**, 255-260.

**Op De Beeck, A. & Dubuisson, J. (2003).** Topology of hepatitis C virus envelope glycoproteins. *Rev Med Virol* **13**, 233-241.

**Op De Beeck, A., Voisset, C., Bartosch, B., Ciczora, Y., Cocquerel, L., Keck, Z., Foung, S., Cosset, F. L. & Dubuisson, J. (2004).** Characterization of functional hepatitis C virus envelope glycoproteins. *J Virol* **78**, 2994-3002.

**Osiak, A., Utermohlen, O., Niendorf, S., Horak, I. & Knobeloch, K. P. (2005).** ISG15, an interferon-stimulated ubiquitin-like protein, is not essential for STAT1 signaling and responses against vesicular stomatitis and lymphocytic choriomeningitis virus. *Mol Cell Biol* **25**, 6338-6345.

**Otto, G. A. & Puglisi, J. D. (2004).** The pathway of HCV IRES-mediated translation initiation. *Cell* **119**, 369-380.

**Owen, D. M., Huang, H., Ye, J. & Gale, M., Jr. (2009).** Apolipoprotein E on hepatitis C virion facilitates infection through interaction with low-density lipoprotein receptor. *Virology* **394**, 99-108.

**Owhashi, M., Taoka, Y., Ishii, K., Nakazawa, S., Uemura, H. & Kambara, H. (2003).** Identification of a ubiquitin family protein as a novel neutrophil chemotactic factor. *Biochem Biophys Res Commun* **309**, 533-539.

**Owsianka, A., Tarr, A. W., Juttla, V. S., Lavillette, D., Bartosch, B., Cosset, F. L., Ball, J. K. & Patel, A. H. (2005).** Monoclonal antibody AP33 defines a broadly neutralizing epitope on the hepatitis C virus E2 envelope glycoprotein. *J Virol* **79**, 11095-11104.

**Paeshuyse, J., Dallmeier, K. & Neyts, J. (2011).** Ribavirin for the treatment of chronic hepatitis C virus infection: a review of the proposed mechanisms of action. *Curr Opin Virol* **1**, 590-598.

**Pang, P. S., Jankowsky, E., Planet, P. J. & Pyle, A. M. (2002).** The hepatitis C viral NS3 protein is a processive DNA helicase with cofactor enhanced RNA unwinding. *Embo J* **21**, 1168-1176.

**Paredes, A. M. & Blight, K. J. (2008).** A genetic interaction between hepatitis C virus NS4B and NS3 is important for RNA replication. *J Virol* **82**, 10671-10683.

**Parent, R., Marion, M. J., Furio, L., Trepo, C. & Petit, M. A. (2004).** Origin and characterization of a human bipotent liver progenitor cell line. *Gastroenterology* **126**, 1147-1156.

**Parent, R., Qu, X., Petit, M. A. & Beretta, L. (2009).** The heat shock cognate protein 70 is associated with hepatitis C virus particles and modulates virus infectivity. *Hepatology* **49**, 1798-1809.

**Parisien, J. P., Lau, J. F., Rodriguez, J. J., Ulane, C. M. & Horvath, C. M. (2002).** Selective STAT protein degradation induced by paramyxoviruses requires both STAT1 and STAT2 but is independent of alpha/beta interferon signal transduction. *J Virol* **76**, 4190-4198.

**Pasare, C. & Medzhitov, R. (2004).** Toll-like receptors: linking innate and adaptive immunity. *Microbes Infect* **6**, 1382-1387.

**Patargias, G., Zitzmann, N., Dwek, R. & Fischer, W. B. (2006).** Protein-protein interactions: modeling the hepatitis C virus ion channel p7. *J Med Chem* **49**, 648-655.

**Paul, D., Romero-Brey, I., Gouttenoire, J., Stoitsova, S., Krijnse-Locker, J., Moradpour, D. & Bartenschlager, R. (2011).** NS4B self-interaction through conserved C-terminal elements is required for the establishment of functional hepatitis C virus replication complexes. *J Virol* **85**, 6963-6976.

**Pavio, N., Taylor, D. R. & Lai, M. M. (2002).** Detection of a novel unglycosylated form of hepatitis C virus E2 envelope protein that is located in the cytosol and interacts with PKR. *J Virol* **76**, 1265-1272.

**Penin, F., Brass, V., Appel, N., Ramboarina, S., Montserret, R., Ficheux, D., Blum, H. E., Bartenschlager, R. & Moradpour, D. (2004).** Structure and function of the membrane anchor domain of hepatitis C virus nonstructural protein 5A. *J Biol Chem* **279**, 40835-40843.

**Perez-Berna, A. J., Moreno, M. R., Guillen, J., Bernabeu, A. & Villalain, J. (2006).** The membrane-active regions of the hepatitis C virus E1 and E2 envelope glycoproteins. *Biochemistry* **45**, 3755-3768.

**Pestka, J. M., Zeisel, M. B., Blaser, E., Schurmann, P., Bartosch, B., Cosset, F. L., Patel, A. H., Meisel, H., Baumert, J., Viazov, S., Rispeter, K., Blum, H. E., Roggendorf, M. & Baumert, T. F. (2007).** Rapid induction of virus-neutralizing antibodies and viral clearance in a single-source outbreak of hepatitis C. *Proc Natl Acad Sci U S A* **104**, 6025-6030.

**Pestka, S., Krause, C. D. & Walter, M. R. (2004).** Interferons, interferon-like cytokines, and their receptors. *Immunol Rev* **202**, 8-32.

**Pestova, T. V., Shatsky, I. N., Fletcher, S. P., Jackson, R. J. & Hellen, C. U. (1998).** A prokaryotic-like mode of cytoplasmic eukaryotic ribosome binding to the initiation codon during internal translation initiation of hepatitis C and classical swine fever virus RNAs. *Genes Dev* **12**, 67-83.

**Petrovic, D., Dempsey, E., Doherty, D. G., Kelleher, D. & Long, A. (2012).** Hepatitis C virus--T-cell responses and viral escape mutations. *Eur J Immunol* **42**, 17-26.

**Pfeifer, U., Thomssen, R., Legler, K., Bottcher, U., Gerlich, W., Weinmann, E. & Klinge, O. (1980).** Experimental non-A, non-B hepatitis: four types of cytoplasmic alteration in hepatocytes of infected chimpanzees. *Virchows Arch B Cell Pathol Incl Mol Pathol* **33**, 233-243.

**Phan, T., Beran, R. K., Peters, C., Lorenz, I. C. & Lindenbach, B. D. (2009).** Hepatitis C virus NS2 protein contributes to virus particle assembly via opposing epistatic interactions with the E1-E2 glycoprotein and NS3-NS4A enzyme complexes. *J Virol* **83**, 8379-8395.

**Phan, T., Kohlway, A., Dimberu, P., Pyle, A. M. & Lindenbach, B. D. (2011).** The acidic domain of hepatitis C virus NS4A contributes to RNA replication and virus particle assembly. *J Virol* **85**, 1193-1204.

**Pietschmann, T., Kaul, A., Koutsoudakis, G., Shavinskaya, A., Kallis, S., Steinmann, E., Abid, K., Negro, F., Dreux, M., Cosset, F. L. & Bartenschlager, R. (2006).** Construction and characterization of infectious intragenotypic and intergenotypic hepatitis C virus chimeras. *Proc Natl Acad Sci U S A* **103**, 7408-7413.

**Pietschmann, T., Lohmann, V., Kaul, A., Krieger, N., Rinck, G., Rutter, G., Strand, D. & Bartenschlager, R. (2002).** Persistent and transient replication of full-length hepatitis C virus genomes in cell culture. *J Virol* **76**, 4008-4021.

**Pileri, P., Uematsu, Y., Campagnoli, S., Galli, G., Falugi, F., Petracca, R., Weiner, A. J., Houghton, M., Rosa, D., Grandi, G. & Abrignani, S. (1998).** Binding of hepatitis C virus to CD81. *Science* **282**, 938-941.

**Ploss, A., Evans, M. J., Gaysinskaya, V. A., Panis, M., You, H., de Jong, Y. P. & Rice, C. M. (2009).** Human occludin is a hepatitis C virus entry factor required for infection of mouse cells. *Nature* **457**, 882-886.

**Pohlmann, S., Zhang, J., Baribaud, F., Chen, Z., Leslie, G. J., Lin, G., Granelli-Piperno, A., Doms, R. W., Rice, C. M. & McKeating, J. A. (2003).** Hepatitis C virus glycoproteins interact with DC-SIGN and DC-SIGNR. *J Virol* **77**, 4070-4080.

**Poordad, F., McCone, J., Jr., Bacon, B. R., Bruno, S., Manns, M. P., Sulkowski, M. S., Jacobson, I. M., Reddy, K. R., Goodman, Z. D.,**

**Boparai, N., DiNubile, M. J., Sniukiene, V., Brass, C. A., Albrecht, J. K. & Bronowicki, J. P. (2011).** Boceprevir for untreated chronic HCV genotype 1 infection. *N Engl J Med* **364**, 1195-1206.

**Popescu, C. I., Callens, N., Trinel, D., Roingeard, P., Moradpour, D., Descamps, V., Duverlie, G., Penin, F., Heliot, L., Rouille, Y. & Dubuisson, J. (2011).** NS2 protein of hepatitis C virus interacts with structural and non-structural proteins towards virus assembly. *PLoS Pathog* **7**, e1001278.

**Post, J. J., Pan, Y., Freeman, A. J., Harvey, C. E., White, P. A., Palladinetti, P., Haber, P. S., Marinos, G., Levy, M. H., Kaldor, J. M., Dolan, K. A., Ffrench, R. A., Lloyd, A. R. & Rawlinson, W. D. (2004).** Clearance of hepatitis C viremia associated with cellular immunity in the absence of seroconversion in the hepatitis C incidence and transmission in prisons study cohort. *J Infect Dis* **189**, 1846-1855.

**Potter, J. L., Narasimhan, J., Mende-Mueller, L. & Haas, A. L. (1999).** Precursor processing of pro-ISG15/UCRP, an interferon-beta-induced ubiquitin-like protein. *J Biol Chem* **274**, 25061-25068.

**Quinkert, D., Bartenschlager, R. & Lohmann, V. (2005).** Quantitative analysis of the hepatitis C virus replication complex. *J Virol* **79**, 13594-13605.

**Quintavalle, M., Sambucini, S., Summa, V., Orsatti, L., Talamo, F., De Francesco, R. & Neddermann, P. (2007).** Hepatitis C virus NS5A is a direct substrate of casein kinase I-alpha, a cellular kinase identified by inhibitor affinity chromatography using specific NS5A hyperphosphorylation inhibitors. *J Biol Chem* **282**, 5536-5544.

**Rabani, M., Levin, J. Z., Fan, L., Adiconis, X., Raychowdhury, R., Garber, M., Gnirke, A., Nusbaum, C., Hacohen, N., Friedman, N., Amit, I. & Regev, A. (2011).** Metabolic labeling of RNA uncovers principles of RNA production and degradation dynamics in mammalian cells. *Nat Biotechnol* **29**, 436-442.

**Ramachandran, P., Fraser, A., Agarwal, K., Austin, A., Brown, A., Foster, G. R., Fox, R., Hayes, P. C., Leen, C., Mills, P. R., Mutimer, D. J., Ryder, S. D. & Dillon, J. F. (2012).** UK consensus guidelines for the use of the protease inhibitors boceprevir and telaprevir in genotype 1 chronic hepatitis C infected patients. *Aliment Pharmacol Ther* **35**, 647-662.

**Randall, G., Chen, L., Panis, M., Fischer, A. K., Lindenbach, B. D., Sun, J., Heathcote, J., Rice, C. M., Edwards, A. M. & McGilvray, I. D. (2006).** Silencing of USP18 potentiates the antiviral activity of interferon against hepatitis C virus infection. *Gastroenterology* **131**, 1584-1591.

**Rao, D. D., Vorhies, J. S., Senzer, N. & Nemunaitis, J. (2009).** siRNA vs. shRNA: similarities and differences. *Adv Drug Deliv Rev* **61**, 746-759.

**Recht, M., Borden, E. C. & Knight, E., Jr. (1991).** A human 15-kDa IFN-induced protein induces the secretion of IFN-gamma. *J Immunol* **147**, 2617-2623.

**Reich, N., Evans, B., Levy, D., Fahey, D., Knight, E., Jr. & Darnell, J. E., Jr. (1987).** Interferon-induced transcription of a gene encoding a 15-kDa protein depends on an upstream enhancer element. *Proc Natl Acad Sci U S A* **84**, 6394-6398.

**Reiss, S., Rebhan, I., Backes, P., Romero-Brey, I., Erfle, H., Matula, P., Kaderali, L., Poenisch, M., Blankenburg, H., Hiet, M. S., Longerich, T., Diehl, S., Ramirez, F., Balla, T., Rohr, K., Kaul, A., Buhler, S., Pepperkok, R., Lengauer, T., Albrecht, M., Eils, R., Schirmacher, P., Lohmann, V. & Bartenschlager, R. (2011).** Recruitment and activation of a lipid kinase by hepatitis C virus NS5A is essential for integrity of the membranous replication compartment. *Cell Host Microbe* **9**, 32-45.

**Reynolds, G. M., Harris, H. J., Jennings, A., Hu, K., Grove, J., Lalor, P. F., Adams, D. H., Balfe, P., Hubscher, S. G. & McKeating, J. A. (2008).** Hepatitis C virus receptor expression in normal and diseased liver tissue. *Hepatology* **47**, 418-427.

**Ridruejo, E., Solano, A., Marciano, S., Galdame, O., Adrover, R., Cocozzella, D., Delettieres, D., Martinez, A., Gadano, A., Mando, O. G. & Silva, M. O. (2011).** Genetic variation in interleukin-28B predicts SVR in hepatitis C genotype 1 Argentine patients treated with PEG IFN and ribavirin. *Ann Hepatol* **10**, 452-457.

**Robertson, B., Myers, G., Howard, C., Brettin, T., Bukh, J., Gaschen, B., Gojobori, T., Maertens, G., Mizokami, M., Nainan, O., Netesov, S., Nishioka, K., Shin i, T., Simmonds, P., Smith, D., Stuyver, L. & Weiner, A. (1998).** Classification, nomenclature, and database development for hepatitis C virus (HCV) and related viruses: proposals for standardization. International Committee on Virus Taxonomy. *Arch Virol* **143**, 2493-2503.

**Roccasecca, R., Ansuini, H., Vitelli, A., Meola, A., Scarselli, E., Acali, S., Pezzanera, M., Ercole, B. B., McKeating, J., Yagnik, A., Lahm, A., Tramontano, A., Cortese, R. & Nicosia, A. (2003).** Binding of the hepatitis C virus E2 glycoprotein to CD81 is strain specific and is modulated by a complex interplay between hypervariable regions 1 and 2. *J Virol* **77**, 1856-1867.

**Roelandt, P., Obeid, S., Paeshuyse, J., Vanhove, J., Van Lommel, A., Nahmias, Y., Nevens, F., Neyts, J. & Verfaillie, C. M. (2012).** Human pluripotent stem cell-derived hepatocytes support complete replication of hepatitis C virus. *J Hepatol* **57**, 246-251.

**Romano, K. P., Ali, A., Aydin, C., Soumana, D., Ozen, A., Deveau, L. M., Silver, C., Cao, H., Newton, A., Petropoulos, C. J., Huang, W. & Schiffer, C. A. (2012).** The Molecular Basis of Drug Resistance against Hepatitis C Virus NS3/4A Protease Inhibitors. *PLoS Pathog* **8**, e1002832.

**Roohvand, F., Maillard, P., Lavergne, J. P., Boulant, S., Walic, M., Andreo, U., Goueslain, L., Helle, F., Mallet, A., McLauchlan, J. & Budkowska, A. (2009).** Initiation of hepatitis C virus infection requires the dynamic microtubule network: role of the viral nucleocapsid protein. *J Biol Chem* **284**, 13778-13791.

**Rubbia-Brandt, L., Leandro, G., Spahr, L., Giostra, E., Quadri, R., Male, P. J. & Negro, F. (2001).** Liver steatosis in chronic hepatitis C: a morphological sign suggesting infection with HCV genotype 3. *Histopathology* **39**, 119-124.

**Rubbia-Brandt, L., Quadri, R., Abid, K., Giostra, E., Male, P. J., Mentha, G., Spahr, L., Zarski, J. P., Borisch, B., Hadengue, A. & Negro, F. (2000).** Hepatocyte steatosis is a cytopathic effect of hepatitis C virus genotype 3. *J Hepatol* **33**, 106-115.

**Russell, R. S., Kawaguchi, K., Meunier, J. C., Takikawa, S., Faulk, K., Bukh, J., Purcell, R. H. & Emerson, S. U. (2009).** Mutational analysis of the hepatitis C virus E1 glycoprotein in retroviral pseudoparticles and cell-culture-derived H77/JFH1 chimeric infectious virus particles. *J Viral Hepat* **16**, 621-632.

**Sadler, A. J. & Williams, B. R. (2008).** Interferon-inducible antiviral effectors. *Nat Rev Immunol* **8**, 559-568.

**Saeed, M., Scheel, T. K., Gottwein, J. M., Marukian, S., Dustin, L. B., Bukh, J. & Rice, C. M. (2012).** Efficient replication of genotype 3a and 4a hepatitis C virus replicons in human hepatoma cells. *Antimicrob Agents Chemother* **56**, 5365-5373.

**Sainz, B., Jr., Barretto, N., Martin, D. N., Hiraga, N., Imamura, M., Hussain, S., Marsh, K. A., Yu, X., Chayama, K., Alrefai, W. A. & Uprichard, S. L. (2012).** Identification of the Niemann-Pick C1-like 1 cholesterol absorption receptor as a new hepatitis C virus entry factor. *Nat Med* **18**, 281-285.

**Sainz, B., Jr., Barretto, N. & Uprichard, S. L. (2009a).** Hepatitis C virus infection in phenotypically distinct Huh7 cell lines. *PLoS One* **4**, e6561.

**Sainz, B., Jr., TenCate, V. & Uprichard, S. L. (2009b).** Three-dimensional Huh7 cell culture system for the study of Hepatitis C virus infection. *Virol J* **6**, 103.

**Saito, K., Ait-Goughoulte, M., Truscott, S. M., Meyer, K., Blazevic, A., Abate, G., Ray, R. B., Hoft, D. F. & Ray, R. (2008a).** Hepatitis C virus inhibits cell surface expression of HLA-DR, prevents dendritic cell maturation, and induces interleukin-10 production. *J Virol* **82**, 3320-3328.

**Saito, T., Owen, D. M., Jiang, F., Marcotrigiano, J. & Gale, M., Jr. (2008b).** Innate immunity induced by composition-dependent RIG-I recognition of hepatitis C virus RNA. *Nature* **454**, 523-527.

**Saito, T., Hirai, R., Loo, Y. M., Owen, D., Johnson, C. L., Sinha, S. C., Akira, S., Fujita, T. & Gale, M., Jr. (2007).** Regulation of innate antiviral defenses through a shared repressor domain in RIG-I and LGP2. *Proc Natl Acad Sci U S A* **104**, 582-587.

**Sakai, A., Claire, M. S., Faulk, K., Govindarajan, S., Emerson, S. U., Purcell, R. H. & Bukh, J. (2003).** The p7 polypeptide of hepatitis C virus is critical for infectivity and contains functionally important genotype-specific sequences. *Proc Natl Acad Sci U S A* **100**, 11646-11651.

**Santiago, Y., Chan, E., Liu, P. Q., Orlando, S., Zhang, L., Urnov, F. D., Holmes, M. C., Guschin, D., Waite, A., Miller, J. C., Rebar, E. J., Gregory, P. D., Klug, A. & Collingwood, T. N. (2008).** Targeted gene knockout in mammalian cells by using engineered zinc-finger nucleases. *Proc Natl Acad Sci U S A* **105**, 5809-5814.

**Santolini, E., Migliaccio, G. & La Monica, N. (1994).** Biosynthesis and biochemical properties of the hepatitis C virus core protein. *J Virol* **68**, 3631-3641.

**Santolini, E., Pacini, L., Fipaldini, C., Migliaccio, G. & Monica, N. (1995).** The NS2 protein of hepatitis C virus is a transmembrane polypeptide. *J Virol* **69**, 7461-7471.

**Sapay, N., Montserret, R., Chipot, C., Brass, V., Moradpour, D., Deleage, G. & Penin, F. (2006).** NMR structure and molecular dynamics of the in-plane membrane anchor of nonstructural protein 5A from bovine viral diarrhea virus. *Biochemistry* **45**, 2221-2233.

**Sarasin-Filipowicz, M., Wang, X., Yan, M., Duong, F. H., Poli, V., Hilton, D. J., Zhang, D. E. & Heim, M. H. (2009).** Alpha interferon induces long-lasting refractoriness of JAK-STAT signaling in the mouse liver through induction of USP18/UBP43. *Mol Cell Biol* **29**, 4841-4851.

**Scarselli, E., Ansuini, H., Cerino, R., Roccasecca, R. M., Acali, S., Filocamo, G., Traboni, C., Nicosia, A., Cortese, R. & Vitelli, A. (2002).** The human scavenger receptor class B type I is a novel candidate receptor for the hepatitis C virus. *Embo J* **21**, 5017-5025.

**Scheel, T. K., Gottwein, J. M., Mikkelsen, L. S., Jensen, T. B. & Bukh, J. (2011).** Recombinant HCV variants with NS5A from genotypes 1-7 have different sensitivities to an NS5A inhibitor but not interferon-alpha. *Gastroenterology* **140**, 1032-1042.

**Schenborn, E. T. & Mierendorf, R. C., Jr. (1985).** A novel transcription property of SP6 and T7 RNA polymerases: dependence on template structure. *Nucleic Acids Res* **13**, 6223-6236.

**Schmidt-Mende, J., Bieck, E., Hugle, T., Penin, F., Rice, C. M., Blum, H. E. & Moradpour, D. (2001).** Determinants for membrane association of the hepatitis C virus RNA-dependent RNA polymerase. *J Biol Chem* **276**, 44052-44063.

**Schmitt, M., Scrima, N., Radujkovic, D., Caillet-Saguy, C., Simister, P. C., Friebe, P., Wicht, O., Klein, R., Bartenschlager, R., Lohmann, V. & Bressanelli, S. (2011).** A comprehensive structure-function comparison of hepatitis C virus strain JFH1 and J6 polymerases reveals a key residue stimulating replication in cell culture across genotypes. *J Virol* **85**, 2565-2581.

**Scrima, N., Caillet-Saguy, C., Ventura, M., Harrus, D., Astier-Gin, T. & Bressanelli, S. (2012).** Two crucial early steps in RNA synthesis by the hepatitis C virus polymerase involve a dual role of residue 405. *J Virol* **86**, 7107-7117.

**Seeff, L. B. (2002).** Natural history of chronic hepatitis C. *Hepatology* **36**, S35-46.

**Seeff, L. B. (2009).** The history of the "natural history" of hepatitis C (1968-2009). *Liver Int* **29 Suppl 1**, 89-99.

**Shah, S. R., Patel, K., Marcellin, P., Foster, G. R., Manns, M., Kottilil, S., Healey, L., Pulkstenis, E., Subramanian, G. M., McHutchison, J. G., Sulkowski, M. S., Zeuzem, S. & Nelson, D. R. (2011).** Steatosis is an independent predictor of relapse following rapid virologic response in patients with HCV genotype 3. *Clin Gastroenterol Hepatol* **9**, 688-693.

**Sharma, N. R., Mateu, G., Dreux, M., Grakoui, A., Cosset, F. L. & Melikyan, G. B. (2011).** Hepatitis C virus is primed by CD81 protein for low pH-dependent fusion. *J Biol Chem* **286**, 30361-30376.

**Shaw, M. L., McLauchlan, J., Mills, P. R., Patel, A. H. & McCruden, E. A. (2003).** Characterisation of the differences between hepatitis C virus genotype 3 and 1 glycoproteins. *J Med Virol* **70**, 361-372.

**Shepard, C. W., Finelli, L. & Alter, M. J. (2005).** Global epidemiology of hepatitis C virus infection. *Lancet Infect Dis* **5**, 558-567.

**Sheppard, P., Kindsvogel, W., Xu, W., Henderson, K., Schlutsmeyer, S., Whitmore, T. E., Kuestner, R., Garrigues, U., Birks, C., Roraback, J., Ostrander, C., Dong, D., Shin, J., Presnell, S., Fox, B., Haldeman, B., Cooper, E., Taft, D., Gilbert, T., Grant, F. J., Tackett, M., Krivan, W., McKnight, G., Clegg, C., Foster, D. & Klucher, K. M. (2003).** IL-28, IL-29 and their class II cytokine receptor IL-28R. *Nat Immunol* **4**, 63-68.

**Shimakami, T., Hijikata, M., Luo, H., Ma, Y. Y., Kaneko, S., Shimotohno, K. & Murakami, S. (2004).** Effect of interaction between hepatitis C virus NS5A and NS5B on hepatitis C virus RNA replication with the hepatitis C virus replicon. *J Virol* **78**, 2738-2748.

**Shimizu, Y. K., Feinstone, S. M., Purcell, R. H., Alter, H. J. & London, W. T. (1979).** Non-A, non-B hepatitis: ultrastructural evidence for two agents in experimentally infected chimpanzees. *Science* **205**, 197-200.

**Shin, K., Fogg, V. C. & Margolis, B. (2006).** Tight junctions and cell polarity. *Annu Rev Cell Dev Biol* **22**, 207-235.

**Shoukry, N. H., Grakoui, A., Houghton, M., Chien, D. Y., Ghrayeb, J., Reimann, K. A. & Walker, C. M. (2003).** Memory CD8+ T cells are required for protection from persistent hepatitis C virus infection. *J Exp Med* **197**, 1645-1655.

**Simister, P., Schmitt, M., Geitmann, M., Wicht, O., Danielson, U. H., Klein, R., Bressanelli, S. & Lohmann, V. (2009).** Structural and functional analysis of hepatitis C virus strain JFH1 polymerase. *J Virol* **83**, 11926-11939.

**Simmonds, P. (2004).** Genetic diversity and evolution of hepatitis C virus--15 years on. *J Gen Virol* **85**, 3173-3188.

**Sledz, C. A., Holko, M., de Veer, M. J., Silverman, R. H. & Williams, B. R. (2003).** Activation of the interferon system by short-interfering RNAs. *Nat Cell Biol* **5**, 834-839.

**Snove, O., Jr. & Rossi, J. J. (2006).** Chemical modifications rescue off-target effects of RNAi. *ACS Chem Biol* **1**, 274-276.

**Song, Y., Friebe, P., Tzima, E., Junemann, C., Bartenschlager, R. & Niepmann, M. (2006).** The hepatitis C virus RNA 3'-untranslated region strongly enhances translation directed by the internal ribosome entry site. *J Virol* **80**, 11579-11588.

**Soriano, V., Peters, M. G. & Zeuzem, S. (2009).** New therapies for hepatitis C virus infection. *Clin Infect Dis* **48**, 313-320.

**Spahn, C. M., Kieft, J. S., Grassucci, R. A., Penczek, P. A., Zhou, K., Doudna, J. A. & Frank, J. (2001).** Hepatitis C virus IRES RNA-induced changes in the conformation of the 40s ribosomal subunit. *Science* **291**, 1959-1962.

**Stapleford, K. A. & Lindenbach, B. D. (2011).** Hepatitis C virus NS2 coordinates virus particle assembly through physical interactions with the E1-E2 glycoprotein and NS3-NS4A enzyme complexes. *J Virol* **85**, 1706-1717.

**Stapleton, J. T., Foung, S., Muerhoff, A. S., Bukh, J. & Simmonds, P. (2011).** The GB viruses: a review and proposed classification of GBV-A, GBV-C (HGV), and GBV-D in genus Pegivirus within the family Flaviviridae. *J Gen Virol* **92**, 233-246.

**Stark, G. R., Kerr, I. M., Williams, B. R., Silverman, R. H. & Schreiber, R. D. (1998).** How cells respond to interferons. *Annu Rev Biochem* **67**, 227-264.

**Staub, O. (2004).** Ubiquitylation and isgylation: overlapping enzymatic cascades do the job. *Sci STKE* **2004**, pe43.

**Steinman, R. M. (2001).** Dendritic cells and the control of immunity: enhancing the efficiency of antigen presentation. *Mt Sinai J Med* **68**, 160-166.

**Steinmann, E., Penin, F., Kallis, S., Patel, A. H., Bartenschlager, R. & Pietschmann, T. (2007).** Hepatitis C Virus p7 Protein Is Crucial for Assembly and Release of Infectious Virions. *PLoS Pathog* **3**, e103.

**Stetson, D. B. & Medzhitov, R. (2006).** Recognition of cytosolic DNA activates an IRF3-dependent innate immune response. *Immunity* **24**, 93-103.

**StGelais, C., Tuthill, T. J., Clarke, D. S., Rowlands, D. J., Harris, M. & Griffin, S. (2007).** Inhibition of hepatitis C virus p7 membrane channels in a liposome-based assay system. *Antiviral Res* **76**, 48-58.

**Street, A., Macdonald, A., Crowder, K. & Harris, M. (2004).** The Hepatitis C virus NS5A protein activates a phosphoinositide 3-kinase-dependent survival signaling cascade. *J Biol Chem* **279**, 12232-12241.

**Sumpter, R., Jr., Loo, Y. M., Foy, E., Li, K., Yoneyama, M., Fujita, T., Lemon, S. M. & Gale, M., Jr. (2005).** Regulating intracellular antiviral defense and permissiveness to hepatitis C virus RNA replication through a cellular RNA helicase, RIG-I. *J Virol* **79**, 2689-2699.

**Swain, S. L., McKinstry, K. K. & Strutt, T. M. (2011).** Expanding roles for CD4(+) T cells in immunity to viruses. *Nat Rev Immunol* **12**, 136-148.

**Tai, C. L., Chi, W. K., Chen, D. S. & Hwang, L. H. (1996).** The helicase activity associated with hepatitis C virus nonstructural protein 3 (NS3). *J Virol* **70**, 8477-8484.

**Takehara, T., Hayashi, N., Mita, E., Hagiwara, H., Ueda, K., Katayama, K., Kasahara, A., Fusamoto, H. & Kamada, T. (1992).** Detection of the minus strand of hepatitis C virus RNA by reverse transcription and polymerase chain reaction: implications for hepatitis C virus replication in infected tissue. *Hepatology* **15**, 387-390.

**Takeuchi, T., Iwahara, S., Saeki, Y., Sasajima, H. & Yokosawa, H. (2005).** Link between the ubiquitin conjugation system and the ISG15 conjugation system: ISG15 conjugation to the UbcH6 ubiquitin E2 enzyme. *J Biochem* **138**, 711-719.

**Takeuchi, T., Kobayashi, T., Tamura, S. & Yokosawa, H. (2006).** Negative regulation of protein phosphatase 2Cbeta by ISG15 conjugation. *FEBS Lett* **580**, 4521-4526.

**Tanaka, T., Kato, N., Cho, M. J., Sugiyama, K. & Shimotohno, K. (1996).** Structure of the 3' terminus of the hepatitis C virus genome. *J Virol* **70**, 3307-3312.

**Tang, Y., Zhong, G., Zhu, L., Liu, X., Shan, Y., Feng, H., Bu, Z., Chen, H. & Wang, C. (2010).** Herc5 attenuates influenza A virus by catalyzing ISGylation of viral NS1 protein. *J Immunol* **184**, 5777-5790.

**Tardif, K. D., Mori, K. & Siddiqui, A. (2002).** Hepatitis C virus subgenomic replicons induce endoplasmic reticulum stress activating an intracellular signaling pathway. *J Virol* **76**, 7453-7459.

**Targett-Adams, P., Boulant, S. & McLauchlan, J. (2008).** Visualization of double-stranded RNA in cells supporting hepatitis C virus RNA replication. *J Virol* **82**, 2182-2195.

**Targett-Adams, P. & McLauchlan, J. (2005).** Development and characterization of a transient-replication assay for the genotype 2a hepatitis C virus subgenomic replicon. *J Gen Virol* **86**, 3075-3080.

**Taylor, J. L., D'Cunha, J., Tom, P., O'Brien, W. J. & Borden, E. C. (1996).** Production of ISG-15, an interferon-inducible protein, in human corneal cells. *J Interferon Cytokine Res* **16**, 937-940.

**Taylor, D. R., Shi, S. T., Romano, P. R., Barber, G. N. & Lai, M. M. (1999).** Inhibition of the interferon-inducible protein kinase PKR by HCV E2 protein. *Science* **285**, 107-110.

**Tedbury, P., Welbourn, S., Pause, A., King, B., Griffin, S. & Harris, M. (2011).** The subcellular localization of the hepatitis C virus non-structural protein NS2 is regulated by an ion channel-independent function of the p7 protein. *J Gen Virol* **92**, 819-830.

**Tellinghuisen, T. L., Evans, M. J., von Hahn, T., You, S. & Rice, C. M. (2007).** Studying hepatitis C virus: making the best of a bad virus. *J Virol* **81**, 8853-8867.

**Tellinghuisen, T. L., Foss, K. L. & Treadaway, J. (2008a).** Regulation of hepatitis C virion production via phosphorylation of the NS5A protein. *PLoS Pathog* **4**, e1000032.

**Tellinghuisen, T. L., Foss, K. L., Treadaway, J. C. & Rice, C. M. (2008b).** Identification of residues required for RNA replication in domains II and III of the hepatitis C virus NS5A protein. *J Virol* **82**, 1073-1083.

**Tellinghuisen, T. L., Marcotrigiano, J., Gorbalenya, A. E. & Rice, C. M. (2004).** The NS5A protein of hepatitis C virus is a zinc metalloprotein. *J Biol Chem* **279**, 48576-48587.

**Tellinghuisen, T. L., Marcotrigiano, J. & Rice, C. M. (2005).** Structure of the zinc-binding domain of an essential component of the hepatitis C virus replicase. *Nature* **435**, 374-379.

**Thimme, R., Bukh, J., Spangenberg, H. C., Wieland, S., Pemberton, J., Steiger, C., Govindarajan, S., Purcell, R. H. & Chisari, F. V. (2002).** Viral and immunological determinants of hepatitis C virus clearance, persistence, and disease. *Proc Natl Acad Sci U S A* **99**, 15661-15668.

**Thimme, R., Oldach, D., Chang, K. M., Steiger, C., Ray, S. C. & Chisari, F. V. (2001).** Determinants of viral clearance and persistence during acute hepatitis C virus infection. *J Exp Med* **194**, 1395-1406.

**Thompson, A. A., Zou, A., Yan, J., Duggal, R., Hao, W., Molina, D., Cronin, C. N. & Wells, P. A. (2009).** Biochemical characterization of recombinant hepatitis C virus nonstructural protein 4B: evidence for ATP/GTP hydrolysis and adenylate kinase activity. *Biochemistry* **48**, 906-916.

**Thompson, A. J., Muir, A. J., Sulkowski, M. S., Ge, D., Fellay, J., Shianna, K. V., Urban, T., Afdhal, N. H., Jacobson, I. M., Esteban, R., Poordad, F., Lawitz, E. J., McCone, J., Shiffman, M. L., Galler, G. W., Lee, W. M., Reindollar, R., King, J. W., Kwo, P. Y., Ghalib, R. H., Freilich, B., Nyberg, L. M., Zeuzem, S., Poynard, T., Vock, D. M., Pieper, K. S., Patel, K., Tillmann, H. L., Noviello, S., Koury, K., Pedicone, L. D., Brass, C. A., Albrecht, J. K., Goldstein, D. B. & McHutchison, J. G. (2010).** Interleukin-28B polymorphism improves viral kinetics and is the strongest pretreatment predictor of sustained virologic response in genotype 1 hepatitis C virus. *Gastroenterology* **139**, 120-129 e118.

**Thompson, M. R., Kaminski, J. J., Kurt-Jones, E. A. & Fitzgerald, K. A. (2011).** Pattern recognition receptors and the innate immune response to viral infection. *Viruses* **3**, 920-940.

**Thomson, B. J. (2009).** Hepatitis C virus: the growing challenge. *Br Med Bull* **89**, 153-167.

**Thomson, E. C., Fleming, V. M., Main, J., Klenerman, P., Weber, J., Eliahoo, J., Smith, J., McClure, M. O. & Karayiannis, P. (2011).** Predicting spontaneous clearance of acute hepatitis C virus in a large cohort of HIV-1-infected men. *Gut* **60**, 837-845.

**Thomson, E. C., Smith, J. A. & Klenerman, P. (2011).** The natural history of early hepatitis C virus evolution; lessons from a global outbreak in human immunodeficiency virus-1-infected individuals. *J Gen Virol* **92**, 2227-2236.

**Tiganis, T., Kemp, B. E. & Tonks, N. K. (1999).** The protein-tyrosine phosphatase TCPTP regulates epidermal growth factor receptor-mediated and phosphatidylinositol 3-kinase-dependent signaling. *J Biol Chem* **274**, 27768-27775.

**Tseng, C. T. & Klimpel, G. R. (2002).** Binding of the hepatitis C virus envelope protein E2 to CD81 inhibits natural killer cell functions. *J Exp Med* **195**, 43-49.

**Ulsenheimer, A., Gerlach, J. T., Jung, M. C., Gruener, N., Wachtler, M., Backmund, M., Santantonio, T., Schraut, W., Heeg, M. H., Schirren, C. A., Zachoval, R., Pape, G. R. & Diepolder, H. M. (2005).** Plasmacytoid dendritic cells in acute and chronic hepatitis C virus infection. *Hepatology* **41**, 643-651.

**Urbani, S., Amadei, B., Fisicaro, P., Tola, D., Orlandini, A., Sacchelli, L., Mori, C., Missale, G. & Ferrari, C. (2006).** Outcome of acute hepatitis C is related to virus-specific CD4 function and maturation of antiviral memory CD8 responses. *Hepatology* **44**, 126-139.

**Vaillancourt, F. H., Brault, M., Pilote, L., Uyttersprot, N., Gaillard, E. T., Stoltz, J. H., Knight, B. L., Pantages, L., McFarland, M., Breitfelder, S., Chiu, T. T., Mahrouche, L., Faucher, A. M., Cartier, M., Cordingley, M. G., Bethell, R. C., Jiang, H., White, P. W. & Kukolj, G. (2012).**

Evaluation of phosphatidylinositol-4-kinase IIIalpha as a hepatitis C virus drug target. *J Virol*.

**Vieyres, G., Thomas, X., Descamps, V., Duverlie, G., Patel, A. H. & Dubuisson, J. (2010).** Characterization of the envelope glycoproteins associated with infectious hepatitis C virus. *J Virol* **84**, 10159-10168.

**Wakita, T., Pietschmann, T., Kato, T., Date, T., Miyamoto, M., Zhao, Z., Murthy, K., Habermann, A., Krausslich, H. G., Mizokami, M., Bartenschlager, R. & Liang, T. J. (2005).** Production of infectious hepatitis C virus in tissue culture from a cloned viral genome. *Nat Med* **11**, 791-796.

**Wang, C., Sarnow, P. & Siddiqui, A. (1993).** Translation of human hepatitis C virus RNA in cultured cells is mediated by an internal ribosome-binding mechanism. *J Virol* **67**, 3338-3344.

**Wang, N., Liang, Y., Devaraj, S., Wang, J., Lemon, S. M. & Li, K. (2009).** Toll-like receptor 3 mediates establishment of an antiviral state against hepatitis C virus in hepatoma cells. *J Virol* **83**, 9824-9834.

**Washburn, M. L., Bility, M. T., Zhang, L., Kovalev, G. I., Buntzman, A., Frelinger, J. A., Barry, W., Ploss, A., Rice, C. M. & Su, L. (2011).** A humanized mouse model to study hepatitis C virus infection, immune response, and liver disease. *Gastroenterology* **140**, 1334-1344.

**Watashi, K., Ishii, N., Hijikata, M., Inoue, D., Murata, T., Miyanari, Y. & Shimotohno, K. (2005).** Cyclophilin B is a functional regulator of hepatitis C virus RNA polymerase. *Mol Cell* **19**, 111-122.

**Watts, J. K., Deleavey, G. F. & Damha, M. J. (2008).** Chemically modified siRNA: tools and applications. *Drug Discov Today* **13**, 842-855.

**Weiner, A. J., Brauer, M. J., Rosenblatt, J., Richman, K. H., Tung, J., Crawford, K., Bonino, F., Saracco, G., Choo, Q. L., Houghton, M. & et al. (1991).** Variable and hypervariable domains are found in the regions of HCV corresponding to the flavivirus envelope and NS1 proteins and the pestivirus envelope glycoproteins. *Virology* **180**, 842-848.

**Williams, B. R. (2001).** Signal integration via PKR. *Sci STKE* **2001**, re2.

**Wolk, B., Sansonno, D., Krausslich, H. G., Dammacco, F., Rice, C. M., Blum, H. E. & Moradpour, D. (2000).** Subcellular localization, stability, and trans-cleavage competence of the hepatitis C virus NS3-NS4A complex expressed in tetracycline-regulated cell lines. *J Virol* **74**, 2293-2304.

**Wozniak, A. L., Griffin, S., Rowlands, D., Harris, M., Yi, M., Lemon, S. M. & Weinman, S. A. (2010).** Intracellular proton conductance of the hepatitis C virus p7 protein and its contribution to infectious virus production. *PLoS Pathog* **6**, e1001087.

**Yamaga, A. K. & Ou, J. H. (2002).** Membrane topology of the hepatitis C virus NS2 protein. *J Biol Chem* **277**, 33228-33234.

**Yanagi, M., St Claire, M., Emerson, S. U., Purcell, R. H. & Bukh, J. (1999).** In vivo analysis of the 3' untranslated region of the hepatitis C virus after in vitro mutagenesis of an infectious cDNA clone. *Proc Natl Acad Sci U S A* **96**, 2291-2295.

**Yao, N., Hesson, T., Cable, M., Hong, Z., Kwong, A. D., Le, H. V. & Weber, P. C. (1997).** Structure of the hepatitis C virus RNA helicase domain. *Nat Struct Biol* **4**, 463-467.

**Yeh, E. T., Gong, L. & Kamitani, T. (2000).** Ubiquitin-like proteins: new wines in new bottles. *Gene* **248**, 1-14.

**Yi, M. & Lemon, S. M. (2003).** Structure-function analysis of the 3' stem-loop of hepatitis C virus genomic RNA and its role in viral RNA replication. *Rna* **9**, 331-345.

**Yi, M. & Lemon, S. M. (2004).** Adaptive mutations producing efficient replication of genotype 1a hepatitis C virus RNA in normal Huh7 cells. *J Virol* **78**, 7904-7915.

**Yi, M., Ma, Y., Yates, J. & Lemon, S. M. (2007).** Compensatory Mutations in E1, p7, NS2, and NS3 Enhance Yields of Cell Culture-Infectious Intergenotypic Chimeric Hepatitis C Virus. *J Virol* **81**, 629-638.

**Yi, M., Ma, Y., Yates, J. & Lemon, S. M. (2009).** Trans-complementation of an NS2 defect in a late step in hepatitis C virus (HCV) particle assembly and maturation. *PLoS Pathog* **5**, e1000403.

**Yoon, J. C., Shiina, M., Ahlenstiel, G. & Rehermann, B. (2009).** Natural killer cell function is intact after direct exposure to infectious hepatitis C virions. *Hepatology* **49**, 12-21.

**Yu, G. Y., Lee, K. J., Gao, L. & Lai, M. M. (2006).** Palmitoylation and polymerization of hepatitis C virus NS4B protein. *J Virol* **80**, 6013-6023.

**Yuan, W. & Krug, R. M. (2001).** Influenza B virus NS1 protein inhibits conjugation of the interferon (IFN)-induced ubiquitin-like ISG15 protein. *Embo J* **20**, 362-371.

**Zech, B., Kurtenbach, A., Krieger, N., Strand, D., Blencke, S., Morbitzer, M., Salassidis, K., Cotten, M., Wissing, J., Obert, S., Bartenschlager, R., Herget, T. & Daub, H. (2003).** Identification and characterization of amphiphysin II as a novel cellular interaction partner of the hepatitis C virus NS5A protein. *J Gen Virol* **84**, 555-560.

**Zeisel, M. B., Koutsoudakis, G., Schnober, E. K., Haberstroh, A., Blum, H. E., Cosset, F. L., Wakita, T., Jaeck, D., Doffoel, M., Royer, C., Soulier, E., Schvoerer, E., Schuster, C., Stoll-Keller, F., Bartenschlager, R., Pietschmann, T., Barth, H. & Baumert, T. F. (2007).** Scavenger receptor class B type I is a key host factor for hepatitis C virus infection required for an entry step closely linked to CD81. *Hepatology* **46**, 1722-1731.

**Zhang, J., Randall, G., Higginbottom, A., Monk, P., Rice, C. M. & McKeating, J. A. (2004).** CD81 is required for hepatitis C virus glycoprotein-mediated viral infection. *J Virol* **78**, 1448-1455.

**Zhao, C., Beaudenon, S. L., Kelley, M. L., Waddell, M. B., Yuan, W., Schulman, B. A., Huibregtse, J. M. & Krug, R. M. (2004).** The UbcH8 ubiquitin E2 enzyme is also the E2 enzyme for ISG15, an IFN-alpha/beta-induced ubiquitin-like protein. *Proc Natl Acad Sci U S A* **101**, 7578-7582.

**Zhao, C., Denison, C., Huibregtse, J. M., Gygi, S. & Krug, R. M. (2005).** Human ISG15 conjugation targets both IFN-induced and constitutively expressed proteins functioning in diverse cellular pathways. *Proc Natl Acad Sci U S A* **102**, 10200-10205.

**Zhao, C., Hsiang, T. Y., Kuo, R. L. & Krug, R. M. (2010).** ISG15 conjugation system targets the viral NS1 protein in influenza A virus-infected cells. *Proc Natl Acad Sci U S A* **107**, 2253-2258.

**Zheng, Y., Gao, B., Ye, L., Kong, L., Jing, W., Yang, X. & Wu, Z. (2005).** Hepatitis C virus non-structural protein NS4B can modulate an unfolded protein response. *J Microbiol* **43**, 529-536.

**Zhong, J., Gastaminza, P., Cheng, G., Kapadia, S., Kato, T., Burton, D. R., Wieland, S. F., Uprichard, S. L., Wakita, T. & Chisari, F. V. (2005).** Robust hepatitis C virus infection in vitro. *Proc Natl Acad Sci U S A* **102**, 9294-9299.

**Zhu, H., Dong, H., Eksioglu, E., Hemming, A., Cao, M., Crawford, J. M., Nelson, D. R. & Liu, C. (2007).** Hepatitis C virus triggers apoptosis of a newly developed hepatoma cell line through antiviral defense system. *Gastroenterology* **133**, 1649-1659.

**Zou, W. & Zhang, D. E. (2006).** The interferon-inducible ubiquitin-protein isopeptide ligase (E3) EFP also functions as an ISG15 E3 ligase. *J Biol Chem* **281**, 3989-3994.